

Past human-landscape interactions in the Netherlands

Reconstructions from sand belt to coastal-delta plain for the first millennium AD

Interacties tussen mens en landschap in het eerste millennium na Chr.

Reconstructies van de Nederlandse kustvlakte, de delta en de zandgebieden

(met een samenvatting in het Nederlands)

PROEFSCHRIFT

ter verkrijging van de graad van doctor aan de Universiteit Utrecht
op gezag van de rector magnificus, prof. dr. G.J. van der Zwaan,
ingevolge het besluit van het college voor promoties in het openbaar te verdedigen
op vrijdag 27 oktober 2017 des middags te 4.15 uur

door

Harm Jan Pierik

geboren op 24 juli 1986 te Zwolle

Past human-landscape interactions in the Netherlands

Past human-landscape interactions in the Netherlands

Reconstructions from sand belt to coastal-delta plain for the first millennium AD

Harm Jan Pierik

Promotoren:

Prof. dr. E. Jansma

Prof. dr. H. Middelkoop

Copromotoren:

Dr. W.Z. Hoek

Dr. E. Stouthamer

Examination committee:

Dr. F. Bungenstock

Niedersächsisches Institut für historische Küstenforschung,
Wilhelmshaven, Germany

Prof. dr. ir. M. Spek

University of Groningen, the Netherlands

Prof. dr. T.E. Törnqvist

Tulane University, New Orleans, USA

Prof. dr. G. Verstraeten

University of Leuven, Belgium

Prof. dr. J. Wallinga

Wageningen University, the Netherlands

ISBN 978-90-6266-483-2

Photo on the front page: human-landscape interactions at 53° 07' 52", 4° 48' 45"

Copyright © 2017 Harm Jan Pierik

Niets uit deze uitgave mag worden vermenigvuldigd en/of openbaar gemaakt door middel van druk, fotokopie of op welke andere wijze dan ook zonder voorafgaande schriftelijke toestemming van de uitgevers.

All rights reserved. No part of this publication may be reproduced in any form, by print or photo print, microfilm or any other means, without written permission by the publishers.

Printed by Ipskamp Printing, Enschede

Contents

1	General introduction	11
1.1	Human-landscape interaction in lowland areas	11
1.2	The Netherlands during the first millennium AD	14
1.3	Problem definition	16
1.4	Aim and general approach	17
1.5	Approach per lowland region	20
2	Geological and geomorphological mapping traditions in the Netherlands	23
2.1	Introduction	23
2.2	Research traditions and resulting maps products	24
2.3	Concluding remarks	36
3	A new GIS approach for reconstructing and mapping dynamic late Holocene coastal plain palaeogeography	39
3.1	Introduction	39
3.2	General approach	41
3.3	Workflow for map compilation and scripted palaeogeography	44
3.4	Results and discussion	56
3.5	Conclusion	60
4	Late Holocene coastal-plain evolution of the Netherlands: the role of antecedent conditions in human-induced sea ingressions	61
4.1	Introduction	61
4.2	Middle Holocene coastal plain evolution	66
4.3	Late-Holocene ingressions	69
4.4	Discussion	78
4.5	Conclusions	84
5	Human-induced drivers of avulsion success in the Rhine-Meuse delta, the Netherlands	87
5.1	Introduction	87
5.2	Materials and methods	89
5.3	Avulsion history results	89
5.4	Anthropogenic controls and feedbacks in avulsion success	91
5.5	Conclusion and implications	93
6	Natural levee evolution in the Rhine-Meuse delta, the Netherlands, during the first millennium AD	95
6.1	Introduction	95
6.2	The Rhine-Meuse delta: setting and natural levee characteristics	98
6.3	Compiling and analysing the natural-levee maps	103
6.4	Spatial and temporal variations in levee geometry	110
6.5	Discussion	115

6.6	Conclusions	122
7	Roman and early-medieval habitation patterns in a delta landscape: the link between settlement elevation and landscape dynamics	125
7.1	Introduction	125
7.2	Materials and methods	128
7.3	Results	133
7.4	Discussion	135
7.5	Conclusions	142
8	Calculating connectivity patterns in delta landscapes: modelling Roman and early-medieval route networks and their stability in dynamic lowlands	145
8.1	Introduction	145
8.2	Route networks and connectivity patterns	147
8.3	Material and methods	149
8.4	Results	157
8.5	Discussion	166
8.6	Conclusion	170
9	Controls on late Holocene drift-sand dynamics: the dominant role of human pressure in the Netherlands	173
9.1	Introduction	173
9.2	Controls in drift-sand formation	175
9.3	Geographical setting	177
9.4	Materials and method	179
9.5	Results	185
9.6	Discussion	197
9.7	Conclusions	200
10	Synthesis	203
10.1	Conclusions on human-landscape interactions	203
10.2	The use of landscape reconstructions in studying past human-landscape interactions	205
10.3	Past human-landscape interactions	209
10.4	Applications and outlook	215
	Summary	219
	Samenvatting	223
	Appendix A: Supplement to chapters 2, 3, and 6 (online only)	229
	Appendix B: Supplement to chapter 5	231
B1	Radiocarbon dating	231
B2	Archaeological reclamation evidence	234
B3	Former peat-surface reconstruction	237

Appendix C: Supplement to chapter 6	243
C1 Methods	243
C2 Maps (online only)	247
Appendix D: Supplement to chapter 9	249
D1 Reconstruction population density	249
D2 Drift-sand dates (online only)	250
Dankwoord	251
References	253
About the author	285

Chapter 1

General introduction

1.1 Human-landscape interaction in lowland areas

Lowland areas comprise coastal plains, peaty wetlands, river deltas, and valleys, surrounded by uplands and coastal waters. Many of these environments nowadays are densely populated, and therefore many people make use of their resources and depend on flooding safety measures in these areas. These lowlands have been shaped naturally by the interplay of fluvial, marine, biotic, and aeolian processes but human pressure increasingly affects the natural processes that shape these low elevated areas. In many wet delta lowlands, such as the Mississippi delta and the Mekong delta, groundwater extraction causes subsidence leading to drowning problems of inhabited areas (Törnqvist et al., 2008; Syvitski et al., 2009). Also, dredging and engineering works in river channels directly affect tidal and fluvial processes, for example by rerouting the water flow or allowing the tide to propagate further landward (Van den Berg et al., 1996; Lesourd et al., 2001). Dam construction in the upstream catchments caused sediment deficits for many downstream deltas, leading to delta erosion and drowning (e.g. Stanley and Warne, 1994; Syvitski et al., 2005; Syvitski & Saito, 2007). Human interferences with wetland ecology (e.g. through deforestation) change flow dynamics, erosional susceptibility, and channel geometry (Corenblit et al., 2007; Osterkamp et al., 2012). Also, outside the coastal and delta plain, deforestation and intensified agriculture can cause soil depletion that may lead to aeolian erosion and further soil degradation (Worster, 1979; Ravi et al., 2010).

Human influence has been a shaping agent on lowland landscapes throughout large parts of history and prehistory. Already thousands of years ago, humans affected lowlands in many parts of the world through deforestation and reclamation for agricultural practices (e.g. Goudie, 2006; Bianchi, 2016). In some cases, people directly affected the course of new river branches by digging channels for irrigation (e.g. Khuzestan plain, Iran; Heyveart & Walstra 2016). More indirectly, deforestation and intensive land use in upstream areas enhanced soil erosion and the eroded sediments that were transported downstream led to accelerated sedimentation in lowland areas. This has been recorded for the Roman period onwards for deltas around the Mediterranean (Maselli & Trincardi, 2013; Anthony et al., 2014), the Danube (Giosan et al., 2006), and the Rhine (Erkens & Cohen, 2009). Outside the wetlands, on higher elevated sandier soils, deforestation and agricultural practices have at least partially controlled drift-sand activity since the late Holocene, for example in Germany and Poland (Kozarski & Nowaczyk, 1991; Tolkendorf & Kaiser, 2012), the UK (Bateman & Godby, 2004), and the Netherlands (Koster et al., 1993).

Natural landscape setting and landscape dynamics were important for the people living in it. In relatively wet lowlands, settlement locations, route corridors, and agricultural practices were mainly concentrated in the higher and drier parts of the landscape. This implies that geomorphological changes, such as drowning, shifting river channels, increased sedimentation, and soil degradation could have far-reaching consequences for these early lowland settlers. Lowland areas contain rich resources and opportunities for trade and transport (e.g. via rivers) and were, therefore, densely populated throughout history and prehistory (the Egyptian Nile Delta — Butzer, 1982; Stanley &



Figure 1.1 | Location of the three study areas and their sub-regions that are dealt with in this thesis. Background palaeogeography AD 800 (Vos & De Vries, 2013).

Warne, 1993; Macklin et al., 2015; Mesopotamia — Wilkinson, 2000; Kuijt & Goring-Morris, 2002 and the Indus valley — Giosan et al., 2012).

Additionally, these areas are specifically susceptible to geomorphological changes, because (i) lowlands are not only directly affected by local changes but also by system disturbances in the upstream parts of the catchments that propagated to the lowland (e.g. deforestation that changed

sediment flux and flood regimes); (ii) gradients in elevation are often small and therefore changes in flood regime, sediment deposition, and groundwater level propagate over larger distances; and (iii) lowlands often consist of soft and unconsolidated substrate (e.g. erodible sands or compaction-prone peat). This makes them more susceptible to erosion by channel dynamics, subsidence, and soil degradation compared to rocky substrates.

Besides being susceptible to forcings, the research potential of deltas and coastal plains for studies on human-landscape interaction is especially high. This is because depositional layers formed through time are stacked, causing the subsequent burial of old landscapes. As a result, these landscapes have been preserved as semi-continuous sedimentary records. Moreover, because archaeological materials in such environments often have remained wet after burial, they often have been preserved well and can be used for reconstructing past human activity.

Because of their vulnerability and their generally rich habitation history, lowlands are interesting areas to study human-landscape interaction, leading to research questions such as: How did early settlers affect the landscape, causing unintended and irreversible effects, such as shifting rivers or drowning? How did people live in vulnerable lowlands and how did they react to environmental changes: did they abandon certain areas or did they adapt to the changing environments? To solve these questions, the impacts and causes of past geomorphological changes have to be assessed and their thresholds are to be identified. Tackling human-landscape interaction in the past also contributes to a better understanding of the current state of lowland areas. This may help to better predict their future geomorphological evolution and contribute to questions that are relevant for society, such as: when will rivers change their paths? Which parts of lowlands will be flooded more often? Which soils are susceptible to land degradation? When the processes involved in these changes are better understood, human-induced effects in lowlands can be better mitigated or adapted to.

Past landscape dynamics of inhabited lowland areas cannot be fully understood without using an integrative approach in which data and methods from the disciplines of physical geography and archaeology are combined. The spatial and temporal patterns of habitation inferred from archaeological records cannot be fully understood without considering the geomorphological setting of the former landscape and the (partly human induced) changes in the abiotic landscape (i.e. on stratigraphy, soils, and geomorphology) and the biotic landscape (i.e., vegetation and animals). To infer causal relations, the timing of these landscape changes is crucial. Besides physical dating methods (radiocarbon, OSL), archaeological finds that are diagnostic for specific archaeological periods can help to determine the age of the geomorphological elements and disturbances in the landscape (e.g. Berendsen & Stouthamer, 2001; Vos & Gerrets, 2005). When the geomorphological changes are known in time and space, archaeological records are needed to assess the effect of human activities on the landscape and the impact of landscape changes on humans. The archaeological records used for dating then have to be independent of records used for deducing these causal relations.

Geoarchaeology and landscape archaeology are interdisciplinary research disciplines that offer tools for better understanding the interactions between geomorphology, environmental history, and archaeology (Butzer, 1982; 2008; Kluiving et al., 2012). In geoarchaeology this is done by applying earth scientific methods (e.g. dating methods, micromorphology, conservation of archaeological materials) to help interpreting and better understand the archaeological record on specific sites (e.g. Rapp & Hill, 2006; Goldberg & Macphail, 2008) and by assessing the influence of environmental factors on archaeology (e.g. Butzer, 1982; Brown, 2008). Many geoarchaeological studies, however, have a strong local focus on archaeological sites or on their direct surroundings. Landscape

archaeology generally comprises a more regional scope focussing on the spatial relation between archaeological sites and other landscape elements (Kluiving et al., 2012; David & Thomas, 2016). Both research disciplines however generally tackle archaeological research questions rather than geomorphological ones. Because in a dynamic lowland landscape geomorphological changes can be majorly human-influenced and in turn can be important drivers for archaeological changes, a more geomorphological perspective on human-landscape interactions is also needed in these areas.

1.2 The Netherlands during the first millennium AD

The Netherlands are situated in a lowland area bordered by the North Sea. Its physical landscape has been shaped since the Late Pleistocene by multiple geomorphological agents, such as the sea, rivers, wind, plants, animals, and humans. The wide coastal plain mainly comprised extensive peat-lands and was interrupted by outlets of the rivers Rhine, Meuse, Scheldt, and Ems and outlets of the tidal area in the northern coastal plain (Figure 1.1). The Netherlands' Pleistocene uplands form the western part of the northwestern European sand belt (Koster, 2005). Considering the interplay between tidal, fluvial, and aeolian processes, this lowland area has a typical and diverse geomorphological evolutionary history. It is a well-studied area where changes in the landscape can be inferred from sedimentological records, geomorphology, and archaeology. As such it provides much data to study the interactions between people and the landscape on a local scale, but also on a larger regional scale compared to many other more confined lowland areas.

Since the introduction of agriculture in the Netherlands (expanding from the loess and sand uplands into the delta and coastal plain over the period 5000-3500 BC; Raemaekers, 2005; Out, 2009), the landscape has been increasingly modified by people, finally resulting in a mainly human-dominated state after ca. AD 1000. This thesis focusses on the first millennium AD as a special period (Figure 1.2), because it saw a strong fluctuation in population pressure and vegetation cover as well as abundant geomorphological changes (Jansma et al., 2014). In the beginning of this period the northern border of the Roman empire (*limes*), was located along the river Rhine in the study area. Here, and also in other parts of the Netherlands, population density was substantially higher than in earlier periods (Louwe Kooijmans, 1995). In the Late Iron Age (250-12 BC) first reclamation works were performed on a small scale: construction of dams, culverts, canals, and ditches (e.g. Ter Brugge, 2002; Van Londen, 2006; Vos, 2009). Since the 4th and 5th centuries AD, however, depopulation occurred, coinciding with the collapse of the Western Roman Empire (Cheyette, 2008; Wickham, 2009; Heeren, 2015), and the large-scale migration of tribes throughout northwestern Europe (e.g. Halsall, 2007). This period has been traditionally referred to as the 'Dark Ages' (e.g. James, 1988), a term that on the one hand refers to a period of cultural decline and disorder, and on the other hand indicates periods from which little written information is available in general, rather than this specific period. The depopulation trend of the 4th and 5th centuries AD caused forest regeneration in many parts of northwestern Europe, including the Netherlands (Teunissen, 1990; Louwe Kooijmans, 1995; Kaplan et al., 2009). The dip in the number of archaeological finds and population density traditionally has been attributed to cultural (political and economic factors – e.g. Halsall, 2007) and climatic factors (Büntgen et al., 2011; 2016; McCormick et al., 2012; Nooren et al., 2017 - Dark Ages Cold period; Figure 1.2). However, also major landscape changes occurred (compare Figure 1.3A and 1.3B), such as sea ingressions (Vos & Van Heeringen, 1997; Vos, 2015), reorganising river networks (Pons, 1957; Törnqvist, 1993; Berendsen & Stouthamer, 2000), and changing hinterland palaeohydrology (Berendsen & Stouthamer, 2000; Erkens et al. 2011; Toonen et al., 2017), which must have affected the inhabitants. From the 7th century onwards the

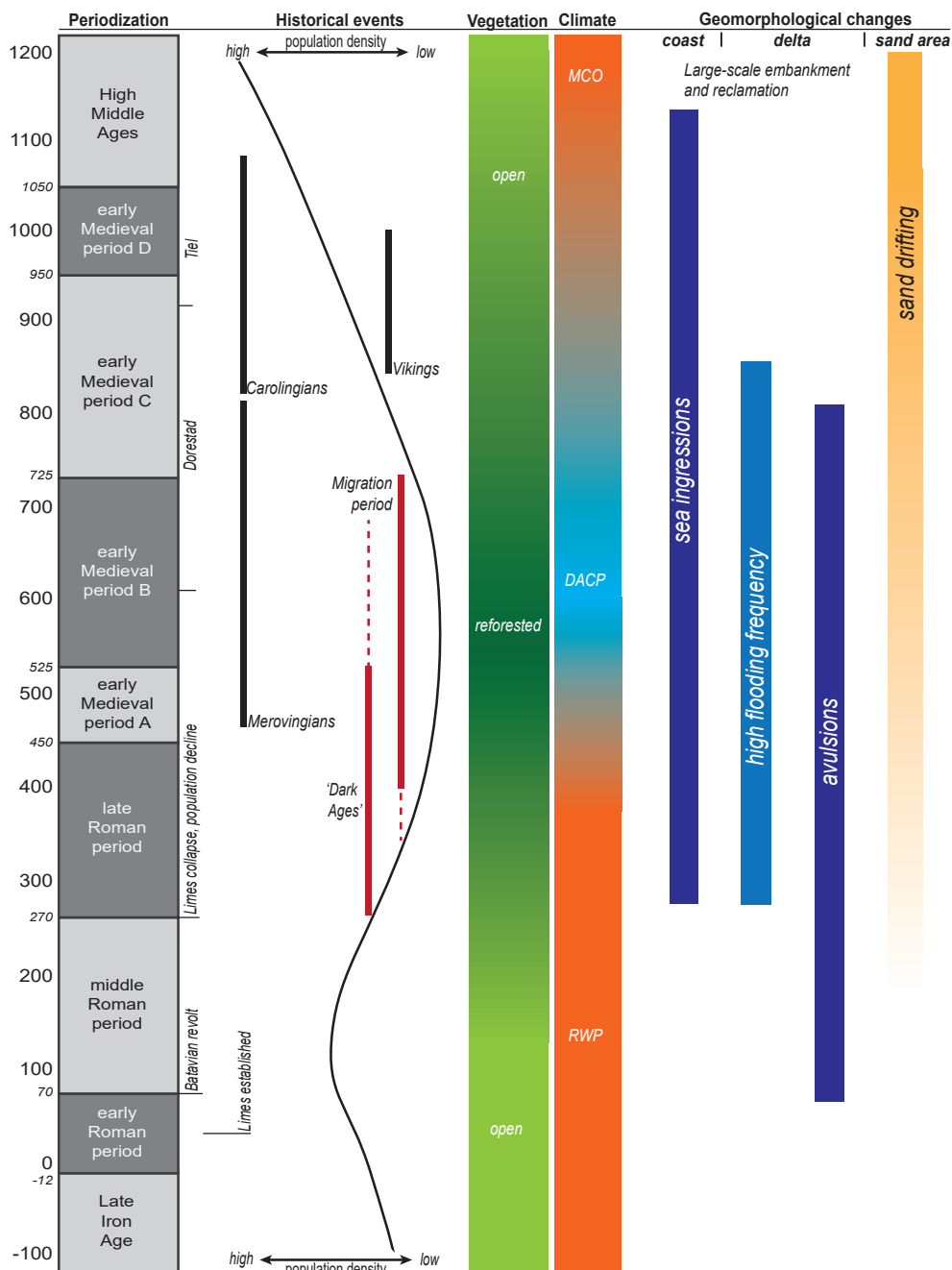


Figure 1.2 | Timeline with periodisation in the first millennium AD in the Netherlands. The depopulation in the Netherlands is coeval with several geomorphological changes. Population density and vegetation openness after Louwe Kooijmans (1995); climate after Buntgen et al. (2016); red = 'warm', blue = 'cold'; RWP = Roman Warm Period, DACP Dark Ages Cold Period, MCO Medieval Climate Optimum. Sea ingressions after Vos (2015a); flooding history after Toonen et al. (2013); avulsions after Berendsen & Stouthamer (2000); Sand drifting after Koster et al. (1993).

population numbers and human pressure on the landscape started to increase again, a trend that persisted throughout the Middle Ages (Van Bavel, 2010). From AD 1100, the fluvial and coastal area were reclaimed and embanked on a large scale. From that time onwards, the natural erosional and sedimentary processes were confined to narrow areas in tidal basins or embanked river plains (Borger, 1992; Hudson et al., 2008; Vos, 2015a) and local wind-erosion prone coastal dune and inland sand areas (Koster et al., 1993; Vos et al., 2015a). As such the first millennium AD represents a transition period from a mainly natural prehistorical lowland landscape that was influenced more and more by people towards a mainly human-dominated landscape with large-scale embankment and reclamation from the High Middle Ages (ca. AD 1050) onwards.

1.3 Problem definition

The sedimentary products and geomorphology resulting from the landscape changes in the Netherlands of the first millennium AD are often well visible in the current landscape and its shallow substrate, for example as tidal channels, clay layers on peat, and drift-sand dunes. In several cases, these changes can be spatially or chronologically linked to the presence or the absence of archaeological artefacts. A tremendous amount of data is available for this area on geology, geomorphology, and human settlements and activities. Also, records of various possible forcings that could have driven these changes have become available, such as storm surges and episodes of Rhine flooding. Despite the striking geomorphological changes that took place, it is unknown to what extent the inhabitants influenced the landscape changes and, vice versa, what the impact of landscape changes was on the people living in it. Solving this requires an integrated overview and chronology of the changes in landscape and human activities, understanding the causes and mechanisms underlying these changes and the feedbacks between them, and an assessment of the relative importance of natural and anthropogenic causes.

The Netherlands has a long research tradition in studying geology, soils, and archaeology, which resulted in a wealth of maps, local reports, and databases of boreholes and datings that are available today. Since 1992, Malta-driven archaeology in the Netherlands has resulted in vast amounts of well-dated archaeological finds and geological data. Most archaeological data are from individual sites and comprise landscape reconstructions on a very local level. Reconstructions of human-landscape interactions on larger scales, therefore, require the integration of all these data to infer new patterns on landscape dynamics and its interaction with humans. This has been done on a regional scale in several reconstructions, sometimes spanning larger parts of the Holocene (e.g. southwestern coastal plain: Vos & Van Heeringen, 1997; central coastal plain wetlands: Van den Biggelaar, 2017; Old Rhine channel belt levees: Van Dinter et al., 2013; 2017; Bergen inlet salt marshes: Van Zijverden, 2017). These studies reconstructed the landscape changes that interfered with human occupation for one specific tidal system or a single channel belt in high detail. However, to assess the forcings that have an effect on larger areas (e.g. flooding in a delta or coastal plain, agriculture in larger areas, climatic impact, etc.), a larger scale approach is required that better suits the scale of the geomorphological effects resulting from these forcings. Additionally, such a regional to national scale approach would allow for comparison of multiple cases with varying conditions (e.g. multiple tidal systems with a varying sediment supply regime). For this purpose, the integration of datasets should be performed on a much larger scale. New techniques on digital Geographical Information Systems (GIS) and the many accumulated datasets that are currently digitally available at the spatial scale of the entire Netherlands make this possible.

This PhD study was executed within the research project 'Dark ages in an interdisciplinary light' (Jansma et al., 2014), which had the goal to reconstruct and understand the interaction between people, landscape, and climate in the first millennium AD. Within the overall project three PhD projects were performed that posed complementary research questions on human-landscape interaction. These focussed on archaeology (Van Lanen, 2017), vegetation and climate (Gouw-Bouman), and on the geomorphological and geological landscape evolution (this thesis).

1.4 Aim and general approach

This thesis aims to study the human-landscape interaction in the Netherlands during first millennium AD by performing the following steps:

- 1) identification of the changes in natural landscape evolution;
- 2) unravelling the natural and anthropogenic causal factors, and the geomorphological feedback mechanisms underlying these geomorphological changes;
- 3) evaluation of the impact of these changes on humans.

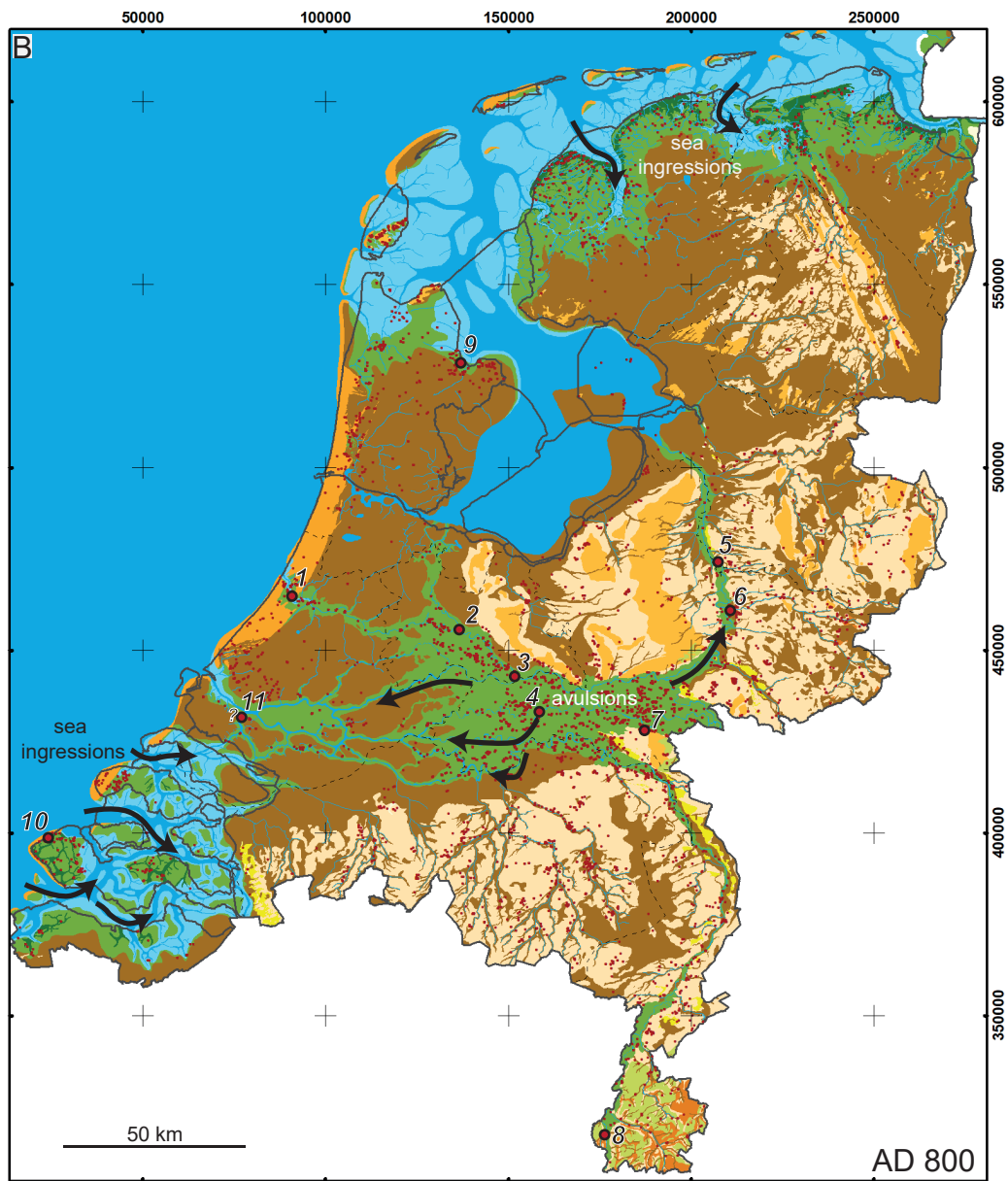
The human-landscape interactions were studied for three research areas within the Netherlands: the coastal area, the fluvial area, and the Pleistocene sand area (Figure 1.1). These areas have distinct physical characteristics and typical landscape elements suitable for habitation and specific land use (e.g. alluvial ridges, peat bogs, or supratidal flats). Also the landscape sensitivity to human influence varies because each region was affected by different geomorphological processes (e.g. peat subsidence or aeolian sand erosion). By comparing the human-landscape interactions between the three regions, the role of the physical landscape setting in these past interactions can be studied. Because each area has its typical human-landscape interactions, it requires area-specific research questions to be solved in order to fulfil the main objectives of the thesis, which are further outlined in the next section.

The regional scale (ca. tens by tens of kilometres) was chosen for all three regions because at this scale many of the geomorphological changes and their causes occurred, but had a different relative effect within these specific research areas. Examples of spatially varying evolution are the large sea ingressions in the southwestern coastal plain compared to other parts of the coastal plain (Vos, 2015a). Also, forcings and their effect can vary on a regional scale, such as floods in the upper and central delta reached higher amplitudes than in the wider lower delta (Cohen et al., 2016). Performing the study on a regional scale is best suited for this research because in this way, the evolution of multiple cases can be compared (i.e. multiple sea ingressions, channel belts) in terms of development, synchronicity, and causal forcings. To this end, this thesis uses landscape regions as a starting point rather than studying the environmental context of specific archaeological sites, as is done in many traditional geoarchaeological studies.

The thesis mainly focusses on the first millennium AD, because this is a transition period from a mainly natural prehistorical lowland landscape towards a state that became mainly human-dominated. The analyses in this thesis were however not always strictly limited to this period because landscape evolution before and after this period had to be understood to judge to what extent the geomorphological changes were typical for this period of increasing human influence. Considering a wider time span was required to assess which developments were the result of natural long-term processes and which would probably not have occurred without human influence. Besides this, the inherited geological and geomorphological setting of the older landscape is important for explaining landscape evolution in the first millennium AD. Considering the younger



Figure 1.3 | Palaeogeographical maps of (a) AD 100 and (b) AD 800 (Vos & De Vries, 2013) with archaeological settlements of the Roman period and early medieval period respectively (Van Lanen et al., 2015a). In B the most visible geomorphological changes are indicated that form a starting point of this thesis. Most important settlements for the Roman period and the Early Middle Ages are numbered A: 1 = Forum Hadriani (Voorburg), 2 = Utrecht, 3 = Nijmegen, 4 = Maastricht. B: 1 = Oestgeest, 2 = Utrecht, 3 = Dorestad, 4 = Tiel, 5 = Deventer, 6 = Zutphen, 7 = Nijmegen, 8 = Maastricht, 9 = Medemblik, 10 = Domburg, 11 = Witla.



periods is necessary to assess the preservation and non-preservation of the first millennium AD landscape, i.e. to determine the locations and spatial extent of erosion by younger rivers or tidal inlets.

To identify the landscape changes in this study, datasets were integrated into reconstruction maps of the physical landscape. These are referred to as palaeogeographical reconstructions, or more specifically as geomorphological reconstructions as they show the former extent of mainly geomorphological units (channels, supratidal ridges, alluvial ridges, etc.). By spatially and temporally comparing the geomorphological changes to varying forcings and the

archaeological record, the causes and effects of these changes were assessed. Soil maps, geological, geomorphological maps, and many local studies were an important input for these reconstructions because they contain information on the spatial outline, age, and stratigraphy of landscape units. To incorporate this fragmented and heterogeneous information into integrated reconstructions, the original focus and research tradition of the input studies had to be considered, as is outlined in chapter 2. In chapters 3 and 6 the methodology of the landscape reconstructions is outlined for the coastal and fluvial environments, respectively, thereby combining the datasets reviewed in chapter 2.

1.5 Approach per lowland region

The state of knowledge of the coastal, fluvial, and Pleistocene sand regions are briefly introduced below. Also the specific research questions are given, which were needed to answer the overall aims of the thesis.

In the coastal plain, large tidal areas were present with channels, shoals, and salt marshes (Figure 1.3). The salt marshes in the coastal plain of the northern Netherlands were inhabited since the Iron Age (800–12 BC) and became one of the most densely populated areas in the Netherlands during the first millennium AD. Habitation was mainly confined to artificial dwelling mounds that protected the inhabitants for the highest water levels (Van Giffen, 1940; Gerrets, 2010; Nieuwhof & Schepers, 2016). Other densely populated areas in the coastal plain were the saltmarshes and silted up tidal creeks around the estuaries of the Rhine, Meuse, and Oer-IJ (Figure 1.3). The tidal areas were fringed by a large freshwater peat swamp at the beginning of the period under consideration. Especially in the southwestern coastal plain and parts of the northern coastal plain, reclamation of these peatlands took place since the Roman period (Vos & Van Heeringen, 1997; Vos & Knol, 2015). These activities caused major landscape changes transforming a large part of the coastal plain peatlands into a tidal area (Vos, 2015a - Figure 1.3B). However, the evolution and spatial extent of these so-called sea ingressions varied, raising the question how human activities and natural factors interacted in this large-scale coastal plain drowning. To this end, the timing of the major drowning events was reconstructed and compared in time and space to the potential causal factors (e.g. timing of peatland reclamation, geomorphological setting of the drowned area). The new GIS-generated palaeogeographical time series that show the late Holocene coastal plain evolution are presented in chapter 3, followed by a discussion on the role of antecedent conditions and human activities in this evolution in chapter 4.

The Rhine-Meuse delta was a densely populated area with many river branches that changed their courses through time (avulsion; Figure 1.3B - Berendsen & Stouthamer, 2000; 2001; Van Dinter et al., 2017). In the transition zone between the coastal plain and the Rhine-Meuse delta, a large peat swamp had developed. For 3000 years, this swamp had separated the Old Rhine and Old Meuse rivers, but at the start of the first millennium AD, two new Rhine branches traversed it (the rivers Hollandse IJssel and Lek), coinciding with increased population pressure in this area. Chapter 5 explores to which extent human interference caused these two avulsions that connected the fluvial area to the Old Meuse estuary. Habitation in the Rhine-Meuse delta mainly occurred on alluvial ridges which were the higher and drier parts of the delta (Modderman, 1948). These alluvial ridges, consisting of crevasse splays and natural levees, were not only essential for delta inhabitants; they also majorly controlled floodwater routing and sediment deposition. Therefore, these landscape elements are essential for understanding delta evolution (Filgueira-Rivera et al., 2007). Changing geomorphological forcings, such as avulsion, variation in flood regime, and sediment supply affected the shape of the alluvial ridges during the first millennium AD. To study this, the extent

and elevation of the natural levees and crevasse splays were mapped in new detailed time series of geomorphological reconstructions for this period. The reconstructions and the geomorphological changes derived from these were matched to the forcings and inheritance effects in chapter 6. After AD 270 severe depopulation and relocation of settlements took place in the fluvial area (Hendrikx, 1983; Willems, 1986). Besides cultural factors, this was possibly influenced by the varying environmental conditions or changes in natural levee morphology. This hypothesis was tested in the next two chapters using the new geomorphological reconstructions of chapter 6. Shifts in settlement elevation throughout the first millennium AD were linked to the evolutionary stages of avulsions and insights in flooding intensity variability in chapter 7. Chapter 8 used the maps to identify accessible corridors in the delta landscape and their possible shifts as a consequence of environmental changes.

The Pleistocene sand area consists of modestly elevated uplands (several meters to tens of meters above sea level) adjacent to the coastal plain and Rhine-Meuse delta (Figure 1.1). A significant geomorphological change in the last thousands of years was the occurrence of drift sands most likely formed as a consequence of deforestation and intense land use (Koster et al., 1993; Sevink et al., 2013). This drift-sand activity locally caused the formation of large drift-sand fields causing part of the land to become useless. Besides intensified land use, episodes of drift-sand activity also seem to coincide with colder and more stormy climate episodes (Jungerius & Riksen, 2010). To explore the relative contribution of climate and land use, the drift-sand dynamics in the Pleistocene sand area were reviewed on a national scale in chapter 9. Their abundance was correlated to population density, deforestation, and climate, whereas their spatial occurrence was linked to known areas with settlements and transport corridors. Chapters 7, 8, and 9 are shared contents with the PhD thesis of Van Lanen (2017) within the same project (his chapters 7, 8, and 11).

In the synthesis (chapter 10), the causes of landscape evolution and its consequences are compared for the three studied areas. The area-specific sensitivity to natural and anthropogenic forcings and the role of feedbacks causing landscape changes are discussed.

Chapter 2

Geological and geomorphological mapping traditions in the Netherlands

In the well-studied Netherlands' coastal plain and Rhine-Meuse delta, many datasets are available regarding the extent, age, and sequential development of Holocene geological and geomorphological elements. Most of these datasets are national and regional map series based on data collection campaigns executed during the last decades of the 20th century (soil maps, geological maps, and geomorphological maps). These datasets have been developed within different research traditions. This chapter reviews the range of mapping traditions behind the datasets that in this thesis were combined into geomorphological and palaeogeographical reconstructions.

While most map datasets describe the current state of the physical-geographical landscape of the Netherlands, they also contain information about the evolution and time depths of the mapped elements. Since, during decades of surveying, the age determinations of landscape elements became increasingly precise, researchers have also produced palaeogeographical map time-series that synthesise Holocene landscape evolution. The production of such map series has benefited from digital-infrastructure developments, facilitating interactive visualisation and dynamic interrogation of the datasets. This has offered important new possibilities for answering applied and fundamental scientific questions, including questions that are not directly related to the original mapping aims.

Currently, knowledge enclosed in many legacy maps, despite the quantity and quality of data underlying it, still remains hidden, fragmented, or under-appreciated. The integration of this information into new landscape reconstructions is needed to re-evaluate and improve the geomorphological and geological understanding of the Dutch delta and coastal plain. Combining information from digital maps using their full potential, requires awareness of the original focus, scale, surveying strategy, and state of knowledge at the time of the original research, which is the topic of this thesis chapter.

H.J. Pierik & K.M. Cohen

2.1 Introduction

Geomorphological reconstructions are a valid tool to identify geomorphological changes, and to study their causes and consequences. This thesis presents new reconstructions to trace landscape evolution in the Netherlands, among others in order to determine the evolution of channels, and supratidal and alluvial ridges over time. These reconstructions build upon a long tradition of mapping-based research in the Netherlands, which has been important for understanding landscape evolution and its controls (e.g. Berendsen, 2007; Cohen et al., 2014a). Previous maps studies include national mapping series (soil maps, geomorphological maps, and geological maps on scale 1: 50,000), many local reports, and theses. These studies provide information about geomorphology,

stratigraphy, and age, which are essential for studying landscape evolution. These studies and their map datasets are however heterogeneous in scale, spatial coverage, and resolution. Additionally, when comparing them it becomes clear that they sometimes have conflicting boundaries and/or different genetic interpretations of the mapped units. This is because the mapping products were made within research traditions that each had specific academic or applied research purposes (e.g. pedological, geological or geomorphological; Figure 2.1A). Additionally, the older maps were produced during periods when the state of knowledge was less well developed, making it hard to derive correct interpretations. Nevertheless, these previous studies have been based on large amounts of source data that nowadays often are inaccessible because of levelled relief or data loss (e.g. borehole data). Despite differences between themes, aims, coverage, and quality, many of the existing datasets contain useful information about geomorphological landscape evolution. Because of its fragmented nature, however, the data have to be combined and integrated into new uniform reconstructions to use its full potential. This requires the reconstructions to be uniform, objective, transparent, and adaptable to new data and insights. Digital GIS environments provide the best opportunity to achieve this (Berendsen et al., 2007).

Integrating information from existing maps into new GIS landscape reconstructions faces the following challenges: (i) converting legend units of original studies to those used in new reconstructions (e.g. from clay (lithology) to salt marsh (geomorphology)); (ii) reconciling element-outline differences for elements mapped by multiple authors at different spatial scale and depth range; (iii) verifying the originally-reported dating information; and (iv) resolve remaining inconsistencies between input maps, due to differences in interpretation.

To tackle these challenges the datasets have to be cross-compared to obtain the right priority rules for combining them. This for example includes assessing which dataset has the most accurate boundaries, or which dataset has the best genetic interpretation of the element. This can only be done successfully when the researcher is aware of the original focus of the studies, their scale and research strategy, and the state of knowledge at the time the studies were performed. Below we present an overview of the research traditions influencing the legacy map data for the Netherlands. First, the research traditions of geological mapping, soil mapping, and geomorphological mapping, which lead to maps that document the currently preserved state of the landscape, are described (Figures 2.2 to 2.5). Next, we introduce the research traditions behind palaeogeographical and GIS-generated time series. The new landscape reconstructions for the Holocene coastal plain and Rhine-Meuse delta presented in this thesis are based on revised and expanded versions of these existing map products. The methodology used for their compilation is described in chapters 3 and 6 and Appendix C.

2.2 Research traditions and resulting maps products

The oldest geological maps of the Netherlands were compiled on a scale of 1:200,000 by Staring (1858–1867), and later by Tesch (1942) on a scale of 1:50,000. Vink (1926) mapped channel belts in the western part of the Rhine-Meuse delta. Since these pioneering works, many map products have been compiled (Figure 2.1A and Table 2.1).

2.2.1 Pedo-geogenetical and pedological mapping traditions

From the 1940s to 1960s, many local and regional studies were produced mapping soil properties, as well as substrate stratigraphy and geological-geomorphological development (Figure 2.1A, Table 2.1). These detailed soil mappings (on scales 1: 10,000 and 1: 50,000) do not cover the entire

Table 2.1 | Mapping research traditions of the physical landscape in the Netherlands, see Appendix A for a more extensive overview. + indicates a strong focus on this aspect, - means almost no focus on this aspect, L = local, R = regional.

Research tradition	Direct observations			Indirect observations		Scale of application
	Geomorphology	Facies	Sequence of facies	Development	Age	
Pedo-genetic traditions	+/-	++	+	+/-	+/-	L
Geomorphology	++	-/+	-	+	-	R
Chronostratigraphy	-	-/+	++	+	++	R
Lithostratigraphy 21 st C.	+	+	++	+/-	+/-	L-R
Palaeogeography	+	++	+	+/-	++	L-R
GIS-generated maps, this thesis	+	++	+	+/-	++	L-R

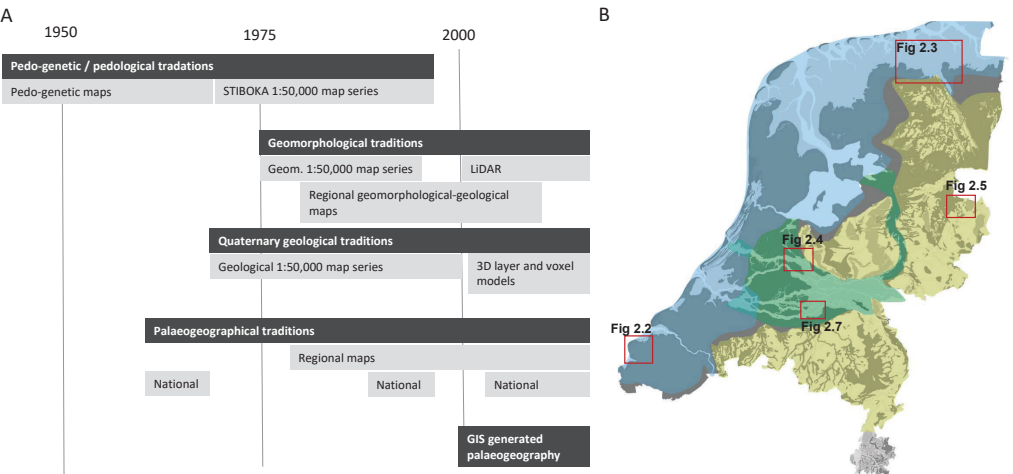


Figure 2.1 | (a) Timeline of parallel mapping research traditions regarding Physical Geography of the Netherlands used since the 1950s. (b) Physical Geographical division used in this thesis (see Figure 1.1), with the location of the example areas used in this chapter. Blue = coastal plain, green = Rhine-Meuse delta, yellow = Pleistocene sand area.

Netherlands, but are available for small parts of the coastal plain (e.g. Van Liere, 1948; Bennema et al., 1952 - Figure 2.2A, Cnossen, 1958; De Smet, 1962), the fluvial area (e.g. Edelman et al., 1950; Pons, 1966 - Figures 2.7B) and the Pleistocene sand area (e.g. Pijls, 1948; Schelling, 1955 - see Appendix A). These pedo-geogenetical studies aimed to characterise the soil and its parent material for agricultural rationalisation. The map products provide information on the lithology of the shallow substrate (upper 1 or 2 meters) in a high spatial detail. Especially landscape elements such as residual channels, alluvial ridges, and tidal levees were mapped in high detail (Figure 2.2A). This detail could be reached because many, nowadays partly lost, borehole data were used, supplemented with geomorphological field observations to draw accurate boundaries. Many mapped elements are not easily traceable anymore in the present-day landscape and in more recent maps, due to

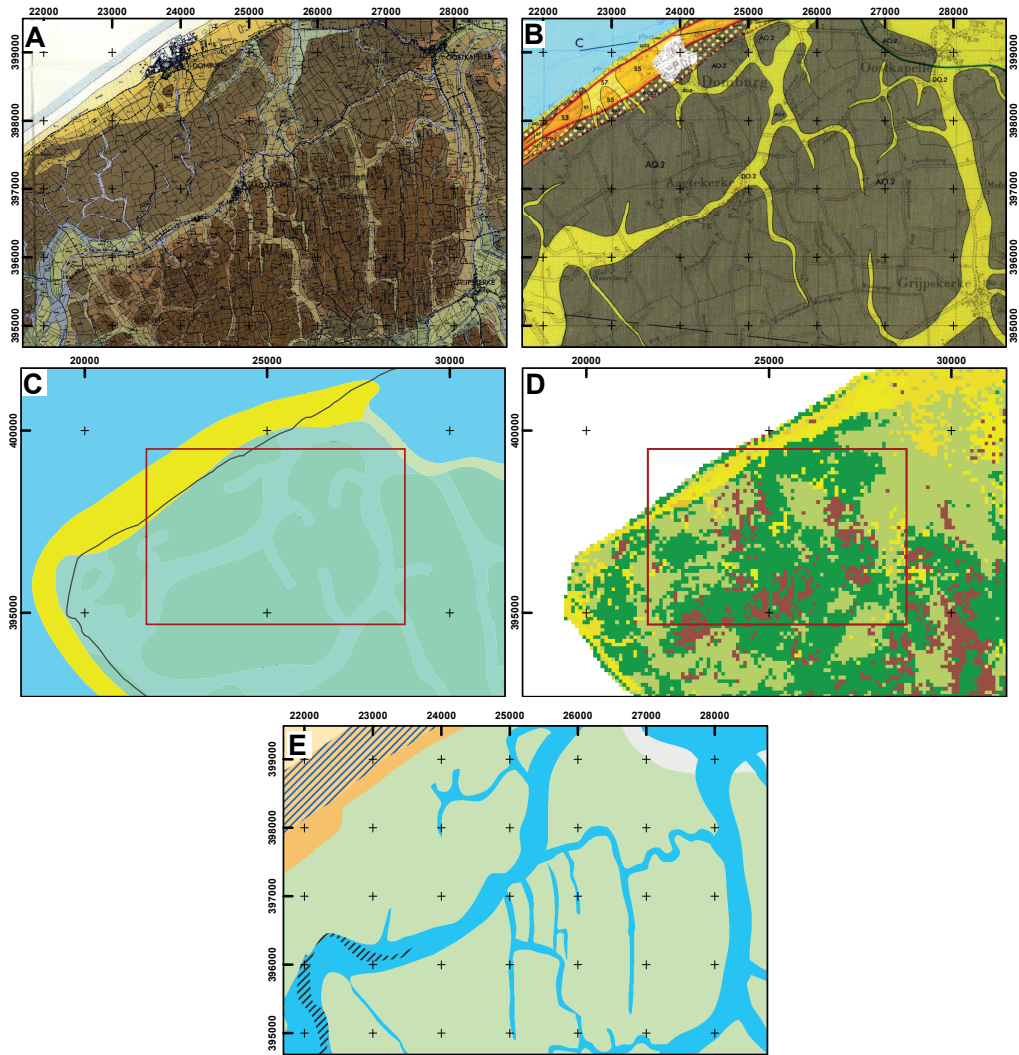


Figure 2.2 | Example area Walcheren, southwestern coastal plain (for location see Figure 2.1B). The area contains a beach barrier in the northwest (yellow and orange), while sandy creeks dissect clayey and peaty flood basins in the back-barrier area (brown and green). (a) Pedogenetic map Bennema et al. (1952; original scale 1:10,000). (b) Geological map (1:50,000). (c) Palaeogeographical map for AD 800 Vos & De Vries (2013). The red outline indicates the extent of Figures 2A, B, E. (d) Voxel-model map GeoTOP (Stafleu et al., 2011) showing the most-probable lithology 0.5-1.0 m below the surface. The red outline indicates the extent of Figures 2A, B, E. (e) GIS-generated palaeogeographical map for AD 800 (chapter 3; Pierik et al., 2016).

agricultural rationalisations or because the areas nowadays have been overbuilt. In addition to soil type and lithology, these studies documented chronological information, landscape evolution, historic land use, and archaeology. Because of the high spatial resolution and the documentation of the soil-genetic properties, these studies provide information about the presence, age, and extent of geomorphological elements mapped in this thesis. The spatial resolution of these datasets, in

general, has not been equalled by more recent studies, the chronology and interpretation of the mapped elements, however, was often much improved in later studies.

The geological, geomorphological, and palaeogeographical insights from these pedology-driven studies were up-scaled to larger parts of the coastal plain by for example Pons and Wiggers (1959/1960), Van Wallenburg (1966), and Pons and Van Oosten (1974). Local pedological terms from the northern and western coastal plain, such as 'knikklei' (Veenenbos, 1949) and 'pikklei' (de Roo, 1953), contain lithological information that can be translated into geomorphological units (e.g. soil formation in 'heavy' clay that formed as a supratidal flat). The deposits in the southwestern coastal plain were divided based on chronostratigraphical, geomorphological, and pedological criteria: (a) the oldest reclaimed areas contain decalcified soils, sandy inversion ridges, and clayey supratidal areas; (b) successively younger embanked tidal flats (mostly formed since the Late Middle Ages) have a higher elevation, contain more sand and have soils that so far remained calcareous (Bennema et al., 1952; Pons, 1965).

A unifying soil-classification system for national use was introduced in the Netherlands in 1966 (De Bakker and Schelling, 1966; De Bakker, 1970; Schelling, 1970), resulting in a STIBOKA 1:50,000 scale map series with a national coverage. Similar to the pre-1966 studies, the system focusses on shallow-soil properties (typically to 1.2 m depth); however it is more distinctly based on descriptive pedological criteria. Despite this shift in focus to uniformly describing the soil profile, the accompanying documentation still contains a substantial review of the shallow geology. These maps are fully available digitally and still used widely. The national coverage of the dataset is a merit, however, the boundaries of the units are relatively inaccurate since the delineations used in earlier detailed local studies were not adopted.

2.2.2 Geomorphological traditions

Geomorphological maps principally show the relief (shape, elevation, slope) of the landscape and additionally contain information about landscape genesis on a general level (e.g. aeolian dune, natural levee, beach ridge). Map sheets have been published since 1977 as a joint effort of the Geological Survey and the 'Stichting voor Bodemkartering' (Ten Cate & Maarleveld, 1977). Since the 2000s, LiDAR imagery has been used to complete the mapping campaign on a national coverage (Koomen & Maas, 2004), and to refine the mapped boundaries (e.g. Berendsen & Volleberg, 2007; Van der Meij, 2014). Geomorphological maps (Figures 2.3B, 2.4A and 2.5A) are widely applied in geoarchaeological studies and landscape planning. For the coastal area, tidal channel belts, supratidal channels and levees, and polders are well-mapped units in this dataset (Figure 2.3B, E). In the central Rhine-Meuse delta, Berendsen (1982) developed a geomorphological-geological map legend that displays the variation in lithofacies of the upper 2 m in a profile-type legend (Figures 2.4B and 2.7B). These maps have a larger emphasis on landscape genesis, i.e. a more detailed break-down of various genetic processes. Therefore they are useful for studying landscape evolution.

2.2.3 Chronostratigraphic traditions

For the coastal plain, a chronological subdivision system was used by geologists throughout the 20th century for categorising the deposits represented on geological maps. This system had originally been developed by Dubois (1924), Tesch (1930) and Tavernier (1946; 1948) for the Flemish and northernmost French coastal-plain area (Figure 2.6). They identified two back-barrier clastic units (the Calais and Dunkirk units, respectively) that in most places were separated by a peat interval. This originally lithostratigraphical division was adopted and extended by the Netherlands' geological survey for application in the coastal area of the Netherlands (e.g. Hageman, 1963; 1969;

Zagwijn & Van Staaldin, 1975). The extension included the recognition of multiple Calais-transgression sub-phases and multiple Duinkerke-transgression sub-phases (Calais sub-units 'I to IV' and Dunkirk sub-units '0 to III'), separated by intervals characterised by the absence of transgressive deposition, with local soil development and peat growth. The sub-phases were distinguished based on radiocarbon dating results rather than on the depositional architecture, resulting in a chronostratigraphic system rather than a lithostratigraphical one. Beds received the sub-unit label throughout the entire coastal plain, regardless of their correspondence to more local tidal systems (Figure 2.6). Consequently, the chronostratigraphical system neglected diachronous lateral shifts in sedimentation resulting from more local effects.

The reliance on radiocarbon dating was based on the assumption that the subunits represent regionally-shared sea-level controlled transgressions, whereas peat intercalations were assumed to correspond to temporary decelerations of sea-level rise. Because these fluctuations were presumed to be climate-driven, this system was also transferred to the Rhine-Meuse delta, assuming that transgressions in the coastal area would be represented as the expansion of clastic sediment in the delta as well. The presumed sea-level rise fluctuations were used to explain phases of habitation in the coastal area (e.g. Louwe-Kooijmans, 1974; Behre, 2004). The 1:50,000 geological mapping campaigns from 1964 onwards used a profile-type legend based on these subdivisions (for detailed references see Appendix A). The first geological maps of these series were compiled in the southwestern Netherlands in the 1960s and 1970s, and showed an essentially chronostratigraphical division. Later mapping campaigns in different parts of the coastal plain and the Rhine-Meuse delta also included back-barrier facies and environmental interpretation as a subdivision (e.g. Dunkirk I; supratidal deposits).

As more radiocarbon dates became available, however, it turned out that the presumed synchronicity of the supraregional regressions and transgressions and the sea-level rise forcing that these implied did not exist (Roeleveld, 1974; Van de Plassche, 1985; Baeteman, 1999; Weerts et al., 2005). Also, the presumed coupling between marine transgression and increased clay deposition in the fluvial area was falsified (Berendsen, 1984ab). The observed pulses of clastic sedimentation in the delta could be linked successfully to avulsion patterns rather than to events synchronously occurring throughout the entire delta and coastal-plain (e.g. Törnqvist, 1993). In addition, gradually increased clastic input resulting from upstream catchment deforestation (Hoffman et al., 2007; Erkens & Cohen, 2009), and generations of tidal systems (Beets & Van der Spek 2000; Vos 2015a) were considered important factors determining the observed variations in sediment deposition throughout the delta.

Geological maps are available for large parts of the coastal plain and the delta, although a few map sheets were never completed. When compared to soil maps and geomorphological maps, they display older and less shallow deposits. Especially in the coastal plain, geological maps provide a consistent dataset displaying the planform geometry and ages of Holocene generations of tidal architectural elements (Figure 2.2B). Their use for geomorphological reconstructions is particularly straightforward for those areas where facies (channel deposits, tidal flat deposits, etc.) were separately mapped (i.e. for the younger map sheets). The original age-attribution was re-evaluated by verifying and complementing the originally used dates (^{14}C , archaeology) with newer additional dating evidence. For the fluvial area, the more recent accurate maps and new borehole data provide information with more detail on lithology, facies architecture, and chronology. Therefore geological maps are less useful here.

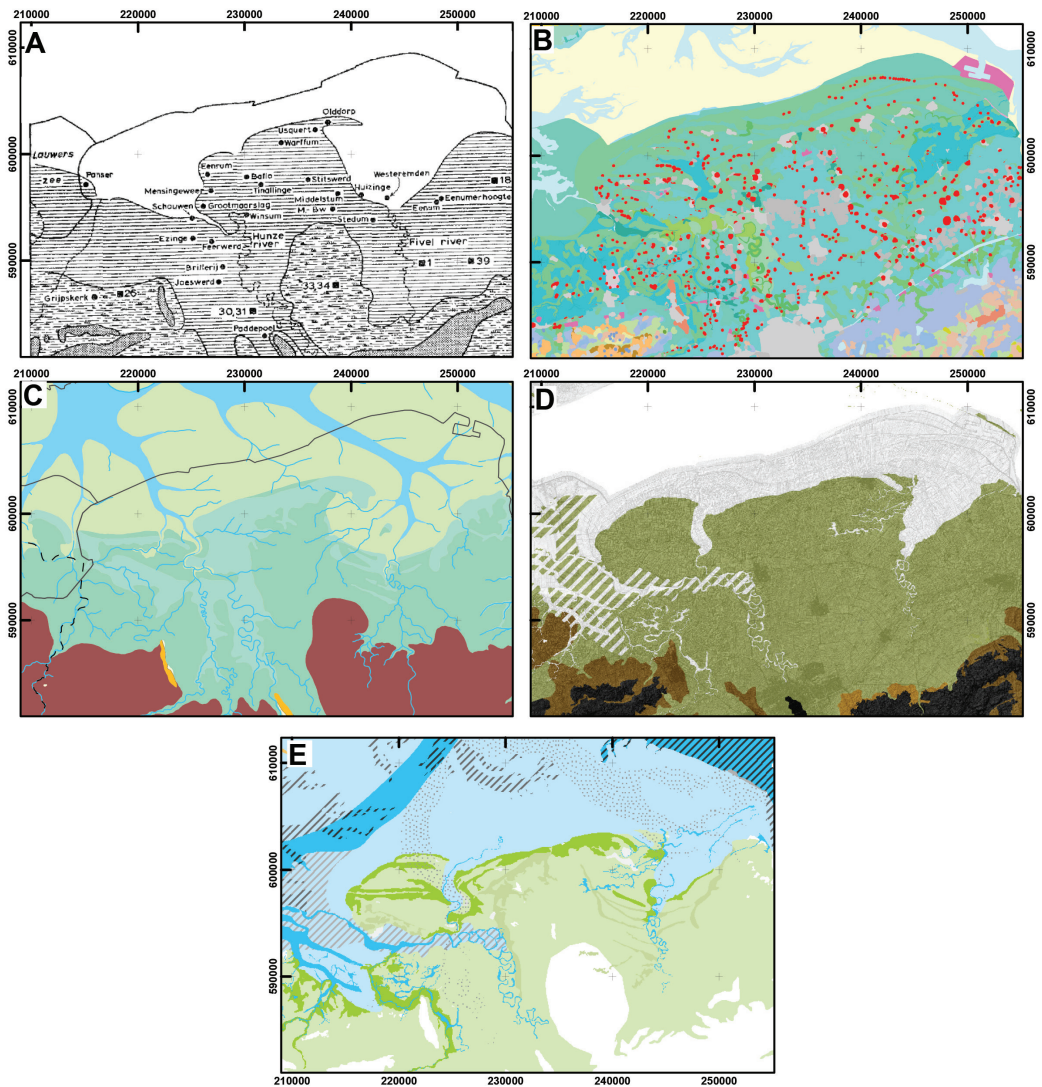


Figure 2.3 | Example area in the northern coastal plain (location see Figure 2.1B). In the north the Wadden sea can be seen with its channels and intertidal flats, south of it supratidal flats and flanking peatlands. (a) Palaeogeographical reconstruction 2000 BP of Roelleveld (1974). (b) LiDAR-based geomorphological map (Koomen & Maas, 2004). (c) Palaeogeographical map for AD 100 Vos & De Vries (2013). (d) GIS-generated landscape time slice map (T3: 1500 BC to AD 900; Cohen et al., 2017a). (e) GIS-generated palaeogeographical map for AD 900 (chapter 3; Pierik et al., 2016).

2.2.4 Lithostratigraphic mapping traditions

Lithostratigraphical schemes divide the substrate into mappable units (Formations, Units, Beds) that have distinct lithological properties and occur at distinct stratigraphical positions (Salvador, 1994). The Dutch lithostratigraphic subdivision was revised in 2000, replacing the Calais/Dunkirk terminology (Weerts et al., 2000). All clastic coastal plain deposits of the barrier and the back-barrier subsystems were assigned to the Naaldwijk Formation (Ebbing et al., 2003; Vos, 2015a).

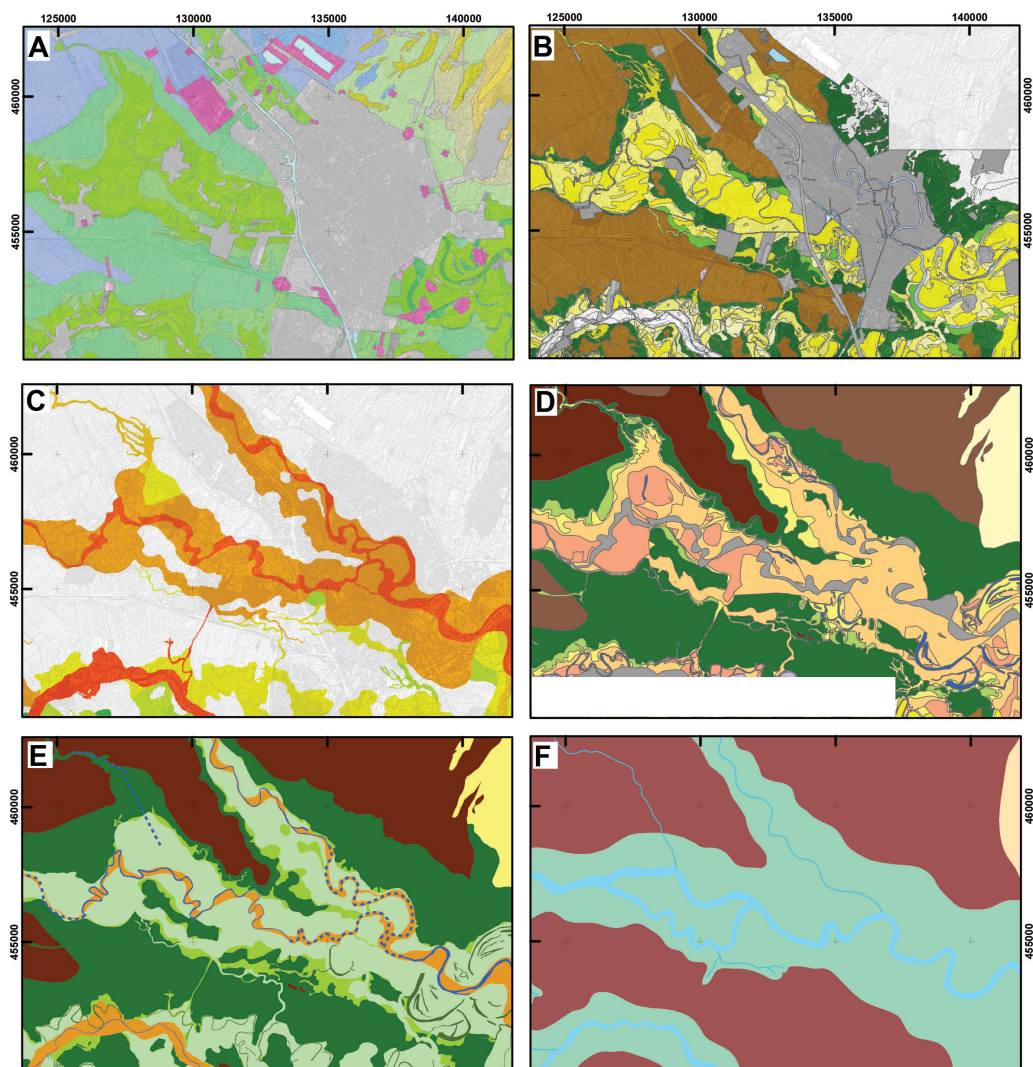


Figure 2.4 | Example area of the Rhine delta around Utrecht (location see Figure 2.1B). The Rhine channel belt splits in a western and northwestern branch, flow direction is towards the west (left). The channel belt (yellowish in B and C) is flanked by flood basins filled with clay and peat (respectively green and brown in maps B, D, E and F). (a) Geomorphological map (original scale 1:50,000 – Koomen & Maas, 2004). (b) Geomorphogenetical map Berendsen (1982; original scale 1:25,000; digitised version). (c) Channel-belt age base map by Cohen et al. (2012). (d) Palaeogeographical map for AD 100 of Van Dinter (2013). (e) GIS-generated palaeogeographical map for AD 900, chapter 6. (f) Palaeogeographical map for AD 100 Vos & De Vries (2013).

Following the original (pre-radiocarbon dating) transgression-phase based subdivision, a lower and upper clastic member were distinguished in the back-barrier area (Wormer and Walcheren Members, respectively Figure 2.6), separated by a main peat layer (Holland peat). Fluvial deposits no longer were chronostratigraphically linked to deposits in the coastal plain: all Holocene fluvial deposits were now attributed to the Echteld Formation, which was further subdivided into

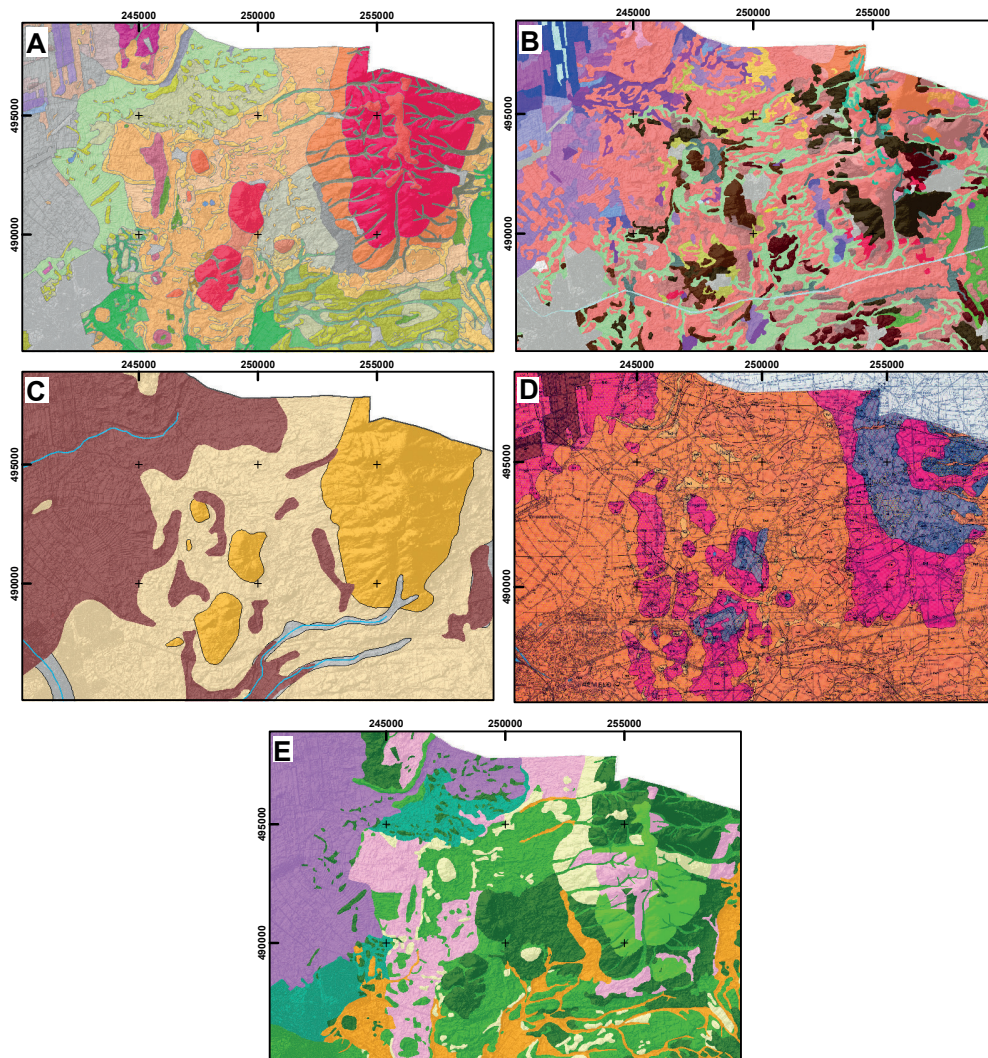


Figure 2.5 | Example area Twente (eastern Pleistocene sand area) (location see Figure 2.1B) containing ice-pushed ridges (dark yellow in C), brook valleys (green in A; grey in C) and (mostly dug) fen peats (purple in B and E; brown in C and D). (a) Geomorphological map (original scale 1:50,000 – Koomen & Maas, 2004). (b) Soil map (original scale 1:50,000 - De Vries et al., 2003). (c) Palaeogeographical map for AD 100 of Vos & De Vries (2013). (d) Geological map (original scale 1:50,000 - Van Den Berg & Den Otter, 1993). (e) Vegetation reconstruction for the Roman period (Van Beek et al., 2015a).

lithofacies units (channel-belt deposits, natural-levee deposits, residual-channel deposits etc.; Weerts, 1996; Weerts et al., 2005). In overview maps these units are grouped by age, origin, and network properties (i.e. channel-belt generation; Berendsen, 1982; Berendsen & Stouthamer, 2001; Cohen et al., 2012).

In contrast to the earlier chronostratigraphical system, no further subdivision into superregional transgressive and regressive units was made in the late-Holocene Walcheren

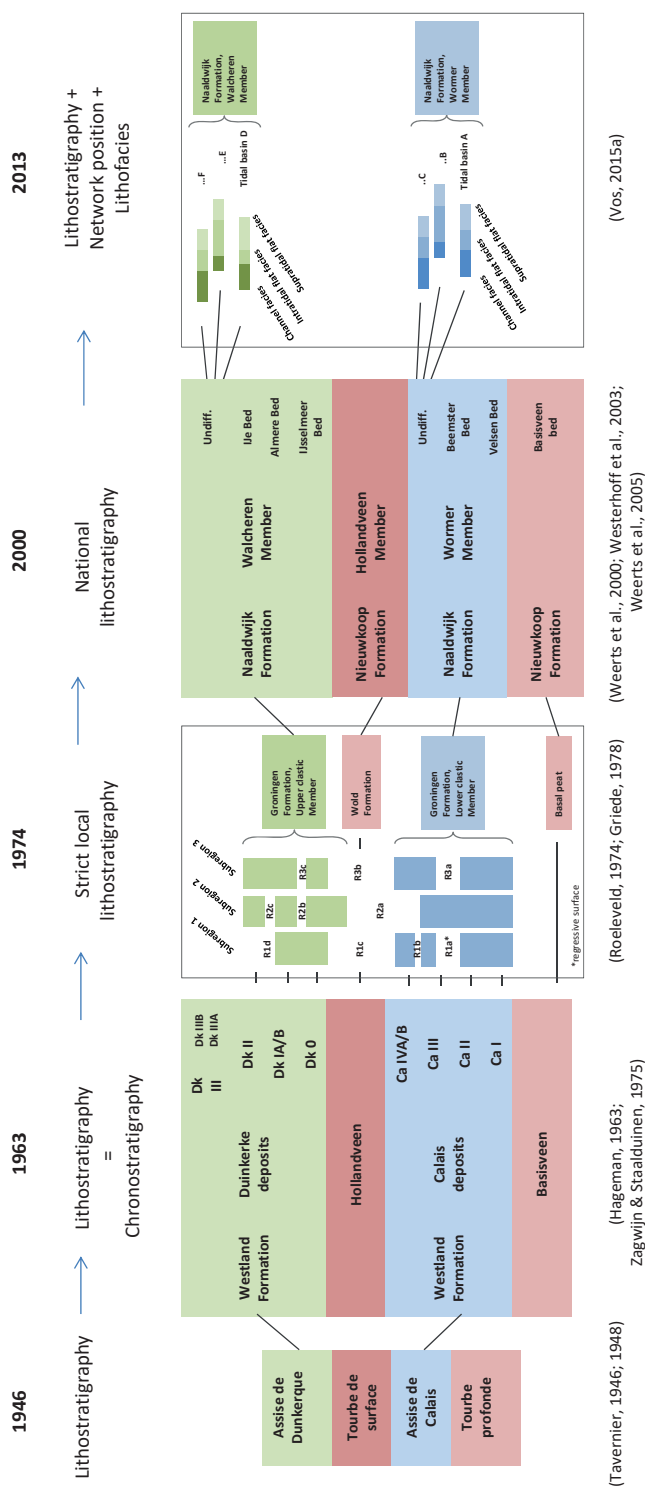


Figure 2.6 | Development of litho- and chronostratigraphical division schemes in Holocene coastal plain geological mapping.

member. Exceptions are the infilling members of the Almere Lagoon in the middle part of the Netherlands (e.g. Almere Bed) and the IJse Bed deposits that represents Medieval clays topping peat around the Almere Lagoon. For specific regions in the coastal plain, Vos et al. (2007), Vos & Eijsskoot (2011), and Vos (2015b) have further distinguished late Holocene coastal clastic members, based on lithofacies properties and network position in a similar way as was done in the fluvial area (Figure 2.6). Using network position means that the mapped deposits and landforms are coupled to a particular tidal system that delivered the sediments, which is the main tidal inlet that was the sediment source of the depositional elements. Within a single tidal inlet system, architectural elements occur with distinct sedimentological characteristics (lithofacies) that can be coupled to a specific depositional environment (e.g. sandy deposits from intertidal flats or clayey deposits from a supratidal flat). Applying this refinement in palaeogeographical reconstructions requires an advanced state of geological mapping because deposits have to be identified and traced over larger areas.

The network-provenance approach in the labelling of individual elements has also been applied in palaeogeographical mapping and the 3D voxel modelling by the Geological Survey (GeoTOP - Stafleu et al., 2011; Van der Meulen et al., 2013 - Figure 2.2D) to distinguish and reconstruct different generations of fluvial and tidal systems in the substrate. The voxel models are currently available for the coastal plain and the fluvial area, they have a $100 \times 100 \times 0.5$ m resolution, with attributes on lithology, lithostratigraphy, and its uncertainty. The 3D models map the substrate using earlier mapped boundaries and stratigraphy of geological elements to enhance borehole data interpolations. Especially for areas of which geological maps at high resolution are not present, the voxel models generate new information on extent and thickness of channel belts or levee complexes. Because interpolations not always resulted in sharp boundaries of the geological elements, the models mainly serve as indications for the extent of elements in geomorphological reconstructions rather than give an updated boundary.

2.2.5 Palaeogeographical mapping

As more chronological data became available, research focus has shifted the last several decades from mapping the current state of the landscape and substrate, towards reconstructing its evolution and the involved geomorphological processes (Figure 2.7). Palaeogeographical maps that show the state of the landscape for distinct time steps (Pons et al., 1963; Zagwijn, 1986; Cohen et al., 2014a; Vos, 2015a) were used as a tool to investigate landscape evolution. Such palaeogeographical reconstructions represent spatial and thematic integrations of knowledge and data from many local and regional studies. Sometimes the reconstructions additionally incorporate interpretations inferred from underlying direct observational data, such as raw borehole logs, outcrop drawings, ^{14}C dates, and archaeological finds. Producing landscape maps for a sequence of time slices requires re-evaluation of the age control and environmental interpretation of the source datasets. In addition, landform inheritance and preservation has to be assessed as well as reconstructing parts of the landscape that have not survived later erosion (Cohen et al., 2014b; Vos, 2015b).

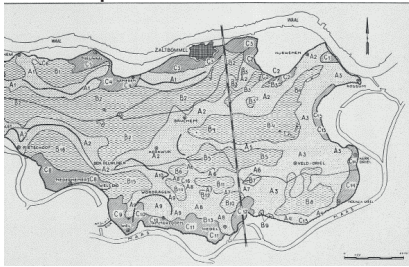
The first palaeogeographical maps for the Holocene coastal plain with a national coverage were compiled by Pons et al. (1963); the second generation was established by Zagwijn (1986). In both publications, the selected time steps in the reconstructions coincided with the presumed transgression periods in the coastal and fluvial areas derived from then prevailing chronostratigraphy. More detailed regional maps were made by Knol (1993 - Northern Netherlands) and Lenselink & Koopstra (1994 - central and northwestern coastal plain). For the Rhine-Meuse delta, a number of regional palaeogeographical maps were compiled to support geoarchaeological

research. These studies mapped the geomorphological units in the landscape, but generally only for the Roman period (Willems, 1986 – Overbetuwe, east; Van Dinter, 2013 – Utrecht-Leiden - Figure 2.4D). Schematic palaeogeographical maps of channel belt evolution were made for specific regions (e.g. Berendsen, 1982; Weerts & Berendsen, 1995 - Figure 2.7C), eventually resulting in GIS-generated maps of channel belt generations for the entire Rhine-Meuse delta (Berendsen & Stouthamer, 2001). Since the 1990s in the context of the Treaty of Malta, an increasing number of local archaeological research projects was carried out in combination with geological and geomorphological research. Results from these projects were integrated in various previous reconstructions of past landscapes of different parts of the coastal-delta plain of the Netherlands, such as by Vos & Van Heeringen (1997 - Zeeland), Vos & Zeiler (2008 – Zeeland), Vos (2008 – Oer-IJ), Cohen et al. (2009 – Gelderse IJssel valley and delta), Vos & Eijsskoot (2011 - Vlaardingen), Ten Anscher (2012 – Noordoostpolder), Vos & Knol (2015 – Northern Netherlands and German Wadden coast), Van Zijverden (2013; 2017 - West Frisia). The palaeogeographical maps from these studies represent smaller parts of the coastal and delta plain, e.g. one tidal system or linked tidal systems. These reconstructions generally used newly collected detailed information from key sites on archaeology, facies architecture, stratigraphy or chronology (Vos, 2015a). The landscape between these key sites was then reconstructed using information from national datasets (mainly LiDAR data). This approach was up-scaled to create a uniform palaeogeographical map series covering the entire Netherlands (Vos, 2006; Vos et al., 2011; Vos & De Vries, 2013; Vos, 2015a - Figures 2.2C, 2.3C, 2.4F, 2.5C). Relatively few palaeogeographical reconstructions exist for the Pleistocene sandy areas of the Netherlands. Here, landscape changes occurred on a smaller scale (e.g. drift sand activity, peat bog growth and reclamation, changes in vegetation), which have been reconstructed by e.g. Casparie & Streefkerk (1992), Spek (2004), Van Beek (2009) and Van Beek et al. (2015ab – Figure 2.5E). These reconstructions were incorporated in the national palaeogeographical map series of Vos & De Vries (2013).

The process of making palaeogeographical maps forces its maker to produce a full 2D coverage of the reconstructed landscape, although the available or accessible data and knowledge on landscape development may neither cover the entire area nor be evenly distributed. Decisions on element inclusion, generalisation, age, and diachroneity underlying existing palaeogeographical reconstructions often were implicit, and generally have been poorly documented on the scale of individual elements. Most palaeogeographical maps are manually produced visualisations of a past landscape, only available for pre-determined time steps or with irregular intervals, depending on the purpose and data availability. This poses some limitations to the full understanding of landscape development. Time series of palaeogeographical maps for the youngest millennia typically encompass shorter time intervals than those representing earlier millennia, because the more recent deposits have been better preserved and have more precise age control. Therefore, elements only active for a shorter period than the time steps between consecutive reconstructions may be missed on the maps. Finally, when the chosen time steps correspond to the time scale at which the elements (e.g. expanding tidal inlets or natural levees) gradually develop towards a mature state,

Figure 2.7 (right page) | Map generations in the Rhine-Meuse delta. Selected maps for the Bommelerwaard example area (south-central delta; see Figure 2.1B). (a) Soil maps of Edelman et al. (1950) and (b) profile type maps of Berendsen et al. (1986). (c) Schematic reconstruction of channel belt activity by Weerts & Berendsen (1995). (d) GIS-generated reconstruction with focus on network history (Cohen et al., 2012, update of Berendsen & Stouthamer, 2001). (e) GIS-generated reconstruction, added focus on natural levees (chapter 6). In the reconstructions, active channel belts are displayed in black, yellow and orange; inactive channel belts as grey and light green.

A: Soil map



Edelman et al. (1950)

- Emphasis on **soil** properties
- **Current state** considered for **archaeology**

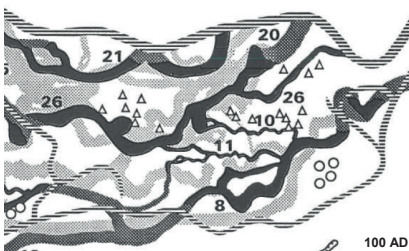
B: Geomorphological-geological map



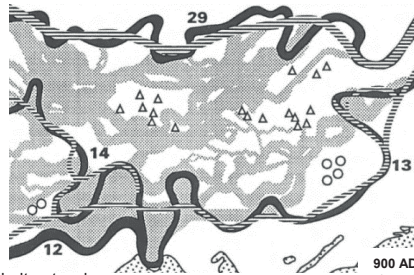
Berendsen et al. (1986)

- Emphasis on **genesis** and **age** of the elements
- Current state considered for archaeology

C: Palaeogeographical cartoon reconstructions



100 AD



900 AD

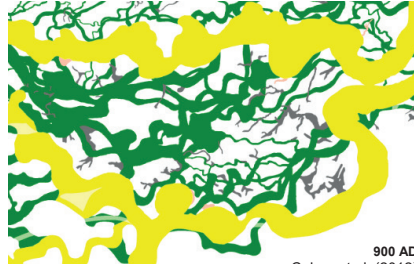
Weerts & Berendsen (1995)

- **Palaeogeographical** cartoon reconstructions of the channel belt network
- Emphasis on **age** of channel belts

D: GIS generated palaeogeography of channel belts



100 AD



900 AD

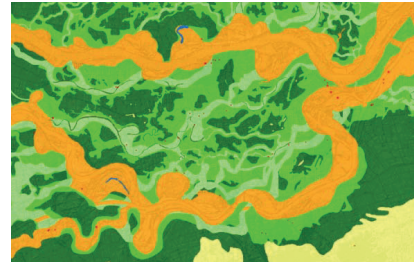
Cohen et al. (2012)

- **Delta wide** reconstructions of the channel-belt network
- **Mapped elements = reconstructed elements**
- Emphasis on age of **channel belts** and sandy crevasse splays

E: GIS generated palaeogeography of channel belts and their natural levees



100 AD



900 AD

Chapter 6

- Palaeogeographical reconstructions
- Mapped elements = reconstructed elements
- Emphasis on age of **all landscape elements**
- **Inherited features** and **post-erosion**
- **Dynamic landscape state** considered for archaeology

the exact spatial extent of such elements on the chosen time step is hard to reconstruct. This can introduce biases when the map series are used for inferring rates of natural landscape changes (e.g. for sediment budgeting studies - Erkens & Cohen, 2009).

2.2.6 GIS-generated landscape reconstruction maps

Since the 1980s, the development of Geographical Information Systems (GIS) has allowed digital map recombination and computer-aided conversion and processing of data (e.g. Burrough, 1986). The GIS methodologies not only provided new techniques for map drawing and visualisation, they also facilitated collecting and managing large amounts of data in one single information system. This made it possible to query, analyse, combine, and update geographic information. Major benefits of using these methodologies for palaeogeographical landscape reconstructions are that GIS can contain much information and the products are more generic, verifiable, and adaptable (Berendsen et al., 2007).

The first scripted digital procedure to construct palaeogeographical maps was performed by Berendsen et al. (2001; 2007) who compiled time series of river-network evolution (latest published version: Cohen et al., 2012 - Figure 2.4C). The dataset documents and summarises a large amount of information on the position and age of subsequent river courses in the Rhine-Meuse delta through the Holocene (Figure 2.7). Over the period 2011-2016, this dataset was expanded to cover the Netherlands' coastal plain outside the Rhine-Meuse delta, introducing additional base maps of pre-deltaic valley landforms (Cohen et al., 2012). Other new datasets following the scripted digital procedure are geoarchaeological predictive maps for the embanked floodplains (Cohen et al., 2014b) and buried Holocene landscapes (Cohen et al., 2017a - Figure 2.3D).

Both traditional and GIS-generated palaeogeographical maps rely on existing maps and require decisions regarding the absolute and relative age of the mapped units. In GIS-derived palaeogeographical maps, the decisions on element age and extent are documented in the scripts and element labelling of the base maps, which facilitates selecting data based on their age. This makes it possible to compose palaeogeographical maps by combining selections of geomorphological elements that were active during the desired time steps or periods. In this way, a direct cross-check is possible between the mapped geology, geomorphology, and the palaeogeography. For example, the geological-geomorphological map of Berendsen & Stouthamer (2001 - Figures 2.4C and 2.7) shows the age of channel belts as well as the palaeogeographical map series of the evolving river network. They are derived from the same base map using scripted recombinations of the same polygons. This allows a palaeogeographical map to be extracted for any time slice in the past, and not only for moments that were a priori decided upon by the map maker. The GIS-generated datasets of the Rhine-Meuse delta have found many scientific applications in themes such as channel belt network dynamics (e.g. avulsion: Stouthamer (2001), Kleinhans et al. (2010), transgressions (Hijma & Cohen, 2011), sediment budgeting (Erkens, 2009; Hobo, 2015), and flooding dynamics (Toonen, 2013)).

2.3 Concluding remarks

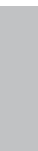
The mapping history of the physical landscape and its substrate in the Netherlands shows different generations of research disciplines, spatial coverage, and resolution, associated information types, and a recent evolution towards GIS-based approaches. The oldest map generations focussed on the geology, geomorphology, or soil type, ranging from very local detailed studies to national overviews. Owing to the introduction of the radiocarbon dating method, maps produced since the

1950s had considerably gained accuracy on age and genetic interpretation of the mapped elements. This resulted in the production of a large number of genetic geomorphological maps, as well as palaeogeographical reconstruction maps (Figure 2.7). After earlier maps and source data (e.g. borehole data) had become digitally available in the early 2000s, new integrated GIS reconstructions have been established. The maps from the research traditions discussed in this chapter generated knowledge for agriculture, landscape planning, and geoarchaeological prospection. Besides, they contributed to fundamental research on landscape evolution or on human-landscape interaction, when confronted with settlement dynamics (e.g. Spek, 2004; Van Dinter, 2013; Van Lanen et al., 2015ab).

To keep knowledge on geomorphological evolution up-to-date, it is important to continue combining existing information and new datasets into integrated overviews. This will in several cases provide new insights or interpretations on age or genesis of mapped units, but sound comparison of different data sets requires awareness of the original focus, scale, research strategy, and state of knowledge underlying each data set. The smart integration following the right combination of priority rules (e.g. which dataset provides the best information on age or extent?) in incorporating these datasets is the best way to disclose the otherwise fragmented knowledge. Using the GIS-generated palaeogeographical mapping system as an iterative tool is an important benefit for studying the geomorphological evolution of past landscapes. The system is generic, verifiable, adaptable, and landscape situations can be extracted for any time slice in the past. During the GIS workflow, inconsistencies in interpretation or input data can be detected and resolved, bearing the background of the research traditions and underlying interpretations in mind. Doing so, enables to harvest most information on landscape evolution from our country's research legacy.

Acknowledgements

This research is part of the PhD thesis of Harm Jan Pierik within the project 'The Dark Ages in an interdisciplinary light' (www.darkagesproject.com) funded by NWO (project nr. 360-60-110). The first author contributed in the following proportions (%) to research design, analysis and conclusions, figures, and writing: 60, 70, 90, 80. We would like to thank Wim Hoek, Esther Jansma, Hans Middelkoop, and Esther Stouthamer for their useful comments on the manuscript.



Chapter 3

A new GIS approach for reconstructing and mapping dynamic late Holocene coastal plain palaeogeography

The geomorphological development of Holocene coastal plains around the world has been studied since the beginning of the twentieth century from various disciplines, resulting in large amounts of data. However, the overwhelming quantities and heterogeneous nature of this data have caused the divided knowledge to remain inconsistent and fragmented. To keep improving the understanding of coastal plain geomorphology and geology, cataloguing of data and integration of knowledge are essential. In this chapter we present a GIS that incorporates the accumulated data of the Netherlands' coastal plain and functions as a storage and integration tool for coastal plain mapped data. The GIS stores redigitised architectural elements (beach barriers, tidal channels, intertidal flats, supratidal flats, and coastal fresh water peat) from earlier mappings in separate map layers. A coupled catalogue-style database stores the dating information of these elements, besides references to source studies and annotations regarding changed insights. Using scripts, the system automatically establishes palaeogeographical maps for any chosen moment, combining the above mapping and dating information. In our approach, we strip the information to architectural element level, and we separate mapping from dating information, serving the automatic generation of time slice maps. It enables a workflow in which the maker can iteratively regenerate maps, which speeds up fine-tuning and thus the quality of palaeogeographical reconstruction. The GIS currently covers the late Holocene coastal plain development of the Netherlands. This period witnessed widespread renewed flooding along the southern North Sea coast, coinciding with large-scale reclamation and human occupation. Our GIS method is generic and can be expanded and adapted to allow faster integrated processing of growing amounts of data for many coastal areas and other large urbanising lowlands around the world. It allows maintaining actual data overview and facilitates new ways of analysis at national, regional, and local scales.

Published as: Pierik, H.J., Cohen, K.M., Stouthamer, E. (2016) A new GIS approach for reconstructing and mapping dynamic late Holocene coastal plain palaeogeography. *Geomorphology* 270, p 55–70. [dx.doi.org/10.1016/j.geomorph.2016.05.037](https://doi.org/10.1016/j.geomorph.2016.05.037).

3.1 Introduction

The evolution of Holocene coastal plain landscapes has been studied extensively worldwide over several decades of research history and from several different scientific disciplines, resulting in a large variety of thematic studies and maps. Some of these studies contain palaeogeographical reconstructions (e.g. Baeteman, 1999; Metcalfe et al., 2000; Fitch et al., 2005; Tanabe et al., 2006; Alexakis et al., 2011; Hijma & Cohen, 2011; Tamura et al., 2012; Tanabe et al., 2015; Vis et al., 2015), in which geological and geomorphological data was incorporated. Although differences in

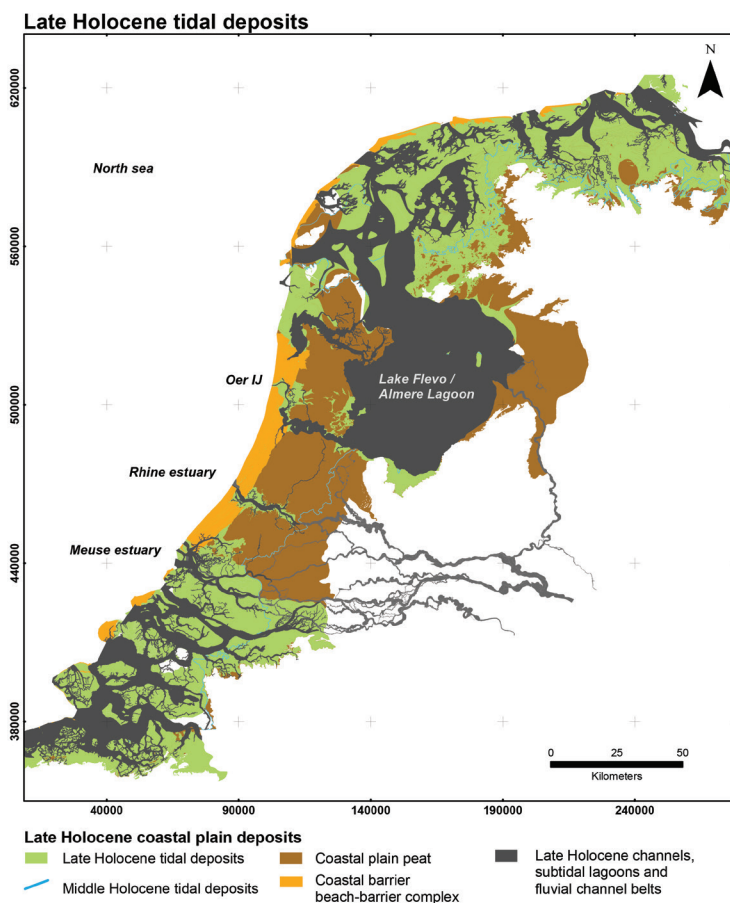


Figure 3.1 | Coastal plain setting of the Netherlands: coastal plain peat and middle Holocene tidal deposits after Cohen et al. (2017a), tidal deposits (this chapter).

approach behind the various palaeogeographical map products exist, they all have been compiled using conceptual insights, based on geological principles and region-specific knowledge, such as history of relative sea level change or shifts in availability of sediment. These (mainly static) maps were compiled to map and illustrate coastal plain development and usually lack a systematic (i.e. verifiable) mapping approach. This limits possibilities to query, verify, update, and expand the reconstructions. Further improvement of coastal plain mapping is generally reckoned to benefit from the integration of heterogeneous data in palaeogeographical maps or uniform databases.

For the Netherlands, many high-density data sets, dissertations, map series, and reports documenting the complex geological subsurface architecture are available (chapter 2; Appendix A). They have been produced over a period of decades and greatly differ in state of knowledge at the time of production, in spatial coverage, and in research focus. Integrated traditional palaeogeographical map products (Pons et al., 1963; Zagwijn, 1986; Vos & Knol, 2015; Vos et al., 2015ab) have found considerable application in geoarchaeological studies (e.g. Knol, 1993; Vos & Van Heeringen, 1997; Gerrets, 2010) and in geological-geomorphological coastal plain studies

(e.g. barrier formation: Beets and Van der Spek, 2000; river avulsion: Kleinhans et al., 2010; transgression and peat growth: Hijma & Cohen, 2011; Bos et al., 2012). The attribution of age to the mapped elements especially is a major source of uncertainty resulting in differences between reconstructions. Even for the densely mapped and dated coastal plain of the Netherlands, the number of elements in reconstruction maps is so large that their majority remains relatively dated only. For all these elements, age-attribution decisions are then taken, often without explicit documentation of the underlying assumptions. This makes adapting these reconstruction maps to new insights and data difficult and hampers integration with maps of adjacent areas. To keep national late Holocene landscape reconstructions up-to-date, a dynamic approach to mapping and dating is required that facilitates producing palaeogeographical maps for any chosen time step and allows us to easily update the elements on the map. To take into account all accumulated knowledge, integration and documentation of maps based on heterogeneous, fragmentary data sets for various parts of the coastal plain are essential. Such a system provides new opportunities to study the geological architecture and evolution of the coastal plain over large regions based on more uniform source data than traditional maps provide.

Since the 1980s, the development of Geographical Information Systems (GIS) has allowed digital map recombination and computer-aided conversion and processing of data (e.g. Burrough, 1986), making it easier to produce coastal plain landform and substrate maps. The GIS methodologies provide the possibility to collect large amounts of data into a single information system in which querying and processing of data and statistical analyses can be done. In this chapter we present an advanced GIS design for geological-geomorphological and palaeogeographical mapping of the late Holocene coastal plain of The Netherlands. Our method elaborates on an earlier developed GIS for reconstructing the river network evolution of the Rhine-Meuse delta (Berendsen & Stouthamer, 2000; Berendsen et al., 2001; Cohen et al., 2012). Our GIS stores the accumulated mapping and attribute data of geological architectural elements in a uniform way. It uses scripts to automatically generate time slice maps based on age information that is stored as element attributes. In this chapter, we restricted the GIS to the late Holocene palaeogeographical development (roughly the last 3500 years) – the youngest period for which data is available at the highest resolution and is most diverse. We explain our workflow for converting architectural-elements and their attributed age into palaeogeographical maps. In the discussion we focus on some of its output products and the research applications of the GIS. The GIS design and workflow to combine geological mapping and production of palaeogeographical reconstructions is a generic one. It is applicable to other Holocene coastal plains and other types of Quaternary sedimentary environments for managing ever-growing heterogeneous data sets, especially when excessive data availability and diversity hamper systematic analysis.

3.2 General approach

The coastal plain of the Netherlands is considered an amalgamation of landforms with barrier systems, tidal inlet systems, and coastal peatland (Figures 3.1 and 3.2). Each tidal system consists of a main inlet channel that connects the open sea to different environments in the back-barrier zone (Figure 3.2). The architectural elements that make up these systems are genetically uniform geological features (e.g. Miall, 1985; element complexes cf. Vakarelov & Ainsworth, 2013) that can be distinguished based on their three-dimensional geometry, scale, and facies. We distinguished several types of architectural elements shown in coastal plain geological maps: beach ridges (topped by dunes), tidal channels (channel belts, subtidal deposits), fluvial channels (in the part of

Table 3.1 | Conversion of existing studies into the GIS, for references see chapter 2. The problems in relative dating and overlap can be minimised by iteratively using the presented GIS.

Themes	Use in GIS	Source	Info from source	Strength	Problems
Lithofacies	In which base map: channel, intertidal flat supratidal flat, beach barrier?	Soil maps	Lithology	Detailed info deposits at the surface	Less detail for deposits below 120 cm below surface
		Dissertations, geological maps, reports TNO/Deltares/ Archaeology	Lithological and geological maps and cross-sections	Detailed	Locally available
Planform geometry	Geometry of features	Soil/ geomorphological /geological maps	Geometry mapped units	Available digitised data easily incorporated in GIS	Units may not overlap, checks needed
Stratigraphy, relative age	Old/middle/young position in GIS, age in database	Geological maps	Chronostratigraphy	Information on surface and deeper deposits	Chronology mixed with facies and stratigraphy: need independent check
		Dissertations, reports TNO/ Deltares/ Archaeology	Lithological and geological maps and cross-sections Information on surface and deeper deposits, shows architecture	Detailed	Local information only
Absolute age	Old/middle/young position in GIS, age in database	Geological maps	Chronostratigraphy	Information on surface and deeper deposits	Chronology mixed with facies and stratigraphy: need independent check
		Dissertations, geological maps, reports TNO/Deltares/ Archaeology	¹⁴ C dates, OSL, pollen, macrofossils, dendrochronology, archaeology	Absolute age, detailed	Local, correlation issues
		Historical sources	Embankment	Detailed, accurate	
Network Position	Geometry of features and connection with main tidal systems	Soil/ geomorphological/ geological maps	Geometry relative to units interpreted as main tidal basins		Correlation based on chronostratigraphy need independent check Erosion hampers correlation
		Soil/ geomorphological/ geological maps, local studies	Lateral distribution of facies relative to units interpreted as tidal basins		

the coastal plain that is affected by the Rhine-Meuse system), intertidal flats (*wadden*), supratidal saltmarsh, and freshwater peatland that occupies the farther inland part of the coastal plain. These architectural elements represent different landforms and former landforms with associated depositional environments (e.g. indicating position relative to tidal range and degree of exposure to waves; Van Straaten & Kuenen, 1957; Reineck & Singh, 1980; Vos, 2015a).

In the last few 1000 years, the formation and abandonment of tidal inlet systems and connecting beach barrier and river systems have been controlled by natural and anthropogenic effects (e.g.

Beets & Van der Spek, 2000; Berendsen & Stouthamer, 2000; Vos, 2015a). The multiple tidal systems that developed during the Holocene resulted in a complex stacked heterogeneous coastal plain subsurface. Bringing down coastal plain sequence mapping to generations of tidal systems not only serves the legend of geological mapping, but also is key to performing palaeogeographical reconstruction with that data.

In the redigitisation process of individual elements from earlier maps, four aspects were considered (Table 3.1): (i) their lithofacies, to decide the type of architectural element and palaeogeographical map legend; (ii) their planform geometry; (iii) a best estimate of their age; and (iv) their network position, i.e. the parent tidal system to which it connects. In some cases, these four aspects all followed straightforward from one single study. However, in many cases earlier mappings left aspects of dating and network position unspecified; here we assessed that information ourselves. For some elements, contradicting interpretations from different studies had to be assessed and judged. This was done element-by-element, taking into account the conceptual background of these studies, the year of map production and availability of new observations (chapter 2; Appendix A). We started with unifying redigitised architectural elements from maps produced in national campaigns (geological, geomorphological, and soil surveys). In general, we retrieved the deeper preserved elements (> 1-2 m below the surface) from geological maps, whereas soil and geomorphological maps were used for the shallowest elements (upper 1-2 m). We then supplemented the information further with more local studies, with higher dating resolution (e.g. Pons & Van Oosten, 1974; Roeleveld, 1974; Vos, 2015a). The extent of shallow elements with topographic expression (supratidal ridges; tidal channel micromorphology, etc.) was cross-verified with LiDAR elevation data, available since 2005. At the most detailed level we stored absolute and relative dating information in a catalogue-style database that is part of the GIS. This includes a considerable amount of chronological data available in the Netherlands (mainly: ^{14}C , archaeology, historical documents; palynology; occasionally: dendrochronology, OSL) from a great number of sampling locations (partial overviews in e.g. Pons & Wiggers, 1959/1960; Berendsen & Stouthamer, 2001; Vos & Knol, 2015; Vos et al., 2015ab).

The GIS stores the planform geometry of the coastal plain architectural elements and their palaeogeographical development of the last ca. 3500 years over four digital map layers, which we call base maps. Each type of architectural element was mapped in a separate base map (see Table 3.2 and Figures 3.3 and 3.4). We used the mapped architectural elements as palaeogeographical (geomorphological) units in the calculated palaeogeographical time series. The elements in each base map thus resemble the past existence of specific environments. The four base maps do not only store elements of different genesis but also of different architectural relations with older elements and the substrate. For example, tidal channels reworked underlying older deposits (erosive contact), whereas supratidal flat deposits nonerosively cover older elements (burial). Therefore, each base map was treated differently when producing palaeogeographical output. The GIS can also manage other landscape units, such as coastal dunes, reed margins, and the flanking peat area. In the current version of the GIS, these are stored in separate layers as static background imagery or overlay data.

The workflow to construct and fill the GIS repeatedly looped through four steps: two manual and two scripted (Figure 3.3). Step 1 involves manual base map editing, labelling, correcting, and visual comparison with earlier mappings of the elements incorporated in the reconstruction. Step 2 is executed in parallel to base map editing and involves editing a catalogue-style database with the age of the architectural elements, their network membership (provenance), and references to original maps. The database also contains reasoning regarding reinterpretations as different dating approaches are suitable, depending on location and type of coastal architectural element

(full overview in Table 3.3). Steps 3 and 4 are the script-automated steps to produce palaeogeographical maps for a user-specified series of time slices. The step 3 script links ages from the database to the elements in the base maps, yielding time-slice selection maps as output (per time slice and per thematic base map). The step 4 script then recombines these time-slice selection maps into palaeogeographical composite maps, producing one map for each time slice.

In the early stages of development, looping through steps 1 to 4 served to debug the script and improve the base map and to catalogue field information. In stages of matured GIS development, the iteration loops served as fine-tuning of relative dating and as resolving apparent inconsistencies between source studies for the same area. The base map assembly of step 1, separate age administration of step 2, and the automatized relabelling in the scripts of steps 3 and 4 together ensure that the output maps result from formalised systematic procedures. All polygons have attributes from calculations that followed the same, retraceable rules in all parts of the map. Section 3 documents further particularities of this workflow, including a discussion of how geological-geomorphological reasoning led to the digitalisation decisions that were taken.

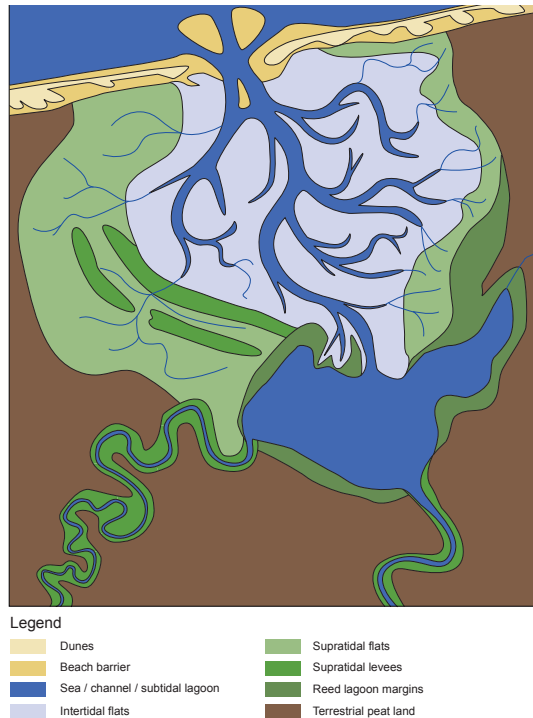


Figure 3.2 | Schematic outline of a coastal plain with different landscape units of one tidal system. The cartoon has been based on the Bergen inlet system (western Netherlands), after Pons & Van Oosten (1974; Figure 11).

3.3 Workflow for map compilation and scripted palaeogeography

3.3.1 Step 1: Assembling base maps holding architectural elements

We here describe design decisions of the four base maps and relate them to the properties of the architectural elements.

Base map 1 – tidal channel belts

Tidal inlets form a dendritic network in inland direction branching into smaller channels (Figure 3.2). Their channels are erosive elements that rework the substrate. They create depositional bodies in incised positions, storing sediments of a subtidal facies (deposited below low water). Lateral migration of the tidal channels forms *channel belts*, depositional elements that are wider than the forming active channel itself. The channel belts consist of a mainly sandy channel facies (Van der Spek, 1996; Martinius & Van den Berg, 2011). The channels are most dynamic and erosive in the vicinity of the tidal inlet, where the channels cut into a sandy substrate and high energy conditions prevail. Notably in the vicinity of the tidal inlets of the Wadden Sea, substrate reworking occurred

Table 3.2 | The GIS uses four manually maintained base maps that store different architectural elements in the coastal plain; the elements in each base map have characteristic lithologies, and geological relations to other features.

GIS Base map	Vertical position	Architectural element and geometry	Dominant lithology	Geological relation to other features
1	Subtidal	Infilled channel bodies, estuaries, creeks (ridges and channels).	Sand, sandy clay	Erodes older features, inherited after abandonment
2	Intertidal/subtidal	Intertidal flats (flats and channels)	Sand, sandy clay	Partly/possibly erodes older features
3	Supratidal	Supratidal flats and Supratidal ridges and levees	(Laminated) clay	Superposed on older features
4	Below EHW	Beach barriers and plains	Sand	Erodes older features (wave reworking)

extensively and former tidal inlet positions were hard to reconstruct. In the GIS we incorporated the reconstruction from Vos & De Vries (2013) for this dynamic area. In other parts of the coastal plain, we obtained channel belt positions from geological mapping. We locally adapted these elements using LiDAR data, which much more clearly identified late Holocene tidal channel belts. Cross-cutting relationships of the channel belts and their related inter- and supratidal elements often allowed identifying the succession of tidal inlet activity. Dating of channel abandonment is relatively straight forward (see Table 3.3), for example, making use of in situ archaeology or dating from residual channel infills (TAQ dates for abandonment, *Terminus Ante Quem*). In the sandy channel belt deposits, dates on intact shells or OSL provide TPQ age control for the abandonment age (*Terminus Post Quem*) to channel activity and termination (e.g. Van der Valk, 1996a; Cleveringa, 2000; Vos et al., 2015b). The timing of initiation of the channel elements is difficult to reconstruct, as with increased longevity their position changes and their dimensions gradually increase, laterally and vertically. Therefore, deposits from the earliest phase of activity, if preserved at all, are not easily identified which prohibits target sampling for direct dating of earliest tidal channel activity. Using iterative visualisation of developments and the intercomparison of developments for adjacent tidal systems that the GIS can provide, we aim to outline palaeogeographical arguments to optimise these initiation ages.

The central lagoon is a particular element that developed in the central coastal plain over the course of the late Holocene by tidal inlet extension and erosion of flanking peatland (Wiggers, 1955). Although the lagoon is not a tidal channel, we stored this element in the same base map because of its subtidal and erosive character. Reconstructions of stepwise erosion of this lagoon system in early phases rely on palaeogeographical arguments (e.g. Vos et al., 2015a). Again, such argumentations can be tested and improved by deploying systematic methods for palaeogeographical analysis.

Base map 2 – intertidal flats

Channels of the tidal system are often flanked by intertidal to supratidal depositional areas (Figure 3.2). Intertidal flats are landforms that form between MLW (mean low water) and MHW (mean high water; Evans, 1965; Amos, 1995; Fan, 2012; Flemming, 2012). Intertidal flat deposits around the North Sea consist of strongly bioturbated sands with mud drapes or muddy sediments with sand lenses (Van Straaten & Kuenen, 1957; Reineck & Singh, 1980; Mauz & Bungenstock, 2007). Because

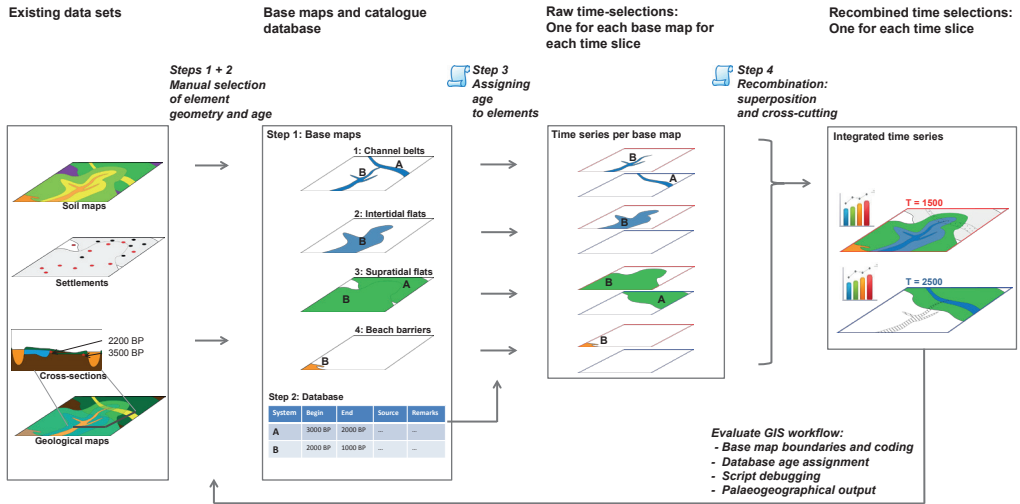


Figure 3.3 | Workflow of the GIS construction. Planform geometry, extension, network position, facies, and stratigraphy are evaluated from the input data and digitised into four thematic base maps (step 1). The database stores attribute information (e.g. age, sources, additional remarks: step 2). Scripted querying is used to assign the ages from the database to the architectural elements in time series maps (step 3). These time series maps are recombined using geological relations (superposition, inheritance, cross-cutting) yielding palaeogeography per time step (step 4). Finally, the output is iteratively evaluated, and the base maps and database are adapted within the possibilities the data provides.

the shoals of the intertidal zone do not necessarily have an erosional base, these elements were stored in a separate base map from the reconstructed tidal channels. Neighbouring tidal channels, however, in areas such as the Wadden Sea and the larger estuaries of the southwestern Netherlands, tend to laterally rework tidal flat deposits rather quickly. In geological mapping campaigns it was therefore often impossible to distinguish between tidal flat shoals and tidal flat channels. In these areas, we recorded them as single amalgamated architectural elements in this base map ('intertidal flats with partial or possible erosive channel belts'). On the landward side, facies are more segregated, and distinction between channel and shoals was often possible, allowing these elements to be stored over base map 1 and 2.

Base map 3 – supratidal flats and ridges

Supratidal depositional areas (salt marshes) trap sediment during storms and springtides (Frey & Basan, 1985; Allen, 2000; Bartholdy, 2012). Their deposits typically consist of pedogenically ripened, rooted, and decalcified clays with spotty iron oxide bands. The clays contain thin sand lamina that is well visible because faunal bioturbation is not as abundant in supratidal areas compared to intertidal areas (Vos & Van Kesteren, 2000). These supratidal deposits do not have an erosional base. Their extent can be recognised in clay occurrences in soil maps or as supratidal facies interpretations from geological maps. On their inland side, the supratidal deposits are usually flanked by peaty deposits from former freshwater fenlands.

Close to the intertidal and channel areas, slightly elevated elongated ridges can occur on the supratidal flats. These tidal levees are formed by regular flooding and storm events (Vos and

Baardman, 1999; Vos & Gerrets, 2005). We mapped them as elements superimposed on former supratidal flats. Their delineations follow from LiDAR-aided geomorphological mapping. Supratidal flats and ridges are both stored in base map 3. A separate attribute field is used to label the polygon as 'supratidal flat' or as 'supratidal flat with a supratidal levee'. Note that part of the supratidal depositional elements overlies fenland peat representing transgressive developments and that other parts overlie intertidal deposits, representing an infilling succession of tidal basins.

In the inland parts of the coastal plain, where supratidal depositional area expanded into and over fenland, age estimates for beginning of deposition typically followed from dating of organic material directly underlying the clay (Table 3.3; e.g. De Mulder & Bosch, 1982; Westerhoff et al., 1987; Vos & Van Heeringen, 1997). We treated such datings with caution, as the clay-peat contact in many places represents a hiatus on the top of the peat. This hiatus is caused by natural terrestrial processes and human activities affecting the fenland surface prior to transgression (causing oxidation of organic topsoil). Top-of-peat dates in such cases overestimate the age of first inundations and landscape change from a freshwater to saltmarsh supratidal environment (Vos & Van Heeringen, 1997). In more seaward parts, supratidal deposits overlie intertidal deposits, and dating of the transition can make use of radiocarbon dating certain molluscs (in *viva* intertidal species, storm-wash displaced fresh specimen; e.g. Vis et al., 2015). The end of supratidal depositional activity in the late Holocene Netherlands setting is associated with human reclamation of the supratidal flats. Therefore, a minimum age for their mature phase can often be derived from archaeology (e.g. Vos & Gerrets, 2005; Gerrets, 2010).

Base map 4 – beach barrier elements

Beach barrier complexes separate the open sea from the coastal plain. A barrier complex consists of beach ridge sandbodies and their near-shore underwater continuations. Beach ridges are shore-parallel, several 100-m-wide, elongated sand ridges formed by wave action (e.g. Otvos, 2000; 2012; Tamura, 2012). Beach barrier complexes can stretch over long distances between major tidal inlets, and individual beach ridges are not tied directly to specific individual tidal systems. Their identification and age administration is therefore kept separate from that of the tidal inlets.

Inland delineation of the individual ridge generations in the barrier complex followed from geological mapping. On the seaward side, older beach ridges show to be truncated by younger erosion. For these beach barrier elements, the delineation in the base map includes extrapolative reconstructions (e.g. Vos & De Vries, 2013).

In the western sector of the coastal plain ('Holland'), successive generations of beach barrier elements amalgamated into a kilometres-wide and 100-km-long barrier complex between 6000 and 3000 years ago (Van Straaten, 1965; Jelgersma et al., 1970; Van der Valk, 1996b; Cleveringa, 2000). In the other sectors along the coastal plain, the barrier complex is less wide and generally younger than 3000 years. Age control on the beach barrier elements was obtained from vertical series of ^{14}C dates on marine mollusc shells (e.g. Beets et al., 1992; Van der Valk, 1996ab; Cleveringa, 2000), besides from radiocarbon dating of local peats in the lows between ridges (e.g. Van de Plassche, 1982) and OSL dating of beach and dune sands (e.g. Vos et al., 2015a).

3.3.2 Step 2: Administrating network provenance and age

Here, we describe how the generations and age of the mapped elements was administered and encoded in the GIS. The age of the elements was obtained through extrapolation from the few intensively studied local sites using *relative dating* arguments (such as superposition and cross-cutting relationships) and established geological conceptual knowledge. Correlating and

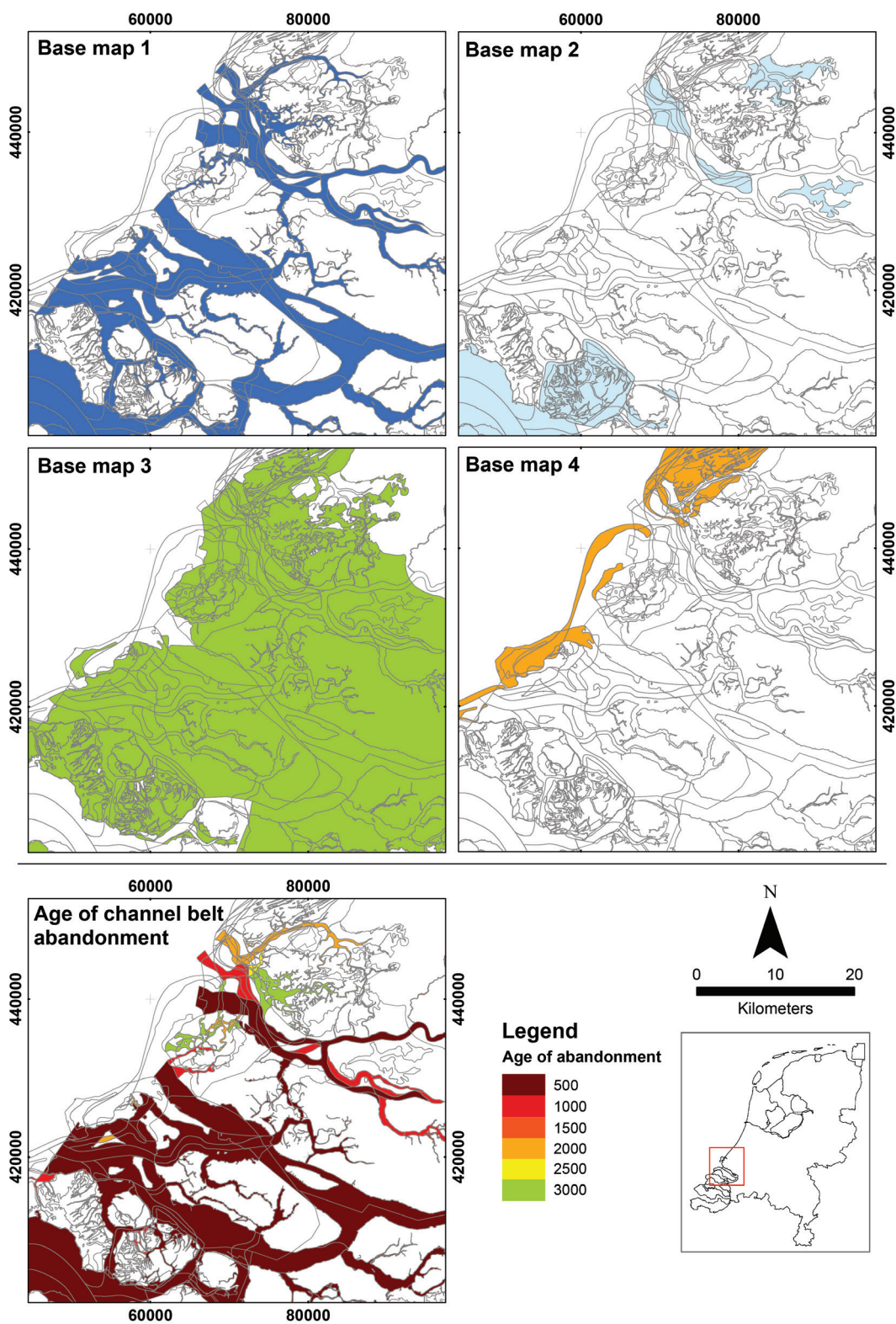


Figure 3.4 (left page) | Four base maps for the Meuse estuary region and age map for channel belts of the Meuse estuary. Four manually created base maps of all late Holocene (base map 1: channel belts; base map 2: intertidal flats; base map 3: supratidal flats; and base map 4: beach barriers). Below: map that shows the age of abandonment of channel belts, ages are in ^{14}C yr BP.

distinguishing separate tidal systems was most simple at distal positions from the tidal inlet. Here, architectural elements have been preserved better, stratigraphic contacts can be traced over considerable distance, and intercalated peat beds provide abundant dating materials.

Dating quality and age resolution

The age resolution of the GIS strongly depends on the dating strategy and number of datings of the incorporated studies, which can vary substantially per element and region. We consider elements with three or more consistent dates to be well-dated, making a 100-year dating resolution possible. We used relative dating for elements that lack independent absolute age control. In these cases, the age assignment was based on burial relations (mainly of supratidal flats) and cross-cut (by channels) relations, still making a 500-year dating resolution possible. Correlation of the undated architectural elements is the most important source of uncertainty in landscape reconstructions and yields differences in reconstructions between authors. The great diversity of dating information and different possible lines of reasoning for age assignments to architectural elements (Table 3.3) makes documentation of the reasoning desirable. This GIS shows the current, most likely age; and its setup helps researchers to optimise age attribution to undated elements. Moreover, the GIS provides the infrastructure to iteratively check presumed element ages, by looping through steps 1 to 4. This allows tracking down inconsistencies on the generated maps and directing where to correct or optimise the reconstruction.

Network membership (provenance)

Based on their platform and stratigraphic position, the digitised elements in the base maps were labelled with ID numbers corresponding to generations of tidal systems. These IDs correspond to the IDs in the database (Figure 3.5), it is a four-digit number that identifies the major feeding tidal inlet and the dendritic subsystems. Additionally temporal phases within the functioning of these tidal inlets could be indicated. This way of labelling makes it easy to query elements from the same tidal inlet or groups of inlets. Up to three generations of tidal systems can be labelled in the base maps. We used this to encode for strong diachroneity, tidal system shifts, and intersections of older and younger (channel) systems.

Catalogue database

In addition to the four base maps, a catalogue-style database was maintained that stores interpreted and summarised information of each tidal system. The database does not store detailed information on each and every described section or measured dating sample, but it contains a discussion on the extent, assigned age, and network position of the tidal system (Figure 3.5). In this discussion, the available dates were evaluated using expert knowledge of the researcher.

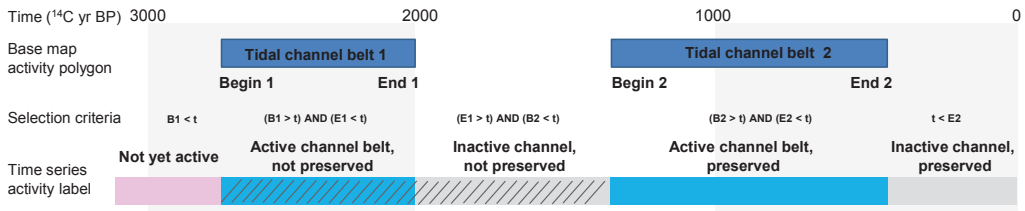
Additionally, referencing to sources providing age and extent information was documented. Using the unique ID, the tidal system ages was later coupled to mapped elements in the base maps during step 3. The scripts in step 4 used these assigned element ages to generate the palaeogeographical maps. Note that, unlike in traditional geological and geomorphological

Subtidal	Channels	Begin			Ad 1: Vos and Van Heeringen (1997)
		1) Indirect, from correlating with elements (e.g. supratidal flats in the hinterland)		- Ad 1: diachroneity between channels initiation and onset distal flat sedimentation	
		2) Historical sources (after AD 1000)		- Ad 1: (proximal) younger channel reworking may hamper correlation	
		Activity		- Ad 1: reservoir effect	Ad 1: Baeteman (2005b)
		1) ¹⁴ C of shells			
		2) OSL			
		End		- Ad 1, 2, 4: TAQ – elements can be inhabited later or at other assumed stage	Ad 1: Vos and Van Heeringen (1997) Ad 2: Use of historical sources: Oost (1995)
		1) Archaeology (last 3000 years)			
		2) Historical sources of embankment (after AD 1000)			
		3) Residual channel dating (¹⁴ C/pollen)		- Ad 3: residual channel fill and overlying peat date provides TAQ	
		4) ¹⁴ C/pollen dating overlying peat		- Ad 1: age of maritime archaeology represents minimal data of presence of open water	Ad 1: Wiggers (1955); Ente et al. (1986); Menke (1998)
	Subtidal lagoons	Begin		1) Maritime archaeology	
		End		1) Historical sources of embankment (after AD 1000)	
		Begin		1) Indirect, from correlating with elements (e.g. supratidal flats in the hinterland)	Ad 1: diachroneity between channels initiation and onset distal flat sedimentation
		2) Historical sources (after AD 1000)		- Ad 1: (proximal) younger channel reworking may hamper correlation	Ad 2: Use of historical sources: Oost (1995)
		Activity		- Ad 1: reservoir effect	
		1) ¹⁴ C of shells			
		2) OSL			
		End		- Ad 1, 2, 4: TAQ – Flats can be inhabited later or at other assumed stage	Ad 2: Oost (1995) Ad 3: Vos and Baardman (1999); Vos and Gerrets (2005); Vis et al. (2015)
		1) Archaeology (last 3000 years)			
		2) Historical sources of embankment (after AD 1000)			
		3) (succession to supratidal flat) ¹⁴ C dating of Hydrobia Ulvae		- Ad 3, 4: reservoir effect	Ad 4: Roelleveld (1974); Griede (1978)
		4) ¹⁴ C/pollen dating overlying peat or soil, if present		- Ad 4: overlying peat date provides TAQ	

Environment	Architectural element	Meaning of age control	Dating strategy	Notes	Selected references
Supratidal	Supratidal flats	Begin	1) (On peat) ^{14}C /pollen top peat 2) On tidal flat: ^{14}C dating of <i>Hydrobia Ulvae</i> 3) Historical sources (after AD 1000)	- Ad 1,2: TPQ – hiatus clay-peat contact	
		End	1) Archaeology (last 3000 years) 2) Historical sources of embankment (after AD 1000) 3) ^{14}C /pollen dating overlying peat, if present	- Ad 2: reservoir effect - Ad 1,2: TAQ – flats can be inhabited later or at other assumed stage - Ad 3: overlying peat date provides TAQ	Ad 1: Vos and Baardman (1999); Vos and Gerretts (2005) Ad 2: Oost (1995) Ad 3: Behre (2004); Griede (1978); Roeleveld (1974)
		Begin	1) (On peat) ^{14}C /pollen top peat 2) On tidal flat: ^{14}C dating of <i>Hydrobia Ulvae</i> 3) Historical sources (after AD 1000)	- Ad 1,2: TPQ – hiatus clay-peat contact - Ad 2: reservoir effect	Ad 3: Oost (1995)
	Supratidal levees and ridges	End	1) Archaeology (last 3000 years) 2) Historical sources of embankment (>AD 1000)	- Ad 1,2: TAQ – Flats can be inhabited later or at other assumed stage	Ad 1: Vos and Baardman (1999); Vos and Gerretts (2005)
Sub-/Inter-/Supratidal	Beach barriers	Accretion (active)	1) ^{14}C dating of shells 2) OSL	- Ad 1: ^{14}C dating of shells: reservoir effect	Ad 1: Van Straaten (1965); Van der Valk (1996a); Cleveringa (2000); Vos et al. (2015b)
		End	1) Archaeology (last 3000 years) 2) Peat/soil on top 3) Oldest aeolian deposits on top	- Ad 1,2,3: TAQ – All these dates are TAQ, hiatuses could occur.	Ad 2: Van Heteren et al. (2000) Ad 1,2,3: Jelgersma et al. (1970); Van de Plassche 1982; Zagwijn (1984); Van Heteren et al. (2000)

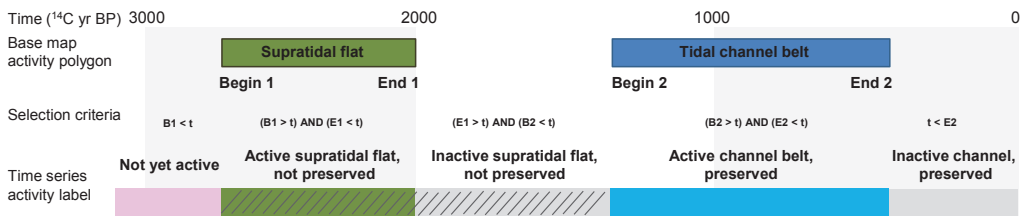
Step 3: single base map solution

(A) Two active channel systems in one base map



Step 4: multiple base map solutions

(B) Step 4: Erosion of supratidal flat by younger channel



(C) Step 4: superposition of supratidal flat on older channel belt

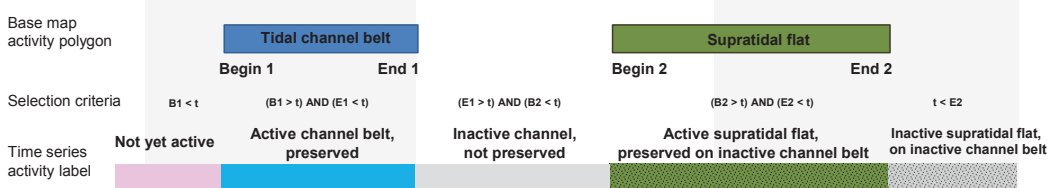


Figure 3.6 | Querying procedure for time series calculation (steps 3 and 4). Possible states for each element are: not yet active, active preserved, active eroded, inactive preserved, inactive eroded, active with inherited channel belt, inactive with inherited channel belt. (a) Example calculation procedure for polygons of base map 1 (channels) with two active tidal systems in step 3. After the systems in the polygons have been assigned an age from the database, the state of the element at the predefined time steps is evaluated. (b) Example calculation procedure in step 4 where a younger channel erodes an older supratidal flat. (c) Calculation procedure in step 4 where an older channel body has been covered by a supratidal flat. B1 = begin of system 1, E1 = end of system 1, B2 begin of system 2, E2 end of system 2. t = predefined time step of which the state is to be calculated.

active' (Figure 3.6), following similar procedures as described in Berendsen et al. (2007). In order to do so efficiently, the procedure starts with linking base map polygons to catalogue entries (using the common ID) and adding new fields to store the activity status (written by the script). Hereto one attribute column for each predefined time step is needed.

Erosion status

The same attribute column also administers whether a past-active element has the status of 'preserved', 'possibly/partially eroded', and 'eroded' status. After processing the activity status per base map, the script verifies at which locations the reconstructed elements have been dissected by younger elements. Adopting the architectural cross-cutting relations in such cases, the script overrules for the older element its previous erosion status, setting it to 'eroded' (in the case of tidal channel elements of base map 1) or to 'possibly/partially eroded' (in the case of intertidal flat

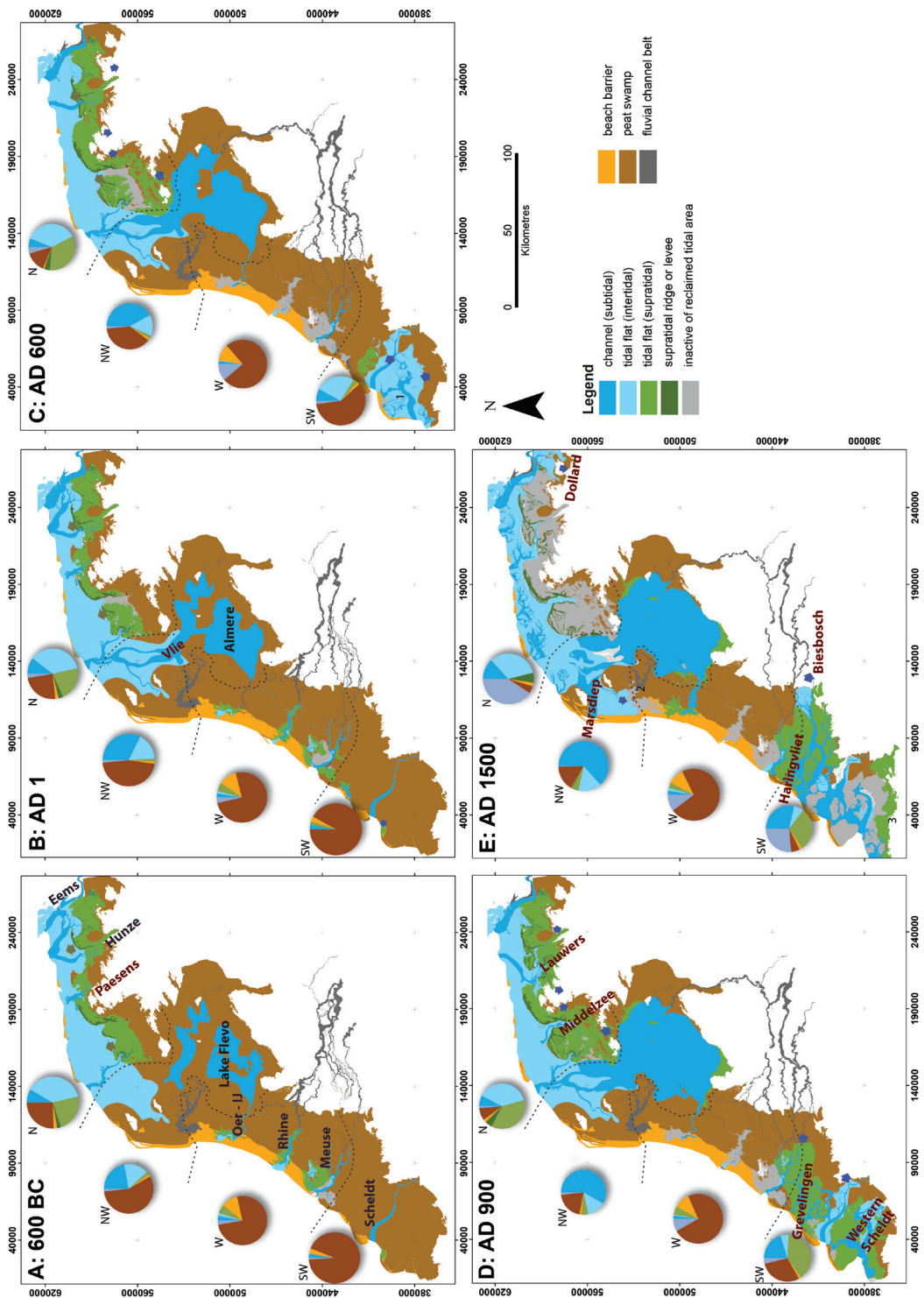


Figure 3.7 (left page) | GIS-derived coastal palaeogeography from 600 BC to AD 1500. Pie charts show relative areal distribution of the palaeogeographical units per coastal plain segment, statistics were derived from the GIS; colours correspond to palaeogeographical units. The GIS reproduces existing reconstructions that show major extension of the tidal area after the Roman period. The fluvial channel belts from the Cohen et al. (2012) datasets are incorporated.

elements). Note that step 3 only evaluates this for relations within base map 1 and 2, it does not yet evaluate potentially conflicting status attribution for overlapping elements from other base maps; that is done when the time-slice selections are recombined in step 4.

3.3.4 Step 4: Scripting the recombination of time-slice selections

In this step, the script reproduces the interrelations between the different types of architectural elements from the base maps (Figures 3.3 and 3.6). This means that the script evaluates which elements cross-cut each other (e.g. tidal channels), which were superimposed (e.g. supratidal flats and levees) and where inheritance of older systems occurred (supratidal flats on top of former channels). Calculations result in a single digital map with polygons with palaeogeographical legend codes for each predefined time step.

The script first combines the four step 3 output maps, with the fields storing activity of the predefined time steps. This results in a 'union mosaic map' with many polygons (in its current state 4000 polygons). Secondly, as in step 3, the script adds attribute fields for each predefined time step. Finally, these attribute fields are systematically filled in with numeric codes representing the type of architectural element and its state of activity. For these fields, a standard legend was designed to display the palaeogeographical map by colouring the polygon mosaic. In that legend, full colour is used for active depositional elements, while cross-hatching is used to indicate the areas that in later time slices will be eroded and where buried landforms imply inherited topographic effects (Figures 3.6-3.8)

The filling of the palaeogeographical legend attribute requires a long series of selection queries and numeric code-writing operations because each possible combination of activity status, erosion status, and base map architectural order has to be considered, according to three situations outlined below (Figure 3.6).

Single polygon situation

This applies when the attributes of the step 4 mosaic map trace back to information from one base map layer only. For example, polygons with only a supratidal depositional activity, meaning that neither a tidal channel, nor intertidal flats, nor beach barriers were active here. The step 4 script once again labels the activity of these polygons 'active', 'no longer active/inherited landform', and as 'not yet active', essentially copying the step 3 written attribute.

Overlapping polygon situation

Where polygons in the step 4 mosaic map trace back to attribute information coming from more than one base map, a more complex evaluation is needed that considers the erosion status. (i) *Erosion* – In this situation the youngest element of the active elements in the time slice considered is an erosive architectural type (i.e. active tidal channel, active tidal flat with channels, active beach system). Attribute fields for older time slices are relabelled into a code that indicates erosion after the element's activity (Figure 3.6B), appearing as a hatched overprint on the map. For the time steps after which the erosive element started, the youngest erosional element is reconstructed. (ii) *Draping*

and geomorphological inheritance – In this situation, the youngest active elements in the time slice considered is nonerosive (i.e. an active supratidal flat; Figure 3.6C). This does not require updating the erosion status for older time slices because the element is considered to be intact. When the script identifies a younger supratidal flat on top of an older, inactive tidal channel belt, the legend attribute is updated to ‘potential tidal channel inversion ridge within supratidal environment’.

3.4 Results and discussion

3.4.1 Output

The GIS automatically generates palaeogeographical time series maps (Figures 3.7 and 3.8). These maps do not only visualise palaeogeography at a specific time step but also show element inheritance from earlier time steps and nonpreservation owing to erosion during later time steps. Other types of output include channel belt age maps (Figure 3.4E) and descriptive areal statistics that can be generated per architectural element and per time step (Figures 3.7 and 3.8). The statistics quantitatively describe the coastal development, by summing the area of the landscape units according to the implemented reconstruction. Similar to the production of the palaeogeographical map series, the calculation of these statistics is scripted and can be recalculated after each major update. As the GIS can identify erosion of elements in later time steps, the noneroded and eroded elements can be summed separately, generating preservation per type of architectural element through time. With this information the rate of development can be quantified. This facilitates comparison of coastal and back-barrier development between regions.

The labelling and design of the base maps and linked database facilitate the user to select elements by region, network position, age, time of activity, and reworking patterns of the architectural elements. For example, statistics can be generated for different subregions (Figures 3.7 and 3.8) and then intercompared. Furthermore, within regions one can quantitatively differentiate between the areal and preservation developments in the coastal barrier zone, e.g. between the seaward part and the landward part of the back-barrier system. Generating such data complements the traditional palaeogeographical map series descriptions that tend to be qualitative only. Such analysis can now be performed on local (one main ingress) and regional scale.

3.4.2 Performance evaluation

A way of evaluating a GIS performance is to compare the palaeogeographical map series output to recent maps that are produced using the traditional approach. In Figure 3.8 this is done on a regional scale for a part of the western Netherlands showing the late Holocene development of the tidal channel and flood-basin area (in both map series). The coastal GIS reproduces the activity and position of the secondary tidal systems around the estuary reconstructed by Vos & De Vries (2013). Differences between the maps result from differences in approach and, at the detailed level, also from interpretation in areas where younger erosion has prevailed. Vos & De Vries (2013) compiled maps on a national scale for archaeologically relevant fixed moments in time, whereas our GIS has a setup that generates maps for any requested time. Vos & De Vries (2013) produced cartographically styled landscape maps redrawn based on geological and geomorphological data and preexisting maps, whereas our GIS digitally stores the original mapped elements and constructs the maps from those.

The shown area in Figure 3.8 contains a well-preserved tidal system from the period 500 BC to AD 500, but also the part of the Meuse estuary that experienced younger natural reworking and, in modern times, the construction of the harbour of Rotterdam. In this area, both approaches

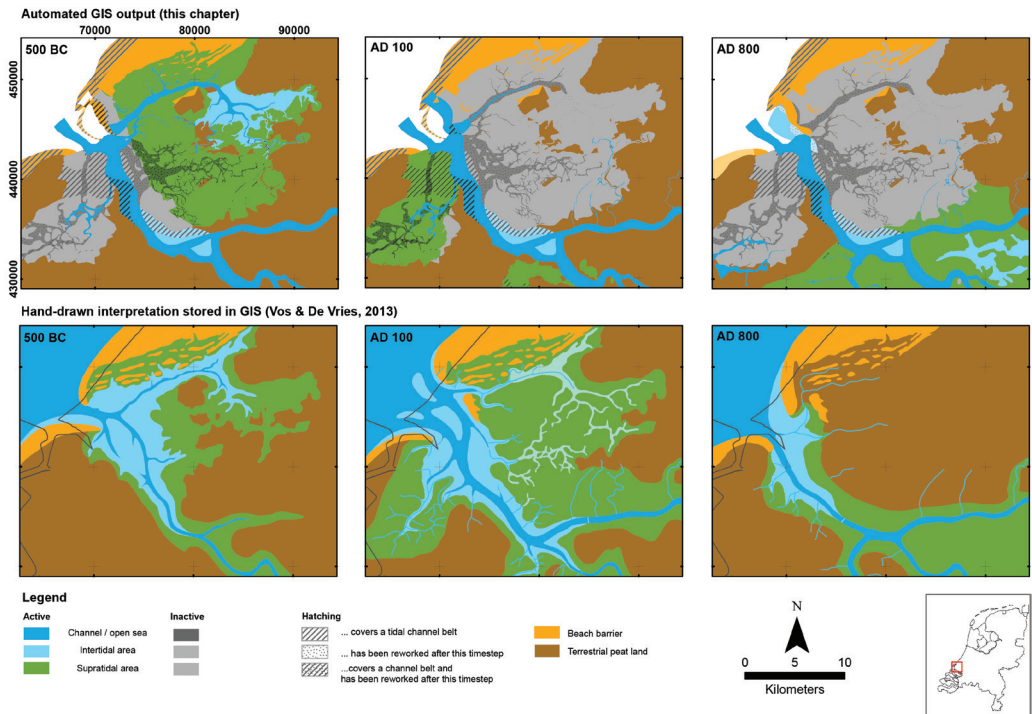


Figure 3.8 | Comparison of the palaeogeographical maps by Vos & De Vries (2013) and our reconstructions at 500 BC, AD 100, and AD 800. Pie charts show relative areal distribution of the palaeogeographical units. Both reconstructions show that the Meuse estuary was rather dynamical: secondary tributaries formed and silted up. Differences in the reconstructions result from deviations in methodology and interpretation of data.

for Holocene palaeogeographical reconstruction have to rely more on conceptual knowledge and extrapolated reconstructions. One such underlying assumption in the maps of Vos & De Vries (2013) is the gradual (diachronous) channel development and tidal areal extension toward the finally preserved maximum extent. In the data entry for our GIS (step 1 and 2), we have not encoded such a mechanism: a tidal system is either active or inactive, and no intermediate stage is displayed where this is not supported by actual dating information. In the few cases that dating information is available or becomes available in the future, the encoding of the tidal system is split up into multiple generations: more subsystems with distinct IDs in step 1, multiple catalogue-database entries in step 2. In our view, this represents the most factual visualisation of the available data. Our GIS also contains inactive inherited elements, whereas Vos & De Vries (2013) only map the reconstructed environment. Because our GIS does not yet include intercalated peat layers between tidal deposits, our AD 800 reconstructions show an ‘inactive tidal area’ instead of ‘peatland’. Any other differences may be the result of other interpretations, or the inclusion of different data, which can be verified through the documentation in the catalogue database and adapted in the future.

3.4.3 Methodological improvements for coastal plain mapping

Our methodology of (i) separated storage of digital mapping and age attribution, and (ii) automated map time series production provides several advantages over traditional geological-geomorphological mapping and palaeogeographical analysis.

First, the setup facilitates a direct cross-check between the mapped record and palaeogeography. The user can put locally dated elements in a regional context to check the output maps for inconsistencies, which may lead to re-evaluating input studies. Inconsistencies may be solved by adapting the base maps or database iteratively, for example by making different choices between conflicting studies or dates, within the possibilities provided by the available data. An update of the age of architectural elements involves a simple adaption of the database, whereas boundaries of elements can be easily updated in the base maps. Then new palaeogeographical maps can be automatically generated, after which the procedure may be repeated. This iterative workflow optimises upscaling local studies to regional and superregional reconstructions for the developer or advanced user. The GIS is therefore an optimizing tool for reducing uncertainty in the age of elements, which is a classical problem in palaeogeographical reconstructions. When new data will be available in the future, adaptations of the extent and the age of tidal systems can easily be made, and new output maps will be automatically calculated. The presented GIS (its content, design, and toolset) should therefore not be seen as an end product but rather as a framework that can be extended and optimised in the future.

The continuous improvement and expansion of the contents of the base maps and catalogue database is an iterative process in which from time to time steps 3 and 4 are also performed again to produce preliminary maps for visual inspection. The user can then check if the base maps polygon labelling and their linked age attributions are consistent and free of data entry errors. The map series is easily regenerated by rerunning the script (Figure 3.3).

A second distinct advantage is that heterogeneous information retrieved from earlier coastal plain mapping is now integrated and made uniform through the choice of storing information systematically at the architectural element level. This is useful for any study that deals with the substrate of the coastal plain, which requires input from different research traditions in this area.

A third advantage is that the system is transparent and reproducible with respect to base map contents, catalogue contents, and script-generated output. The planform geometry of the elements is stored independently of further geological data (e.g. age), description (e.g. naming, reasoning), and metadata (e.g. referencing to earlier publications). Consequently, output palaeogeographical maps from the GIS can be traced back to the primary input components, and combination rules helps verification and accuracy validation of the generated palaeogeographical maps. With our GIS design, future communal maintenance of a national palaeogeographical map series is better served than in the workflow of traditional reconstructions.

3.4.4 Limitations and opportunities for improvements

In the future, the GIS will benefit from further growth of data: more dates, better resolved stratigraphy, and further locally verified facies interpretations. Further inspection of existing source data (e.g. borehole data, CPTs, and archaeological sites) will result in enhanced reconstructions. For areas where erosion prevailed, the age, spatial extent and correlation of suspected former elements unavoidably will remain uncertain. Erosion took place especially close to tidal inlet systems, clearing the evidence of older generations of tidal systems. As a first step to visualise the reconstruction of eroded architectural elements, the GIS highlights the areas that were reworked in a later time step (Figures 3.7 and 3.8), i.e. where the eroded area of the elements had to be reconstructed. The chronology of such tidal inlets can be enhanced when the dating of distal elements (e.g. clay layers in peat) is improved and subsequently better correlated to the eroded tidal inlet.

The GIS treats activation of architectural elements of the same tidal system as instantaneous and simultaneous events. This means that all elements of the same generation of tidal system (by

ID) have the same activation age. Continuous extension of tidal flats or migration of channels can only be incorporated in distinct phases in the GIS. For preserved deposits, reconstructing the exact position of the boundaries of the elements per time step would require an extremely densely dated data set and many assumptions. Improved chronology of phases within channel belt bodies by ^{14}C dating of shells or OSL dating can indicate channel dimensions at time steps and hence channel dynamics (e.g. Baeteman et al., 2002; Vos et al., 2015a). This will work for silting up channels with little reworking.

Another method that can improve chronology is using case study models of hydrodynamical processes and sedimentation balance, indicating how fast tidal inlets can develop and silt up (Van den Berg et al., 1996). Additionally, studies based on local event stratigraphy (flooding frequency Rhine; Toonen, 2013) and storm marker chronology (e.g. Cunningham et al., 2011; Van den Biggelaar et al., 2014) could improve vertical time control of deposits that leads to improving the time-resolution and rate of deposition in tidal systems. These studies require palaeogeographical and geomorphological initial conditions, which the GIS output can provide, and their results can improve the GIS chronology and landscape evolution considerably.

Extension of the GIS to adjacent coastal areas of comparable genesis in Germany and Belgium will be a good opportunity to support research on coastal development on a macroregional scale. Tidal inlets with a similar geological setting can be compared, such as the Jade Busen and Dollard (Wartenberg et al., 2013; Vos & Knol, 2015), in order to increase our understanding of the controls involved in their development. In Germany and Belgium the coastal plain has been mapped in a different way than in the Netherlands, based on a strict lithostratigraphical profile type legend (Streif, 1972; Barckhausen et al., 1977; Streif, 1978; Baeteman, 2005a; Bertrand & Baeteman, 2005). The map units show the sequence of clastic and organic layers; whereas thickness, age, and lateral variation in thickness is not included in the legend. To incorporate these units in a similar GIS as presented in this study, the information deduced from lithostratigraphical maps can be extended with data from cross sections and additional local studies.

3.4.5 Applications of the GIS

The presented GIS is a tool to compare and analyse the evolution of tidal inlet systems. It facilitates improving the understanding of the coastal plain evolution controls, such as sea level rise and human impact (Vos, 2015a). Also, ongoing projects of three-dimensional mapping of the Dutch subsurface (Stafleu et al., 2011; 2013; Gunnink et al., 2013; Van der Meulen et al., 2013) may benefit from the geological mapping and stratigraphical information that the GIS provides. Archaeological prospection and preservation surveys may benefit from landscape reconstructions, especially for periods before large-scale reclamation activities started in the eleventh century. Additionally, by comparison to independent archaeological data, the output may also be used to study the interaction between landscape development and settlements dynamics. This will lead to a better understanding of human-induced processes in coastal development (e.g. peat subsidence) and will extend the knowledge about population dynamics related to the landscape.

Using architectural elements as the basic entity in a GIS setup would work for palaeogeographical reconstruction in many sedimentary environments – especially when the two-stepped selection-recombination approach from the scripting is adopted. The GIS solution is especially suitable for advanced mapping of delta and coastal areas that are composites of multiple sedimentary environments in which sediment transport and deposition segregates over subaquatic and terrestrial system elements. Many of such coastal plains (e.g. urban deltas) are under pressure

of increased population, sea level rise, changes in sediment budgets, and subsidence (e.g. Törnqvist et al., 2008; Syvitski et al., 2009). Ongoing research in these regions makes that they are increasingly data rich and intensively studied from various disciplines. As the amount of data becomes larger, the need for smart integration of this data and the mapping products increases in order to make better management decisions to protect these areas.

3.5 Conclusion

This chapter presents a GIS that integrates a large amount of existing fragmented and heterogeneous data on coastal plain architecture and development. The new GIS provides an overview and integration of previously fragmented knowledge on coastal development and allows for unambiguous regional reconstruction and comparison of coastal plain development.

The GIS contains four manually maintained thematic base maps with the geometry and generation identity of the architectural elements (step 1). A database is maintained in which the age of the tidal systems and the considerations in mapping and age decision are documented (step 2). Then a scripted procedure follows that first connects the base maps to the age from the database, creating palaeogeographical maps per thematic base map (step 3). Secondly, the script integrates the four base maps by mimicking geological relations such as cross-cutting, superposition, and inheritance (step 4). This workflow makes many extractions possible, for example of geological maps (age maps), palaeogeographical time series (geomorphology back in time), and areal statistics.

Rather than manually drawn, fixed-time-step traditional maps, our GIS is a transparent and systematic tool for geological mapping and palaeogeographical reconstruction. It facilitates querying, verifying, updating, and expanding the reconstructions. The optimised palaeogeographical reconstructions minimise the uncertainty in the age of the reconstructed architectural elements and make the workflow of the reconstruction transparent. Additionally, the products offer a framework to analyse late-Holocene coastal system evolution on centennial to millennial time scales, which is particularly dominated by sea ingression dynamics. The formalised workflow is also suitable for other coastal sections where smart integration of existing data is required. The GIS solution presented in this chapter organises an overview in mapping and understanding the geomorphology and substrate of coastal plains, which is valuable information for decision making on protecting vulnerable coastal systems.

Acknowledgements

This chapter is part of the project ‘The Dark Ages in an interdisciplinary light’ funded by NWO (project nr. 360-60-110). The first author contributed in the following proportions to research design, data collection, GIS design, analysis and conclusions, figures, and writing: 60, 75, 60, 60, 80, 60. The authors thank Peter Vos (Deltares) for the exchange of ideas on coastal plain palaeogeography and Freek Busschers (TNO Geological Survey of the Netherlands) for providing the digital geological datasets. We thank Friederike Bungenstock (Niedersächsisches Institut für historische Küstenforschung) for her comments on an earlier draft of the chapter. Finally, we thank Hans Middelkoop (Utrecht University) and an anonymous reviewer for their useful comments on the manuscript.

Chapter 4

Late Holocene coastal-plain evolution of the Netherlands: the role of antecedent conditions in human-induced sea ingressions

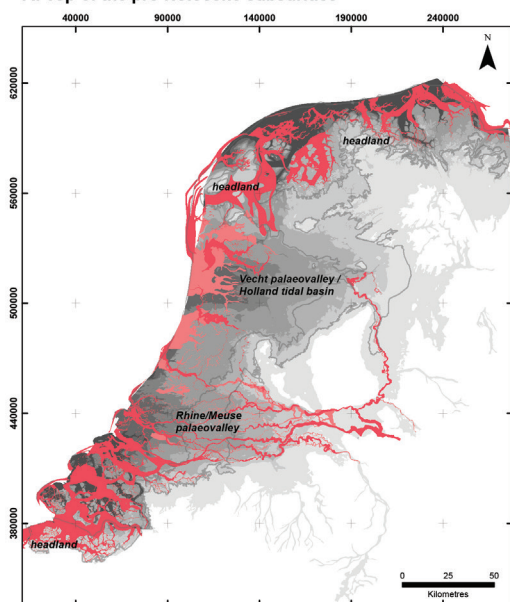
This chapter demonstrates the decisive role of antecedent conditions on the formation of large late Holocene sea ingressions in peaty coastal plains along the North Sea's southern shores. Geological and archaeological evidence shows that these sea ingressions (expansion of new tidal systems) were mainly caused by land subsidence, which occurred due to intensified agricultural use of artificially drained peatlands since the Late Iron Age (250–12 BC). This made the coastal plain sensitive to storm-surge ingression through weak spots, e.g. at the location of existing creeks, in the coastline. Using the Netherlands as a case study, we show that antecedent conditions (i.e. the geological setting at the time of ingression) played a key role in the pacing and extent of tidal area expansion. Ingressive tidal systems eventually reached most far inland in coastal segments with wide peaty back-barrier plains. In contrast, sea ingression formation was hampered in coastal segments with well-developed natural ingression-protecting geomorphic features (e.g. beach-barriers, supratidal levees). Feedback mechanisms, such as additional peat subsidence by loading of sediment imported into the new tidal area, caused further tidal prism increase and created accommodation space for tidal deposits. These combined effects caused irreversible sea ingression over large areas that consequently became unsuitable for habitation for many centuries. Improved understanding of such sea-ingression mechanisms and their facilitating conditions are essential for the assessment of the sensitivity of many densely populated coastal plains, which experience major human-induced subsidence, eventually leading to coastal plain drowning.

Published as: H.J. Pierik, K.M. Cohen, P.C. Vos, A.J.F. Van der Spek & E. Stouthamer (2017) Late Holocene coastal-plain evolution of the Netherlands: the role of natural preconditions in human-induced sea ingressions, *Proceedings of the Geologists' Association*, 128(2) p.180-197, [dx.doi.org/10.1016/j.pgeola.2016.12.002](https://doi.org/10.1016/j.pgeola.2016.12.002).

4.1 Introduction

The Holocene evolution of coastal plains and barrier systems around the world is generally considered to be driven by inherited topography, post-glacial sea-level rise, background subsidence or uplift regime, and sediment distribution by waves, tides, and rivers (e.g. Goodbred & Kuehl; 1999; Giosan et al., 2006; Rossi et al., 2011; Hanebuth et al., 2012; Gao & Collins, 2014; Vos, 2015a). During the last millennia, simultaneously acting natural and human-affected sedimentary processes led to increased coastline progradation in several European deltas resulting from increased sediment load caused by deforestation (e.g. Po and Rhône delta – Stefani & Vincenzi, 2005; Maselli & Trincardi, 2013; Anthony et al., 2014), whereas in other regions human activity (e.g. the construction of dams) caused sediment deficit and subsequent flooding (e.g. Nile delta –

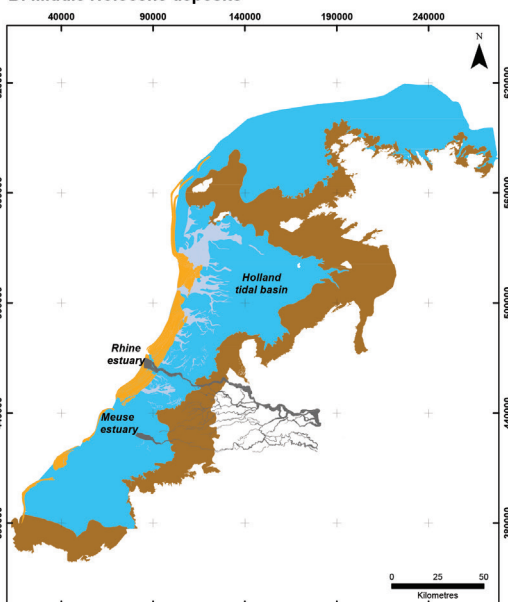
A: Top of the pre-Holocene subsurface



Contours of the coastal plain base (m relative to modern sl)

-35 to -25	-10 to -5	middle-Holocene erosion
-25 to -20	-5 to 0	late-Holocene erosion
-20 to -15	0 to +10	
-15 to -10		

B: Middle Holocene deposits



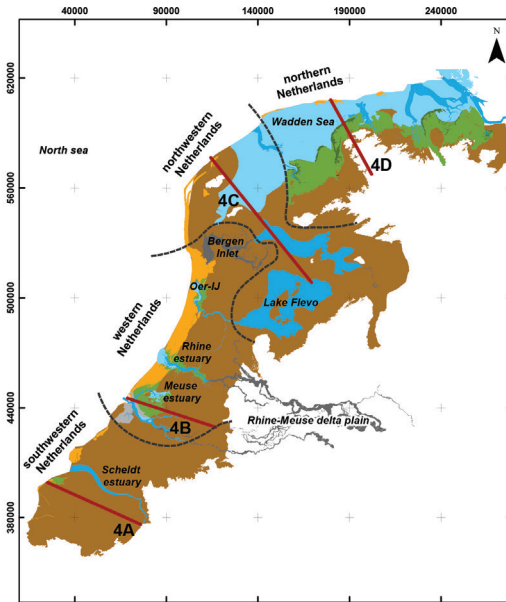
Middle Holocene coastal plain deposits

beach-barrier complex before 2500 BP
middle Holocene tidal deposits (older than 4000 cal BP)
middle Holocene tidal channels
coastal plain peat
active Rhine-Meuse channel belts around 5000 BP

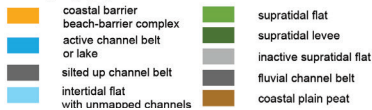
Figure 4.1 | (a) Top of the pre-Holocene subsurface after Vos (2006). The major headlands and the major palaeovalleys mentioned in the text are indicated. The position of late Holocene erosive tidal channels were taken from chapter 3, the middle Holocene channels were taken from Cohen et al. (2017a). The grey line indicates the extent of the middle Holocene deposits and the coastal peatlands of Figure 4.1B. (b) Extent of the middle Holocene deposits and peat area, from Cohen et al. (2017a). The Rhine-Meuse channel belts were taken from Cohen et al. (2012).

Stanley & Warne, 1994, Nile and Ebro deltas – Syvitski et al., 2005; the coastal plain north of the Po delta – Zecchin et al., 2009). Nowadays many densely populated coastal plains experience major human-induced subsidence leading to coastal plain drowning (e.g. Törnqvist et al., 2008; Syvitski et al., 2009). In many northwestern European coastal plains, human-affected developments began relatively early (roughly 2000 years BP), coevally with episodes of transgression (*large-scale landward lateral expansion of back-barrier tidal depositional sedimentary environments*). These late-Holocene transgressions have been documented for the Flemish coast (Baeteman, 2005b), the UK Fenlands (Brew et al., 2000), the UK Romney Marsh (Long et al., 2006), Northern Brittany, France (Regnaud et al., 1996), and the Bay of Biscay, France (Clavé et al., 2001). These authors discuss potential natural triggers such as intensified storm regimes and facilitating conditions such as decreased sediment availability and human peatland reclamation. Antecedent conditions include the geological setting (e.g. coastal plain extent, stratigraphical architecture, sediment delivery) at the time of ingress. These conditions also affect the occurrence and extent of transgression, but the degree to which they facilitated or prevented transgression has hardly been considered.

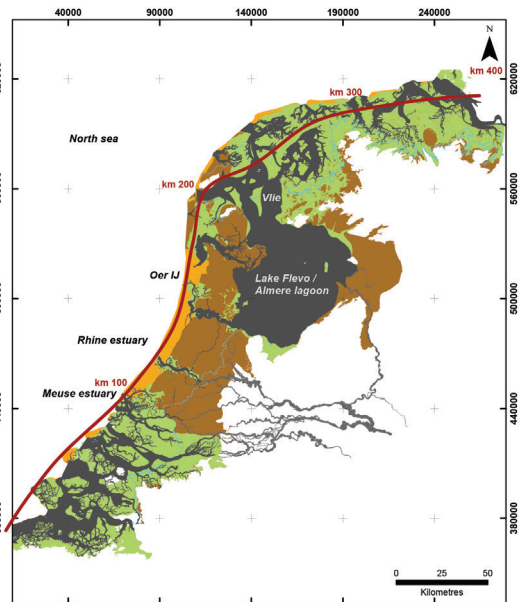
A: Landscape reconstruction 600 BC



Palaeogeography



B: Late Holocene tidal deposits



Late Holocene coastal plain deposits



Figure 4.2 | (a) Landscape reconstruction at the onset of late-Holocene transgression (around 600 BC – chapter 3). The red lines and figure numbers correspond to segments in Figure 4.4. (b) Extent of the middle and late Holocene tidal deposits including channels and beach barriers (after Cohen et al. (2017a); chapter 3). The red line corresponds to the position of the longshore diagram of Figure 4.5.

The coastal plain of the Netherlands is the largest coastal plain of NW Europe and therefore contains a variety of antecedent conditions (Figures 4.1 and 4.2A). Situated in the depocentre of the Southern North Sea, the length of the coastal plain is not bound to inherited valleys, but stretches over hundreds of kilometres along the shore. Also, the width reaches tens of kilometres inland, where – different to many smaller coastal plains – vast peatland areas occur (Figures 4.1B and 4.2). These peatlands were reclaimed for agricultural use from about 250 BC onwards, causing human-induced subsidence (Borger, 1992; Vos & Van Heeringen, 1997; Vos, 2015a). Major sea ingressions (*landward lateral expansion of a new single tidal system*¹) have been recorded in geological and archaeological studies of these human-occupied coastal plains. The availability of age-specific archaeological artefacts and well-mapped deposits in the coastal plain makes this region very suitable to assess the timing of landscape developments and human activities (e.g. Van Liere, 1948; Knol, 1993; Vos & Van Heeringen, 1997; Vos & Gerrets, 2005; Vos, 2015a; Pierik et al., 2016; chapter 3).

1) A tidal system is a back-barrier tidal environment, connected to open sea through an inlet channel (containing tidal channels, tidal flats, salt marshes, or lagoons).

Peat-surface lowering was triggered by peatland reclamation that involved ditch cutting to drain the topsoil making it suitable for agriculture (Vos, 2015a; Erkens et al., 2016). The start of the reclamations across the coastal plain varies from Late Iron Age to early medieval times (250 BC to AD 1050). The reclamations were wide-spread, and had affected the entire coastal plain by ca. AD 900 (Vos, 2015a). Natural forcings, such as wave and tidal regime show minor variations regionally and are not considered to have varied majorly during the last 4 to 5 millennia (e.g. Van der Molen & de Swart, 2001ab). Major regional differences exist, however, in the antecedent conditions, i.e. geological and geographical setting along the coastal plain. These regional differences also occur in the timing, degree, and impact of sea ingressions. This raises the question how the antecedent conditions affected the pacing and final extent of the mainly human-triggered coastal plain changes. Data coverage on the geological situation of the Dutch coastal plain nowadays is quite even (e.g. Vos, 2015a; chapter 3). Therefore it provides an ideal area to geographically intercompare the evidence and to assess the mechanisms and controls of late Holocene coastal-plain transgressions.

4.1.1 Aim and approach

This chapter aims to 1) reconstruct the antecedent conditions for late Holocene sea ingressions; 2) reconstruct the late Holocene ingressive development, and 3) identify the mechanisms of ingressive developments in relation to different antecedent conditions. The study area reaches from the coastline inland and includes areas with tidal deposits and their flanking peat swamps (Figures 4.1 and 4.2). We focus on the late-Holocene period when peat-surface habitation and coeval ingression development repetitively occurred at multiple locations (Vos, 2015a). We tested the influence of antecedent conditions on sea ingression development. Therefore, we compared the divergent ingressive developments between four main segments of Netherlands' coastal plain that faced contrasting late-Holocene developments and had different antecedent conditions (i.e. landscape settings around 600 BC before large-scale reclamation – Figure 4.2A). The defined segments are:

- The *southwestern* part of the Netherlands (SW-NL). This peat area witnessed major sea ingressions since ca. 2000 cal yrs BP (e.g. Vos & Van Heeringen, 1997);
- The *western* part of the Netherlands (W-NL), with a wide sequence of beach barriers, interrupted by estuaries (Beets et al., 1992). We position its borders in the peat area directly south of the Meuse estuary, and just north of the former Bergen tidal basin. The inland boundary of this segment is positioned at the most inland location of perimarine crevasse splays around the Rhine and Meuse channel belts indicating significant tidal influence, after Cohen et al. (2017a);
- The *northwestern* Netherlands (NW-NL), which experienced coastal retrogradation in the west during the late Holocene and at the same time, westward expansion of the Wadden-Sea tidal area in its eastern part. During the late Holocene, the Almere lagoon was connected to the Wadden Sea and it was therefore included in this segment (Zagwijn, 1986);
- The *northern* Netherlands (N-NL) that maintained a barrier-tidal basin coast during the entire Holocene (Vos & Knol, 2015).

To understand the mechanisms controlling the development of tidal systems and sea ingressions, we describe the coastal evolution with its specific local details. In the analysis we used geological information from various national datasets, in which the results of many previous studies have accumulated. The local details unavoidably are selective and incomplete, for further information and additional argumentation we refer to the original publications in the text, for more extensive references see also Vos (2015a) and chapters 2 and 3. Even in our long-studied research

area, the available age control does not allow absolute dating of all stages per individual tidal system. Dates have often been collected at one location per tidal system only, while peat reclamation and tidal channel expansion mainly occurred diachronously. To optimize coastal evolution age control, we used a recently-developed GIS that stores all relevant late-Holocene coastal plain geological mapping, palaeogeography, and local study referencing (chapter 3). In the GIS, the extent of coastal plain architectural elements was mapped, a database with dating information was maintained separately. This information was then automatically combined by generating time slice palaeogeographical maps for each desired time slice, which were iteratively improved. This GIS further allowed to reconstruct and quantify the evolution of individual tidal systems and beach barrier segments, as well as intercomparison between the subregions. From the sea ingressions cases in the study area, we compiled a conceptual model for their evolution that will be used in the discussion to outline the mechanisms and the influence of antecedent conditions on sea ingressions evolution.

4.1.2 Geographical setting and boundary conditions

The coastal plain of the Netherlands mainly comprises middle and late Holocene back-barrier deposits, overlapping a modestly sloping pre-Holocene substrate (Jelgersma, 1979; Beets & Van der Spek, 2000). The coastline encompasses a chain of beach-barrier complexes and tidal inlet systems (Van der Spek & Beets, 1992; Beets & Van der Spek, 2000; Vos, 2015a; Figure 4.2B). This barrier complex established between 6000 and 5000 BP, after an initial middle-Holocene phase of marked sea-level rise (Van de Plassche, 1982; Hijma & Cohen, 2011; Lambeck et al., 2014) and marks the change to coastline stabilization when relative sea-level rise decelerated towards the modest present-day rates. After 3000 cal yr BP, the trapping of fine-grained sediment from the Rhine and Meuse in fluvial-deltaic environments (Erkens & Cohen, 2009) and neighbouring peat areas (De Boer & Pons, 1960) started to increase. This clay deposition is understood to result from an increase in sediment supply received from upstream (i.e. external control; Cohen, 2005; Gouw & Erkens, 2007; Hoffmann et al., 2007; Erkens & Cohen, 2009).

Conditions along the coastline are micro to mesotidal (1.5 to 4 m tidal range), with significant wave energy (cf. Davis & Hayes, 1984; Van der Spek & Beets, 1992). The Dutch coast is exposed to predominant westerly winds and wave fields and consequently experiences a dominant north to northeastern oriented net longshore sediment transport (Beets et al., 1992; Beets & Van der Spek, 2000). These dominant winds facilitated wave-driven sediment transport from the shallow sea floor to the coast. The tidal range varies from over 3 m in the southwestern and northern Netherlands to 1.5 m in the western Netherlands. Open-sea tidal conditions have remained more or less stable since at least 6000 yrs BP (Van der Molen & de Swart 2001ab). An increase in wave energy has been reported for the last 6000 years in the western part of the Netherlands attributed to steepening of the shoreface (Van Heteren et al., 2011). Gottschalk (1975) documented increased storm activity between AD 1400–1600 in the SW Netherlands based on historical records, whereas Sorrel et al. (2012) reported intervals of increased storminess (relatively high frequency of intense storms) in NW Europe for 1350–450 BC, AD 50–900, and AD 1350–1700 based on sedimentological evidence. Apart from that, hydrodynamical conditions are assumed to have been quite constant over the last millennia (Beets et al., 1992).

Relative sea-level rise (RSLR) over the last 2000 years varied between 0.5 and 1.0 m (Van de Plassche, 1982; Roep & Beets, 1988). In these youngest millennia, RSLR was predominantly controlled by tectonic and glacio-isostatic background subsidence (Kiden et al., 2002; Vink et al., 2007; Koster et al. 2016a). Small fluctuations of the eustatic sea-level possibly occurred during the

late Holocene mainly resulting from steric sea-level movement due to climate fluctuations (Van Geel et al., 1996; Behre, 2004, 2007; Gehrels, 2010; Van de Plassche et al., 2010; Kopp et al., 2015). Most authors however, do not attribute a major forcing role to this, as they consider the rates of peatland-surface lowering and autogenic tidal and sedimentary changes to be larger (see discussions in Weerts et al., 2005; Bungenstock & Weerts, 2010; Baeteman, 2008; Baeteman et al., 2011; Vis et al., 2015).

4.2 Middle Holocene coastal plain evolution

This section describes the middle-Holocene evolution of the four coastal segments, determining the antecedent conditions for the late Holocene human-triggered coastal landscape changes. Ages are presented in calibrated years before present (cal yr BP), unless otherwise specified.

4.2.1 Pre-Holocene inherited setting and middle-Holocene transgression

During post-glacial sea-level rise, continental shelves submerged forming vast wetlands where both organic and clastic sedimentation occurred (Shepard, 1932; Jelgersma, 1979; Smith et al., 2011; Bicket & Tizzard, 2015). The Pleistocene and early-Holocene topography that underlies the coastal plain deposits served as substrate for this middle-Holocene transgression (Pons et al., 1963; de Gans & Van Gijssel, 1996). This moderately sloping pre-Holocene substrate was intersected by two wide fluvial valleys (ca. 30 km) in the western Netherlands and smaller valleys in other parts of the study area (Figure 4.1A). The large valleys provided ample Holocene accommodation space and served as major sediment sinks for coastal and fluvial sediments. These inherited palaeovalleys inundated from about 9500 BP onwards (Hijma & Cohen, 2011; Vos et al., 2015a; Koster et al., 2016a). The Rhine-Meuse palaeovalley (Figure 4.1A) filled up relatively quickly with estuarine and fluvial sediments (Erkens & Cohen, 2009; Hijma et al., 2009, 2010). The absence of a large river and the subsequent low sediment input caused the Vecht palaeovalley to be transformed into an embayment, where infilling occurred at significantly lower rates (Holland tidal basin, Jelgersma, 1983; Van der Spek & Beets 1992; Beets & Van der Spek, 2000). Here, subtidal clays were the first preserved clastic marine deposits (Pons & Wiggers, 1959/1960; Beets et al., 2003).

Currently offshore positioned remains of tidal inlets indicate the position of an old beach barrier around 7000 BP (Rieu et al., 2005; Hijma et al., 2010); formed when decreasing sea-level rise reduced the creation of accommodation space. The back-barrier basins started to fill in with sandy channel sediments and intertidal tidal flat deposits (Pons & Wiggers, 1959/1960, de Mulder & Bosch, 1982, Hijma et al., 2009). In the southwestern and northern Netherlands a similar stratigraphical sequence of initial transgressive subtidal clays to sandy subtidal and intertidal deposits developed (de Jong et al., 1960; Vos & Van Kesteren, 2000).

The higher elevated parts of the pre-Holocene substrate were situated in the southern part of the southwestern Netherlands and in the northwestern Netherlands (Figure 4.1A; de Gans & Van Gijssel, 1996). They were headlands during the middle Holocene and acted as sediment sources for coastal evolution (e.g. Beets et al., 1992, 1994; Cleveringa, 2000). They were inundated relatively late during the middle Holocene creating a relatively thin Holocene coastal wedge (generally less than 5 m thick peat and clastic tidal deposits). At present, 65% of the coastal plain area contains middle Holocene tidal deposits (Figure 4.1B). The tidal areas were flanked by extensive peatlands on the Pleistocene substrate (ca. 35% of the coastal plain area). The peats contain intercalated clay layers representing distal tidal system deposits (Jelgersma, 1961; Streif, 1978; Allen, 2000; Bertrand & Baeteman, 2005).

4.2.2 Middle-Holocene turnover to highstand

The decreasing rate of sea-level rise reduced the creation of back-barrier accommodation space from about 6000 BP onwards. During the late Holocene the relative importance of eustatic sea-level rise decreased and land subsidence became more important (Beets & Van der Spek, 2000; Cohen, 2005; Hijma & Cohen, 2011; Koster et al., 2016a). The continuing sedimentation in the back-barrier area and especially the expansion of the intertidal flats, caused a decrease in tidal storage volume of the tidal basins, to which the tidal inlets adapted by filling in. In the western and southwestern Netherlands this eventually led to their closure and the formation of an elongated uninterrupted beach barrier complex (Van Straaten, 1965; Beets et al., 1992; Van der Spek et al., 2007; Van Heteren et al., 2011). In the back-barrier area of these coastal segments a fining-upward trend is found in the top of the middle Holocene tidal deposits, recording a transition from intertidal to supratidal conditions and a decrease of tidal energy (Pons & Wiggers, 1959/1960; Westerhoff et al., 1987; Hijma et al., 2009). In the northern Netherlands, the tidal area never fully silted up, tidal inlets persisted and the chain of barrier islands did not amalgamate into an uninterrupted beach-barrier complex (Beets & Van der Spek, 2000).

Table 4.1 | Areal extent (in 1000 ha) of peat and tidal deposits per segment of coastal plain during the middle Holocene, 600-250 BC and AD 2000. Numbers are given as integers.

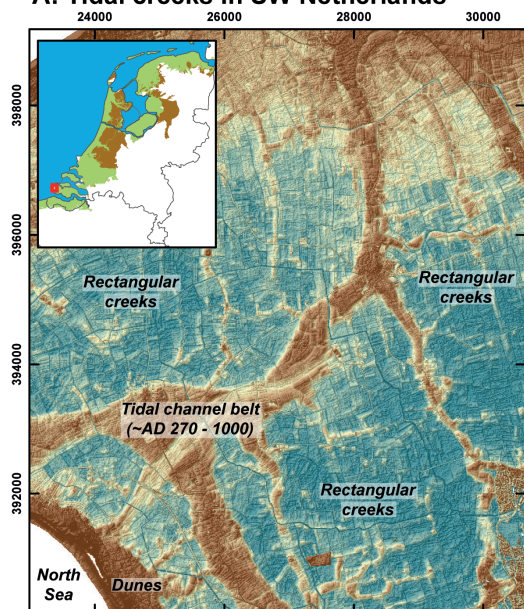
	Total coastal plain ^{a)}	Middle Holocene (MH) ^{b)}		600 – 250 BC		AD 2000
		Tidal deposits	Peat	Tidal deposits	Peat ^{c)}	Tidal deposits
SW	435	282	153	30	405	420
W	551	443	108	134	417	157
lake Flevo/ Almere lagoon ^{d)}	396	140	256	285	363	558
NW	252	149	103			
N	500	382	117	372	128	477
Total	2133	1396	737	372	1312	1612

a) Derived from the sum of middle Holocene (MH) peat and MH tidal deposits; b) Values represent the total area of MH tidal deposits (i.e. not at a specific time step) and are derived from the GIS data shown in Figures 4.1B and 4.2A.; c) Calculated by subtracting tidal deposits area from total coastal plain area; d) The NW Netherlands and lake Flevo were separated areas during the middle Holocene and therefore split up in the table. During the late Holocene the Flevo Lake/Almere lagoon connected to the NW coastal segment, and is therefore considered as part of this segment.

4.2.3 Late Holocene mature highstand

The closure of the Holland beach-barrier complex ended tidal dynamics and sedimentation in the largest part of the back-barrier area (Beets et al., 1994), thereby facilitating large-scale peat formation on top of the silted-up tidal systems, especially in the western, southwestern, and northwestern coastal plain segments (Pons et al., 1963; Pons, 1992). At the onset of large-scale peatland reclamation (e.g. between 600 and 250 BC, see Table 4.1), ca. 60% of the coastal plain area consisted of peatland, draining to a few river outlets and remaining tidal inlets. At a distance from large rivers and tidal channels, peat bogs had developed that were modestly elevated (2-4 m) above high tide and storm-surge sea levels (Bennema et al., 1952; Pons, 1992; Vos et al., 2015a; Erkens et al., 2016). These bogs acted as local watersheds that are regarded to have stabilised the positions of peat-drainage channels that linked up to the tidal creeks and the sea. In the northern Netherlands

A: Tidal creeks in SW Netherlands



Legend

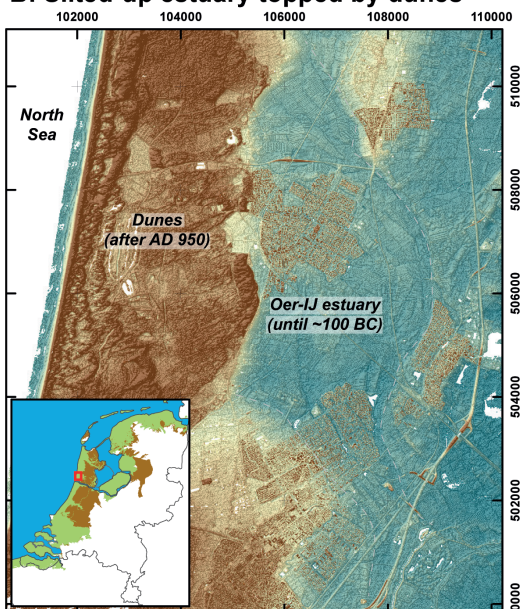
Surface elevation (m O.D.)

Low: -1 High: 1



0 0.5 1 2
Kilometres

B: Silted-up estuary topped by dunes



Legend

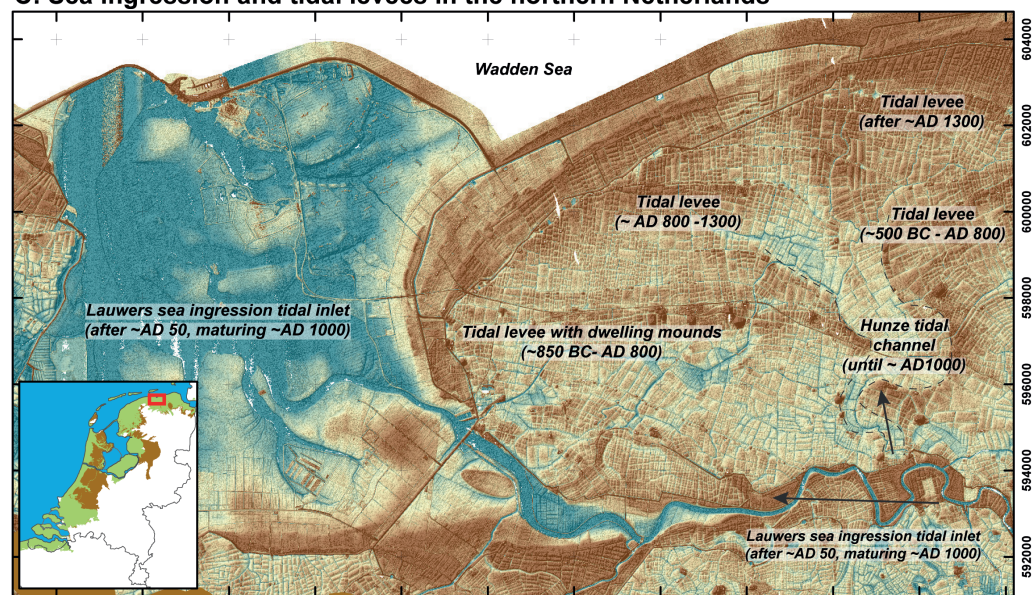
Surface elevation (m O.D.)

Low: -1.5 High: 5



0 0.5 1 2
Kilometres

C: Sea ingression and tidal levees in the northern Netherlands



Legend

Surface elevation (m O.D.)

Low: -0,5 High: 1,5



0 0.5 1 2 3 4 5
Kilometres

Figure 4.3 (left page) | LiDAR images of three parts of the coastal plain. The small location maps are after Figure 4.2B): green: late Holocene tidal deposits, brown: coastal plain peatlands. (a) Rectangular tidal inversion ridges in the former reclaimed peatlands in the SW Netherlands, representing Roman ditches later filled in with sand. Ages after Vos & Van Heeringen (1997). (b) Silted-up estuary western Netherlands covered by parabolic dunes. Ages after Vos et al. (2015a). (c) Multiple generations of supratidal levees protected the coastal plain (ages after Vos & Knol, 2015; chapter 3). They were interrupted by small tidal inlets such as the Hunze, which silted up after the Lauwers sea ingression formed during the Early Middle Ages (AD 450-1050).

the barriers of the Wadden Sea remained interrupted by tidal inlets, whereas along the inland side of the tidal basins supratidal levees developed after 700 BC that facilitated peat areal expansion (Vos & Gerrets, 2005).

The large Holland tidal basin was not completely filled in by the end of the middle Holocene (Bergen Inlet system, Figure 4.2A, Pons et al., 1963; Van der Spek & Beets, 1992; De Gans & Van Gijssel, 1996; Van Zijverden, 2017). In the inland distal central part of this basin (over ca. 40 km away from the coastline), an extensive lake remained ('lake Flevo'), surrounded by peat fens and swamps. Waves eroded and reworked the peat edges of this lagoon into lake detritus that mixed with sand from the locally-eroded outcropping Pleistocene substrate (Pons & Wiggers, 1959/1960; Van Loon & Wiggers, 1975). After the Bergen Inlet silted up (around 1500–1100 BC, De Mulder & Bosch, 1982; Beets et al., 1996; Van Zijverden, 2017), lake drainage occurred via the Oer IJ inlet (Vos et al., 2015a). When drainage shifted northwards to the Wadden Sea by the formation of the Vlie, the Oer IJ inlet silted up as well (around the last century BC), (Figure 4.2; Vos et al., 2015a). This marked the beginning of lake Flevos' transformation into the Almere lagoon in late Roman and earliest medieval times. In the western Netherlands, two river outlets were present in the Rhine-Meuse delta (Figure 4.2A). The major branch of the Rhine occupied a northernmost route since 6000 BP (Berendsen & Stouthamer, 2000). Because of its long maintained position, a mature fluvial channel belt was present that had steadily supplied sand to the barrier coast, contributing to the beach barrier progradation and the formation of a subaquatic delta. Behind the barriers, dendritic secondary tidal creeks successively formed and silted up along the Rhine estuary, both at its very mouth and at distance inland (Pruissers & De Gans, 1985; Berendsen, 1982; Van Dinter, 2013). The smaller river Meuse debouched into a southerly estuary near Rotterdam throughout the Holocene (Hijma et al., 2009), supplying a relatively small amount of sediment to the coast. Here too, secondary tidal creeks branched off the main Meuse estuarine channel.

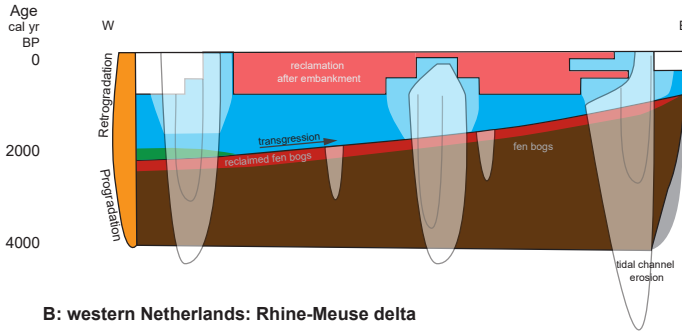
4.3 Late-Holocene ingressions

After the relatively stable period characterised by large-scale peat formation, large-scale sea ingressions into the peat area occurred from the Roman period onwards (12 BC to AD 450 – Vos, 2015a). Since then, the area containing tidal deposits expanded from 40% to 75% of the coastal plain (Table 4.1). In this section, we describe the late-Holocene evolution per coastal segment, focussing on the timing of initiation, maturation, and silting up the sea ingressions. This location-specific information, as well as the general trends, are illustrated by Figures 4.3–4.7.

4.3.1 Southwestern Netherlands

In the southwestern Netherlands, beach barriers dating to the beginning of the late Holocene have hardly been preserved, due to extensive post-Roman erosion. Therefore, the exact width of the

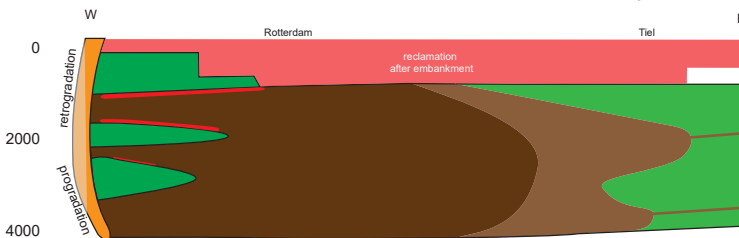
A: southwestern Netherlands



Second phase ingressions: 14th century
First large scale embankments: 11th century
First rehabilitation: late 8/9th century

Onset ingressions: AD 250
Onset peat habitation: Early Roman age

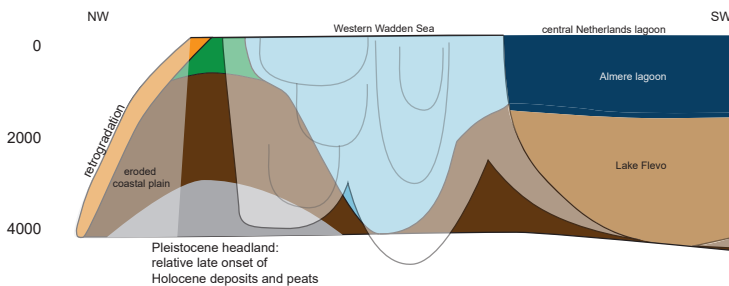
B: western Netherlands: Rhine-Meuse delta



Meuse estuary: Late Medieval ingressions

Natural ingressions before 500 BC

C: northwestern Netherlands

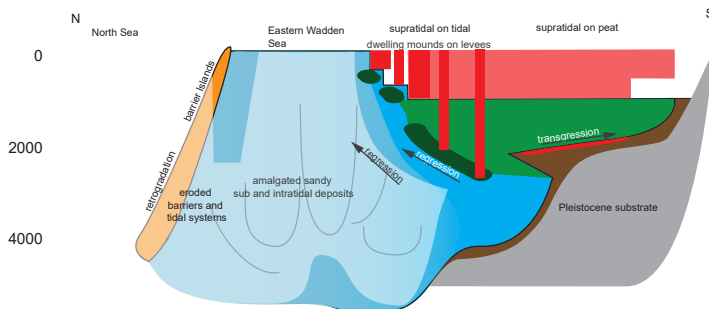


Clay on peat: AD 800 AD

Full connection Almere lagoon to Wadden Sea: 400 BC - AD 1

Continuous transgression and barrier retrogradation

D: northern Netherlands



Embankment: 10th century

Habitation peat: 200 BC - AD 300

Legend

intertidal/subtidal deposits	supratidal deposits	peat
intertidal/subtidal deposits, sandy facies	supratidal levees	gyttja
coastal beach barrier	archaeology/reclamation	lagoon

Figure 4.4 (left page) | Time-space cross-sections of coastal segments. Four conceptual cross-shore space-time diagrams illustrating the regional differences of the four coastal plain segments (location Figure 4.2A). (a) After cross-section of Vos & Van Heeringen (1997: Appendix I, profile B). Reclamation and habitation of the vast peatlands caused flooding and expansion of the tidal area. After several centuries of tidal sedimentation gradual embankment of the area took place. (b) After Hijma & Cohen (2011). Beach barriers projected from The Hague, after Cleveringa (2000); Van der Valk (1996a). Intercalated clay layers from secondary tidal systems formed around the Meuse estuary after Van Staaldin (1979) and Vos & Eijsskoot (2015), and were inhabited since 600 BC (Van Liere, 1950; Van Londen, 2006). In the Late Middle Ages large-scale embankment and peat reclamation took place (Borger, 1992; De Bont, 2008) whereas in the areas south of the Meuse sea ingressions occurred. (c) Northwestern Netherlands. The distal lagoonal area was a remnant of the middle Holocene Vecht Embayment and became only part of the northwestern Netherlands coastal segment after ca. 400 BC when the Vlie connected lake Flevo to the Wadden Sea (Figures 4.5 and 4.7). (d) After space-depth profile (Van der Spek, 1996; Figure 5). Here, beach barriers never closed, amalgamated channel deposits occur in the intertidal area. The expansion of the tidal area in the landward part of this coastal plain occurred diachronously after the Roman period, whereas more seaward supratidal levees accreted (Vos & Gerrets, 2005; Vos & Knol, 2015).

beach barrier complex at the time is unknown, but is assumed to be a few kilometres at maximum (Vos & Van Heeringen, 1997). In the back-barrier area, an extensive peatland was situated. In the top of the peat sequence mainly fen peat has been found (indicating formerly raised bogs), which contains abundant evidence of Roman reclamations and habitation. The earliest evidence of peat reclamation in this area is placed during the Late Iron age (Bennema & Van der Meer, 1952; Vos & Van Heeringen, 1997).

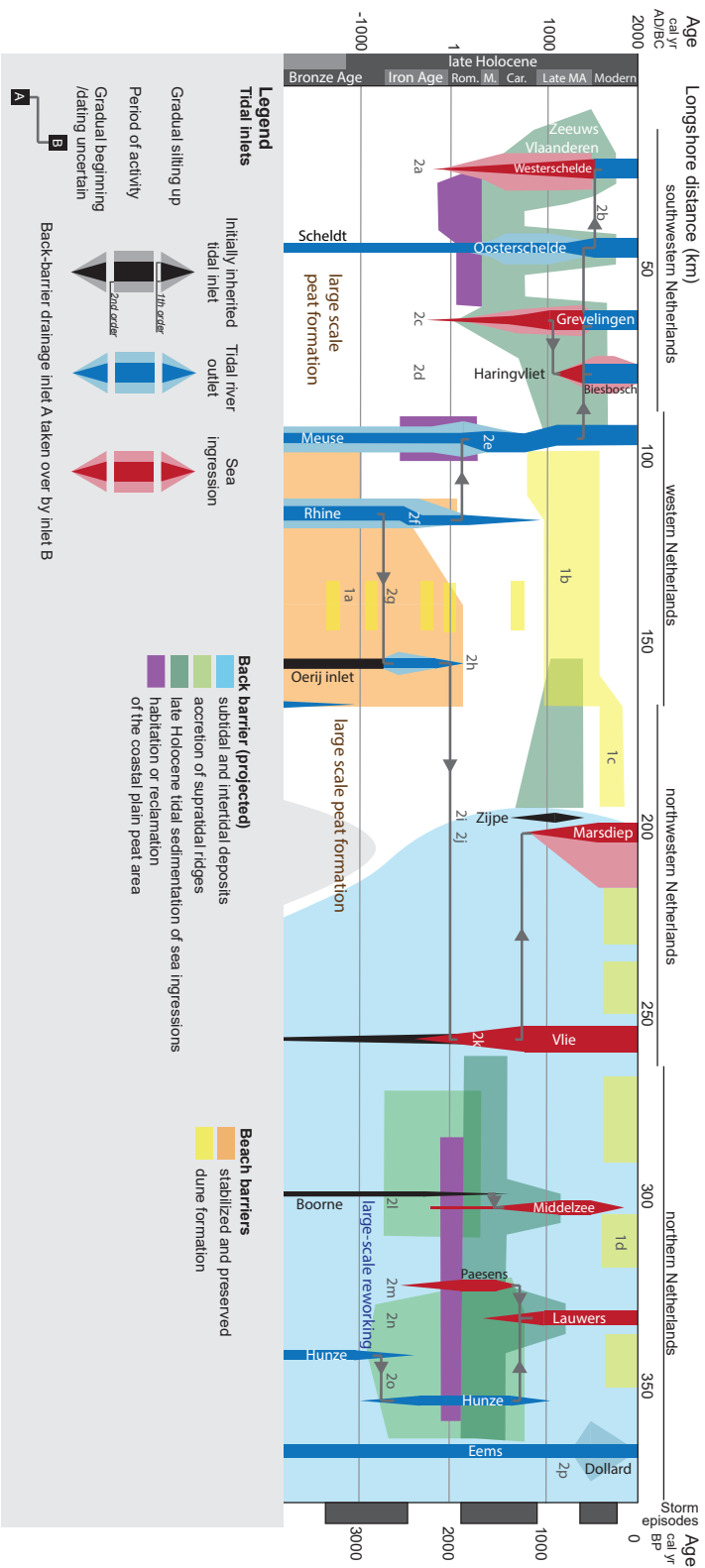
Around 500 BC, the first small ingressions took place into this peat area along the mouth of the Scheldt estuary (Figures 4.4A, 4.5, 4.6A, 4.7A). More large scale deposition of clastic material on the strongly subsided peat began approximately at ca. AD 250 and reached further inland at AD 500 (Figures 4.4A, 4.5, 4.6A, 4.7C; Vos & Van Heeringen, 1997; Vos, 2015b). The wide-spread clay deposits positioned directly on the peat indicate relatively low energy environments during the first stages of inundation (Pons, 1965). The rectangular pattern of many tidal tributaries (preserved as tidal channel inversion ridges – Figure 4.3A) indicate the usage of a Late Iron Age or Roman ditch-network that offered a preferential pathway for transgression (Vlam, 1942; Bennema & Van der Meer, 1952; Vos & Van Heeringen, 1997). With the drowning of the back-barrier area large tidal inlets developed (compare Tables 4.1 and 4.2, Figures 4.4A and 4.6A) eventually reaching depths up to several 10s of metres (De Jong et al., 1960). From the moment of drowning onwards, sandy material was deposited in the intertidal areas and channels. This material mainly originated from reworking inherited middle Holocene tidal channel belts as well as from a strong retrogradation of the coast between Walcheren and the adjacent Flemish coast (Ebbing & Laban, 1996; Denys, 2007; Mathys, 2009; Vos, 2015b), leading to scouring of the relatively shallow Pleistocene substrate in this area. The new large tidal channels caused sand to be transported efficiently into the tidal basins. In the 8th century, infilling of the tidal area was advanced to a supratidal level facilitating the first settlements on the silted-up tidal channel belts (Vos & Van Heeringen, 1997). Since the 12th century the supratidal area was embanked in successive phases, starting with the then highest elevated supratidal areas at a distance from major channels (Figures 4.4A and 4.6). The late medieval tidal deposits became more enriched in sand indicating an increase in depositional energy (Pons, 1965), corresponding to the expansion of the tidal area and the increase in tidal inlet size. After the intertidal shoals and smaller channels had silted up to supratidal level they successively could be embanked as well. In the Late Middle Ages (AD 1050–1500), the Scheldt river avulsed

to the Western Scheldt as a consequence of continuous backward ingression of the latter (Van der Spek, 1997; Vos, 2015b). While in Late Middle Ages, new areas were embanked, new land losses also took place. These late medieval ingressions especially affected the more inland part of the coastal plain in the subsided peat area of the northern part of the southwestern Netherlands, as well as the southernmost edge of this segment. The confinement and planform smoothing of the tidal area by dikes caused high water levels to increase, posing more flooding risks to adjacent embanked areas (Van der Spek, 1997). Additionally, the dikes were generally not well maintained when the disasters took place (Zonneveld, 1960; Verbraeck & Bisschops 1971; Kleinhans et al., 2010; Missiaen et al., 2016; Figure 4.7E).

4.3.2 Western Netherlands (Holland)

Unlike the other segments, no large sea ingression occurred in the western Netherlands during the late Holocene, mainly because of the presence of a wide beach-barrier complex. This barrier complex was dissected by three estuaries (Meuse, Rhine, Oer IJ; Figure 4.7A), from which secondary tributaries branched out into the flanking peat area. In the Meuse estuary, the levees and supratidal areas of the active tributaries were inhabited since the Iron Age (Van Liere, 1950; Van Londen, 2006). After Roman times most of these secondary tidal systems silted up and were overgrown by peat (Figure 4.4B; Van Trierum, 1986; Beets et al., 1994; Dijkstra, 2011; Vos

Figure 4.5 (right page) | Longshore time-space section of coastal development. The diagram shows the evolution of tidal inlets in time and space related to presence of rivers and coastal plain habitation. The cross-section is situated along the coastline (Figure 4.2B), tidal inlet locations are indicated in Figure 4.7. In the northern Netherlands, the line is projected along the intertidal- supratidal transition to visualize back-barrier development. Episodes of increased storm frequencies are taken from Sorrel et al. (2012). We subdivide the tidal inlet systems into three genetic classes after Vos & Knol (2015): 1) inherited tidal inlets formed during early-middle Holocene sea-level rise (black); 2) estuaries (blue); 3) natural or human induced late Holocene sea ingressions. Bright colours indicate the 1st order inlets, which are directly connected to the sea, paler colours indicate the presence of their secondary tributaries. Abbreviations of the archaeological periods on the y-axis: Rom. = Roman period, M. = Merovingian period, Car. = Carolinian period. Numbers refer to the following sources: Archaeology: Southwestern Netherlands – (Vos & Van Heeringen, 1997); Meuse estuary – (Van Londen, 2006); northern Netherlands – (Miedema, 1983; Knol, 1993; Gerrets, 2010). Beach barriers and dunes – 1a: Beach barriers western Netherlands – (Van Straaten, 1965; Beets et al., 1992; Van der Valk, 1996ab; Cleveringa, 2000; Vos et al., 2015a); 1b: Younger Dunes – (Jelgersma et al., 1970; Zagwijn, 1984; Vos et al., 2015a); 1c: Schoorl (1999); 1d: Jelgersma & Ente (1977). Tidal inlets – 2a: Onset youngest transgression southwestern Netherlands – (Bennema & Van der Meer, 1952; Vos & Van Heeringen, 1997); 2b: Avulsion Eastern Scheldt to western Scheldt – (Van der Spek, 1997; Vos & Van Heeringen, 1997); 2c: Initiation Grevelingen – (Vos, 2015b); 2d: Initiation Haringvliet – (Vos, 2015b); 2e: Extension tidal basin around Meuse estuary – (Van Staalduinen, 1979; Van Trierum, 1986; Vos & Eijsskoot, 2015); 2f: Rhine estuary dynamics – (Van Dinter, 2013); 2g: Avulsion Utrechtse Vecht (Rhine tributary) into the Oer IJ (Bos et al., 2009); 2h: Closing Oer-IJ inlet: (Vos et al., 2015a); 2i: Activity Zijpe – (Schoorl, 1999; Vos, 2015a); 2j: Initiation Marsdiep – (Ente et al., 1986; Schoorl, 1999; Vos, 2015a); 2k: Vlie – (Ente et al., 1986; Schoorl, 1999; Vos, 2015a); 2l: Boorne and Middelzee – (Cnossen, 1958; Van der Spek, 1995; Vos & Gerrets, 2005; Vos & Knol, 2015); 2m: Paesens – (Griede, 1978; Vos & Knol, 2015); 2n: Lauwerszee – (Roeleveld, 1974; Griede, 1978; Vos & Knol, 2015); 2o: Hunze (Roeleveld, 1974; Vos & Knol, 2015); 2p: Dollard – (Homeier, 1977; Behre, 1999; Vos & Knol, 2015). Supratidal ridges – (Roeleveld, 1974; Vos & Gerrets, 2005). Late Holocene transgression – southwestern Netherlands: (Vos & Van Heeringen, 1997; Vos, 2015b); northwestern Netherlands – (Westerhoff et al., 1987; Vos, 2015a); northern Netherlands – (Gerrets, 2010; Vos & Knol, 2015).



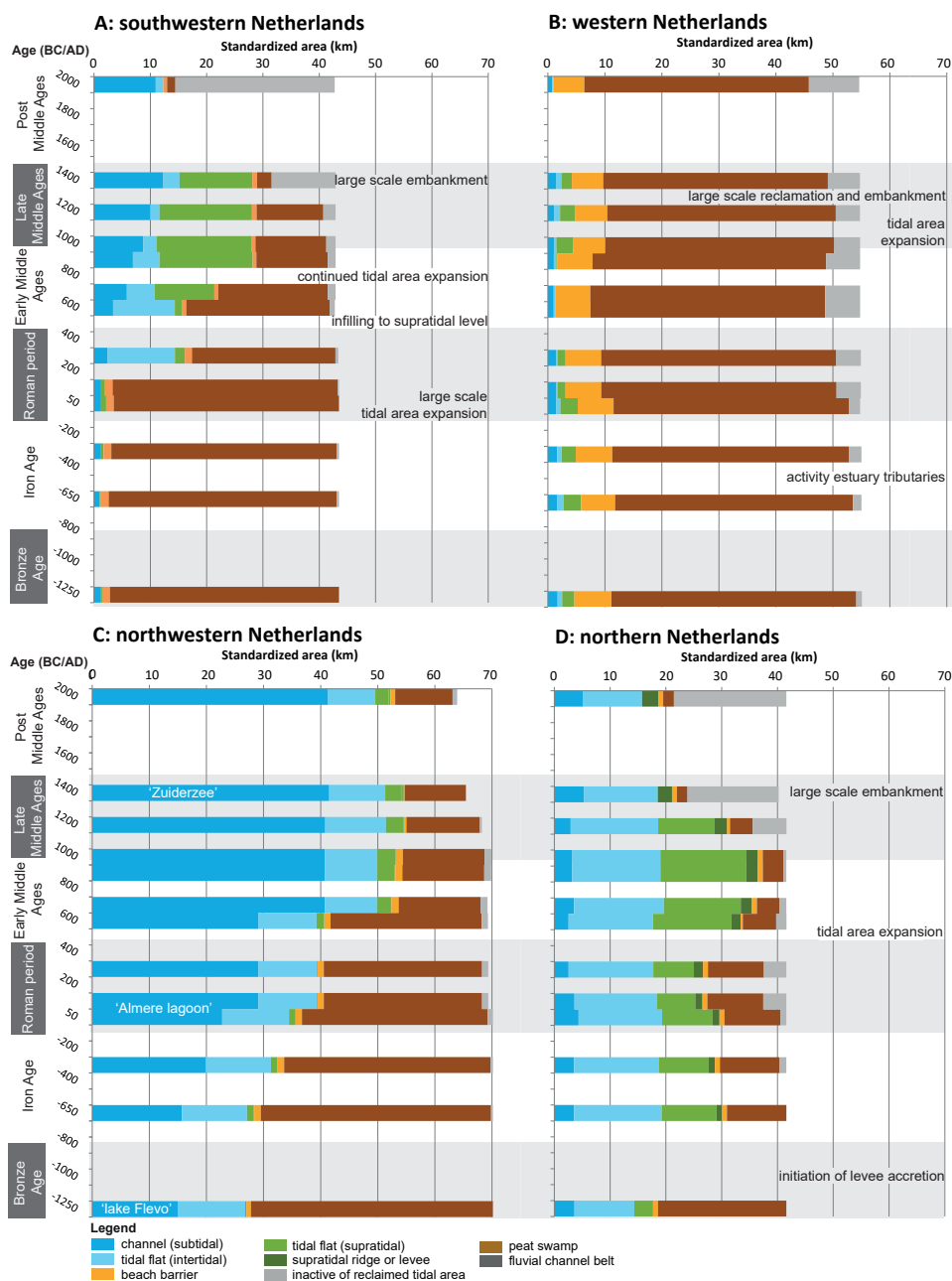


Figure 4.6 | Areal statistics of sedimentary domains. Regional comparison of the timing and impact of tidal area expansion since 1250 BC. The units were derived from Figure 4.7, and their colours correspond to Figure 4.7. The areal extent was standardized per km coastal length to correct for the different sizes of the coastal plains by dividing the summed area of the landscape units by longshore coastal section length. Transgression in the northwestern Netherlands mainly comprises the expansion of the Almere lagoon.

& Eijsskoot, 2015). Around 2000 BP the Oer IJ and Rhine estuaries silted up and beach-barrier progradation stopped along this coastal segment. Waves reworked the seaward bending beach ridges near the former Rhine estuary, leading to local coastline retrogradation (Figure 4.4C; Van Straaten, 1965; Cleveringa, 2000). Coastal retrogradation has been attributed to a decrease in sediment supply from the shallow offshore area caused by depletion of the offshore sand volume as a result of continued wave transport towards the coastal barriers during the millennia before (Roep, 1984; Beets et al., 1994; Van Heteren et al., 2011). Additionally, it coincided with avulsion of the Rhine towards the Meuse estuary after the Roman period (Berendsen & Stouthamer, 2000; Stouthamer & Berendsen 2001), resulting in a loss of direct fluvial sand supply to the beach barrier complex around the former Rhine estuary. Afterwards, the Meuse estuary received more discharge and sediment load (e.g. Erkens & Cohen, 2009; Hijma et al., 2009). It is quite possible that these sediments contributed to the silting up of the tidal areas of the late-medieval sea ingressions in the northern part of southwestern Netherlands. Iron Age and Roman habitation was mainly confined to the barriers, the tidal levees, and possibly also to the edges of the peatlands. From the Middle Ages onwards, large scale peat reclamation took place (Borger, 1992; Vos et al., 2015a).

4.3.3 Northwestern Netherlands

The present coastal barrier in this segment is composed of relatively narrow mainly post-medieval beach ridges. Behind the barrier system, back-barrier peat is covered by clastic deposits of medieval age (Zagwijn, 1986; Vos, 2015a), whereas tidal deposits from the Iron Age and Roman period have not been found. Due to continuous erosion, the timing of developments in this area is less known. This erosion is documented by historical sources that describe a medieval and post-medieval retrograding trend of the coastline and the expansion of tidal inlets (Schoorl, 1999). Coastal plain erosion and tidal deposition in this area not only occurred directly as a result of ingressions from the North Sea. On the eastern side, expansion of the Wadden Sea tidal flats in the peat area took place (Eisma & Wolff, 1980). Similar to the other coastal sections, this medieval tidal area expansion (probably since AD 800) has been registered in the northern part of Noord-Holland as a clay cover on peat and is associated with peat reclamation (Figure 4.5; Vos et al., 2015c). In a final phase of tidal area expansion, during the Late Middle Ages, the Marsdiep inlet was formed (Figures 4.5 and 4.7), which since then drained a large part of western Wadden Sea (Ente et al., 1986; Schoorl, 1999). Meanwhile, waves continuously eroded the peaty shores, causing the lagoonal area to expand (Figures 4.4C and 4.7). The remaining peatland surrounding the lagoon became covered with clay during the Middle Ages (Veenenbos, 1949; Pons & Wiggers, 1959/1960; Westerhoff et al., 1987; Van den Biggelaar et al., 2014).

4.3.4 Northern Netherlands

In the northern Netherlands, barrier islands alternated with tidal inlets that each drained large intertidal areas of the Wadden Sea (Figures 4.2 and 4.7). The occurrence of back-barrier tidal-channel deposits underneath the barrier islands (Oost, 1995; Van der Spek, 1996; Vos & Van Kesteren, 2000), and remnants of tidal channels in the current offshore realm (Beets et al., 1994) demonstrate that the barrier-island coastline retrograded during the last millennia. This retrogradation provided sand for the back-barrier intertidal area. Along the most inland part of the intertidal area, supratidal levees accreted between 700 BC and AD 500 (Roeleveld, 1974; Griede, 1978; Vos & Gerrets, 2005; Figures 4.3C, 4.4D, 4.5, and 4.6). Their clayey texture made them relatively resistant to lateral erosion by tidal channels and they probably also hampered the drainage of the surrounding subsiding peatland (Knol, 1993). Between ca. AD 300 and AD 600 the inland

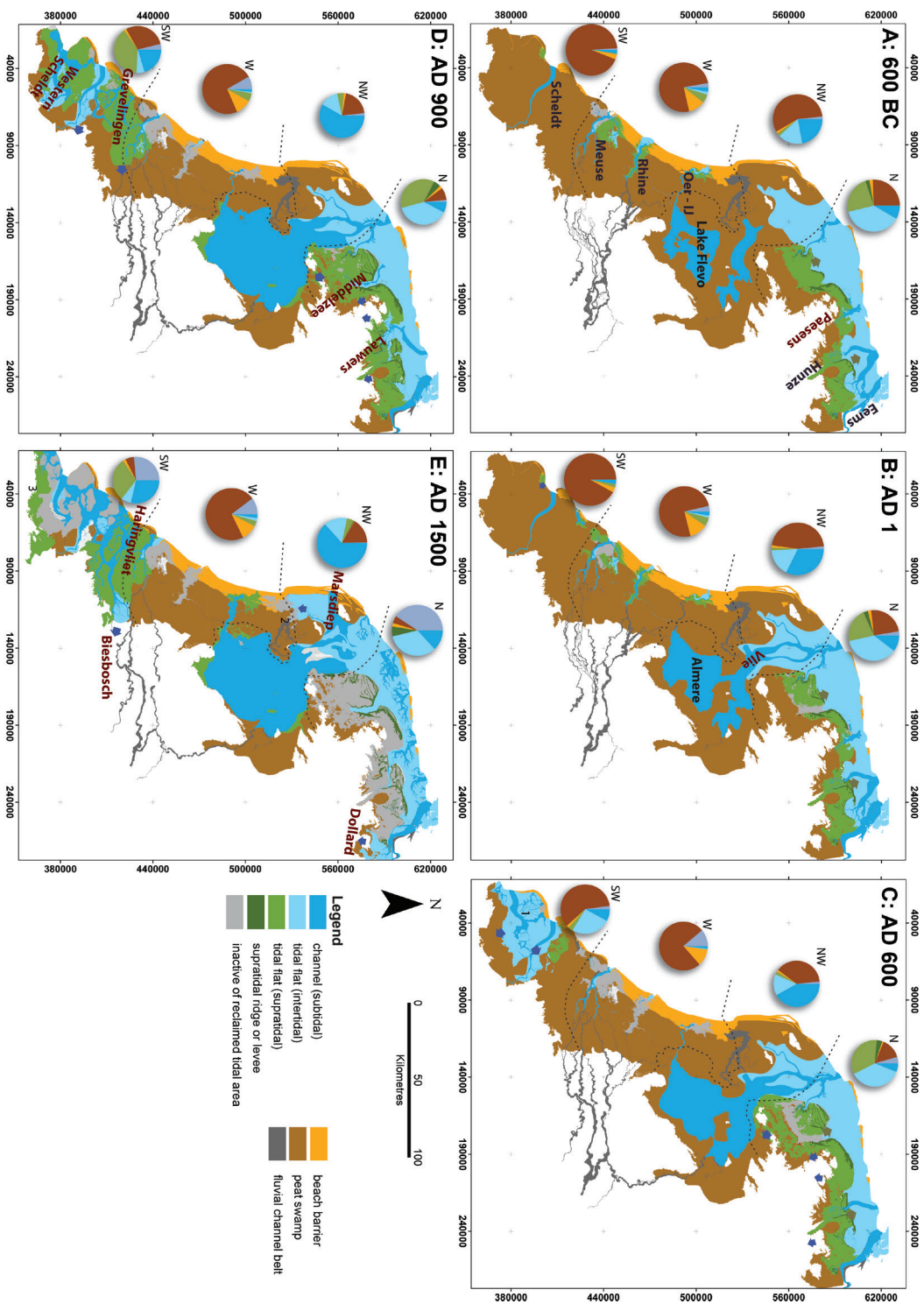
peatlands became regionally covered by a transgressive clay layer (Tables 4.1 and 4.2, Figures 4.6 and 4.7C; Veenenbos, 1949; Veenenbos & Schuylenborgh, 1951; Roeleveld, 1974; Knol, 1993). This clay deposition is attributed to peat-surface subsidence mainly resulting from reclamation activities and peat mining during the Late Iron Age (250–12 BC) and the Roman period (Figure 4.4D; Griede, 1978; De Groot et al., 1987; Gerrets, 2010; De Langen et al., 2013). The deposits are associated with newly-formed ingressions tidal inlets such as the Lauwers and Middelzee. Their size and depth expanded, caused by the increased tidal prism initiated by subsidence of the peat area (Knol, 1993; Van der Spek, 1995; Vos & Knol, 2015). In the tidal sediment sequences, this expansion is observed as a gradual upward increase in sand content (Pons, 1965). The new ingressions reached their maximum extent approximately AD 1000, after which they were embanked in different phases (Van der Spek, 1995). It is presumed that they initiated in the Roman period (Vos & Knol, 2015) taking over the drainage of local small channels from the previous generation of tidal inlets (Figure 4.5). Compared to regions in the southwestern Netherlands, the late Holocene transgressed area in the northern Netherlands was small and therefore the number of new ingressive systems was smaller as well. New tidal depositional areas connected to these inlets were also smaller than those in other coastal sections and furthermore better protected from the sea by the supratidal levees (Figure 4.5, 4.6, and 4.7). Similar to the southwestern Netherlands, a second generation of extensive land losses in the embanked former tidal areas occurred. The most dramatic example is the land loss owing to the 15th to 16th century ingressions along the river Ems known as the ‘Dollard’ (Homeier, 1977; Behre, 1999; Vos & Knol, 2015).

Table 4.2 | Increase in tidal channel and total tidal flooded area (channels, intertidal and supratidal flats) in average $1.0 \times 10^4 \text{ m}^2$ per yr, derived from the palaeogeographical reconstructions of Figure 4.7.

	600-300 BC	300 BC-AD 50	AD 50-300	AD 300-600	AD 600-900	AD 900-1200	AD 1200-1500
SW NL	13	18	466	0 ^{a)}	416 ^{a)}	0 ^{b)}	40 ^{b)}
SW NL tidal area increase							
SW channel increase	7	0	38	28	117	102 ^{b)}	78 ^{b)}
N NL tidal area increase	0	0	0	230	104	- ^{b)}	6 ^{b)}
N NL channel increase	0	-20	0	0	27	- ^{b)}	- ^{b)}

a) The pacing of tidal areal increase in the southwestern Netherlands after AD 300 is uncertain; b) land loss compensated by embankments, only new losses are shown.

Figure 4.7 (right page) | GIS generated palaeogeography. GIS-derived coastal development since 600 BC (chapter 3): blue arrows: tidal areal expansion; green arrows: salt marsh ridges expansion; black names: inherited middle Holocene estuaries and lakes; brown names: newly formed sea ingressions. Pie charts demonstrate relative areal extent of the landscape units per coastal segment, colours correspond to the map legend units. Footnotes: 1 – Walcheren, 2 – northern part Noord Holland, 3 – Zeeuws-Vlaanderen.



4.4 Discussion

4.4.1 Evolution of sea ingression tidal systems: mechanisms, timing, and pacing

From the series of examples encountered in the Netherlands, it is observed that quite a large coastal plain area was flooded instantaneously by major storms, but that the tidal channels took a few centuries to reach their equilibrium dimensions before the tidal system finally silted up (Figures 4.4, 4.5, 4.7). To better understand sea ingression evolution we summarised the facilitating controls, triggering mechanisms, and feedbacks, derived from the cases in our study area, into a conceptual model showing the evolution of a typical late Holocene tidal system (Figure 4.8). In our conceptual model we distinguish the following key phases:

Phase 0 – pre-triggering phase

Before sea ingression took place, natural or anthropogenic developments caused subsidence in the coastal plain, making it susceptible to sea ingression (phase 0 in Figure 4.8). At least for the southwestern and northern Netherlands we consider human-induced subsidence of the peatland to be the prerequisite for sea ingressions in our study area, based on the timing of initial tidal sediment deposition after peatland occupation and the unprecedented scale of the sea ingressions (Pons, 1992; Vos & Van Heeringen, 1997; Eryvncx et al., 1999; Vos, 2015a). This subsidence ranged

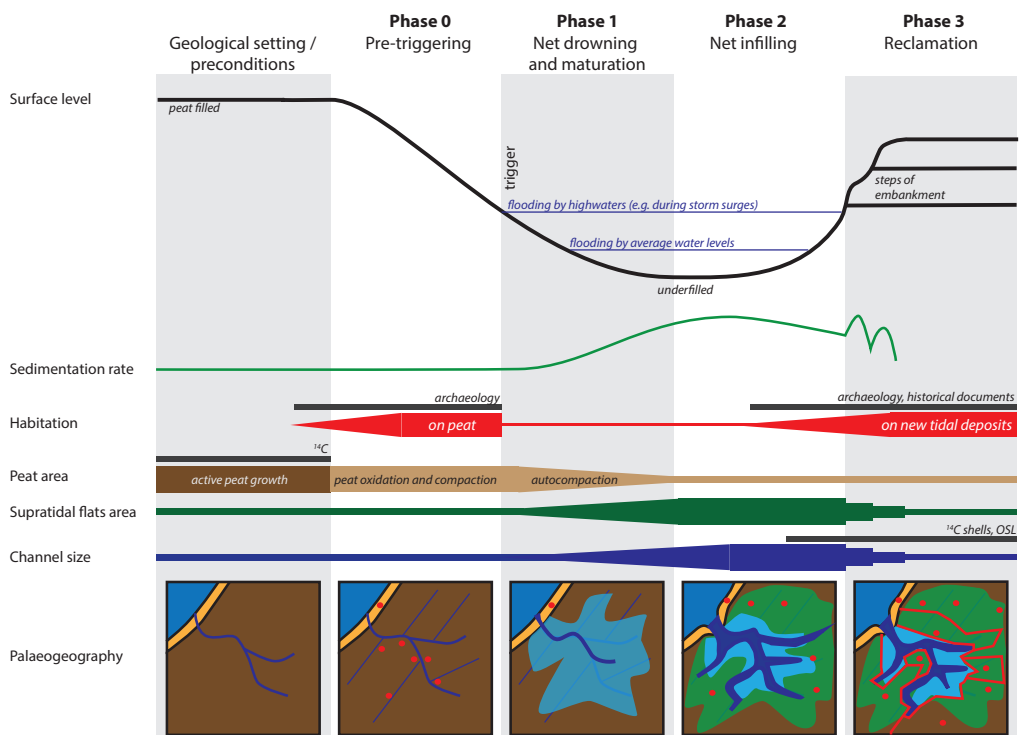


Figure 4.8 | Infographic on the development of a sea ingression, for new ingressions in reclaimed peatland. For further explanation see text.

from several decimetres to up to several metres and resulted from oxidation and compaction caused by groundwater table lowering (Erkens et al., 2016). In a later stage, subsidence was further aided by peat digging for salt mining (e.g. Griede, 1978; Jongepier et al., 2011). The large-scale surface lowering was not immediately compensated for by sedimentation and therefore caused irreversible drowning and transgression.

Natural factors have also been postulated for sea ingression initiation. An increased discharge of rivers would have caused widening or deepening of estuaries, facilitating sea ingressions (e.g. Pons, 1992; Baeteman, 2005b). In our study area, this would apply to the Meuse estuary that received more river discharge due to the avulsion of Rhine channel belts towards the Meuse estuary. Here, however, the opposite is observed: increased river discharge coincided with large scale peat formation around the estuary rather than sea ingression (section 4.2). Moreover, most sea ingressions in our study area occurred in absence of these major rivers or even at new positions along the coast (Figure 4.5) making it unlikely that this played a major role for the sea ingressions considered in this study. Depletion of offshore sediment sources where coastal barriers were narrow made the coastal plain more prone to back-barrier tidal area expansion. This mechanism has been discussed for the Flemish coast – Baeteman (2005b), UK Fenlands – Brew et al. (2000), UK Romney Marsh – Long et al. (2006) as well as for the Holland coast (section 4.3.2). This could also have played a role in the northwestern Netherlands, although the ingressions seem to follow periods of reclamation as well (Vos, 2015a). The extent and timing of the reclamation and the sea ingression in this segment remains to be established more accurately to assess the role of this facilitating antecedent condition (Vos, 2015a).

Phase 1 – net drowning and maturation

Ingression triggering: The subsiding peat area provided storage capacity, initially for storm water, later for diurnal high tide water, and in some cases even for permanent water. This large-scale flooding took place after the peatlands became connected to tidal or fluvial systems, most likely triggered by storms or spring tides (start of phase 1). Several studies attribute the increased influence of marine conditions to an increase in regional storm intensity (e.g. Regnaud et al., 1996 – Brittany, France, Long et al., 1998 – Humber estuary, UK; Clavé et al., 2001 – Gironde estuary, France). As demonstrated in Figure 4.5, documented NW European episodes of increased storminess (after Sorrel et al., 2012) coincide with two phases of sea ingressions in our study area (1900–1050 BP and 600–250 BP), whereas a third episode of enhanced storminess (3300–2400 BP) hardly had an effect on coastal plain development. This suggests that the facilitating conditions of large scale peat subsidence in enlarging back-barrier storage capacity after 2000 BP was an essential prerequisite for the sea ingressions. The tidal storage generated by this facilitating condition was necessary to cause water flow through existing weak spots along the coastline (e.g. small channels, lower spots in barriers or levees) to develop into new large tidal inlets at the observed scale (Figure 4.5). Single storms or episodes of enhanced storminess may have accelerated sea ingression or triggered the beginning of sea ingression, but they are unlikely to be the main cause behind the sea ingressions.

Sea ingression maturation: The creation of accommodation space in the back-barrier area provided an increase in tidal prism to which the size of the sea ingression tidal channels adapted proportionally during phase 1 and 2. For empirical relations considering channel dimensions in relation to tidal discharge, we refer to O'Brien (1931, 1969), Jarrett (1976), and Van der Spek (1995). In our reconstructions, we observe that the areal extent of the drowning part of the coastal plain is proportional to the size of the tidal channel belts (Table 4.2 and 4.3, Figure 4.7). During this stage,

an erodible sandy substrate allowed fast adaptation to the new back-barrier tidal area, whereas in more resistant clay and peat channel adaptation took longer. The gradual maturation is reflected in the sedimentary record by the upward increasing sand content of clays in the southwestern and northern Netherlands indicating an increase in energy.

Initial infilling and autocompaction feedback: the growing accommodation space has been filled with sediments supplied through the expanding tidal channels. The weight of clastic deposits caused compaction of the underlying peat by loading resulting in additional subsidence. This positive feedback created a further increase of the tidal prism and accommodation space. Its effect is proportional to the thickness of peat deposits at the time of inundation (e.g. Allen, 1999, Van Asselen et al., 2011). The thickness of the peat therefore controls the amount of accommodation space resulting from sediment loading and hence the timing of the shift from net drowning to the net infilling of the tidal system (phase 1 to 2).

Flanking area feedbacks: Another positive feedback includes the collapse of flanking unreclaimed peat areas caused by lowering of the groundwater table in the adjacent area after ingressions. The areal extent of this feedback and its pacing is unknown, but it may have played a role in further expanding ingressions. Furthermore, in response to the expanding ingressions, peat-land habitation can shift towards more inland positions, inducing new local land subsidence, which further enlarges the ingressions prone area. Developing a detailed chronology of drowning in the northern part of the southwestern Netherlands and in the northwestern Netherlands may help further understanding of this mechanism.

Phase 2 – net infilling

In the study area, tidal basins had a tendency to fill in as a result of tidal asymmetry and additional feedbacks (e.g. scour lag, settling lag – Van Straaten & Kuenen, 1958; Van den Berg et al., 1996). The timing of the shift from phase 1 to 2 is determined by sediment availability, but also by accommodation space and its feedbacks as described above (auto-compaction and flanking area feedbacks), which delay the net infilling. We expect sediment import to be proportional to channel size, i.e. the sediment will be most efficiently distributed over the tidal system when the size of the channels is adapted to the tidal prism of the tidal system.

Phase 3 – reclamation by embankment

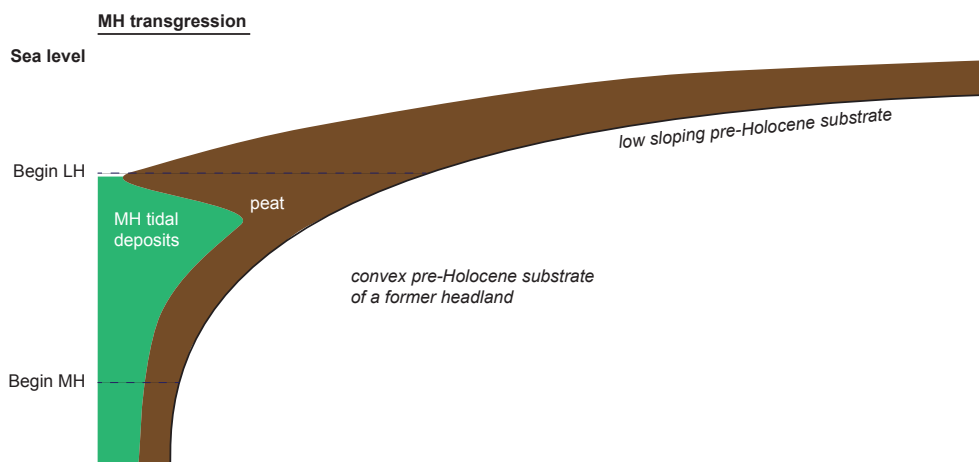
After sediment accretion had caused the tidal area to be sufficiently elevated, the area could be inhabited, reclaimed or successively embanked. Despite the increased supply of suspended sediment, not all late Holocene created accommodation space has been filled in and embanked today (e.g. Westerschelde, Oosterschelde, Dollard, Eastern Wadden Sea).

4.4.2 Antecedent conditions controlling the pacing and extent of sea ingressions

Several antecedent conditions control the development of sea ingressions and the resulting new tidal areas. We use the phases of Figure 4.8 to outline the relative contribution of antecedent conditions, which are also summarised in Table 4.3.

Coastal-plain width: a large coastal peat area results in a relatively large potential for the creation of tidal storage and accommodation space during phase 0, which will eventually develop in a large transgressed area during phase 1 (Table 4.3). This explains the large extent of the transgressed area in the southwestern part (30 km per km coastal length – Figure 4.6) compared to the northern Netherlands (10 km per km coastal length) Figure 4.5. When the areal extent of drowned peat is large, more sediment is required to push the tidal area from phase 1 to phase 2 (Figure 4.8).

A: Situation during the beginning of the late Holocene



B: Situation after late Holocene sea ingression

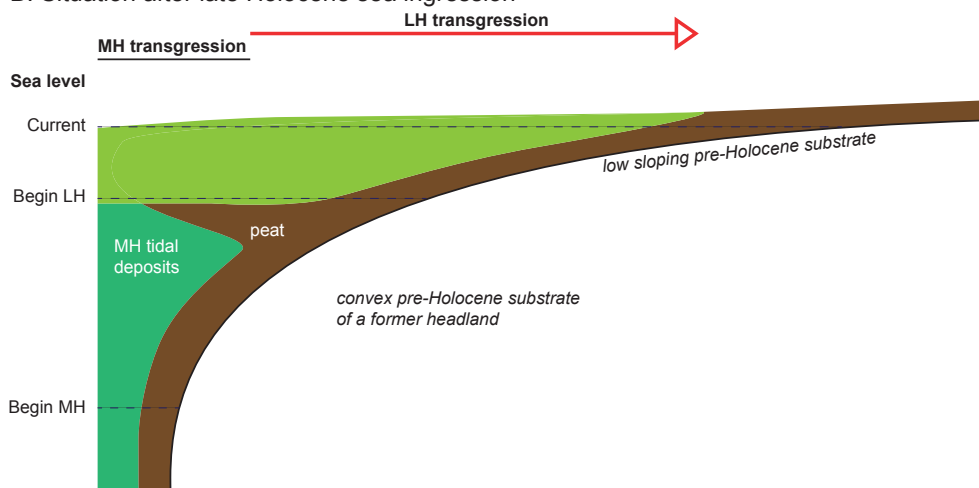


Figure 4.9 | Infographic on the development of a sea ingression on a convex sloping pre-Holocene substrate. This situation represents pre-Holocene headlands indicated in Figure 4.1A where the sea ingression can reach relatively far during the late Holocene compared to the middle Holocene tidal systems. This is a result of the low sloping shallow part of the pre-Holocene substrate.

Furthermore, within the considered coastal segments, the slope of the pre-Holocene substrate of the most inland part of the coastal plain controlled the inland extent of the late Holocene tidal deposits during phase 1 (Figure 4.9). When late-Holocene gradual RSLR and peat collapse took place, the presence of a flat and shallow Pleistocene surface (i.e. former headlands), topped by a thin middle Holocene peat layer facilitated the sea ingressions to penetrate deeper inland compared to the middle Holocene tidal areas (Figures 4.2B and 4.9). This is observed in the northwestern Netherlands and on a smaller scale in the southern part of the southwestern Netherlands (in the

areas indicated as *headland* in Figure 4.1A) and in the peat area of the northern Netherlands. The underfilled Flevo lakes in the coastal plain in the northwestern part have never entirely been filled up by peat, making them sensitive to a different natural transgression mechanism: peat erosion by wave activity. This facilitated large scale late-Holocene expansion of the lagoon (Almere) and the growth of the proportionally large Vlie channel (Figure 4.7).

Protecting elements: Three types of protecting geomorphological features have counteracted coastal ingressions of human-reclaimed land: beach barriers, supratidal levees, and inherited tidal tributaries. In the aftermath of storm surges, such elements delayed or prevented the formation of a permanent tidal channel connecting flooded subsidence-prone land to the sea (phase 0 towards 1 in Figure 4.8). They also delayed lateral expansion of the newly forming tidal channels (during phase 1 and 2). In the western Netherlands, the wide beach-barrier complex topped by coastal dunes prevented large-scale flooding and the formation of new tidal inlets. Peat-filled back-barrier areas in the southwestern and northwestern Netherlands had less wide beach barriers and were more sensitive to flooding and subsequent formation of sea ingressions. Other protecting elements were the inherited secondary tidal systems along the long-active estuaries (Meuse, Old Rhine, Oer IJ; Figure 4.5). In the millennia before reclamation, these systems had formed a more elevated levee-like topography around the estuaries inhibiting sea ingressions (Pons, 1992). The long presence of tides in these rivers caused floodwater to be relatively high on a regular basis, probably allowing the natural levees to build up relatively high (several decimetres). In addition to this effect, this already naturally auto compacted ribbon zone was less prone to subsidence compared to peatlands and therefore less sensitive to ingressive erosion. These elements probably became especially important from AD 1000 onwards, when the flanking peatlands were reclaimed at large scale around the Rhine and Meuse estuary. In the northern Netherlands supratidal clayey levees formed a line of protection. This probably delayed channel formation, causing the tidal channels to mature relatively late compared to the southwestern Netherlands (Figure 4.5). The position and elevation of protecting elements did not only influence the pacing of sea ingressions, but also the location of the late Holocene sea ingression tidal inlets. They mainly formed at new positions relative to their precursors (e.g. Lauwers, Middelzee, Westerschelde Figure 4.5), i.e. at weak locations in the protecting elements, possibly taking advantage of already-existing small creeks.

In the Late Middle Ages (AD 1050-1500), the first Roman to early medieval generations of sea ingressions that formed relatively close to the sea had silted up, to a level that made them suitable for human activities. They also formed protecting elements for the remaining inland peatlands. This could not prevent a second late medieval generation of ingressions taking place further inland in already embanked areas (Biesbosch, Dollard, Zeeuws Vlaanderen; Figures 4.5 and 4.7E). In contrast to the earlier ingressions, the position of the dikes in the landscape controlled the ingression extent and modulated the tidal amplitude (section 4.3.1), whereas their state of maintenance controlled the sensitivity for failure.

Sediment delivery to the back-barrier area was determined by overall sediment supply and by the proximity of the inundated area to main paths of tidal flow and wave activity. During the natural preconditional phase, sediment supply facilitated the presence of protecting elements as described above. When the ingression took place, it co-controlled the transition from net drowning to net infilling (transition from phase 1 to 2) and finally reclamation (phase 3). After the creation of additional accommodation space by autocompaction during phase 1 the balance shifted towards net infilling when sediment supply is abundant. In our study area, sources of sand mainly included reworked material from pre-Holocene headlands and the seafloor (Beets & Van der Spek, 2000), consisting of overstepped back-barrier deposits (Hijma et al., 2010). Suspended material was mainly

imported through the tidal inlets from the sea, where it was originally supplied from river mouths. As a result of deforestation in the upstream catchments, the amount of suspended load trapped in the Rhine-Meuse delta gradually increased since 500 BC, up to 3 Mton/y by AD 1000, which is twice the amount compared to the middle Holocene (Erkens & Cohen, 2009). We presume that the amounts of clays and silts transported to the sea and consequently available for sedimentation in the coastal plain must have increased as well, most likely causing relatively faster silting up of the new tidal systems. Around AD 1400 the avulsed Rhine system directly supplied sediments to the southwestern Netherlands (Biesbosch; Kleinhans et al., 2010), accelerating the rate at which the young tidal system could fill in (8-10 mm/a proximal to the river) and lost peatland could be reclaimed as fresh supra-tidal surface (Figure 4.4). Finally, the development of many new tidal channels favoured efficient sediment distribution over large parts of the coastal plain during phase 2 and 3 (in the southwestern Netherlands). In contrast, coastal parallel-transgressed areas (clay on peat areas in the northern Netherlands) drained by a comparatively smaller number of channels, hampered sediment distribution (especially sands) over the distal part of the coastal plain.

4.4.3 Outlook

Within our study area, several topics deserve additional research. A first topic is the non-linear response of flanking unreclaimed peat collapse feedback after initial ingressions. Continued dating effort in geoarchaeological contexts will show how far the entire peat area is affected by possibly rather local human-induced subsidence. Other unresolved issues are the role of a potential storm-frequency and intensity increase in triggering sea ingressions, and the complex interplay between

Table 4.3 | Relative contribution of antecedent conditions on flooding, the formation of sea ingressions and infilling of the coastal plain.

Antecedent conditions	Enhance LH flooding or sea ingressions initiation	Enhance far inland LH transgression?	Enhance LH infilling?	Remarks/feedbacks	Example
Low sloping Pleistocene substrate (result: wide peat filled plain)	0	++	0	Shallow peat, but far inland	NW-NL, N-NL
Thick peat	No initial effect	No initial effect	-	Subsidence by loading	SW-NL, W-NL
Small MH beach barriers	+	0	0	Enhance MH peat growth, and thus LH flooding potential	SW-NL, NW-NL
Wide MH beach barriers	-	-	+	Reworked beach barrier material for sea ingressions infilling	W-NL
Supratidal levees	-	-	0		N-NL
MH presence of large rivers	-	0	0	Clastics flanking estuaries	W-NL (Meuse, Rhine)
LH presence of rivers	?	?	+	Estuary remains open, sediment source	W-NL (Meuse)

MH = middle Holocene, LH = late Holocene, + positive effect, - negative effect, 0 no effect.

tidal, storm and river-discharge conditions controlling sea ingressions around larger rivers. For this, further refining of storm-event records around the North Sea for the entire late Holocene, flood records from rivers, and refining the timing of river branches and tidal inlet maturing will provide new insights. The mechanisms derived from the palaeogeographical reconstructions may be tested using numerical models.

The mechanisms and suitable antecedent conditions for transgression reconstructed for the Dutch coastal plain can be used to study drowning coastal plains in other areas in the world. In these areas boundary conditions may be different or the substrate could consist of another subsidence-prone lithology (e.g. unconsolidated clays). Successful maturation of ingressions could be related to either lack of sediment supply (e.g. Stanley & Warne, 1993; Zecchin et al., 2009) or creation of additional accommodation space (Törnqvist et al., 2008, this chapter). Despite these possible differences, these drowning coastal plains have in common that a rapid human-induced transgression results in sea ingressions with comparable feedbacks. This pushes the system into a long state of drowning and land loss until sedimentation compensates for this. Considering the role of antecedent conditions in these mechanisms as in our approach can help to assess the differential impact of coastal plain subsidence and drowning.

4.5 Conclusions

Large-scale coastal plain subsidence causes a major impact, both on the landscape and on habitation. We demonstrate this impact for the Netherlands' coastal plain, where mainly human-induced sea ingressions took place since the late Roman period continuing in the Middle Ages, on a remarkably large scale. Unlike the middle-Holocene transgression, these late-Holocene ingressions occurred in a peat filled back-barrier area and were not forced by rapid sea-level rise. In our study we identified the role antecedent conditions (i.e. geological setting) in the coastal plain changes caused by human-induced subsidence area for different coastal sections with varying antecedent conditions. The contrasting developments in coastal plain evolution in the different coastal sections are used to derive generic mechanisms of the initiation and maturing stages of sea ingressions:

- Wide coastal plains filled with subsidence-prone peat are most sensitive to surface lowering which facilitated ingressions after reclamation. The formation of such wide coastal plains is facilitated by a low sloping pre-Holocene substrate. Cutting of ditches during reclamation lowers groundwater tables, which causes peat oxidation and compaction. The resulting surface lowering rate outpaces by far the rate of regional eustatic sea-level rise and is therefore considered a much more important factor for sea ingressions. Late Holocene tidal-system ingressions can reach tens of kilometres far inland when all controlling factors add up.
- Coastal plain subsidence yields an increase of tidal storage in the back-barrier area. This can cause weak points in the coastline (e.g. creeks, lower parts of barriers or levees) to grow into new tidal channels, that grow proportionally to the back-barrier drainage area. Additional feedbacks such as subsidence by sediment loading lead to extra tidal prism increase and accommodation space for tidal sediments. These combined effects result in irreversible sea ingressions over large areas that become unsuitable for habitation.
- In some segments of the coast, certain protecting elements (barriers, supratidal levees) in the landscape control the location of sea ingressions that can develop in their weak spots. Moreover, protecting elements can delay or even prevent channel formation between the sea and the subsiding back-barrier area. Peat areas around estuaries are also less susceptible because they

are protected by a zone of erosion resistant clayey deposits from estuary tributaries that coevally formed during peat accumulation.

- Many coastal segments only partially fill in after sea ingression. Filling in the newly formed tidal area to a level that is suitable for habitation takes several centuries. The time required for this development is controlled by the extent of the ingressed area, sediment supply, and the strength of the peat area degradation or subsidence feedbacks. Large drowned areas with thick peat sequences, at distal positions to sediment supply take several centuries longer to fill in.
- When the oldest generation of ingressions is filled in with tidal deposits, these areas are less prone to new ingressions and become suitable for habitation again. Further inland however, vulnerable peatlands can still face younger generations of sea ingressions. In contrast to the earlier ingressions their extent is limited by the location of dikes rather than by natural feedback mechanisms.

Acknowledgements

This study is part of research program ‘The Dark Age of the Lowlands in an interdisciplinary light: people, landscape, and climate in the Netherlands between AD 300 and 1000’ funded by the Netherlands Organization for Scientific Research (NWO, section Humanities – project nr. 360-60-110). The first author contributed in the following proportions (%) to research design, data collection, analysis and conclusions, figures, and writing: 60, 75, 60, 80, 60. The authors would like to thank the participants of the workshop ‘Coastal evolution’ of April 2014 and Esther Jansma, Hans Middelkoop, and Cecile Baeteman for feedback on earlier drafts of this chapter. Finally we would like to thank two anonymous reviewers for their useful comments on the manuscript.



Chapter 5

Human-induced drivers of avulsion success in the Rhine-Meuse delta, the Netherlands

The shifting of deltaic river branches (avulsion) is a natural process that has been increasingly influenced by humans over the last millennia. Still, the impact of early human activities as controls of avulsion success has remained poorly explored. This study demonstrates how two avulsions in the Rhine-Meuse delta, the Netherlands, were stimulated by human activities already in the first millennium AD. By step-wise rerouting of nearly all Rhine discharge towards the expanding Meuse estuary, these avulsions led to a total reorganisation of the delta-river network. We show that peatland reclamation induced land subsidence in the lower delta. This effect, together with human-induced increased suspended loads from the upstream basin and tidal backwater effects, caused expansion of and eventual connection between tidal ingressions and fluvial crevasse channels across extensive deltaic peatlands. We identify the feedback loops between overbank sedimentation, tidal incursion, and land drainage subsidence that have led to avulsion success. The unravelled chain of processes and feedbacks are generic and relevant to many other deltas, where ongoing subsidence may cause tidal incursion and connection to rivers potentially causing unexpected avulsions.

H.J. Pierik, E. Stouthamer, T. Schuring, & K.M. Cohen

5.1 Introduction

Humans are known to be responsible for intended and unintended river avulsion, the formation of new channels, in deltas (e.g. Syvitski & Saito, 2007). Whereas natural drivers and triggers are usually split into upstream and downstream controlling factors (e.g. Smith et al., 1989; Jones & Schumm, 1999; Stouthamer, 2001; Makaske et al., 2012), human controls are harder to put in these terms. Here we describe two successful avulsions in the lower Rhine delta in the 1st millennium AD, driven by downstream tidal processes, upstream fluvial processes, and omnipresent humans. The resulting river branches crossed 30 km of freshwater peatland and connected to the tidal channels of the Old Meuse estuary (Figure 5.1). The avulsions occurred in a period of increased suspended sediment delivery from the upstream river basin, increased tidal incursion from the downstream direction, and increased population and intensified land use across the delta plain. The avulsions caused a large-scale river network reorganisation in the delta, redistributing discharge, floodwater, and sediment. Remarkably, these were the first lower-delta avulsions that managed to cross extensive alder peat swamps, which had separated the Old Rhine and Old Meuse river mouths in the preceding 3000 years. While eutrophic Rhine flood waters had fed these swamps, the crevasse splays reaching into them never developed into successful avulsions, meaning that floodwater flow velocities were effectively reduced and that crevasse-channel progradation was hampered by the peat substrate and abundant vegetation (Makaske et al., 2007). Deforestation and reclamation of the peatlands from the Late Iron Age onwards (250 BC) altered this situation, shortly after which

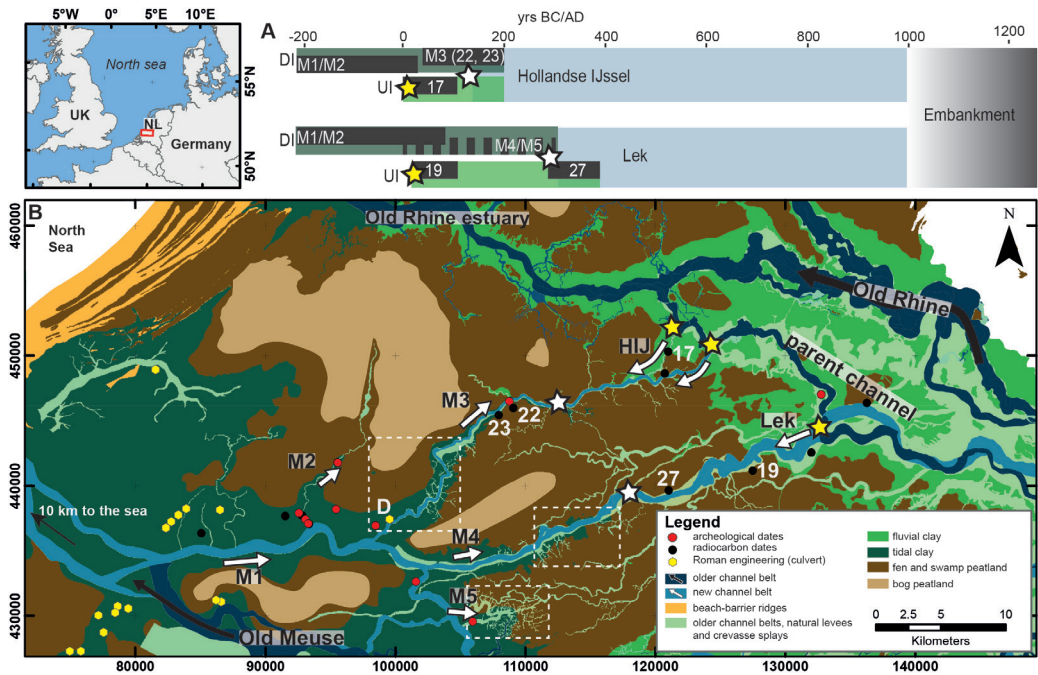


Figure 5.1 | (a) Timeline of stage development of the Hollandse IJssel (HIJ) and Lek avulsions, highlighting the initiation phases at the downstream (DI) and upstream (UI) sides. M1-M5 resemble different tidal creeks from the Old Meuse estuary, white extents indicate occurrence of rectangular creek networks. White stars indicate presumed tidal-fluvial connection locations, yellow stars UI crevasse-avulsion nodes. (b) Superficial geological map of the study area showing the old river courses (dark blue) and the new courses (light blue) (Cohen et al., 2012); flood-basin extent (green), raised peat bogs (light brown) (Van Dinter et al., 2014). Anthropogenic features of the youngest 1000 years were stripped from the map. Selected dates (white numbers), relevant archaeological sites mentioned in the text, and inferred stages of avulsion are indicated. See Appendix B for a full description of age-control.

the studied avulsions occurred (Figure 5.1). This raises the question if and how humans stimulated these avulsions by performing these land-use practices. Therefore, the objective of this study was to determine how natural and human controls, both acting from upstream and downstream sides, contributed to the development and eventual success of these avulsions. Hereto we mapped and dated downstream tidal ingressions and upstream crevasse splay progradation, identified locations of peatland reclamation, and identified the drivers, that eventually led to successful avulsion. If indeed humans contributed importantly, our case would be an early example of human-controlled avulsion and one that allows studying the full completed process. As such the Rhine-Meuse delta case serves as an example for younger human-induced avulsion in other deltas that are either in progress or waiting to happen and will have lasting socio-economic implications.

5.2 Materials and methods

Previous studies have mapped and documented in great detail the age, position, and styles of channel belts and their natural levees, crevasse splays, and tidal creek landforms in the Rhine-Meuse delta (e.g. Berendsen & Stouthamer, 2000; Gouw & Erkens, 2007; see also chapter 2). We expanded this dataset for the two avulsion cases by sampling and ^{14}C dating the top of peat immediately below overbank deposits (Törnqvist & Van Dijk, 1993) at multiple locations along the branches Hollandse IJssel (HIJ) and Lek (see Table B1 in Appendix B). All dates are reported in standard calibrated form in YR BC/AD with 1σ range. Based on these datings, we identified the stages of channel initiation at either end of the branches and the maturation stages after upstream and downstream initiated channel features connected (Figure 5.1). We correlated these events to human activity using archaeological artefacts that were found on the natural levees and on top of the peat. Peatland-surface elevation before avulsion was reconstructed for each ^{14}C sampled site (including compaction correction, see Appendix B3), to assess gradient advantages at the time of established connection.

5.3 Avulsion history results

Antecedent conditions: In the last millennium BC, two upstream induced processes determined the geomorphological setting for our study. In the central delta Rhine, avulsions towards the Meuse estuary developed along the eastern margin of the peatlands (Figure 5.2A). Additionally, human deforestation of the hinterland resulted in increased supply of fine-grained sediment towards the delta after ca. 500 BC (Erkens et al., 2011), affecting the delta plain and its estuarine outlets. Along the peatlands, this caused the Rhine branches to raise their levees by ca. 1 m between 1000 and 1 BC (Figure 5.2C) and it caused crevasse splays to grow larger than their precursors. This accelerated the initial stages of avulsion and thus increased the chance that the crevasse splay could develop into an avulsion. The increased sediment load and enhanced connection of Rhine channels along the peatlands towards the Meuse outlet resulted in a larger sediment transport towards to this estuary (Berendsen & Stouthamer, 2000).

Upstream crevassing initiation (UI): The parent channel belt for the HIJ and Lek avulsion was the secondary Rhine branch that ran along the northern edge of the peatland as had developed in prior times (Figures 5.1B and 5.2A). Around settlements on these channel belts as well as in the flood basins, riparian deforestation for wood use was common practice during Roman age (Van Dinter et al. (2014). Once swamps were deforested and sediment supply had increased, crevassing was no longer restricted to the channel belt margins but the systems could further penetrate into the flood basin. Avulsion-belt formation by crevassing along HIJ began between 50 BC–AD 50 (date 17) and along the Lek around AD 24 ± 34 (date 19; Figure 5.1).

Downstream creek initiation (DI): From 200 BC onwards, tidal deposition along the Old Meuse estuary expanded and multiple creeks ingressed into the peatlands from the southwest (M1-M5 in Figure 5.1). Archaeological artefacts on top of this peat provide evidence for habitation and reclamation of this environment between 250 BC and AD 250 (Figure 5.1B; Table B2 in Appendix B). The intensified agricultural use of the artificially drained peatlands caused surface lowering. A Roman hollow-tree valve-culvert (Roman engineering work) found at site D (AD 150–200) along M3, and 16 other culverts found more downstream in the Meuse estuary (Ter Brugge, 2002 Figures 1) provide evidence that the land was artificially drained during low tide. The valves allowed drainage during low tide, and prevented a return flow during high tide, indicating that reclamations caused land-surface lowering to below high tide water levels. In places, Roman-aged small-scale

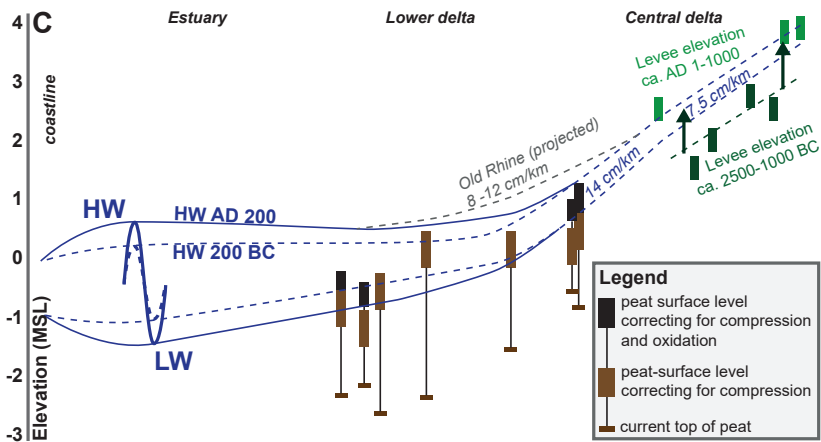
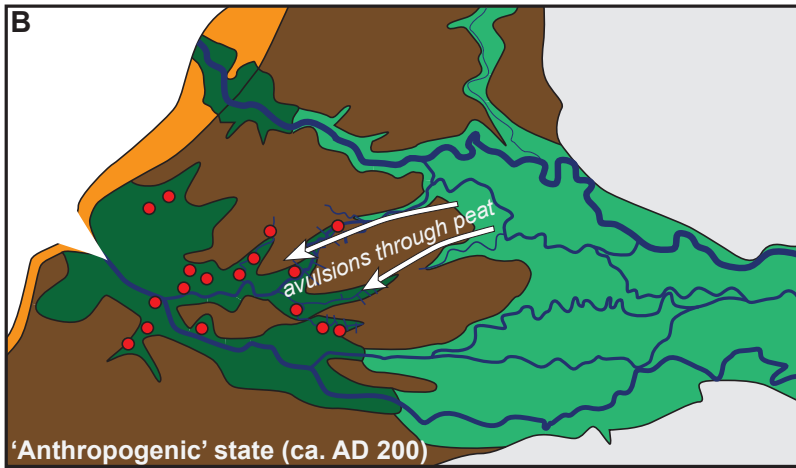
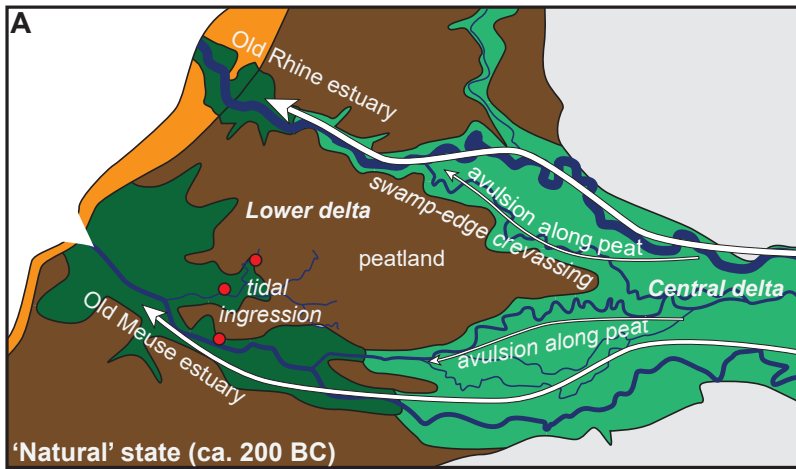


Figure 5.2 (left page) | (a) Simplified map of the delta network in last natural state around 200 BC. (b) Simplified map of the delta network in the first anthropogenic state around AD 200. Colors as in Figure 5.1, red dots indicate settlement locations. (c) Reconstruction of pre-avulsion surface elevation along HIJ and Lek paths. The approach is outlined in Appendix B3. Upstream: mapped levee elevation (green and dark green), Central: top of peat, Downstream: tentative tidal incursion, increasing with tidal creek ingressive progradation from 200 BC to AD 200 (Vos, 2015a). Projected Old Rhine gradient was measured along its residual channels, after Cohen et al. (2012).

creek ridges follow straight courses that are strikingly perpendicular to the larger natural channels, suggesting inheritance of man-dug ditch patterns. This pattern was observed in the lower reaches of the HIJ and Lek rivers, and the Alblas system (in the white dotted rectangles in M3-5 in Figure 5.1), in analogue to sites in the southwestern Netherlands (Vos, 2015a). Peatland subsidence increased the tidal prism and triggered tidal-creek expansion, making the area increasingly sensitive to severe storm-surge floods (e.g. Vos, 2015a; Pierik et al., 2017a; chapter 4). These developments caused more sediment to be imported into the flood basins, leading to additional surface lowering as the accumulation of supplied sediment could not compensate for the subsidence of the underlying peat. Subsurface lowering due to sediment loading ranged from 1 to 2 meter (Figure 5.2C) along the avulsion path. The resulting estuarine channel and creek network expansion at the downstream side (M1-M5) shortened the path distance that crevasse splays from upstream had to cross to connect downstream (Figure 5.1B).

Connection and beginning of maturation: Ingressing creeks reached the central part of the peatlands around AD 1–100, at least along the path of branch HIJ (dates 22 and 23; Figure 5.1). Not much later, crevasse-splay progradation reached this area from the east and connection of tidal and fluvial subsystems occurred at the white star indicated approximate location (Figure 5.1B). Especially with swamp forests removed, a slight hydraulic energy gradient advantage arose for the cross-over route towards the Meuse estuary. After AD 300 a final second connection was established by the river Lek (date 27; Figure 5.1), similar to the Hollandse IJssel. The Lek route towards the Old Meuse estuary was shorter compared to the HIJ route, and therefore the Lek river became the dominant of the two.

5.4 Anthropogenic controls and feedbacks in avulsion success

The double case of HIJ and Lek avulsion success marked a major change in delta-plain network configuration (Figure 5.2), shortly following first extensive anthropogenic deforestation and reclamation of the lower-delta swamp and fen lands. Apparently, human impact - peatland subsidence and increased suspended sediment load - on the river, estuary, and peatlands changed the odds in favour of avulsion success.

In the initial phase, as well as after the connection, several interacting feedback loops caused the avulsion to succeed (Figure 5.3). In both the upstream and downstream realms, enhanced peat subsidence created more accommodation space for floodwater, leading to larger crevasse and creek channels. These facilitated additional sediment transport and deposition onto the peatlands, causing further subsidence. Upstream (UI) the loop was initiated by crevassing (sediment loading), whereas downstream (DI) this loop was initiated by peatland subsidence (Figure 5.3). Once a connection had established, channels matured and natural levees formed that were resistant to lateral erosion. Additionally, their weight caused further peat compression further hampering lateral channel development and moving the channel system to an equilibrium size (blue arrows in Figure 5.3). A positive feedback of tidal-fluvial connectivity is the delivery of more sediment to the estuary, further

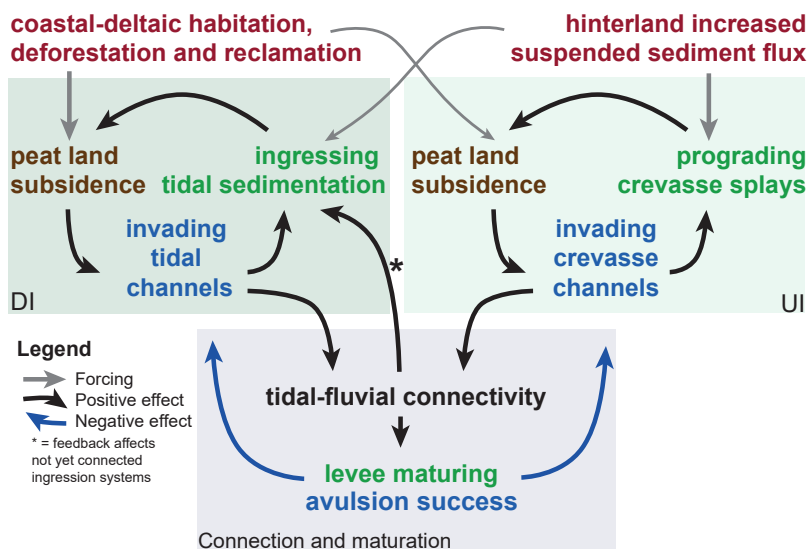


Figure 5.3 | Conceptual diagram of the human-induced feedback mechanisms that lead to avulsion success. Tidal incursion started with downstream human-induced peatland subsidence (DI). Meanwhile, human-enhanced suspended sediment load increased from upstream (UI). When successive avulsions increasingly routed sediments towards the estuary and its ingressing creeks, more sediment was available here as well to develop creeks and load onto the peat, accelerating the next avulsion (connection and maturation).

accelerating peat subsidence and the ingression of creeks that were not yet connected to a river (*in Figure 5.3). This is how an avulsion could help a next avulsion to develop: starting before BC (Figure 5.2A) along the southern swamp edge, followed by the HIJ and finally the Lek.

One may argue that topographic gradient advantages are not decisive to lowland river avulsions in natural delta plains, because elevation differences are very small (e.g. Kleinhans et al., 2013). Nevertheless, for the human-impacted situation of the lower Rhine delta in the first millennium AD, our results show that (i) Old Meuse estuary tidal channels had invaded the flood basin by 15-25 km, bringing the point where the river connects to marine base level further inland (Figure 5.2C), (ii) a millennium of maturation with ever increasing overbank sedimentation of the parent channel upstream had raised its levees by ca. 1 meter (Figure 5.2C), and (iii) deforestation and subsidence caused the peatland to lose its function as a topographic separation with a high hydraulic roughness. This increased the flood-basin gradient from ca. 4 cm/km to ca. 14 cm/km, yielding a slight gradient advantage to the parent channel slope (Old Rhine) of 8-12 cm/km upstream of Utrecht (Figure 5.2C). Landward penetration of the tides due to this gradient advantage combined with a decreased vegetation roughness caused the effective energy gradient to increase significantly, especially during low tide in combination with high river discharge and water levels (Figure 5.2C). This not only allowed for ‘connection’ of initiating secondary system, but also for maturation of the HIJ and Lek tidal-fluvial channels.

5.5 Conclusion and implications

Our historical case study demonstrates that human impact in the low-gradient Rhine-Meuse delta plain was the main driver of avulsion success. Tidal incursion into the lower delta peatland was caused by human-induced peatland subsidence. Avulsion progress was further aided by human-enhanced suspended sediment load from upstream, which allowed for accelerated crevasse splay and channel development, expanding across the peatland towards the estuary. When successive avulsions increasingly routed sediments towards the estuary and its ingressing creeks, more sediment was available here as well to develop creeks and load onto the peat, accelerating the next avulsion.

Tidal ingression resulting from subsidence often is not included in avulsion models but can be a major control as demonstrated for this historical case. As subsidence currently is ongoing in many deltas in the world, that additionally face threats from cyclones and sea-level rise (e.g. Syvitski et al., 2009), tidal ingression will presumably become increasingly important for causing unexpected avulsions. Especially natural floodplains with a subsidence-prone substrate (clay and peat) will become more sensitive to storm-surge flooding and sea incursions.

Acknowledgements

This research was funded by NWO (project nr. 360-60-110). The first author contributed in the following proportions (%) to research design, data collection, analysis and conclusions, figures, and writing: 60, 75, 60, 80, 60. We thank Arjan van Eijk, Marjolein Gouw-Bouman, Rowin van Lanen, Kay Koster, Tim Winkels, and Hessel Woolderink for assistance in the field. We additionally thank Wim Hoek for his instructions in the lab, Hanneke Bos and Nelleke van Asch for selecting the macrofossils, and the Centre of Isotope Research in Groningen for dating the radiocarbon samples. This chapter benefited from discussions with Kay Koster (Utrecht University / Geological Survey of the Netherlands), Ton Guiran, and Jurrien Moree (Bureau Oudheidkundig Onderzoek Rotterdam), and from useful suggestions by Hans Middelkoop and Esther Jansma.



Chapter 6

Natural levee evolution in the Rhine-Meuse delta, the Netherlands, during the first millennium AD

This chapter presents reconstructions on natural-levee development in the Rhine-Meuse delta, the Netherlands, during the first millennium AD, covering the full delta plain. It is the first study that performs this on a delta scale, which allows seeing the delta-wide trends on levee forming controls and their feedbacks. We mapped the levee morphology and elevation by combining LiDAR imagery, lithological borehole data, soil mapping, radiocarbon dates, archaeological data, and GIS-reconstruction techniques. From the detailed levee reconstructions we quantified natural-levee dimensions and evaluated the temporal changes therein. The dimensions and the changes therein were then linked to external forcings (increasing suspended sediment load, variable flooding intensity) and to antecedent conditions (e.g. delta-plain width, flood-basin configuration).

We show that antecedent conditions are an important control on levee shape. This is demonstrated for the upper delta where the relatively narrow delta-plain combined with strong compartmentation (i.e. the occurrence of many alluvial ridges and enclosed flood basins) caused the flood levels to be amplified allowing the natural levees to grow relatively high. Compartmentation also seems to have stimulated trapping of coarse-grained overbank sediments, explaining the clear downstream trend in levee width. This effect was probably further aided by the clearance of the riparian forests, mainly in the upstream and central delta, which caused the coarser fraction of the suspended load to be further dispersed into the flood basin leading to wider levees. In the first millennium AD several new river courses formed that avoided the areas of natural-levee relief of abandoned alluvial ridges. On these fossil alluvial ridges, the topographical expression gradually reduced due to widespread flood-basin trapping of overbank sediment, which led to topographic levelling. The natural levees that formed during this period along the new courses appear to be relatively high compared to precursor generations in the upper and the central delta. This is most likely related to the increased suspended sediment supply and intense flooding regime during their formation. The hypotheses generated with this new delta-wide overview help to better understand the controls in the development of levees, which are important elements in river landscapes and in fluvial sedimentary records.

Published as: Pierik, H.J., E. Stouthamer, & K.M. Cohen (2017) Natural levee evolution in the Rhine-Meuse delta, the Netherlands, during the first millennium CE, *Geomorphology* 295, p 215–234. [dx.doi.org/10.1016/j.geomorph.2017.07.003](https://doi.org/10.1016/j.geomorph.2017.07.003).

6.1 Introduction

Natural levees are pronounced geomorphological features in the low-relief floodplain topography of river and delta landscapes (e.g. Fisk, 1947; Allen, 1965). Because of their relief expression, natural levees affect floodplain hydraulics and overbank sedimentation. As such, they are also key elements

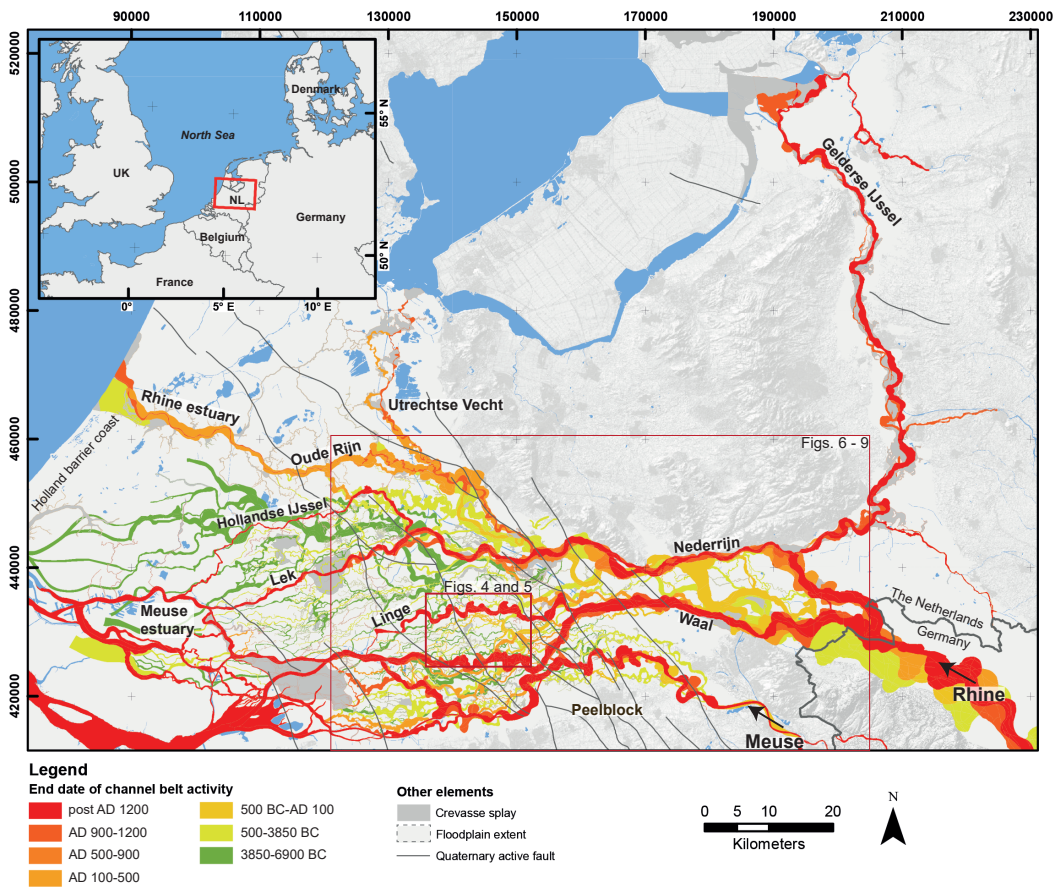


Figure 6.1 | Location of the study area within the Rhine-Meuse delta. Network of channel belts after Berendsen & Stouthamer (2000) and Cohen et al. (2012).

in the formation of channels and fluvial sedimentary records (e.g. Brierley et al., 1997; Törnqvist & Bridge, 2002; Filgueira-Rivera et al., 2007). As natural levees are the main areas of human occupation in wet delta landscapes, they are also important for understanding the interaction between the active delta landscape and coeval human occupation (e.g. Modderman, 1948; Hudson, 2004; Guccione, 2008; Funabiki et al., 2012; Van Dinter et al., 2017; Pierik & Van Lanen, 2017; chapters 7 & 8). The size, shape, and height of natural levees strongly varies between rivers and within deltas, owing to differences in sediment supply, duration of sedimentation, and flood regime (Hudson & Heitmuller, 2003; Adams et al., 2004). Their formative controls have typically been analysed as case studies for specific selected meander bends, mainly for active sedimentary environments (e.g. Cazanacli & Smith, 1998; Törnqvist & Bridge, 2002; Hudson & Heitmuller, 2003; Filgueira-Rivera et al., 2007; Smith & Perez-Arlucea, 2008; Smith et al., 2009; Heitmuller et al., 2017). These studies mainly provide insight into short-term sedimentary processes involved in local levee formation. The diverse morphology of levees, however, also is a product of regional variation in antecedent conditions – the geomorphological setting of the delta and the flood basins – (e.g. Kleinhans et al., 2013; Klasz et al., 2014; Lewin & Ashworth, 2014; Van Asselen et al., 2017) that is often missed in local case studies. The regional variation in the antecedent conditions includes

differences in delta-plain width, flood-basin configuration, substrate, and the prior avulsion history. These conditions affect typical flood height that in turn controls levee height and shape, and makes overbank sedimentation vary within the delta, along channels and through successive stages. This setting needs to be studied on a regional scale before dimensions of individual levees can be well understood. A delta-wide analysis therefore is necessary to study the variation in dimensions of natural levees and their formative controls in space and time.

In this chapter we map the natural levees of the Rhine-Meuse delta in the Netherlands (Figure 6.1) and interpret the inferred patterns as the outcome of the inherited setting, external forcings, and internal geomorphic process factors. This is a suitable area to conduct such a study, because of data abundance: LiDAR surface datasets, dense subsurface data from borehole databases, and well-developed age control on landscape development (e.g. Berendsen and Stouthamer, 2000; Gouw, 2008; Cohen et al., 2012). Natural levees in this delta – as in other deltas – have been studied before, but mostly as local case studies only. Natural levees show up as elements in individual detailed local mapping projects that seldom cover areas larger than 50 km². Levee extent and thickness have also been investigated using detailed local cross-sections (e.g. Törnqvist & Bridge, 2002), delta-wide cross-sections (e.g. Gouw & Erkens, 2007), and regional geomorphological and geoarchaeological mapping (e.g. Berendsen, 1982; Willems, 1986; Van Dinter, 2013; chapter 2). When comparing these studies, which each have slightly different methods and definitions when distinguishing the levees, the large diversity in levee width, elevation, and distribution across the Rhine-Meuse delta becomes evident. A uniform mapping and synthesis of the levee characteristics across the Rhine-Meuse delta, so far has not been attempted, and the factors that explain levee shape variability have remained unexplored on the delta scale.

In the next sections, we (i) determine and quantify the changes in natural-levee patterns, shape, distribution, and elevation in the Rhine-Meuse delta throughout the first millennium AD, and (ii) use these results to assess the role of varying forcings, antecedent conditions and feedbacks in the development of natural levees in this area. The levee geomorphology was mapped for consecutive time slices in the first millennium AD (AD 100, 500, and 900) because the landscape from this period has been well preserved and is best resolved using LiDAR and borehole data. The large-scale construction of dikes from ca. AD 1050 onwards caused sedimentation to be restricted to the narrow corridors of the embanked floodplain (Hesslink et al., 2003; Hudson et al., 2008). This caused the fossil levee landscape in the rest of the delta plain to remain at a rather shallow depth below the current surface, which enhanced the possibilities for mapping the levees.

The antecedent conditions in the beginning of the first millennium AD (e.g. the width of the delta plain and the substrate composition) vary greatly between the upper and central regions of the delta. Over the studied period, major geomorphological changes occurred to which the levees presumably adjusted. For example, a series of avulsions redistributed discharge of Rhine water and sediment over the delta (Stouthamer & Berendsen, 2001), suspended sediment load was higher than in previous periods (Erkens et al., 2011), and the frequency of large floods increased (Toonen et al., 2013). These independently reconstructed varying antecedent conditions and external forcings were compared to natural-levee shape and the developments therein observed in the levee reconstructions. The time steps of the reconstructions (AD 100, 500, and 900) equally divide the first millennium and the phasing of the avulsions and changing forcings. By comparing the differences in levee shape across the entire delta throughout the first millennium AD, the regional controls on levee formation are inferred. This leads to a more complete identification of the processes and controls involved in levee formation.

Table 6.1 | New avulsed rivers in the Rhine-Meuse delta between 500 BC and AD 1000 compiled from overviews in Berendsen & Stouthamer (2001), Cohen et al. (2012; 2016). More specific references are given in the table. The start of the initiation and mature phases were inferred from radiocarbon dates and relative dating. Location of the rivers is indicated in Figure 6.1.

New river branch	Start of the initiation phase	Start of the mature phase
Nederrijn	ca. 500–20 BC ¹⁾	After AD 310 ¹⁾
Linge	ca. 250–20 BC ²⁾	After AD 20 ²⁾
Hollandse IJssel	ca. AD 0–100 ³⁾	Before AD 800 ³⁾
Lek	ca. AD 40–300 ³⁾	Around AD 700 ³⁾
Waal	ca. AD 220–450 ²⁾	After AD 450 ²⁾
Gelderse IJssel	ca. AD 550–650 ¹⁾	Around AD 900 ¹⁾

¹⁾Based on Teunissen (1988; 1990); Makaske et al. (2008); Cohen et al. (2009). ²⁾Based on Törnqvist (1993); Weerts & Berendsen (1995). ³⁾Based on Berendsen (1982), Guiran (1997) and chapter 5.

6.2 The Rhine-Meuse delta: setting and natural levee characteristics

6.2.1 Delta evolution

The Rhine-Meuse delta extends from its apex in the Dutch-German border region westward to the Holland barrier coast (Figure 6.1). Near the delta apex, the Rhine floodplain is up to 20 km wide, but in downstream direction it first narrows to ca. 10 km (near X = 190,000; Figure 6.1) before widening again to 50 km in the central and lower parts of the delta. The thickness of the Holocene deposits increases from a few meters in the upper delta to about 20 m near the coastline. This deltaic wedge contains flood-basin clays and peat intersected by sand bodies of multiple generations of channel belts topped and flanked by levee complexes (e.g. Törnqvist, 1993; Weerts, 1996; Gouw & Erkens, 2007; Makaske et al., 2007). In the upstream delta, wide alluvial ridges enclose relatively small flood basins, whereas westward, increasingly confined alluvial ridges separate much larger flood basins (Törnqvist, 1993; Makaske et al., 2007; Gouw, 2008). In the upstream part the overbank material is more silty, and the presence of vegetation horizons indicates mainly non-permanent inundation of the flood basins (Egberts, 1950; Havinga, 1969), whereas in the downstream part, peat indicates semi-permanent and permanent flood-basin inundation.

Individual channel belts typically were active for some 100 to 1000 years, whereas trunk channels (e.g. Oude Rijn in Figure 6.1) could be active for multiple thousands of years (Stouthamer & Berendsen, 2001; Stouthamer et al., 2011). Repeated avulsions caused new river courses to form, leaving the old channel belt abandoned. The remaining alluvial ridges of such abandoned river courses were gradually buried by overbank sedimentation from the younger channels, which caused the ridges to lose their topographic expression over time (Figure 6.2 – Cazanagli & Smith, 1998; Van Dinter & Van Zijverden, 2010). The burial of older alluvial ridges was driven by relative sea-level rise (RSLR) and upstream sediment supply. This burial took place relatively quickly in the beginning of the middle Holocene and gradually slowed down afterwards due to declining RSLR (Van Dijk et al., 1991). In the downstream parts of the delta, aggradation decreased from ca. 1 m/kyr around 5000 cal BP to ca. 0.3 m/kyr around 2000 cal BP. In the central and upper delta fluvial aggradation was ca. 0.8 m/kyr around 5000 cal BP and ca. 0.3 m/kyr around 2000 cal BP (Cohen, 2005; Stouthamer et al., 2011; Koster et al., 2016a).

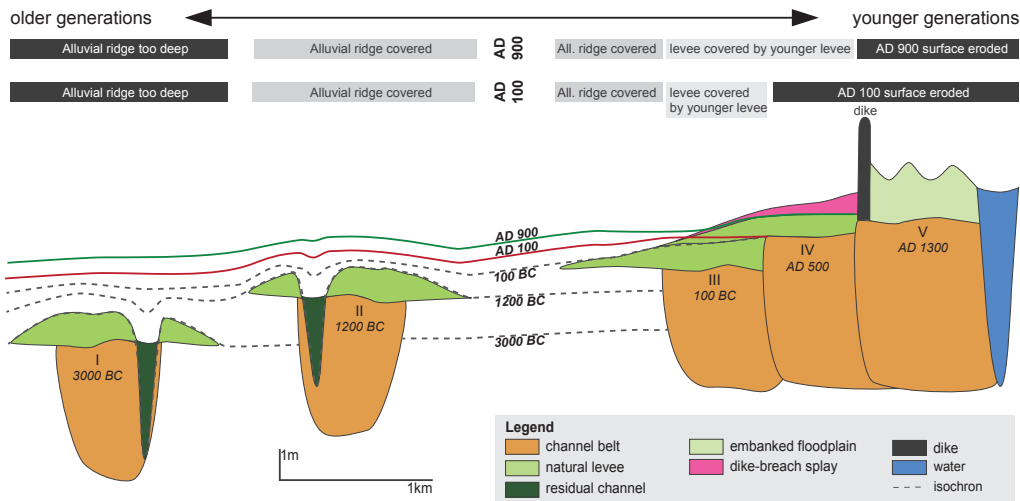


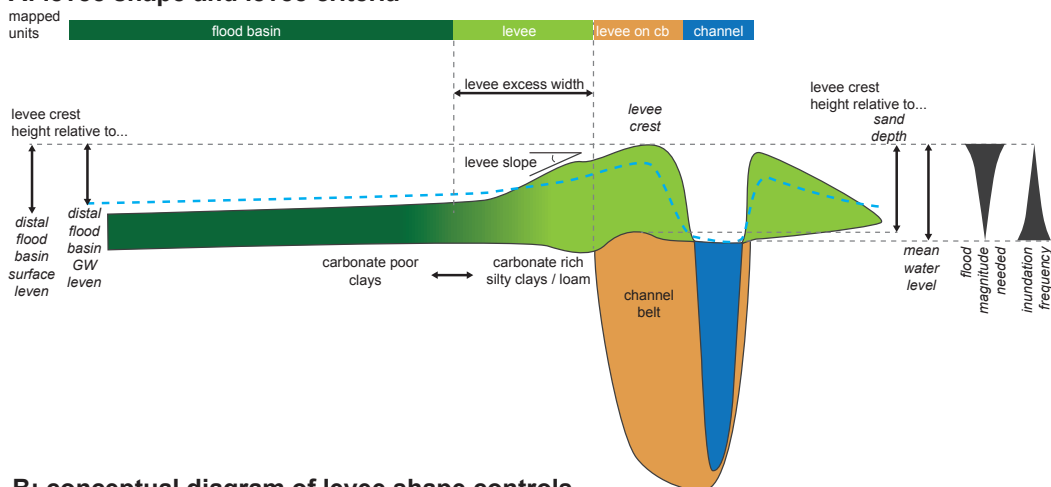
Figure 6.2 | Schematic cross-section showing age-depth relations between generations of natural levee complexes and channel belts. Older generations of levees (I–III) get buried by continued accumulation of levee and non-levee overbank deposits associated with younger channel belt generations and the flooding regime during their activity. The AD 900 surface roughly corresponds to the modern surface found in the LiDAR data, i.e. it matches the pre-embankment surface. Exceptions are the dike-breach deposits (post AD 900) and artificial elements such as roads, dikes, etc.

Due to deforestation in the upstream catchment, the supply of fine-grained sediments – which levees typically are composed of – increased considerably in the youngest millennia (Erkens & Cohen, 2009; Erkens et al., 2011). Notably the contribution of silt in the supplied sediment remarkably increased (Erkens et al., 2013). Another distinct change is the increased frequency of large floods in the Lower Rhine, particularly in the period AD 300–800 (Toonen et al., 2013; 2017; Cohen et al., 2016). The increased suspended load and higher flooding frequency together resulted in increased overbank sedimentation in the central and upper delta: here, aggradation rates were mainly controlled by sediment delivery from the upstream basin rather than by RSLR (Cohen et al., 2005; Erkens et al., 2011; Stouthamer et al., 2011). Increased sediment supply also resulted in the expansion of clastic sedimentation both in upstream and downstream directions over the last ca. 3000 years (Pons, 1957; Cohen, 2005; Gouw & Erkens, 2007). These developments concurred with channel network changes (Table 6.1 – Berendsen, 1982; Stouthamer & Berendsen, 2001; Stouthamer et al., 2011; chapter 5) and anomalously large meander lengths in the rivers of the first millennium AD (Weerts & Berendsen, 1995; Stouthamer et al., 2011).

6.2.2 Natural levee characteristics

Natural levees form the upper part of alluvial ridges and constitute semi-continuous zones of relatively higher (1–2 m) terrain. They flank infilled residual channels and active channels, and gradually slope downward toward the adjacent flood basins (Figure 6.3A). Alluvial ridges of the Rhine typically have levees with dominant clay-loam textures and are rich in calcium carbonate (Havinga, 1969; Weerts, 1996; Gouw, 2008). Their height and width are controlled by hydraulic and sedimentary conditions that act on a delta scale, such as the rivers' flood regime, upstream sediment delivery, and the delta-plain geometry – Figure 6.3B). Levees incrementally grow in height until

A: levee shape and levee criteria



B: conceptual diagram of levee shape controls

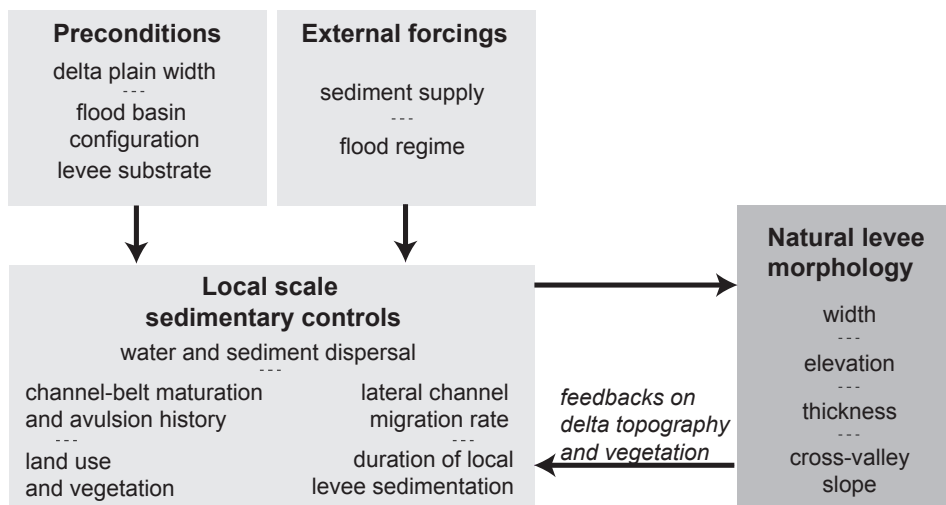


Figure 6.3 | (a) Levee shape and criteria. Idealised cross section of a channel belt and its levee in which the dimensions of levee shape are indicated. For levee width we primarily use lithological criteria, for height we use the elevation relative to the distal flood-basin groundwater. (b) Conceptual diagram of controls on levee morphology. Natural-levee morphology is influenced by local sedimentary controls that are in turn affected by antecedent conditions, i.e. delta-plain geomorphological setting (delta-plain width, flood-basin configuration, and substrate) and external forcings (flood regime, sediment supply). Delta-plain setting determines how water and sediments are dispersed throughout the flood basins (e.g. by controlling flood amplitude, trapping efficiency). The substrate determines lateral channel-migration rate, controlling the duration of local levee sedimentation and thereby levee morphology. Channel-belt maturation and avulsion history control the location and pace of new levee formation. Vegetation and land use (e.g. deforestation) affect levee sedimentation patterns, e.g. dense vegetation can trap more overbank sediments close to the channel. When levee shape changes, the local relief changes as well causing feedbacks on flood-flow, vegetation patterns, and land-use strategies.

they reach an elevation that is overtopped by rare high floods only. Therefore, the crest mean height of a mature natural levee is attributable to regularly recurring floods (bankfull discharge), and local crest maxima to the rare highest floods (Filgueira-Rivera et al., 2007 – Figure 6.3A).

Crevasse splays are a specific type of overbank features that forms in the flood basin when a levee breaches during floods. Although crevasse splays have a more complex sedimentological structure than natural levees (Smith et al., 1989; Farrell, 2001; Stouthamer, 2001; Shen et al., 2015), they can be lithologically and topographically difficult to distinguish, at least with the current data availability. This is because they can amalgamate with natural levees, which is the especially the case in the upstream and central parts of the Rhine-Meuse delta where the levees are relatively wide and the density of alluvial ridges is high.

Levee height in the study area ranges from 0.5–1.5 m above the adjacent surface of the flood basins (Berendsen, 1982). Around the Rhine apex, levees are generally higher: 1.5–2.5 m (Erkens et al., 2011). Levees are typically 1–2 m thick where they overlie channel belt sands, a contact that is usually gradational (Allen, 1965; Berendsen, 1982). Where a levee overlies compaction-prone substrate next to channel belts (e.g. peat), its thickness can be up to 4 m (Makaske et al., 2007; Van Asselen, 2011), which is considerably larger than their topographic relative height.

In the Rhine-Meuse delta, natural levees reach some 50 to 500 m into the flood basin, measured from the channel belt edge (excess width in Figure 6.3A). Lateral thinning of the levee deposits results in a gradual and diffuse transition between the levee and the flood basin (Figure 6.3A – Weerts, 1996; Törnqvist & Bridge, 2002; Gouw, 2007). Natural levee width is determined by factors such as channel size and discharge, sediment supply, vegetation, substrate, and flood-basin configuration (Figure 6.3B – e.g. Törnqvist & Bridge, 2002; Adams et al., 2004). Vegetation roughness results in steeper decreasing stream-power gradients from the channel to the flood basin, causing most sediment to be deposited close to the channel (e.g. Simm & Walling, 1998; Corenblit et al., 2007; Klasz et al., 2014), presumably resulting in narrow and steeper levees. Once formed, the levee relief in turn affects the local riparian vegetation patterns and flood hydraulics in its surroundings (i.e. by forming obstacles for flood flow) (Figure 6.3B).

When comparing multiple meanders within the same channel belt, levee shape tends to vary with meander geometry, rate of channel migration, local crevasse formation, and local interaction with pre-existent bank morphology and substrate (Figure 6.3B – Hudson & Heitmuller, 2003). Downstream decrease in levee width over large distances has been reported for the Mississippi delta (Kolb, 1963), the Blue River USA (Lecce, 1997), and the Pánuco Basin, Mexico (Hudson & Heitmuller, 2003). These authors link this trend to downstream fining of sediment associated with a longitudinal sediment depletion and decreasing stream power because of the declining floodplain gradients. In the Rhine-Meuse delta, reconstructions by Gouw & Erkens (2007) and Erkens & Cohen (2009) show a decrease in volume of overbank deposits by roughly a factor 2 between the upstream and downstream end of our study area – matching the trends in the above-mentioned studies.

Steepness (i.e. cross-valley slope) is a function of levee width, levee crest height and flood-basin height (Figure 6.3A). It can either directly be an important parameter for delta hydraulics and avulsion chances (Bryant et al., 1995; Heller & Paola, 1996; Mohrig et al., 2000) or more indirectly when compared to the downstream valley slope (Allen, 1965; Slingerland & Smith, 1998; Jones & Schumm, 1999). Although higher levees most likely favour initiation of avulsion, a critical threshold cannot be represented by one single value (cf. Törnqvist & Bridge, 2002), because avulsion triggering is affected by many other factors, such as flood-basin topography (Aslan et al., 2005; Lewin & Ashworth, 2014; Toonen et al., 2016).

Table 6.2 | Lithology (USDA classification) and geometry of architectural elements in the Rhine-Meuse delta (adapted after Weerts, 1996; Hesselink et al., 2003; Gouw, 2008).

Architectural element	Lithology	Geometry	References
Channel-belt deposits	Very fine to coarse sand. Occasionally gravel and sandy-silty-clay. Fining-upward sequence.	5–10 m thick 50–2000 m wide	Berendsen and Stouthamer (2000); Cohen et al. (2012)
Residual-channels deposits	Peat, humic clay, sandy to silty clay. Sometimes sandy loam and fine sand.	1–3 m thick 10–80 m wide 0.5–10 km long	Havinga & op 't Hof (1983); Toonen et al. (2012)
Natural-levee deposits	Horizontally laminated silty clay, clay loam, or loam, occasionally with layers of clay or fine sand. Fining-upward sequences are common.	0.5–1.5 m thick, thicker towards the channel belt 50–500 m wide, flanking channel belt	<i>This study</i>
Crevasse-splay deposits	Silty clay, clay loam, or loam, channels: sand.	Splay: 1–2 m thick 0.1–5 km wide Channels (erosive): 1–8 m thick 0.1–10 km long 10–200 m wide	Smith et al. (1989); Makaske et al. (2007); Stouthamer (2001); Van Dinter & Van Zijverden (2010)
Flood-basin deposits	Thin laminated to homogeneous clay and humic clay. Vegetation horizons.	1–5 m thick 0.1–10's km wide	Havinga & op 't Hof (1983); Edelman et al. (1950); Steenbeek (1990)
Organic beds	<i>Alnus</i> or <i>Phragmites</i> peat, can contain up to 70% of clastic material (De Bakker & Schelling, 1989).	0.1–5 m thick 0.1–10 km wide	Pons (1992)
Embanked floodplain deposits	Very fine to very coarse sand, with clay or sandy clay layers. Fining-upward sequences are common.	5–10 m thick 200–1500 m wide	Hesselink et al. (2003); Cohen et al. (2014)
Dike-breach deposits	Sandy to silty clay, sand or gravel admixture. Occasionally with sand lenses.	0.5–1.5 m thick 0.1–3 km wide	Pons (1953); Berendsen (1982); Hesselink et al. (2003)

During and after deposition, only modest soil development took place in the levees due to their short periods of surface exposure in the dynamic sedimentary delta environment (Edelman et al., 1950; Van Helvoort, 2003). Ripening (i.e. initial soil formation; Pons & Zonneveld, 1965) already occurred during levee formation, repetitively after the waning stage of each flood. Compaction of underlying flood-basin sediment and peat by levee loading mainly occurred while the levee formed, therefore ripening and compaction had only limited influence on the accuracy of the palaeo-elevation reconstructions in this chapter. Surface lowering as a result of groundwater-table management since ca. 1000 AD has mainly affected flood-basin areas (Havinga & Op 't Hof, 1983). This caused occasional re-exposure of buried alluvial ridges, but it has not significantly affected the elevations of the Common Era alluvial ridges as compaction had occurred already, mainly while the levees were forming. Only the distal parts of natural levees in the compaction-prone flood basins

have lowered along with the subsiding flood-basin surface, which hampers the reconstruction of past levee steepness.

6.3 Compiling and analysing the natural-levee maps

6.3.1 Approach and materials

To assess the patterns of levee geometry through the delta, we established (i) maps of reconstructed geomorphology of the landscapes around AD 100, 500, and 900, with the spatial distribution of natural levees and other elements in planform (Figure 6.4); and (ii) two palaeo Digital Elevation Models (DEMs) showing the topography of this levee landscape for AD 100 and 900 (Figure 6.5).

For the two datasets, we developed methodologies to (i) integrate existing heterogeneous geomorphological data (see chapter 2 and Appendix A) into new uniform maps, (ii) quantify burial depth of older levee surfaces where they are covered by younger and more distal overbank flood deposits, and (iii) determine whether buried older levee surfaces retained morphological expression at the time of reconstruction (Figure 6.2). The essentials of the methods are described in this section, and details are contained in Appendix C1.

The geomorphological reconstructions were compiled from several thematic base map layers, each containing the spatial extent and age of architectural elements in the delta subsurface (e.g. channel belts, levees). The levee base map is the primary base map in which the location and age of the levees were stored. In addition, base maps with the following architectural elements were compiled: (i) residual channel deposits that interrupt the levee cover on channel belts (Toonen et al., 2012); (ii) channel-belt sand bodies underlying levees (from Berendsen & Stouthamer, 2000; Cohen et al., 2012); (iii) outcropping sandy Pleistocene deposits (from Cohen et al., 2017ab); (iv) flood-basin deposits (clay or peat facies: e.g. Van Dinter, 2013); and (v) dike-breach deposits (Tables 6.2 and 6.3; Figure 6.2). These elements were mapped and stored in separate base map layers and together with the levee base map, merged into the integrated geomorphological reconstruction maps (Appendix C1.2).

The maps were based on borehole queries, LiDAR data (Figure 6.4C), and existing maps (e.g. soil maps, geomorphological maps, and palaeogeographical maps – Berendsen, 2007). For a complete description including resolution, coverage, scale, and references of the various types of data used in this study, the reader is referred to Appendix A.

6.3.2 Geomorphological reconstructions

Mapping the levee extent

Based on general levee characteristics, three criteria were considered for identification of natural levees in the study area (Figure 6.3A; Table 6.2): (i) lithology: silty clay, clay loam, or loam, (ii) elevation relative to floodplain level: 1-2 meter, and (iii) pedology: the levee material is calcareous. Distinguishing levees by carbonate content generally is less reliable as calcium carbonate was partly leached during later surface exposure; moreover, the criterion does not apply to the carbonate-poor natural levees of the Meuse. The use of elevation criteria can lead to diffuse boundaries when levees are wide and have low slopes. Levee boundaries also vary with the selected delta-plain gradient. Therefore lithology was chosen as the most clear and objective primary criterion for levee identification.

To identify the boreholes with natural levees, we first queried the borehole database for the criterion 'at least 40 cm thick layer of silty clay, clay loam and/or loam in the upper 2 meters

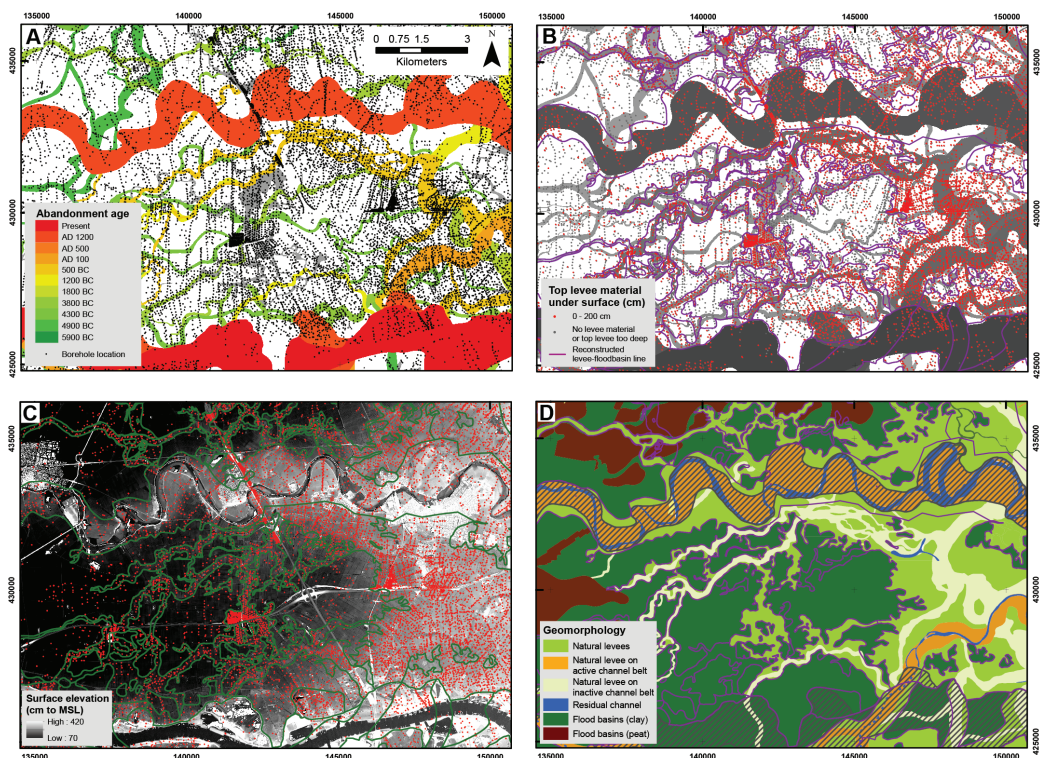


Figure 6.4 | Production steps in the natural-levee extent map. The location of the example area is indicated in Figure 6.1. (a) High-density borehole data projected on the channel belt map of Figure 6.1. This borehole data was the main source for the geomorphological levee map (b) Queried borehole results (presence levee/crevasse splay deposits) within 200 cm below the current surface and manually digitised boundary between floodplain and levee (purple lines, also in panels C and D) (c) LiDAR image used to refine the levee to flood-basin boundary derived from the borehole data. (d) Landscape reconstruction with the channel belt base map and levee base map combined, the diagonal line pattern indicates reworking by younger channels.

below the surface’ (Appendix C1.1). We then used LiDAR imagery, showing the shallow levees, as a secondary criterion (Berendsen & Volleberg, 2007; De Boer et al., 2008), to manually digitize the levee delineations from the borehole queries and the earlier maps. Crevasse splays were treated as part of the natural levee complex as they are lithologically and topographically mostly indistinguishable on the considered scale.

Age attribution

Assigning the correct age to the mapped levees is important in order to trace their development and to link their activity to changing forcings such as changes in floods, sediment load regimes or phases of habitation. On-site age control was provided by over 300 ^{14}C dates (Berendsen & Stouthamer, 2001; Cohen et al., 2012; Van Dinter et al., 2017), ca. 70 sites with pollen records (e.g. Teunissen, 1988; Törnqvist, 1990), and numerous independently dated archaeological sites (e.g. Willems, 1986; Berendsen & Stouthamer, 2001). Because the presence and extent of architectural elements is relatively well known, relative dating methods provided further age constraints, for example by

correlating features in detailed cross sections (e.g. Törnqvist, 1993; Weerts & Berendsen, 1995; Cohen, 2003; Gouw & Erkens, 2007). The combined architectural mapping and dating strategies are described extensively in Berendsen (1982), Törnqvist & Van Dijk (1993), Gouw & Erkens (2007); and further references in Table 6.3. The levees either overlying the channel belts or directly flanking them were assigned the age of the associated channel belt. We manually assigned begin and end ages of activity to the digitized polygon elements of the new natural levee base map. Similarly, we manually assigned ages to residual channel polygons in the second base map.

Time-sliced reconstructions assembled from base maps

To compile reconstructions of the natural-levee landscape, both the actively forming and the fossil levees (younger than 2500 BC) were selected for AD 100, 500, and 900 based on their assigned ages. Levees of older channel-belt generations were presumed to lack any surface expression during the first millennium AD (Figure 6.2 generation II and III). The < 2500 BC criterion was chosen based on the levee surface expression of various levee generations inferred from delta-wide cross sections (Gouw & Erkens, 2007), this was later verified in section 6.3.3. Furthermore, younger elements, such as eroding channels or younger generation of levees, were removed from the reconstruction. Our GIS method is an extension of the approach described earlier in Berendsen et al. (2007) and chapter 3 and is further outlined in Appendix C1.2.

6.3.3 Natural levee palaeo-topography

Palaeo-DEM calculation

Once the levee extent was reconstructed for AD 100, 500, and 900, we compiled two palaeo-DEMs (digital elevation models) for AD 100 and 900. We started with the natural levee palaeo-topography in AD 900, using the LiDAR elevation at the locations of boreholes where levees were encountered in (i.e. within the levee landscape zones in Figures 6.2 and 6.5). Where artificial landscape elements (e.g. roads, dikes, cities) were present, we used the original surface elevation derived from the original borehole description (for ca. 10% of the boreholes).

For the AD 100 palaeo-DEM, the vertical position (relative to the surface) of the top of the levee material was queried from the 70,000 boreholes (Figure 6.5A). This does however not directly represent surface level at a given time step, as clay draping has occurred after levee abandonment (Figure 6.2). We therefore assessed distal clay deposition on top of the older levees, by assuming a linear accumulation rate towards the AD 900 surface (this procedure is further outlined in Appendix C1.3). Both DEMs show landscape surface level relative to MSL. They were obtained by interpolating the reconstructed surface level at the borehole locations by quadratic inverse distance weighting, using a maximum of 10 nearest points within a 2 km radius. The delineations of the levee to flood-basin transition and of the residual channels from the geomorphological reconstructions were used as break lines for the interpolation procedure (Figure 6.5B, E). In areas close to modern rivers, where deposits were formed by sedimentation of younger natural levees and dike breaches, we added a mask that highlights overestimation of the levee surface level (Figure 6.5C).

Converting palaeo-topography to relative elevation

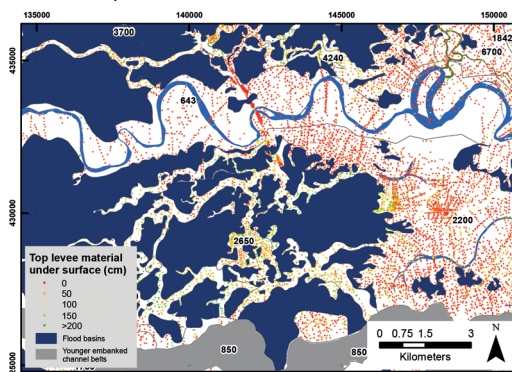
The AD 100 and 900 DEMs (in m NAP; NAP = Dutch Ordnance Datum \approx MSL) were normalised to the floodplain gradient, producing DEMs of relative elevation (Figure 6.5C, E, Appendix C1.3). As the reference plane for normalisation, we used relatively smooth groundwater level reconstructions for the first millennium AD (Cohen, 2005; Koster et al., 2016a). These interpolated grids are a

Table 6.3 | Age attribution to the three sets of architectural elements in the Rhine-Meuse delta. TAQ = *Terminus ante quem* (date indicating minimum age), TPQ = *Terminus post quem* (date indicating maximum age).

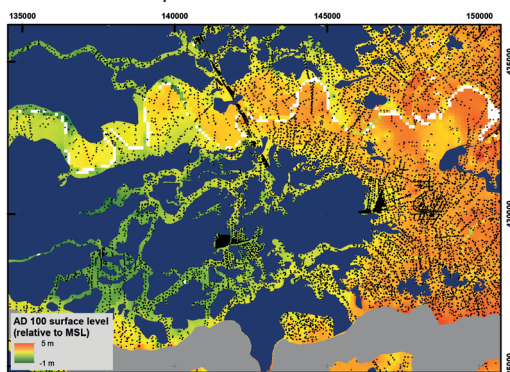
Phase	Indirect dating	Direct dating	Potential errors	References
Channel belts and crevasse channels – Channel belt base map (Berendsen & Stouthamer, 2001; Cohen et al., 2012; and further updates)				
Begin (initiation, avulsion belt)	Deduced from dating flood basin organics, overlain by overbank deposits with non-erosive contacts (TPQ)	OSL from channels of avulsion-belt complex.	Time lag between accumulation of organics and burial by overbank clastics	Verbraeck (1970); Berendsen (1982); Törnqvist & Van Dijk (1993)
Activity (maturation)	From dating 'Begin' and 'End'. Also from archaeological dates: trapped water-bound archaeology or deduced from sites undercut by riverbank erosion (TAQ).	1) OSL from point bar facies; 2) ¹⁴ C on reworked material from bar facies or thalweg lag deposit (TPQ); 3) dating washed-in organics at contact pointbar-levee (TAQ).	1) single ¹⁴ C dates of reworked material are often much older than the begin age; 2) OSLs show a bias towards the younger half of the period of activity, owing to river migration and reworking.	Berendsen (1982); Hesselink et al. (2003); Cohen et al. (2014b).
End (abandonment)	Deduced from 1) base residual channels (TAQ) or ; 2) organics on top of flood-basin deposits; 3) begin ages of upstream new-avulsed channels; 4) correlation to high-magnitude events.	1) OSL on plug bars and residual-channel associated point bar; 2) archaeology (TAQ).	Slow initial abandonment leading to delayed onset of accumulation of organic residual channel facies.	Verbraeck (1970); Berendsen (1982); Törnqvist & Van Dijk (1993); Toonen et al. (2012); Cohen et al. (2016).

Phase	Indirect dating	Direct dating	Potential errors	References
Residual channel infills – Residual channel base map (this chapter)				
Begin (base)	1) Adopting dates for End-of-Channel belt activity, obtained outside residual channels; 2) Pollen-evidence from base of infill.	¹⁴ C date of base of infill.	Carbonaceous clay-gyttja organic sediment are susceptible for hard water effect – this can be avoided by picking riparian macrofossil for AMS ¹⁴ C dating.	Verbraeck (1970; 1984); Berendsen (1982); Törnqvist & Van Dijk (1993); Berendsen & Stouthamer (2001).
Activity (silting up)	1) From dating 'Begin' and 'End'; 2) pollen-evidence from within infill; 3) change of infill facies correlated network change.	1) ¹⁴ C date in infilling; 2) archaeology in infilling; 3) recognising event-beds major floods in infilling.	Reactivations by crevasse and chute-channels, cause hiatuses in the infill.	Teunissen (1988); Törnqvist (1990); Hoek (1997); Toonen et al. (2012); Toonen et al. (2013); Minderhoud et al. (2016); Cohen et al. (2016).
End (top)	Soil horizons or archaeological layers in top of the fill.	¹⁴ C date top infilling (TAQ).	Final stages of lacustrine infill very local and diachronic over the residual channel element.	Verbraeck (1970); Berendsen (1982); Törnqvist & Van Dijk (1993); Hoek (1997).
Natural levees and crevasse splays – Natural levee base map (this chapter)				
Begin (initiation, avulsion belt)	Deduced from dating flood-basin organics, overlain by overbank deposits with non-erosive contacts (TPQ).	Buried archaeology (TPQ).	Time lag between accumulation of organics and burial by overbank clastics.	Verbraeck (1970); Berendsen (1982); Törnqvist & Van Dijk (1993).
Activity (maturation)	Pollen in levee deposits (TAQ).	Archaeology within levee deposits (TAQ).	Levee preservation bias to younger half of activity period, owing to river migration and reworking – affects long-lived largest river channels mainly.	Verbraeck (1970); Berendsen (1982).
End (silting up)	1) Deduced from associated res. channel 'Begin' dates (TAQ). 2) By adopting channel belt 'End' dates (TAQ).	Archaeology in the top of the levee deposits (TAQ).	Early abandonment stages of channel belt (narrowing channel) may be last pulses of levee aggradation, especially near bifurcations.	Verbraeck (1970); Willems (1986); Berendsen (1982); Törnqvist & Van Dijk (1993); Van Dinter (2013).

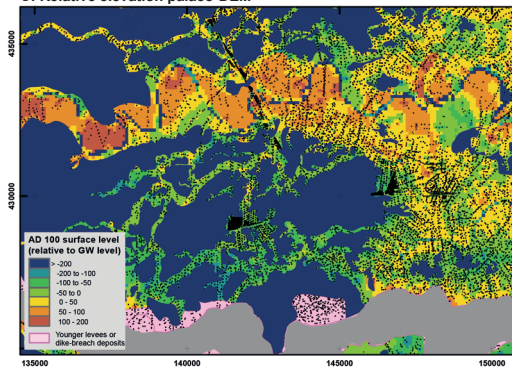
A: Borehole queries



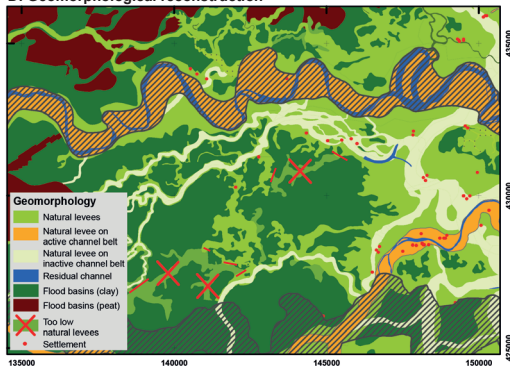
B: Absolute elevation palaeo-DEM



C: Relative elevation palaeo-DEM



D: Geomorphological reconstruction



E: schematic workflow

Borehole description queries

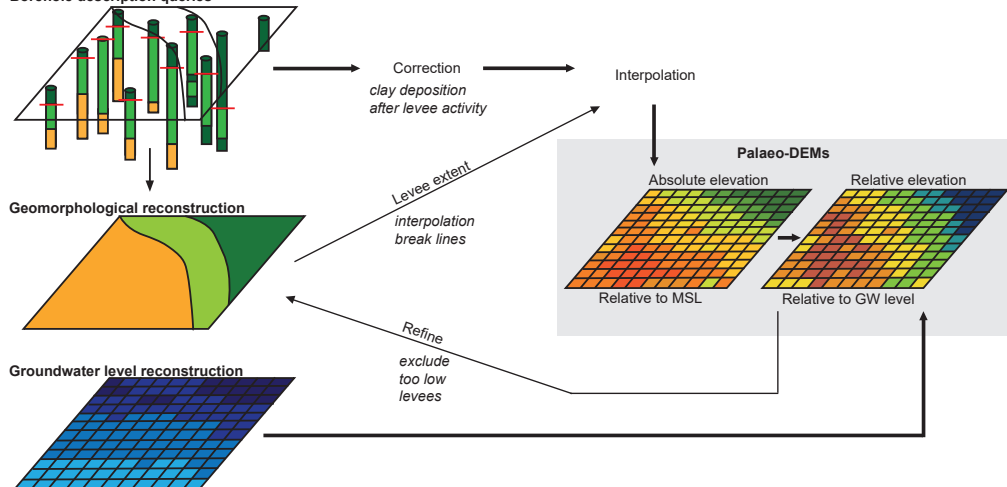


Figure 6.5 (left page) | Palaeo-DEM production steps, location of example area indicated in Figure 6.1. (a) Source data for palaeo-elevation map: borehole database query results for the vertical position of the top of the levee (depth in the borehole) and age of the levee complexes (obtained from channel belt age maps Figure 6.4A). The query results were corrected for burying flood-basin sedimentation after levee sedimentary activity (Appendix C1.3). (b) Elevation of the top of the levees (m OD). (c) Relative elevation of the top of the levees, using a reconstructed groundwater surface 2000 cal BP as reference plane (Cohen, 2005; Koster et al., 2016a). (d) Confrontation with natural levee extent mapping, dark tone alluvial ridges with red crosses indicate too deeply buried levees (> 2 m relative depth), these are considered to have had no surface expression in the floodplains of the first millennium AD (also confirmed by absence of archaeological settlement finds from that period, red dots were taken from Pierik & Van Lanen, 2017). (e) Outline of the workflow of Figure 6.5A-D, explained in a diagram.

uniform delta-wide dataset and have a vertical accuracy of ca. 13 cm (Cohen, 2005). These grids were considered more suitable than reference planes based on present-day surface LiDAR data, which suffers from differential surface lowering effects in downstream polders (e.g. Erkens et al., 2016) and post-embankment dike-breach fans that could cause elevation artefacts along modern rivers. The reconstructed groundwater surfaces are some decimetres below the average levee crest elevations, which is in agreement with soil formation observations (e.g. Edelman et al., 1950) and past human land use as inferred from archaeology (e.g. Willems, 1986). At the transition from levees to flood basins (relative elevation = 0), the water tables approximate the reconstructed surface level. To calculate the natural levee elevation relative to groundwater level at AD 100 and 900, the groundwater level reconstructions for 2000 and 1000 cal years BP (50 BC resp. AD 950) were subtracted from, respectively, the AD 100 and 900 DEMs. For discussion of the accuracy of the resulting palaeo-DEM, see Appendix C1.3.

Inactive channel belts that were abandoned before 2500 BC were initially incorporated in the reconstructions (section 6.2.3; Figure 6.2). From the paleo-elevation reconstruction, we could then compare the vertical positions of these older levees relative to the reconstructed groundwater level. We considered natural levees that occurred deeper than 1 meter below the reconstructed groundwater level as buried ‘too deep’ to have had full surface expression in terms of natural soil formation and human land use. Therefore, we manually labelled such areas as ‘inactive’ in the levee base map (red crosses in Figure 6.5D) and subsequently repeated the procedure in section 6.3.2 to update the levee extent of the geomorphological map resulting in Figure 6.6. The too-low top of these levees is confirmed by the absence of Roman settlements on these locations (chapters 7 and 8).

6.3.4 Regional-scale analysis

Based on the map products, we divided the delta into three main segments: (i) a narrow upstream segment with wide levees and narrow flood basins (U1-U4), (ii) a widening middle segment containing multiple channel belts with abundant and wide levees (C1-C4), and (iii) a wide downstream segment (D) with wide flood basins and narrow levees (Figures 6.6-6.9). Within these segments we made a further subdivision based on our newly mapped characteristic levee morphology, e.g. levee surface area, average alluvial ridge elevation (Figure 6.10). For each delta segment we quantified the areal cover, the average elevation, and the variation in elevation of the levee landscape. We additionally isolated 13 single-generation channel belts throughout the delta (indicated with white lines in Figure 6.9), of which we derived metrics on levee width, asymmetry, and relative elevation. Width and asymmetry in width were inferred by comparing excess levee widths (i.e. distance from the channel belt to the flood basin – Figure 6.3A) measured every downstream kilometre. After quantifying these differences in levee shape, we compared these across

Figure 6.6 (*right page*) | Geomorphological reconstructions for AD 100, 500, and 900, for the central and upper Rhine-Meuse delta (Figure 6.1). See Appendix C2 for large version.

the entire delta to the independently reconstructed controls (e.g. flooding regime, sediment supply, avulsions) that varied during the studied period. From this comparison the levee-forming processes were inferred.

6.4 Spatial and temporal variations in levee geometry

6.4.1 Delta-wide longitudinal trends

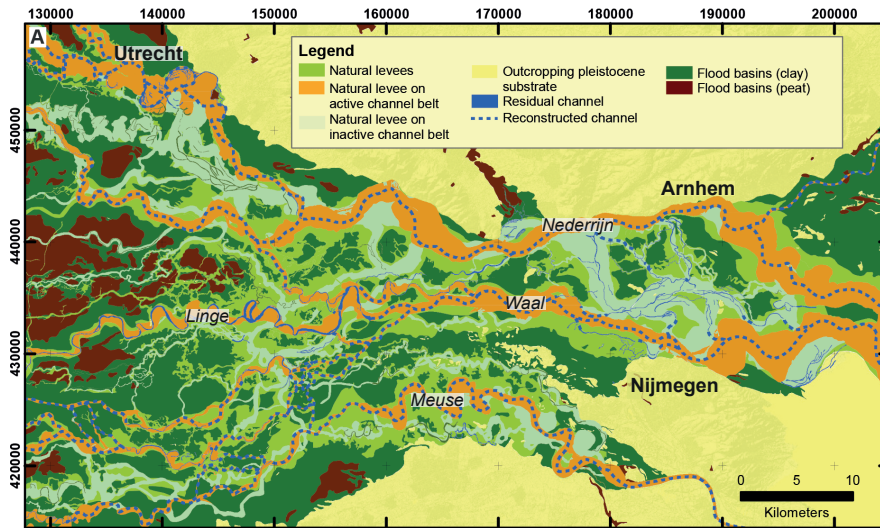
In the upstream part of the study area (segment U1), relatively high levees (1–2 m) are present in both the AD 100 and 900 reconstructions (Figures 6.7A, B and 6.9B). This is also the area where delta-plain width decreases in downstream direction from 30 km around the apex to 13 km in segment U1 (Figure 6.1 and red triangle 1 upstream in Figure 6.9B). Going downstream, around U2 and U3 the delta-plain becomes wider again (from 13 km to 20 km) coinciding with lower levees elevated on average 20–30 cm in U2. In the downstream part of U2 narrowing occurs (20 to 9 km Figure 6.9B, red triangle 2), this corresponds to levee heights of 0.5–1 m around the narrow part downstream of U2. We interpret the high levees as products of relatively higher flood-water levels that formed when flood propagation was hampered when floods reached the narrowing of the delta plain in segment U1. The amplified flood levels, allowed overbank sedimentation to reach relatively high elevations resulting in higher natural levees above the regional groundwater level. In U1, flood amplitudes were likely further increased by three N-S oriented alluvial ridges that hampered flow in the delta plain (Figures 6.8B, C). The levee heights indicate that the typical morphology-forming flood would have reached 0.5–1 m higher in the narrow segments, compared to wider segments (U2) and segments further downstream.

The average cover of alluvial ridge area in our maps ranges from 67% in the upstream sections (U1–U4), to 62% in the central delta (C1–C5), to 14 % in the downstream part (D). Segment C3 proportionally contains the most levees and crevasse splays (75–80% of 314 km² Figure 6.8C). Roughly 75% of the levees in this segment date from rivers that were active during the last millennia BC, which caused this segment to be a relatively high part in the delta from the first millennium AD onwards (Figure 6.7A, B). The abundant levees can be seen as the result of repeated avulsions and failed avulsions known to be concentrated in this area (Stouthamer, 2001; Bos & Stouthamer, 2011), associated with neotectonic subsidence downstream of the Peelblock and Peel Boundary Faultzone (Figure 6.1; Berendsen & Stouthamer, 2000; Cohen et al., 2005; Stouthamer et al., 2011).

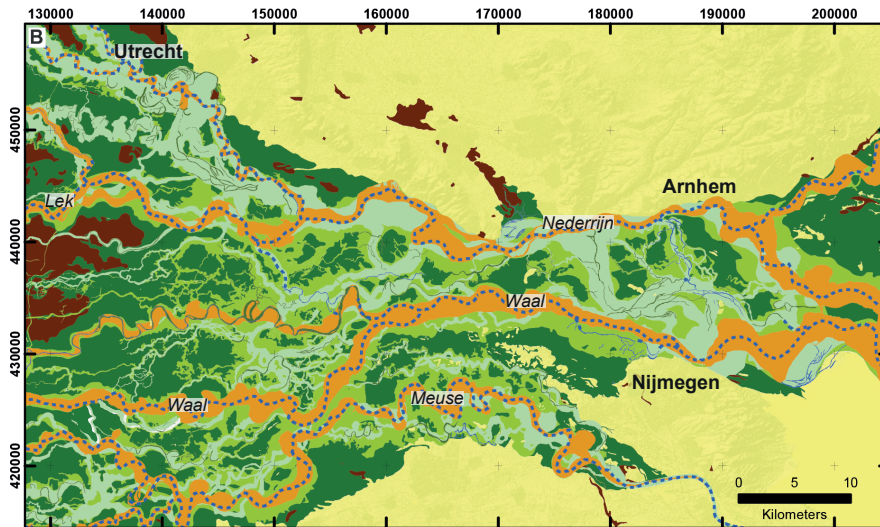
Levee-excess width decreases in a downstream direction (Figures 6.6 and 6.10C), also the boundaries from levee to flood basin become sharper in a longitudinal direction. In our results, the relation between levee-excess width and downstream position was relatively strong ($R^2 = 0.79$; $n = 13$ – Figure 6.10C). This implies that downstream position is the most dominant predictor for average levee width along a channel belt, in our case it is more important than channel-belt width (Figure 6.10D; $R^2 = 0.13$). The abundancy of levees in the upstream and central parts of the delta combined with their decreasing widths, suggests that coarse-grained overbank deposits were probably relatively efficiently trapped here.

6.4.2 Levee development between AD 100 and 900

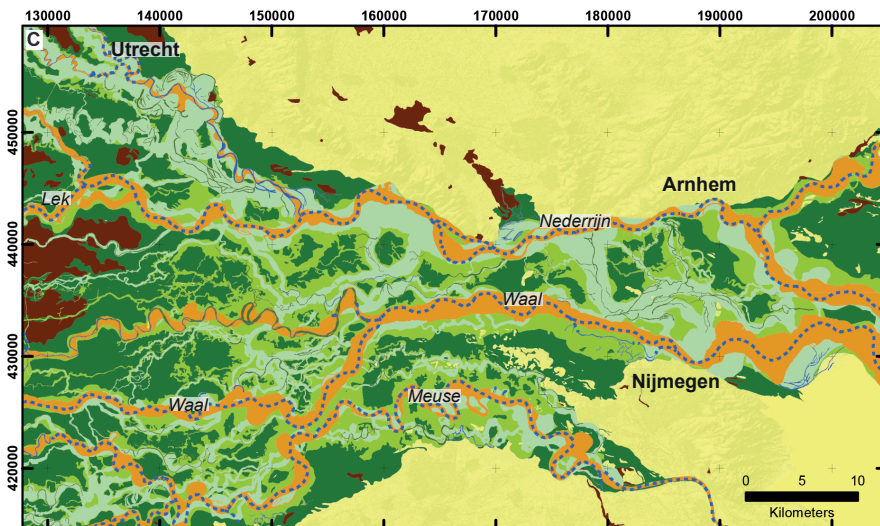
Avulsion during the first millennium AD caused levee depocentres to shift: the new river courses replaced flood-basin areas with levees, increasing their areal portion from 57 to 64 % of the total



AD 100



AD 500



AD 900

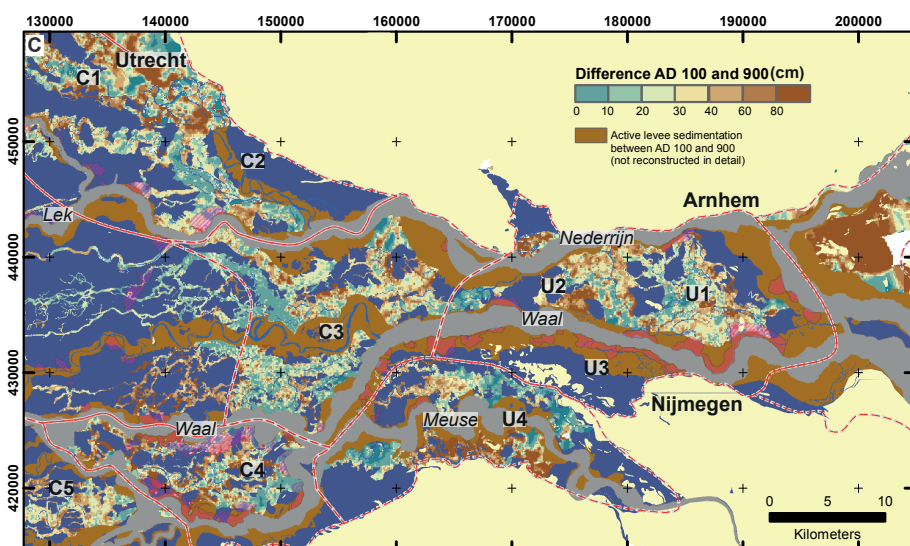
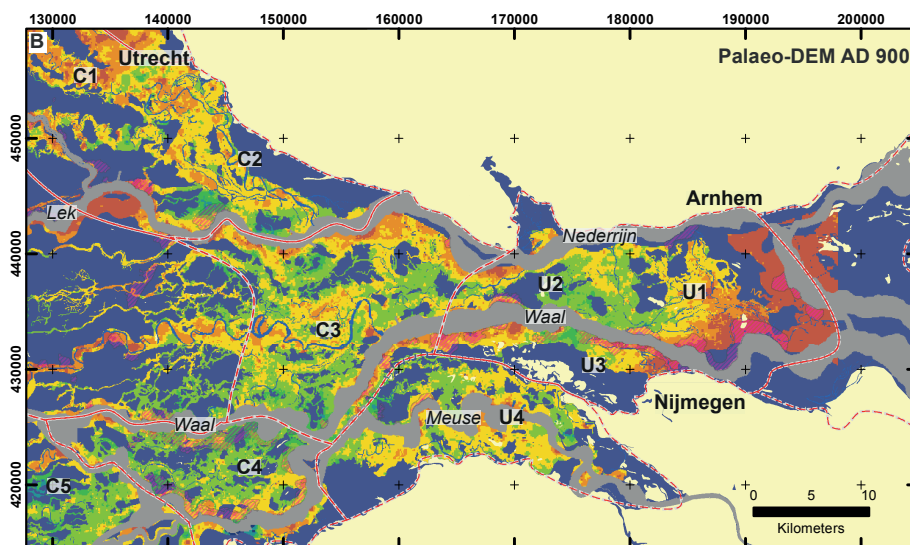
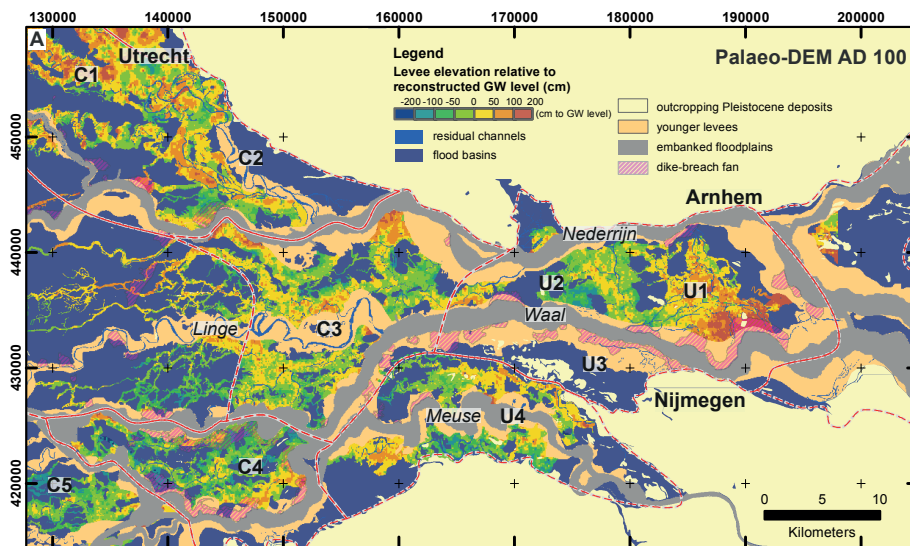


Figure 6.7 (left page) | Palaeo-DEMs for the central and upper Rhine-Meuse delta (Figure 6.1), showing the relative elevation of the natural levees at (a) AD 100 (0 m = groundwater level 2000 BP) and (b) AD 900 (0 m = groundwater level 1000 BP), and (c) the elevation difference of the levees between AD 100 and 900. See Appendix C2 for larger files.

area in the C and U segments. Routing of the new channels was determined by the levee topography in the delta: it explains the position of the new river Waal which was diverted around area C3 towards the low-lying segment C4 (Figure 6.7). Development of avulsions within the enclosed basins was limited because splay development was blocked by a neighbouring channel belt (cf. Toonen et al., 2016). Clay draping on fossil natural levees (i.e. of the inactive channel belts) at more distal positions from the active channels raised these levees by a few decimetres over the studied period (39 ± 32 cm on average delta-wide). The clay layer on the higher fossil levees was thinner than on the lower levees and the flood basins, causing topographical levelling (Figure 6.7C). No downstream trend was found in the amount of clay deposited on the fossil levees in this study (compare orange and green bars in Figure 6.10A). The topographical levelling of the old levee landscape contrasts with the high new levees along the active channels. As an example, in section U3 and along the river Lek in section C2, the new levees locally appear about a meter higher compared to the levees of their precursors (Figures 6.7, 6.9, and 6.10A).

6.4.3 Trends along individual channel belts

Levee width varies considerably along individual channel belts, regardless of longitudinal position, age, or channel-belt width (Figures 6.6-6.9). Remarkably, levee width of N-S oriented alluvial ridges is asymmetric, the most notable cases in the upper and central delta are indicated as W2 in Figure 6.8. The levees on the western side of these channel belts are 500 to 1500 m wide, whereas those on the eastern side are at most a few hundreds of metres wide. This asymmetry changes with channel-belt axis orientation relative to the E-W trending delta-plain slope ($R^2 = 0.63$; $n = 13$ – Figure 6.10B). This relation was found in all segments of the delta, although less pronounced at first sight downstream where levees are less wide. The preferential overbank sediment transport in the direction of the overall delta-plain slope indicates that levee dimensions were controlled by flow patterns in the flood basins. They most likely formed during a high flood stage when flood-basin throughflow had established. In the upstream and central segment (C3), the presence of these N-S directed channel belts caused the flood basins to be enclosed. During floods, breaching of these N-S oriented channel belts, created E-W oriented overflow channels (e.g. Est, Ommeren; blue arrows in Figure 6.8D, E – Havinga and op 't Hof (1983), again showing that considerable flow occurred in these flood basins, at least during the most severe floods of the first millennium AD.

Generally, levee complexes tend to be widest in the upstream parts of channel belts, i.e. just downstream of their avulsion points (500–1500 m – indicated with W1 in Figure 6.8A, B). Most likely, these features formed as multi-channel avulsion belts during the initial stage of channel-belt activity (Smith et al., 1989; Stouthamer, 2001; Makaske et al., 2007), rather than representing levees from the single-channel mature phase of these channel belts. The avulsion belt deposits are especially well-preserved along relatively narrow and short-lived channel belts.

Within single channel belts, significant differences in elevation occur. Generally, levees on top of channel belts are highest (compare elevation inside and outside channel belts, black dotted lines in Figure 6.9), but when they overlie flood-basin deposits they can also be relatively high. Where residual channels have preserved as pronounced meanders, the dataset allows to compare levee size along the inner bends (e.g. covering point-bar channel deposits) and along outer the bends. Levees

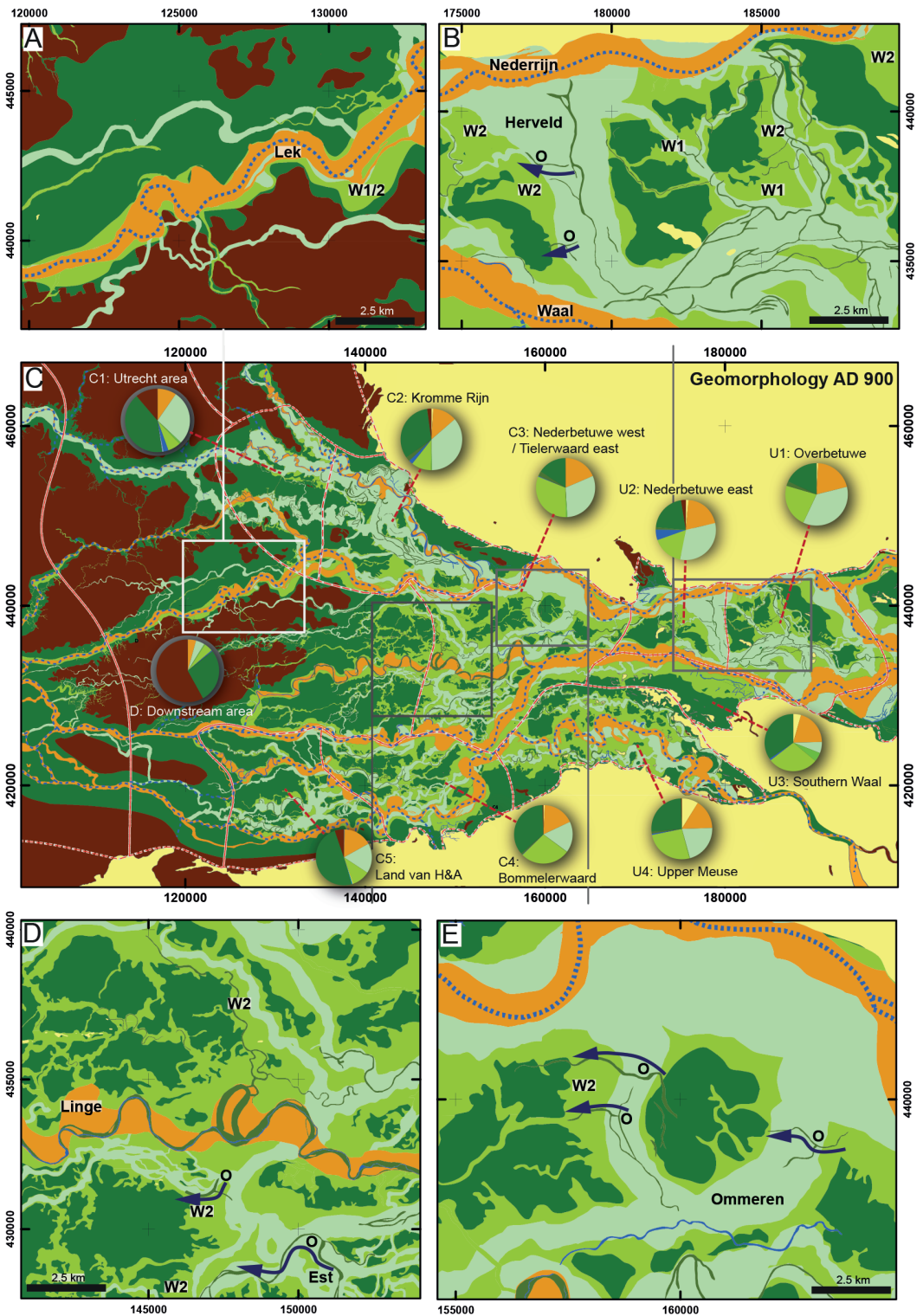


Figure 6.8 (left page) | Geomorphological reconstruction for AD 900, with pie charts indicating areal proportions of landscape units per segment, for legend see Figure 6.6A. O = overflow channel, W1 = Wide levee/crevasse splay in upstream part channel belt, W2 = wide levee flanking S-N oriented channel belt, forming in line with regional westward sloping delta-plain gradient.

in the inner bends of meanders are relatively high (1 to 1.5 m), whereas along the outer bend levees are narrow and lower (around flood-basin level and max. 100 m wide – e.g. Linge, Alm/Werken channel belts in Figure 6.9A, C). The lower and narrower levees on the outer bends appear to contradict the hydraulic concept of cross-channel water-level setup towards the outer bends owing to flow momentum, which would generate higher and wider outer bend levees (Leopold & Wolman, 1960; Hudson & Heitmuller, 2003). The causes of higher levees in the inner bends compared to the outer bends, can be sought in (i) topping up of the original levees with additional silty sediments as an abandonment overprint, in the final stages of ephemeral flow activity, in a narrowing channel and at reduced flow velocities (e.g. Toonen et al., 2012; Van Dinter et al., 2017), and (ii) post-depositional compaction of flood-basin sediments underlying the outer bend levees (e.g. Van Asselen, 2011). These mechanisms can explain the differences in height between the inner and outer bends. The controls behind the narrow outer-bend levees, however, remain to be further explored.

6.5 Discussion

6.5.1 Controls on natural-levee shape

From the reconstructions, we inferred that natural-levee morphology was controlled by spatially varying antecedent conditions and temporally varying forcings. In the results section the levee dimensions and configuration were described, together with the hydraulic and sedimentary processes that formed them. This discussion section builds on this by formulating hypotheses on the relative importance of antecedent conditions (delta-plain width, substrate), external forcings (variation in discharge and sediment load) (Figures 6.3B and 6.11), and downstream trapping that controlled levee shape in the first millennium AD.

Role of antecedent conditions: Our results strongly suggest that levee dimensions were not solely determined by the flooding regime and channel dynamics of the Rhine branches. They were also controlled by conditions occurring in the inundated flood basins. The higher levees that formed in the narrow parts of the delta are a clear example of this. The inference that in our case, the narrowing of the upper delta floodplain caused higher flood amplitudes, differs from studies on levee morphology carried out in more confined valley systems of a few kilometres wide (e.g. Magilligan, 1985 – Galena river, US; Lecce, 1997 – Blue river, US; Kiss et al., 2011 – Danube, Hungary). In these examples, floodplain narrowing, besides raising the water level, also led to increased stream power, keeping sediments in suspension and subduing overbank aggradation (i.e. keeping the levees relatively low). In the 1 to 2 km-wide reaches of the anastomosing Columbia River valley (Canada, Filgueira-Rivera et al., 2007), confinements also caused significant flood heights and flow velocities, which limited levee width, but allowed them to aggrade relatively high and to become relatively steep. In the Rhine-Meuse delta, the narrowed reach of the delta plain is a factor 10 wider than the valley examples, and additionally the upstream segments contain alluvial ridges that cross over the entire delta plain (i.e. compartmentalisation of the delta plain). These differences in antecedent conditions caused the through-flow velocities in the flood basins (i.e. stream power) in the upper Rhine-Meuse delta to be less strongly raised compared to the valley examples. Numerical hydraulic modelling could further test the critical levels of delta-plain

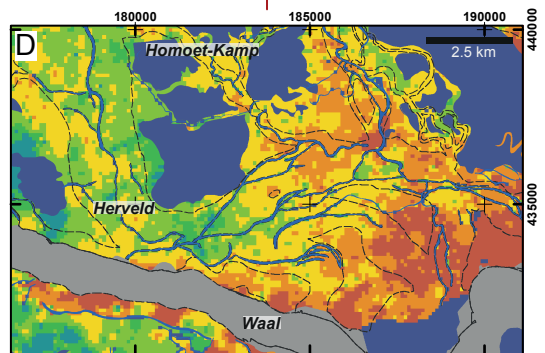
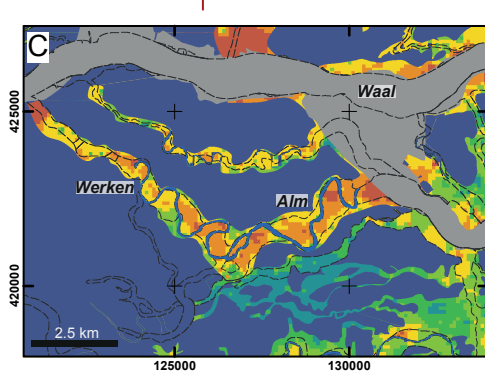
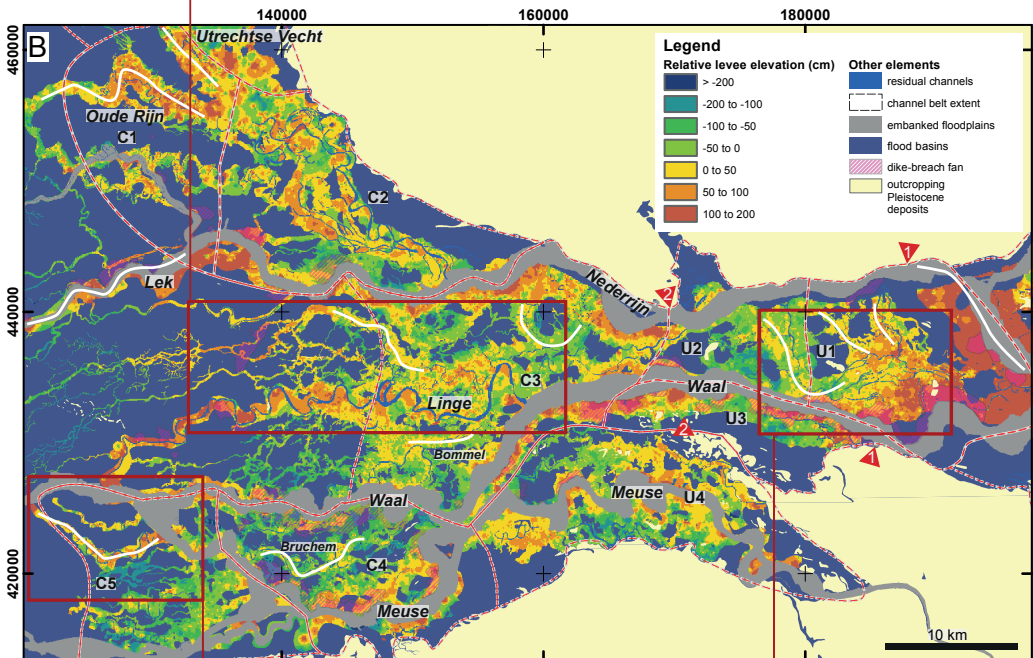
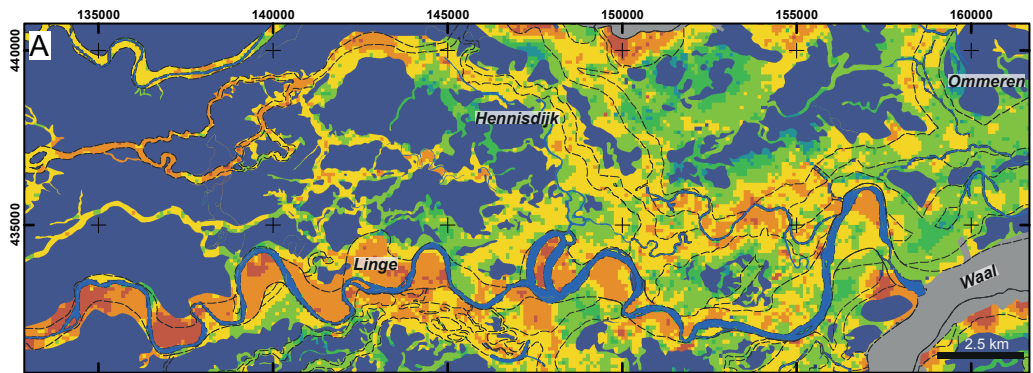


Figure 6.9 (left page) | Examples of relative levee elevation AD 900. White lines indicate the channel belts that were analysed on levee-excess width, the red triangles indicate the two reaches of delta-plain narrowing. (a) and (c) show examples of variation in levee height on a meander-belt scale. (b) overview of natural-levee relative heights across the delta (calculated above surrounding flood basin mean groundwater level). White lines indicate channel belts used for the analysis in Figure 6.10. (d) zoom to the confined flood basins of the upper delta, with their high, accentuated levees. The names of channel belts discussed in the text are indicated.

narrowing, valley gradient, and obstacle height (alluvial ridges) that cause levees to grow higher or cause their development to be subdued by overflow. Such studies can use the reconstruction maps as realistic input topography to further test the basic principles of delta-plain width and flood-water level and its implications for overbank sediment dispersal and deposition.

Another antecedent condition that influenced levee geometry is the substrate adjacent to the channel belt and underlying the levee (Figures 6.2B and 6.11), especially in the more downstream segments where the levees overlie compacted peat. Subsidence of the underlying peat in response to loading with levee sediment created extra accommodation space for overbank sedimentation (Van Asselen, 2011). Furthermore the erosion-resistant properties of peat retarded channel-bank erosion and hence caused the channel position to be fixed (Makaske et al., 2007) and levee sedimentation for long periods at the same place. Subsidence and channel fixation combined resulted in narrow but rather thick levees that did not become very high.

Role of external forcings changing over time: Especially in the upstream parts of the study area, the crests of the youngest levee generations, formed along newly avulsed main river branches, are clearly higher (0.5 to 1 m above groundwater level in segments U1, U2, U4, and C2 – Figure 6.10A), than levees along similar sized precursor channels. This is in part the result of the interaction of floods with the delta plain width and compartmentalisation described above. The high elevation of the younger levees may be additionally attributed to the greater availability of suspended sediments in the first millennium AD compared to the millennia before (Figure 6.11; Erkens & Cohen, 2009; Erkens et al., 2011) and the intensified flood regime after ca. AD 250 observed by Toonen et al. (2013; 2017). The observation that the volume of overbank sedimentation in levee complexes and flood basins (Erkens & Cohen, 2009) increased by a factor 1.6 to 2 from the last millennia BC to the first millennium AD, supports the idea that the young levees are larger because more levee building material was supplied (especially the silt fraction of the suspended load – Erkens et al., 2013). To explain the relative higher elevations, however, also frequent high flood levels are required as has been suggested for other river settings (Filgueira-Rivera et al., 2007). This principle is confirmed by our data: the AD 900 levees were formed in a period of increased frequency of large and moderate flooding of the Rhine, which locally caused levee crests to become ca. 1 m higher relative to the flood basin compared to their processors. The levees in the AD 100 landscape were lower as they had not experienced these large floods. Delta-wide, when comparing the average elevation of the entire levee areas (i.e. from the flood-basin limit to the channel, so not only the highest crests; Figure 6.2A) the differences between the AD 100 and 900 levees are smaller (compare yellow and purple bars in Figure 6.10A). This indicates a large spread in elevation within the youngest levee generation. Besides the levees, also the flood basins silted up (especially the lower parts by ca. 50 cm) aided by the increased sediment supply (Figure 6.11). The occurrence of severe floods is not regarded as important for the filling of the lower parts of the flood basins as it is for levees. This is because the lower flood basins were also inundated during lower or modest magnitude floods. Therefore, sediments will have reached the flood basins via crevasses and lower parts of the levees regularly (e.g. Makaske et al., 2002; Filgueira-Rivera et al., 2007).

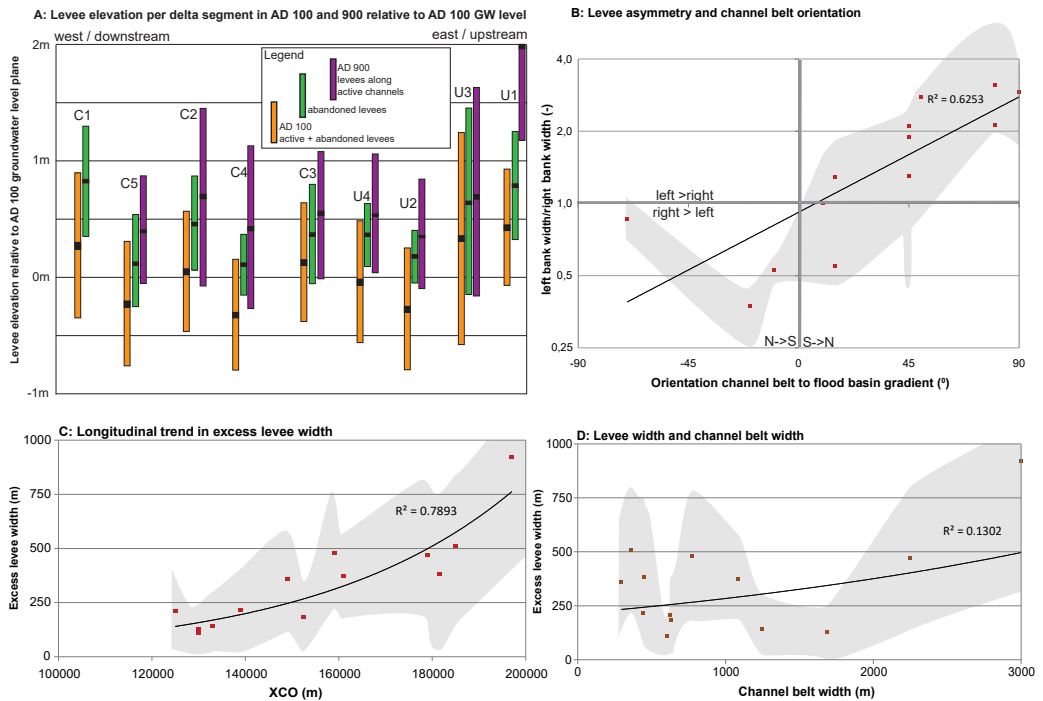


Figure 6.10 | (a) Levee elevation per delta segment in AD 100 (yellow bars) and AD 900 (green bars: all levees, purple bars: active levees only) relative to the AD 100 ground-water level, see also Table C1. (b) – (d) show metrics of levees along 13 channel belts throughout the entire delta (indicated in Figure 6.9). (b) Levee asymmetry is a function of channel-belt orientation: a larger angle of the channel belt relative to the flood-basin gradient yields more asymmetric levees (wider larger downslope). (c) A clear trend is observed in longitudinal position of a channel belt (mean position of the X-coordinate was taken) and the average levee width along the channel belt. (d) A weak relation is found between channel-belt width and excess-levee width.

It is well possible, that the higher levees along the new branches, induced feedbacks on channel morphology and avulsion probability. Considering channel morphology, previous studies have noted that the rivers of the first millennium AD developed larger meander wavelengths than their older counterparts (Weerts & Berendsen, 1995; Berendsen & Stouthamer, 2000), suggesting that these rivers could route more discharge through the river bed than their precursors. One can explain this increase in bankfull discharge carrying capacity as a consequence of the raised levees along the channels. Following this explanation, no major changes in mean-annual discharge supply to the delta would be required to generate such meander wavelengths. When the levee elevation relative to the flood basin increased without becoming much wider, it is possible that increasing the cross-channel slope accelerated avulsion. For example, the Waal and Meuse avulsions (Table 6.1) along either side of segment C4 (Figure 6.6C) could have been aided by the levee superelevation at their avulsion points. However, the wide spread in elevation implies the presence of lower parts of the levees sensitive to overtopping, which raises the question whether these highest crests really determined avulsion chances in our case.

Sediment trapping and role of vegetation: The narrowing of levees from the upstream to the downstream parts of the delta, matches the downstream volume reduction of late Holocene levee

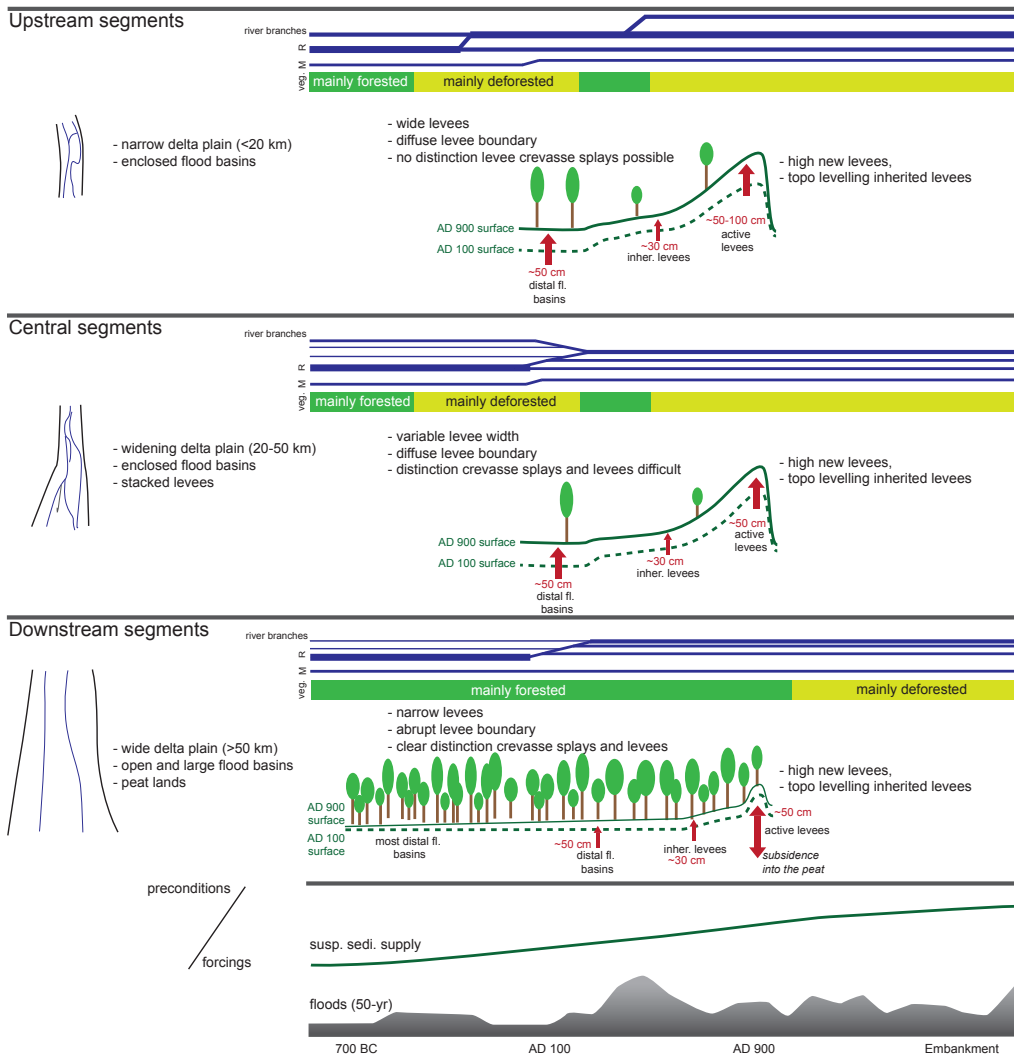


Figure 6.11 | Conceptual diagram on levee shape evolution during the first millennium AD throughout the Rhine-Meuse delta. Suspended sediment supply from Erkens & Cohen (2009), 50-yr flood recurrence floods from Toonen et al. (2013). Levee width after Figures 6.8 and 6.10C, riparian vegetation after Teunissen (1988) and Kooistra et al. (2013). Sedimentation rates of levees and fossil levees from Figure 6.10A, in distal flood basins after Gouw & Erkens (2007). Active river branches R = Rhine, M = Meuse) after Berendsen & Stouthamer (2000).

and crevasse splay deposits (Gouw & Erkens, 2007; Erkens & Cohen, 2009). The preserved volume per km² of silty clays and clay loams was reconstructed to be two times less in the downstream part compared to the upstream part of the delta. In comparison, volumes of flood-basin clay as distal overbank deposits, is rather evenly distributed between the upstream, central, and downstream parts of the delta. From this it appears that the upstream deltaic reaches were relatively more efficient in trapping silt fractions (and probably also the finest sand fractions) than in trapping clay. A longitudinal decrease in levee size has been observed in other river systems as well, where it has

been explained by a downstream decrease in availability of suspended material (i.e. the sediment concentrations of flood water leaving the channel – Kolb, 1963; Hudson & Heitmuller, 2003; Thonon et al., 2007). Our findings imply that the loss of sediment to levee building in upstream reaches, is the reason that the excess levee width drops so strongly in downstream sectors. The occurrence of abundant flood basins enclosed by alluvial ridges in the upstream and C3 segments is a likely setting to promote the high trapping efficiency for the silt fraction. In these areas the fossil alluvial ridges (i) slowed down the flow of incoming water that overpassed the alluvial ridges; and (ii) prevented floodwater outflow when the water levels in the flood basin started to drop in the final stages of the flood, allowing clays but also relatively much silt and the finest sand fractions to settle. While the absolute amount of sediments available for levee formation decreased in a longitudinal direction, the downstream levee width trend was likely enlarged by a positive land-use feedback concerning riparian vegetation (Figure 6.11). The large areal coverage of alluvial ridges in the upstream and central delta, were attractive places for people to live (Pierik & Van Lanen, 2017), leading to deforestation of the area since ca. 500 BC (Teunissen, 1988). The absence of a dense riparian vegetation resulted in a smaller lateral flow velocity gradient of the overbank flow, facilitating overbank fines to be conveyed further into the flood basin. This deposition further expanded the levee area in the upper and central delta segments. Once larger amounts of coarse-grained sediments could reach the flood basins, the levees became wider and the transition to the flood basin became more gradual. In the downstream parts of the delta, marsh and swamp vegetation remained largely intact (Kooistra et al., 2013), and interactions of flood dynamics with vegetation were more natural. As a result, the flow velocity gradient from the channel towards the flood basin would have been steeper here, generating narrower levees. This may well explain the occurrence of the remarkable narrow outer bend levees in the peatlands, trapping by vegetation in the flood-basin would then be more important than channel hydraulics.

6.5.2 Map information value, potential, and implications

In our data-driven geomorphological approach we reconstructed and analysed a palaeo-levee landscape of which much data is available at the scale of an entire delta. By quantifying the levee characteristics from these reconstructions in a uniform way across the entire delta, our map products allow assessing the role of regional flood-basin configuration, delta confinement, and spatially varying flood amplitudes on levee shape. This section discusses the benefits and limitations of our methodology and gives recommendations for further research.

In the reconstructions, the location and extent of the levees are generally known within tens of meters to maximal hundreds of meters, due to the availability of more than 100,000 lithological borehole descriptions and abundant map datasets. For more detailed use, e.g. to study levee width for smaller levees, it is important to have a clear definition of the distal levee boundary in the mapping. We considered this as the line where modestly inundated floodbasin water tables (i.e. the regional groundwater reconstructions) intersected the levee relief, rather than a particular break or convexity in transverse slope.

The precision of age control of the mapped levees varies across the study area. It was based on some 300 dates from site locations, from which the ages were transferred to the levees. This was done by comparing the orientation and position of levee complexes relative to the channel belts or by tracing levee deposits in cross-sections. Assigning ages to levees was hampered by diachronous activity within individual generations of channel belts. This concerns the pace in which levees expand in a cross-channel direction into the flood basin as well as vertical levee aggradation over time (see Appendici C1.2 and C1.3). Considering this we estimate that mature levee complexes

in the period of interest can be dated with a precision of ± 200 years, which is slightly less than the precision at which the according channel systems can be dated (± 100 years; Stouthamer & Berendsen, 2001). This makes the 400-year interval between the AD 100, 500, and 900 maps the most suitable time steps for levee planform comparison within the available data. For the palaeo-DEMs additional assumptions on vertical levee aggradation had to be made. Considering the present state of geological dating control, the AD 100 and 900 elevation maps are considered to be the most optimal time steps. The accuracy of relative levee elevation reconstructions is estimated to be ± 17 cm based on errors in individual lithological borehole descriptions and the groundwater level reconstructions used as the reference surface (see Appendix C1.3). The age and surface expression are more uncertain for older natural levees positioned deeper in the substrate, and for stacked levees that occur in areas where the channel-belt density is high (such as in the upstream and central delta segments). The relative elevations resulting from our reconstructions were compared to those of archaeological settlements known to be positioned on the higher parts of the levee landscape (Roorda & Wiemer, 1992; Wiemer, 2002, updated in chapter 8). The settlement finds are most abundant above or around the reconstructed groundwater level (chapters 7 and 8), supporting the suitability of the reference surface in expressing levee height as relative elevation. Although the reconstructions proved to be valuable on a delta scale and for comparing individual channel belts, it cannot be always fully assessed at this stage to what extent variation in local height (within smaller parts of individual alluvial ridges) represents real relief undulation or error noise. Nevertheless, it can be comfortably stated that levee dimensions show considerable variation on the scale of individual channel belts. This confirms the conclusion of Törnqvist & Bridge (2002) that many levees do not show idealized dimensions (e.g. widths or slopes), which are easily quantified and that would serve as a critical threshold for predicting avulsion. The pacing of lateral-levee development as well as distinguishing between initial stage crevasse splays and mature channel-belt levees could be further refined by detailed local sedimentological and geoarchaeological research focussed on the stratigraphy of single channel-belt generations. This could also help to better distinguish multiple generations of stacked levees and to include their dimensions in the already found delta-wide trends.

Identifying and isolating the roles of different levee forming processes and their controls from the reconstructed palaeo-landscape maps remains a challenge. Process-based modelling (e.g. Nicholas et al., 2006) might be used as a complementary approach to test the relative importance of controls on levee evolution, such as the role of valley width, flood-basin configuration, or riparian vegetation. Vice versa, the presented reconstructions can serve as validation for those modelling studies for scenarios with comparable initial and boundary conditions. Besides using numerical models, the mechanisms and controls proposed in the present study could be further tested by performing more detailed sedimentological research on selected isolated channel belts that were predominantly influenced by single controls. For such work, the maps of this study provide a way to select such test locations, where presumed controls are best expressed in levee shape. Sedimentological analysis on targeted channel belts could improve quantification of the development of levee growth through time, and could help unravelling the relative roles of levee-forming controls. Examples of paired selections of channel belts to isolate the effect of the controls are the varying distribution of discharge over bifurcating channels (levees of the Nederrijn vs. Waal channel belts; Figure 6.7), the effect of downstream decreasing delta-plain slope (levees of the Homoet/Kamp vs. Hennisdijk vs. Alm/Werken channel belts; Figure 6.9A, C, D), or increased sediment load (levees of the pre-AD 100 Herveld vs. AD 900 Nederrijn channel belts; in Figure 6.8B). Combining delta-wide geomorphological studies with results from selected case studies and

process-based modelling studies will further enhance the understanding on levee development as important components in fluvial geomorphology.

6.5.3 Further applications

The advanced mapping of natural levees as executed in this study, is only possible in deltaic and coastal areas for which large amounts of data have been collected and integrated. Because geomorphological and lithological data are generally most abundant for the shallow parts of a delta, mapping works best for relatively young deposits. The mapping could be extended to older deposits (formed in the first millennium BC or earlier), but because data density is lower for these deposits -owing to erosion or burial by younger elements- the method will only yield comparable quality as the current study for smaller well-preserved and well-explored areas (e.g. as done by Arnoldussen, 2008).

With our palaeo-DEMs, it is now possible to systematically distinguish between lower and higher parts of the levee landscape (i.e. within alluvial ridges of single channel-belt generations) – for the first time at delta scale. The levee reconstructions of our study therefore provide a starting point for archaeological prediction maps (e.g. Cohen et al., 2017ab) and modelling studies that focus on human-landscape interactions in the delta (e.g. Van Lanen et al., 2015ab; Groenhuijzen & Verhagen, 2016). The maps also provide a landscape zonation template for vegetation reconstructions (Peeters, 2007; Brouwer Burg, 2013; Van Beek et al., 2015a), which in turn may be used to further enhance hydraulic modelling scenarios of delta-flood dispersal (e.g. Van Oorschot et al., 2015). Including vegetation-morphology interactions would be an important step to test the hypotheses on variable levee morphology generated in this study.

6.6 Conclusions

In this chapter we explored the controls on natural levee formation in the Rhine-Meuse delta. The detailed delta-wide reconstructions of natural-levee surface elevation for the first millennium AD revealed levee patterns from which the following conclusions can be drawn:

- Our results strongly suggest that delta-scale antecedent conditions – delta-plain confinement, flood-basin configuration and substrate – were important controls in levee shape. Levee dimensions are not solely determined by channel dynamics, but also by the hydraulic conditions in the inundated flood basins. This is demonstrated for the upper delta where delta-plain confinement (from > 20 to 10 km wide) and the presence of older alluvial ridges amplified flood levels that generated higher natural levees (1–2 m above distal flood-basin groundwater levels). The importance of flood-basin hydraulics is confirmed by the strong tendency for wider levees in the direction of the decreasing flood-basin slope along N-S oriented channel belts, suggesting that flood-basin slope affected levee forming hydraulics. Examples of the influence of the substrate were found in the downstream delta. Here, presence of peat close to the channel and under the levees led to levee subsidence and channel fixation, resulting in narrow but rather thick levees.
- Natural levees in the central to lower delta parts show a considerable decrease in width. This is due to a downstream depletion of suspended load caused by efficient sediment trapping of coarse-grained overbank sediment. This was facilitated by hampered flow and sediment-rich water trapping in the upstream enclosed flood basins. Most likely, the effect was further aided by differences in riparian vegetation density: in the deforested upstream part, the smaller lateral

reduction in flow velocity allowed conveyance of overbank material farther away from the channel, leading to wider levees.

- Avulsions in the first millennium AD led to the formation of new levee complexes along the newly formed river channels over a considerable area in the former flood-basins. The new river courses avoided the higher elevated areas with abundant fossil alluvial ridges in the landscape. On these fossil ridges, topographic levelling occurred resulting from widespread flood-basin trapping of overbank sediment. Increased flooding frequencies combined with large suspended sediment loads during the first millennium AD, caused the newly formed local levee crest heights to be 0.5 to 1.0 m higher than their predecessors. These higher levees possibly increased the chances for avulsion by enhancing cross-channel slope, and enlarged meander wavelength, because higher levees increased bankfull discharge.

Our new GIS-based reconstruction maps of the natural-levee landscape serve as a starting point for more detailed sedimentological research and as field evidence for process-based numeric modelling studies. They additionally facilitate new opportunities for compiling palaeoenvironmental and geoarchaeological maps to further study the interaction between the past geomorphological processes, vegetation, and habitation.

Acknowledgements

This chapter is part of the project 'The Dark Ages in an interdisciplinary light' funded by NWO (project nr. 360-60-110). The first author contributed in the following proportions (%) to research design, data collection, GIS design, analysis and conclusions, figures, and writing: 60, 75, 60, 60, 80, 60. The authors thank Bart Makaske (Wageningen University) for the first version of the new geomorphological map of the river area and Marieke van Dinter (Utrecht University/ADC) for the palaeogeographical map of the area around Utrecht. This chapter benefited from discussions with Marjolein Gouw-Bouman, Marieke van Dinter (Utrecht University/ADC) and the participants of the workshop Dark Ages of the Lowlands 2015 listed on: <http://darkagesproject.com/conferences>. We would like to thank Hans Middelkoop, Bart Makaske, and three anonymous reviewers for their useful comments on the manuscript.



Chapter 7

Roman and early-medieval habitation patterns in a delta landscape: the link between settlement elevation and landscape dynamics

Settlement locations in delta landscapes change through time because of cultural and natural dynamics. We assessed the impact of natural-landscape dynamics on settlement-location shifts for the Rhine-Meuse delta in the Netherlands during the Roman and early-medieval periods (12 BC–AD 450 and AD 450–1050 respectively). During this time interval major landscape and cultural changes occurred in this area, with river avulsions and changes in flooding frequency coinciding with changing settlement patterns. In the delta plain, the relatively high and dry alluvial ridges of abandoned or active rivers were most favourable for habitation. Settlement location and elevation patterns were reconstructed in these landscape units using a high-resolution elevation map of the alluvial ridges. By integrating high-resolution palaeo-environmental and archaeological datasets for this period, we were able to spatially analyse the trends and to assess the effect of environmental changes on habitation. Results show that settlements progressively shifted towards higher areas between AD 250 and 750, on average by 20 cm over this period deltawide, which was coeval with an increased frequency of severe Rhine floods. The observed spatial differences demonstrate that this trend is most notable in the least-elevated segments of the study area. In areas where new large river branches developed, settlements show a strong shift towards higher-elevated parts of the landscape or even became completely abandoned. The river probably caused floods to be more frequent and more severe in these areas. Despite the clear link between changing settlement positions and floods during the studied time interval, floods do not seem to have caused long-term abandonment of major parts of the study area.

Based on article in press: H.J. Pierik & R.J. Van Lanen (2017) Roman and early-medieval habitation patterns in a delta landscape: The link between settlement elevation and landscape dynamics. *Quaternary International* (in press). [dx.doi.org/10.1016/j.quaint.2017.03.010](https://doi.org/10.1016/j.quaint.2017.03.010)

7.1 Introduction

River and delta landscapes were among the most densely-populated areas in the world throughout all archaeological periods. In these areas, settlement patterns were susceptible not only to cultural processes (e.g. socio-economic, political) but also to environmental factors (e.g. flooding, elevation, avulsions – e.g. Butzer, 1982; Brown, 1997; Von Nagy, 1997; Guccione, 2008; Funabiki et al., 2012; Hill, 2014; Howard et al., 2015; Pennington et al., 2016). These fluvial landscapes provided fertile substrates and natural resources, and hosted abundant land and water routes for long-distance transport (e.g. Cunliffe, 2004; McCormick, 2007; Van Es & Verwers, 2010; Van Lanen et al., 2016a).



Figure 7.1 | Location and palaeogeography for AD 900. Pleistocene uplands and peat extent after Vos & De Vries (2013); tidal areas, alluvial floodplains and channels are after chapters 3 and 6; situation Gelderse IJssel: after Cohen et al. (2009). Newly formed river channels in the first millennium AD are indicated with arrows (see Table 7.2 for ages of initiation); red dots indicate avulsion sites.

However the people living in these wet and dynamic landscapes often were confronted with flooding events. When the frequency or magnitude (flooding regime) of these floods changed, people can be expected to have adapted to this by relocating settlements to more suitable areas. For wetland regions all over the world changes in human-activity have indeed been linked to changes in flooding regimes (e.g. UK: Macklin, 1999; Gila River, Arizona: Waters 2008; Elbe, Germany: Schneeweiss & Schatz, 2014; Nile delta: Marriner et al., 2013; Macklin et al., 2015). On a larger scale even the rise and fall of civilizations have been attributed to changes in flooding regime (Yangtze delta: Zhang et al., 2005; Shanghai area: Wu et al., 2014). In some areas however increased episodes of flooding do not seem to have affected settlement dynamics (e.g. in the Roman Rhône delta:

Arnaud-Fassetta et al., 2010). All these studies correlate trends observed in archaeological and sedimentological records, however deltawide geomorphological approaches have not been carried out as this would require the presence and integration of large amounts of data. For most of these areas, data is currently not always available on the desired resolution or spatial coverage and often remains rather fragmented.

In the fluvial-dominated part of the Dutch Rhine-Meuse delta (Figure 7.1), large-scale cultural and landscape changes have occurred during the late-Roman period (LRP: AD 270–450 – Table 7.1) and the early-medieval period (EMP: AD 450–1050) (e.g. Hendrikx, 1983; Willems, 1986; Teunissen, 1988; Jansma et al., 2014). After the abandonment of the Roman *limes* in the delta, which was located along the river Rhine, large-scale depopulation occurred and settlements were relocated (e.g. Willems, 1986; Heeren, 2009; Vos, 2009; Van Dinter, 2013; Verhagen et al., 2016). This coincided with some remarkable environmental changes: (i) the avulsion of the major Rhine branch from its northern course to its currently active southern Waal branch (e.g., Table 7.2 – Berendsen & Stouthamer, 2000; Van Dinter et al., 2017; chapter 5); and (ii) an increase in flooding frequency of the river Rhine between AD 250 and 850 (Toonen et al., 2013; Cohen et al., 2016). This raises the question to what extent these environmental changes, next to cultural factors, influenced habitation in the area. Recent studies focusing on local settlement dynamics in specific parts of the delta (Bronze Age: Arnoldussen, 2008; Roman and Early medieval situation for the city of Utrecht: Van Dinter et al., 2017) conclude that the flooding regime temporally could have altered settlement distribution, forcing people to move to higher places or leading to abandonment of the area.

For the Rhine-Meuse delta, recent developments in integrating large-scale archaeological datasets (Van Lanen et al., 2015a) and the sedimentary-geomorphological perspective (e.g. Cohen et al., 2012; Toonen et al., 2013; chapter 6) for the first time allow the combination of high-resolution cultural and geoscientific data on a delta-wide scale. Here we combine new geomorphological reconstructions, recently assessed environmental changes in the delta, and changing settlement patterns through time. The aims are: 1) to analyse the shifts of settlement location over areas with different elevation through time; and 2) to assess the role of natural dynamics in these settlement shifts.

Already from the Bronze Age (2000–800 BC) onwards the relatively dry and elevated alluvial ridges with their natural levees and crevasse splays in the Rhine-Meuse delta were the most favourable areas for habitation (Modderman, 1948; Edelman et al., 1950; Hendrikx, 1983; Verbraeck, 1984; Willems, 1986; Arnoldussen, 2008; Van Dinter & Van Zijverden, 2010; Van Dinter et al., 2017). Therefore the alluvial ridges are considered to be key landscape elements to study the human-landscape interactions in the delta. However the spatial extent and elevation of the alluvial ridges in this delta are rather variable. Settlements positioned on the ridges therefore experienced different flooding frequencies and amplitude regimes during high-water events. Assuming that settlement elevation determined the sensitivity of the settlement to changes in flooding regime, a more detailed distinction between high and low parts of alluvial ridges is required to better understand the interaction between landscape and settlement dynamics. Because the height of settlements was not always recorded in the archaeological datasets consulted in this study, we inferred settlement elevation from the new high-resolution palaeo-DEMs presented in chapter 6. Integrating geoscientific and archaeological datasets is an important step towards further understanding of the relative contribution of environmental factors (e.g. floodings) to explain settlement distribution in the Rhine-Meuse delta.

7.2 Materials and methods

Settlement data for the Roman and early-medieval periods were collected, updated and enhanced for the study area (Van Lanen et al., 2015ab; chapter 8). Next we determined the landscape units where the settlements were located and assigned a palaeoelevation to each settlement using geomorphological-reconstruction and palaeo-topography maps. Finally settlement persistency and settlement elevation shifts throughout the first millennium were analysed.

7.2.1 Archaeological source materials

Archaeological data on settlements in the research area were extracted from the Archaeological Information System of the Netherlands (ARCHIS). This system contains a national overview of reported archaeological finds (Roorda & Wiemer, 1992; Wiemer, 2002). For the study area this dataset was expanded and enhanced with archaeological data published in regional overview studies, which in general contain more detailed (meta)data on the settlements: Bechert & Willems (1995), Verwers (1998), and LGL World Heritage Database (2010). Both the ARCHIS and external data were integrated into a single dataset to obtain maximal chronological resolution and spatial accuracy of all available settlement data in the study area. Duplicate records were selected, compared and removed based on the appliance of a 100 metres buffer around each settlement (for a more detailed description of this method see: Van Lanen et al., 2015a; chapter 8). Next overviews of active settlements were created per archaeological period (Roman Period, Early Middle Ages) and subperiod (e.g. early-Roman period, middle-Roman period) as specified by the Archaeological Basic Register (ABR, Table 7.1).

Settlement data were compiled for seven ABR-defined subperiods which each roughly cover 100 to 200 years (see section 7.2.2. and Table 7.1). We chose these short time intervals to match changing settlement patterns to developments in the landscape with a high-chronological resolution. Settlements dating to an unidentifiable part of the period, i.e. broadly classified as RP or EMP only, were excluded from the analysis since their chronological resolution is too low to yield significant results when comparing settlement patterns to landscape changes on the considered time scale.

Table 7.1 | Roman and early-medieval periods and subperiods as defined by the Archaeological Basic Register (ABR) and their chronological projection on the geomorphological reconstructions.

Archaeological Period	Subperiod	Abbreviation	Age	Geomorphological reconstruction
Roman period (RP)	early-Roman period	ERP	12 BC to AD 70	AD 100
	middle-Roman period	MRP	AD 70 to 270	
	late-Roman period	LRP	AD 270 to 450	AD 500
Early Middle Ages (EMP)	early-medieval period A	EMPA	AD 450 – 525	
	early-medieval period B	EMPB	AD 525 – 725	
	early-medieval period C	EMPC	AD 725 – 950	AD 900
	early-medieval period D	EMPD	AD 950 – 1050	

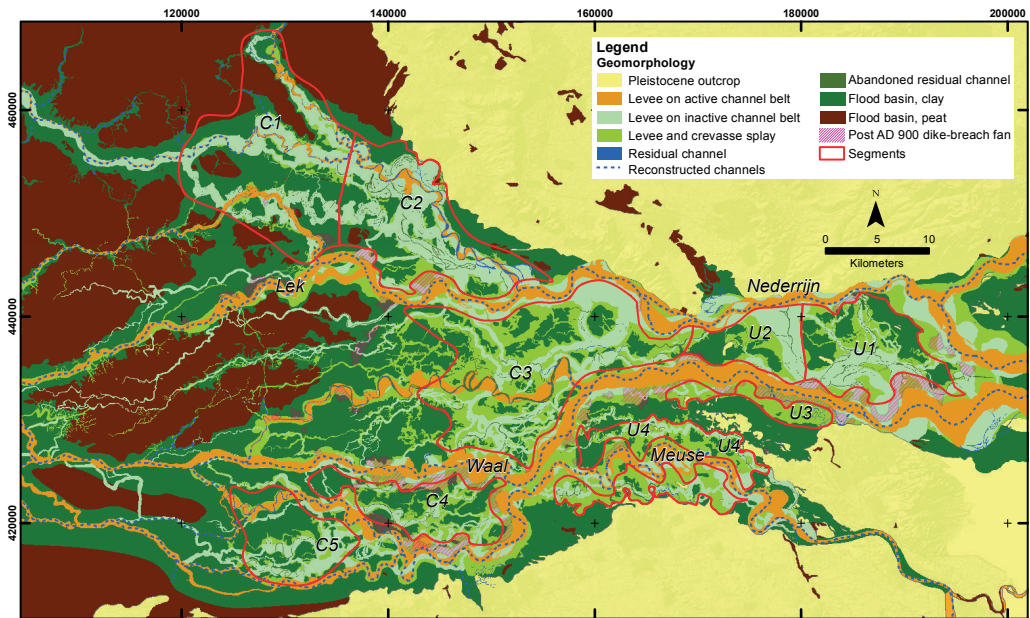


Figure 7.2 | Geomorphological reconstruction for AD 900 (after chapter 6). Segments C1-C5, D, and U1-U4 are based on geomorphological criteria (Table 7.4).

7.2.2 Geomorphological and palaeo-surface reconstructions

To assign elevation values to settlements and to assess their geomorphological setting across the delta landscape, two types of recently developed geomorphological reconstructions were used, which both cover the whole of the Rhine-Meuse delta: i) palaeogeographical maps (geomorphological reconstruction maps) for the time slices AD 100, 500, and 900; and ii) two palaeo-DEMs (Digital Elevation Models) representing the surface topography for AD 100 and 900. These time steps equally divide the first millennium and the phasing of these developments. The first time step comprises the initial stage of a series of avulsions in the delta (Table 7.2); the second time step fits with the stage of ongoing avulsions and increased flooding frequencies; the last interval represents the last natural state before embankment with matured new channel belts of a more-or-less completed avulsion. Their compilation method is explained in chapter 6 and summarised below.

The maps show the extent and distribution of the alluvial ridges present in the past landscape, which consist of natural levees and crevasse splays either on top of or flanking channel belts (Figure 7.2). The maps also include residual channels, zones of younger reworking by river activity, and dike-breach splays that cover the old landscape (Figure 7.2). The landscape elements were mapped based on the lithological and geomorphological criteria following methods of Berendsen & Stouthamer (2000), Berendsen et al. (2007), Van Dinter (2013). The lithological information was obtained from an extensive borehole database maintained by Utrecht University, whereas LiDAR images provided modern elevation of the landscape (Berendsen & Volleberg, 2007). The age of the mapped landscape elements was assessed from ^{14}C dates, archaeology and relative dating (Berendsen & Stouthamer, 2000; Gouw & Erkens, 2007; Cohen et al., 2012; Van Dinter et al., 2017).

Table 7.2 | New river branches in the Rhine-Meuse delta between in the first millennium AD, compiled after overviews in Berendsen & Stouthamer (2001), Cohen et al. (2012; 2016), more specific references are given in the table. The start of the initiation and mature phases are inferred from radiocarbon dates and relative dating. The location of the rivers is indicated in Figure 7.1.

New river branch	Start of the initiation phase	Start of the mature phase
Hollandse IJssel	ca. AD 0–100 ¹⁾	before AD 800 ¹⁾
Lek	ca. AD 40–300 ¹⁾	around AD 700 ¹⁾
Waal	ca. AD 220–450 ²⁾	after AD 450 ²⁾
Maas (Meuse)	after AD 270 ²⁾	after AD 270 ²⁾
Gelderse IJssel	ca. AD 550–650 AD ³⁾	after AD 735 ³⁾

¹⁾Based on Berendsen (1982), Guiran (1997), and on chapter 5; ²⁾based on Törnqvist (1993); Weerts & Berendsen (1995); ³⁾based on Makaske et al. (2008); Cohen et al. (2009).

To determine alluvial ridge and settlement elevation we used reconstructions of the palaeo surface on a 100 × 100 m resolution for AD 100 and AD 900, which both represent the situation just before large-scale embankment of the rivers around AD 1100 (Hesselink et al., 2003). The AD 100 surface level, derived from borehole data, was buried by flood sedimentation afterwards. The AD 900 surface level was mapped from current surface expression in LiDAR datasets. Absolute elevation (meters above O.D.) was converted to relative elevation (meters above a reference plain with a floodplain gradient) in order to facilitate comparison of changing settlement elevation on alluvial ridges throughout the delta. As a reference plane, we used an interpolated palaeo-groundwater level reconstruction (Cohen, 2005; Koster et al., 2016a), selecting the reconstructions for 2000 BP and 1000 BP (i.e. early-Roman period and Early Middle Ages) (Figures 7.3–7.5).

The total vertical error of the surface reconstruction is estimated to be ca. 17 cm per individual grid cell (Appendix C1.3). Its main components are the core sampling error and the maximum error of the groundwater reconstruction. The palaeo-surface reconstruction is most accurate on the higher parts of the alluvial ridges where most settlements were situated. Data density in general is somewhat lower for built-up areas. Given the amount of data points used for the interpolation (n = 80,000), these errors are cancelled out when considering larger areas.

After AD 100 only limited sedimentation of clay took place in the research area (some cm on the inherited natural levees to max. 30 cm in the lower flood basins), which in general did not

Table 7.3 | Scenarios used to assigning elevation to the settlements.

	Scenario 1	Scenario 2	Scenario 3
Input datasets	DEM100 (OD) GW2000 ¹⁾	DEM100 (OD) GW2000 ¹⁾	DEM100 (OD) GW2000 DEM900 (OD) GW1000 ²⁾
Spatial varying overbank sedimentation and groundwater level rise?	-	-	v
100 m smoothing	-	v	-

¹⁾GW2000 was subtracted from DEM with elevation relative to OD, ²⁾The interpolated value of groundwater-level reconstructions between 1000 and 2000 BP was subtracted from the interpolated value between DEM100 (OD) and DEM900 (OD) per time slice.

significantly affect the distribution of high and low areas throughout the landscape (Gouw & Erkens, 2007). Close to the active rivers, however, post-Roman sedimentation rate was significantly higher, with active levees and dike breach deposits reaching a height of some tens of cm to max. 2m (Hesselink et al., 2003; Gouw & Erkens, 2007). Because of the uncertainty in sedimentation rate in these areas, they were excluded from the analyses, which implies that a small number of settlements located in these areas were not taken into account. We used the delineations of these younger geomorphological elements of chapter 6 as boundaries for our analyses (Figure 7.2).

7.2.3 Assigning elevation to settlements

For each time slice we assigned the reconstructed landscape elevation to the settlements and subsequently determined the changes in settlement elevation observed between the time slices. Per DEM grid cell in the palaeo-surface reconstructions the maximal error is ca. 17 cm (see section 7.2.2). The mean elevation error of a selection of cells (i.e. those with settlements), depends on the number of cells (i.e. settlements) considered N , and was estimated as:

$$d\bar{x} = \frac{dx}{\sqrt{N}}$$

For the case with the smallest number of samples ($N = 11$ samples in EMPA in segments C4 and C5), the uncertainty of the mean equals 4.5 cm, which we assume the most conservative case.

To account for possible errors in the source datasets we developed three scenarios (Table 7.3). By comparing these scenarios we tested the accuracy of the two DEMs and the settlement-shift trends. Scenario 1 and 2 use two input datasets (GW2000 and DEM100 (OD)), whereas scenario 3 additionally uses groundwater and surface-level reconstructions of AD 900. For *scenario 1* we used the reconstructed AD 100 DEM for the settlement elevation of all time slices. This assumed that the elevation differences between higher and lower areas remained constant after AD 100. *Scenario 2* was performed to test the influence of local errors which either originate from location administration errors in the archaeological database or from administrative outliers in individual boreholes. These types of error were compensated for by taking the average value of the 9 grid cells within 100 m surrounding the cells on which the settlement was positioned. In *scenario 3* we assume a linear floodplain-sedimentation rate on the alluvial ridges between AD 100 and embankment around AD 1100, by assigning the interpolated value between the AD 100 and the AD 900 DEM to the settlements per time slice. From the results we subtracted the interpolated value of groundwater-level reconstructions between 1000 and 2000 BP. In this scenario a thicker layer of overbank clay is deposited on the lower ridges than on the higher ridges (chapter 6).

Some settlements were positioned on dwelling mounds (e.g. Edelman et al., 1950) that were not mapped on the DEMs. Therefore, settlements located on known dwelling mounds were selected manually and their elevation was corrected using the mounds' present surface elevation as the RP and EMP elevation. A two sample t-test (with unequal variances) was performed to assess the significance of the differences between average settlement elevation in the subsequent periods.

7.2.4 Calculating settlement persistence

Other important aspects of settlement dynamics are persistence, abandonment, and settling in new areas. In this context persistence is defined as the degree of spatial correlation in settlement locations between two successive subperiods. We regard settlement locations in use during two successive subperiods (e.g. the early-Roman period and middle-Roman period) within the same

100 m area as persistent (cf. Schlanger, 1992). The term refers to the long-term use of a specific area, i.e. not necessarily continuous use by the same inhabitants.

To analyse these aspects we spatially buffered the settlement locations for all periods using a 100 m buffer. For each subperiod, we evaluated whether the point settlement overlaps with the 100 m buffer area around the point settlement from the preceding subperiod. This buffer reflects the minimum surface area of a settlement, i.e. settled area (cf. Van Lanen et al., 2015b) of the ARCHIS settlement point data. In addition this buffer compensates for possible administration inconsistencies in location coordinates that are present in the original datasets.

The next step was to evaluate the elevation difference between abandoned and persistent settlements. We performed the comparison for all subperiods on the AD 100 DEM under the assumption that the relative elevation in the landscape did not change after AD 100 (section 7.2.1). A t-test (with unequal variances) was used to test the significance of the results.

7.2.5 Selecting delta segments

To test the influence of landscape settings (e.g. delta plain width, alluvial ridge configuration, or position of river branches) on settlement dynamics we divided the delta plain into 10 segments. We followed the existing segments of chapter 6, which are based on distinct landscape settings. Regarding delta-plain width we distinguished three major segments: the upper delta (U: confined delta plain), the central delta (C: widening delta plain), and the lower downstream part of the delta (D: wide delta plain, large flood basins) (Figure 7.2). The central delta was divided further into five spatial segments, based on areal percentages of the alluvial ridges and the avulsion history of the major rivers (Table 7.4). Settlements within these segments that were situated on post-Roman embanked floodplains, levees and dike-breach deposits were excluded from the analysis (also see 2.1). The lower delta plain, which is characterized by extensive peat areas and narrow alluvial ridges,

Table 7.4 | Delta segments and their geomorphological criteria (also see Figure 7.2).

Main segment	Delta width	Segment code	Geographical name	Alluvial ridge elevation relative to delta plain gradient	Alluvial ridge area ¹⁾ (areal % of the segment)	Flood-basin area ²⁾ (areal % of the segment)	Remarks
Upper	ca. 10 km	U1	Overbetuwe	High	60	35	
		U2	Nederbetuwe (east)	Low	68	29	
		U3	Southern bank Waal	Average	86	9	
		U4	Upper Meuse	Average	77	19	
Central	10–40 km	C1	Utrecht	Average	40	59	Large river silts up
		C2	Kromme Rijn	Average	61	33	
		C3	Nederbetuwe west/ Tielerswaard east	Average	74	22	Large river forms
		C4	Bommelerwaard	Low	52	46	
		C5	Land van Heusden Altena	Low	52	46	
Lower	> 40 km	D	Alblasserwaard, Krimpenerwaard	Low	-	-	Not considered

¹⁾ Alluvial ridges include natural levees, crevasse splays and levees on channel belts in Figure 7.2; ²⁾ Flood-basin area includes lower clayey and peaty flood basins in Figure 7.2.

does not contain sufficient archaeological data for the studied periods. Therefore this segment was excluded from the analysis.

7.3 Results

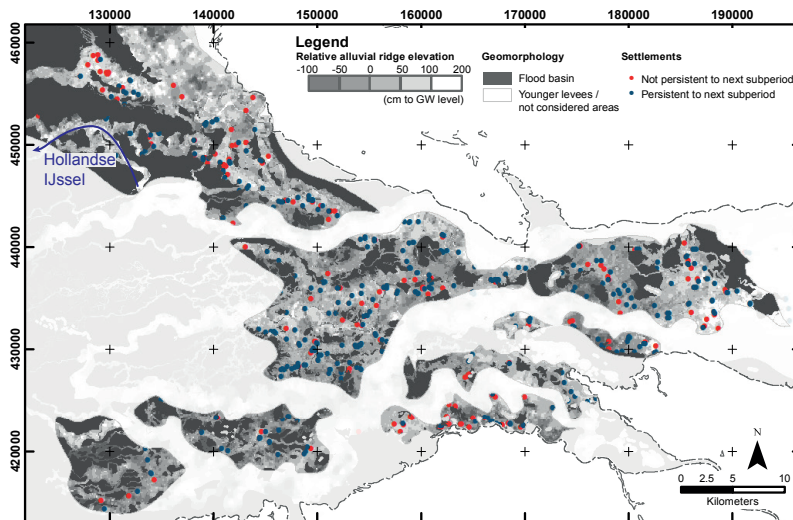
Settlements in both the RP and EMP generally were located on the higher parts in the landscape, 99% being located on top of natural levees or crevasse splays, of which 60% was situated on top of channel belt sand bodies (Figures 7.6A and 7.7D). Within these landscape units some shifts in settlement location and therefore also settlement elevation from the RP to the EMP can be observed (Figures 7.5 and 7.7). The changes in settlement elevation through time are described below and linked to the most important landscape developments. The deviations in scenarios are indicated in Figure 7.5, indicating the robustness of the analysis.

ERP-MRP: Compared to the ERP, during the MRP settlement numbers increased by 40% throughout the study area (Figures 7.6A, B and 7.7A). No significant difference in settlement elevation can be observed between the ERP and MRP (Figure 7.7E). In terms of large floods and river avulsion both periods were relatively quiet (Figure 7.7B, C – Toonen et al., 2013).

MRP-LRP: From the MRP to LRP the number of settlements dramatically decreased by 66%, coinciding with the abandonment of the *limes* around AD 270 (e.g. Alföldi, 1967; Heeren, 2015; Verhagen et al., 2016) (Figure 7.6A, B). Only 33% of the MRP settlement persisted to the LRP (Figure 7.6C). Throughout the entire delta settlements shifted on average to 5–9 cm higher positions during the LRP (Figure 7.7E). The MRP settlements that persisted to the LRP were situated ca. 8 cm higher than settlements that became abandoned, a trend that is statistically significant (Figure 7.7F). This shift seems to have been strongest in the lowest segments (U2, C4, and C5 – Figure 7.5). During the LRP it coincided with an increase in flooding frequency (50–100 yr recurrence time) and a large flood around AD 282 (Toonen et al., 2013). Locally this shift is also observed in the southern part of segment C1 (Figure 7.5) where the river Hollandse IJssel and Lek were reactivated between AD 100 and 300 (Table 7.2; Figure 7.7C – Cohen et al., 2012).

LRP-EMPA: Towards and during the EMPA the number of settlements decreased even further by 35% (Figure 7.6A, B). Similar to the preceding period the persistence of settlements was still very low (Figure 7.6C). No delta-wide rising trend in settlement elevation can be observed between the LRP-EMPA (Figure 7.7E). However given the contrast between individual persistent and abandoned settlements, persistent settlements were located on average 13 cm higher than settlements that were abandoned (Figure 7.7F). Combined with the absence of an average rise in settlements this implies that new settlements most likely were situated on similarly low elevations as settlements abandoned during the LRP.

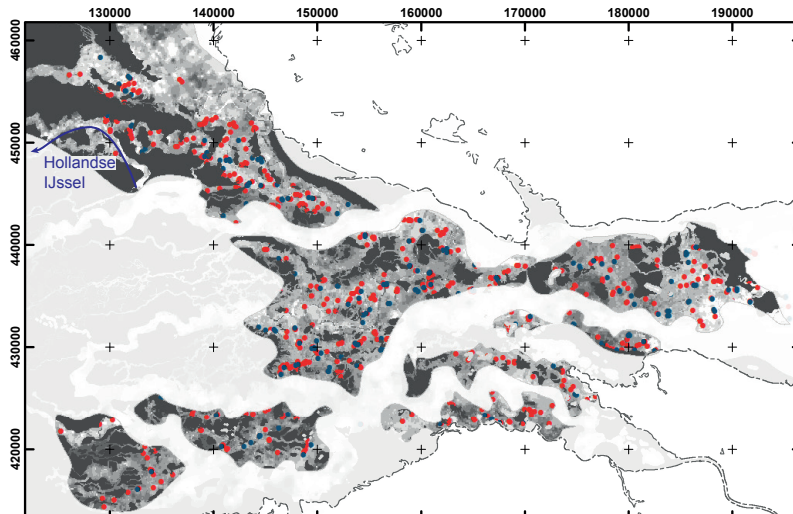
EMPA-EMPB: After the EMPA the number of settlements increased by 39% (Figure 7.6A, B). Throughout the research area the average EMPA-EMPB settlement elevation increased by 4–7 cm (Figure 7.7E). About 50% of the EMPA settlements persisted into the EMPB. These persisting settlements were located on average about 27 cm higher than the abandoned settlements (Figure 7.7F). One of the largest millennial floods in the research area occurred during the EMPA-EMPB (ca. AD 685; Toonen et al., 2013). The most notable shifts towards higher grounds occurred in segments C3–C5 and U3 (Figure 7.5). These trends correspond with the formation of the river Waal as the major Rhine branch. As segments C3 and U3 were located directly next to or just downstream of the Waal, they most likely were affected by higher and more frequent yearly floods conveyed through this new river branch. The effect of the formation of the Waal is further underlined by the abandonment of many existing settlements along this new river branch between the EMPA-EMPB.



ERP

n = 531

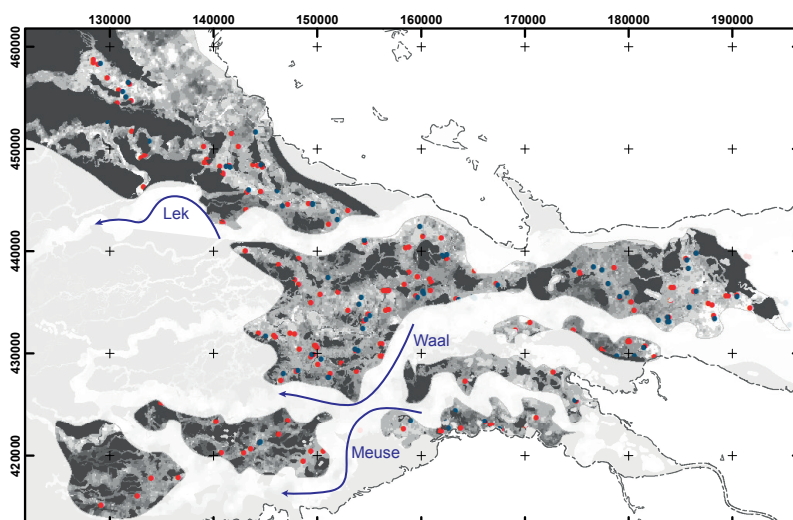
pers to MRP = 71%



MRP

n = 745

pers to LRP = 29%



LRP

n = 246

pers to EMPA = 34%

A similar trend is observed in the northern part of segment C3 corresponding with the increasing discharge of the river Lek (Figures 7.3 and 7.4).

EMPB–EMPC: The number of settlements further increased during this period by 78%. The EMPB–EMPC settlement persistence is 60% (Figure 7.6). Throughout the research area settlement elevation increased further (Figure 7.7), with no clear spatial differences throughout the study area. Looking at persistent versus non-persistent settlements we observe a statistically significant 20 cm difference in settlement elevation. Presumably the large millennial flood of ca. AD 785 (Toonen et al., 2013) contributed to this rising settlement elevation.

EMPC–EMPD: In the EMPD the number of settlements decreased by 16% (Figure 7.6B). This decline is best explained by 1) increased clustering of settlements and houses within these settlements (Numan, 2005) and 2) the lack of excavation data for this period. The trend of settlement movement to higher elevated areas stagnated and in some segments the average position of settlements even slightly decreased (C2, U2, U3, and U4). Persistent settlements were located 3 cm higher on average than non-persistent settlements (Figure 7.7F). Newly-founded settlements appear to have been located on lower grounds. These observations are best explained by the combination of increased reclamation activities and water management during this period, enabling the colonisation of previously unsuitable areas (Lascaris & De Kraker, 2013), and the relatively small number of severe floods during this period (Figure 7.7).

7.4 Discussion

7.4.1 Factors causing settlements shifts

The results show that from the RP to EMP settlements steadily shifted towards higher areas in the landscape. When comparing all subperiods except the ERP to MRP transition, persistent settlements on average were located higher than settlements that became abandoned. These shifts are most clear in the lowest segments in the MRP to LRP interval (U2, C4, and C5), and in the segments dating to the EMPA to EMPB transition close to a new river branch (C3 and U3). This suggests that during these periods water levels expressed by groundwater-level table, regular floods and extreme floods were important factors determining settlement location. The relative importance of these three factors is discussed below.

Influence of increased frequency of large floods

From the LRP onwards the study area experienced an increase in flooding frequency after centuries characterized by relatively few (large) floods (Figure 7.7B). Trends in settlement elevation from the MRP to LRP are mainly observed in the lowest areas of the delta (U2, C4, and C5 in Figure 7.5). From this we conclude that floods during the LRP must have affected the habitation conditions in the lowest areas in the study area, although they certainly will not have been the only cause of the depopulation. After the LRP, the lowest areas are much less populated and possible influences of major flooding events only are observed in the somewhat higher elevated segment C3, where a shift towards higher areas occurred until the EMPC (Figure 7.5).

Segment U1 is the most confined delta segment, causing floodwater to be higher than in other segments. This suggests that settlements in this area must have flooded more frequently and that even during regular, less extreme floods the water levels were higher (chapter 6). This area does not

Figure 7.3 (left page) | Persistent (abbreviated as pers) and non-persistent settlements for the Roman period plotted on the palaeo-surface reconstruction of AD 100 (for colour version see Figure 7.5), with the settlements per time slice. Masked areas are not included in the analysis. The most important avulsions are indicated, for the segment codes see Figure 7.2.

show significant trends in shifting patterns (Figure 7.5), presumably because during the Roman period settlements in this region already were located on the highest possible positions (as can be observed in Figures 7.3 and 7.4). Since segment U1 was never completely abandoned, its inhabitants probably were able to adapt relatively well to floods. Also in segment U4 no shift towards higher areas was observed for the MRP-LRP. This is best explained by the fact that this area was influenced by the regime of the river Meuse. Its flooding regime is yet unknown but as the river is smaller, floods can be expected to be less high compared to those of the river Rhine.

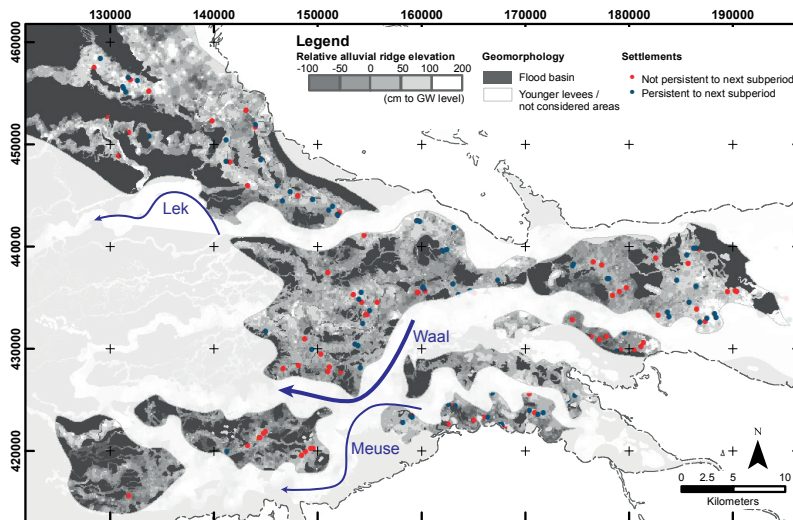
In summary, major floods caused settlements in the study area to shift upwards. These floods appear to have influenced settlement elevation shifts, but did not cause large areas to become permanently abandoned. The recorded floods are rare high-magnitude events and did not occur more frequently than once in several decades. Despite their possibly large impact, the relatively low frequency of these events probably made it possible for the delta inhabitants to return towards less elevated and therefore flooding-prone areas. This may explain why the settlements in the lowest areas in all cases were least persistent and why newly founded settlements often were located exactly here.

Position along a major river branch

The formation of the southern Waal course of the Rhine (Figures 7.1, 7.3, and 7.4) and the subsequent silting up of the former main branch of the Rhine in the north around AD 450 (Weerts & Berendsen, 1995; Berendsen & Stouthamer, 2000; Van Dinter et al., 2017) caused the main discharge of the Rhine to flow through segments C4 and C5 instead of segments C1 and C2 (Figures 7.3 and 7.4). This shift of the main channel from the northern part of the central delta towards the southern segment caused more frequent and higher floods in the southern areas and less severe flooding regimes in the northern part of the central delta. This is reflected in the trends of settlement shifting to higher sites, as observed in segments C4, C5, and U3 and also in the southern part of C3 and C1 (Figure 7.5, section 7.3). This is further underlined by the position of the settlements located in areas C4 and C5, which after the LRP mainly were confined to dwelling mounds. Although their absolute elevation through time (i.e., phases of dwelling mound elevation) is not known in detail, the trend of moving to higher areas is evident.

The configuration of large river branches affected settlement distribution by modulating both the distribution of flood water from large floods as well as from regular flooding events. Although the amplified effect of these events around rivers cannot be independently validated, as these lower-magnitude floods are not well recorded in the sedimentological record, they form the most likely explanation for the observed settlement shifts susceptibility close to major rivers compared to areas further away from rivers. The higher-frequency occurrence of these floods probably made them easier to be remembered by inhabitants of the delta. It is also possible that locally more permanent higher groundwater levels occurred as observed by Van Asselen et al. (2017) for flood basins where a new river branch formed in segments C3 and D between 6000–4000 cal BP. Despite the upward settlement shifts observed throughout the entire delta, no major areas seem to have become depopulated as a result of the environmental changes.

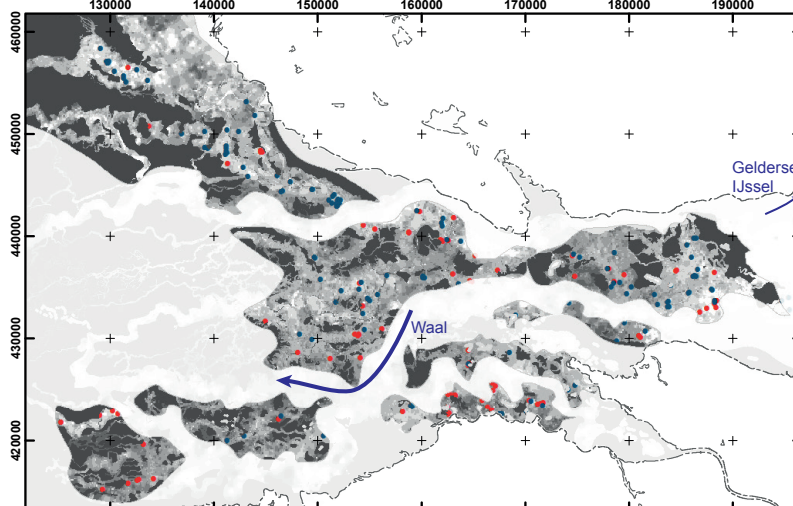
Figure 7.4 (right page) | Persistent (abbreviated as *pers*) and non-persistent settlements for the Early Middle Ages plotted on the palaeo-surface reconstruction of AD 100 (for colour version see Figure 7.5), with the settlements per time slice. Masked areas are not included in the analysis. The most important avulsions are indicated, for the segment codes see Figure 7.2.



EMPA

n = 160

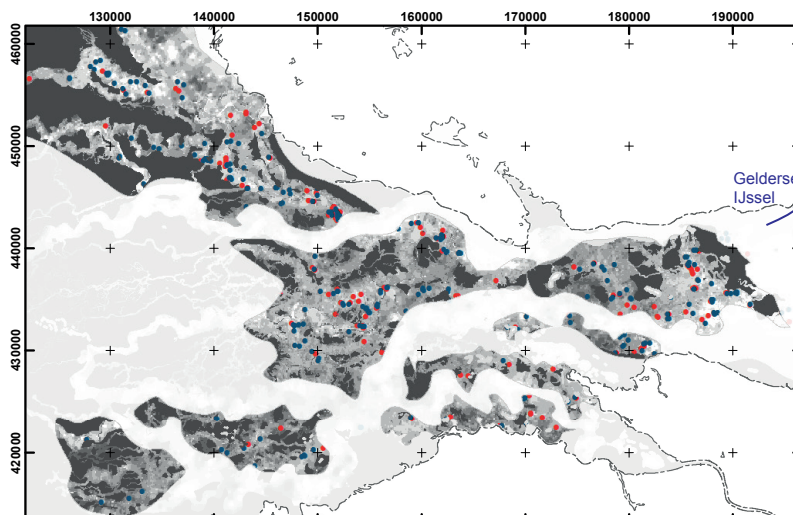
pers to EMPB = 52%



EMPB

n = 222

pers to EMPC = 61%



EMPC

n = 397

pers to EMPD = 53%

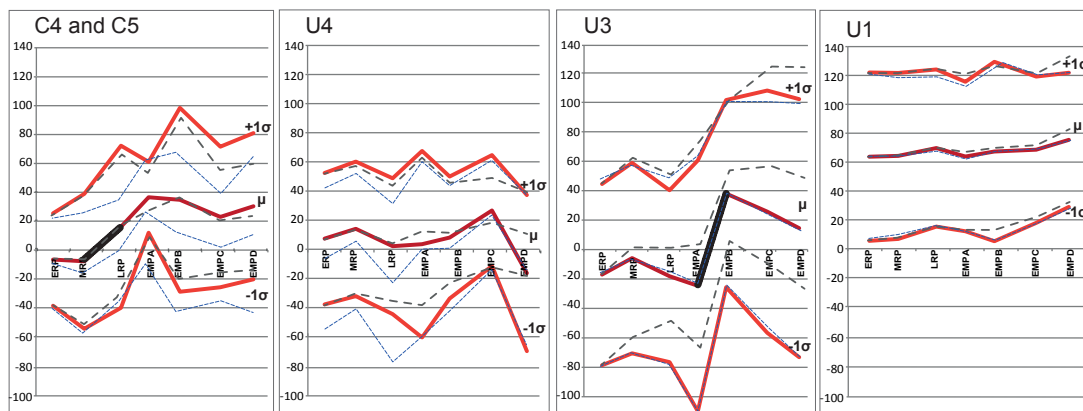
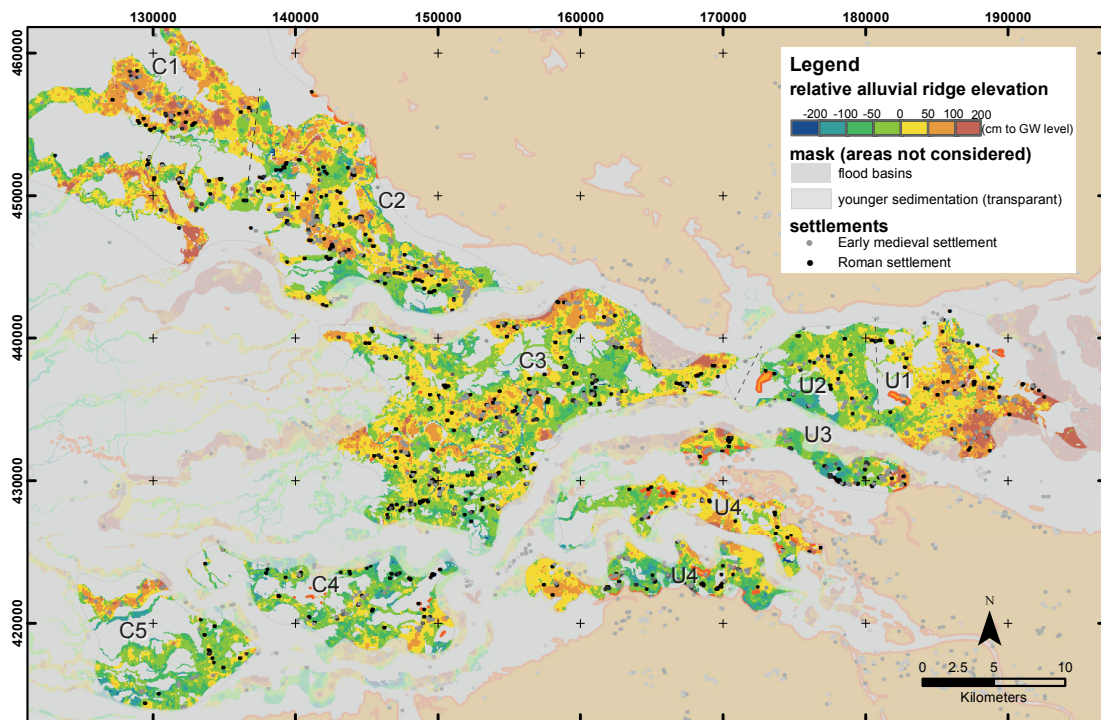
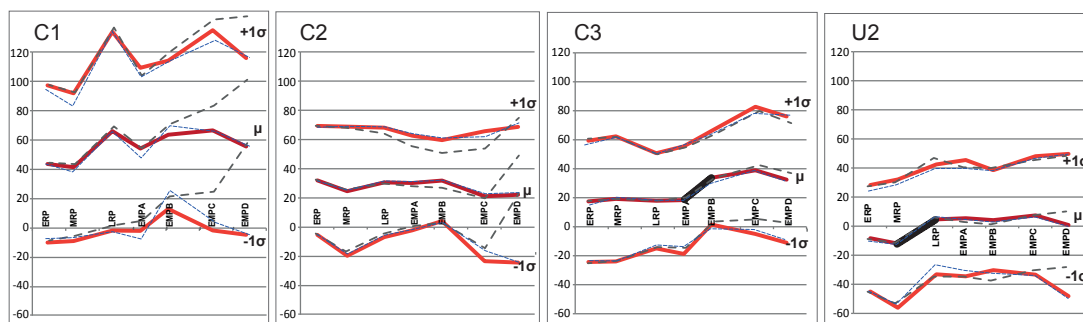
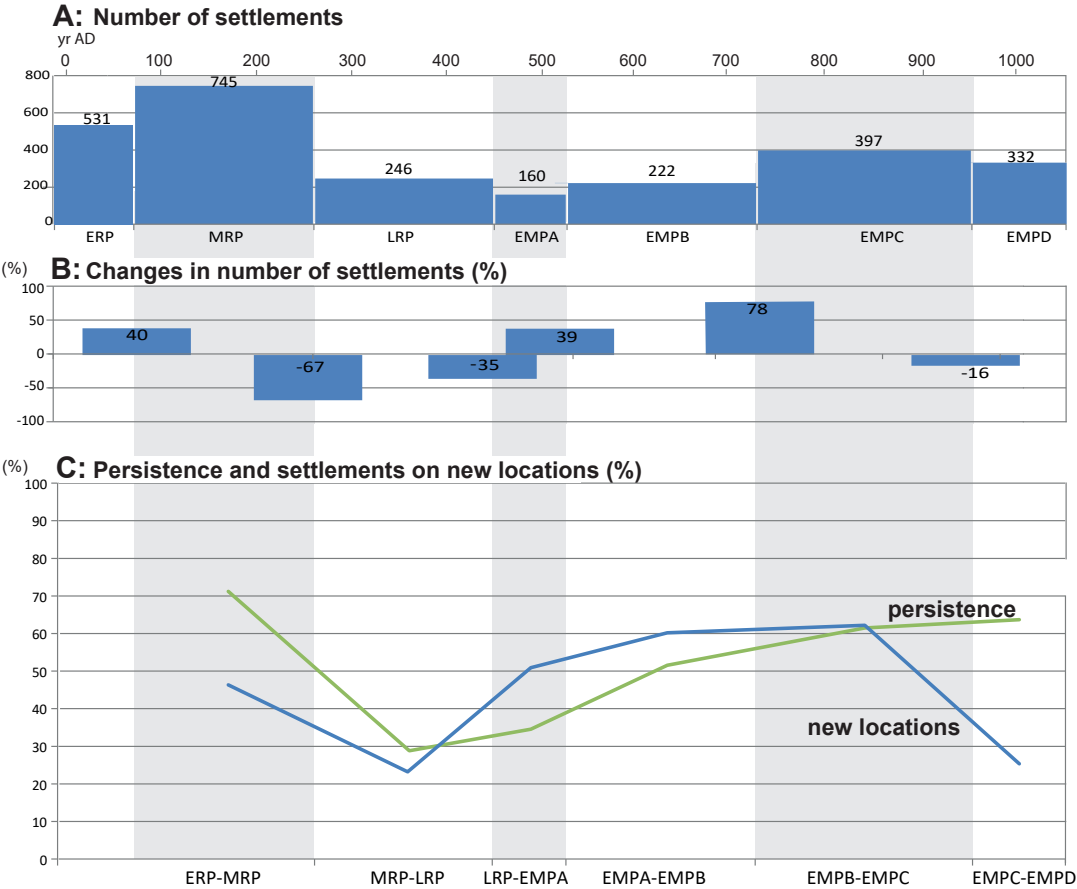


Figure 7.5 (left page) | Average settlement elevation (μ) and 1σ (68% of settlements) for the segments per subperiod on the AD 100 DEM. Areas not included in the analysis are masked transparent. Red lines: average settlement elevation (scenario 1); blue dashed lines: average and standard deviations of scenario 2 (section 7.2.3) grey dashed lines: average and standard deviations of scenario 3 (section 7.2.3); black lines: significant average differences for $p \leq 0.05$.

Figure 7.6 (below) | (a) Number of settlements in the research area; (b) percentage difference in number of settlements between subsequent time slices; (c) percentage of persistent settlements and settlements on new locations.



Gradually rising groundwater levels

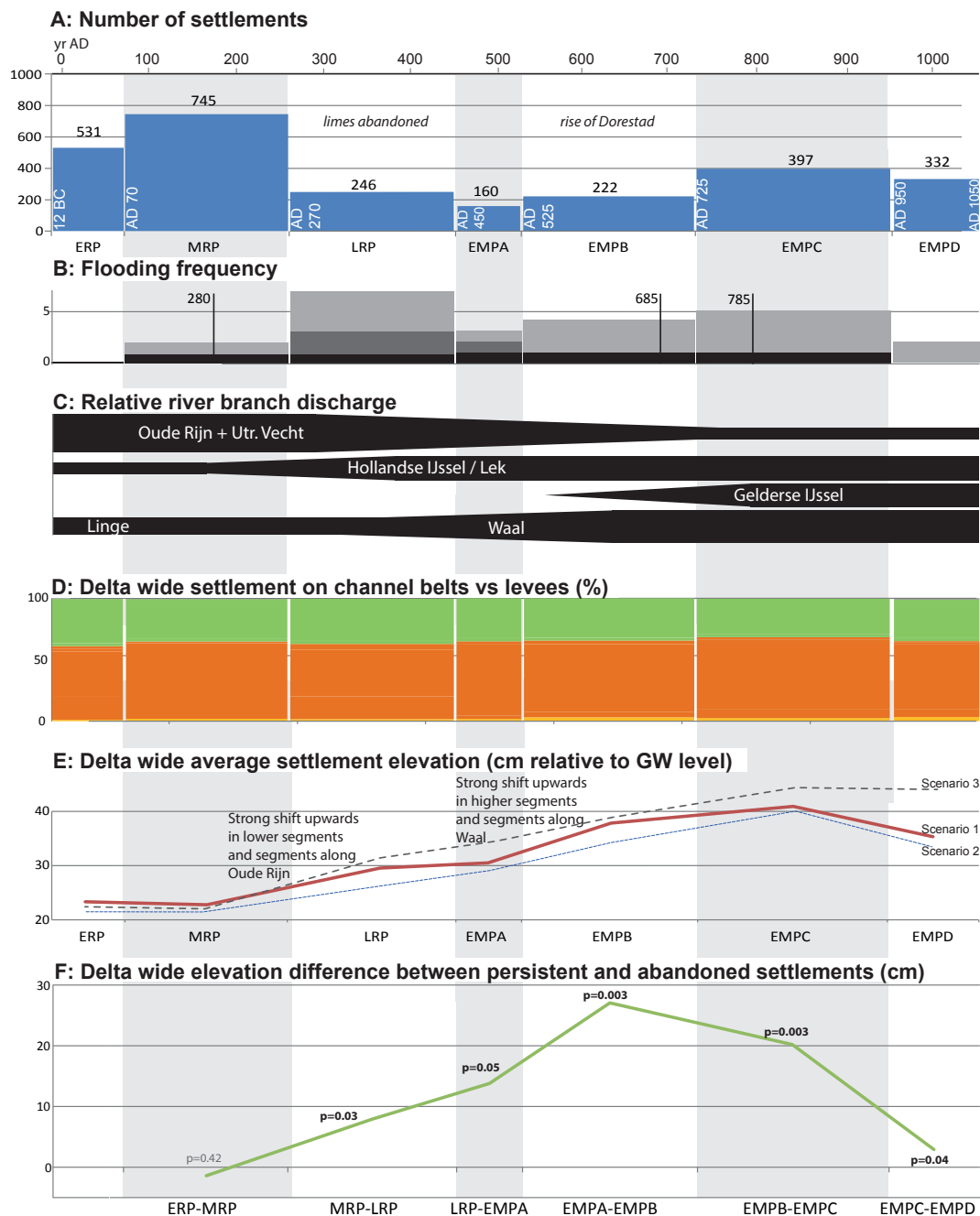
Rising groundwater levels could have triggered the establishment of settlements on higher elevated locations. In the central and upper part of the delta groundwater-level rise was mainly forced by continuous sedimentation rather than by absolute sea-level rise during the first millennium BP (Cohen, 2005; Gouw & Erkens, 2007), i.e. while the surface area was being elevated by clay sedimentation, the groundwater-level also rose at a similar rate causing the groundwater level relative to the surface to remain more or less constant. In chapter 6 this was confirmed by demonstrating that sedimentation on the alluvial ridges between AD 100 and river embankment around AD 1100 on average was 38 cm, which corresponds to the results of groundwater-level rise modelled by Cohen (2005). In this study, scenario 1 assumes equal pacing of groundwater and surface elevation, whereas scenario 3 actually tests this assumption using independent datasets on surface elevation and groundwater level reconstructions for AD 100 and AD 900 (see section 7.2.3; Table 7.3). When both scenarios are compared, it seems that sedimentation and groundwater level indeed kept the same pace, since both scenarios show comparable and consistent upward-shifting trends (Figure 7.5). From this we conclude that at least on the location of the settlements, the groundwater level relative to the surface did not significantly rise. Locally, in the lowest parts of the alluvial ridges, gradual groundwater-level rise may have been a minor forcing. This mechanism, however, cannot fully explain the observed major settlement shifts in the study area and the differences between the segments.

Despite the dynamic nature and changing environmental conditions of the delta landscape, cultural patterns (e.g. route networks) seem to show signs of long-term persistence as can be seen in the connectivity patterns in the study area (also see chapter 8).

7.4.2 Reflections on the scale and data resolution

The upward shift of settlements during the studied time interval are visible both on delta scale and in the individual segments of the delta. In addition for all three scenarios the differences in elevation between the subperiods are rather consistent (Figures 7.5, 7.7E). The introduction of AD 900 surface level and groundwater levels in scenario 3 in addition to the AD 100 surface level and groundwater level used in scenarios 1 and 2 (Table 7.3) indicates that the latter input datasets are reliable. Administrative errors in settlement location appear to have a minor influence on the results (compare scenarios 1 and 2 in Figures 7.5 and 7.7E). In segments C4, C5, and U4 some more deviation between scenarios 1 and 2 is observed, however the magnitude and timing of these changes remain similar.

Figure 7.7 (right page) | (a) Number of settlements in the research area; (b) Holocene recurrence time of floods from black to light grey: 250 yr (very severe flood), 100 yr (severe flood), 50 yr (moderately severe flood), after: Toonen et al. (2013); Cohen et al. (2016); Toonen (personal communication); here the events are grouped per archaeological subperiod and the ages of the three largest floods are indicated; (c) activity of major rivers in the research area after Cohen et al. (2012), Van Dinter et al. (2017), and chapter 5; (d) percentage of settlements on geomorphological units on map of Figure 7.2. Orange: settlements on levees or crevasse splays on sandy channel belts, green: settlements on levees or crevasse splays outside sandy channel belts; (e) delta-wide average settlement elevation; (f) elevation difference between persistent and abandoned settlements for scenario 1, including p-values describing the significance of the results of the t-test, with values statistically significant at $p \leq 0.05$ accentuated.



The individual flood events generally have been dated with an accuracy of 30 to 150 years using ^{14}C dating and correlation techniques (Cohen et al., 2016), which corresponds to the chronological precision of the archaeologically dated settlements, i.e. a 20 to 200 years resolution. Cohen et al. (2016, p.43) state that the occurrence of major flood events in the ERP and MRP are highly unlikely considering the sedimentological and archaeological evidence. The chronological recording of settlement data is most accurate for the Roman period. This is due to: 1) a shorter time interval per subperiod; and 2) the fact that typologies based on Roman material culture in our study area are well developed and allow precise dating. In addition large-scale analyses in our study area are bound to specific ABR chronological boundaries (i.e. on average 100–200 yr. intervals, Table 7.1). Although locally more detailed dating is available, when performing large-scale analyses the least accurately dated sites are the bottleneck of the analysis. Methods by Verhagen et al. (2016) who explored a detailed and statistical approach for the Roman period, appear to be promising to increase chronological resolution of settlements and to better understand settlement abandonment, continuity and persistence for the first millennium AD.

7.4.3 Outlook

Since the LRP, settlements steadily shifted towards higher areas while the lower elevated settlements became abandoned. The observed elevation differences are small but appear to be robust. To further test the impact of floods on habitation conditions, hydraulic flood-modelling studies can be performed. These studies address flood-water dispersal through the delta assessing flooding frequency and intensity per gridcell. The palaeo-DEMs can serve as input layer for such a study. Following the approach in this chapter, segments in the delta can be compared and the role of delta plain width and avulsion in flooding frequencies can be further assessed.

The results of our study can be locally validated using information from studies characterized by a higher chronological and spatial resolution. When these studies focus on absolute settlement elevation and indications for wetter conditions (e.g. clay layer by flooding), the link between settlement dynamics (i.e. elevation trends and persistence) and floods can then be further evaluated.

The patterns observed in this chapter can be compared to more detailed large-scale historical and archaeological studies regarding e.g. early-reclamation activities, land use, demography, political settings, and transport. This will further improve our understanding of past human-landscape interactions.

7.5 Conclusions

Settlement data from integrated archaeological databases were combined with geomorphological reconstructions and records of environmental changes in the Rhine-Meuse delta. This delta-wide approach demonstrates that:

- During the first millennium AD habitation mainly occurred on the higher parts of the alluvial ridges, with 40% of the settlements being situated on alluvial ridges without an underlying channel belt.
- Between AD 270 and 750 settlements shifted towards higher locations. Between AD 270 and 450 this development mainly occurred in relatively low-elevated delta segments. From AD 450 onwards the somewhat higher-elevated central delta was affected as well. This settlement shift coincided with an increased frequency of severe floods.

- Areas close to newly-formed large river branches between AD 270 and 750 were characterised by a strong relocation trend of settlements towards higher-elevated positions or even by settlement abandonment. Close to rivers, settlements appear to be relatively more susceptible to low-magnitude floods (yearly to decadal) because here these floods occur more regularly and reach higher levels than in areas further away from the river channel.
- The presented integrated approach clearly is useful for correlating environmental events to the settlement dynamics in the Rhine-Meuse delta during the first millennium AD. Although cultural factors must also have played a role in the observed geographical and altitudinal shifts of settlement locations, these can only be fully explained by including landscape dynamics in the analyses.

Acknowledgements

This chapter is part of the PhD theses of H.J. Pierik and R.J. Van Lanen, within the project ‘The Dark Ages in an interdisciplinary light’ (www.darkagesproject.com) funded by NWO (project nr. 360-60-110). The first author contributed in the following proportions (%) to research design, data collection, analysis and conclusions, figures, and writing: 60, 50, 60, 80, 70. The authors would like to thank Willem Toonen for kindly providing flooding frequency data. We would like to thank Kim Cohen, Marjolein Gouw-Bouman, Bert Groenewoudt, Esther Jansma, Hans Middelkoop, and Esther Stouthamer for their comments on earlier drafts of the chapter. Finally we thank two anonymous reviewers for their useful comments on the manuscript.

Chapter 8

Calculating connectivity patterns in delta landscapes: modelling Roman and early-medieval route networks and their stability in dynamic lowlands

River landscapes can be regarded as amongst the most densely populated regions in the world. Despite their dynamic nature and their susceptibility to natural hazards, pull factors such as fertile soils and trade connections always have attracted people to these regions. During the Roman (12 BC–AD 450) and early-medieval periods (AD 450–1050) the Rhine-Meuse delta in the Netherlands underwent significant simultaneous cultural and environmental changes such as changing settlement patterns, the collapse of the Roman *limes*, changing flooding regimes and river avulsions. Past route networks are influenced by both cultural and natural dynamics and are therefore a useful tool to better understand the complex interaction between these dynamics. By applying and enhancing recently-developed methods of modelling route networks in dynamic lowlands, this study reconstructs connectivity patterns in the Rhine-Meuse delta. Based on newly-available high-resolution geoscientific and archaeological data, network-friction maps and route networks were calculated for three time slices: AD 100, 500, and 900. These modelled networks were validated using archaeologically-excavated infrastructural and isolated finds. Additionally the amount of network stability between these networks was calculated. Results show that for each of the route zones a clear correlation exist between the modelled network and the occurrence of infrastructural and isolated finds. Although clear periodic differences between these correlations percentages are visible. Despite the dynamic nature of the research area the routes show clear signs of network stability, with 80% of the AD 500 network being persistent with their AD 100 counterparts. Between AD 500 and AD 900 the persistence percentage slightly rises to 81% indicating a similar level of network stability. This shows that large parts of the Rhine-Meuse delta were persistently used during the Roman period and Early Middle Ages despite local settlement dynamics and changing natural settings.

Based on article in press: R.J. Van Lanen & H.J. Pierik (2017) Calculating connectivity patterns in delta landscapes: modelling Roman and early-medieval route networks and their stability in dynamic lowlands. *Quaternary International* (in press). [dx.doi.org/10.1016/j.quaint.2017.03.009](https://doi.org/10.1016/j.quaint.2017.03.009)

8.1 Introduction

Many river and delta landscapes in the past were densely populated, since they provided fertile substrates and easily-maintainable geographical boundaries, and provided ample opportunities for long-distance transport networks (e.g. Cunliffe, 2004; McCormick, 2007). The Rhine-Meuse delta in the Netherlands is such a wetland landscape. It already was relatively densely populated

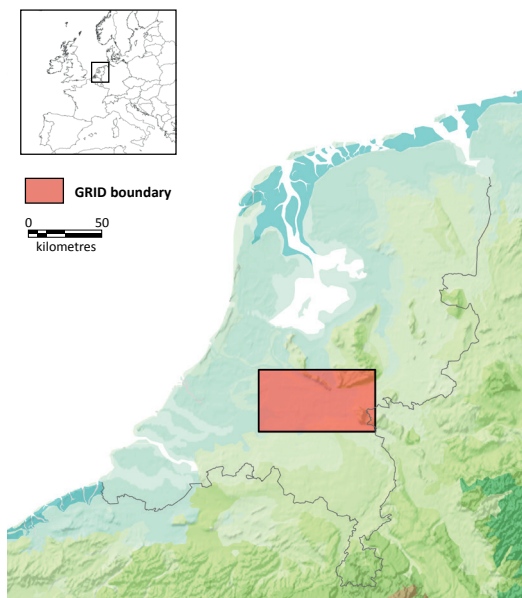


Figure 8.1 | The location of the study area (in red) within the current Netherlands. The coastline represents the Roman period. The study area reflects the spatial boundaries visible in Figures 8.3, 8.4, 8.6–8.10.

during the Bronze Age (2000–800 BC; Louwe-Kooijmans, 1974; Arnoldussen, 2008) and formed a crucial transport corridor functioning in long-distance connections between the mainland of Northwest Europe and the British Isles (Figure 8.1; Cunliffe, 2004). Rivers in the Netherlands frequently have been described as crucial Roman and early-medieval trade routes (e.g. Van Es & Verwers, 2010; Dijkstra, 2011). However low-lying, dynamic landscapes also were challenging for their inhabitants, confronting them with amongst other regular flooding and changes in river courses (e.g. Cohen et al., 2016; Van Dinter et al., 2017).

During the late-Roman and early-medieval periods (AD 270–1050), large-scale cultural and natural changes occurred in the fluvial-dominated part of the Rhine-Meuse delta (e.g. Hendriks, 1983; Willems, 1986; Van Es & Verwers, 2010; Jansma et al., 2014; Van Dinter et al., 2017). After the collapse of the Roman *limes* around AD 275 large-scale depopulation and settlement-relocation took place (e.g.

Alföldi, 1967; Willems, 1986; Van Dinter, 2013; Heeren, 2015). These developments corresponded with large-scale landscape changes such as the avulsion of the Rhine to its southern course, the river Waal (Weerts & Berendsen, 1995), and increasing flooding frequency and intensity (Toonen et al., 2013; Cohen et al., 2016; Van Dinter et al., 2017). These cultural and natural changes clearly affected settlement patterns (Pierik & Van Lanen, 2017; chapter 7) and also must have had a significant impact on the geographical position and functioning of route networks in the landscape and on resulting cultural connectivity patterns.

In this chapter we model Roman and early-medieval route networks in a delta landscape as an expression of environmental and cultural changes. The aims are to: 1) calculate the level of persistence between the reconstructed Roman and early-medieval route networks; 2) determine to what extent the dynamic nature of delta landscapes influenced patterns of connectivity during this period; and 3) determine to what extent a network-friction model (NFM; section 8.2) can be applied to model Roman and early-medieval route networks on a more detailed regional scale and in densely populated areas. This was performed by applying a regional multidisciplinary approach: integrating large-scale archaeological and geoscientific datasets in combination with evidence-based route-network reconstructions. Our approach was based on the network-friction method presented by Van Lanen et al. (2015ab) which we further developed and tested.

We used the network-friction method introduced by Van Lanen et al. (2015a). This method was specifically designed to model suitable areas for potential route networks, i.e. movement corridors, in dynamic lowland areas. Van Lanen et al. (2015a, p. 200–201) define network friction as: “..the variable that determines potential regional accessibility based on the comparison of local and

surrounding landscape factors”. A network-friction model (NFM) calculates local accessibility based on a combination of high-resolution geoscientific datasets (e.g. palaeogeography, geomorphology, soil map, elevation model) and shows the potential movement corridors in the past. By combining a NFM with large-scale archaeological data it is possible to calculate and validate Roman and early-medieval route networks on a supra-regional scale. Van Lanen et al. (2015b) already stressed the importance of applying the network-friction method on a more local, detailed scale, especially in densely populated regions, in order to test its applicability for reconstructing past-route networks and human-landscape interaction.

The amount of archaeological data on the Roman period and, especially, the Early Middle Ages in northwest Europe has grown substantially over the last few decades. However, large-scale spatial patterns (e.g. settlement patterns, route networks, land-use systems) and their dynamics through time on delta-covering scale have not been studied in detail. Davis & McCormick (2008) and McCormick (2008) have already suggested that the next step should be to compare and analyse these newly available, vast amounts of data and collaborate better within and across scientific disciplines (e.g. geosciences, history, biology). For the Rhine-Meuse delta well-documented archaeological and detailed landscape reconstructions are now available and allow us to for the first time to study these spatial patterns on delta-covering scales using multi- and interdisciplinary approaches (e.g. Van Dinter, 2013; Van Dinter et al., 2017; chapters 6 and 7).

8.2 Route networks and connectivity patterns

Roads can be defined as narrow, fixed communication and transport lines connecting different places, whereas routes have been characterized as broad and vaguely delimited zones of communication and transport (Van Lanen, 2016; Van Lanen et al., 2016b). With the exception of the Roman *limes* road, there is little evidence for the presence of Roman and early-medieval roads in the Rhine-Meuse delta (e.g. Van der Heijden, 2016). Almost all Roman and early-medieval routes were unpaved and hence not rigidly anchored in space (e.g. Bell & Lock, 2000; Horsten, 2005). Route zones are spatial zones in which, often unpaved, bundles of tracks, paths or roads are located. These zones formed as a result of travellers frequently shifting to adjacent lanes because of e.g. weather conditions or general wear of the carved-in tracks. Although the general orientation of past roads and routes were similar, route networks spatially were more dynamic and therefore they should be regarded as corridors rather than as single lines.

Route networks are spatial elements connecting settlements by land or water through the surrounding landscape on local, regional and supra-regional scales (Van Lanen et al., 2015ab). In our study area the higher and relatively dry alluvial ridges provided the best places to live (e.g. Willems 1986; chapter 7) and also functioned as the movement corridors in the landscape. Movement corridors are defined as areas where landscape units provide people with connectivity options such as route zones to other places of interests (e.g. settlements, forts, mining areas, religious centres). The spatial layout of these movement corridors through time has been influenced by both environmental as well as cultural factors and therefore their chronological development is key to understand the complex interaction between these dynamics. As environmental conditions changed, the accessibility of these alluvial ridges also may be expected to have changed and in this manner the movement corridors and settlements situated there. This especially holds true for past delta landscapes due to the relatively large number of settlements and because the dynamic-fluvial environment forced people to adapt to rapidly changing environmental conditions

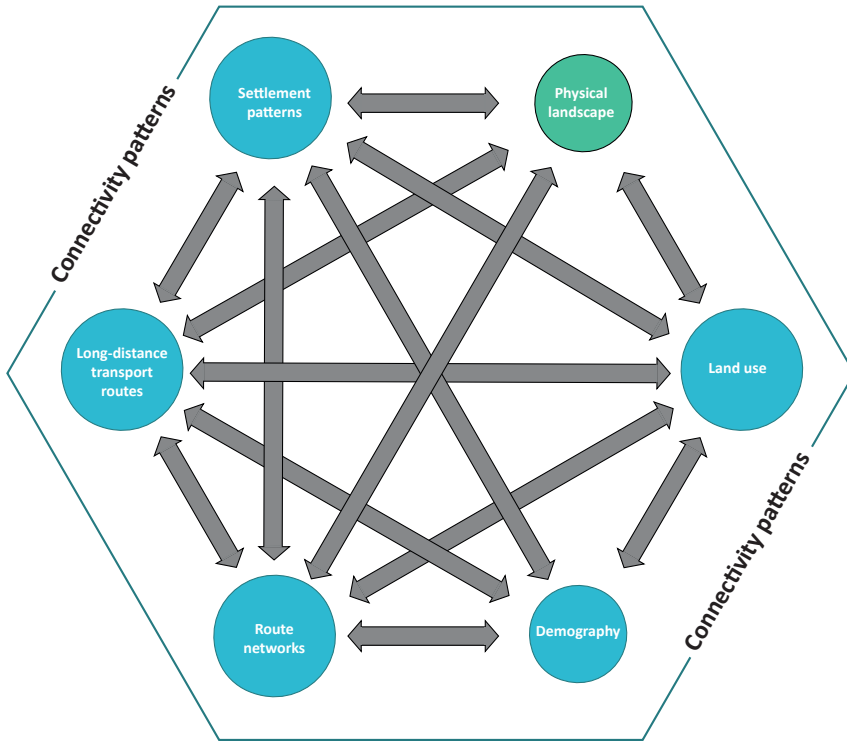


Figure 8.2 | Connectivity patterns: schematic overview of the interrelationships between important connectivity-pattern factors: physical landscape, settlement patterns, long-distance transport routes, route networks, demography and land use. The relative size of each factor node reflects the numbers of connections within the system, i.e. smaller nodes have less interrelationships. Each factor is connected to the other factors in the system, with the exception of the physical landscape and demography between which, excluding catastrophic events, no direct connection exists. Changes within one (or more) of the factors influence the interrelationships within the system and may cause changes in other factors, making connectivity patterns a complex system with countless dynamic, path-dependent connections.

Route networks are not merely connecting zones in the landscape but are an integral part of connectivity patterns. Here we define connectivity patterns as the dynamic spatial and social interrelation and interaction between the following landscape-influencing factors: settlement patterns, land use, demography, route networks, long-distance transport routes and physical landscape-formation processes (Figure 8.2). Changes in one of the factors within this system (may) cause a far-reaching ripple effect within the system, which implies that these patterns are connected and characterized by a level of path dependency and in general function on larger spatial and chronological scales. Although connectivity patterns are a complex collection of seemingly countless entwined relations, studying the changes of individual connectivity-pattern factors, such as settlement patterns and route networks allows to unravel this complexity. Therefore route networks, or connectivity patterns in general, are key for studying large-scale human-landscape interactions.

The reconstruction of historical route and road networks has been the focus point of many studies dealing with spatial modelling and Geographical Information Systems (GIS) software (e.g. Gietl et al., 2008; Zakšek et al., 2008; Verhagen & Jeneson, 2012; White & Barber, 2012; Verhagen, 2013; Breier, 2013; Vletter, 2013; 2014; Groenhuijzen & Verhagen, 2015). Traditionally the modelling of historical route networks using GIS has been limited to relatively theoretical exercises to determine technological possibilities and practical applications, and to calculate cost-surface modules and least-cost paths (e.g. Zakšek et al., 2008; Herzog & Posluschny, 2011; Murrieta-Flores, 2012; Herzog, 2013abc; Verhagen, 2013; Herzog, 2014). Many of these studies focus on regions characterized by large elevation differences, i.e. mountainous areas, and focus mainly on slope calculations, in this manner limiting the usefulness of the developed techniques for application in delta landscapes. Recently, it has been suggested that especially in these landscapes other environmental (e.g. soil type, groundwater levels) and non-environmental (e.g. political, socio-economic, religious) formative processes are of influence on the spatial layout of past route networks (e.g. Bell & Lock, 2000; Llobera, 2000; Herzog, 2013a; Van Lanen et al., 2015b; Vletter & Van Lanen, in review). The research focus therefore increasingly has shifted towards the need for integrated, explanatory and complementary models which can be validated using archaeological or historical data (e.g. Verhagen & Whitley, 2011; Citter, 2012; Herzog, 2013a; Fovet & Zakšek, 2014; Van Lanen et al., 2015b; 2016a). In order to study connectivity patterns, which are defined by cultural and natural processes, such models combining multiple proxies are required.

It is generally accepted that the (micro-)regional level is the optimal spatial entity to study the interaction between settlement and landscape dynamics from a long-term perspective using a landscape-archaeological approach (e.g. Spek, 2004; Kluiving et al., 2012; Kluiving & Guttmann-Bond, 2012; Van Beek & Groenewoudt, 2011). Van Lanen et al. (2015b) recently reconstructed Roman and early-medieval routes on a supra-regional level using multiple proxies. One of the findings was that this approach is unsuitable for application to the Rhine-Meuse delta, due to high settlement density in this region during the first millennium AD. The relatively high number of settlements, i.e. the ratio of settlements per km² higher than the national average, requires a spatially more detailed approach in order to accurately calculate route zones (Van Lanen et al., 2015b). This is now possible in our study area because: (i) newly-developed geoscientific input data with an unprecedented spatial and temporal resolution have become available (chapter 6), (ii) the grid-cell resolution of the NFM can be enhanced, i.e. from 500 × 500 m to 100 × 100 m and (iii) the study area reflects a region where settlement-density differences are minimal, i.e. settlements equally divided in the landscape.

8.3 Material and methods

Routes and network stability were calculated following the methods developed by Van Lanen et al. (2015ab). The first step was to create a NFM based on high-resolution geoscientific datasets (sections 8.3.1. and 8.3.2.). Next, archaeological data were integrated into the model by overlaying these data on network-friction maps, and routes were calculated for the time slices: AD 100, 500, and 900 (sections 8.3.3. and 8.3.4.). The resulting network reconstruction was to determine persistence of the reconstructed route network and validate the results based on the occurrence of infrastructural and isolated finds (sections 8.3.5. and 8.3.6.).

Since route networks were reconstructed based on archaeological and geoscientific data, the first were converted to match available geoscientific chronology. Archaeological data in our study area are recorded using chronological specifications from the Archaeological Basic Register (ABR).

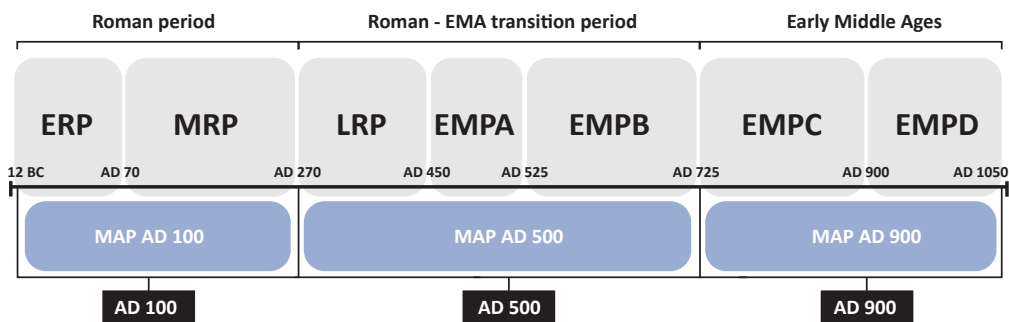


Figure 8.3 | Chronological division of subperiods based on the Archaeological Basic Register: early-Roman period (ERP), middle-Roman period (MRP), late-Roman period (LRP), early-medieval period A (EMPA), early-medieval period B (EMPB), early-medieval period C (EMPC) and early-medieval period D (EMPD). Each of the subperiods were linked to one of the geomorphological-landscape reconstructions for AD 100, 500, or 900.

Based on these chronological divisions and the newly-developed high-resolution geomorphological reconstructions we converted archaeological data to fit three time slices: AD 100, AD 500, and AD 900 (Figure 8.3). Data were divided based on two major cultural events during the first millennium AD: (i) the collapse of the Roman *limes* and coinciding diminishing of Roman authority and economy; and (ii) the cultural integration of the study area into the Carolingian empire. Each archaeological subperiod was linked to the geomorphological time slice optimally representing the specified period (Figure 8.3). We linked the Roman period (12 BC–AD 270), consisting of the early and middle-Roman periods, to the AD 100 time slice. The late-Roman period and early-medieval periods A to B, summarised as the Roman-EMA transition period (AD 270–725), was linked to the AD 500 time slice. Early-medieval periods C and D, the final part of the early-medieval period (AD 725–1050), were linked to the AD 900 time slice.

8.3.1 Geomorphological and palaeo-elevation reconstructions

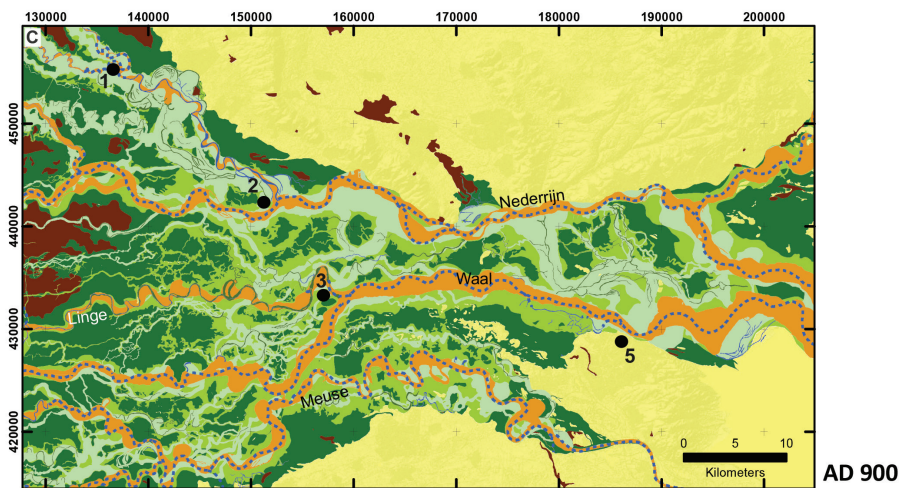
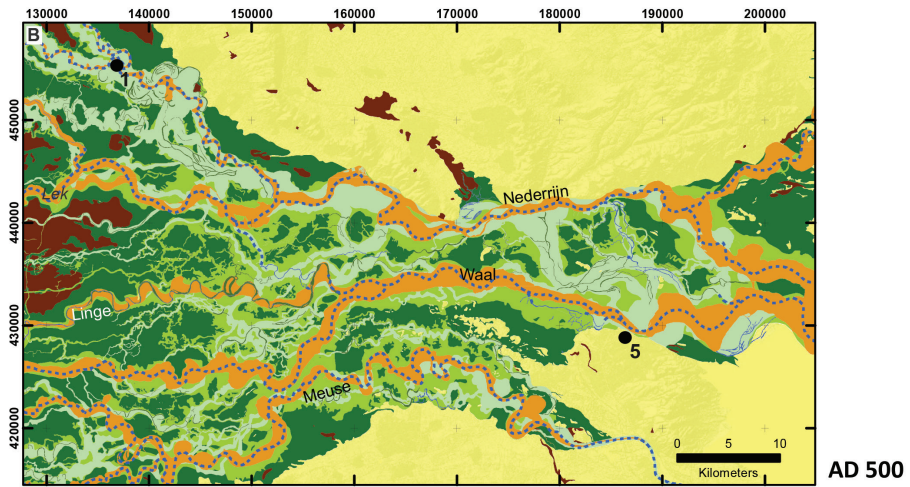
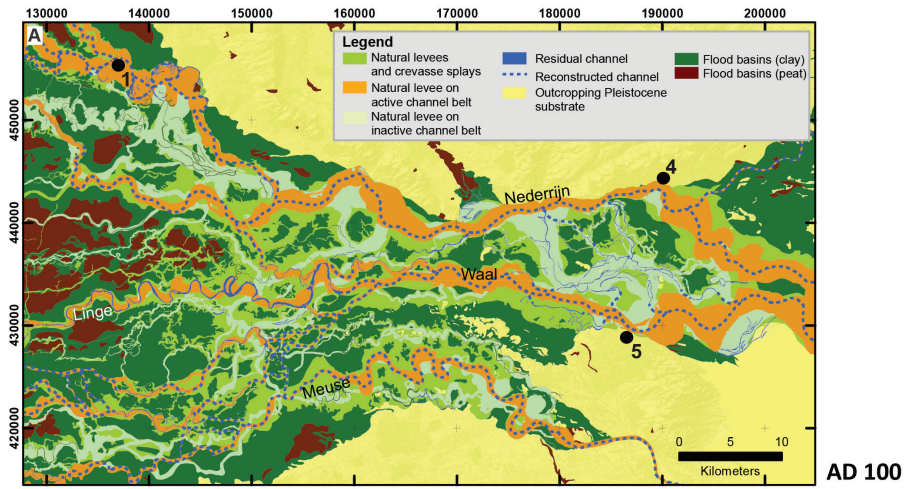
The network-friction maps presented in this chapter were based on recently developed geomorphological reconstructions and palaeo-elevation models, which are described below.

Geomorphological reconstructions

The geomorphological maps developed in chapter 6 represent reconstructions of the extent, distribution and orientation of the alluvial ridges present in the past landscape for the time slices AD 100, 500, and 900. The time steps 100, 500, and 900 CE equally divide the first millennium and the phasing of these developments. The first time step comprises the initial stage of a series of avulsions in the delta; the second time step fits with the stage of ongoing avulsions and increased flooding frequencies; the last interval represents the last natural state before embankment with matured new channel belts of a more-or-less completed avulsion.

Each of these maps in unprecedented detail show the spatial extent of channel belts including the well-accessible alluvial ridges (including natural levees and crevasse splays) and less-accessible flood basins (Figure 8.4). These reconstructions expand on existing regional studies (e.g. Willems,

Figure 8.4 (right page) | Geomorphological landscape reconstructions for the Rhine-Meuse delta around AD 100, 500, and 900 of chapter 6. The names of the major rivers and towns mentioned in the text are given for each time slice. 1 = Utrecht, 2 = Dorestad, 3 = Tiel, 4 = Arnhem, 5 = Nijmegen.



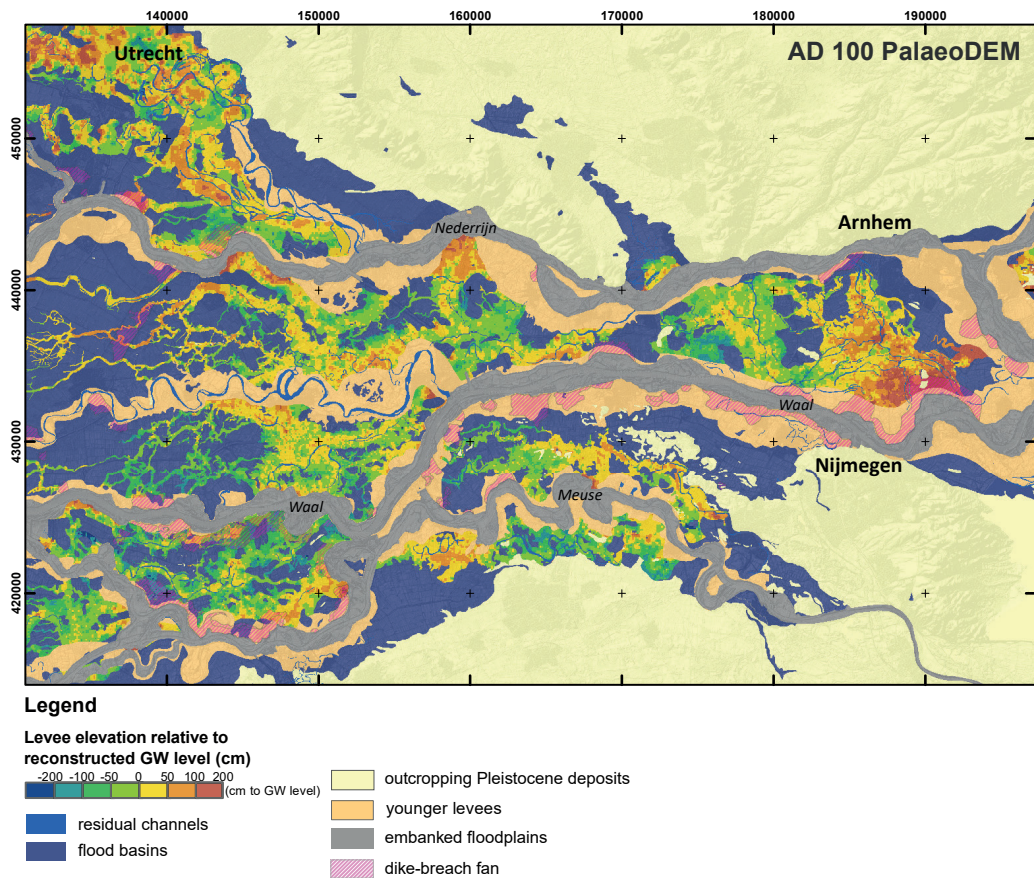


Figure 8.5 | Palaeo-DEM (relative to the groundwater level) for the Rhine-Meuse delta around AD 100 (chapter 6).

1986; Van Dinter, 2013; Van Dinter et al., 2017, see chapter 2) to delta scale in a uniform manner. The geomorphological elements were mapped using lithological and geomorphological datasets: lithological information was obtained from an extensive borehole database maintained by Utrecht University, whereas LiDAR images provided modern elevation data of the landscape (Berendsen & Volleberg, 2007). Alluvial ridges were taken from borehole data as loam or sandy clay intervals of at least 40 cm thick, that are elevated ca. 1-2 meter above to floodplain level (chapter 6). The sandy channel belts were taken from Berendsen & Stouthamer (2000), Cohen et al. (2012). In order to reconstruct past water routes, the position of former river channels was outlined by identifying elongated depressions in the LiDAR with a clayey and peaty infill.

The age of the mapped elements is relevant to evaluate the presence of specific elements during the reconstructed time steps. It was derived from ca. 300 ^{14}C dates, archaeology, and relative dating (Berendsen & Stouthamer, 2000; Cohen et al., 2012). The majority of the alluvial ridges had been formed before AD 100 (blue to red alluvial ridges in Figure 8.4). The age uncertainty of the younger alluvial ridges in Figure 8.4 relates to the dating accuracy of the initiation and the maturation of the according channel belts, which is generally maximal several centuries (Berendsen & Stouthamer, 2000). The maps have a higher spatial resolution than previous reconstructions, representing a

higher level of accuracy and include more landscape elements. Compared to existing supra-regional reconstructions for the first millennium AD by Vos (2015a) they include an additional time step, AD 500.

Palaeo Digital-Elevation Model (palaeo-DEM)

Higher and lower areas in the study region were distinguished using a palaeo-surface reconstruction for AD 100 with 100 × 100 m grid-cell resolution. This palaeo-surface topography (palaeo-DEM) was compiled by interpolating the vertical position of the top of the typical natural-levee and crevasse splay lithology, derived from the lithological borehole data (chapter 6). This dataset has been corrected for younger clay sedimentation on abandoned alluvial ridges and has been normalised for delta plain gradient (around +8 m OD in the east to around -1 m OD in the west). This normalization was performed by subtracting groundwater level reconstructions for 2000 yrs BP (Cohen, 2005; Koster et al., 2016a) from the palaeo-surface reconstruction. The resulting map shows the elevation of the landscape relative to the reconstructed past groundwater level in the delta (Figure 8.5).

Zones with actively-forming natural levees, embanked floodplains and dike-breach deposits of post-Roman active rivers have been omitted from the analysis, because they hampered the detailed reconstruction of former landscape elevation in this area. We therefore excluded the narrow strip of these elements and only used the inherited alluvial ridge landscape to update the NFM. The masked delineations of the levees were derived from the mapped boundaries of the geomorphological elements developed in chapter 6 (Figure 8.4).

8.3.2 Rhine-Meuse delta network-friction model (NFM)

Network friction was developed to identify geographical ‘push’ (unattractive areas for travelling: e.g. peat marshes, flood basins) and ‘pull’ (attractive areas for travelling: e.g. high, dry alluvial ridges) factors for possible translocation through the delta in the past. High-resolution geoscientific data on the Roman and early-medieval physical landscape were integrated into one network-friction model (NFM), which is described below.

Grid model

In order to develop the NFM we created a GRID model covering the fluvial dominated Rhine-Meuse delta region. The GRID model consists of 331,800 individual grid cells of 100 × 100 m, with each cell containing 21 data fields (Table 8.1). Each grid cell was assigned a unique identifier and corresponding grid-cell identifier from the supra-regional NFM developed by Van Lanen et al. (2015a; Table 8.1: #1 and #2). Geomorphological-reconstruction data on land and water units and accessibility values were recorded for each of the three time slices (Table 8.1: #3–#14). Elevation data derived from the palaeo-DEM and corresponding accessibility values were recorded in fields #15–#18 (Table 8.1). Network-friction values were calculated combining accessibility values from all geoscientific datasets.

Accessibility and network-friction calculation

In the NFM we used the five network-friction classes defined by Van Lanen et al. (2015a) (Table 8.2). Network-friction values were calculated for each individual grid cell by first selecting geomorphological units as reconstructed in chapter 6 that are archaeologically and historically known to be well suited for routes (e.g. high-elevated alluvial ridges), which were designated accessible (Table 8.2: 5). Grid cells located in areas clearly not suited for routes (e.g. wet peat areas,

Table 8.1 | Design of the NFM in the study area.

#	Field name	Description
1	GRID_100_ID	Unique identifier for each individual grid cell
2	GRID_500_ID	Corresponding identifier field in NFM Van Lanen et al. 2015b
3	LA_AD100_Unit	Geomorphological reconstruction unit AD 100
4	LA_Nfv_AD100	Accessibility based on land unit AD 100
5	LA_AD500_Unit	Palaeogeographical land unit AD 500
6	LA_Nfv_AD500	Accessibility based on land unit AD 500
7	LA_AD900_Unit	Geomorphological reconstruction unit unit AD 900
8	LA_Nfv_AD900	Accessibility based on land unit AD 900
9	WA_AD100_Unit	Geomorphological reconstruction water unit AD 100
10	WA_Nfv_AD100	Accessibility based on water unit AD 100
11	WA_AD500_Unit	Geomorphological reconstruction water unit AD 500
12	WA_Nfv_AD500	Accessibility based on water unit AD 500
13	WA_AD900_Unit	Geomorphological reconstruction water unit AD 900
14	WA_Nfv_AD900	Accessibility based on water unit AD 900
15	Palaeo_Elevation	Elevation based on the palaeoDEM AD 100
16	Nfv_AD100_PalaeoDEM	Accessibility based on elevation AD 100
17	Nfv_AD500_PalaeoDEM	Accessibility based on elevation AD 500
18	Nfv_AD900_PalaeoDEM	Accessibility based on elevation AD 900
19	LA_Nfv_AD100_Avg	Average network-friction value AD 100
20	LA_Nfv_AD500_Avg	Average network-friction value AD 500
21	LA_Nfv_AD900_Avg	Average network-friction value AD 900

flood basins) were designated inaccessible (Table 8.2: 1). Next, all remaining landscape units were classified as reasonably accessible (Table 8.2: 3). Since the network-friction value of a cell is not only defined by local but also immediately the surrounding landscape units, network-friction values were upgraded or downgraded based on their proximity to accessible or inaccessible areas, using a 100 m buffer (cf. Van Lanen et al., 2015a).

Importing the geomorphological reconstructions

Network friction has been designed to model the maximum amount of accessibility in the past. Therefore in the procedure of assigning friction values to the grid cells in the NFM, landscape units archaeologically known to be important for possible routes were imported into the model first (Table 8.3). In this conversion, even when only a small part of the grid cell intersected with such landscape units, the complete cell was assigned this specific value. In delta landscapes this approach ensures that small movement corridors such as very narrow alluvial ridges (< 100 m wide) are included in the resulting reconstruction. Since land and water transport require opposite landscape units, some areas are well suited for land routes but equally form an obstacle for water transport (and vice versa). Therefore land and water routes were separately calculated in the NFM (Table 8.3).

The geomorphological data for AD 100, 500, and 900 developed in chapter 6 were clustered into 10 generalized landscape units (Table 8.3). These landscape units were imported into the NFM by spatially overlaying their geographical outlines with the grid cells. Intersecting cells were selected and updated with corresponding geomorphological data using the unique GRID_ID. This process was repeated for each of the landscape units and time slices.

Table 8.2 | Network-friction values as defined by Van Lanen et al. (2015a).

Description	Network-friction value
Inaccessible	1
Poorly accessible	2
Moderately accessible	3
Reasonably accessible	4
Accessible	5

Table 8.3 | Generalized landscape units of the geomorphological reconstructions in chapter 6. For each of the legend units the import sequence into the NFM, the legend ID in the original dataset, corresponding descriptions and assigned network-friction values (1 = inaccessible, 3 = moderately accessible, or 5 = accessible) are presented.

Import seq. Land routes	Import seq. Water routes	ID legend (chapter 6)	Description geomorphological unit (chapter 6)	Network-friction value Land routes	Network-friction value Water routes
1	1	x	Reconstructed active channel	1	5
2	2	6	Open residual channel	1	5
3	x	5	Natural levee	5	x
4	x	3	Natural levee on inactive channel belt	5	x
5	x	4	Crevasse splay	5	x
6	x	1	Outcropping pleistocene substrate	5	x
7	x	7	Abandoned residual channel	3	x
8	3	2	Active channel belt/with immature natural levees	3	3
9	x	8	Clay-filled floodbasin	1	x
10	x	9	Peat-filled floodbasin	1	x

Palaeo-DEM import

Within the alluvial ridges (Figure 8.3), further distinctions regarding accessibility were made using the reconstructed relative surface elevation of the palaeo-DEM. We assumed that more elevated areas had lower-groundwater levels and were less prone to floods. Elevation data in the palaeo-DEM was recorded using 100 × 100 m grid-cell resolution, which corresponds to the resolution of the NFM. These data were included by calculating the relative surface elevation for each NFM-grid cell and further refining the network-friction values, i.e. lower areas (< -0.5 m) were manually given a value of 2 and grid cells with an elevation between -0.5 m and 0 m and > 0 m, values 4 and 5 respectively. Including this dataset allowed us to take elevation differences within these landscape units into account. Areas with post-Roman alluvial ridges (i.e. close to post-Roman active rivers) were not reconstructed in the palaeo-DEM and therefore were not adapted further. The low-lying flood basins already had been designated as less suitable for routes and therefore also remained unchanged. In addition the younger reworked landscape units were not differentiated using the palaeo-DEM.

8.3.3 Archaeology

Archaeological data on the location, chronology and type of Roman and early-medieval settlements, burial sites, shipping (e.g. shipwrecks) and isolated finds were collected through the Archaeological Information System of the Netherlands (ARCHIS), the dendrochronological repository DCCD, and the Electronic Archiving System (EASY). ARCHIS contains a national overview of archaeological finds (Roorda & Wiemer, 1992; Wiemer, 2002). In order to increase data accuracy we expanded and enhanced this dataset with archaeological data published in regional overview studies (e.g. Bechert & Willems, 1995; Verwers, 1998) and the LGL World Heritage Database (2010). Additional data on shipwrecks were collected through the heritage-based online dendrochronological repository DCCD (Jansma et al., 2012; Jansma, 2013) and from overviews made by Brouwers et al. (2013; 2015). EASY is an online archiving system for archaeology and contains a wide variety of excavation data (e.g. reports, figures, photos, GIS files).

8.3.4 Modelling past routes

Land and water route networks were calculated for AD 100, 500, and 900 by combining the settlement data and the NFM. Using the method of Van Lanen et al. (2015b) we modelled route zones between settlements in the manner described below.

Modelling land routes

We modelled land-route zones following the method presented by Van Lanen et al. (2015b). By calculating the shortest path between neighbouring settlements or burial sites (nearest neighbour) following the average highest network-friction values (i.e. highest level of accessibility, least friction) route zones of 100 m wide were computed. Since Roman and early-medieval burial sites always were located near settlements (i.e. at a minimum distance of 300 m from the settlement; Van Es, 1981; Verlinde, 1987; Verwers, 1998; Hiddink, 2003; Heeren, 2009; Van Beek, 2009), in case of missing settlement data we used burial sites as an indication of nearby habitation. In order to obtain maximum accuracy within the used datasets, settlement data were selected from ARCHIS only when: 1) at least five finds were recorded for that site; and 2) the chronological resolution reflects the ABR subperiod division (e.g. early-Roman period, early-medieval period B). In this respect the modelled network shows a minimum amount of probable connections to settlements, since only settlements dating to specific subperiods were included in route calculations. Therefore additional movement corridors calculated by the NFM, which based on geoscientific data were well suited for route zones but lacked (reliable) archaeological data, were not part of the route-network reconstructions.

Modelling water routes

Water-route zones were modelled based on data representing shipwrecks and water-adjacent settlements (i.e. settlements within 100 m from active channel belts). Through dendrochronology many shipwrecks have been dated accurately, and therefore this find category was used as a high-resolution record of active transport routes. Water routes were modelled by calculating the shortest path between water-adjacent settlements and shipwrecks along the reconstructed active rivers around AD 100, 500, and 900, i.e. grid cells with network-friction value 5 for water transport (Table 8.3). Grid cells containing navigable rivers but without known water-adjacent settlements were excluded from the route-network reconstruction.

8.3.5 Route persistence

Route-network persistence was calculated by comparing the spatial layout of route-zone sections within the networks during the different time slices. In line with Van Lanen et al. (2016b) we define the term “persistence” as the long-term use of specific locations in the landscape. These areas, although not necessarily continuously in use, reflect locations which are at least frequently reused and ‘never’ completely abandoned. Even if these route zones or movement corridors were at some point abandoned they are expected to survive in the collective memory. In order to calculate persistence, the networks were converted into individual line sections, i.e. unique lines between nodes never exceeding 200 m in length, which were then spatially compared to route-zone sections from the two other periods. We used the 100 m wide route-zone sections for the persistence calculations, since these reflect the most accurate buffers and therefore yield the most conservative persistence results.

8.3.6 Route validation

The reconstructed route networks were validated using three route-zone scales: 100 m, 250 m and 500 m, the latter corresponding with the average width of the larger alluvial ridges (Figure 8.3). For each of the time slices the percentage of infrastructural and isolated finds located within the route zone was calculated. Infrastructural finds, e.g. remnants of roads, tracks, jetties and harbours, are indicative for the presence of past-route networks. Isolated finds such as pottery sherds, *fibulae* and jewellery, represent past material unconnected to any (known) larger archaeological complex (e.g. settlement, temple), but nonetheless indicate human activity on a specific location (cf. Van Lanen et al., 2015b). Therefore, if routes have been modelled correctly the percentages of infrastructural and isolated finds located within the route zones should be relatively high as compared to the complete set of infrastructural or isolated finds found in the study area.

We determined the relative accuracy of the validation results by comparing them to the spatial dimensions (i.e. width) of individual landscape elements, such as alluvial ridges which function as movement corridor. First, the surface area of each route zone of 100 m, 250 m, and 500 m (rz100, rz250 and rz500 respectively) was divided by the total surface area of the NFM. Next, the numbers of infrastructural finds and isolated finds located within the route zone were divided by the total number of similar finds located in the study area. In order to assess the performance of the model and determine the robustness of these validations we calculated gain values (G) based on Kvamme (1988) using the following equation:

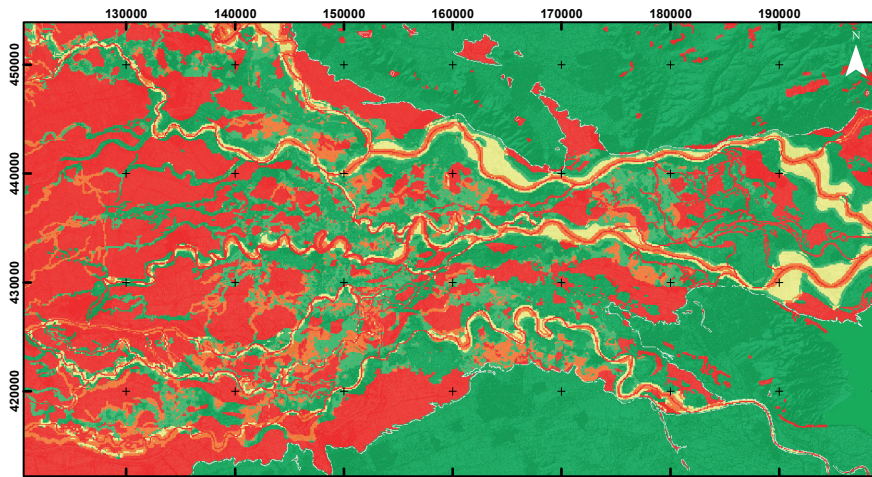
$$G = 1 - \frac{Pa}{Pf}$$

Where Pa is the proportion of the surface area of each route zones (100 m, 250 m, and 500 m) compared to the total surface area of the NFM and Pf is the proportion of infrastructural or isolated finds within that zone of interest.

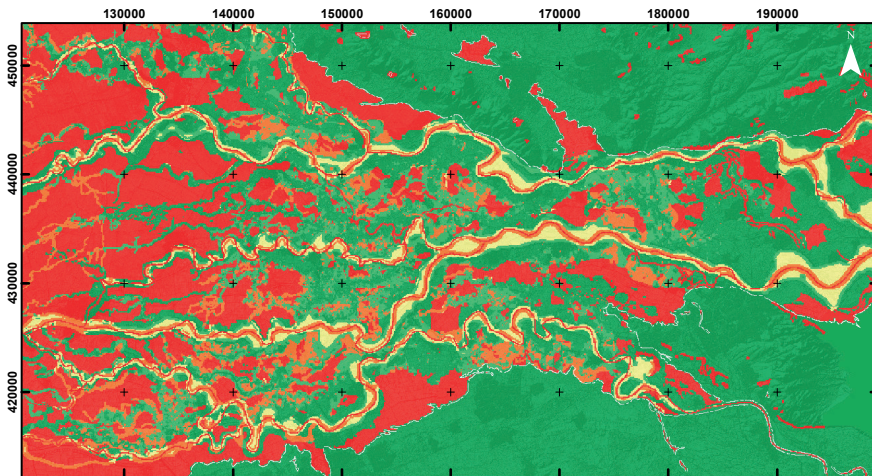
8.4 Results

8.4.1 Network friction

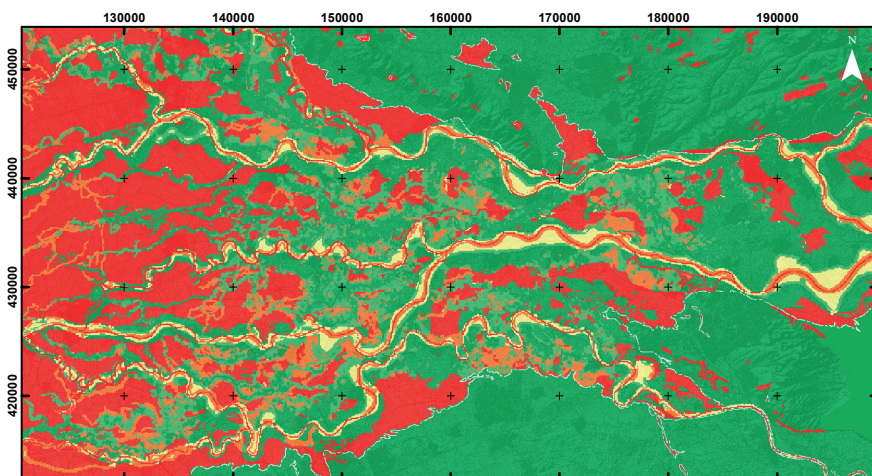
The NFM shows that most accessible regions in AD 100, 500, and 900 were located in the eastern and central part of the study area (Figure 8.6). In the western part, which was dominated by clayey and peaty flood basins, small and less-accessible alluvial ridges and rivers formed narrow movement



AD 100



AD 500

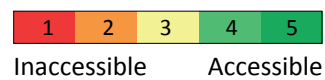


AD 900

Network-friction maps

Rhine-Meuse delta (NL)

158



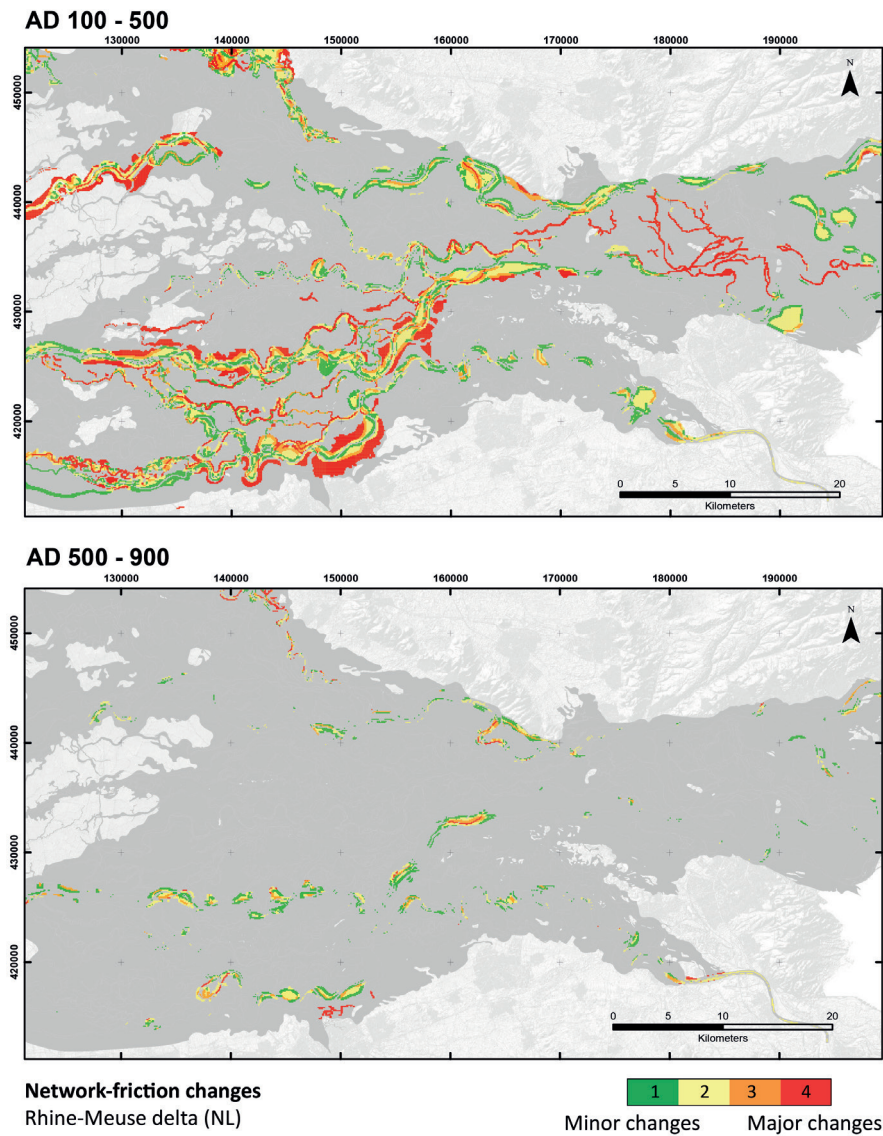
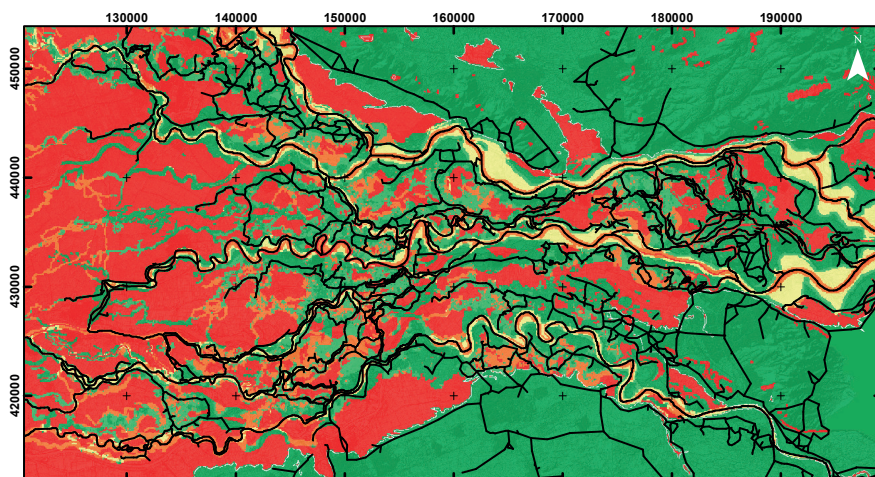
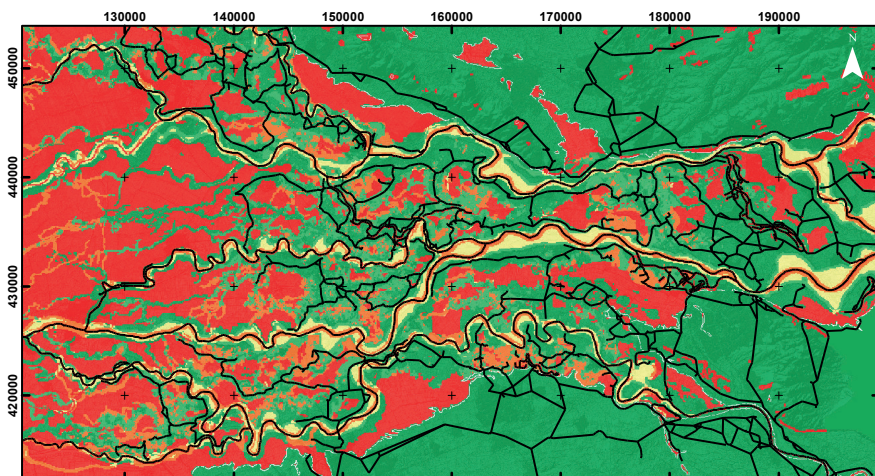


Figure 8.6 (left page) | Network-friction maps for the Rhine-Meuse delta around AD 100, 500, and 900. The white line shows the division between the Holocene and Pleistocene parts of the study area.

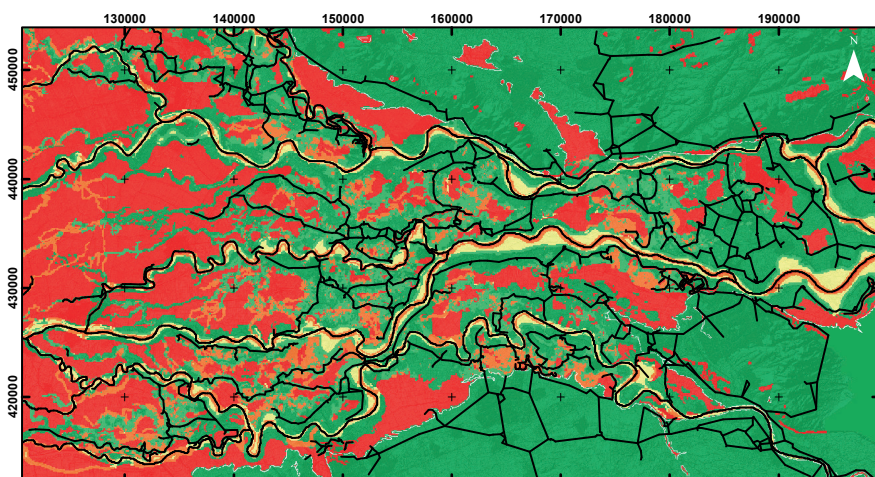
Figure 8.7 (above) | Overview of network-friction changes in the Rhine-Meuse delta between AD 100 to 500 and AD 500 to 900.



AD 100



AD 500



AD 900

Route networks

Rhine-Meuse delta (NL)

Route network

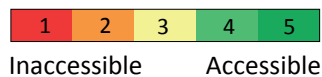


Figure 8.8 (left page) | Route networks (land and water) in the Rhine-Meuse delta around AD 100, 500, and 900 projected on the corresponding network-friction maps.

corridors for land or water routes to the west. In this area landscape settings strongly must have limited route orientation.

Through the NFM we were able to locate regions where accessibility changed between AD 100, 500, and 900 and calculate the severity of these changes (Figure 8.7). The most notable changes occurred between AD 100 and 500, especially in the south-western and north-western parts of the study area. Between AD 500 and 900 accessibility changes appear to have been less severe, with the largest changes being restricted to the north-western, south-western and north-eastern part of the Rhine-Meuse delta. Changes in accessibility during the first millennium AD appear to have been linked to meander migration and avulsion activity. These changes can be attributed to avulsions of the river Waal, Maas, and Lek, which especially affected the western part of the study area (Stouthamer & Berendsen, 2001, Stouthamer et al., 2011, Cohen et al., 2012). The new river courses must have cut off older routes, but at the same time must have provided new opportunities for water routes and, when the natural levees matured, eventually for land routes. The older river courses must have silted up and therefore became less accessible for water transport.

8.4.2 Network characteristics

Spatial patterns

During the first millennium AD route networks connected almost all parts of the Rhine-Meuse delta (Figure 8.8). Land routes were mainly east-west oriented and located on the alluvial ridges. The delta could be crossed in a north-south direction in the eastern part of the study area, most notably on the movement corridors near the current cities of Arnhem and Nijmegen (Figures 8.3 and 8.8). Towards the west, in the central part of the delta, land routes mainly ran towards the northwest and the southwest. The most western option to switch route zones and cross the entire delta in a north-south direction appears to have been in the centre of our research area, near the early-medieval towns of Dorestad and Tiel. These two locations were characterized not only by well-connected land routes running north-south and east-west, but also by abundant water-transport possibilities as they were located on important river bifurcations (Kosian et al., 2016; Oudhof et al., 2013). In the Roman period, the presence of many open residual channels caused water routes in the study area to be oriented in line with many land routes on the alluvial ridges (Figures 8.3 and 8.8). When new rivers formed, these older channel silted up leaving only a few navigable connections towards the north-west and south-west from the centre of the study area. With the exception of the eastern and central parts of the delta during the Roman period, water routes running north-south were almost non-existent (Figures 8.3 and 8.8).

The reconstructed route networks point towards a remarkable high level of connectivity in the Rhine-Meuse delta. Almost all movement corridors contain one or more route zones, which suggests that the delta landscape was used to its full potential. Despite the dynamic nature of the landscape and the likelihood of floods, the areas' pull factors (section 8.1) appears to have continuously drawn people to settle in this area, resulting in all parts of the delta to be well connected and isolated areas to be non-existent. Major events such as the avulsion of the river Rhine to its southern course, the river Waal, initially will have limited the number of accessible land routes in the south-western part of the study area, but equally facilitated new water-route connections

Table 8.4 | Overview of surface calculations of the modelled route networks. For each of the networks the surface area and corresponding percentage compared to the total research area are given.

Route zone	Surface AD 100 (km ²)	% of AD 100 surface	Surface AD 500 (km ²)	% of AD 500 surface	Surface AD 900 (km ²)	% of AD 900 surface
100 m	211.9	6.4%	173.3	5.2%	167.1	5.1%
250 m	503.8	15.2%	419.0	12.7%	405.9	12.3%
500 m	906.5	27.4%	779.7	23.6%	762.8	23.1%
Total study area	3,306.8					

Table 8.5 | Persistence and long-term persistence between route networks using 100 m-wide route zones. Persistence percentages are based on: the surface area of the complete route-networks (i.e. 50 m buffer) compared to the surface area of the route sections that are in use during (persist to) the next time step. Long-term persistence is presented for the youngest route network of AD 900 and shows the percentage of route sections in use during all researched time slices.

Route network	Surface area (km ²)	% Surface area
AD 100	211.9	100.0%
AD 500	173.3	100.0%
AD 900	167.1	100.0%
Persistence between time slices		
Persistence AD 500 (compared to AD 100 network)	138.3	79.8%
Persistence AD 900 (compared to AD 500 network)	134.6	80.5%
Long-term persistence		
Long-term persistence within AD 900 network (route sections in use during all time slices)	118.5	70.9%

towards the southwest. Here the natural levees were not mature yet, which is underlined by the lack of archaeological finds on these relatively young landscape units.

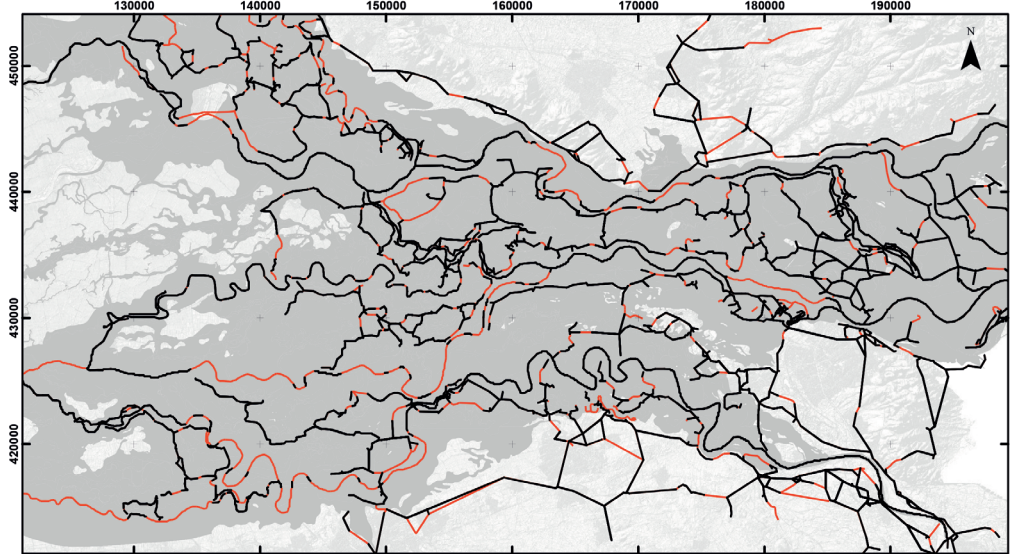
Surface areas

Route-zone density was determined for the combined land and water route networks (Table 8.4). Results show that the Roman-route zones around AD 100 covered the most land. A decreasing trend in route-zone surface area is visible towards the AD 500 and AD 900 time slices. The pattern between AD 100 and AD 500 is best explained by demographic decline during the post-Roman periods. Despite a probable population increase after AD 500, the pattern between AD 500 and AD 900 is still rather consistent, this is most likely due to increased settlement size and the clustering of settlements towards the Middle Ages (e.g. Dekker, 1983; Rutte & Abrahamse, 2015; chapter 7).

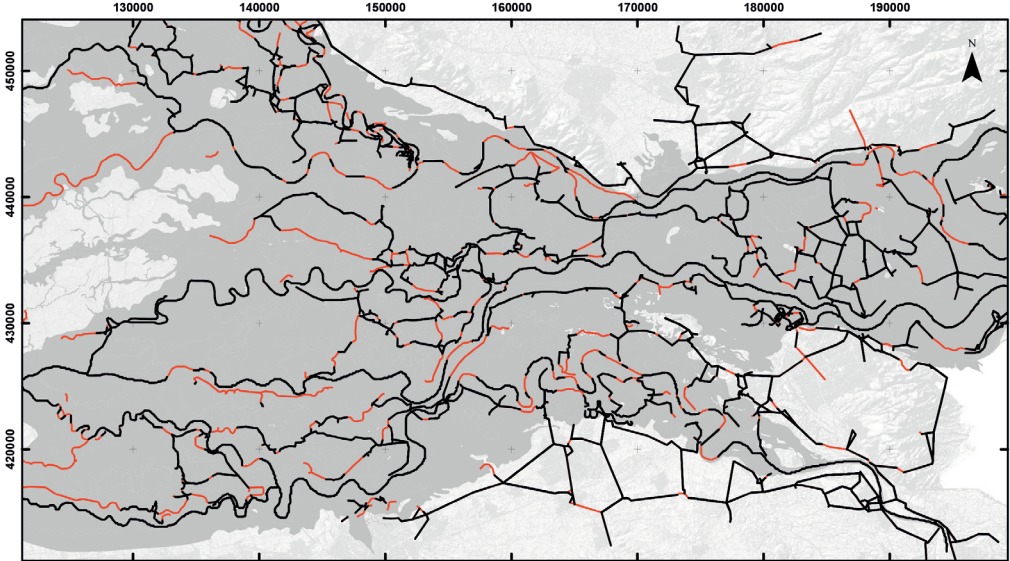
8.4.3 Route-network changes and persistence

Despite the dynamic nature of the study area, 79.8% of the modelled AD 500 network shows persistence with route sections from the AD 100 network (Table 8.5; Figure 8.9). In the subsequent period persistence slightly increased, resulting in 80.5% of the AD 900 route sections showing persistence with their AD 500 predecessors (Table 8.5; Figure 8.9).



Persistence AD 100 - 500



Persistence AD 500 - 900



Route-network persistence
Rhine-Meuse delta (NL)

-  Complete route network
(A = AD 500 network, B = AD 900 network)
-  Persistent route sections

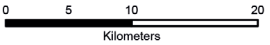


Figure 8.9 | Persistent-route sections (in black) projected on the AD 500 and AD 900 route networks (in red) in the Rhine-Meuse delta. Persistence was calculated between the AD 100 and AD 500 route networks (above) and the AD 500 and AD 900 route networks (below).

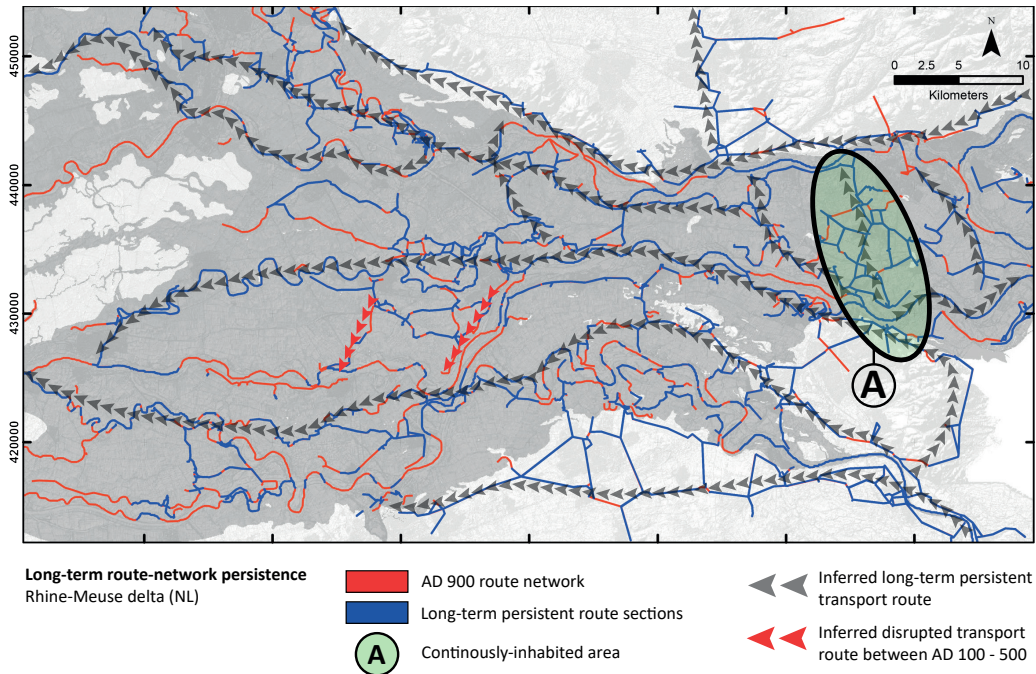


Figure 8.10 | Long-term persistent route sections (in blue) projected on the AD 900 route network (in red) in the Rhine-Meuse delta. For each of the movement corridors long-term persistent transport routes were inferred (in grey). Major disruptions in these transport routes between the Roman and early-medieval periods are presented in red.

Long-term persistence

Long-term persistence between all three time slices was calculated for the youngest time slice, the AD 900 network. By comparing AD 500 to 900 persistence (80.5%; Table 8.5) to AD 100 and 500 persistence we calculated that 88.1% of the AD 900 persistent-route network is long-term persistent, i.e. in-use during all three periods (Table 8.5; Figure 8.10). This equals to 70.9% of the complete AD 900 network. Results show that the majority of the route sections in the first millennium AD were persistent and located in movement corridors that appear to form core regions within the study area. Within these regions the majority of the persistent settlement were situated. During periods with strong demographic decline, i.e. the LRP, EMPA, and EMPB periods, habitation appears to have clustered within these parts of the movement corridors and route-zone orientation remained relatively stable.

8.4.4 Route-network validation

Table 8.6 shows overviews of the validation results for each of the modelled route zones and time slices (Table 8.6; Figure 8.11A). Additional percentages of finds located outside the largest route zone, i.e. 500 m, are also presented. Although these 500 m route zones represent the least strict validation, their spatial extent corresponds best with the width of the movement corridors, i.e. representing the smallest levees. Results show that for infrastructural finds derived from locations within the route zones the validation percentages are lowest for the AD 100 time slice. At this 100 m route-zone level results for the AD 500 and 900 time slices are more-or-less comparable (Table

Table 8.6 | Overview of the validation results and gain values for Roman and early-medieval infrastructure (upper) and isolated finds (lower). For each route zone either the percentage of correctly modelled finds within the route network or gain value is given.

Route zone	AD 100 network		AD 500 network		AD 900 network	
Validation: infrastructural finds within route zone						
	N	%	N	%	N	%
100 m	98	48.8%	38	60.3%	28	63.6%
250 m	135	67.2%	50	79.4%	38	86.4%
500 m	180	89.6%	60	95.2%	40	90.9%
Outside 500 m	21	10.4%	3	4.8%	4	9.1%
Validation: isolated finds within route zone						
	N	%	N	%	N	%
100 m	2372	35.9%	590	38.1%	557	29.0%
250 m	4081	61.7%	896	57.8%	954	49.6%
500 m	5255	79.5%	1163	75.1%	1287	66.9%
Outside 500 m	1357	20.5%	387	25.0%	637	33.1%
Route zone	AD 100 network		AD 500 network		AD 900 network	
Gain values: infrastructural finds						
100 m	0.87		0.91		0.92	
250 m	0.77		0.84		0.86	
500 m	0.69		0.75		0.75	
Gain values: isolated finds						
100 m	0.82		0.86		0.82	
250 m	0.75		0.78		0.75	
500 m	0.66		0.69		0.66	

8.6). In contrast, the validation percentages for finds located outside the 500 m route zones are more comparable for the AD 100 and 900 networks. In general validation results for AD 100 are high but slightly lower than for AD 500 and 900. The relatively low 100 m route-zone validation percentages for the AD 100 time slice are best explained by the fact that during the Roman occupation infrastructural works were often issued by a central government despite less favourable landscape settings (e.g. Van der Heijden, 2016). The current NFM does not include these variables sufficiently to model these deviations correctly. The test results increase drastically between the 100 m and 250 m route zone validations, with the best results for the AD 900 network. Gain values were also calculated for each time slice and modelled route zone (Table 8.6). None of the gains are lower than 0.5 and most values relatively close to 1, meaning that the modelled route zones are a good representation of human activity in the landscape. Showing potential for predicting yet undiscovered archaeology. The performance of our model appears to be better than gain values calculated for the Indicative Map of Archaeological Values of the Netherlands (IKAW; Verhagen, 2007).

When comparing the validation for the infrastructural and isolated finds the following differences are observed: the correlation between the spatial layout of isolated finds and the modelled route zones is generally lower for all periods. Additionally, the highest percentages of isolated find within the route zones occur in the Roman period, whereas the infrastructural finds

in this period show the lowest correlation (Table 8.6; Figure 8.11A). This pattern also was visible in the supra-regional analysis by Van Lanen et al. (2015b: Table 8.4 and Figure 13). The exact reasons behind this pattern shift are unclear, but it is probably best explained by: a) the different nature of isolated finds in the three periods (i.e. relatively high number of recognisable coins in the Roman period) and b) the probable culturally-defined differences in depositional and post-depositional processes, i.e. processes influencing the degradation and retrievability of archaeological material (e.g. Schiffer, 1976; 1987). Most notable are the relative low validation percentages for the AD 900 network, with 33.1% of the isolated finds located outside the 500 m route zone.

Calculating probability of the networks

When the route-zone width is increased from 100 m to 250 m, the validation results, i.e. the number of infrastructural and isolated finds located in the route-zone buffers, greatly increase (Figure 8.11B). Most graphs show a slight flattening-out between rz250 and rz500 and reach good results for the latter. This suggests that 250 m as a route zone is the most accurate resolving resolution for route-width reconstructions. The validation using infrastructural finds show better results compared to the isolated-find validation, which is understandable since infrastructural finds are a direct representation of active route networks. Figure 8.11B also shows the most notable, almost linear trend for correctly located infrastructure during the Roman period as compared to the post-Roman periods. This trend probably shows the deviating development of infrastructural works during the Roman period, i.e. infrastructural works located on less predictable locations because of Roman centralized governing.

8.5 Discussion

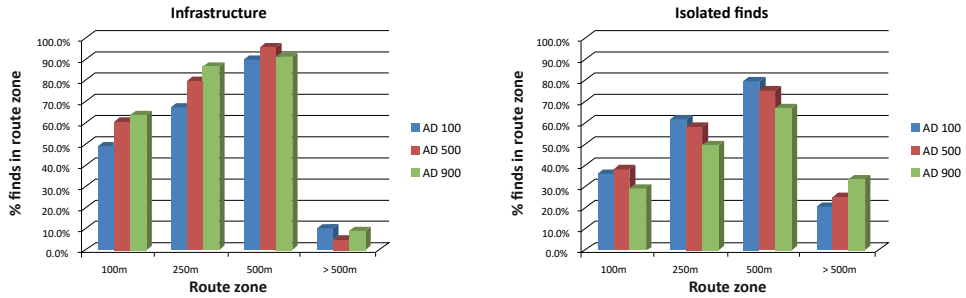
8.5.1 Connectivity patterns in the Rhine-Meuse delta

The NFM for the Rhine-Meuse delta shows a clear intra-regional variability between the eastern and western parts (Figure 8.6). The eastern parts of the delta landscape were relatively well accessible throughout the first millennium AD. The western parts generally were less accessible and appear to have been much more susceptible to landscape dynamics, mainly avulsion, most notably between AD 100 and 500 (Figures 8.6 and 8.7).

Landscape settings clearly influenced regional accessibility during the first millennium AD. Areas which contained extensive flood basins, which were not interrupted by accessible alluvial ridge corridors (e.g. western delta), formed a large barrier in the landscape (Figure 8.8). Areas with abundant accessible alluvial ridges that were well connected to each other on the other hand facilitated multiple movement corridors. The abundance and orientation of the ridges determined the connectivity in the central and upper Rhine-Meuse delta and facilitated transport from and towards multiple directions. Therefore this region can be regarded as a transport hub characterized by east-west corridors as well as several north-south connections (Figure 8.10).

Despite the dynamic nature of the delta landscape, its modelled route networks between AD 100 and 900 were characterized by a surprising degree of stability (Table 8.6; Figure 8.9). The main reasons for this are: (i) the route-networks were generally located on the older, more stable alluvial ridges; (ii) although strong population decline following the Roman period must have led to decreasing demographic pressure on the landscape, in the study region settlements shifted locally rather than disappearing completely as was also shown by Verhagen et al. (2016) and in chapter 7; and (iii) the lower demographic pressure after the Roman period on the landscape allowed the delta inhabitants to locate to the ideal (i.e. safest) settlement locations, probably partially forced by

A



B

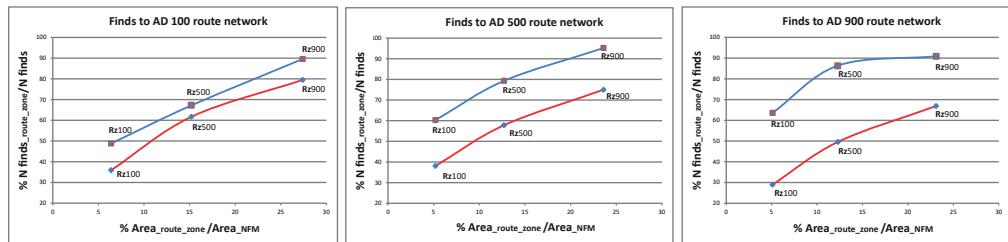


Figure 8.11 | (a) Percentages of infrastructural (left) and isolated finds (right) located within the 100 m, 250 m and 500 m route zones for AD 100, 500, and 900. (b) Overview of validation results using infrastructural (blue) and isolated finds (red). For each of the route zones: 100 m, 250 m, and 500 m (Rz100, Rz500, and Rz900 respectively) the correlation between route-zone surface area, finds located within that zone and the complete dataset (area_NFM and N finds respectively) area given.

increased flooding between AD 270–850 (Toonen et al., 2013; Cohen et al., 2016). As a result, many parts of the route networks remained in use and the impact of increased flooding frequencies on the development of the route networks appears to have been limited.

Most parts of the modelled route networks in the study area show clear signs of long-term persistence, with the exception of the southwest of the study area (Figure 8.10: red arrows). The robustness of route-network persistence could be further assessed in the future using more detailed archaeological settlement data. Our results are in agreement with findings by Hendriks et al. (in press: Table 7.12), who used a detailed regional approach to study changing Roman and early-medieval settlement patterns in the central and southern Netherlands. They have shown that certain parts of our study area (Figure 8.10: region A) were continuously inhabited during each of the cultural subperiods (Figure 8.5). As such these continuously-inhabited regions even cross the archaeologically defined chronological boundaries and can be useful to study long-term route-network development.

Avulsions appear to have been very influential on route-network development, most notably through the newly-formed river Waal and Meuse in the south-western part of the study area. Here we see route-network persistence is low and settlement density after the Roman period decreasing (chapter 7). There are several reasons to classify this part of the delta as more sensitive to physical-landscape changes. First, the new river Waal cut through all existing corridors, i.e. through land routes as well as water routes. Second, the presence of this largest river in the delta made the area more prone to floods (chapter 7). In this area existing land and water routes will have been cut off,

effecting the stability of route networks (section 8.4.1; Figures 8.7 and 8.10), but at same time this river provided new (long-distance) water-based connections.

Equal to settlements, route networks were formed by a combination of cultural and natural factors. The relatively high number of infrastructural and isolated finds located within the reconstructed route zones confirms the hypothesis that natural setting, i.e. the occurrence of alluvial ridges and navigable channels, was a key factor for route-network development. Although natural forcings, such as floods, must have led to countless local adaptations in settlements patterns (e.g. chapter 7; Hendriks et al., in press) and route sections on a local scale, natural-forcing factors, appear to have been of little influence on the persistence of the networks. This is probably due to the fact that interconnecting route zones and movement corridors function on a more regional scale and therefore appear to have been persistently reused throughout the first millennium AD. From this we infer that the overarching delta-wide connectivity patterns appear to have remained the same, i.e. reflecting dynamics on a local scale (e.g. settlement patterns) but at the same time mirroring persistence on a larger scale (e.g. route networks).

The results demonstrate the strong link between settlement location, route orientation and the physical landscape. The network-friction method has proven itself very helpful in better understanding dynamics between these factors on these varying spatial and chronological scales. Spatial structures such as route networks and settlement patterns in the Rhine-Meuse delta point towards a persistence in overarching connectivity patterns in the area. Regions with abandoned routes or settlements appear to have been prone to be reused for similar functions in later periods (functioning as pull factor), showing a degree of path dependency to one another. In the future, the NFM therefore could be slightly adapted to function as predictive map pinpointing regions with an increased likelihood of containing archaeological remains of as yet undiscovered settlements, burial sites or shipwrecks (section 8.4.4).

8.5.2 The network-friction method on regional scale

The presented results contributed to refining route-network modelling in delta landscapes (section 8.3.1; Figure 8.3). The results of this integrated view, combining high-resolution archaeological and geoscientific data, are promising for route-network modelling since they clearly show that local accessibility in the first millennium AD can considerably vary in space and in time in this dynamic landscape.

When the validation outcomes are compared with the supra-regional analysis by Van Lanen et al. (2015b), it becomes clear that data quality between the different input datasets is crucial. The models' accuracy using the most detailed route zone of 100 m is relatively low compared to the other modelled-route zones (Table 8.6; Figure 8.11A). Figure 8.11B shows that within the available data resolution the route-zone width of 250 m is probably most suited for route-network modelling using a NFM. Furthermore the results show that we can accurately reconstruct the route location within 500 m, but the data is less suitable for modelling route zones with 100 m accuracy. This is mainly due to the regional scale and archaeological data applied in the current NFM. Gain values however show that the models' performance in locating infrastructural and isolated finds is generally higher than the scores calculated by Verhagen (2007) for the national predictive model in the area, the IKAW (section 8.4.3). Although the high-resolution geomorphological data used in the NFM were specifically designed for the study area, the archaeological data in the model originate from supra-regional overviews and as such create a disbalance. Data stored in ARCHIS have not been developed for studies with this level of detail, and should be improved upon when applying a

regional or smaller approach to route-network modelling. These improvements should incorporate amongst other settlement hierarchy and enhanced chronological resolution.

Although the current NFM successfully models persistency of movement corridors, it would benefit from a more extensive analysis using traditional GIS-based route or path-modelling techniques. This includes network analysis and least-cost path calculations, in order to model route networks and network hierarchy within these movement corridors more precisely (e.g. Gietl et al., 2008; Murietta-Flores 2012; Herzog, 2013a; 2013b; Verhagen, 2013; Groenhuijzen & Verhagen, 2015; 2016). Such an approach would also probably more accurately reconstruct the multi-scale variability within route networks, i.e. thoroughfares versus more local secondary routes (cf. Vletter & Van Lanen, in review).

Vletter & Van Lanen (in review) already concluded that the network-friction method is most suited for the reconstruction of supra-regional connections, but less successful in the modelling of secondary paths or tracks, i.e. connections functioning on a finer scale than reconstructed in this study. Since the route networks in this chapter were calculated based on the spatial distribution of settlements, differences in settlement patterns directly influence the models' outcome. The demographic decline that characterized the early-post Roman periods (i.e. LRP to EMPB; Verhagen et al., 2016), combined with the increased size and clustering of settlements during the EMPC and EMPD (e.g. Dekker, 1983; Rutte & Abrahamse, 2015; chapter 7) further hampers route-network modelling using network friction, since less nodes are available. For these post-Roman periods route-network modelling based on the NFM will mainly reconstruct primary connections and have an increased chance of missing more local, secondary paths or tracks. This might explain the relatively low validation results for the isolated finds in these later periods (Table 8.6).

We assumed that lower areas are generally wetter and also more prone to inundation during floods. It should be noted that detailed data on flooding frequency per NFM grid cell, and the general influence of flooding on the cultural landscape in the study area during the Roman and early-medieval periods, are still unknown. Including these data in the future will further enhance modelling results. However the current lack of these data is not a problem for the reconstruction of connectivity patterns, since network persistence will probably only slightly decrease as the archaeological data, i.e. mainly settlements, are key for these analyses and settlement dynamics occur on local scales only (chapter 7). In the Rhine-Meuse delta settlement patterns thinned out but remained situated on movement corridors, i.e. the higher and accessible alluvial ridges (chapters 6 and 7). Although movement corridors might have gotten narrower through landscape dynamics such as flooding, they will have persisted in the landscape. As such these stable movement corridors increase the likelihood of persistent-route sections occurring in these areas.

8.5.3 Outlook

This chapter focused on modelling connectivity factors in delta landscapes by calculating route networks and route-network stability in the Rhine-Meuse delta during the Roman period and Early Middle Ages. However, connectivity patterns encompass more than route networks only (Figure 8.2). Chapter 7 already showed that settlements patterns, another factor within connectivity patterns, on the local scale show much less persistence than route networks. In order to understand these differences between settlements and route networks, in the future a more detailed analysis of settlement persistence in the study area is necessary. In addition, other connectivity-pattern factors such as demography, land use should be studied in more detail in order to better understand their mutual relations/interaction and general.

Although floods appear to have been of limited influence on the route-network evolution in the study area, the developed NFM could benefit from a more detailed analysis of the impact of severe floods on the landscape. The consequences of the flood episodes on landscape suitability for routes can be modelled using results from flood-hydraulic models. Such models can further quantify the assumption that lower areas are more prone to flood levels and can better predict the propagation of floods through the delta. Subsequently, data regarding this increased flooding variability then can be incorporated into route-network modelling using a NFM, allowing the quantification of flooding impact on route-network evolution and leading to more detailed reconstructions of route-network probability in the Rhine-Meuse delta.

8.6 Conclusion

The network-friction method can be applied on a regional scale in order to obtain high-resolution NFMs able to model route networks and network stability in the past. The approach proves itself to be very well suited for locating movement corridors and obstacles in past landscapes. However, the current approach appears to be best suited for supra-regional analyses and would benefit from a combination with other route-network modelling techniques in order to also allow regional or micro-regional reconstructions. By integrating high-resolution archaeological and geoscientific data we created a regional NFM showing the complex interaction between route networks and landscape dynamics in densely populated areas. The models' validation results showed that the NFM is able to calculate the link between route networks, settlement patterns and the physical landscape. The model is an important first step towards reconstructing overarching connectivity patterns within the study area.

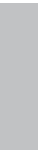
Despite the dynamic nature of the landscape in the Rhine-Meuse delta, persistence between the route networks is remarkably high. By applying network friction to the study area, we quantified the level of (long-term) route-network persistence. Results showed that with the exception of the southwestern part of the study area, the majority of the movement corridors remained in use throughout the Roman and early-medieval periods. In the southwest of the research area, the exceptional scale and orientation of the newly-developed river Waal will have led to great changes in the physical as well as the cultural landscape, which are reflected in route-network instability in this area. The overarching connectivity patterns in the other parts of the Rhine-Meuse delta appear to be relatively stable as became clear by the calculated route-network stability. This points towards possibly more continuity and at least a degree of path dependency in the development of settlement patterns and route networks between the Roman period and Early Middle Ages.

Connectivity patterns function on a variety of scales and link the physical and cultural landscapes. Our research shows that studying these patterns increases our understanding of the complex interplay between processes of change and persistence on varying scales. Connectivity patterns should be studied by combining numerous (large-scale) datasets. The current NFM was developed on a regional scale and showed the need for a quality balance between datasets, since the least accurate data determines the level of detail that can be obtained. The NFM did however show the added value of, and need for, more evidence-based and multi-proxy approaches when researching connectivity patterns or solely route networks in the past.

Acknowledgements

This chapter is part of the PhD theses of R.J. Van Lanen and H.J. Pierik, within the project 'The Dark Ages in an interdisciplinary light' (www.darkagesproject.com) funded by NWO (project nr. 360-60-110). The second author

contributed in the following proportions (%) to research design, data collection, analysis and conclusions, figures, and writing: 40, 50, 30, 30, 30. The authors thank Marjolein Gouw-Bouman, Bert Groenewoudt, Esther Jansma, Hans Middelkoop, and Esther Stouthamer for their comments on earlier drafts of the chapter. Finally, we like to thank the two anonymous reviewers for their useful comments on the manuscript.



Chapter 9

Controls on late Holocene drift-sand dynamics: the dominant role of human pressure in the Netherlands

Holocene drift-sand activity is commonly directly linked to population pressure (agricultural activity) or to climate change (e.g. storminess). In the Pleistocene sand areas of the Netherlands small-scale Holocene drift-sand activity began in the Neolithic, whereas large-scale sand drifting started during the Middle Ages. This last phase coincides with the intensification of farming and demographic pressure, but also is commonly associated with a colder climate and enhanced storminess. This raises the question to what extent drift-sand activity can be attributed to either human activities or natural forcing factors. In this study we compare the spatial and temporal patterns of drift-sand occurrence for the four characteristic Pleistocene sand regions in the Netherlands for the period between 1000 BC and AD 1700. To this end we compiled a new supra-regional overview of dates related to drift-sand activity (^{14}C , OSL, archaeological and historical), which were compared to reconstructions of soil properties, historical-route networks, vegetation, and climate. Results indicate a constant but low drift-sand activity between 1000 BC and AD 1000, interrupted by a remarkable decrease in activity around the BC/AD transition. It is evident that human pressure on the landscape was most influential on initiating sand drifting: this is supported by more frequent occurrences close to routes and the uninterrupted increase of drift-sand activity from AD 900 onwards, a period of high population density and large-scale deforestation. Once triggered by human activities, this drift-sand development was probably further intensified several centuries later during the cold and more stormy Little Ice Age (AD 1570-1850).

H.J. Pierik, R.J. Van Lanen, M.T.I.J. Gouw-Bouman, B.J. Groenewoudt, J. Wallinga & W.Z. Hoek (in review): Controls on late Holocene drift-sand dynamics: the dominant role of human pressure in the Netherlands, *The Holocene*.

9.1 Introduction

Drift sands are relatively young Holocene aeolian deposits, which originate from local re-working of terrestrial Pleistocene sand deposits (Koster, 1982). Throughout the Holocene, expansion of drift-sand fields has been a prominent geomorphological phenomenon in the northwest European sand belt (Koster, 2009; Tolksdorf & Kaiser, 2012 – Figure 9.1). Drift-sand formation often led to the loss of suitable farming land (Lascaris, 1999; Ravi et al., 2010), and sometimes even caused settlement abandonment (Heidinga, 1987; Mikkelsen et al., 2007; Derese et al., 2010). Neolithic occurrence of small-scale drift-sand activity was demonstrated by Tolksdorf & Kaiser (2012) and Willemse & Groenewoudt (2012), whereas large-scale drift-sand activity started from the Middle Ages onwards when human impact (e.g. deforestation and intensification of farming) on the landscape increased (Koster et al., 1993). Therefore, Holocene drift-sand activity is commonly linked to population

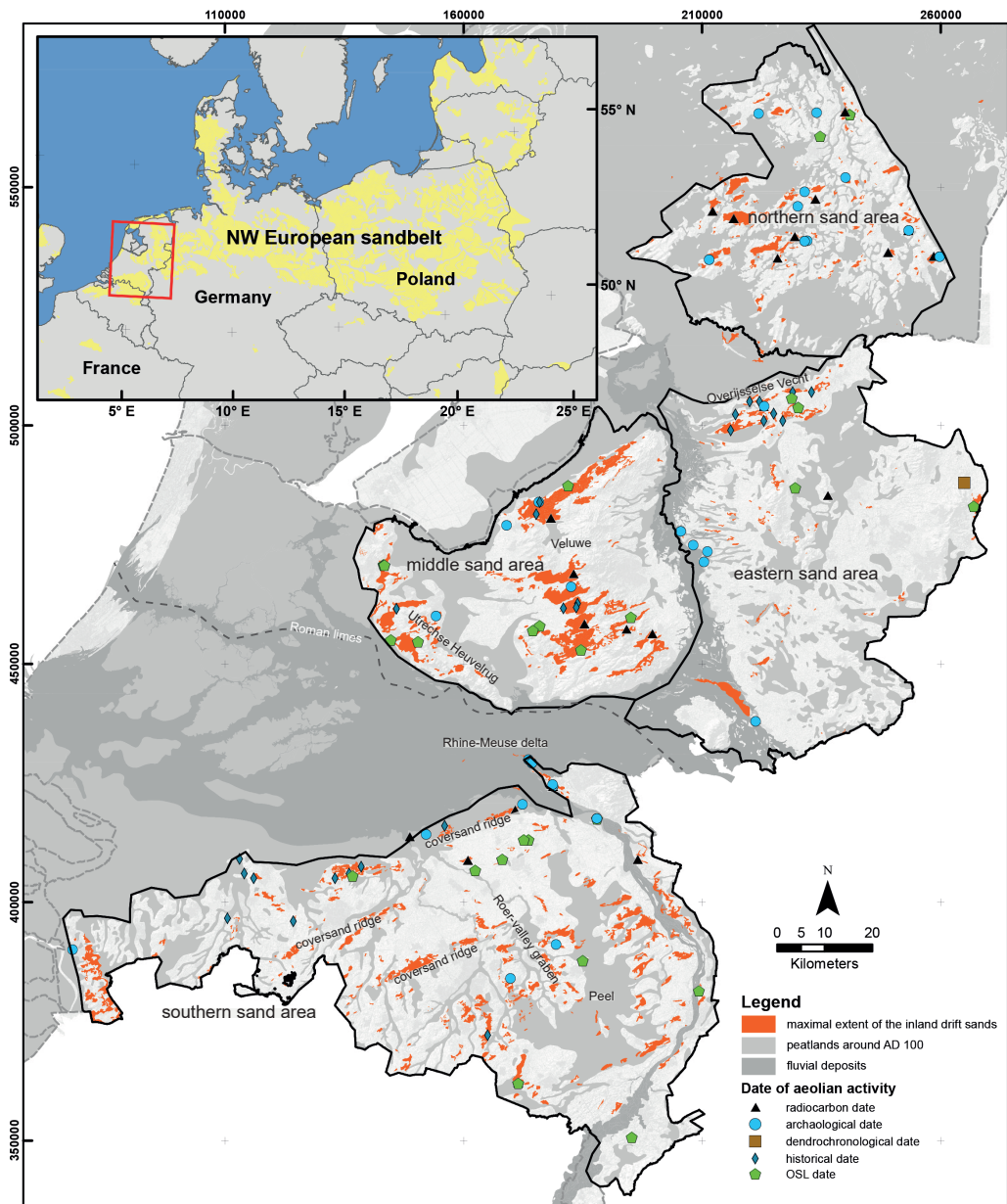


Figure 9.1 | Location of the study area and the four regions distinguished in this study.

pressure and agricultural practices (e.g. Koster et al., 1993; Kolstrup, 1997; Tolksdorf & Kaiser, 2012). However, other studies consider changes in climate or storminess to be an important control (e.g. Bateman & Godby, 2004; Charman, 2010; Jungerius & Riksen, 2010). This raises the question to what extent drift-sand activity can be attributed to either natural or human factors, or to a combination of these.

Many studies that link drift-sand occurrence to fluctuations in climate or human pressure consider only few sites in high detail. The information from these sites not always necessarily represents regional trends. Large supra-regional studies have resulted in useful overviews of multiple sites mainly by chronologically comparing patterns of forcing factors and drift sands (e.g. Koster et al., 1993; Tolksdorf & Kaiser, 2012). Few studies, however, analysed the spatial patterns of drift-sand activity and their forcings on a regional scale. Further understanding of past drift-sand activity would additionally benefit from complementing such overview studies with new data from different disciplines.

In this chapter we explore the role and the relative importance of environmental factors (e.g. landscape setting, climate) and demographic pressure (population density, deforestation) on the formation of drift sands. We focus on four Pleistocene sand regions in the Netherlands, which comprise the western part of the northwest European sand belt (Figure 9.1). For this area abundant data on climate, vegetation development, human occupation, and drift-sand activity are available. The four studied areas, all ca. 50×100 km in size, share common past climate trends but are different in many cultural and geomorphological aspects. We compiled an integrated supra-regional overview of drift-sand related dates, either directly or indirectly indicating drift-sand activity or its absence using ^{14}C and OSL, as well as archaeological and historical dates. Using this new data overview we performed analyses of: (i) the temporal changes in drift-sand activity between the areas, and (ii) the local spatial patterns of drift-sand activity within these regions. For the first analysis, the regional drift-sand chronology was compared to reconstructions of regional population density and forest cover. For the second analysis, the location of drift-sand activity was compared to areas with higher demographic pressure, indicated by the presence of past main route networks. The study focuses on the period between 1000 BC and AD 1700, because the population density and vegetation cover strongly changed during this time span (Teunissen, 1990; Louwe Kooijmans, 1995; Jansma et al., 2014), allowing a comparison between these factors and drift-sand occurrence. Furthermore, this time frame provides the most data regarding drift-sand activity, palaeoclimate data, and demographic pressure, which enables to discriminate between forcing factors and resulting drift-sand activity. Before the selected time frame (before 1000 BC) data on sand drifting and possible forcings are scarce. After ca. AD 1700 the dune fields became so large and the pressure of people on the landscape so high, that an approach using written sources and historical maps would be more adequate, which is beyond the scope of this chapter. The dune fields reached their maximum extent in the 19th century, after which they were confined and reduced through the establishment of large-scale pine plantations (Riksen et al., 2006; Koster, 2009). The regional scale and the period 1000 BC –AD 1700 provides the best opportunity to test the relation between drift-sand activity and climate, demography, and land use. As such, this chapter contributes to further understanding human-landscape interactions in sandy areas.

9.2 Controls in drift-sand formation

Several prerequisites of drift-sand initiation have been identified in previous studies (Figure 9.2 – Schelling, 1955; Koster, 1978). First of all, sand drifting requires the presence of dry, fine and relatively well-sorted sand at the surface (Marzolf, 1988; Pye & Tsoar, 2008). Second, vegetation cover has to be low (generally lower than 30%; Ash & Wasson, 1983), not only at the surface of the sand source, but also in its surroundings. In order to transport the sand, the wind needs a fetch of around 500 m (Steckhan, 1950). When these antecedent conditions are met, strong winds

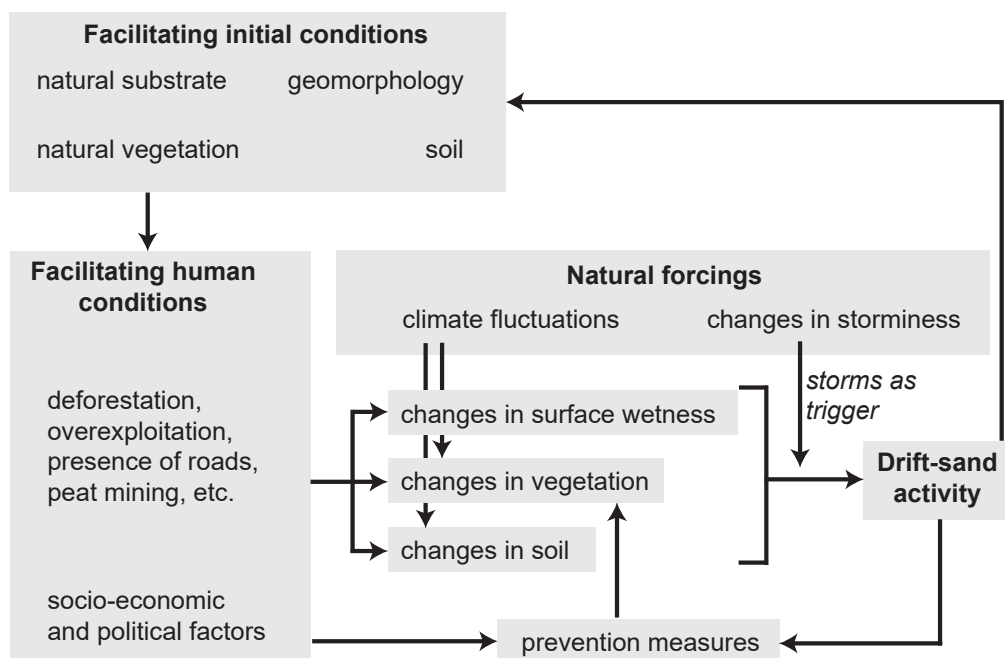


Figure 9.2 | Conceptual diagram summarising the controls on Holocene drift-sand formation that are treated in this study, for explanation see text.

(especially above 5.5 m/s) can generate large-scale sand transport (Livingstone & Warren, 1996). Fine sands with non-cohesive grains are most easily transported by the wind (Bagnold, 1941; Pye & Tsoar, 2008).

Heidinga (1984ab) and Jungerius & Riksen (2010) suggested severe drought as a climatically facilitating condition that could have made the soil more prone to sand drifting. In the NW European sand belt, sand drifting has been linked to land-use changes such as deforestation and especially to the presence of bare soil in croplands from which sand can deflate (Figure 9.2 – e.g. Castel et al., 1989; Kozarski & Nowaczyk, 1991; Spek, 2004; Koster, 2009). The area of bare soil and the seasonal timing varies per region and crop and determines the risk of sand drifting. Overexploitation by grazing, burning practices and the use of *plaggen* (sods digging) from heathlands are also land-use practices associated with sand drifting (Lascaris, 1999; Koster, 2009). Also, roads and cattle and sheep drifts have been suggested as drift-sand nuclei (Heidinga, 1984a; Spek, 2004). The occurrence of these land-use practices can be influenced by socio-economic factors, as are prevention measures (e.g. use of hedges) that prevent drift-sands once formed (Figure 9.2; e.g. Heidinga, 1987; De Keyzer, 2016).

Besides a research focus on facilitating controls that make the substrate more prone to sand drifting, much focus has been on the triggers causing it (Figure 9.2). Large-scale reactivation of both inland and coastal dune systems has been linked to climatic change, in particular to the frequency of intense storms ('storminess'; Clemmensen et al., 2009; Costas et al., 2012; Sorrel et al., 2012). These periods seem to match reasonably well with colder climate episodes. Especially for the Little Ice Age (LIA, AD 1570-1850), which is associated with more severe storms in NW Europe (Clarcke & Rendell, 2009; Costas et al., 2012). Enhanced inland and coastal dune formation has been found

in the UK for this period (Bateman & Godby, 2004; Charman, 2010), along the French Atlantic coast (Clarke et al., 2006), in the Netherlands (Jungerius & Riksen, 2010), in Portugal (Clarke & Rendell, 2011; Costas et al., 2012, and in Denmark (Clemmensen et al., 2001; 2007; 2009). Many of these studies focussed on coastal settings where marine-influenced factors also played a role (e.g. Van Vliet-Lanoë et al., 2015), nevertheless these cold and stormy climates might have caused inland sand drifting as well. Because the observed large-scale dune formation also coincided with increasing population density and enhanced human pressure in both inland and coastal landscapes, it is remarkable that in most of these studies the human factor was considered to a limited extent only. Therefore, in the present study an integrative approach is applied, which considers the role and relative importance of the forcings (natural and human-induced) and initial conditions in Figure 9.2.

9.3 Geographical setting

9.3.1 Geological and geomorphological setting

Inland drift sands in the Netherlands are mainly reworked Weichselian periglacial coversands (Schelling, 1955), which form the largest outcropping unit in the Pleistocene sandy area (Van der Hammen et al., 1967; Kasse, 2002; Schokker et al., 2007). Peat formed during the Holocene, either in brook valleys (Bisschops et al., 1985) or in other lower and wet areas, could develop into large oligotrophic fen peatlands (Figure 9.1 – Casparie and Streefkerk, 1992; Van Beek et al., 2015b). Within the Pleistocene sand area we distinguish four areas that have distinct geological substrates and are separated by fen peat wetlands or large river floodplains: the northern, eastern, middle, and southern sand area (Figure 9.1).

The substrate of the *northern sand area* contains till of Saalian age (Rappol, 1987), capped by up to two meters of coversand (Bosch, 1990). The substrate is loamy and wet due to the presence of the impermeable till. The main drift-sand activity in this area was reconstructed to have taken place after ca. AD 1200 (Castel et al., 1989; Castel, 1991).

In the *eastern sand area* relatively small isolated coversand ridges are present. The first indications of drift-sand activity date back to the Neolithic period (Table 9.1) and occurred on relatively high Pleistocene river dunes flanking small rivers (Willemse & Groenewoudt, 2012). At present, the largest drift-sand fields, which mainly are post medieval, are situated along the Overijsselse Vecht (Bruins, 1981; Neefjes et al., 2011).

A large part of the *middle sand area* consists of ice-pushed ridges formed during the Saalian; the Veluwe and Utrechtse Heuvelrug (Busschers et al., 2008). Although they are very well drained and thus dry, their coarse sandy and gravelly substrate makes them less likely sources for sand drifting. On the western side, however, the ice-pushed ridges are flanked and partly covered by thick coversands, which are prone to sand drifting (Koster, 1978; Sevink et al., 2013). Early evidence of drift-sand activity around 4500 BC was found by Sevink et al. (2013). Especially on the western flanks of the ice-pushed ridges, large drift-sand fields developed after AD 1200, which developed into the largest drift-sand fields of the Netherlands (Koster, 1978; Heidinga, 1984ab; 1987).

In the *southern sand area* the Roervalley Graben contains thick coversand deposits with quite shallow loamy impermeable deposits, causing the soils to be relatively wet (Bisschops et al., 1985; Schokker et al., 2007). Here, three long WSW-ENE oriented coversand ridges occur which locally have been reworked into drift-sand dunes (Figure 9.1). The earliest Holocene sand drifting has been dated around 4000 BC in this area (Van Mourik, 1988; Van Mourik et al., 2010).

Table 9.1 | Subdivisions of archaeological periods since the Neolithic period used in this study.

Period	Subperiod	Start	End
Neolithic period (5300–2000 BC)	Early-Neolithic period	5300 BC	4200 BC
	Middle-Neolithic period	4200 BC	2850 BC
	Late-Neolithic period	2850 BC	2000 BC
Bronze age (2000–800 BC)	Early-Bronze Age	2000 BC	1800 BC
	Middle-Bronze Age	1800 BC	1100 BC
	Late-Bronze Age	1100 BC	800 BC
Iron Age (800–12 BC)	Early-Iron Age	800 BC	500 BC
	Middle-Iron Age	500 BC	250 BC
	Late-Iron Age	250 BC	12 BC
Roman period (12 BC–AD 450)	Early-Roman period	12 BC	AD 70
	Middle-Roman period	AD 70	AD 270
	Late-Roman period	AD 270	AD 450
Middle Ages (AD 450–1500)	Early Middle Ages	AD 450	AD 1050
	Late Middle Ages	AD 1050	AD 1500
Modern period (AD 1500–present)	Modern period A	AD 1500	AD 1650
	Modern period B	AD 1650	AD 1850
	Modern period C	AD 1850	Present

9.3.2 Vegetation development and population

Until the Neolithic period (Table 9.1), vegetation development and soil formation in coversand deposits took place without significant human interference (Doorenbosch & Van Mourik, 2016). From the Late Neolithic period onwards, forest vegetation gradually developed into heathland (Janssen, 1972; Casparie & Groenman-Van Waateringe, 1980; Louwe Kooijmans, 1995; Van Geel et al., 2017), coinciding with soil depletion and podzol development (Waterbolk, 1964; Spek, 1996; Sevink et al., 2013). The first small-scale sand drifting took place on high and dry river dunes in the Neolithic period; it became more widespread since the Middle-Bronze Age (Willemse & Groenewoudt, 2012). In all four areas population density gradually increased towards the Roman period (Louwe Kooijmans et al., 2011), coeval with the decrease in forest cover. This pattern changed during the 4th and 5th centuries AD, when major depopulation and reforestation occurred (Teunissen, 1990; Groenewoudt et al., 2007; Cheyette, 2008; Kalis et al., 2008; Wickham, 2009). The latter trend was most pronounced in the areas south of the Roman *limes* (Figure 9.1) in the southern sand area, where it started from AD 270 onwards, a century later it also occurred in the other three areas. From the 7th century onwards population density and the corresponding pressure on the landscape started to increase again, a trend which generally persisted throughout the entire Middle Ages (e.g. Van Bavel, 2010). As a result, the forested area decreased again, with the lowest forest cover occurring during the Modern period (Teunissen, 1990; Spek, 2004; Van Beek et al., 2015a; Engels et al., 2016). From the Late Middle Ages onwards the southern sand area became the most densely populated sand area in the Netherlands (Spek, 2004).

9.3.3 Climate

During the last three millennia several warmer and colder periods occurred in northwestern Europe with temperature fluctuations of 1 to 2 degrees Celsius. The transitions between these

periods usually were gradual and differ in timing between the various records from which they were derived. Before 500 BC climate was relatively warm, followed by a colder episode between 500 and 300 BC, and subsequently by a warmer period between 300 BC and AD 500 (inferred from a Greenland ice core by Kobashi et al., 2011). This later warm period, the Roman Warm Period (RWP) is recorded in proxy records across NW Europe (Büntgen et al., 2011). An abrupt cooling has been identified around AD 500 (Dark Ages Cold Period DACP – AD 500-700: Ljungqvist, 2010; Büntgen et al., 2016), and was followed by the relatively warm Medieval Climate Optimum (MCO – AD 700-1570) and subsequently by the colder Little Ice Age (LIA – AD 1570-1850; Lamb, 1972; Mann, 2003). Accurate precipitation reconstructions are scarce; Büntgen et al. (2011) indicate normal conditions during the Iron Age (800-12 BC – Table 9.1), a wetter RWP and first part of the DACP (Dermody et al., 2011; McCormick et al., 2012), and a relatively dry second part of the DACP for NW Europe. The MCO is often reconstructed as relatively wet. Periods of prolonged drought could lead to the dying of vegetation or fires, both resulting in bare soils susceptible to aeolian erosion (Doorenbosch & Van Mourik, 2016). Sorrel et al. (2012) have inferred periods of increased storminess in NW Europe from sedimentological archives of coastal records, with increased storminess occurring in 1100-400 BC, AD 100-950 and AD 1400-1750. The latter period also has been documented as relatively stormy in historical records in the Netherlands dating from around AD 1400 onwards (Berendsen, 1984c; Buisman & Van Engelen, 1996; 1998; 2000; Vos, 2015b). Although the first historical storm references date from the 8th century, the record is only reliable after around AD 1300 for deriving long-term trends.

9.4 Materials and method

In order to establish the relationship between drift-sand activity and human pressure between 1000 BC and AD 1700, the temporal patterns per region were analysed as outlined in the first methodological section. This was done by comparing the occurrence of 140 investigated drift-sand events to population-density data and forest cover trends. The occurrence and intensity of sand drifting in the Pleistocene coversand area were derived from ca. 340 dates related to drift-sand activity (Figure 9.1; Table 9.2). In the second methodological section we outline how the location of the events of drift-sand activity was compared to zones of intensified demographic pressure.

9.4.1 Assessing temporal patterns per region

Collecting dates on events of drift-sand activity

Several techniques are available that can be used to directly or indirectly date (the absence of) drift-sand activity (Table 9.2). These dates were collected from the literature (e.g. Koster et al., 1993; Tolksdorf & Kaiser, 2012; Willemse & Groenewoudt, 2012), the LumiD database (www.lumid.nl) and archaeological reports (see Appendix D2). Only dates of inland drift sands were used (i.e. omitting events affected by coastal dynamics; e.g. Vos et al., 2015).

Archaeological finds (usually pottery) below the drift-sand deposits, e.g. Van Beek (2009); Van Gijn & Waterbolk (1984); Willemse & Groenewoudt (2012), were used as indirect *Terminus Post Quem* dates (TPQ, providing an earliest possible age). Archaeological finds on top of the drift-sand deposits were used as *Terminus Ante Quem* (TAQ, providing a youngest possible date). Since drift sands rarely contain organic material, direct radiocarbon-dating opportunities of drift phases are limited. We excluded radiocarbon dates of humic acids from intercalating soils (Van Mourik, 1988; Castel, 1991), as these proved to be up to 1500 years too old when compared to OSL dates (Van

Table 9.2 | Dating methods for drift sands (TAQ = *Terminus Ante Quem*, TPQ = *Terminus Post Quem*, TL = Thermoluminescence) and how the drift-sand events were derived from them. Earlier used dating methods that are too inaccurate and therefore not used in this study are also included.

Dating strategy	Notes	Begin date sand drift ¹⁾	End date sand drift ¹⁾	Selected references
Begin				
¹⁴ C of humic acids from the A-horizon under drift sand	TPQ – considered generally 1500 years too old.	Not used	Not used	Van Mourik (1988)
AMS ¹⁴ C macrofossils from the A-horizon under drift sand	TPQ	Not used	Not used	Castel (1991)
¹⁴ C of peat or charcoal under drift sand	TPQ best method, first sand influx in peat. Charcoal can yield too old dates.	DATE ²⁾	DATE + 250 ¹⁾	Castel (1991); Teunissen (1988; 1990)
Archaeology directly under the drift sand		Mean of arch period(s)	Mean of arch period(s) + 500	Van Gijn & Waterbolk (1984); Willemse & Groenewoudt (2012)
Pollen		Not used	Not used	
Dendro of trees buried under drift sand	Low-resolution date	DATE	DATE + 250	Den Ouden et al. (2007)
Activity				
TL	Systematic underestimation of 20-40%	Not used	Not used	Dijkmans et al. (1988; 1992); Dijkmans & Wintle (1991)
OSL	Mixing by bioturbation, saturation.	DATE - 125	DATE + 125	Wintle (2008); Wallinga et al. (2013)
Historical sources	Accurate age, location not always. After ca. AD 1400	DATE - 125	DATE + 125	Bruins (1981); De Keyzer (2016); Leenders (2016)
End				
¹⁴ C of humic acids from the A-horizon in drift sand	TAQ	Not used	Not used	Van Mourik (1988)
AMS ¹⁴ C macrofossils from the A-horizon in drift sand		Not used	Not used	Castel (1991)
Archaeology on top of drift sand		Mean of arch. period(s) – 500	Mean of arch. period(s)	Van Gijn & Waterbolk (1984); Willemse & Groenewoudt (2012)
Dendro on top of drift sand		DATE - 250	DATE	Verlinde (2004); Den Ouden et al. (2007)

¹⁾Begin and end date inferred from the dating evidence in cases that no additional dates or indications are present. ²⁾ The mean date is taken.

Mourik et al., 2010; Wallinga et al., 2013). Dates of peat below drift sands, however, provided more accurate TPQ ^{14}C dates, especially AMS ^{14}C dates (Castel, 1991; Koster et al., 1993),

Optically Stimulated Luminescence (OSL) is a reliable direct dating tool of drift-sand activity (Wallinga et al., 2007), it has been applied to inland drift sands by e.g. Bateman & Huissteden (1999); Hilgers (2007); Derese et al. (2010); Van Mourik et al. (2010); Sevink et al. (2013); Vandenberghe et al. (2013); and Wallinga et al. (2013). Usually multiple samples are taken within in a single drift-sand sequence, in order to determine the rate and duration of sand deposition. Equivalent doses are obtained using the *Single Aliquot Regenerative* dose protocol (Murray & Wintle, 2003), with measurement parameters differing for each of the individual sites that contribute to the dataset. The vast majority of analyses were performed at the *Netherlands' Centre for Luminescence Dating* (NCL sample codes), where dose rates are calculated from radionuclide activity concentrations determined by gamma-ray spectrometry (see the original publications listed in Appendix D2 for further details of the measurement procedures).

Historical documents (i.e. written sources) recording drift-sand activity on a specific location are also used as dates for active sand drifting (e.g. Bruins, 1981; De Keyzer, 2016; Leenders, 2016). These records have the highest chronological accuracy, but the exact location of the described sites is not always clear and written sources on drift-sand activity are only available from around AD 1400 onwards.

Determining drift-sand events and establishing drift-sand intensity

The chronological information was incorporated into a database, registering the dating method and the literature reference (Appendix D2). From this information the most likely periods of drift-sand activity were derived (Table 9.2), which were summed into drift-sand intensity per century. The beginning of drift-sand events was set at the mean TPQ age (if available), and the end of activity at the mean TAQ age (if available). If direct dating evidence was available, the drift-sand activity was clustered around these dates. When either the begin or end date was not available, we assumed a period of 250 years for drift-sand activity (Table 9.2). This period was derived from empirical studies that resulted in multiple OSL dates for single drift-sand sequences, since the results pointed to periods of activity ranging from decades to a maximum of ca. 250 years (Derese et al., 2010; Sevink et al., 2013; Vandenberghe et al., 2013). Within this time frame, multiple short drift-sand events can occur with hiatuses in between which are hard to identify. Therefore we generally considered one single section or point location as a single event with a resolution of 250 years. For direct dates (OSL, historical records) we assumed that the beginning of the event took place 125 years before this date and that the end occurred 125 years after this date. For TPQ dates based on radiocarbon dating of peat underneath drift sand, we assumed that no hiatus occurred between peat formation (cf. Koster et al., 1993) and sand influx. For archaeology buried by drift sand, the mean of the archaeological dating range was taken as the begin age, and the end age was set 500 years later in order to account for the possible large hiatus between the archaeological age and the drift-sand event. For finds on top of drift sands we took the central age of the archaeological period as the end age and set the start date 500 years earlier. If additional evidence suggested that the sand drifting occurred during a shorter or much longer period (e.g. when multiple datings are present), begin and end ages were adapted accordingly.

To reconstruct drift-sand intensity from the combined data over time, we summed the intensity of all drift-sand events per century. The intensity per individual event (I) was set proportional to the reconstructed duration of the reconstructed drift-sand period (taken as the difference between its begin age (t_b) and end age (t_e)):

$$I = \frac{1}{t_e - t_b}$$

This method incorporates the precision of the events: events that were dated within a small time frame (i.e. more precisely dated events) received a high weight, whereas events that had a much more uncertain time frame were assigned a lower weight. Applying this step weights down the contribution of less well-dated events in the resulting intensity curve.

This approach results in an overview of currently known sites with sand-drift activity, which is unavoidably biased due to research traditions and availability of the dates (e.g. historical dates only are available for the last centuries). To assess the relative contribution of each dating method, the intensity curve shows the contribution of the different dating techniques. To partially overcome biases in the reconstructed drifting, we also used evidence regarding the lack of this phenomenon, among others derived from dated peat sequences and well-dated hiatuses between drift-sand stages (e.g. between Late Glacial coversand and drift sand). This was incorporated in the temporal analysis as evidence of sand-drift absence (brown and grey bars in Figures 9.3-9.6).

Reconstructing population density

Population density per period (PD) was calculated using existing population estimates for the Roman period of Van Beek & Groenewoudt (2011), and for AD 1500 and 1600 using estimates of Spek (2004). We estimated population for the less-known periods in between by means of interpolation, taking into account the number of archaeological settlements in this period, following Zoetbrood et al. (2006). This procedure is further explained in Appendix D1.

Assessing the areal extent of deforestation

The degree of deforestation was used as a proxy for human pressure on the vegetation and hence on the landscape. The relative amount of deforested area was derived from the arboreal pollen percentages (AP%-values) in existing well-dated and detailed pollen diagrams from point locations per sand area. Empirical studies demonstrate that the AP%-values of modern vegetation assemblages are related to landscape openness (Groenman-Van Waateringe, 1986; Frenzel et al., 1992; Frenzel, 1994; Doorenbosch, 2013). Because this relation is strongly influenced by the pollen source area and the vegetation type and pattern, the AP%-values were only used as an indication of relative landscape openness rather than as an absolute percentage of forest cover (Broström et al., 1998; Sugita et al., 1999; 2010; Doorenbosch, 2013;). Therefore, we did not compare absolute values between areas but assessed the long-term deforestation trends per region by identifying periods with rising and falling AP%-values.

The pollen diagrams were selected using the Dutch Pollen Database (Donders et al., 2010), based on representability of the regional vegetation trend following comparisons with other sites and studies (e.g. Groenewoudt et al., 2007; Brinkkemper, 2013), robustness of the chronology and detail of the analyses. We only selected pollen diagrams from undisturbed peat sequences, to eliminate the influence of fluvial transported pollen and human interference. For the northern sand area we selected the Mekelermeer pollen diagram (Figure 9.3). The record from this pingo remnant covers the period from ca. 1200 BC to AD 1100 and was originally published by Bohncke (1991). For the eastern sand area a pollen diagram from a raised bog was chosen: the Engbertdijksveen (Figure 9.4) covering the period 950 BC to AD 950 (Van der Molen & Hoekstra, 1988). The

vegetation development for the middle sand area was best reflected in the pollen diagram from the Uddelermeer pingo remnant (Figure 9.5 – Engels et al., 2016; unpublished data Gouw-Bouman). For the southern sand area we chose a pollen diagram from the peat infill of an abandoned Pleistocene channel without Holocene fluvial influx, Berkenhof which shows the vegetation trend from BC 1500 to AD 1850 (Figure 9.6 – Teunissen, 1990). The chronology of all pollen records is supported by radiocarbon dates reported in Appendix D2 (Table D6). Although pollen percentage values can vary strongly between sites, the trends in AP%-values are reasonably similar to pollen records from other natural and relatively undisturbed sequences (De Jong, 1982; Berendsen & Zagwijn, 1984; Teunissen, 1990; Engels et al., 2016). This indicates that the selected sites represent the regional trends well.

The arboreal pollen percentages of the different studies were digitised and recalculated using a uniform pollen sum to enable comparison. To capture regional vegetation trends, we chose a pollen sum comprising upland types only (i.e. vegetation from dry areas), excluding wetland pollen types such as Alder to minimise the effects of local vegetation dynamics. The original chronology of the record was updated using linear interpolation between the sequence calibrated original radiocarbon dates (Bronk Ramsey, 2009; Niu et al., 2013; Reimer et al., 2013).

9.4.2 Spatial analysis

To investigate the relation between population pressure and the occurrence of sand drifting, spatial zones with increased human activity were identified based on route-network reconstructions (Van Lanen et al., 2015ab; 2016b). This analysis was performed for soils susceptible for sand drifting for three time slices: roughly corresponding to the Roman period, the Early Middle Ages and the Late Middle Ages.

Determining sand-drift susceptibility

The spatial analysis was performed for soils that are susceptible for sand drifting only (i.e. the drier sandy soils). The areal distribution of susceptible soils was derived from national datasets of soil maps and palaeogeographical maps (chapter 2) using the criteria listed in Table 9.3. Dry soils with fine sands with a poor loam content are considered most susceptible. Moderately dry, more loamy sands or gravelly sands are considered moderately susceptible. Using GIS we recategorised these soil map units from the digital national soil map (De Vries et al., 2003) into drift-sand susceptibility classes (Table 9.3). Since the Roman period and especially the Middle Ages the extent of peatlands diminished due to oxidation as a result of artificial drainage and excavation leaving behind more sandy soils prone to sand drifting (Casparie & Streefkerk, 1992). Therefore, drift-sand susceptibility maps were compiled for three periods in time. We derived the fen bog extent from the Vos & De Vries (2013) palaeogeographical maps for the three periods (using the AD 100, 800, and 1500 peat extent – Table 9.4) and assigned these landscape units as ‘not susceptible’.

The current extent of fossil drift-sand dune-fields was derived from the palaeogeographical map for AD 1500 (Vos & De Vries, 2013) that shows the presumed distribution of active drift-sand fields. This information is supplemented with pedological criteria (occurrence of young, incipient or undeveloped soils – cf. Koster, 1982) using the national soil map (De Bakker & Schelling, 1989; De Vries et al., 2003). The fossil dune fields derived from these datasets represent the maximal spatial extent of the dune fields during the Holocene, which roughly corresponds to the extent of active dunes in the 17th to the 19th century. We included these areas as susceptible soils in the AD 100, 800, and 1500 reconstructions.

Table 9.3 | Criteria for susceptibility of the soil to aeolian erosion (after Hack-Ten Broeke et al. (2009) and Hessel et al. (2011)). Units from the national soil map were converted based on three criteria: groundwater level, median grain size and silt fraction. For each criterion three susceptibility classes were distinguished. Polygons that are susceptible based on all three criteria (i.e. low groundwater level, fine sandy, poor in silt) are marked as susceptible. If only one or two criteria are met (e.g. low groundwater but with silty sand or gravelly sand), the soil is considered to be moderately susceptible. Soils that had clay or peat at the surface during the reconstructed time step are considered to be unsusceptible. Silt percentages and median grain sizes: after De Bakker & Schelling (1989).

	Susceptible	Moderately susceptible	Not susceptible
Groundwater level	Low (> 40;> 120)	Moderate (< 40; 80-120)	High (surface; < 40,0-120)
Median grain size	50-210 µm	210-2000 µm	Silt and clay
Silt fraction	< 17.5%	17.5-50%	> 50 %
Wetlands	-	-	Clay, peat

Table 9.4 | Drift-sand activity ranges, route network, and soil susceptibility maps used for the three studied periods in the spatial analysis. The three periods roughly correspond to the Roman period, Early Middle Ages and Late Middle Ages.

ABR period	Drift-sand activity range	Zones of increased human activity	Soil susceptibility
Roman period 12 BC-AD 450	100 BC-AD 450	AD 100 route network (Van Lanen et al., 2015b)	Current soil map + Peat extent AD 100
Early Middle Ages AD 450-1050	AD 450-950	AD 800 route network (Van Lanen et al., 2015b)	Current soil map + Peat extent AD 800
Late Middle Ages AD 1050-1500	AD 950-1700	AD 1600 historical route network (Horsten, 2005; Van Lanen et al., 2016b)	Current soil map + Peat extent AD 1500

Comparing sand-drift locations to corridors of human activity

For the Roman period we used drift-sand events ranging from 100 BC to AD 450, a time frame that reflects the absolute onset and end of Roman occupation in the Netherlands. The Early Middle Ages, ranging from AD 450 to 950, roughly cover the period after Roman occupation until the end Carolingian rule. For these two periods we used zones around the AD 100 and 800 route networks of Van Lanen et al. (2015a). These networks have been calculated based on (a) the spatial distribution of excavated archaeological settlements and (b) the spatial distribution of movement corridors, i.e. well-accessible areas, in the landscape derived from soil and geomorphological maps. Verification against independent archaeological finds (i.e. infrastructural and isolated finds) has shown that the majority of these finds were uncovered within 1000 m around these route networks (< 85% and < 72% around AD 100 and 800 respectively; Van Lanen et al., 2015b). This indicates that these route networks reflect zones with a high level of human activity. Additionally, routes (always located in these zones) themselves can directly cause sand drifting (Lascaris, 1999; Spek, 2004). Therefore we used these route zones to determine the spatial link between sand drifting and population pressure.

The third time slice ranges from the end of the Early Middle Ages to the beginning of the modern period, i.e. AD 950 to 1700. At the end of the Early Middle Ages habitation started to

cluster and in the sand areas became fixed on stable positions (Waterbolk, 1980; Hamerow, 2002; Van der Velde, 2004). Some of these settlements after AD 1300 developed into larger towns (Spek, 2004; Keunen, 2011; Rutte & IJsselstijn, 2014). Because most settlements were established by the end of the Early Middle Ages, route networks are expected not to have changed significantly afterwards, even when urbanisation took place (Van Lanen et al., 2016b). Major changes in the route networks did occur after the introduction of railways in AD 1848 (Horsten, 2005). Therefore we used a historical road map of the AD 1600 route network reconstructed by Horsten (2005) and digitally made available by Van Lanen et al. (2016b) as representative for the period AD 950-1700. This overview of roads in the Netherlands mainly was based on a variety of old maps showing contemporaneous data on roads. These data have been integrated into an overview of main thoroughfares, and therefore do not include secondary roads and local paths. Although the AD 1600 road network has a high spatial accuracy, this network does not – in contrast to the reconstructions made by Van Lanen et al. (2015b) – connect all known settlements from that period (Van Lanen et al. 2016b). Still, the network does reflect the main thoroughfares and therefore the areas where land transport and associated population pressure on the landscape were highest.

We compared the number of drift-sand events within and outside a 1000 m buffer around the routes. These buffers represent (i) the uncertainty in route-network location (AD 100 and 800) and (ii) the expected impact zone of population pressure (settlements, arable fields, etc.) around these routes (Van Lanen et al., 2015b). Next, we calculated the spatial distribution of drift sand in and outside the zone of increased human pressure. This was done by determining the ratio of the number of sites inside and outside the buffer, corrected for the areal ratio in susceptible substrates within and outside the buffer (moderately susceptible and susceptible soils). The resulting factor expresses how often sand drifting was identified inside the buffer relative to its occurrence outside the buffer, with < 1 expressing predominant occurrences outside the buffer and > 1 expressing predominant occurrence within the buffer zone. To further test the statistical significance of the calculated factor values, we performed an exact binominal test. We took the assumption that drift-sand sites occurred as often within and outside the buffers per areal unit as a null-hypothesis.

9.5 Results

9.5.1 Temporal patterns in drift-sand activity

The results show that abundant drift-sand activity took place during Late Bronze Age and Iron Age (Figures 9.3-9.6), in the middle sand area this phenomenon was less prominent in these periods. All areas show a gradual decrease in forest cover and population density since the Late Bronze Age towards the Roman period, in line with reconstructions by Teunissen (1988), Louwe Kooijmans (1995), and Spek (2004).

Between AD 1 and 400 (the largest part of the Roman period), the data of drift-sand activity show a remarkable decrease on a national level (Figures 9.3-9.6). This trend is observed in the northern and eastern sand areas (AD 1-400; Figures 9.3 and 9.4) and in the southern Netherlands (AD 200-600; Figure 9.6). In the middle sand area no drift-sand activity occurred before AD 800 (Figure 9.5). The Roman dip in drift-sand activity is confirmed by observed peat growth without sandy influx at several sites (brown bars in Figures 9.3-9.6). This timing is counter-intuitive since it coincides with a relatively high population density and a low forest cover. In the southern sand area the dip occurred somewhat later, but still at a time that population density was relatively high and forest cover was low (Figure 9.6).

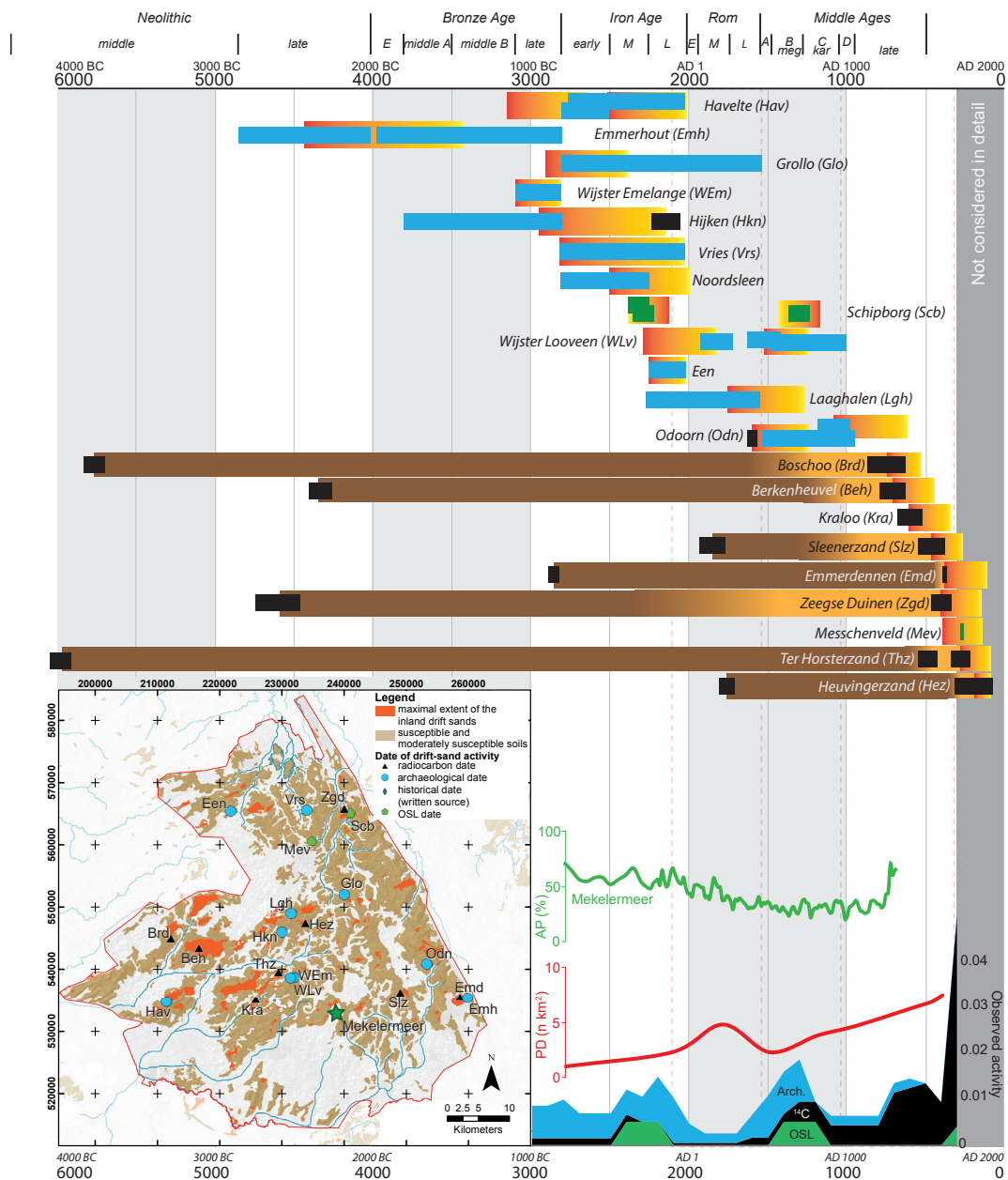


Figure 9.3 | Drift-sand activity in the northern sand area. Ages are in B2k (before AD 2000), for legend see Figure 9.4. The narrow bars indicate drift-sand dates 1 σ range (Appendix D2), the wider yellow-orange bars indicate estimated drift-sand activity. The observed intensity graph (bottom right) shows the sum of all dates in the figure visualised per type of date (colour corresponds to the colours of the narrow bars). Population density (PD) estimates are explained in Appendix D1, the arboreal pollen percentage (AP%) is used as an indication for openness (see text).

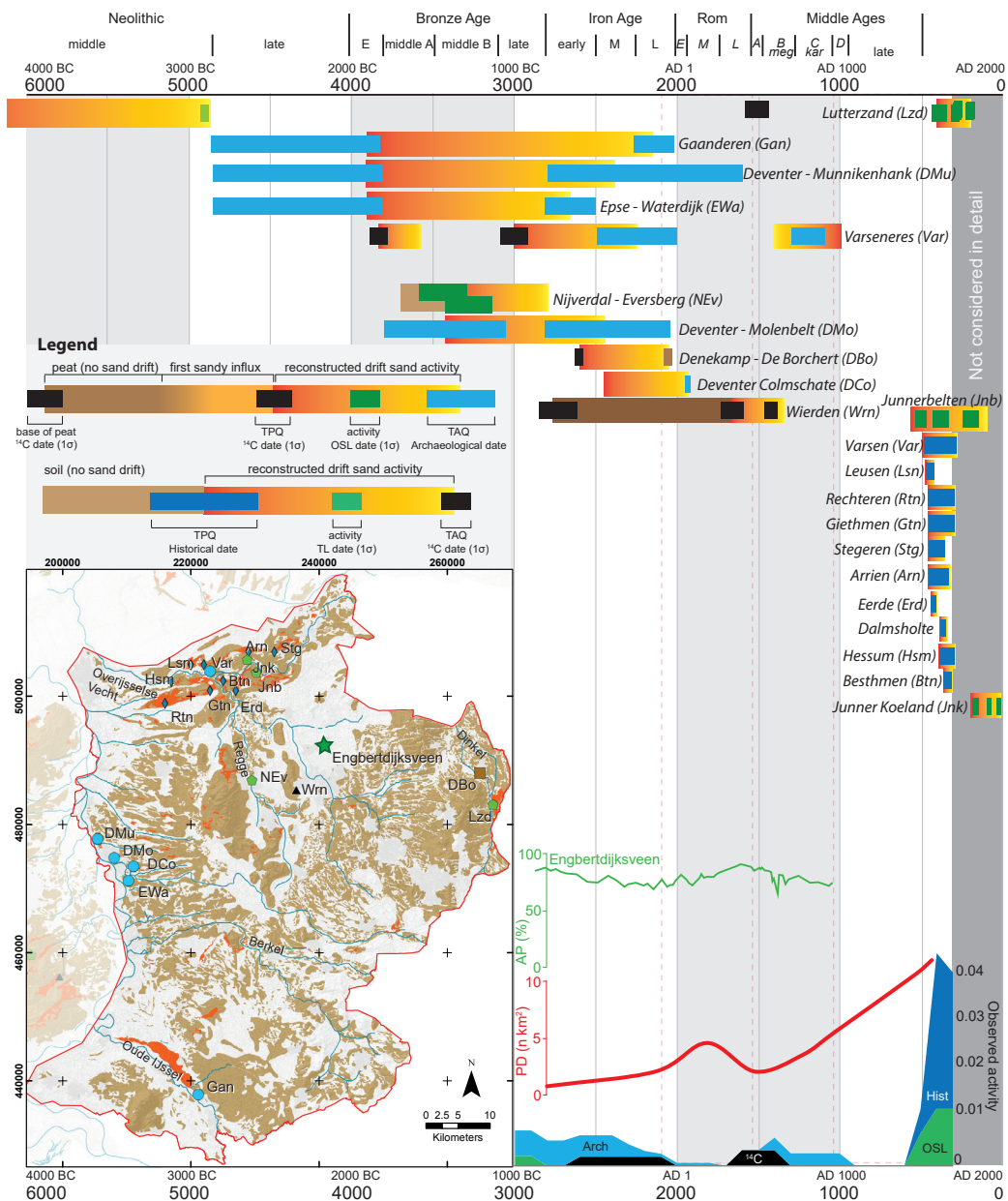


Figure 9.4 | Drift-sand activity in the eastern sand area, ages are in B2k (before AD 2000). Brown square (DBo) = dendrochronological date. The narrow bars indicate drift-sand dates 1σ range (Appendix D2), the wider yellow-orange bars indicate estimated drift-sand activity. The observed intensity graph (bottom, right) shows the sum of all dates in the figure visualised per type of date (colour corresponds to the colours of the narrow bars). Population density (PD) estimates are explained in Appendix D1, the arboreal pollen percentage (AP%) is used as an indication for openness (see text).

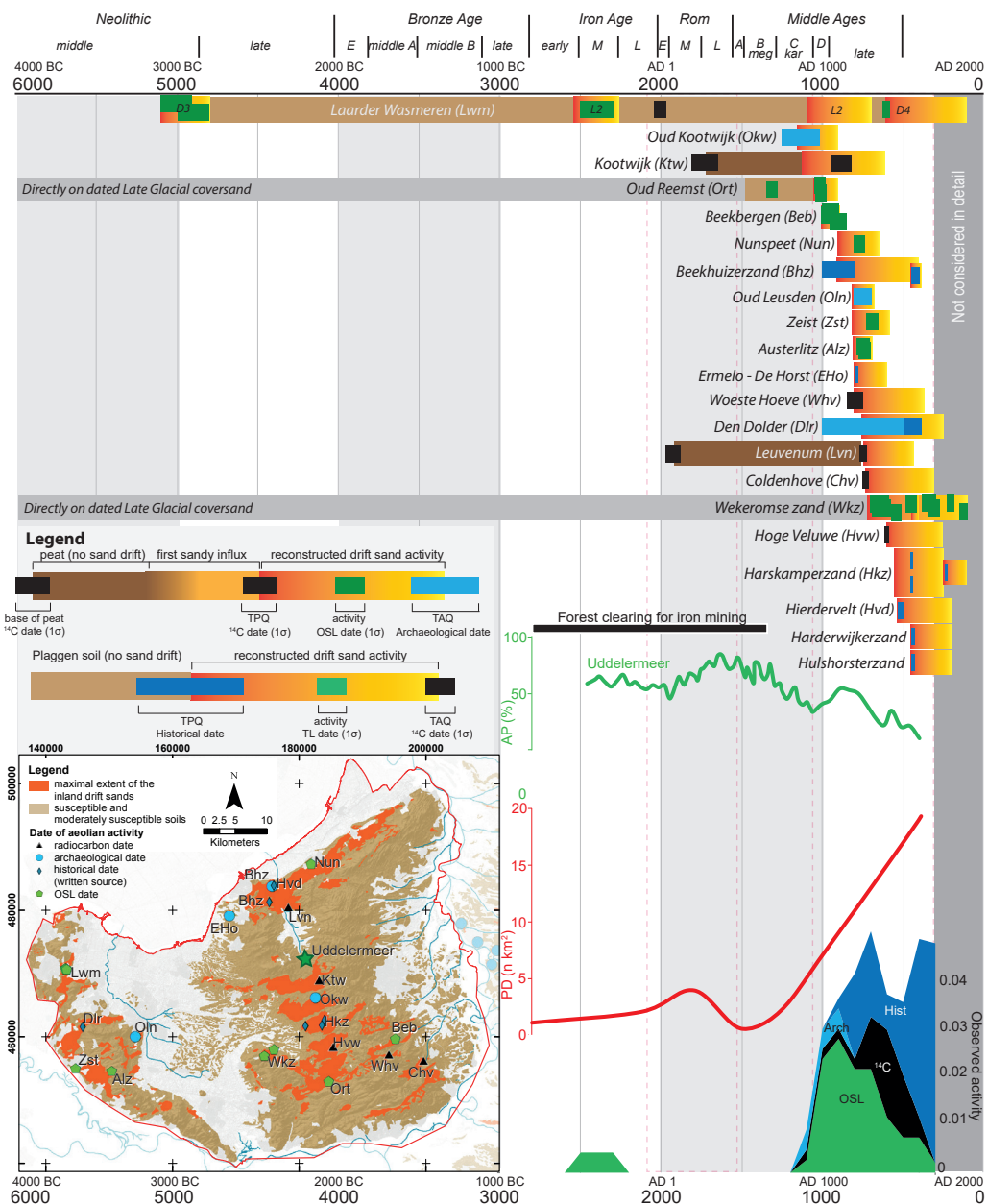


Figure 9.5 | Drift-sand activity in the middle sand area. Ages are in B2k (before AD 2000). The narrow bars indicate drift-sand dates 1σ range (Appendix D1), the wider yellow-orange bars indicate estimated drift-sand activity. The observed intensity graph (bottom right) shows the sum of all dates in the figure visualised per type of date (colour corresponds to the colours of the narrow bars). Population density (PD) estimates are explained in Appendix D1, the arboreal pollen percentage (AP%) is used as an indication for openness (see text).

Table 9.5 | Spatial distribution of drift-sand sites inside and outside the route zones in Figures 9.7-9.10.

Region	Period	% susceptible area within 1 km routes	% susceptible area outside 1 km routes	# sites within 1 km buffer	# sites outside 1 km buffer	Factor comparing drift sand sites inside and outside 1 km buffer	p-value (n)
northern sand area	RP	25.7	74.3	2	6	1	0.650 (8)
	EMA	25.8	74.2	4	4	> 10	0.126 (8)
	LME	22.9	77.1	2	8	0.8	0.706 (10)
eastern sand area	RP	30.1	69.9	3	0	> 10	0.027 (3)
	EMA	28.2	71.8	1	1	2.5	0.485 (2)
	LME	41.1	58.9	5	7	1	0.593 (12)
middle sand area	RP	25.6	74.4	1	0	-	-
	EMA	21.0	79.0	1	1	3	0.377 (2)
	LME	46.9	53.1	6	17	0.4	0.988 (23)
southern sand area	RP	40.3	59.7	2	3	1	0.668 (5)
	EMA	30.5	69.5	2	2	2.3	0.358 (4)
	LME	35.9	64.1	11	11	1.8	0.125 (22)

P-value for H_0 : drift sand activity occurs as frequent within as outside the 1000 m buffer. Lower p-value indicates trend towards more drift sand within buffer, $p < 0.05$ indicates significantly more drift sand within the buffer.

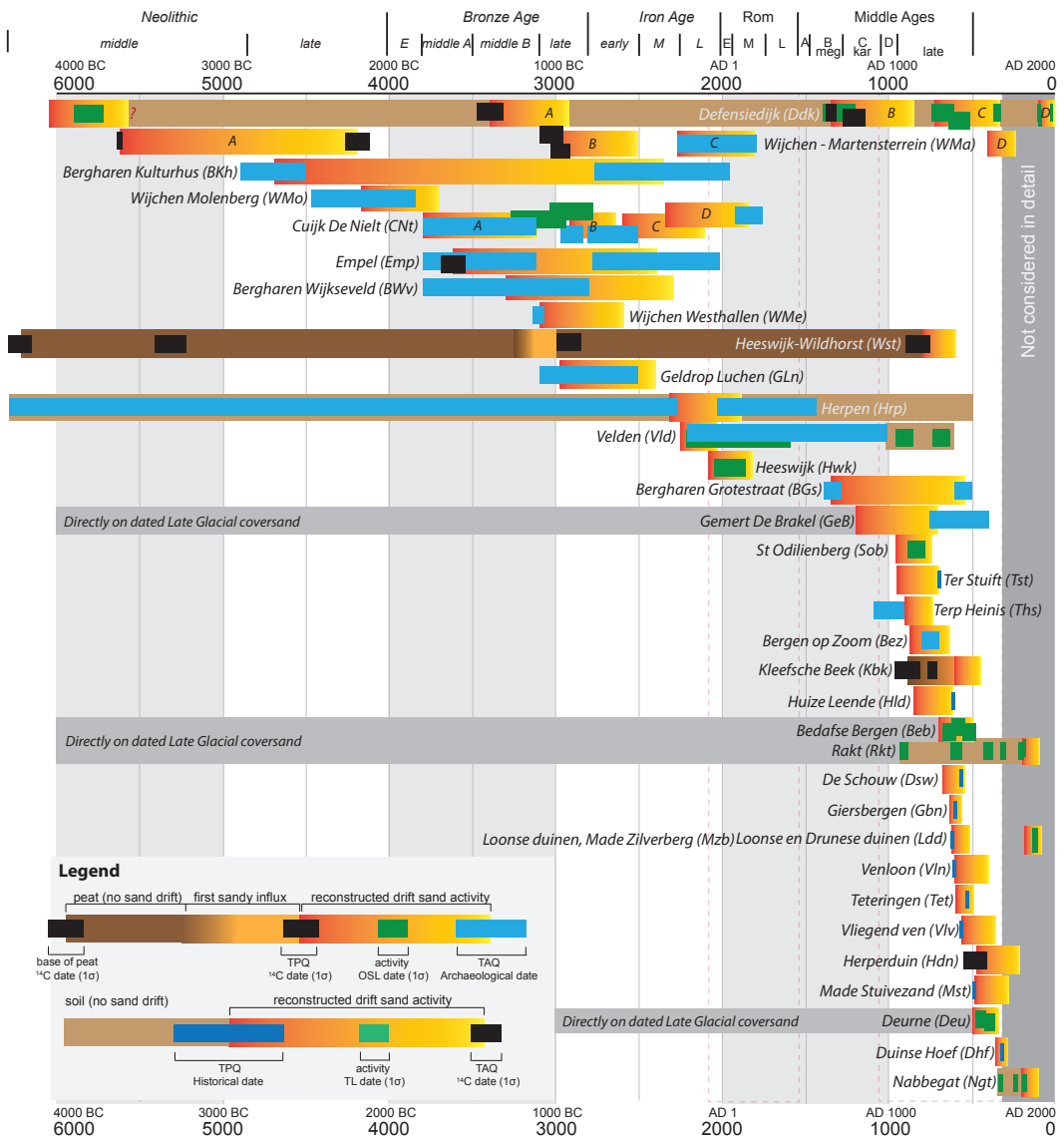
Between AD 600 and 900 the observed drift-sand activity increased to the prehistoric level. This seems in line with the vegetation trends, which during this time interval show renewed deforestation. After AD 900 sand drifting shows a sharp rise, especially in the middle and southern sand areas (Figures 9.5 and 9.6). In the northern and eastern sand areas the drift-sand activity remained moderately low, until after AD 1500 a sharp rise in the number of active sites occurred here as well (Figures 9.3 and 9.4). The change in timing of this major increase between the regions is consistent for all dating methods and therefore most likely represents a real trend rather than a sampling bias. The difference in timing it is best explained by the increase in population density that was higher in the southern and middle sand areas than in the eastern and northern areas.

On a national level the number of point locations where sand drifting occurred did not increase from AD 1300 onwards. This does not imply that drift-sand activity stabilized; the surface of existing drift sites increased (e.g. Lascaris, 1999).

9.5.2 Spatial patterns in drift-sand activity

The locations of sand drifting are not randomly distributed over the areas with susceptible soils, but seem to occur more often close to routes (Figures 9.7-9.10). When comparing the number of active sites inside and outside the 1000-m buffer around reconstructed route networks, taking only the areas susceptible to sand drifting into account, most sites are indeed located relatively close to route zones. For the cases where more sites are available, the southern sand area for AD 1600 and the northern sand area for AD 800, have > 1.8 times more activity close to routes (Table 9.5).

Few sites with sand drifting were found for the period between 100 BC and AD 450 ($n = 18$). The northern and southern sand areas contain 8 and 5 sites respectively. These are situated relatively close to the route network, but in each area only two sites are located within the defined 1000-m buffer (Figures 9.7A, D and 9.10A). The eastern and middle sand areas contain few sites, which all are located within the buffer (Table 9.5; Figures 9.8A and 9.9A). Between AD 450 and 950 drift-sand



frequency was low (generally $n < 4$), mostly occurring close to routes. In the northern sand area (Figure 9.7B) 8 sites are present with a strong spatial tendency towards the routes ($p = 0.126$; Table 9.5).

For the Late Middle Ages and early Modern period (until ca. AD 1700) more sites have been identified, and clear relations between drift-sand occurrence and human presence can be observed. In the southern sand area, 50% of the drift sites (11 out of 22) occur within the 1000-m buffer, which differs close to significantly from a random distribution (exact binomial test, $p = 0.125$ – Figure 9.10C, D; Table 9.5). In the northern sand area and the Overijsselse Vecht area in the eastern sand area, drift-sand activity was remarkably aligned along routes (Figures 9.7C and 9.8D). However in this area several outliers occur (remote sites), which reduces the overall spatial correspondence

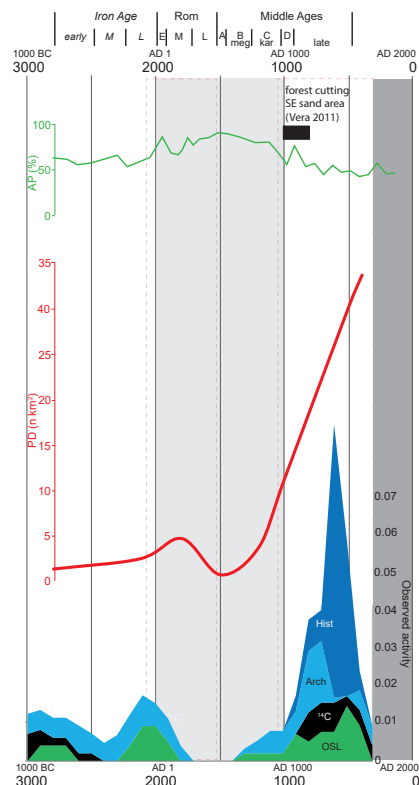
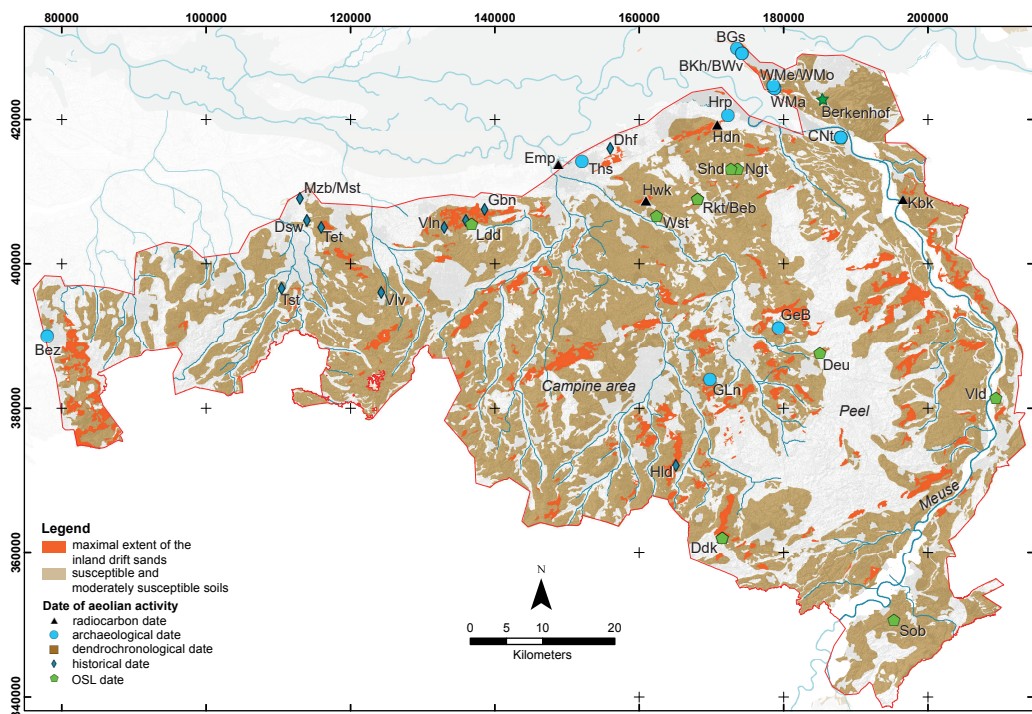


Figure 9.6 (left page and this page) | Drift-sand activity in the southern sand area. Ages are in B2k (before AD 2000). The narrow bars indicate drift-sand dates 1 σ range (Appendix D2), the wider yellow-orange bars indicate estimated drift-sand activity. The observed intensity graph (bottom right) shows the sum of all dates in the figure visualised per type of date (colour corresponds to the colours of the narrow bars). Population density (PD) estimates are explained in Appendix D1, the arboreal pollen percentage (AP%) is used as an indication for openness (see text).

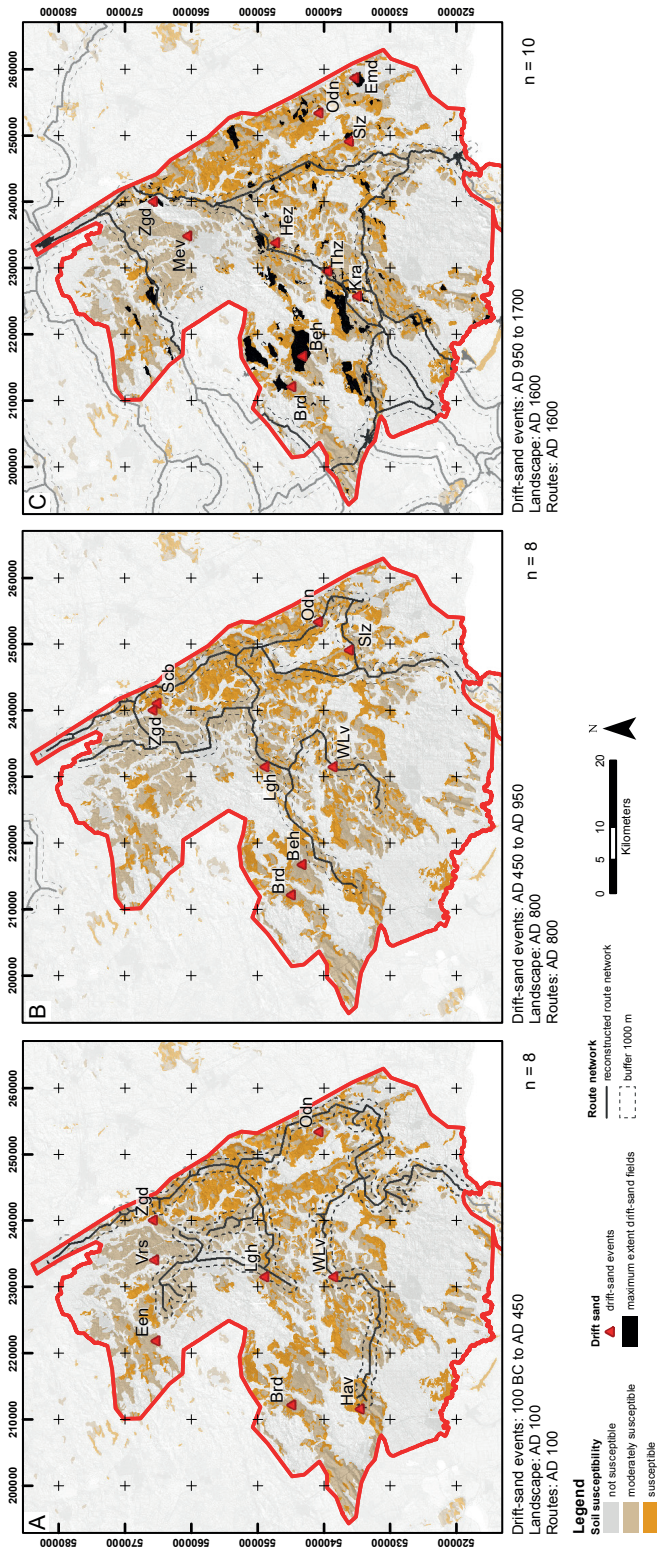


Figure 9.7 | Position of sand-drifting events relative to the route networks in the northern sand area. For codes of the sites, see Figure 9.3. A: AD 100, B: AD 800, C: AD 1600. For all time slices, the sites show a rather good correspondence to the location of the route networks, except for some remote outliers in AD 1600.

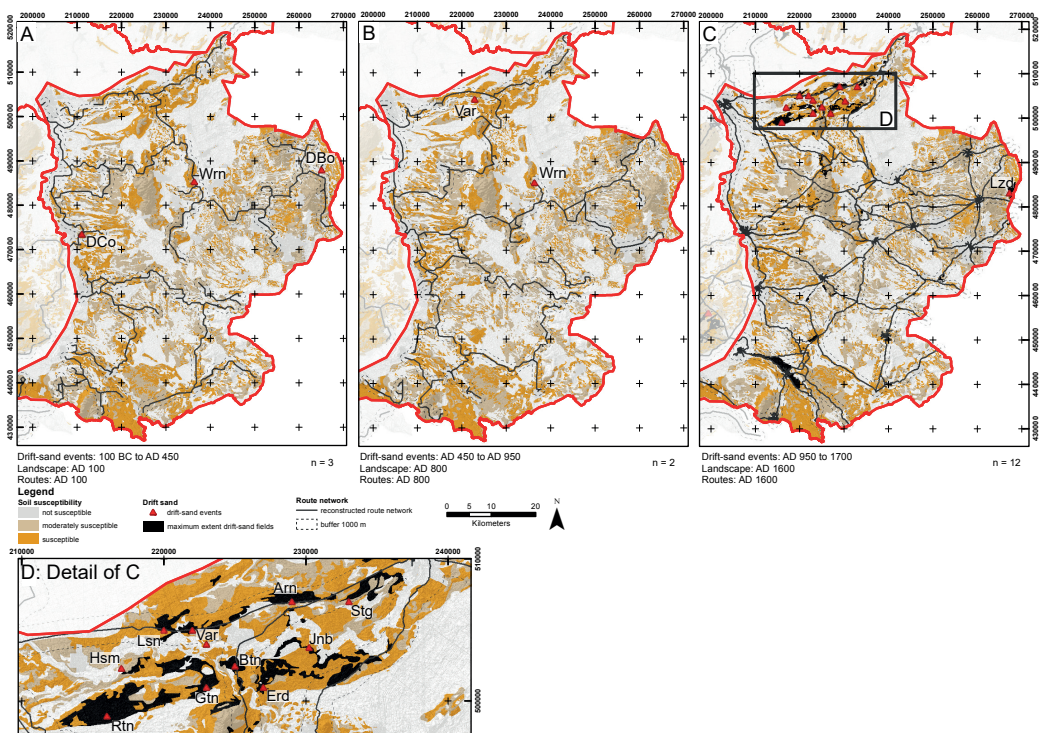


Figure 9.8 | Position of sand-drifting events relative to the route networks in the eastern sand area. For codes of the sites, see Figure 9.4. A: AD 100, B: AD 800, C: AD 1600, D: detail of the Overijsselse Vecht area for AD 1600. For AD 100 and 800 the few sites present show a rather good correspondence to the location of the route networks. For AD 1600, the correspondence is low.

between route networks and drift sites (Table 9.5). This is probably caused by drift-sand occurrence in remote sites or by the fact that not all routes have been mapped.

For the Veluwe in the middle sand area the opposite trend is observed: especially in the area around the largest dune fields most sites are located relatively far away from routes (Figure 9.9C; Table 9.5). The most likely reason is that these dune fields became so large that the roads had to be diverted around them as demonstrated for the Kootwijk (*Ktw* in Figure 9.9) area by Heidinga (1987). The AD 1600 roads represent the situation after significant extension of drift-sand fields and do therefore not reflect the initial spatial layout of the routes. The original route zones probably are buried under the fossil drift-sand fields. Around the western edge of the Veluwe (i.e. upwind, Nunspeet, Zeist), the same pattern emerges as in other areas. Here, relatively many drift-sands are found close to routes. The reason is that the sand mostly was blown towards the east, and therefore these roads were not affected/relocated.

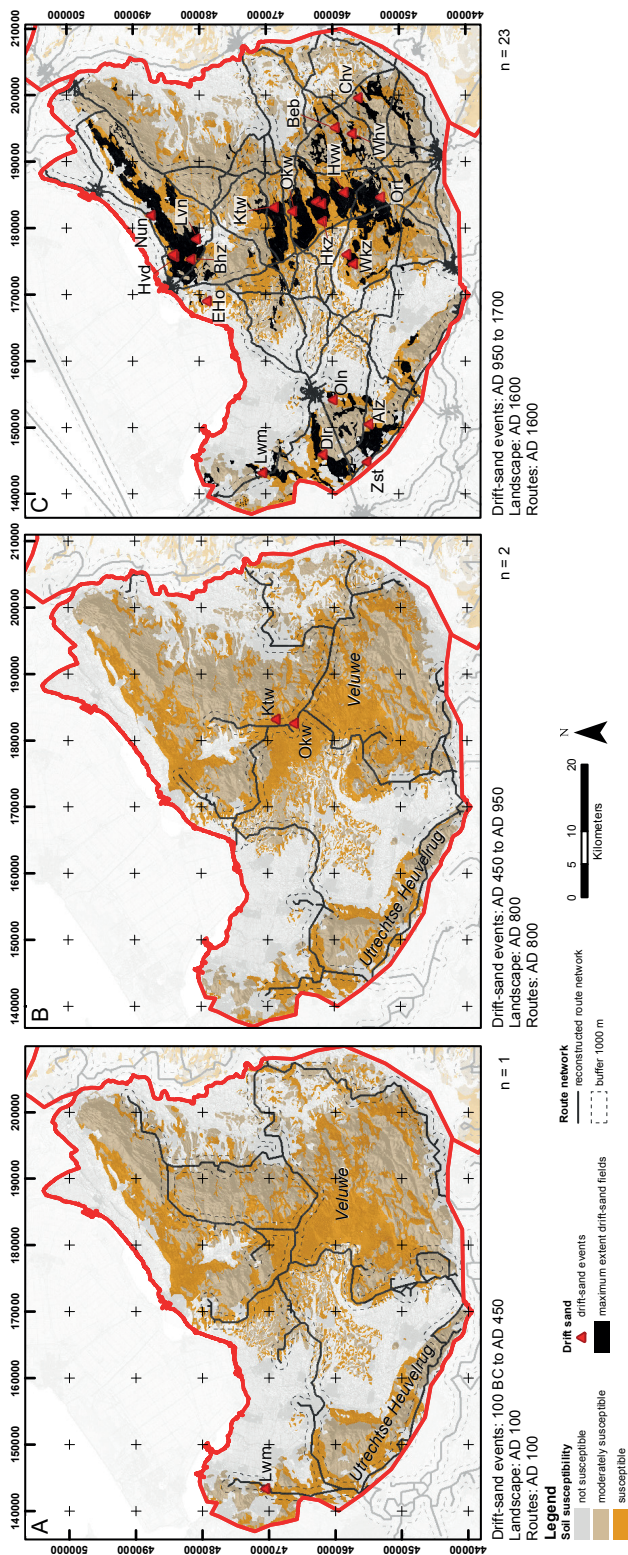


Figure 9.9 | Position of sand-drifting events relative to the route networks in the middle sand area. For codes of the sites, see Figure 9.5. A: AD 100, B: AD 800, C: AD 1600. For AD 100 and 800 the few sites present show a rather good correspondence to the location of the route networks. For AD 1600, the sites are mostly located far away from the route networks.

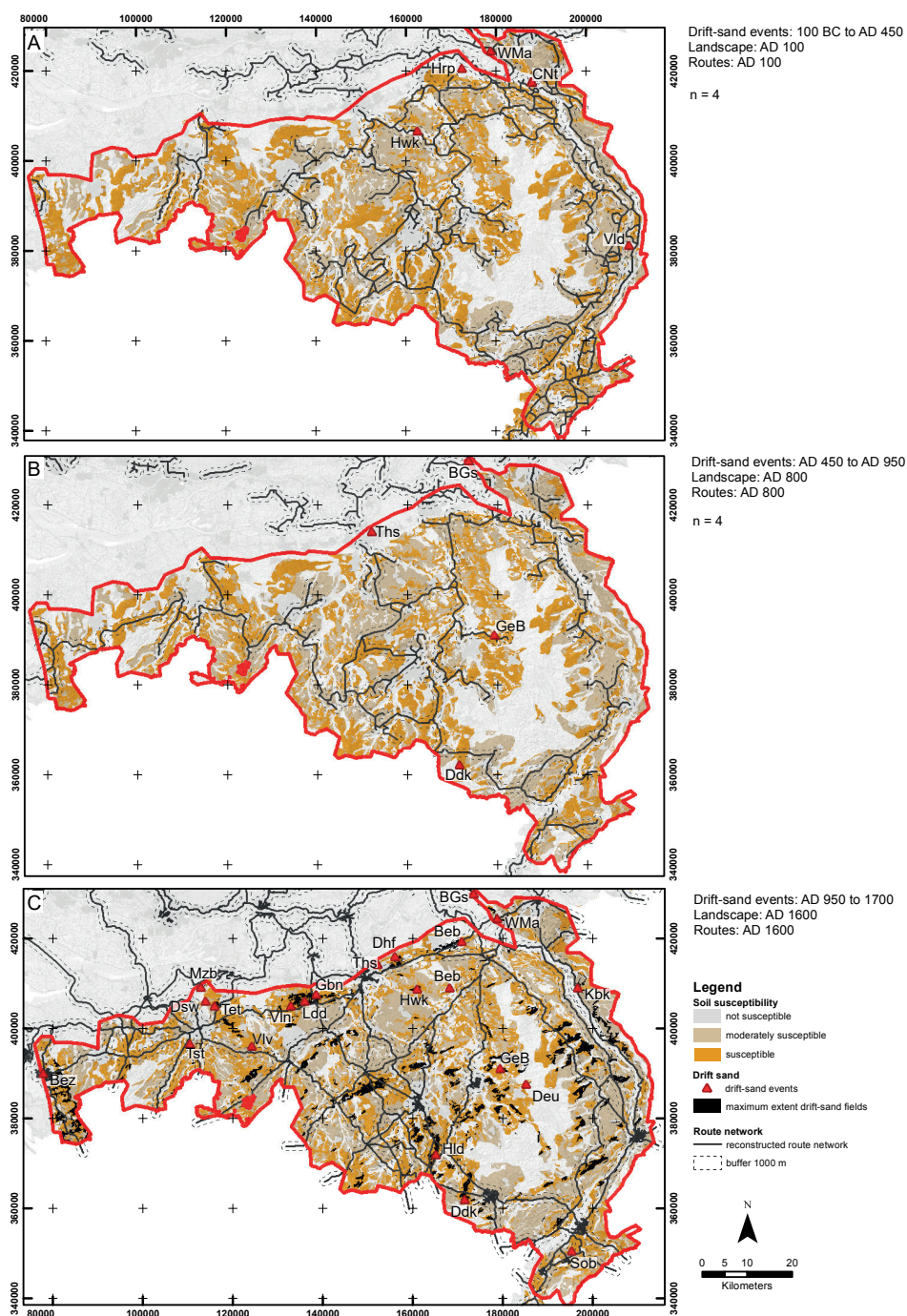


Figure 9.10 | Position of sand-drifting events relative to the route networks in the southern sand area. For codes of the sites, see Figure 9.6. A: AD 100, B: AD 800, C: AD 1600. For AD 100 and 800 the few sites present show a rather good correspondence to the location of the route networks. For AD 1600, mainly concentrate on the northern edge of the area with a good correspondence to the route networks.

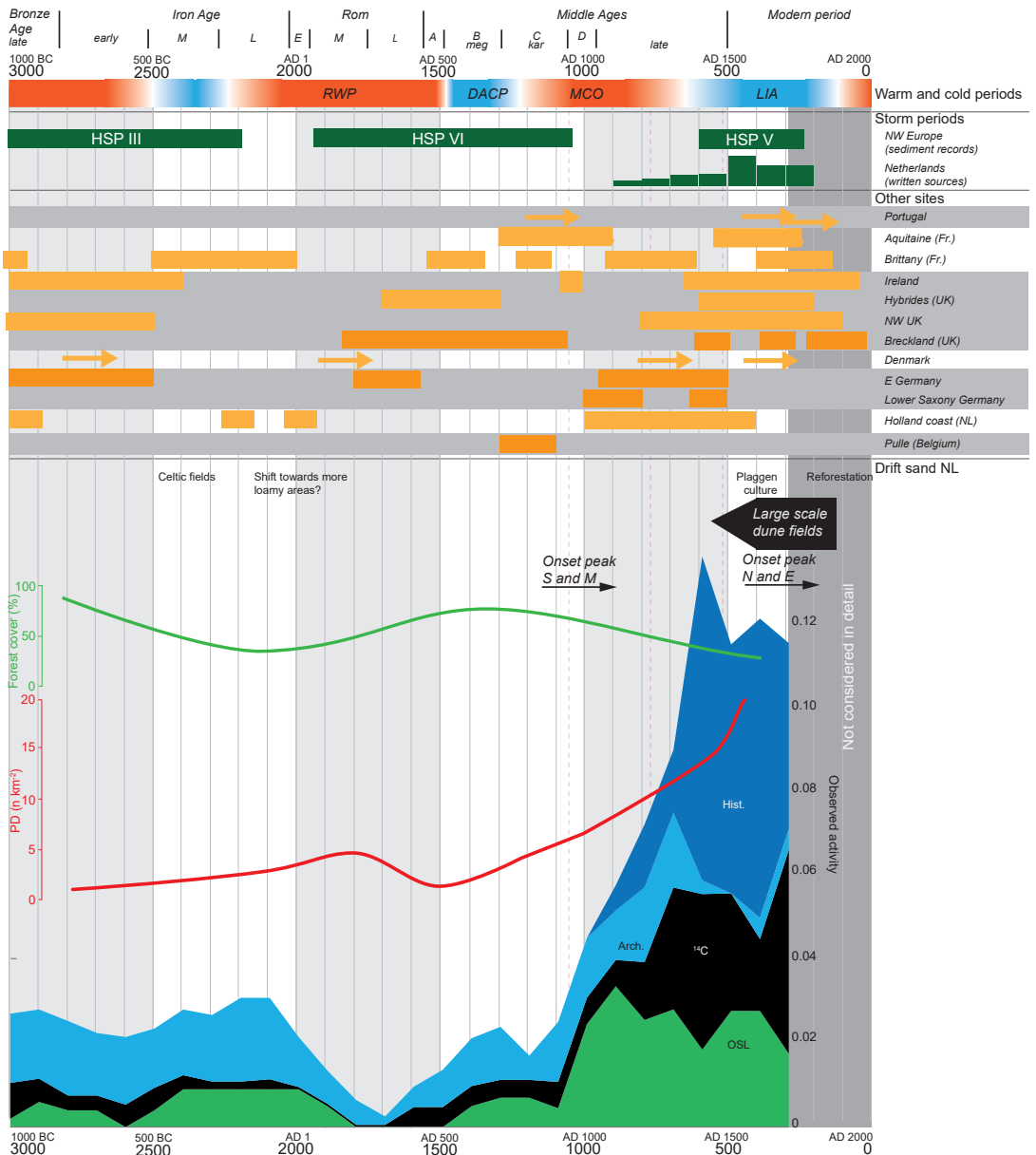


Figure 9.11 | Timing of drift-sand formation for all four sand areas in the Netherlands combined and its forcings compared to other sites in NW Europe. Warmer (red) and colder (blue) periods 1000 BC-AD 1 after Kobashi et al. (2011) – Greenland ice core, 1 AD-AD 2000 after Büntgen et al. (2016). RWP = Roman Warm Period, DACP = Dark Ages Cold Period, MCO = Medieval climate optimum, LIA = Little Ice Age. NW European Holocene storm periods (HSPs) after Sorrel et al. (2012), Dutch storms from written sources after Berendsen (1984c), Buisman & Van Engelen (1996; 1998; 2000). Light orange bars are coastal dune sites, dark orange sites are inland drift sands: Portugal – Costas et al. (2012), Aquitaine, France – Clarke et al., 2002, Brittany, France – Van Vliet-Lanoë et al. (2015), Ireland – Wilson et al. (2004), Hybrides, NW Scotland – Gilbertson et al. (1999), northwestern UK – Pye &

Neal (1993); Orford et al. (2000), Brecklands – Bateman & Godby (2004), Denmark – Clemmensen et al. (2009), eastern Germany and Lower Saxony – Tolksdorf & Kaiser (2012), Holland coast – Jelgersma et al. (1970); Zagwijn (1984), Pulle, Belgium – Derese et al. (2010). Forest cover after Louwe Kooijmans (1995); population density (PD) and drift-sand intensity – this study. The drift-sand intensity graph shows the sum of all dates for the four study areas, visualised per type of date. Moderate drift-sand activity has been present at least since 1000 BC, with a clear dip between AD 1 and 500. After AD 900 the drift-sand activity increases uninterruptedly. Together with several Belgium and German sites, this increase occurs earlier than in many other parts of NW Europe and does not seem to be related to climate or storm trends.

9.6 Discussion

9.6.1 Natural and anthropogenic causes

In this section the role of natural and human facilitating conditions and natural forcings for sand drifting is outlined using the conceptual diagram of Figure 9.2 and the results from our study area summarised in Figure 9.11.

Facilitating initial conditions – Large dune fields can develop most easily in a sandy and dry substrate (Figure 9.2) and when this substrate covers a large area. This explains why in the eastern sand area small isolated coversand outcrops are most prominent, and drifting is confined to smaller areas. An exception is the Vecht area (eastern sand area) with large W-E oriented coversand ridges (Figures 9.4 and 9.8), since due to the predominantly western wind regime and the long fetch through the E-W oriented valley, large drift sands could easily develop here. Southwest of the Veluwe thick coversand deposits occur. Here the largest drift-sand fields of the study area developed, which were active until the 19th century. The peat bogs flanking and covering sandy areas were mainly excavated or reclaimed from the Late Middle Ages onwards. This probably lowered the local groundwater level, further facilitating sand drifting. This mechanism could have played a role along the edges of large sand areas: the northern edge of the southern sand area (Figures 9.6 and 9.10) and the western edge of the Veluwe (Heidinga, 1984ab) and Utrechtse Heuvelrug (Sevink et al., 2013; Figures 9.5 and 9.9).

Natural forcings (climate and storms) – The hypothesis that colder climatic events coincided with episodes of drift-sand activity (possibly through weaker vegetation – Figure 9.2) is not confirmed with our data. The rise in drift-sand activity around AD 400 took place before the cold DACP (AD 500-750) started. Moreover the most pronounced rise in drift-sand intensity of the studied period after AD 900, especially occurring in the southern and middle sand area, is not concurrent with a cold period but with the warm MCO (AD 750-1570 – Figure 9.11).

In order to identify periods with enhanced storminess, historical written sources can only be used after ca. AD 1400 and we therefore have to rely on sedimentary records for comparing drift-sand activity to storms. Sorrel et al. (2012) reconstructed a stormy Roman period in NW-Europe (Holocene Storm Period (HSP) VI in Figure 9.11), while during this period in the Netherlands the lowest drift-sand activity of the past 3 millennia occurred. This sharp rise in drift-sand activity during the MCO after AD 900 does also not match a presumed NW European storm period, it falls between HSP VI and V in Figure 9.11. The inland rise after AD 900 is in line with late-medieval inland drift sands recorded in Germany (Tolksdorf & Kaiser, 2012 and references therein) and dune phases along the Dutch coast from around AD 1000 onwards (Jelgersma et al., 1970; Vos et al., 2015). All these drift-sand activity phases occurred earlier than the onset of the cold LIA and

inferred storm periods in NW Europe. It is nevertheless possible that once drift sands were initiated, they further expanded during the colder and more stormy LIA from ca. AD 1500 onwards. For this colder period higher storm frequencies and much dune activity has been recorded throughout many sites in the Netherlands and for many other parts of northwestern Europe (Figure 9.11).

When comparing storm periods to phases with increased drift-sand intensity on a NW European scale, still several methodological problems arise: (i) many of the sites of the Sorrel et al. (2012) study are situated in coastal dunes or in tidal areas, which are also sensitive to autogenic sediment dynamics such as supply from the shallow sea (Jelgersma et al., 1970, 1995; Zagwijn, 1984; Van der Valk, 1992; chapter 4); (ii) the effect of individual storms that occur outside the period of enhanced storm activity on coastal and inland sand drifting can be overlooked. These storms could push an already vulnerable system state (e.g. intensively used dry sandy soils) across a threshold, causing a non-linear response in the form of drift-sand formation; (iii) within NW Europe or even within the Netherlands, individual storms can have different magnitudes and impact. Not all storms that may have been important are recorded in independent sedimentary records or historical records; (iv) dating uncertainty of drift-sand events (several centuries) does not often allow linking them to individual storms (Clarke & Rendell, 2009).

The issues discussed above highlight the importance of independent storm records and reconstructions (i.e. not inferred from aeolian dunes) on a regional scale rather than on a NW European scale. With the exception of the LIA, the discrepancies between presumed periods of enhanced storminess, colder or drier climate and drift-sand events indicate that changes in climate conditions still were small compared to the optimum temperature or wetness range of vegetation. Therefore climate conditions are considered not to be the main cause behind drift-sand activity in the Netherlands.

Facilitating human conditions – Generally, higher population densities will result in more intense land use (deforestation, overexploitation) leading to more sand drifting. When comparing the period before and after AD 1000 in terms of drift-sand activity and population density, it is clear that higher population densities indeed coincided with high drift-sand activity. This is further underlined by the early timing of large-scale drift-sand activity in the middle and southern sand areas, which were characterized by higher population densities than the other study areas. The higher population densities in the south are best explained by the development of flourishing medieval Flemish cities nearby. In the middle sand area, settlements mainly were located near the area boundaries, close to the densely-populated river area. We also see a clear link between forest cover and drift-sand activity. Periods of decreasing forest cover generally coincided with periods of increased drift-sand activity, for example in the southern sand area during the Iron Age and the 11-13th centuries (Vera, 2011) (Figure 9.6). In the middle sand area a low forest cover after AD 900 coincided with high drift-sand activity. Modest forest clearings for iron mining between the Iron Age and the 6/7th century in this area does not seem to have caused much drift-sand activity (Heidinga, 1987; Doorenbosch & Van Mourik, 2016; Figure 9.5).

The consistent dip in drift-sand activity during the Roman period strongly suggests that population increase and deforestation did not automatically lead to more drift-sand activity. This dip is observed both south as well as north of the Roman *limes*. Besides possibly low storm activity during this period, the type of land use could play a role. After the Iron Age, Celtic fields were abandoned, indicating a shift in agricultural practices (Van Gijn & Waterbolck, 1984; Roymans & Gerritsen, 2002; Spek et al., 2003). In the eastern and northern sand area this coincided with a settlement shift towards areas with more loamy and fertile substrates (Groenewoudt, 1989; Spek,

2004). The same type of shift has been documented by Roymans & Gerritsen (2002) and Kluiving et al. (2015) for the southern sand area. These trends could not be reproduced by Wolthuis & Arnoldussen (2015), but they did notice a settlement shift trend towards areas comprising more wet soils during the Late Iron Age and the Early Roman period. These shift in the Roman period may have decreased human pressure on the most sensitive sandy areas. More research should further explore this hypothesis, also for other sandy areas within the NW European sand belt.

The introduction of different agricultural techniques from the Early Middle Ages onwards, such as more advanced ploughs leading to increased soil destruction (Larsen, 2016), could have made the land more prone to sand drifting. From the 15th century onwards, heather sods (*plaggen*) were used as natural fertilizers in the southern sand area. These *plaggen*, with a high organic content, were collected by removing the vegetated organic top soil, causing the bare sandy substrate to become exposed to wind erosion. Around a century later this technique was introduced in the middle and eastern sand areas, and during the 17th century it was applied in the north (Groenman-Van Waateringe, 1992; Lascaris, 1999; Spek, 2004; Van Mourik et al., 2011). Initially, *plaggen* activities most likely took place close to settlements and routes. Later, *plaggen* material had to be collected from more remote areas as well. These areas generally contained the poorest and driest soils, and therefore, already were most prone to sand drifting. The large-scale destruction of the protecting top soil allowed drift-sand fields in these areas to develop into their final maximal extent during the 19th century, also in more remote areas.

Besides population density, also the type of land use (e.g. agricultural techniques, specialization, ratio arable farming-animal husbandry) was an important driver for sand drifting (Figure 9.2). Socio-economic and political factors such as institutional arrangements, property structures, power balances, and commercial strategies play an important role when it comes to the initiation and prevention of drift sand (e.g. De Keyzer, 2016; De Keyzer & Bateman, in review). These factors determine activities enhancing or preventing sand drifting, such as the use of *plaggen*, deforestation, and the construction of hedges and wooden fences.

From the cases presented in this study, it can be concluded that human pressure on a sandy landscape was the most important facilitating condition for drift-sand activity. When the landscape is more sensitive due to the human pressure, sand drifting can be enhanced by colder climate or higher storm intensity. Whether sand actually will start to drift or continue to drift depends strongly on how the land is used (e.g. deforestation, use of prevention measures), which is besides population pressure influenced by many cultural factors. This causes the relation between population density, deforestation, and drift sand activity to be strongly non-linear.

9.6.2 Reflection on data quality

In this study regional patterns of drift-sand activity were assessed by combining information from many point locations. This approach is sensitive to sampling biases, because the coverage of the earlier research this work was based on may vary in space and time depending on past research traditions. A source of undersampling are the *plaggen* soils in which drift sands have become homogenised by ploughing (Spek, 2004). When low drift-sand activity is found (e.g. the Roman period), bias caused by undersampling can be minimised by (i) considering regional patterns (i.e. by comparing multiple regions and other locations in NW Europe), and (ii) considering evidence of *absence* of drift sands (e.g. peat records), as was done in this study. Using the latter kind of evidence also minimises the overrepresentation of younger drift-sand events caused by reworking of older generations of dunes. The reworking bias could still have a local effect, but from peat records and dated soil horizons it is clear that increasing drift-sand intensity in the Netherlands after AD 900

represents a real trend. To consider oversampling effects during observed high aeolian intensity (e.g. influenced by detailed records in written sources dating from AD 1400 onwards), the events were split up according to their dating method in which the increase is still evident (Figure 9.11).

Especially after AD 1500, not the amount of drift-sand sites, but the size of the drift-sand dune fields becomes a more important indicator of human impact on the landscape and people. This makes the point location approach used in this chapter gradually less suitable for the period after AD 1500. Therefore, the growing dune fields are not well reflected in our study, and even resulted in the apparent decrease of site events in Figure 9.11 after ca. AD 1400. Historical records mentioning the size and scale of the dunes therefore should be considered more suitable for this interval. In addition for the interval after AD 1800, historical maps can be used for drift-sand reconstruction.

Despite the low amount of drift-sand data around AD 100 and 800, it appears that sand drifting occurred more often close to route networks. Although the reconstructed route networks due to a lack of data only reflect parts of the original networks, they do show a spatial correspondence with drift-sand activity for the investigated period. Also for AD 1600 the results indicate that areas flanking these routes contained more drift-sand sites than areas further away, but this spatial trend cannot be proven statistically on a regional scale. This is partly because during this period more activities causing sand drifting took place at increasing distance from the main roads (e.g. digging of *plaggen*), as most likely is reflected by several clusters of sites further away from these routes. For drift-sand sites near settlements, results probably can improve by including secondary roads and local paths in the AD 1600 route network, and by improving the chronological depth of the analyses.

9.6.3 Outlook

Including more exact dates from local site studies (preferentially OSL) would further unravel the chronological and spatial patterns of past aeolian activity. Additionally, sand influx data from continuous peat records will provide a good record of both the presence and absence of sand drifting. Further independent storm records (i.e. not inferred from dunes) will help to assess the role of storms in episodes of drift-sand formation. Such records may include shell layers in coastal dunes (representing wave height – Jelgersma et al., 1995; Cunningham et al., 2011) or lagoon-derived sand layers (Van den Biggelaar et al., 2014; Degeai et al., 2015). Although these were mainly influenced by wind direction and resulting water setup rather than absolute wind strength, they can help to understand the role of storm events in drift-sand formation.

Comparing sand drifting north and south of the Roman *limes* based on more sites would probably further help to understand the (lack of) impact of anthropogenic and natural conditions during the Roman period. Combining such local studies in an interdisciplinary manner, also taking into account the occurrence of human activity and vegetation, will improve the understanding of the relation between people and landscapes of the past. To achieve this, spatial vegetation reconstructions including drift sands will be helpful (e.g. Van Beek et al., 2015a). Historical studies from AD 1500 onwards can unravel the political and economic factors behind land use strategies (Spek, 2004; De Keyzer, 2016). These detailed local studies can be integrated into regional and supraregional studies as done in this study or further extended towards adjacent areas in the NW European sand belt.

9.7 Conclusions

This chapter presents an integrated overview of inland Holocene drift-sand activity in the Netherlands, aiming to assess the relative importance of natural and anthropogenic factors in this region on aeolian drift-sand activity.

- From the cases presented in this study it can be concluded that human pressure on a sandy landscape was an important facilitating condition for drift-sand activity. Prehistoric sand drifting occurred since the Late Neolithic period under increasing population densities and deforestation. The uninterrupted increase of drift-sand activity from ca. AD 900 onwards coincided with a growing population density and decreasing forest cover compared to preceding periods. This effect was strongest in the most densely-populated southern and middle sand areas.
- Human pressure as an important forcing is also demonstrated by the proximity of sand drifts to routes, which represent areas with intense human activities. In these areas road density, agricultural activities and overexploitation are presumed to have been most intense, enhancing drift sand formation. After AD 1500, drift-sand activity not only took place close to habitation but also on more remote sites, especially where *plaggen* digging led to the large-scale expansion of active dune fields.
- The relation between population density, deforestation, and drift sand activity is non-linear. Whether sand actually started to drift, continued to drift, or was prevented from drifting, depended on the manner in which the land was used. For example, the shifting of habitation throughout the Iron Age towards less drift-sand susceptible areas could explain the observed dip in drift-sand activity during the densely populated Roman period. The type of land use furthermore depended on political and economic factors facilitating overexploitation or leading to prevention measures.
- Sand drifting likely was enhanced, but not initiated, by colder climate and higher storm intensity. These conditions accelerated the expansion of dune fields during the Little Ice Age after ca. AD 1500, although original facilitating conditions were provided by population pressure and type of land use.

Acknowledgements

This chapter is part of the PhD theses of H.J. Pierik and R.J. Van Lanen, within the project ‘The Dark Ages in an interdisciplinary light’ (www.darkagesproject.com) funded by NWO (project nr. 360-60-110). The first author contributed in the following proportions (%) to research design, data collection, analysis and conclusions, figures, and writing: 60, 60, 70, 90, 70. The authors would like to thank Theo Spek and Maïka de Keyzer for the useful discussions and Hans Middelkoop and Esther Jansma for their comments on earlier drafts of the chapter.

Chapter 10

Synthesis

In this thesis human-landscape interactions in the Netherlands during the first millennium AD were studied. During this period a mainly natural, prehistorical lowland landscape became increasingly influenced by people. The first centuries of the first millennium (Roman period), were characterised by a high human pressure on the landscape, followed by a period with depopulation and less human influence ('Dark Ages'). Eventually human influence increased again and the landscape reached a mainly human-dominated state after embankment, large-scale reclamation, and population growth from the High Middle Ages (ca. AD 1050–1200) onwards (Jansma et al., 2014).

This research on human-landscape interactions during the first millennium AD has a broad areal focus, dealing with three distinct physical geographical regions within the Netherlands: the coastal plain, the fluvial area (Rhine-Meuse delta), and the Pleistocene sand area (Figure 10.1). The aims were to: 1) identify the changes in natural landscape evolution; 2) unravel the natural and anthropogenic causal factors as well as the geomorphological feedback mechanisms underlying these changes; and 3) to evaluate the impact of these changes on humans. An integrative approach was used in which data and methods from the disciplines of physical geography and archaeology were combined. To identify landscape changes, map datasets were integrated into reconstruction maps of the physical landscape that show the former extent of geomorphological elements (channels, supratidal ridges, alluvial ridges, etc.). By spatially and temporally comparing observed geomorphological changes to varying external forcings and the archaeological record, the causes and effect on humans were inferred.

The three studied regions each have a typical geomorphological setting. In the coastal plain estuaries, tidal wetlands, and peatlands were situated, the fluvial area was characterised by a river network with alluvial ridges and wet flood basins, and the sand area consisted of sandy uplands, brook valleys, and peat bogs. In these areas various geomorphological changes took place (e.g. tidal-areal expansion, river avulsion, or drift-sand activity). Both the different geomorphological settings and the varying processes between the regions resulted in regionally characteristic human-landscape interactions. In this final chapter, these interactions are discussed and compared between the three regions.

Section 10.1 lists the main overarching and region specific conclusions. Section 10.2 discusses the reconstruction methods applied in this thesis and their use for unravelling human-landscape interactions. Section 10.3 elaborates on human-landscape interaction in all three regions, by conceptualising the respective roles of the inherited landscape, active natural and human-induced processes, and implications for settlement dynamics. In section 10.4 recommendations for further research are presented.

10.1 Conclusions on human-landscape interactions

10.1.1 Overarching conclusions

Based on the study of three research areas within the Netherlands the following overarching conclusions are drawn on human-landscape interactions for the first millennium AD:

- Anthropogenic land-use activities played an important role in the evolution of all studied landscapes. After a period in which the landscape was made more susceptible to geomorphological change by human influence (e.g. through deforestation or soil subsidence), unintended geomorphological changes took place (e.g. sea ingressions, avulsion, and sand drifting). Storms and floods functioned as triggers, but were not the primary causes of these landscape changes. Although a more frequent occurrence of these triggers may have accelerated the processes, the increased sensitivity of the landscape caused by humans was a prerequisite for these changes.
- In the coastal and fluvial areas, human impact during the first millennium AD was large compared to the preceding periods. The human forcings that made the landscape more susceptible to the changes had already been initiated in the preceding centuries, e.g. by reclamation of peatlands or increased sediment load due to deforestation. In the sand area human impact on sand drifting was comparable to the preceding periods. It mainly occurred locally and probably shortly after the overexploitation that caused it.
- The scale on which geomorphological changes occurred depended on antecedent conditions in the landscape (i.e. the substrate composition and geomorphology). These determined the sensitivity of the landscape to human influence and the strength of geomorphological feedbacks. Anthropogenic impact could be initiated locally, for example through soil subsidence of peatlands after reclamation. Later, the effects could spread regionally via non-linear response and feedback mechanisms. During the studied period, sea ingressions in the coastal plain had the largest effect on landscape evolution, transforming a major part of the coastal plain peatlands into a tidal area. Avulsion had a moderate effect by changing sediment depocentres and delta-network properties. Finally, sand drifting occurred on a more local scale.
- The impact of landscape changes on humans depended on the scale, irreversibility, and recovery time of the geomorphological change, and hence varied across the lowland area. In the coastal plain, sea ingressions caused large-scale settlement abandonment. In the fluvial area, modest settlement shifts are observed in reaction to wetter conditions. In the sand area, no major settlement shifts occurred due to the drift sands.

10.1.2 Regional conclusions

For each of the three research areas, the following conclusions are made on the human-landscape interactions for the first millennium AD:

Coastal plain (chapters 3-5)

- Late-Holocene sea ingressions in the peaty coastal plain of the Netherlands were the effect of subsidence caused by prehistoric peatland reclamation and groundwater level lowering. In these areas, inlet channels were initiated during storm surges and these increased in size by erosion of the tidal flow, leading to considerable loss of land.
- Filling in a newly-formed tidal area to a level suitable for habitation took several centuries. The filling time depended on the extent of the ingressed area, sediment supply by local reworking or fluvial input, and subsidence feedbacks.
- The presence of wide peatlands in the coastal plain facilitated the formation of large sea ingressions, whereas other antecedent conditions, such as the presence of beach barriers or supratidal levees, explains their absence or small extent.
- Because large areas in the coastal plain were drowned for multiple centuries, large parts of this plain were abandoned by people.

Rhine-Meuse delta (chapters 5-8)

- Human-induced peat subsidence and wetland deforestation caused the success of the avulsion of the Hollandse IJssel and Lek rivers between ca. AD 1–300. These rivers were the first Rhine branches that fully crossed the peatland in the downstream part of the delta since several thousands of years. Human-induced increased suspended sediment supply towards the rivers and estuaries caused additional peat subsidence by loading processes in the lower delta, thereby accelerating the avulsion process. Increased sediment load also caused the natural levees to be larger along the active channels and probably facilitated avulsions by enhanced crevasse-splay progradation.
- In the upper and central parts of the delta, avulsion paths were controlled by flood-basin and natural-levee topography. While the levees along young branches grew relatively high during the first millennium AD, the flood basins and fossil levees collected a substantial clay cover causing delta-topography levelling.
- Antecedent conditions (e.g. flood-basin configuration) were an important control in the shape of natural levees. Delta-plain confinement and the presence of older alluvial ridges amplified flood levels in the upper delta generating higher natural levees. This configuration also led to efficient upstream trapping of overbank sediments yielding wide levees upstream and smaller levees downstream. The importance of flood-basin hydraulics for levee shape is further confirmed by the strong tendency for wider levees in the direction of the decreasing flood-basin slope.
- In the Roman and early-medieval periods, the alluvial ridges were densely inhabited and hosted route networks. Between AD 270 and 850, preferred settlement locations on the alluvial ridges contracted and shifted towards the higher parts of the ridges, which is attributed to increased flooding intensity during this period. These settlement shifts hardly affected the route networks, since almost all alluvial ridges remained habitable and accessible.
- Along the banks of new, steadily enlarging rivers such as the Waal (since ca. AD 450), settlements appear to have been more susceptible to regular floods. Along these branches relatively many settlements were abandoned, and the route networks were reorganised after the late-Roman period.

Pleistocene sand area (chapter 9)

- Drift-sand activity was triggered by human presence. This is evident from the peak in activity after ca. AD 900 that coincided with higher population densities, larger-scale deforestation, and a more frequent occurrence of this activity close to settlements and route corridors. Different types of land use strongly influenced the occurrence of drift-sand activity by either provoking or preventing it. For the first millennium AD no direct match was found between climatological variation and drift-sand activity.
- Drift-sand activity and its impact on people in the first millennium AD were restricted to the local scale. When overexploitation of arable fields increased in the Middle Ages, the drift-sand dune fields became larger.

10.2 The use of landscape reconstructions in studying past human-landscape interactions

Studying the interaction between people and the landscape requires an integrated analysis of the chronology of landscape changes and human activities. The landscape changes described in this



Figure 10.1 | Landscape changes in the first millennium AD in the three studied regions and their subregions discussed in this thesis. Human land-use activities in the red areas triggered most landscape changes in larger surrounding areas in the coastal plain (blue) and the Rhine-Meuse delta (green). The yellow squares indicate local drift-sand activity, locally human induced.

thesis were a product of regional variation in the interaction between external forcings, autogenic processes, and antecedent conditions (geomorphological and geological setting) that are often unexplored in local case studies. A regional-scale analysis, therefore, is necessary to study the landscape changes and their formative controls in space and time. The natural landscape changes

were reconstructed by integrating stratigraphical, geomorphological, and chronological data from accumulated and formerly fragmented data (chapter 2). This was done for the three study areas, where different approaches were used, tailored to the type of landscape and the quality and quantity of the available data. The new landscape reconstructions contain more spatial and chronological detail than previous studies, they are additionally spatially uniform, generic, and adaptable. The reconstructed timing of geomorphological changes was linked to the antecedent conditions, settlement dynamics, and known natural forcings. The relative importance and interaction of generic process rules shaping the landscape (for example peat subsides when drained) were then identified from the spatial and temporal correspondence of landscape changes to its forcings. The quality of these reconstruction-based studies heavily depends on the resolution of the underlying landscape reconstructions and on the resolution of the presumed forcings, which is discussed in this section.

10.2.1 Mapping past landscapes

The development of new tidal and river channels, and their flanking natural levees, tidal flats, and salt marshes represent the most prominent geomorphological changes in the studied coastal-deltaic plain. The abundance and quality of data (e.g. borehole data, existing maps) in the Netherlands are unprecedented compared to many other areas in the world. Therefore, the spatial extent of the end situation (mature state) of the natural levees and tidal systems is rather well-known. Their deposits form traceable clastic layers in the substrate that can be absolutely dated and correlated over large distances (chapters 2, 3, and 6). The last phases of sedimentary activity are also visible as channels or tidal or alluvial ridges in the current landscape. In the fluvial area the fossil alluvial-ridge landscape is mostly pre-Roman, except for the direct area around modern rivers. In the coastal plain, the final extent of the established late Roman to early-medieval sea ingressions also is well expressed in the current relief of the landscape. This data abundance allowed the creation of integrated landscape reconstructions with a uniform spatial coverage, based on existing fragmented information from regional studies and numerous local studies. Even in cases where age control and/or detailed stratigraphy only was available for point locations, the geomorphological expression enabled making regional reconstructions for the youngest elements, geological data allowed this for the older and buried elements. In the coastal plain mainly existing maps were used, whereas in the fluvial area high-quality borehole data were used, providing a higher spatial and chronological resolution in this area. In the sand area, the spatial extent of drift-sand dune fields was not reconstructed. Rather than a uniformly covering reconstruction, a more site-based approach was applied, especially for drift sands that occurred before the 17th century. This is because the geomorphology of the currently preserved drift-sand dune fields mostly represents the maximum state of drift-sand activity during the 17th to 19th centuries, obscuring the older phases of drift-sand activity on these locations. Moreover, drift-sand activity often only occurred on a local scale and phases of activity, therefore, often cannot be correlated over large distances.

10.2.2 Assigning ages to geomorphological elements

When assigning ages of activity to sea ingressions and channel belts, the following challenges had to be overcome: (i) uncertainty of the dating method; (ii) gaps between the date and the actual event (e.g. too old dates due to peat oxidation); (iii) diachronicity in the elements' development; and (iv) lost record due to reworking by maturing channels (i.e. non-preservation of deposits from initial channel forming stages). Combining multiple dates, allowing for a ca. 200-yr dating resolution, reduced the overall uncertainty of an elements' date. Reworking by younger channels hampered

the reconstruction of the stages of initiation and the preceding state. This especially occurred close to tidal inlets where high-energy conditions prevailed and a sandy substrate facilitated lateral channel movement. By relative dating and the use of well-dated archaeological finds from the top of the silted-up tidal system, it was nevertheless possible to identify the age of the activity of the tidal system within an uncertainty range of several centuries. Compared to the coastal area, in the river area more systematic dating had been performed, making reconstruction of channel-belt generations easier. In addition, compared to the coastal plain, reworking in the river area was much more confined to the channel belts, leaving most parts of the old landscape intact. Many peat beds used for dating tidal or fluvial initiation in the first millennium AD, however, suffer from oxidation. This hampers the reconstruction of the tidal inlets and rivers and makes further differentiation of development phases within a single river or tidal system (e.g. longitudinal trends) difficult.

For the activity of drift sands, other age issues had to be overcome. Because the natural archive of drift sands contains many hiatuses and the known dates still represent a small portion of drift-sand activity, inevitable bias will occur in the data. The best way to reconstruct geomorphological changes in this type of landscape is to use as many sites as possible to infer general trends. This can be supplemented with drift-sand dates from more continuous records (e.g. peat with datable sand pulses). Drift-sand activity on individual sites can currently be dated with a 500-yr precision when few indirect dates are available. It can be dated within several decades precision when using OSL dates (Optically Stimulated Luminescence) and/or historical references. As we compiled trends using information from ca. 140 sites and 340 dates the observed overall trends in drift-sand activity have a maximum age uncertainty of 1 to 2 centuries.

10.2.3 Inferring processes from geomorphological changes

From the reconstructions, the antecedent conditions and landscape changes were inferred. The forcings that could have driven these changes were derived from the archaeological record (indicating human activities) and independent records on floods. The spatial and temporal correspondence of these changes to the forcings was used to derive the causal relations between them (identifying processes via induction). To achieve this, geomorphological changes and the forcings that presumably caused the changes had to be placed in time as precisely as possible. Variation in sediment supply to the delta was dated within 500-yr increments by Erkens & Cohen (2009). Individual severe floods generally were dated more precisely with 30-150 yrs precision, whereas archaeology tends to be dated at 20-200 yrs precision (Toonen, 2013; Cohen et al., 2016). When archaeology was used as an indication of human pressure or reaction to landscape change in the coastal area, a chronological hiatus between the reconstructed habitation and landscape change may occur. Because landscape changes can be traced over larger distances in the geological and geomorphological record, collecting additional dates reduces this uncertainty.

In this thesis, archaeological finds were not only used to date geomorphological changes but also to determine if human activities forced geomorphological changes. To avoid circular reasoning, independent additional proof of new absolute dates and stratigraphical correlations in the data-rich study area were used. For example, archaeological finds in the coastal plain on top of peat covered by clay layers indicate reclamation activity. They were additionally used to date the peatland drowning indicated by the clay layers, assuming that peatland reclamation caused the drowning. The causal relation then had to be proven independently, for example by assessing additional evidence of the identified reclamation (rectangular in-filled tidal channels) and by using additional dates of associated materials (e.g. ^{14}C of the peat or shells inside the tidal deposits).

Other challenges in inferring geomorphological processes from reconstructions is that multiple processes can lead to similar outcomes or that local processes propagating to larger areas may be overlooked. This is partly circumvented by comparing the changes for multiple cases (rivers, tidal systems, sand areas), with well-known differing antecedent conditions and forcings. Mechanistic understanding can be further improved when more detailed case studies are added in which the results from regional studies are explicitly tested. This can be done by expanding the research area and increasing the number of cases, as well as by process-based modelling testing the sensitivity of the landscape to the forcings (see section 10.4).

10.3 Past human-landscape interactions

Landscape evolution occurred in response to different types of ‘slow forcings’ that gradually pushed the landscape into a state susceptible for geomorphological change. One of such slow forcings is autogenic behaviour (e.g. channel belt maturation, increasing levee height with time) (Stouthamer & Berendsen, 2007). These developments were overprinted by generally unintended human-induced changes through slow forcing processes such as deforestation and agricultural practices

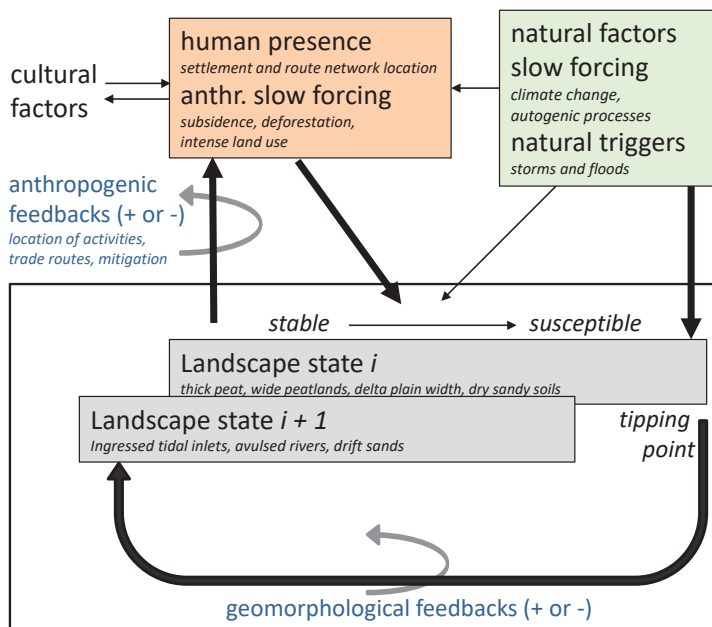


Figure 10.2 | Components of human-landscape interaction and their relations. Landscape change occurs when forcings and triggers act upon the landscape. Slow forcings can be either naturally or human-induced, they make the landscape more susceptible to triggers, pushing the landscape into a different state. The moment when this occurs is called a tipping point. After the tipping point, geomorphological feedbacks can enhance this change and the state of the landscape changes (from i to $i+1$). From this new situation the interaction starts again: the landscape change affects people in the landscape, who respond by adapting to the change or by abandoning the area. This new settlement configuration, in turn, affects where and how people influence the landscape from then onwards, leading to potential new landscape change. Examples from this thesis are in Table 10.1.

Table 10.1 | Causes, consequences, and feedbacks of geomorphological changes studied in this thesis for the coastal plain, the delta plain and the sand area. The chapters in which these are discussed are indicated in parentheses.

	Coastal plain	Delta plain	Sand area
Most important antecedent condition	presence of peatlands (4, 5).	delta plain width, flood-basin and alluvial-ridge configuration (6).	presence of dry sands (9).
Anthropogenic forcing	reclamation induced land subsidence (4, 5).	deforestation, in delta and catchment area.	deforestation, intensive land use (e.g. ploughing) (9).
Natural trigger	storm surge, spring tide (4, 9).	discharge peak (5, 6, 7).	storm (9).
Landscape change/geomorphological response	loss of land to ingression by inundation or erosion (4, 5).	more frequent flooding, river network reorganisation due to avulsion, increase natural-levee area (5, 6).	drift-sand dunes or dune fields (9).
Geomorphological feedbacks	(+) peat collapse surrounding areas, (+) subsidence by loading, (-/+ tidal channels allow sediment import for extra loading (+) and infilling (-), (-) limited by peat thickness.	(+) more sediment trapping, faster subsidence, avulsion and sea ingression, (-) reduction of flood intensity by diversion and spreading over new river branches.	(+) open landscape more susceptible to new sand drifting, (-) aeolian denudation reaches groundwater table.
Impact	large-scale abandonment of inhabited areas (4).	local shift of settlements, avulsion facilitates trade network (7,8).	local relocation of roads and settlements (9).
Anthropogenic feedbacks	(+) shifting habitation to flanking peat, (-) re-embankment decreases tidal area (4).	(+/-) shifting zones of habitation, and location of deforestation, embankment. (-) embankment.	(-) settlement shifts to less drift-sand prone areas, (-) prevention measures.

(Figure 10.2). These exerted a pressure on the landscape, initially without having a direct effect, but over time they made the landscape more susceptible until a tipping point was reached. This is the moment that the landscape shifts into a different state (from state *i* to state *i*+1 - Figure 10.2). Such a characteristic change for this period was the transformation from peatlands into tidal areas in the coastal region, as a result of progressive lowering of the land surface due to artificial drainage. Such shifts occasionally were aided by triggers (storms or floods). After which a cascade of positive feedbacks caused the landscape to shift into a new state with a new arrangement of landscape elements and habitation.

This section outlines the interplay between the antecedent conditions (geological and geomorphological setting), slow forcings, and triggers (Figure 10.2), comparing the examples from the three lowland areas treated in this thesis (Table 10.1; Figure 10.3). First, natural and anthropogenic causes (forcings and triggers) are discussed, next the focus is on geomorphological consequences and feedbacks, and finally the impact for people and the associated feedbacks are outlined.

10.3.1 Forcings, triggers, and landscape sensitivity

Slow forcings that act upon the antecedent landscape can either be naturally or anthropogenically induced (Figure 10.2). Once the slow forcing sets in, the landscape becomes more susceptible to triggers such as storms and floods (Figure 10.2). In the coastal plain, peatland reclamation and water-level lowering were slow anthropogenic forcings that caused subsidence of these areas (Figure 10.3A). This process was locally initiated since Late Iron Age (250-12 BC), but the consequences started after AD 250 as soon as the first storm surge reached this lowered peatland, eventually leading to the large-scale development of new tidal systems (chapter 4) and river courses (chapter 5).

In the coastal dune and inland drift-sand areas, deforestation and intensive land use enhanced the susceptibility to aeolian erosion by storms (chapter 9). Under Holocene climatic conditions and natural vegetation development, a bare substrate required for sand drifting can hardly be formed. The local drift-sand occurrences during the first millennium AD, therefore, must have been mainly human induced (Figure 10.3A). In contrast to the human forcings in the coastal plain and the sand area, the human-induced slow forcings in the river area were not induced in the area itself, but occurred far more upstream (Figure 10.3A), where deforestation in the catchments caused increased sediment supply towards the delta since ca. 500 BC (Erkens et al., 2011). This caused accelerated overbank deposition and stimulated avulsion, a mainly natural process that was accelerated by the human-induced increase in sediment supply (chapters 5 and 6 - Figure 10.3A).

Storms and floods regularly occur, their frequency and intensity can however change as a function of climate and catchment dynamics (natural slow forcing - Figure 10.2). Besides the human-induced changes in landscape sensitivity, more intense storms or floods may have affected geomorphological development as well. Storms were especially important for the coastal and sand areas. The stormy conditions during the Little Ice Age (LIA; AD 1570-1850) for example, probably helped to form marine incursions. The incursions, however, could only have happened because the land had already subsided and dikes were weak. Storms could also have increased drift-sand intensity, but this did not take place before the land was overexploited by humans. In the Rhine-Meuse delta, the human-enhanced increased sediment supply combined with episodes of frequent high Rhine floods between ca. AD 250 and 850 are two slow forcings that enhanced overbank deposition (chapter 6). Similar to the effect of storms in the coastal and sand areas, individual floods can serve as triggers for avulsion in the fluvial area, forming breaches in natural levees. Once this tipping point was reached and a new channel had initiated, floods often played a role in channel maturation by enlarging the channel stimulating avulsion success (Makaske et al., 2012; Cohen et al., 2016). A large flood determining avulsion success may be a second tipping point in the avulsion. Whereas large Holocene floods had been identified in the upper and central delta (Toonen et al., 2013; 2017), sedimentological records of individual floods in the lower delta and coastal plain are sparse. For tidal systems, reconstructing high water levels is especially complicated, since they strongly depend on tidal and storm dynamics. Additionally, tidal resonance effects determined by estuary and tidal-basin shape also affect flood levels. To incorporate the shape of these tidal systems, the palaeogeographical situation has to be known in a high detail.

In the three study areas, geomorphological changes took place after a period during which human influence made the landscape more susceptible to triggers (e.g. by deforestation, soil subsidence). The tipping points were caused by one of these triggers, but these were generally not the primary causes of the observed landscape changes. Although a more frequent occurrence of triggers can accelerate such processes of change, the enhanced susceptibility of the landscape was

the primary cause to become more susceptible to these triggers. In the coastal plain and delta, the first millennium AD resembles a period in which human impact was clearly large, considering the period before the embankments took place. The landscape changes were the result of slow forcings driven by human impact that were occurring already for several centuries. The landscape in the coastal area became more susceptible when reclamation started, several centuries before the actual drowning took place. In the delta, avulsion took place once in every few centuries. Sediment load increase over the preceding centuries, however, resulted in more frequent avulsion during the first millennium AD. In contrast, drift-sand intensity in the sand area was rather comparable to the preceding centuries, it occurred rather locally and probably reacted shortly after the overexploitation that caused it.

10.3.2 Geomorphological changes and feedbacks

Settlements were widely spread in the Netherlands throughout the first millennium AD, but only at distinct locations human land-use practices led to landscape change (Figure 10.3). Geomorphological change often occurred as a progressively large response to a relatively small trigger and forcing (Phillips, 2003; Verstraeten et al., 2017). Whether a change occurred and how non-linear the change was, largely depended on the geomorphological feedbacks that are characteristic for the substrate and the geomorphology of the area (Figure 10.2).

In chapter 4 it was shown that the size of a coastal-plain peatland was a dominant precondition determining the extent of sea ingressions that invaded it. After 250 BC the areal planform of tidal areas increased from 30% to 75% of the coastal-plain area, making it the largest geomorphological change (considering areal extent) that occurred in the Netherlands in the first millennium AD. The tidal area even expanded beyond the extent of the initially reclaimed and subsided areas where the sea ingressions were provoked (compare red and blue areas in Figure 10.1). Three strong positive feedbacks - linked to the geological and geomorphological setting of the area - made this transformation irreversible (chapter 4): (i) tidal incursion in the peat area caused higher water-level differences, leading to stronger flow enlarging the tidal channels; (ii) the weight of the imported sediments caused additional subsidence by loading (peat compression is limited by the thickness of the peat); (iii) flanking peatlands could collapse by drainage when the reclaimed peatlands had subsided (limited by the areal peatland extent). Initially only very high water levels reached the back-barrier, but as the tidal channels became larger, regular high-water tides could also contribute to flooding the peatlands. Sediment import initially caused further peat subsidence (positive feedback) and compensated for this process only several centuries later (negative feedback), eventually transforming the area into a totally different landscape with tidal channels, levees, and tidal flats. Besides the type of substrate, also the geomorphological setting of the area was important. Sea-ingression formation in the coastal plain was hampered by protecting back barriers in the western parts of the Netherlands and by tidal levees in the western and northern Netherlands. This explains why large sea ingressions did not develop in all back-barrier areas with wide peatlands (chapter 4).

Sea ingression occasionally caused short-cutting of drainage routes from the Pleistocene upland or hinterland rivers towards the sea. Expanding tidal channels could connect to existing streams and brooks in these areas. Examples of new tidal channels that functioned as new outlets for fluvial discharge are the Lauwers ingression in the northern coastal area (from ca. 500 AD onwards) and Honte-Westerschelde in the southwestern Netherlands (from ca. 1500 AD onwards). On a larger scale, the same happened within the Rhine-Meuse delta, where creeks of the Old Meuse estuary invaded the adjacent peatlands already in the Iron Age (800-12 BC; Vos, 2015a). The expansion of

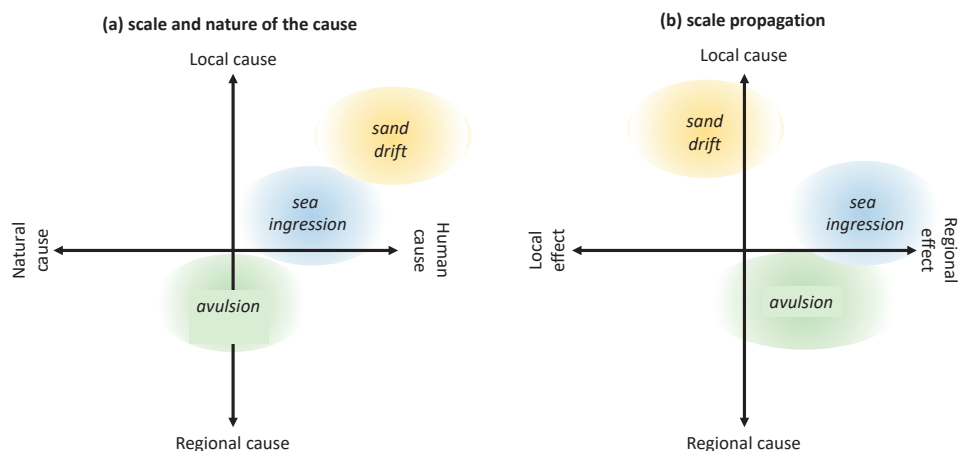


Figure 10.3 | (a) Spatial scale on which the cause of a landscape change took place and relative importance of human influence. Avulsion was controlled by local levee and flood-basin topography as well as by upstream sediment supply and flood regime. Sea ingressions and drift sands were more locally induced. Avulsion was a relatively natural process that was partly stimulated by human activity. Sea ingressions and especially drift sands, on the other hand, were to a larger degree human-induced. (b) Scale of the geomorphological effects and causes of landscape changes. Drift sands were locally induced, and mostly only expanded to much larger areas after AD 1500. Avulsion had a moderately large impact on the delta: it redistributed water and sediment to a distinct part within the delta. Sea ingression had the largest effect, transforming the largest part of the coastal plain from peatlands into a tidal landscape.

the Old Meuse estuary, at least from late Iron Age onwards, is due to peatland reclamation, causing the success of the avulsions of the Hollandse IJssel (after AD 1), and the Lek (after AD 300) (chapter 5). The positive feedbacks owing to peat substrate and tidal activity described above were similar to those occurring in other parts of the coastal plain. However, avulsion was further stimulated by the human-enhanced sediment supply from upstream, causing the crevasse splays to prograde faster and facilitating the sediment-loading feedback in the peat area. Additionally, deforestation in the lower delta reduced the hydraulic roughness and caused the tidal wave to propagate further inland. These human-influenced factors made that the new rivers gained energy advantage over the old courses, leading to avulsion success of these lower-delta rivers. In the central and upper delta, alluvial ridge and floodplain morphology determined the position of new river branches (chapter 6). The Waal course in the central part was one of these that formed after AD 450 in a relatively low part of the delta (chapters 6 and 7). The development of the new river branches caused the Oude Rijn, which had been the main Rhine branch in the delta until the first millennium AD, to gradually silt up (Van Dinter et al., 2017).

Unlike sea ingressions in the coastal plain, avulsions did not transform the delta into a totally different landscape (Figure 10.3B). Still, avulsions reorganised the delta network, for example by annexation of new areas and connecting these to the Rhine-Meuse delta (e.g. the Lek/Hollandse IJssel and Gelderse IJssel; Stouthamer & Berendsen, 2000; Cohen et al., 2009; chapter 5), thereby

affecting the distribution of sediment through the delta. Along the new river branches, levees developed, and the total area of natural levees increased by ca. 5% during the first millennium AD (chapter 6). Especially these young levees built up relatively high, whereas the topographical expression of more distal-inherited natural levees gradually reduced. A distal downstream effect of the lower delta avulsions is that they routed more sediments towards the Meuse estuary and the southwestern coastal plain. The increased supply of sediments probably accelerated the infilling of the tidal systems to a supra-tidal level suited for habitation (chapter 4).

Geomorphological changes in the Pleistocene sand area (Figure 10.1) were small before human influence started. The sandy substrate, however, became susceptible to aeolian erosion when deforestation and overexploitation took place (chapter 9). In the first millennium AD, drift-sand activity mainly occurred locally and shortly (Figure 10.3B). As in the fluvial and coastal areas, positive feedbacks enhanced sand drifting in the Pleistocene sand area. Once a large storm had caused a part of the sands to be laid bare, these parts were more susceptible to the next storm, a process that finally resulted in the formation of large, active dune fields. This feedback was especially effective when the storm frequencies increased and vegetation was less well recovered. The drift-sand activity became irreversible when the spatial extent of drift-sands after 1500 AD increased, reaching a climax in the 19th century (Koster, 2009). Compared to the surface affected by sea ingressions and new river branches, however, these dune fields were still relatively small (i.e. not larger than several square kilometres).

In summary, both substrate and surrounding geomorphology controlled the extent in which geomorphological feedbacks occurred in the coastal, fluvial, and sand areas. Anthropogenic slow forcings could start locally, as was the case with soil subsidence of peatlands after reclamation, and later spread regionally via non-linear response and feedback mechanisms. Sea ingressions in the coastal plain had the largest effect on the landscape during the studied period, avulsion had a moderate effect on delta evolution, and sand drifting occurred on a relatively small scale.

10.3.3 Impact of landscape changes on inhabitants and anthropogenic feedbacks

When the impact of landscape changes on humans is expressed as settlement shifts, it becomes clear that the impact of landscape change on its inhabitants generally was proportional to the area over which the change took place. Some changes had a negative effect on habitation or on the accessibility of the landscape, whereas others had a positive effect (Figure 10.2).

The formation of new tidal inlets and systems into a former freshwater peat swamp transformed this landscape into a brackish tidal area, which had major implications for the ecosystems and population in this area. In the southwestern coastal plain people lived on such drowning peatlands. Not only the former peat area was abandoned, but also the flanking coastal dune areas that probably became more isolated. Filling in the newly-formed tidal areas to a level suitable for habitation took several centuries depending on the surface size of the inundated area, sediment supply, and subsidence feedbacks (chapter 4). In the northern coastal plain large supratidal areas were situated, to which the human population was mainly confined (living on dwelling mounds). Therefore the direct impact of sea ingressions was much smaller in these areas. However, the drowning of the flanking peatlands may have hampered their accessibility, obstructing the connection between the northern coastal plain and the northern sand area. Avulsions in the delta redistributed flood water, directing larger water volumes to new river channels with less mature natural levees. This caused more frequent inundation of the surrounding fossil levees, a mechanism explaining the early-medieval abandonment of settlements close to the young Waal (chapter 7).

Landscape changes could have accelerated already ongoing cultural changes (political and economical factors). In the second half of the 3rd century depopulation in the Netherlands started, coeval with the abandonment of the Roman Rhine-based frontier, the *limes*. This was most likely strongly influenced by political developments, but it is clear that the impact of floods also changed the habitation conditions in the delta at that time. A period of intense floods occurred between AD 250 and 850, which must have influenced habitable areas and at least caused local-settlement shifts to somewhat higher parts of alluvial ridges in most parts of the delta. Evidence of settlement abandonment on entire alluvial ridges after the most severe of these floods, which occurred around AD 260/280, 680, and 780 (Cohen et al., 2016), is restricted to the inherited alluvial ridges near large rivers. Most alluvial ridges remained in use as route-network corridors throughout the first millennium AD (chapter 8), indicating that overall people seem to have been rather resilient to floods and changes in the landscape.

A positive economic effect of the formation of new tidal and fluvial channels was the formation of potential trade routes over water (Figure 1.3B). From the southwestern part of the coastal plain towards the Meuse estuary new channels were formed. The Lek and Hollandse IJssel provided new route connections that later (after the 7th century) provided the early-medieval city of Dorestad in the central Netherlands with suitable (long-distance) transport options fundamental to its development. The expanding Vlie inlet and Almere lagoon and the formation of the Gelderse IJssel (since the 7th century) connected the upstream part of the delta to the northwestern and northern coastal plain. Along the new Gelderse IJssel after ca. AD 800 cities such as Zutphen and Deventer emerged (e.g. Groothedde, 2013).

Landscape impact in the sand area was relatively small; local communities seem to have easily dealt with drift sands by the local communities. This process did not clearly affect the landscape and its inhabitants before the Late Middle Ages (AD 1050-1500). In the sand areas, any changes in settlement patterns therefore most likely were mainly culturally induced. Only after ca. AD 1500 onwards, drift-sand activity became a supra-local phenomenon since extensive drift-sand dune fields developed, making larger areas unsuitable for land use and transport. The way in which these landscape changes were managed by humans differs from other areas. In the sand areas, relatively small adaptations in land use could already prevent sand drifting (i.e. maintaining small hedges). Such mitigation was for example more difficult in the coastal plain peat areas, where subsidence generally occurred on a scale too large to perform effective measures.

In short, the impact of landscape changes on people depended on the scale, irreversibility, and recovery time of the geomorphological system. Large-scale sea ingressions in the coastal plain caused large-scale abandonment of settlements. In the fluvial area, settlements modestly shifted after avulsions and changing flooding frequencies. In the sand area no settlement shifts can be linked to drift-sand activity.

10.4 Applications and outlook

Human-affected landscape changes not only occurred in the past, they also take place today in many other lowland areas (e.g. Syvitski & Saito, 2007). Most currently-drowning coastal plains have in common that rapid human-induced transgression (Törnqvist et al., 2008; Syvitski et al., 2009) has resulted in sea ingressions with comparable feedback mechanisms to those presented here. In the landscape changes described in this study the system is pushed into a new state, causing effects that can be better mitigated or restored when the involved processes are well understood.

The conditions (e.g. climate, substrate, tidal regime, ecology), extent, and initiation of human impact may be different for these areas. But still the generic processes, mechanisms, and feedbacks inferred from this study can be used to better understand comparable non-linear geomorphological responses and their impact on humans in ancient, current, and future comparable lowland landscapes. To transfer the insights from the Netherlands to other areas, the roles of region-specific antecedent conditions, forcings, and cultural factors have to be identified, separated, and quantified as much as possible as demonstrated in this thesis. When the contributions and interactions of these components are better understood, the results from this region can be applied for realistic scenarios for other areas, as the nature laws that operate within these boundaries are universal.

Besides generic knowledge, the new and more detailed reconstructions in this thesis can serve geological and geomorphological mapping projects within the Netherlands (e.g. Koomen & Maas, 2004; Van der Meulen et al., 2013), geoarchaeological prospection maps (e.g. Cohen et al., 2017ab; Rensink et al., 2016), and vegetation reconstruction maps (Van Beek et al., 2015a). The planform geometry, stratigraphy, and age of the geomorphological elements stored in the reconstructions can refine these datasets. The results of this thesis can help answer questions on the surrounding environment of site-specific geoarchaeological studies, a topic that is not always directly studied in archaeology. This will help to solve research questions such as: Are land-use changes and settlement dynamics driven by external natural or cultural factors, or by internal factors? Why do similar land-use practices lead to different geomorphological responses in other areas? Why are certain coastal and delta areas more affected by floods than others? How do delta-wide floods affect water-related infrastructural works such as harbours, quays, and revetments before river embankment? Such questions cannot be answered with local studies only, therefore comparative studies with a regional scope are necessary.

To further refine the reconstructed human-landscape interactions and to better compare them to other areas in the world, the following topics deserve attention: (i) chronology of identified landscape changes and their forcings and triggers – The landscape reconstructions presented in this thesis will improve when new dates and site descriptions (e.g. on facies and stratigraphy) are incorporated. To achieve this, the reconstructions have to be continuously synchronised with newly-available data from fragmented studies. In this manner, the reconstructions will remain ‘state of the art’ and therefore usable within applied and academic research. The processes driving landscape changes can be better understood when the timing, frequency, and magnitude of the forcings and triggers is further refined. Crucial information on storm and flood chronology can be inferred from sedimentological records of flood layers in residual channels, lagoons or on clay drapes covering well-dated settlements. Especially for the lower delta plain and many parts of the coastal plain this type of data is currently sparse. If suitable material for dating (organic materials or sand layers) is found in these records, flood and storm events can be dated absolutely. For the most recent 10 to 12 centuries historical written sources are available, which supplement the geomorphological data allowing for better and chronologically more detailed inferences of landscape changes and their forcings (e.g. Toonen et al., 2015). Combining geomorphological and historical sources also is useful assessing storm events in time and space in the sand area, since independent sedimentological records on storms in this area are sparse.

(ii) understanding geomorphological processes – For deepening our understanding of coastal evolution on a 1000-yr time scale, more in-depth studies are needed on the role of tidal activity, sediment supply, and climate change. This can be realised in several complementary ways: (a) performing detailed sedimentological studies of individual tidal systems and channel belts to refine the reconstruction of their evolution and to investigate the connection to identified forcings.

In this way, pulses of overbank and tidal deposition can be better linked to regional events (e.g. already identified floods) and local effects (e.g. proximity and geometry of a channel). The regional landscape reconstructions presented in this thesis will be useful to select suitable sites. They will also help to put the results from the local studies into a regional context. (b) When the regional reconstructions are spatially up-scaled to adjacent coastal plains in Germany and Belgium, more data on cases of tidal systems will become available. These can be used to better assess the role of human pressure, antecedent conditions, ecology, and varying strengths of forcings (e.g. more variation in tidal amplitudes) in landscape evolution. When a larger time span is studied, the effect of human activity on the landscape could be further explored. This can be done by comparing the results for the first millennium AD to earlier periods characterised by less human impact and to more recent historical periods with increased human impact. (c) The processes inferred from comparing observed landscape changes to natural and human forcings could be tested using numerical models. This approach allows for isolating individual forcings to further test their relative importance (e.g. Karssenberg & Bridge, 2008; Hajek & Wolinsky, 2012). Detailed geomorphological reconstructions of past tidal-basin morphology can serve as input for models that reconstruct water levels using tidal-wave propagation rules. From their output the implications of water-level changes for habitation as a function of tidal basin geometry can be assessed. A similar approach can be followed in the delta using flood modelling, where past morphology is much better known than in the coastal plain.

Iteratively combining local and more regional overview studies will allow for further assessment of geomorphological processes that interact between both scale levels. Besides integrating studies from different scales, further integration of geoscientific, archaeological, ecological, and historical data and approaches on landscape changes as performed in this thesis will improve the understanding of human-landscape interactions. Such integrated approaches will be key to better understand the role of humans in landscape changes and their adaptations to it. This is the case for human-landscape interactions in the past as well as in the future, for all areas where human pressure on the landscape is increasing.

Summary

Problem definition and aims

Lowland areas have been shaped by the interplay of fluvial, marine, biotic, and aeolian processes. Because many lowlands nowadays are densely populated, many people at present make use of their natural resources and depend on flooding safety. Already for millennia, humans have affected the landscape in such areas, among others through deforestation and reclamation for agricultural practices. In the Netherlands, the first millennium AD represents a transition period from a mainly natural prehistorical lowland landscape that was increasingly influenced by people towards a mainly human-dominated landscape from the High Middle Ages (ca. AD 1050) onwards.

This thesis focusses on the reconstruction of human-landscape interactions in the Netherlands during first millennium AD by performing the following steps: 1) identify the changes in natural landscape evolution; 2) unravel the natural and anthropogenic causal factors, and the geomorphological feedback mechanisms underlying these geomorphological changes; 3) evaluate the effect and impact of these changes on humans.

Human-landscape interactions were studied for three research areas within the present-day Netherlands: the coastal area, the fluvial area, and the Pleistocene sand area. These areas have distinct physical characteristics and therefore the sensitivity of their landscapes to human influence varied, because they each were shaped and affected by different geomorphological processes (e.g. peat subsidence or aeolian sand erosion). An integrative approach was used in which data and methods from the disciplines of physical geography and archaeology were combined. To identify landscape changes, map datasets were integrated into geomorphological reconstruction maps of the physical landscape that show the former extent of mainly geomorphological elements (channels, supratidal ridges, alluvial ridges etc.). By spatially and temporally comparing observed geomorphological changes to varying forcings and the archaeological record, the causes and effects of these changes were assessed. The study was performed on a regional scale, to allow for the comparison of the geomorphological evolution of different rivers, sand areas, and tidal systems that resulted from varying human and natural induced forcings.

In the well-studied Netherlands' coastal plain and Rhine-Meuse delta, many datasets on the extent, age, and sequential development of Holocene geological and geomorphological elements are available, including soil maps, geological, geomorphological maps, and many local studies. These were developed within various research traditions and were an important input for the new reconstructions, because they contain information on the spatial outline, age, and stratigraphy of landscape units. However, the overwhelming quantities and heterogeneous nature of these data have caused much information to remain inconsistent and fragmented. Combining information from digital maps using their full potential, requires awareness of the original focus, scale, surveying strategy, and state of knowledge at the time of the original research. To this end, chapter 2 reviews the range of mapping traditions behind the datasets that were combined into the geomorphological and palaeogeographical reconstructions presented in this thesis.

Human-landscape interaction in the coastal plain

In chapter 3 a GIS is presented that incorporates the accumulated data of the Netherlands' coastal plain reviewed in chapter 2. The GIS stores redigitised architectural elements (beach barriers, tidal channels, intertidal flats, supratidal flats, and coastal freshwater peat) from earlier mappings in separate map layers. A coupled catalogue-style database stores the dating information of these

elements. Using scripts, the system automatically generates palaeogeographical maps for any chosen past time slice, combining the earlier mapping and dating information. This enables a workflow in which the maker can regenerate maps iteratively, which speeds up the fine-tuning and thus the quality of palaeogeographical reconstruction. In chapter 4 this GIS is used to demonstrate the decisive role of antecedent conditions on the formation of large late-Holocene sea ingressions in the peaty coastal plain. These ingressions (expansion of new tidal systems) were mainly caused by land subsidence, which in the coastal plain occurred due to intensified agricultural use of artificially-drained peatlands since the last centuries BC. As a result, the coastal plain became sensitive to storm-surge ingression through weak spots in the coastline, e.g. at the location of existing creeks. Using the Netherlands as a case study, we show that antecedent conditions (i.e. the geological setting at the time of ingression) played a key role in the pacing and extent of tidal-area expansion. Ingressive tidal systems eventually reached furthest inland in coastal segments with wide peaty back-barrier plains. In contrast, sea-ingression formation was hampered in coastal segments with well-developed natural ingression-protecting geomorphic features (e.g. beach-barriers, supratidal levees). These combined effects caused sea ingression over large areas that consequently became unsuitable for habitation for many centuries. Human-induced peat-land subsidence additionally caused a major reorganization of the river network of the lower Rhine-Meuse delta in the first millennium AD. The Hollandse IJssel and Lek river branches invaded extensive peatlands, thus rerouting a major part of the Rhine discharge and sediments towards the Meuse-estuary tidal inlet. Chapter 5 outlines the role of human activities in connecting marine ingressions and fluvial crevasse channels, through reclamation-induced peat-land subsidence and enhanced sediment load. Feedback mechanisms, such as additional peat subsidence by loading of sediment imported into the new tidal area, caused further tidal prism increase and created accommodation space for tidal deposits.

Human-landscape interaction in the Rhine-Meuse delta

In chapter 6 the controls on natural levee development were identified in the Rhine-Meuse delta during the first millennium AD. From detailed levee reconstructions we quantified natural-levee dimensions, and evaluated the temporal changes therein. These developments were then linked to external forcings (increasing suspended-sediment load, variable flooding intensity, riparian deforestation) and to inherited intrinsic geographical controls (delta-plain width, compartmentalization). These new detailed geomorphological reconstructions were based on the existing datasets presented in chapter 2, as well as on LiDAR data and large amounts of lithological borehole data. Natural levees in the upper delta were relatively high: 1–2 m above distal flood basin groundwater levels. This is due to the relatively confined floodplain width in this delta segment, which increased hydraulic resistance to floodwaters, causing them to be relatively raised. Natural levees in the central to lower delta parts showed a considerable decrease in width. This is explained by a downstream depletion of suspended load carried in the channel at flood stage, most likely aided by differences in riparian vegetation density and the presence of many enclosed flood basins upstream (i.e. abundant channel belts). The youngest natural levees, formed along new channels that matured during the first millennium AD, have local crest heights that are 0.5 to 1.0 m above their preceding levee generations. This is attributed to the more abundant suspended sediment supply and increased flooding intensity during their formation. Alluvial-ridge areas with older levee relief along abandoned channels clearly affected the paths of the new avulsed channels. Avulsions led to the formation of new levee complexes along the river over a considerable area in former flood

basins. Meanwhile, the topographical expression of inherited alluvial ridges gradually reduced due to widespread flood-basin trapping of overbank sediment, causing topographic levelling.

In chapter 7 the impact of the natural-landscape dynamics described in chapter 6 on the settlement distribution within the fluvial area is discussed. During this time interval, major landscape and cultural changes occurred in this area, with river avulsions and changes in flooding frequency coinciding with changing settlement patterns. In the delta plain, the relatively high and dry alluvial ridges of abandoned or active rivers were most favourable for habitation. Settlement location and elevation patterns were reconstructed in these landscape units using the high-resolution elevation map of the alluvial ridges introduced in chapter 6. By integrating high-resolution palaeo-environmental and archaeological datasets for this period, we were able to spatially analyse the trends and to assess the effect of environmental changes on habitation. Results show that settlements progressively shifted towards higher areas between AD 250 and 750, on average by 20 cm over this period delta wide, which was coeval with an increased frequency of severe Rhine floods. The observed spatial differences demonstrate that this trend is most obvious in the least-elevated segments of the study area. In areas where new large river branches developed, settlements show a strong shift towards higher-elevated parts of the landscape or even became completely abandoned. Probably, flooding occurred more frequently and was more severe in these areas. Despite the clear link between changing settlement positions and floods during the studied time interval, floods do not seem to have caused long-term abandonment of major parts of the study area. In chapter 8 network-friction maps and route networks were modelled based on the geomorphological and archaeological datasets presented in chapters 6 and 7 respectively. Past route networks were influenced by both cultural and natural dynamics and are therefore a useful source of information to increase understanding of the complex interaction between these dynamics. Despite the dynamic nature of the research area, the reconstructed routes show clear signs of network stability. This demonstrates that large parts of the Rhine-Meuse delta were persistently occupied during the Roman period and Early Middle Ages despite local settlement dynamics and changing natural settings.

Human-landscape interaction in the Pleistocene sand area

In chapter 9 human-landscape interactions are discussed for the Pleistocene sand area. Here, drift-sand occurrence was a significant geomorphological activity during the last millennia. This locally caused the formation of large active dune fields causing part of the land to become useless. In order to better assess the causes we compared the spatial and temporal patterns of drift-sand occurrence, we compiled a new supra-regional overview of dates related to drift-sand activity. These were compared to available information on soil properties, historical-route networks, vegetation, and past climate. Results indicate a constant but low aeolian activity between 1000 BC and AD 1000, interrupted by a remarkable decrease in aeolian activity around the BC/AD transition. It is evident that sand drifting was strongly related to human pressure on the landscape, since it occurred most frequently close to routes and increased uninterruptedly from AD 900 onwards, coeval with rising population density and large-scale deforestation.

Concluding remarks

In all studied landscapes, human preconditioning of the landscape played an important role in its evolution. After a period during which human activities had made the landscape more vulnerable (e.g. through deforestation or soil subsidence) to natural geomorphological processes, unintended geomorphological changes took place, such as sea ingressions, avulsion, and sand drifting. The

tipping points concurred with natural triggers, such as storms and floods, but these were not the primary causes behind the observed landscape changes. Although a more frequent occurrence of triggers could have accelerated the processes, the more sensitive state of the landscape was a prerequisite for these changes.

Human impact on the landscape could start locally, such as the occurrence of soil subsidence of peatlands after reclamation, and later could spread regionally via non-linear response and feedback mechanisms. The scale on which geomorphological changes occurred was co-controlled by the substrate of the area and its surrounding geomorphology. This determined the sensitivity of the landscape to human influence and the strength of geomorphological feedbacks (e.g. peat subsidence feedbacks). Sea ingressions in the coastal plain had the largest effect in the studied period, transforming major peatlands into tidal areas. Avulsion had a moderate effect on delta evolution, rearranging the delta network and building new alluvial ridges. Sand drifting only occurred on a relatively small scale. The impact of landscape changes on people depended on the scale and irreversibility of the change, and on the recovery time of the landscape after the change. The sea ingressions in the coastal-plain peatlands caused large-scale abandonment. In the fluvial area modest settlement shifts were observed in reaction to wetter conditions. In the sand area in general no major shifts of settlements can be linked to changes in the landscape during this period.

This study provides more insights in the circumstances under which impact of human action on the landscape was largest. Better understanding of human impact on the natural landscape in the past is especially relevant to better cope with threats from floods or sea-level rise, especially in densely populated and subsiding deltas. The regional, integrative approach on studying human-landscape interaction performed in this thesis can be expanded by adding results from more detailed case studies and by extending the approach to adjacent areas in Belgium and Germany. Such studies can either involve further refining the timing of forcings (e.g. storms episodes, human land-use practices) and geomorphological responses, or testing the sensitivity of the landscape using processes-based models. Iterative integration between local and regional scale processes, while combining multiple disciplines, will further improve the understanding of human-landscape interaction.

Samenvatting

Probleemstelling en doel van het onderzoek

Laaglandgebieden worden gevormd door het samenspel tussen rivieren, zee, wind en biologische processen. Deze gebieden zijn veelal dichtbevolkt vanwege hun voedselrijkdom en transportmogelijkheden zowel over water als over land. Ze zijn echter ook gevoelig voor overstromingen, wat implicaties heeft voor de veiligheid van de bewoners. Al sinds duizenden jaren wonen mensen in dergelijke landschappen en beïnvloedden ze ook hun ontwikkeling, onder andere door ontbossing en ontginningen voor de landbouw. In Nederland is het eerste millennium na Christus (Romeinse tijd en Vroege Middeleeuwen) een overgangperiode waarin een overwegend natuurlijk laaglandlandschap omvormde naar een steeds meer door mensen beïnvloed landschap. In de hierop volgende periode, de Hoge Middeleeuwen (vanaf ca. 1050 na Chr.), begon de mens steeds meer de dominante landschapsvormende factor te worden, vooral door grootschalige bedijkingen, inpolderingen en ontginningen. De impact en timing van de menselijke invloed verschilde echter sterk voor verschillende plekken in Nederland in het eerste millennium.

Dit proefschrift richt zich op de interactie tussen de mens en het landschap in Nederland tijdens het eerste millennium na Christus. Dit is een periode waaruit al veel bekend is over de ontwikkeling van het landschap en de mens, maar nog weinig over hun samenspel. Met andere woorden: hoe belangrijk was de mens in de ontwikkeling van het landschap en wat was de invloed van landschapsontwikkelingen op de mens? Om deze vragen te beantwoorden zijn de volgende stappen gevolgd: 1) het identificeren van de veranderingen in het natuurlijke landschap; 2) het ontrafelen van de natuurlijke en door de mens gestuurde oorzaken hierachter en het beschrijven van de natuurlijke terugkoppelingseffecten die hierop volgden; 3) het evalueren van de effecten van deze veranderingen op de mens.

De mens-landschapsinteracties zijn bestudeerd in drie onderzoeksgebieden in Nederland: de kustvlakte, de Rijn-Maas delta en het Pleistocene zandgebied. Deze gebieden hebben elk een typische ondergrond (bv. zand of veen) en verschillende landvormen (ruggen of vlaktes) waardoor hun gevoeligheid voor menselijk ingrijpen varieerde. Er is een geïntegreerde aanpak gevolgd waarbij gegevens en werkwijzen vanuit de fysische geografie en archeologie zijn gecombineerd. Om de landschapsveranderingen te identificeren zijn in dit proefschrift verschillende bestaande gegevens gecombineerd tot nieuwe landschapsreconstructies (paleogeografische kaarten) die de verbreiding en ontwikkeling van verschillende landschapseenheden (veengebieden, geulen, kwelders, ruggen, etc.) door de tijd weergeven. Door de landschapsveranderingen zowel in de tijd als in de ruimte te vergelijken met wisselende forceringen en archeologische vondsten, konden de oorzaken en gevolgen van de landschapsveranderingen worden afgeleid. Het onderzoek is op een regionale schaal verricht om de ontwikkelingen van verschillende rivieren, getijsystemen en zandgebieden onderling goed te kunnen vergelijken.

Nederland kent een rijke onderzoekstraditie van de bodem en ondergrond. De afgelopen decennia zijn er vele lokale studies en kaartseries verschenen waar nuttige informatie over de verbreiding, ouderdom en opeenvolging van diverse landschapseenheden in verwerkt zit. Deze studies zijn verricht vanuit onderzoekstradities waarbij op één of enkele aspecten van de ondergrond en het landschap de nadruk werd gelegd en een geïntegreerd overzicht vaak ontbreekt. De grote hoeveelheid kaarten, bijbehorende rapporten en achterliggende gegevens zijn ook niet altijd geheel consistent, vaak gefragmenteerd of alleen beschikbaar voor kleinere deelgebieden. Om deze gegevens goed te kunnen combineren is daarom bewustzijn nodig van de oorspronkelijke

focus, het doel, de onderzoeksstrategie en de staat van kennis op het moment van uitvoeren van het originele onderzoek. Daarom wordt eerst een overzicht gegeven van de onderzoekstradities achter de gebruikte gegevens in hoofdstuk 2, voordat deze tot de paleogeografische en geomorfologische kaarten in dit proefschrift gecombineerd zijn.

Mens-landschapsinteractie in de kustvlakte

In hoofdstuk 3 wordt een nieuw Geografisch Informatie Systeem (GIS) gepresenteerd. Hierin zijn de kaartbeelden en de achterliggende kennis over landschapsontwikkeling in de Nederlandse kustvlakte uit hoofdstuk 2 voor het eerst consistent samengebracht. In het GIS zijn gedigitaliseerde landschapselementen in de kustvlakte (strandwallen, getijgeulen, wadden en kwelders) uit eerdere karteringen opgeslagen en voorzien van informatie over hun ouderdom en ontstaanswijze. Het GIS kan informatie over de ruimtelijke verspreiding en ouderdom van gekarteerde landschapselementen aan elkaar koppelen om zo automatisch gegenereerde paleogeografische kaarten voor iedere gewenste tijdstap te produceren. Deze methode maakt de werkwijze transparant en reproduceerbaar en versnelt het proces van karteren. Dit maakt het mogelijk om snel afwijkingen in het kaartbeeld en in de brondata op te sporen en op te lossen.

De gegenereerde kaarten zijn vervolgens gebruikt in hoofdstuk 4 om de geomorfologische ontwikkeling van de kustvlakte te bestuderen. In de bestudeerde periode vonden er grootschalige zee-inbraken plaats in uitgestrekte veengebieden door toedoen van de mens. Door ontginningen van het veengebied sinds de late IJzertijd (250-12 voor Chr.) vond grootschalige bodemdaling plaats. Hierdoor werden grote delen van het veengebied direct achter de kustlijn gevoelig voor zee-inbraken volgend op stormen, waardoor het getijgebied op sommige plekken aanzienlijk kon uitbreiden. Dit leidde tot verdrinking van grote delen in het kustgebied (met name in Zeeland, maar ook in noord Nederland) die hierdoor voor enkele eeuwen onbewoonbaar werden. In dit hoofdstuk wordt aangetoond dat de landschappelijke uitgangssituatie van doorslaggevend belang is voor de schaal waarop de zee-inbraken zich voordeden. De inbraken waren het meest verbreid waar de veengebieden groot waren en waar de strandwallen en kwelderwallen het zwakst waren of het minst ontwikkeld.

In hoofdstuk 5 wordt aangetoond dat de door de mens veroorzaakte zee-inbraken ook voor riviervleggingen in het benedenstroomse deel van de Rijn-Maas delta zorgden. De Rijntakken Hollandse IJssel en Lek doorbraken een groot veengebied waardoor vanuit de Rijn, afvoer richting het Maasestuarium geleid werd. Dit zorgde voor een veranderende afwatering in de gehele delta. Ontginningsactiviteiten in de benedenloop van deze rivieren speelden een doorslaggevende rol in deze riviervleggingen, naast de toegenomen sedimentlast vanaf bovenstroomse gebieden. Overal waar zee-inbraken en nieuwe riviertakken in het veen ontstonden traden terugkoppelingen in werking die het proces versterkten. Een voorbeeld hiervan is de extra veendaling die optrad door het extra gewicht van riviersediment in het veengebied, naarmate de geulen groter werden en meer sediment konden aanvoeren.

Mens-landschapsinteractie in de Rijn-Maas delta

In hoofdstuk 6 worden de factoren beschreven die de oeverwallen in de Rijn-Maasdelta hebben gevormd. Oeverwallen zijn hoger gelegen elementen in het landschap die tijdens overstromingen worden gevormd op de overgang van de rivier naar de lager gelegen komgebieden. Daarom zijn ze belangrijk voor zowel de ontwikkeling van het rivierengebied als voor de mensen die er wonen. Om de vormen en de ontwikkeling van deze oeverwallen te beschrijven is gebruik gemaakt van nieuw ontwikkelde gedetailleerde reconstructies van het landschap. Deze ontwikkelingen zijn

vervolgens gelinkt aan veranderende overstromingen en sedimentlast en aan verschillen in vegetatie en de overgeërfde landschappelijke situatie (geometrie van de delta, vorm van het reeds aanwezige oeverlandschap). De landschapsreconstructies ontwikkeld in dit hoofdstuk zijn grotendeels gebaseerd op een uitgebreide database met boorbeschrijvingen, gedetailleerde hoogtebeelden en bestaande datasets besproken in hoofdstuk 2. De reconstructies laten zien dat oeverwallen in het bovenstroomse deel van de delta relatief hoog zijn. Dit is het gevolg van het opgestuwde waterniveau door de vernauwing van de delta op deze plek, waardoor tijdens overstromingen de oevers hoger opgebouwd kunnen worden. In de nieuwe landschapsreconstructies is ook te zien dat de breedte van oeverwallen afneemt in benedenstroomse richting. Dit wordt toegeschreven aan de afname van fijn sediment (klei en silt) in het overstromingswater in benedenstroomse richting omdat dit bovenstrooms relatief efficiënt ingevangen wordt. Daarnaast spelen verschillen in vegetatiedichtheid en grootte van de komgebieden hierin vermoedelijk een rol. De jongste oevers (gevormd in het 1e millennium na Chr.) hebben relatief hoge delen omdat ze gevormd zijn in een periode met veel sedimentaanvoer en relatief veel grote overstromingen. Grote oeverwalcomplexen die al in het landschap aanwezig waren vormden een belangrijk obstakel en bepaalden zo de ligging van nieuwe rivierlopen, zoals bijvoorbeeld de Nederrijn vlak voor het begin van de jaartelling en de Waal rond 450 na Chr. Deze nieuwe rivierlopen zorgden op hun beurt weer voor de vorming van hoge oeverwallen op geheel nieuwe plekken in de delta. Ondertussen werd tijdens overstromingen vooral klei afgezet op de lage delen van de oude oeverwallen. Hierdoor werd het reliëf in deze verder van de actieve rivier afgelegen gebieden minder uitgesproken.

In hoofdstuk 7 wordt ingegaan op de gevolgen van de landschapsveranderingen in het rivierengebied voor de mens. Tijdens de onderzochte periode vonden er naast riviervleggingen en toegenomen overstromingen ook grote culturele veranderingen plaats. Dit had gevolgen voor de mensen die op de hoger gelegen oeverwallen woonden, dit is o.a. te zien in de verschuivingen van nederzettingen die optraden in het rivierengebied. In dit hoofdstuk worden archeologische gegevens gecombineerd met gegevens over landschapsontwikkeling, waarbij we focussen op het verschuiven van de nederzettingen in het landschap. Hierbij is gebruik gemaakt van de reliëfreconstructie van de bewoonde oeverwallen uit hoofdstuk 6. Het blijkt dat nederzettingen in de gehele delta langzaam verplaatsen naar hoger gelegen delen tussen 250 na Chr en 750 na Chr., tegelijk met een geregistreerde toename in de intensiteit van overstromingen. Deze trend is het sterkst te zien in de lagere delen van de delta. Ook in de directe nabijheid van plekken waar nieuwe riviertakken ontwikkelden (met name de Waal) is duidelijk te zien dat nederzettingen verplaatsen en dat er zones geheel verlaten raakten. Zeer waarschijnlijk zorgden deze nieuwe riviertakken voor het vaker overstromen van gebieden die eerst verder van de hoofdtakken af lagen.

In hoofdstuk 8 worden routenetwerken en verplaatsingscorridors gereconstrueerd in de delta gebaseerd op de geomorfologie en de nederzettingslocaties uit hoofdstuk 6 en 7. Omdat deze verbindingszones afhangen van zowel het landschap als culturele factoren vormen ze een interessante schakel om de mens-landschapsinteractie te onderzoeken. Ondanks de in hoofdstuk 7 aangetoonde link tussen nederzettingsverplaatsing en overstromingen lijkt het er niet op dat grote delen echt verlaten zijn geraakt en bleven de grootschalige verbindingszones vrijwel allemaal intact. Dit toont aan dat de meeste plekken in de delta bewoond bleven tijdens de Romeinse tijd en de Vroege Middeleeuwen en suggereert dat er hooguit aanpassingen hebben plaatsgevonden om de veranderingen het hoofd te bieden.

Mens-landschapsinteractie in het Pleistocene zandgebied

In hoofdstuk 9 wordt de mens-landschapsinteractie in het zandgebied besproken, waar met name het optreden van stuifzand een belangrijke landschapontwikkeling was. Op bepaalde plekken in het landschap konden er zelfs grote aaneengesloten duingebieden ontstaan die ervoor zorgden dat delen van het landschap onbruikbaar werden. Om de oorzaken achter het stuiven beter te kunnen achterhalen is een nieuw overzicht gemaakt van alle bekende aanwijzingen van stuifzandactiviteit op nationale schaal uit overzichtsstudies en vele lokale studies. Op basis hiervan zijn vervolgens de patronen in ruimte en tijd met menselijke activiteit vergeleken, waarbij gebruik is gemaakt van schattingen over bevolkingsdichtheid uit de archeologie en historische bronnen en locaties van routes in het landschap. Daarnaast is er ook gekeken naar ontbossing en klimaat als mogelijke factoren. Uit de analyse blijkt dat er tussen 1000 voor Chr. en 1000 na Chr. een constante hoeveelheid stuifzandactiviteit plaatsvond, die veelal lokaal en kleinschalig van aard was. Dit patroon werd onderbroken in de Romeinse tijd (12 voor Chr. tot 450 na Chr.), waar een opvallend lage hoeveelheid stuifzandactiviteit geconstateerd is. Mogelijk speelt de verplaatsing van nederzettingen naar minder stuifgevoelige delen in het landschap tijdens de voorafgaande periode hierin een rol. Er komt verder naar voren dat stuifzandactiviteit gedurende de laatste twee millennia duidelijk gelinkt is aan de plekken waar mensen het landschap het meest intensief gebruikten. Ook de ononderbroken toename in stuifzandactiviteit na ongeveer 1000 na Chr. valt duidelijk samen met een stijgende bevolkingsaantallen en hogere mate van ontbossing.

Conclusie

In alle bestudeerde deelgebieden in Nederland vonden grote landschapsveranderingen plaats, waarbij de mens vooral vooraf een grote rol speelde door het landschap gevoeliger te maken. Dit gebeurde bijvoorbeeld door ontbossing van zandgronden zodat ze gevoeliger werden voor verstuiving, of door het ontwateren van veengebieden waardoor deze inklonken en de bodem hier daalde. Dit bracht onbedoelde landschapsveranderingen teweeg zoals zee-inbraken, rivierverleggingen en zandverstuivingen. Een grote storm of een overstroming zorgde vaak voor het laatste zetje in een gevoeliger geworden landschap. Hoewel het vaker voorkomen van stormen of overstromingen het proces kon versnellen, waren deze gebeurtenissen meestal niet van doorslaggevend belang voor de landschapsveranderingen. Stormen of overstromingen zorgden voor het omslagpunt waarna de landschapsverandering daadwerkelijk ingezet kon worden, maar dat was niet mogelijk voordat het landschap vatbaarder was geworden voor deze regelmatig voorkomende stormen en overstromingen.

De invloed van de mens op het landschap begon in sommige gevallen lokaal en kon zich verder verspreiden door allerlei versterkingsmechanismen. De aard van het landschap en de ondergrond speelde hierbij een grote rol. Zo konden zee-inbraken in gevoelige veengebieden het landschap volledig veranderen in grote getijgebieden. Rivierverleggingen, die deels door de mens zijn veroorzaakt, zorgden voor een belangrijke verandering van het riviertakkenpatroon in de delta, maar zorgden in mindere mate voor een totale transformatie van het landschap, zoals in het kustgebied. Zandverstuivingen vonden in de onderzochte periode slechts lokaal plaats. De gevolgen van de landschapsveranderingen voor de mens waren afhankelijk van de schaal waarop deze plaatsvonden en de onomkeerbaarheid ervan. De zee-inbraken in het kustgebied zorgden voor het grootschalig verlaten raken van de eerdere veengebieden. In het rivierengebied is de verplaatsing van nederzettingen in reactie op nattere condities waarneembaar, maar geen grote gebieden raakten verlaten. In het zandgebied zijn vooralsnog geen verschuivingen in nederzettingenpatronen te linken aan stuifzandactiviteit voor de onderzochte periode.

Deze kennis uit het verleden geeft ons meer inzicht in de omstandigheden waaronder de impact van de mens op het landschap het grootst is en wanneer mensen zich daaraan moeten aanpassen. Ook in deze tijd is dit samenspel tussen de mens en het landschap nog belangrijk, bijvoorbeeld in dichtbevolkte delta's die te maken hebben met grootschalige bodemdaling, zeespiegelstijging en toenemende overstromingen.

De regionale, geïntegreerde aanpak bij het bestuderen van de interactie tussen de mens en het landschap kan in de toekomst verder worden uitgebreid door meer resultaten van detailstudies toe te voegen of juist het onderzoek op te schalen naar aanliggende gebieden in België of Duitsland. Dit kan gaan om studies die de timing van menselijk handelen of stormen verfijnen en gevolgen hiervan voor het landschap bestuderen. Maar ook kunnen modelstudies gebruikt worden om de gevoeligheid van het landschap voor menselijke handelen of het vaker voorkomen van grote stormen te testen. Het blijven combineren van verschillende typen data vanuit meerdere disciplines voor zowel grote als kleine schaal zal zorgen voor een beter beeld van het samenspel tussen de mens en het landschap.

Appendix A

Supplement to chapters 2, 3, and 6: input materials to the reconstructions

Available on the Utrecht University Repository via:
<http://dspace.library.uu.nl/handle/1874/354561>

Appendix B: Supplement to chapter 5

This Appendix contains data and processing details belonging to the chapter 5. The first section provides details regarding the radiocarbon dating strategy for the course of events of the Hollandse IJssel (HIJ) and Lek avulsions. The second section treats the use of archaeological data. The last section provides details regarding the land-surface reconstruction at the time of the initiation of the avulsions, for the research sites in nowadays subsided polder land.

B1 Radiocarbon dating

In the main text the formation of the Lek and Hollandse IJssel and the abandonment of pre-existent river branches between 500 BC and AD 1000 are discussed. The ages of these events followed from combined direct dating (of ^{14}C dated samples from relevant stratigraphical positions) and relative dating (i.e. by tracing sedimentary layers and applying cross-cutting relationships). The Rhine-Meuse delta has a long research history in mapping and dating of the river network, for overview compilations we refer to Berendsen & Stouthamer (2000), Stouthamer & Berendsen (2000) and Cohen et al. (2012) (ca. 1500 ^{14}C dates related to ca. 200 river branches). Dates collected in the 1970s to early 1990s were usually performed on larger volume bulk samples using conventional ^{14}C dating (e.g. Berendsen, 1982; Törnqvist & Van Dijk, 1993), whereas smaller volume AMS ^{14}C -dating of selected terrestrial botanical macrofossils has been common since the 1990s.

We collected multiple new *Terminus Post Quem* (TPQ) AMS ^{14}C -dates for the Hollandse IJssel and Lek branches at various positions along the channel belt (Figure B1). The fieldwork sites were located as close as possible to the channel belt, where a gradual, i.e. a non-erosive stratigraphic boundary was observed. Prior to picking the interval to select and date macrofossils from, Loss-On-Ignition (LOI; e.g. Teunissen, 1990; Heiri et al., 2001) was measured over consecutive 1-cm intervals on subsamples, to measure mass percentage organic contents (insets in Figure B1). Those intervals that record increasing clastic input were selected for terrestrial macrofossils sampling. Dates were calibrated using the IntCal13 curve of Reimer et al. (2013) in OxCal (Bronk-Ramsey & Lee, 2013). All dates are reported in standard calibrated form in yrs BC/AD with a 1σ range.

The main calibrated radiocarbon dates used for the phases of avulsion in this study are visualised chronologically in Figure B2, together with their interpreted phases of avulsion related to the phases in Figure 5.1. Table B1 lists all dates regarded relevant for the dating of the Hollandse IJssel and Lek branches, taken from past research, from our own fieldwork, and from previous archaeological investigations. It includes dates directly relating to the onset of deposition (avulsion), as well as supporting dates that relate to older or younger stratigraphic levels, serving verification and support of the newly obtained dates. Where we rejected earlier collected dates as TPQ ages, our argumentation for this is reported. Several conventional ^{14}C bulk dates were rejected where newer obtained AMS dates indicate them to suffer from ageing effects. Rejected usage also applies to some AMS dates, where they were collected from peat beds that suffered from recent oxidation. At such locations, we still used the LOI and age results to perform peat-surface reconstructions (see section on former peat surface reconstruction).

Table B1 | Results, stratigraphy, and meaning of the ¹⁴C dates used in this study. Numbers correspond to the numbers in Figures S1 and S2.

nr	Sample name	Lab code	X/Y ¹⁾	Lat./Long.	¹⁴ C Age	Calendar age	Type	Stratigraphy	Meaning	Reference
1	Snelrewaard	GrA-64318	122464 448834	N 52° 1' 36.8" E 4° 54' 47.3"	2650 ± 45	829 BC ± 38	AMS	Top of the peat below clay Hollandse IJssel	oxidized, too old surface level reconstruction (HJ)	This study
2	Over Oudland 1	KIA-43210	132740 447000	N 52° 0' 39.3" E 5° 3' 46.7"	2560 ± 45	693 BC ± 89	AMS	Base residual channel Over Oudland	Phase predecessor Hollandse IJssel (HJ)	Bouman et al. (2012)
3	Oudekerk 2	GrA-64321	103618 439348	N 51° 56' 24.8" E 4° 38' 23.9"	2550 ± 70	659 BC ± 105	AMS	Top of the peat below clay Hollandse IJssel	oxidized, too old surface level reconstruction (M3)	This study
4	Schiedam Volkstuinencomplex	GrN-23225	84961 436589	N 51° 54' 48.2" E 4° 22' 9.3"	2480 ± 50	640 BC ± 72	Conv ²⁾	Top of the Holland peat	TPQ Schie (M1)	Moree et al. (2002)
5	Oudekerk 1	GrA-64564	103618 439348	N 51° 56' 24.8" E 4° 38' 23.9"	2390 ± 30	480 BC ± 76	AMS	Top of the peat below clay Hollandse IJssel	oxidized, too old surface level reconstruction (M3)	This study
6	Jaarsveld 1	GrA-67120	127420 443380	N 51° 58' 41.3" E 4° 59' 8.8"	2265 ± 35	309 BC ± 60	AMS	Humic clays below clay Lek	most likely erosive contact, too old surface level reconstruction (Lek)	This study
7	Nieuw Lekkerland 1	GrA-64317	107533 433761	N 51° 53' 25.3" E 4° 41' 51.6"	2260 ± 35	305 BC ± 59	AMS	Top of the peat below clay Lek	oxidized, too old surface level reconstruction (M4)	This study
8	Willige Langerak	GrN-08708	122402 439900	N 51° 56' 47.8" E 4° 54' 47.1"	2220 ± 35	293 BC ± 62	Conv ²⁾	Top of the peat below clay Lek	TPQ Lek: Conventional, too old	Berendsen (1982 p136, 185)
9	Rotterdam Blaak 2	GrN-21282	93340 437050	N 51° 55' 6.7" E 4° 29' 27.4"	2220 ± 30	294 BC ± 61	Conv ²⁾	Peat below clay Rotte several dms below top	M1/M2 TPQ	Guiran (1997)
10	Streefkerk 1	GrA-62966	112608 436097	N 51° 54' 42.3" E 4° 46' 16.0"	2190 ± 30	275 BC ± 57	AMS	Top of the peat below clay Lek	oxidized, too old surface level reconstruction (Lek/ M4)	This study
11	Jaarsveld 2	GrA-67212	127420 443380	N 51° 58' 41.3" E 4° 59' 8.8"	2190 ± 35	272 BC ± 60	AMS	Humic clays below clay Lek	most likely erosive contact, too old surface level reconstruction	This study
12	Rotterdam St Jacobsplaats 2	GrN-22343	92820 437720	N 51° 55' 28.1" E 4° 28' 59.7"	2190 ± 30	278 BC ± 65	Conv ²⁾	Peat below clay Rotte several dms below top	M1/M2 TPQ	Guiran (1997)
13	Ameide 2	GrA-62997	127453 441165	N 51° 57' 29.6" E 4° 59' 11.2"	2160 ± 30	241 BC ± 77	AMS	Top of the peat below clay Lek	oxidized, too old or distal part of flood basin clays. Surface level reconstruction (Lek)	This study
14	Rotterdam St Jacobsplaats 1	GrN-22444	92820 437720	N 51° 55' 28.1" E 4° 28' 59.7"	2140 ± 30	222 BC ± 95	Conv ²⁾	Top of the peat below clay Rotte	M2 TPQ	Guiran (1997 p30)
15	Rotterdam Terbregge	GrN-21279	95547 441771	N 51° 57' 40.3" E 4° 31' 19.9"	2070 ± 30	101 BC ± 46	Conv ²⁾	Top of the peat below clay Rotte	M2 TPQ	Guiran (1997 p30)
16	Rotterdam Emplacement CS	GrN-28992	91508 437669	N 51° 55' 25.9" E 4° 27' 51.1"	2045 ± 40	66 BC ± 59	Conv ²⁾	Top of the peat below clay	M1/M2 TPQ	BOORrapporten 318

17	Lange Linschoten	GrA-62969	120955 450321	N 52° 2' 24.6" E 4° 53' 27.6"	2000 ± 30	AD 2 ± 34	AMS	Top of the peat below clay Lange Linschoten	HIJ TPQ	<i>This study</i>
18	Rotterdam Blaak 1	GrN-21283	93340 437050	N 51° 55' 6.7" E 4° 29' 27.4"	1990 ± 50	AD 1 ± 52	Conv ²⁾	Top of the peat below clay Rotte	M2 TPQ	Guiran (1997 p30)
19	Ameide 3A	GrA-64635	127453 441165	N 51° 57' 29.6" E 4° 59' 11.2"	1975 ± 30	AD 24 ± 34	AMS	Very top of the peat below clay Lek	Initial crevassing Lek or distal part of flood basin clays. Surface level reconstruction	<i>This study</i>
20	Nieuwegein 2	GrA-64632	136246 446378	N 52° 0' 19.7" E 5° 6' 50.7"	1965 ± 35	AD 33 ± 40	AMS	Base of the peat below clay Lek	(-) TAQ older system, supporting date for sequence calibration (Lek)	<i>This study</i>
21	Lek	GrN-08707	136212 446375	N 52° 0' 19.6" E 5° 6' 48.9"	1950 ± 30	AD 44 ± 30	Conv ²⁾	Top of the peat below clay Lek	Lek TPQ, bulk too old	Berendsen (1982 p136, 185)
22	Gouda Groenakker	Ua-37219	109066 445975	N 52° 0' 0.9" E 4° 43' 5.9"	1945 ± 35	AD 50 ± 37	AMS	Alder wood from top of the peat below clay Hollandse IJssel	M3 TPQ	Eimermann et al. (2009)
23	Gouderak	GrA-62970	107948 445419	N 51° 59' 42.6" E 4° 42' 7.6"	1895 ± 30	AD 113 ± 41	AMS	Top of the peat below clay Hollandse IJssel	M3 TPQ	<i>This study</i>
24	Over Oudland 2	Poz-41826	132740 447000	N 52° 0' 39.3" E 5° 3' 46.7"	1870 ± 30	AD 144 ± 45	AMS	Vegetation horizont under the clay Hollandse IJssel or Lek	Lek TPQ; possibly younger shortcut (local avulsion)	Bouman et al. (2012)
25	Nieuwegein 1	GrA-64240	136246 446378	N 52° 0' 19.7" E 5° 6' 50.7"	1830 ± 30	AD 183 ± 43	AMS	Top of the peat below clay Lek	Lek TPQ; possibly younger shortcut (local avulsion)	<i>This study</i>
26	Kleidek Hollandse IJssel	GrN-07577	120702 448637	N 52° 1' 30.1" E 4° 53' 14.9"	1805 ± 50	AD 214 ± 73	Conv ²⁾	Top of the peat below clay Hollandse IJssel	HIJ TPQ; possibly younger shortcut (local avulsion)	Berendsen (1982 p136, 187)
27	Schoonhoven	GrA-62968	120993 439623	N 51° 56' 38.5" E 4° 53' 33.4"	1715 ± 30	AD 324 ± 44	AMS	Top of the peat below clay Lek	Lek TPQ	<i>This study</i>
28	Lexmond 2	GrA-64323	131974 442570	N 51° 58' 15.8" E 5° 3' 7.6"	1515 ± 40	AD 534 ± 56	AMS	Roots	Lek	<i>This study</i>
29	Lexmond 1	GrA-64319	131974 442570	N 51° 58' 15.8" E 5° 3' 7.6"	930 ± 45	AD 1104 ± 50	AMS	Top of the peat below clay Lek	Lek	<i>This study</i>

¹⁾X,Y are given in the Dutch coordinate system (Rijksdriehoekstelsel), position in meters. ²⁾Conv = conventional

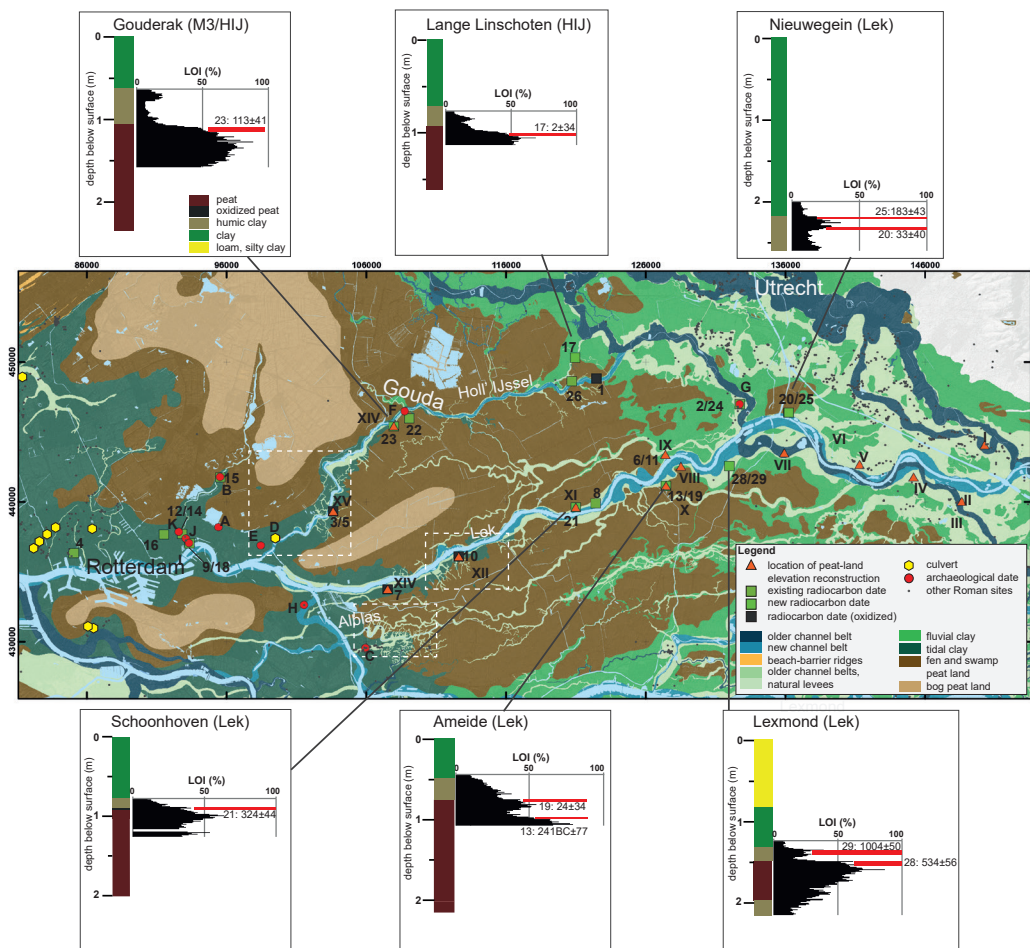


Figure B1 | Location of the radiocarbon sample sites. For the newly sampled sites the vertical position and calibrated age AD are indicated in a borehole log and LOI curve. White dashed rectangles indicate the extent of Figure B3. Numbers refer to radiocarbon dates in Table B1, letters to archaeological dates in Table B2, Roman numbers to locations of surface elevation in Tables B3 and B4.

B2 Archaeological reclamation evidence

We use archaeological artefacts to indicate zones of human activities in the landscape and link these to the timing of avulsion (Table B2). Evidence of habitation directly on the peat is known from multiple sites in the study area (labelled A, B, D, E, F, J in Figure B1), and humans were also abundantly present on tidal levee ridges bordering and penetrating the peatland (sites C, I, K in Figure B1). Along the Rotte tidal creek (M2; sites A, B, I-K), for example, habitation existed since the Iron Age (800–12 BC) on the tidal levees, and expanded into more distal positions on the peat during the Roman Age (12 BC–AD 450), after which local clay deposition occurred (Carmiggelt & Guiran, 1997). The expansions of habitation and clay cover took place into eutrophic wood peat

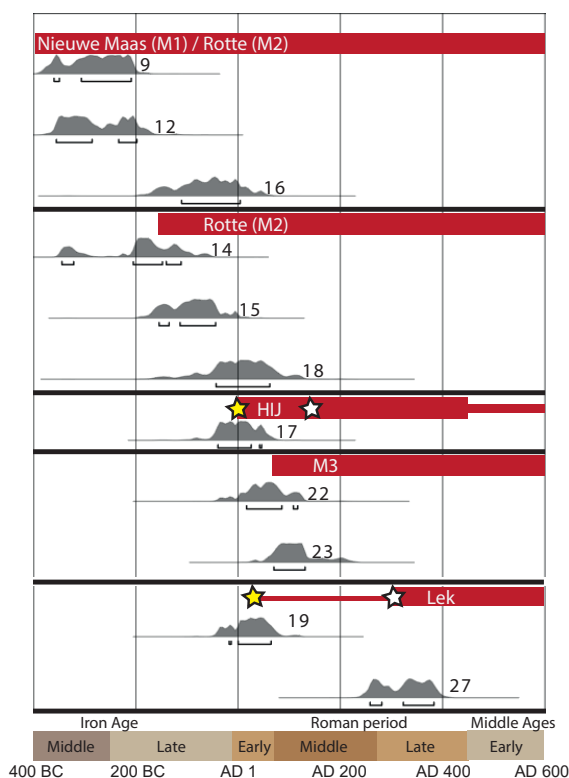


Figure B2 | Calibrated radiocarbon dates and the inferred phases of activity (red bars) of the Meuse sea ingressions (M), Hollandse IJssel (HIJ) and Lek, also shown in Figure 5.1. HIJ and Lek shortcuts indicate two local avulsions that occurred after the first connection. Numbers of the dates correspond to Table B4.

areas close to the alluvial ridges (formed under high nutrient influxes supplied by tidal and fluvial floods), with mesotrophic to oligotrophic peat areas at a greater distance from the channels as nutrient sources (Markus, 1984). Fourteen culverts next to the creeks (#9 in Figure B1, of which site D is located directly along the Hollandse IJssel) date from this time of expansion (Ter Brugge, 2002). These water management works were used to drain the water from the reclaimed lands during low tide and to prevent water flowing in during high tide. They testify that shortly after peatland reclamation, people were forced to cope with a progressively lowering land surface. Human impact on the peatlands during Roman Age was not restricted to the areas that were cultivated by digging ditches: swamp forest clearing to collect wood as building material may have affected additional areas of peatland (Van Dinter et al., 2014, Kooistra et al., 2013).

Regularly spaced, rectangular patterns observed in LiDAR and soil mapping of the study area, bear further indication for human activity in the peatland. These are clay infilled dendritic creek-ridge networks connected to the main channels of the Meuse estuary (Figure B3). A prime example is the occurrence of creek ridges along the Alblas tidal channel (M5; Figure B3C), that nowadays lie somewhat higher than the surrounding land. This is due to relief-inversion that had taken place because, compared to the silted up creeks, the surrounding peat soils were more prone to land subsidence (see also last section). Their presence is an indication that the tidal creeks developed as local ingressions during the Roman Age and Early Middle Ages, following pre-existent regular ditch networks dug in the Late Iron Age to Roman Age. Human presence in this area is supported

Table B2 | Archaeological dates and indication of habitation.

Site	Site name	X/Y ¹⁾	Lat./Long.	Material	Age ²⁾	Meaning	Reference
A	Kralingen	95412 438195	N 51° 55' 44.5" E 4° 31' 15.1"	Pottery on top of the peat	3 rd -1 st C BC	(i) Proof of habitation on top of the peat (on thin clay layer), (ii) TAQ Rotte (M2)	Guiran (1996); Carmiggelt & Guiran (1997)
B	Terbregge	95533 441782	N 51° 57' 40.6" E 4° 31' 19.1"	Pottery on top of the peat	3 rd -1 st C BC	(i) Proof of habitation on top of the peat (on thin clay layer), (ii) TAQ Rotte (M2)	Moree & Van Trierum (1992); Carmiggelt & Guiran (1997)
C	Alblasserdam	105927 429558	N 51° 51' 8.8" E 4° 40' 29.8"	Pottery on top of a channel belt	ROM (12 BC-AD 450) most likely before AD 270 ¹⁾	(i) Proof of habitation on a channel belt adjacent to the peat area (M5)	Hallewas (1986 p305)
D	Capelle Middelwatering West	99550 437410	N 51° 55' 20.6" E 4° 34' 52.1"	Dam with 3 culverts	Begin 2 nd century-begin 3 rd century	(i) Proof of habitation and water management on top of the peat, (ii) TAQ Hollandse IJssel (M3)	Jacobs et al. (2001); Moree et al. (2002 p133); Moree et al. (2010 p127)
E	Capelle 's Gravenland	98450 436900	N 51° 55' 3.8" E 4° 33' 54.8"	Pottery (no context)	ROM (12 BC-AD 450) most likely before AD 270 ¹⁾	(i) Indication of habitation on top of the peat, (ii) TAQ Hollandse IJssel (M3)	Moree et al. (2002 p133)
F	Gouderaksedijk	108750 446500	N 52° 0' 17.8" E 4° 42' 49.1"	Pottery charcoal and wood on top of the peat	ROM (12 BC-AD 450) most likely before AD 270 ¹⁾	(i) Indication of habitation on top of the peat, (ii) TAQ Hollandse IJssel (M3)	Van Dasselaar (2006); Eimermann et al. (2009)
G	Over Oudland	132740 447000	N 52° 0' 39.3" E 5° 3' 46.7"	Pottery under clay cover	1 st to 3 rd century	TPQ Lek/Hollandse IJssel	Bouman et al. (2012)
H	Ridderkerk-Slikkeveer	101550 432630	N 51° 52' 46.7" E 4° 36' 39.4"		ROM (12 BC-AD 450) most likely before AD 270 ¹⁾	(i) Proof of habitation on a channel belt adjacent to the peat area (M5)	Moree et al. (2002)
I	Rotterdam Wijnhaven	93290 437075	N 51° 55' 7.4" E 4° 29' 24.7"	Pottery (no context)	ROM (12 BC-AD 450) most likely before AD 270 ¹⁾	(i) Indication of habitation on top of the peat, (ii) TAQ Hollandse IJssel (M1/M2)	
J	Rotterdam Hoogstraat	93080 437400	N 51° 55' 17.9" E 4° 29' 13.5"	Settlement on top of the peat	Middle of the 2 nd century	(i) Proof of habitation on top of the peat (on thin clay layer), (ii) TAQ Hollandse IJssel (M1/M2)	Carmiggelt & Guiran (1997); Moree et al. (2002 p133); Moree et al. (2010 p132)
K	Rotterdam Spoortunnel	92570 437870	N 51° 55' 32.9" E 4° 28' 46.5"	Pottery (no context) reworked by the Rotte	ROM (12 BC-AD 450) most likely before AD 270 ¹⁾	(i) Indication of habitation on top of the peat, (ii) TAQ Hollandse IJssel (M1/M2)	Carmiggelt & Guiran 1997; Moree et al. (2002 p108)

¹⁾X/Y are given in the Dutch coordinate system (Rijksdriehoekstelsel), position in meters. ²⁾The bulk of roman finds in the Rhine-Meuse delta dates from early and middle Roman period (12 BC-AD 270).

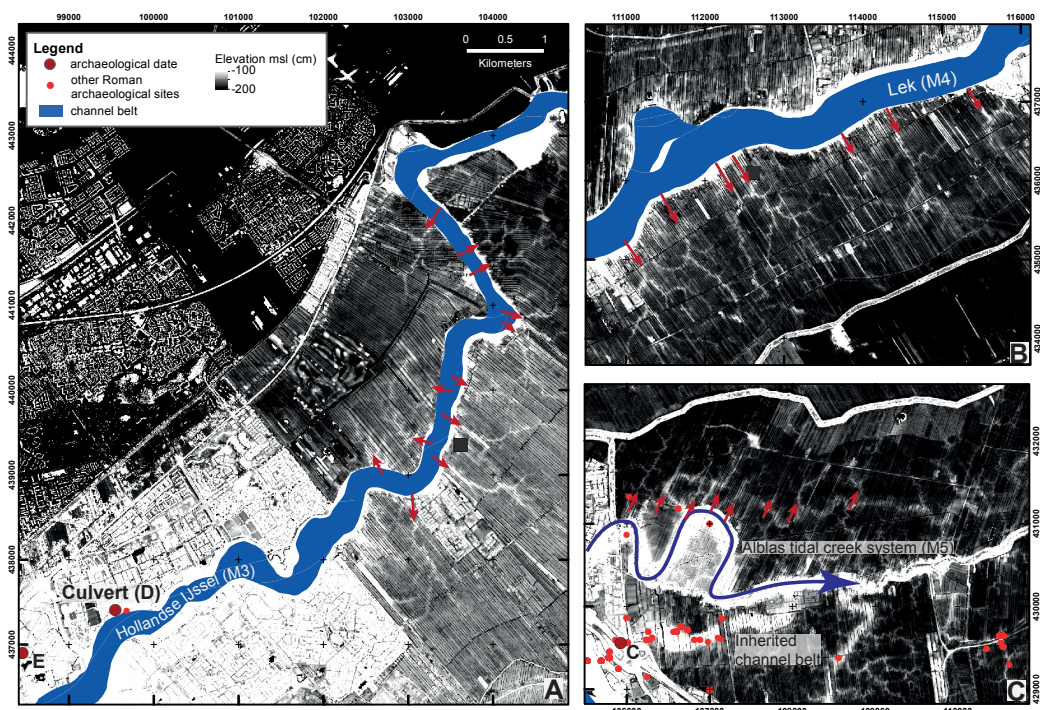


Figure B3 | LiDAR images of the tidal creek patterns in the downstream part of the Hollandse IJssel (M3; A), Lek (M4; B), and Alblas (M5; C). Archaeological finds indicate Roman habitation on the creek ridges or directly next to them on the peat. Red arrows indicate remarkable straight ridges spaced on a regular distance pointing towards former reclamation ditches. Locations are indicated in Figures 5.1C and B1.

by Roman archaeological sites on and along the Alblas main alluvial ridge (Louwe Kooijmans, 1974; Figure 5.3C). Similar such networks associated with Roman archaeological finds have been found in the southwestern Netherlands in the peatlands (Bennema et al., 1952; Vos & Van Heeringen, 1997; Pierik et al., 2017a). Similar regularly spaced, rectangular patterns of tidal creeks into peatland are also observed on either side of the downstream reaches of the Hollandse IJssel and Lek tidal-river avulsed channels (M3 and M4; Figure B3). However, a more natural development of these creek ridges cannot be fully ruled out, since modern natural tidal environments may exhibit a similar a rectangular planform arrangement of tidal creeks.

B3 Former peat-surface reconstruction

This section presents calculations to derive reconstructions of the original peatland surface elevation at the time of initiation of the rivers Hollandse IJssel and Lek. This was performed to assess the longitudinal gradient advantage of the pre-avulsion peat landscape relative to the active river-bed gradient of the Oude Rijn from which the Hollandse IJssel and Lek took over the largest portion of discharge.

Coastal plain peatlands in the study area were reclaimed locally in the Iron Age and Roman period – before the avulsions took place (see section above). Systematic reclamation of the entire area followed about 1000 years later – after the avulsions, from ca. AD 1100 onwards (e.g.

Borger, 1992; De Bont, 2008; Erkens et al., 2016). These two phases of reclamation combined with sedimentation from the avulsion described in this chapter, have resulted in considerable land-surface lowering. This makes that the depths of dated clay-on-peat contacts at sample locations need to be corrected before they can be used as indicators for former land-surface elevation.

To this end, we used geomechanical insights on peat consolidation that led to surface lowering in response to water-table lowering (Schothorst, 1977; Erkens et al., 2016). Peat consolidation (volume loss caused by compression) takes place when sediments are deposited on top of the peat (e.g. clays) or when the peat is drained. The calculations that reconstruct the state of the peat before consolidation took place, use the following properties from our sampled field sites as input: current vertical position of the clay-on-peat contacts, age and type of the buried peat, and thickness of the overburden.

Besides consolidation, oxidation above the phreatic groundwater level is an important component in peat loss. This process will persist as long as organic matter is available above the water level, and as subsidence in cultivated peatlands will provoke more drainage, it becomes a self-perpetuating process (Erkens et al., 2016). This component cannot be directly quantified, and it causes a hiatus in the top of the peat leading to too old TPQ dates in Table B1. Field descriptions and LOI measurements on peat (Figure B1) already indicate whether the peat is encountered in a compressed state and whether (prehistoric) oxidation has affected the top of the peat below clastic overburden. The peat appears black and the organic content is relatively low (relative enrichment in clays after oxidation).

Besides reconstructing the original surface height, the calculations in this section serve to estimate how much peat had disappeared due to oxidation. And to verify that too old dates were indeed caused by oxidation, rather by diachronic clay deposition in a lateral direction from the river channel or in a longitudinal direction relative to the avulsion point. Where the reconstructed elevation of these samples plots well below the reconstructed elevation based on the non-oxidized samples that retrieved younger TPQ ages, this age can indeed be attributed to a hiatus resulting from oxidation.

B3.1 Role of vegetation composition

The vegetation composition of peat determines at what accuracy it can be related to an original groundwater level at the time the peat formed. The study area is dominated by woody peat types (*Alnus* and *Salix*) that indicate former presence of swamps fed by eutrophic Rhine floodwaters. These peat types generally form around multi-year-averaged, mean annual lowest groundwater level (Den Held et al., 1992). At the time of formation, the Rhine-Meuse delta swamp peat surfaces are regarded to have followed a very gentle regional elevation gradient from central delta towards the coast (estimated at 2 to 5 cm/km; Van Dijk et al., 1991; Cohen, 2005; Koster et al., 2016a), around the same elevation as the mean-water surface in open river channels connecting the inland delta to the estuaries and sea. Other types of peat (e.g. mesotrophic and oligotrophic mossy peat) are known to have formed bog domes in distal sectors of the Rhine-Meuse delta plain along the edges of the study area (Pons, 1992; Figure B1). These bogs stored rainwater and held up local peat surface and groundwater tables at higher elevation than the surrounding swamps. Their elevation during the first millennium AD is estimated to have been 2-3 meter above that of the surrounding, irregularly flooded swamp peatland (Pons, 1992). Past occurrence of oligotrophic vegetation is a clear indication that in natural conditions such areas were not flooded by river or tidal waters.

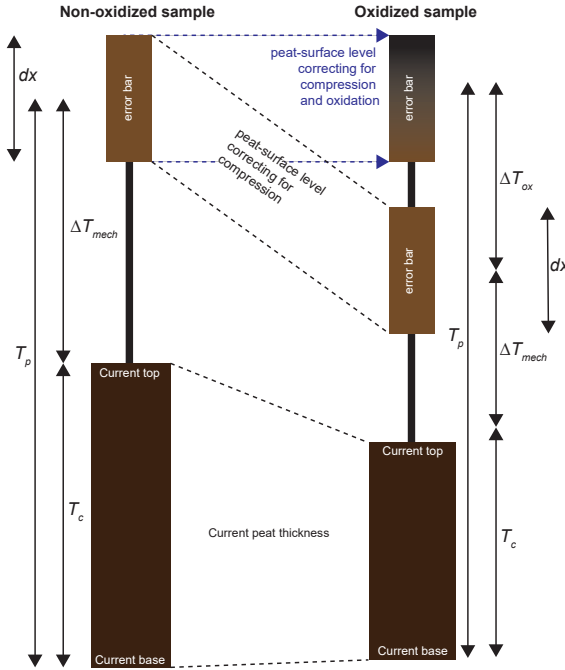


Figure B4 | Reconstruction of the former peat level (Figure 5.2C) using the current peat thickness, the calculated mechanical peat loss component, and the estimated oxidation loss component for oxidized samples. For parameters see text.

B3.2 Calculation procedure

The past surface-level elevation was reconstructed by calculating the thickness of the pristine wood peat T_p (i.e. before the avulsions took place). This was done using the current peat thickness T_c , the loss of peat thickness due to mechanical properties ΔT_{mech} , and the loss of peat thickness due to oxidation between the moment the sample was taken and the moment just before the avulsion ΔT_{ox} (Eq. 1; Figure B4). This latter component could not be directly calculated; the oxidized samples (i.e. samples with a clear black appearance in their top) were used as a minimum surface level estimate. T_c was derived from borehole data on the site. ΔT_{mech} was calculated using empirically derived relations between thickness of the current peat T_c and its geomechanical properties (Koster et al., 2016b; in prep; Eqs. B2-4). This was done using the void ratio (i.e. ratio between non-solid and solid components) of the current e_c and pristine peat e_p (Eq. B2). For e_p a vertical stress of 3.7 kPa was taken as a typical value in fresh peat (Koster et al., 2016b). The current, compressed state void ratio e_c of the peat was determined by its current vertical effective stress (σ') exerted on the peat after its burial (Eq. B3: Koster et al., 2017). σ' was quantified in Eq. B4 by multiplying the combined thickness of overburden and the peat with standard values of lithology specific total stress per meter thickness (see below). Because groundwater in the pores counteracts the effective stress, the water pressure was subtracted for the saturated parts of the overburden. Overburden thickness ($T_{overburden}$) was derived from borehole data on the site. Thickness of the saturated overburden ($T_{saturated}$) was derived from the groundwater level measured during coring or alternatively from the groundwater level indications on the soil map (Markus, 1984). Table B4 shows the calculation results.

$$T_p = T_c + \Delta T_{mech} + \Delta T_{ox} \quad \text{Eq. B1}$$

$$\Delta T_{mech} = T_c \times (1 - \frac{e_c}{e_p}) \quad \text{Eq. B2}$$

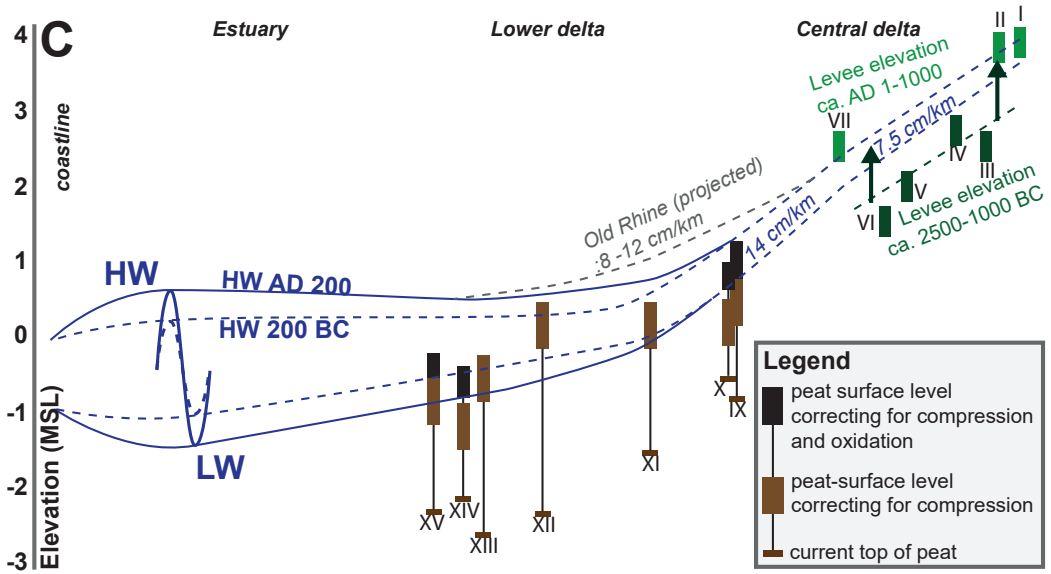


Figure B5 | Reconstruction of pre-avulsion surface elevation along Hollandse IJssel and Lek courses (extended version of Figure 5.2C). Upstream: mapped levee elevation (Roman numbers indicate codes in Table B3), Central: top of peat (Roman numbers indicate codes in Table B4), Downstream: tentative tidal incursion, increasing with tidal creek ingressive progradation from 200 BC to AD 200 (Vos, 2015a). Projected Old Rhine gradient after Cohen et al. (2012).

$$e = 1.38 \sigma_v^{-0.433} \quad \text{Eq. B3}$$

$$\sigma' = (T_{\text{overburden}} \times S_{\sigma'}^{\text{SEDIMENT}}) - (T_{\text{saturated}} \times S_{\sigma'}^{\text{WATER}}) \quad \text{Eq. B4}$$

with

T_c =	thickness of peat in compressed state	[m]
e_c =	void ratio in compressed state	[-]
e_p =	void ratio in pristine state	[-]
σ_v =	vertical effective stress	[10^3 kg m^{-2}]
$T_{\text{overburden}}$ =	thickness of overburden	[m]
$S_{\sigma'}$ =	standard value total vertical stress per meter thickness, taken as 11 for peat, 15.1 for clay, and 10 for water, as in Kruiver et al. (2017)	[10^3 kg m^{-3}]

The peat-surface reconstruction calculated using T_c and ΔT_{mech} yields some errors regarding determining the surface level ($E1$), and sampling error of the depth of the top of the peat ($E2$). Both are assessed to be < 0.1 m. Additional error ($E3$) estimated at 0.6 m comes from errors in determining the current groundwater level and the base of the peat. The total maximal error of the reconstructed peat surface level due to compression is estimated at $dx = \sqrt{E_1^2 + E_2^2 + E_3^2} = 0.53$ m, and this value is indicated as the vertical range in Figures 5.2C, B4, and B5.

The surface-level reconstructions of the two peat samples without oxidation ($\Delta T_{\text{ox}} = 0$ for XI and XV), were used for the gradient lines. This was supported by the sea level downstream and the top of

the levees adjacent to the peat area upstream (Table B3). The disappeared thickness of the oxidized peat could not be calculated, but it could be roughly estimated by comparing the age and position of the oxidized and the reconstructed non-oxidized surface level and the ground-water level rise at time of the peat formation. The time-equivalent of the disappeared peat could be determined when comparing the dates inferred from the oxidized peat to dates without oxidation. For example when the top of the peat under flood-basin clay of the Lek was oxidized and dated at 200 BC, while from other locations along the Lek non-oxidized peat yielded a date of AD 300. This means that a hiatus of 500 years occurs in the oxidized sample. When plotted in Figure 5.2C it appears that this time hiatus corresponds to approximately 0.5 meter (see also Table B4), which roughly corresponds to groundwater-level rise of ca. 0.6-0.3m/kyr during the period when the peat formed between 3000 and 2000 BP (Cohen, 2005; Koster et al., 2016a).

Table B3 | Reconstructed alluvial ridge surface levels before the avulsion of the alluvial ridges flanking the peatland on the upstream side.

Site name	Code ¹⁾	X/Y ²⁾	Lat./Long.	Age ³⁾	Z surface (msl)	Levee elevation ⁴⁾
Wijk bij Duurstede	I	150250 444066	N 51° 59' 5.9" E 5° 19' 5.0"	800 BC	4	3.9
Beusichem	II	148610 440028	N 51° 56' 55.2" E 5° 17' 39.4"	AD 570	4	3.8
De Molenkampen	III	147535 438800	N 51° 56' 15.4" E 5° 16' 43.1"	1343 BC	2.8	2.5
Culemborg	IV	145175 441775	N 51° 57' 51.5" E 5° 14' 39.3"	2600 BC	2.9	2.7
Schalkwijk	V	141300 442690	N 51° 58' 20.8" E 5° 11' 16.2"	2600 BC	2.2	2
Molenbuurt	VI	139620 445380	N 51° 59' 47.8" E 5° 9' 47.8"	2250 BC	1.78	1.51
Hagestein	VII	135900 443493	N 51° 58' 46.3" E 5° 6' 33.1"	AD 10	1.78	2.5

¹⁾Roman numbers can be found in Figure B1. ²⁾X/Y are given in the Dutch coordinate system (Rijksdriehoekstelsel), position in meters. ³⁾ages from Cohen et al. (2012). ⁴⁾Levee elevation after chapter 6 and Pierik et al. (2017b).

Table B4 | Reconstructing peat surface level before the Hollandse IJssel and Lek avulsions.

Site name	Code ¹⁾	X/Y ²⁾	Lat./Long.	Z surface (msl)	Ground-water level	Clay thickness	Current peat thickness	Reconstructed peat thickness	Z surface past	Years of peat oxidized ³⁾
Jaarsveld	IX	127420 443380	N 51° 58' 41.3" E 4° 59' 8.8"	0,45	0,8	1,3	2	2,9	0,05	500
Ameide 1	X	127453 441165	N 51° 57' 29.6" E 4° 59' 11.2"	0,02	0,5	0,5	2,5	3,2	0,22	500
Schoonhoven	XI	120993 439622	N 51° 56' 38.5" E 4° 53' 33.4"	-0,6	0,6	0,8	4,5	6,08	0,18	none
Streefkerk	XII	112608 436097	N 51° 54' 42.3" E 4° 46' 16.0"	-1,7	0,6	0,65	5	7,53	0,18	550
Gouderak	XII	107948 445419	N 51° 59' 42.6" E 4° 42' 7.6"	-1,7	0,9	1	5	7,2	-0,5	none
Nw. Lekkerland	XIV	107533 433761	N 51° 53' 25.3" E 4° 41' 51.6"	-1,55	0,4	0,6	3	3,73	-1,42	600
Oudekerk	XV	103618 439348	N 51° 56' 24.8" E 4° 38' 23.9"	-1,7	0,5	0,55	2,5	3,7	-1,05	750

¹⁾Roman numbers can be found in Figure B1. ²⁾X/Y are given in the Dutch coordinate system (Rijksdriehoekstelsel), position in meters. ³⁾Difference between the inferred river age (from unoxidized top peat samples along the same river) and the age of the d top peat sample.

Appendix C: Supplement to chapter 6

C1 Methods

This chapter presents two types of geomorphological reconstruction for the Rhine-Meuse delta: (i) three palaeogeographical maps (geomorphological reconstruction maps), for the time slices: AD 100, 500, and 900; and (ii) two palaeo-DEMs, for AD 100 and 900. The method in compiling these maps is given in section 6.3. Several technical detailed aspects that go beyond the scope of the main text are further outlined in this sections. Section C1.1 gives further details on the lithological criteria used of levee mapping, section C1.2 considers the integration of diachronously inherited, younger landscape elements into the reconstructions. Lastly, section C1.3 deals with technical details on corrections on the palaeo-DEM.

C1.1 Lithological criteria for mapping levee extent

To map levee extent, the borehole data was queried for two criteria: (i) presence silty clay, clay loam, or loam (textures LK, ZZL, and MZL; De Bakker & Schelling, 1989; Berendsen & Stouthamer, 2001) over a minimal combined thickness of 40 cm; that (ii) occur at shallow depth below present surface, 2 meters below the current surface at max.

We used 40 cm as a minimal thickness separating the natural levee area from its gradual transition into the flood basin. This meant that boreholes with clay loam intervals thinner than 40 cm alternating with ‘heavy’ clay (textures MK and ZK) were not considered part of the levees. Experiments querying for smaller thickness criteria resulted in test maps with very irregular levee-flood basin boundaries. The 2 meters maximum depth criterion was taken to include all levees that would have had surface expression at the time of the first time slice (AD 100), based on the depth of the 2000-BP isochron in levee areas in the cross-sections of Gouw & Erkens (2007). In a later stage of the research the vertical position of the top of the mapped levee was verified by calculating the palaeo-topography and matching with archaeological settlements (section 3.3.2; 5.2).

C1.2 Older feature inheritance and younger element masking

Inheritance of geomorphological elements

Inherited features are present in landscape reconstructions for AD 100, 500, and 900. These include: (i) buried natural levees and (ii) residual channels of channel belts, both from systems that had functioned in the 2500 years before (based on ages of parent channel belts, section A1.4, (iii) outcropping tops of buried inland-dune topography (‘donken’), and (iv) flood basin peats.

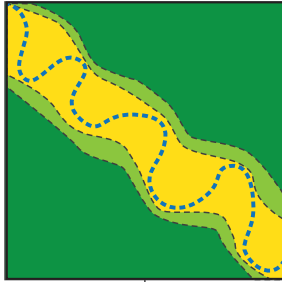
Ad (i): For these older natural levees, we initially assumed that river systems actively forming since roughly 2500 BC had surface expression in the earliest periods interest. The actual burial depth and degree of surface expression of these levees were evaluated in section 3.3.2 of the main text.

Ad (ii): After a river channel was abandoned, its residual channels can contain water for many centuries before entirely silting up (e.g. Stouthamer, 2001; Toonen et al., 2012). Even when they have silted up (with clay or peat - for sedimentological criteria see Toonen et al., 2012) they remain in the landscape as elongated depressions for a considerable time. These geomorphological elements were stored in a separate digital layer and used to cut the surrounding natural levee landscape. Similar to the levees, we mapped these elements from

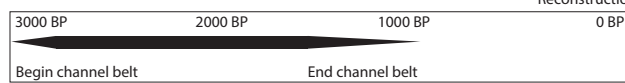
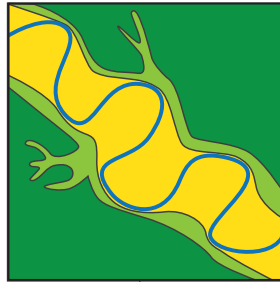
Administrative solutions for mapping-reconstruction issues

Diachronous elements

Reconstruction 2000 BP

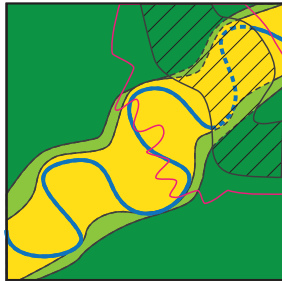


Reconstruction 1000 BP

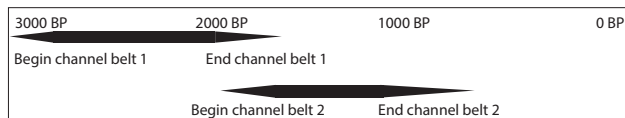


Eroded and covered elements

Reconstruction 2000 BP



Reconstruction 1000 BP



Elements in base maps

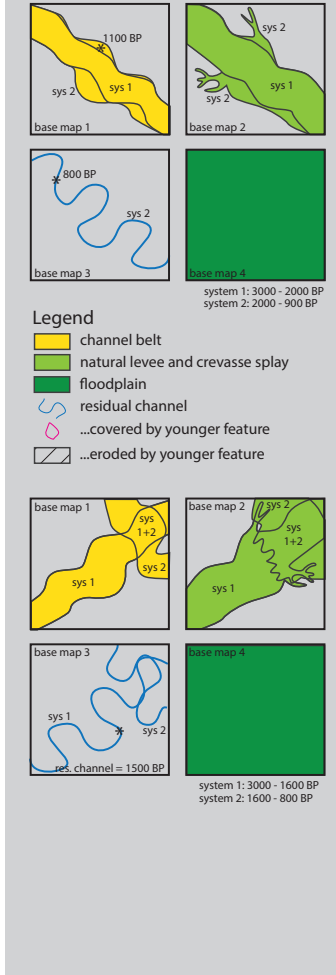


Figure C1 | Administrative solutions for mapping-reconstruction issues. Upper panel: earlier stages of channel belts were reconstructed using conceptual knowledge on the development of meandering rivers and dates. Lower panel: younger generations of channel belts partly cover and erode older phases. The extent of the covered phases can be derived from borehole data and cross-sections.

LiDAR datasets (A1.3), local soil maps (A1.7), and UU boreholes (A1.1) that contain the probable presence of residual channel fills (for > 1 m thick clays and peat occurrence on mapped sand belts).

Ad (iii): These sandy dune complexes formed in the Late Glacial along Rhine and Meuse channels in the floodplain of that time (e.g. Bennema & Pons, 1951; Kasse, 1995; Berendsen et al., 1995) and were buried by deltaic deposits since. Their long-lived sandy outcrops have been mapped separately before in soil maps, geological maps, and geomorphological maps. We

used a recently created compilation (Cohen et al., 2017ab) that assembled the outcrops from these earlier mappings.

Ad (iv): Peat occurrence was directly taken from the national soil maps and Van Dinter (2013).

Diachroneity of geomorphological elements

The natural levee polygons in the base map relate to their final preserved extent, by administering a *Begin* and an *End* age in two separate attribute fields the timespan of sedimentary activity of the features is stored. The values for *Begin* and *End* age were in turn based on correlation to the channel belt base map (section A1.4) and its documentation (Berendsen & Stouthamer, 2001; Cohen et al., 2012; further updates). Levees are not only vertically but also laterally diachronous (Figure C1): in the initial phase of natural levee sedimentary activity its extent was smaller than in the mature stage (i.e. preserved and thus mapped stage). Similar to levees, the gradual lateral growth applies to the channel belt too as meanders also increase in size over time. Lacking explicit storage of this lateral diachronous development generates limitations when time-sliced palaeogeographical maps are created as direct queries from these base maps. These limitations were circumvented in three ways: (i) by using relative late estimates for the begin ages of the levees and allowing to treat natural levees as multiple-generation stacked levees (Figure 6.2), (ii) by coding complex long-lived, presumably laterally expanding levee complexes as multiple polygons (spatially differentiated begin ages, mixing interpretative with strictly observational aspects of mapping in the base map), and (iii) by applying masking techniques in later stages of the reconstruction process.

Younger burial or erosion

Natural levees present in the past often have been subject to either burial or erosion in younger times. Younger mainly non-erosive elements include levees, crevasse splay or dike-beach deposits from rivers active after the time step of reconstruction. Because the younger levee were stored in the same base map (Figure C1), the levee base map was queried for levees younger than the time step under consideration, indicating areas where burial is to be expected. Areas next to these youngest channel belts developed relatively thick overbank deposits, raising the elevation of the old levee. This also applies to dike-breach splays, which formed after embankment covering the levee landscape (Pons, 1953; Hesselink et al., 2003). Their delineation was taken from detailed soil maps, geological maps, and borehole descriptions in which the top layer has been labelled as ‘dike-breach deposit’ during the process of borehole logging in the field.

A similar procedure was performed for the channel belts bearing in mind that younger channel belts erode older features. In our case, former levee areas occupied by channel belt polygons in younger times (queried from the channel belt base map, section A1.4), are considered to have been eroded (Figure C1). We used existing cross-sections, surrounding geomorphology and borehole information to reconstruct the situation before the activity of the younger elements in the geomorphological maps, in the Palaeo-DEMs these areas were masked.

C1.3 Palaeo-topography correction for sedimentation

To compile the palaeo-DEMs we used data combination processes described in the main text and sections of the appendix above. This concerns the following steps: (i) the depth of encountering the top of levee deposits (see C1.1) was queried (for borehole locations), (ii) the age of these levees was assigned (by architecturally correlating the levee to a parent channel belt system with a documented age of abandonment; see C1.2), and (iii) the encountered top of the levee was converted to a surface level at AD 100 and 900. This last step is explained in this section.

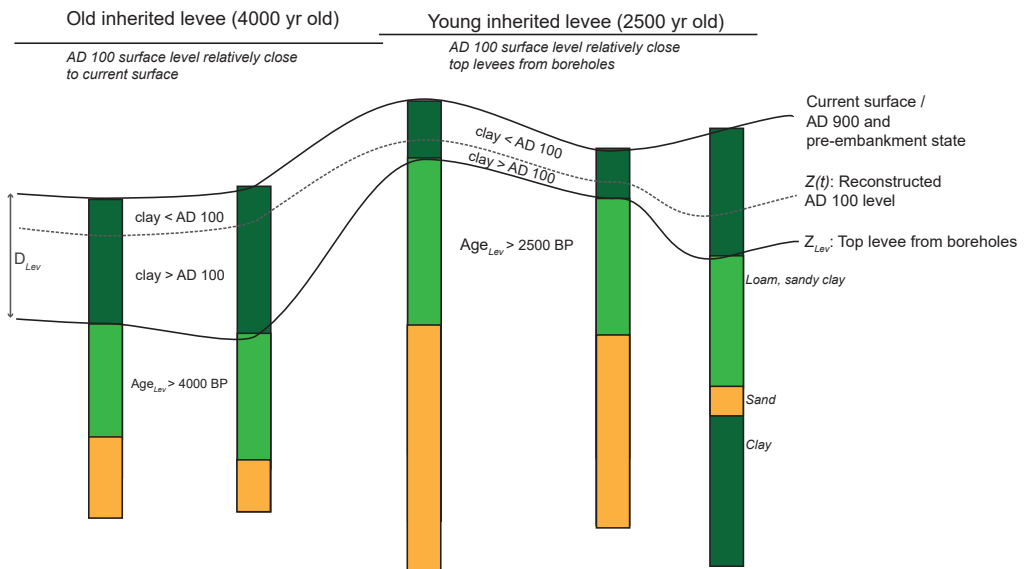


Figure C2 | Calculating palaeo topography from borehole data using levee age, vertical position of the levees' top, and pre-embankment surface level and age.

The present elevation is known (from LiDAR data) and in most of the study area representative for the elevation at ca. 850 BP (= AD 1100, just centuries after AD 900). To minimise the error in estimated surface elevation, we updated all values with values from LiDAR data, except for the localities on artificially elevated structures (e.g. cities, dikes, and roads ca. 10% of the input points). Here, we adapted the originally assigned surface elevation.

For levees known to be older than AD 100 - or any arbitrary moment in time (t) - a last step before interpolation of the reconstruction DEM was to pinpoint the surface level of that time within the burying deposits $Z(t)$ (Figure C2). This was performed by a calculation, that assumes a linear sedimentation rate between the end of levee sedimentation (Age_{Lev}) and embankment ($T_{Embankment}$). The equation below was then used to correct the levee elevation (Z_{Lev} ; in m OD) from the raw borehole query, with a proportion burial thickness (D_{Lev} ; in m) to give an elevation at the moment t (i.e. AD 100 = 1850 BP):

$$Z(t) = Z_{Lev} + D_{Lev} \frac{Age_{Lev} - t}{Age_{Lev} - T_{Embankment}} \quad \text{Eq. C1}$$

After applying this correction, most levees were elevated several centimetres, the surface of the oldest levees is several dms higher than the raw query (occasionally up to 90 cm).

Sampling error per grid cell dx is calculated to be 0.17 m by combining the following components of error. E_1 LiDAR error (0.1 m), E_2 field sampling error (0.05 m) and E_3 groundwater level error (0.13 m).

$$dx = \sqrt{E_1^2 + E_2^2 + E_3^2} \quad \text{Eq. C2}$$

When sampling multiple grid cells (N) for analysing larger areas, the error range $d\bar{x}$ strongly reduces by the following relation:

$$d\bar{x} = \frac{dx}{\sqrt{N}} \quad \text{Eq. C3}$$

A methodological bias was encountered in a small part of segment D between (130,000 < X < 140,000; 435,000 < Y < 445,000). Here the relative elevation of old channel belts shows up as too high (Figure 6.7). This bias originates from the groundwater-level plane, which estimates in the eastern flank of the peat area too low because control points (i.e. basal peat or old surfaces) are missing here. This part was therefore not considered in the analyses.

Table C1 | Characteristic levee properties for the defined segments in the delta. Negative values: most alluvial ridge surfaces are positioned relatively close to or slightly below GW level, in accordance with sparse archaeology. Relative portion of levee and flood-basin area increase is mainly due to the formation of new channels in the former flood basins.

Segment code	Geographical name	Relative elevation first millennium AD	AD 100 Levee area ¹⁾ (%)	AD 100 Flood basin area ²⁾ (%)	AD 900 Levee area ¹⁾ (%)	AD 900 Flood basin area ²⁾ (%)	AD 100 Levee elevation ⁴⁾ (cm to 2000 BP GW level)	AD 900 Inherited levee elevation ⁵⁾ (cm to 1000 BP GW level)	AD 900 Total delta levee elevation ⁶⁾ (cm to 1000 BP GW level)
<i>Upper (~10 km wide)</i>									
U1	Overbetuwe	High	67	16	79	18	43 ± 50	50 ± 46	105 ± 88
U2	Nederbetuwe (east)	Low	70	24	68	24	-25 ± 39	-11 ± 23	-2 ± 34
U3	Southern bank Waal	Average	56	38	58	36	33 ± 90	37 ± 80	51 ± 93
U4	Upper Meuse	Average	61	30	61	30	-3 ± 52	7 ± 27	14 ± 37
<i>Central (10 – 40 km wide)</i>									
C1	Utrecht	Average	45	53	45	52	27 ± 62	54 ± 47	60 ± 55
C2	Kromme Rijn	Average	52	31	60	35	6 ± 52	17 ± 41	25 ± 55
C3	Nederbetuwe west/ Tielervaard east	Average	75	22	82	15	5 ± 51	8 ± 43	15 ± 48
C4	Bommelerwaard	Low	44	55	64	34	-32 ± 48	-17 ± 26	-9 ± 48
C5	Land van Heusden Altena	Low	34	65	44	55	-23 ± 53	-14 ± 39	-2 ± 46
<i>Lower (> 40 km wide)</i>									
D	Alblasserwaard, Krimpenerwaard	Low	12	88	14	86	³⁾	³⁾	³⁾

¹⁾levee area includes crevasse splays and levees on channel belts in Figures 6.6 and 6.8; ²⁾flood basin area includes clayey and peaty flood basins in Figures 6.6 and 6.8. ³⁾Levee-properties and subdivisions have not been studied in detail for this area; ⁴⁾mean and 1σ of the relative elevation of the inherited levee landscape AD 100 (i.e. the levees formed before AD 100 – for mask see Figure 6.7C). The delta-wide mean and spatial difference is 11 ± 63 cm; ⁵⁾relative elevation of AD 900, the delta-wide mean and spatial difference of only the inherited levee landscape is 20 ± 53 cm; ⁶⁾the delta-wide mean and spatial difference of the total levee landscape (inherited and actively forming) at AD 900 is 28 ± 65 cm.

C2 Maps

Geomorphological reconstructions of AD 100, AD 500, and AD 900.
Palaeo-DEMs of AD 100 and 900.

Available on the Utrecht University Repository via:
<http://dSPACE.library.uu.nl/handle/1874/354561>

Appendix D: Supplement to chapter 9

D1 Reconstruction population density

Estimates of population density (PD in p/km²) are shown in Table D1 and Figures 9.3-9.6. These were based on (i) published population numbers and densities inferred from archaeological settlement data. Benchmark for pre-AD 1000 periods were the Roman period (AD 200) population reconstructions based on detailed micro-regional studies (Van Beek & Groenewoudt, 2011). (ii) Published population numbers and densities based on written sources (only after AD 1500).

For the less-known periods: 1000 BC, 100 BC, AD 500 and AD 800, population density estimates (PD) were based on the number of known archaeological settlements (Zoetbrood et al., 2006), relative to the number of Roman-period settlements. We corrected for differences in the duration of the different archaeological periods and took the period-specific differences in discovery potential of settlements (Groenewoudt, 1994; Deeben et al., 2005) into account.

Estimated numbers were validated and (if necessary) adjusted by comparing them to long-term demographic trends published by Roymans & Gerritsen (2002), Louwe Kooijmans et al. (2011) and Van Munster (2012), and for the Late and post-Medieval periods Faber (1965); McEvedy and Jones (1978); Paping (2009). In the case of (published) settlement density ranges, we choose the mean value, unless long-term demographic trends (Louwe Kooijmans et al., 2011; Van Munster, 2012) make higher or lower numbers more likely. This reconstruction gives a relative trend of PD through time, more detailed micro-regional studies that estimate the number of people from the archaeological record would further improve these reconstructions. Below the estimates are further outlined per period:

Early Iron Age (ca. 800 BC)

Population density for the Early Iron Age was estimated to be 50% of the Late Iron Age population on a national level based on (Louwe Kooijmans et al., 2011).

Late Iron Age (ca. 200 BC)

The number of Iron Age settlements is 37% less relative to the number of Roman settlements (341 Iron Age and 452 in the Roman age on a national scale) (Zoetbrood et al., 2006), because Iron Age sites are less well recognisable, which negatively influences the discovery rate (Groenewoudt, 1994; Deeben et al., 2005; Verhagen & Borsboom, 2009) we estimate PD to be 50% relative to the Roman Age.

Roman Period (ca. AD 200)

During this period population density (PD) was relatively high, especially in the river area. In the sandy area, population numbers were lower but also increased. For these areas Van Beek & Groenewoudt (2011) reconstructed a mean PD of 4.9 p/km².

Early Post-Roman period (ca. AD 500)

After the Roman period a strong depopulation occurred, however some major differences can be seen between the study regions (Van Munster, 2012). Based on the number of settlements from the Early Post-Roman period relative to the number of settlements known from Roman period (Zoetbrood et al., 2006; Van Munster, 2012) we reconstructed a population decline of around 90% in the southern and middle sand areas and of 50 % in northern and eastern sand areas.

Early Middle Ages: Carolingian period (ca. AD 800)

After the population decline around AD 500, population numbers increased towards AD 800, but did not reach the level of the Roman period. The strongest increase is found in the southern and middle sand areas. Based on the number of settlements (Zoetbrood et al., 2006) (corrected for differential settlement discovery rate) it was estimated that – on a national scale - 80% of the Roman-period population is present around AD 800. Assuming an equal distribution over the different sand areas, we projected this percentage on the population in the sand area as well.

Early Middle Ages: Ottonian period (ca. AD 1000)

Numbers based on interpolation between numbers AD 500 and 1500, taking into account the long-term demographic trend (Louwe Kooijmans et al., 2011; Van Munster, 2012).

Late Middle Ages AD (AD 1500)

Numbers AD 1600, minus 10% (see below). Strong population growth from AD 1500 to 1600 of ca. 50 % has been reported for mainly for the large towns in the Netherlands (Faber, 1965; McEvedy & Jones, 1978). These towns are however not situated in sandy areas, therefore the AD 1500 to 1600 population growth much lower here, estimated at 10%. The sharp rise in population numbers in the southern sand area can be explained by the rise of nearby Flemish towns (Theuws, 1989; Spek, 2004: 981-983; Vangheluwe & Spek, 2008; Van Bavel, 1999).

Late Middle Ages AD (AD 1600)

Population densities mentioned by Spek (2004: p966) derived from historical sources (Slicher van Bath, 1957; Bielemans, 1987; Arts, 1993; 1999; Kossmann, 1986). Ranges from these sources and their best guesses are indicated in Table D1.

Table D1 | Reconstructed population density in people per km². For explanation, see text.

	800 BC	125 BC	AD 200	AD 500	AD 800	AD 1000	AD 1500	AD 1600
Northern sand area	1.2	2.4	4.9	2.4	3.9	4.6	6.3	6.0-8.0 (7.0)
eastern sand area	1.2	2.5	4.9	2.5	3.9	5.9	10.8	12.0
Middle sand area	1.2	2.4	4.9	0.5	3.9	7.6	17.0	15-25 (17.0)
Southern sand area	1.2	2.5	4.9	0.5	3.9	12.3	33.3	25-50 (37.0)
All sand areas	1.2	2.5	4.9	1.3	3.9	7.2	15.3	19.6

D2 Drift-sand dates

Available on the Utrecht University Repository via:
<http://dspace.library.uu.nl/handle/1874/354561>

Dankwoord

Allereerst wil ik mijn begeleiders hartelijk danken voor het mogelijk maken van mijn promotieonderzoek, voor hun betrokkenheid, aanmoedigingen en feedback. Mijn promotoren Esther Jansma en Hans Middelkoop wil ik bedanken voor het helpen ontwikkelen van de grote lijn van het onderzoek en de cruciale details in de laatste fase van het schrijven. Esther, bedankt voor het initiëren van het project en je persoonlijke betrokkenheid gedurende het hele traject. Hans, bedankt voor al je tips over 'de grote vragen' en hun framing. Ook wil ik mijn dagelijkse begeleiders Esther Stouthamer en Wim Hoek bedanken. Al vroeg in mijn studie Aardwetenschappen wisten jullie mijn enthousiasme voor het vakgebied aan te wakkeren. Tijdens mijn promotie was het niet anders, na ieder overleg explodeerde het aantal ideeën of vonden we juist de beste focus. Graag wil ik ook Kim Cohen bedanken. Al vanaf mijn master heb je me alles geleerd over GIS en over de ondergrond en paleogeografie van Nederland. Door regelmatig even binnen te lopen en een veelheid aan ideeën te spuien hielp je mee het onderzoek vorm te geven en goed op papier te krijgen.

Marjolein en Rowin, jullie waren zowel mijn projectgenoten als kamergenoten. Ik kijk terug op een mooie en zeer prettige samenwerking en veel gezelligheid. Marjolein, bedankt voor al je gezelligheid, steun en inhoudelijke suggesties. Rowin, je bezoeken waren kort en krachtig. We bespraken dan het hele project, alle mogelijke strubbelingen en de archeologische wereld. En dat alles in hyperbolen, 'groots' was het. Kay, Tjalling, Marieke en Kees wil ik graag bedanken voor alle interessante en inhoudelijke discussies over respectievelijk 'vergeten' literatuur, estuaria, archeologie in het rivierengebied en strandwallen in Mexico. Jullie, maar ook alle mede-AIO's en overige collega's bij het departement Fysische Geografie: bedankt voor jullie support en tips bij de lange weg van het schrijven van een thesis. Dank ook voor alle gezelligheid bij de koffie, de lunchwandelingen en het plezier tijdens de cabaretjes.

Graag wil ik mijn medeauteurs van hoofdstuk 4, Peter Vos en Ad van der Spek, bedanken (beiden Deltares). Peter, bedankt voor het mij bijbrengen van alle ins en outs over de ontwikkeling van de Nederlandse kustvlakte, Ad bedankt voor al je suggesties die me hielpen een goede focus te vinden. Bert Groenewoudt (RCE) en Jakob Wallinga (WUR) wil ik bedanken voor hun bijdragen aan hoofdstuk 9. Tim Schuring, Tim Winkels, Hessel Woolderink en Arjan van Eijk, bedankt voor jullie hulp bij het veldwerk in het rivierengebied. Tim Schuring, dank voor het bellen van de boeren en je bijdrage aan de dateringen van de riviertakken voor je afstudeerproject. Hanneke Bos en Nelleke van Asch (ADC), dank jullie wel voor het uitzoeken van de macroresten voor de dateringen. De collega's bij TNO, Deltares, RCE, BOOR, RUG, WUR en diverse (archeologische) adviesbureaus wil ik bedanken voor de kennisuitwisseling en hun inspirerende ideeën tijdens de projectworkshops en daarbuiten. Margot Stoete wil ik bedanken voor haar hulp bij de opmaak van het proefschrift.

Vrienden en familie, bedankt voor jullie interesse, afleiding en gezelligheid. Medetonelers van toneelgroep Sporen: ik heb genoten van onze producties en in mijn drukke laatste jaar was het een fantastische afleiding! Pap en mam, bedankt voor jullie onvoorwaardelijke steun en voor het altijd stimuleren van mijn interesses en een open blik op de wereld. Eveline, dank voor al je steun en liefde, dat we nog maar lang samen de wereld om ons heen mogen blijven ontdekken.

References

- ADAMS, P.N., R.L. SLINGERLAND & N.D. SMITH (2004) Variations in natural levee morphology in anastomosed channel flood plain complexes. *Geomorphology*, 61(1 – 2), pp. 127 – 142.
- ALEXAKIS, D., A. SARRIS, T. ASTARAS & K. ALBANAKIS (2011) Integrated GIS, remote sensing and geomorphologic approaches for the reconstruction of the landscape habitation of Thessaly during the neolithic period. *Journal of Archaeological Science*, 38(1), pp. 89 – 100.
- ALFÖLDI, A. (1967) *Studien zur Geschichte der Weltkrise des 3 Jahrhunderts*, Darmstadt.
- ALLEN, J.R.L. (1965) A review of the origin and characteristics of recent alluvial sediments. *Sedimentology*, 5, pp. 89 – 191.
- ALLEN, J.R.L. (1999) Geological impacts on coastal wetland landscapes: some general effects of sediment autocompaction in the Holocene of northwest Europe. *The Holocene*, 9(1), pp. 1 – 12.
- ALLEN, J.R.L. (2000) Morphodynamics of Holocene salt marshes: a review sketch from the Atlantic and Southern North Sea coasts of Europe. *Quaternary Science Reviews*, 19(12), pp. 1155 – 1231.
- AMOS, C.L. (1995) Siliciclastic tidal flats. In G.M.E. Perillo, ed. *Geomorphology and Sedimentology of Estuaries*. Elsevier bv, pp. 273 – 306.
- ANTHONY, E.J., N. MARRINER & C. MORHANGE (2014) Human influence and the changing geomorphology of Mediterranean deltas and coasts over the last 6000 years: From progradation to destruction phase? *Earth-Science Reviews*, 139, pp. 336 – 361.
- ARNAUD-FASSETTA, G., N. CARCAUD, C. CASTANET & P.G. SALVADOR (2010) Fluvial palaeoenvironments in archaeological context: Geographical position, methodological approach and global change – Hydrological risk issues. *Quaternary International*, 216(1 – 2), pp. 93 – 117.
- ARNOLDUSSEN, S. (2008) *A Living Landscape: Bronze Age settlements in the Dutch river area (c. 2000-800 BC)*. Rijksuniversiteit Groningen.
- ARTS, P. (1993) De gemeentegrootte in West- en Zuid-Europa. Een kwantitatieve benadering. *Tijdschrift van de Belgische vereniging voor aardrijkskundige studies*, 62, pp. 377 – 404.
- ARTS, P. (1999) De grootte van de parochies in het hertogdom Brabant in de eerste helft van de zestiende eeuw. *Noordbrabants Historisch Jaarboek*, 16, pp. 141 – 159.
- ASH, J.E. & R.J. WASSON. (1983) Vegetation and sand mobility in the Australian desert dunefield. *Zeitschrift für Geomorphologie*, 45, p.7 – 25.
- ASLAN, A., W.J. AUTIN & M.D. BLUM (2005) Causes of River Avulsion: Insights from the Late Holocene Avulsion History of the Mississippi River, U.S.A. *Journal of Sedimentary Research*, 75(4), pp. 650 – 664.
- BAETEMAN, C. (1999) The Holocene depositional history of the IJzer palaeovalley (Western Belgian coastal plain) with reference to the factors controlling the formation of intercalated peat beds. *Geologica Belgica*, 2(3 – 4), pp. 39 – 72.
- BAETEMAN, C. (2005)(a) The Streif classification system: a tribute to an alternative system for organising and mapping Holocene coastal deposits. *Quaternary International*, 133 – 134, pp. 141 – 149.
- BAETEMAN, C. (2005)(b) How subsoil morphology and erodibility influence the origin and pattern of late Holocene tidal channels: case studies from the Belgian coastal lowlands. *Quaternary Science Reviews*, 24(18 – 19), pp. 2146 – 2162.
- BAETEMAN, C. (2008) Radiocarbon-dated sediment sequences from the Belgian coastal plain: testing the hypothesis of fluctuating or smooth late-Holocene relative sea-level rise. *The Holocene*, 18(8), pp. 1219 – 1228.
- BAETEMAN, C., D.B. SCOTT & M. VAN STRYDONCK (2002) Changes in coastal zone processes at a high sea-level stand: a late Holocene example from Belgium. *Journal of Quaternary Science*, 17(5 – 6), pp. 547 – 559.

- BAETEMAN, C., M. WALLER & P. KIDEN (2011) Reconstructing middle to late Holocene sea-level change: A methodological review with particular reference to "A new Holocene sea-level curve for the southern North Sea" presented by K.-E. Behre. *Boreas*, 40(4), pp. 557 – 572.
- BAGNOLD, R.A. (1941) *The physics of blown sand and desert dunes*, London: Methuen & Co.
- BARCKHAUSEN, J., H. PREUSS & H. STREIF (1977) *Ein lithologisches Ordnungsprinzip für das künstenholozän und seine Darstellung in Form von Profiltypen*, Geologischen Landesämtern in der Bundesrepublik Deutschland.
- BARTHOLDY, J. (2012) Salt Marsh Sedimentation. In R.A. Davis & R.W. Dalrymple, eds. *Principles of Tidal Sedimentology*. Dordrecht Heidelberg London New York: Springer Science, pp. 151 – 186.
- BATEMAN, M.D. & J. VAN HUISSTEDEN (1999) The timing of last-glacial periglacial and aeolian events, Twente, eastern Netherlands. *Journal of Quaternary Science*, 14(3), pp. 277 – 283.
- BATEMAN, M.D. & S.P. GODBY (2004) Late-Holocene inland dune activity in the UK: a case study from Breckland, East Anglia. *The Holocene*, 4, pp. 579 – 588.
- BECHERT, T. & W.J.H. WILLEMS (1995) *De Romeinse rijksgrens tussen Moezel en Noordzeekust*, Utrecht.
- BEETS, D.J. & A.J.F. VAN DER SPEK (2000) The Holocene evolution of the barrier and the back-barrier basins of Belgium and the Netherlands as a function of late Weichselian morphology, relative sea-level rise and sediment supply, *Netherlands Journal of Geosciences – Geologie & Mijnbouw*, 79(1), pp. 3 – 16.
- BEETS, D.J., L. VAN DER VALK & M.J.F. STIVE (1992) Holocene evolution of the coast of Holland. *Marine Geology*, 103, pp. 423 – 443.
- BEETS, D.J., A.J.F. VAN DER SPEK & L. VAN DER VALK (1994) *Holocene ontwikkeling van de Nederlandse kust*, Haarlem.
- BEETS, D.J., T.B. ROEP & W.E. WESTERHOFF (1996) The Holocene Bergen Inlet: closing history and related barrier progradation. *Mededelingen Rijks Geologische Dienst*, 57, pp. 97 – 131.
- BEETS, D.J., T.A.M. DE GROOT & H.A. DAVIES (2003) Holocene tidal back-barrier development at decelerating sea-level rise: a 5 millennia record, exposed in the western Netherlands. *Sedimentary Geology*, 158(1 – 2), pp. 117 – 144.
- BEHRE, K.-E. (1999) Die Veränderung der niedersächsischen Küstenlinien in den letzten 3000 Jahren und ihre Ursachen. Probleme der Küstenforschung in südlichen Nordseegebiet. *Isensee Verlag*, 26, pp. 9 – 33.
- BEHRE, K.-E. (2004) Coastal development, sea-level change and settlement history during the later Holocene in the Clay District of Lower Saxony (Niedersachsen), northern Germany. *Quaternary International*, 112(1), pp. 37 – 53.
- BEHRE, K.-E. (2007) A new Holocene sea-level curve for the southern North Sea. *Boreas*, 36(1), pp. 82 – 102.
- BELL, T. & G.R. LOCK (2000) Topography and cultural influences on walking the Ridgeway in later prehistoric times. In G.R. Lock, ed. *Beyond the map: archaeology and spatial technologies*,. IOS Press, pp. 85 – 100.
- BENNEMA, J. & L.J. PONS (1951) Donken, fluviatiel laagterras en eemzeeafzettingen in het westelijk gebied van de grote rivieren, pp. 126 – 137.
- BENNEMA, J. & K. VAN DER MEER (1952) De genese van Walcheren. *Boor & Spade*, pp. 245 – 255.
- BENNEMA, J., K. VAN DER MEER, C. DORSMAN & J.P. VAN DER FEEN (1952) *De bodemkartering van Walcheren*, Staatsdrukkerij Uitgeverijbedrijf.
- BERENDSEN, H.J.A. (1982) *De genese van het landschap in het zuiden van de provincie Utrecht*. Utrecht: Utrecht University.
- BERENDSEN, H.J.A. (1984)(a) Quantative analysis of radiocarbon-dates of the perimarine area in the Netherlands. *Geologie & Mijnbouw*, 63(4), pp. 343 – 350.
- BERENDSEN, H.J.A. (1984)(b) Problems of lithostratigraphic classification of Holocene deposits in the perimarine area of the Netherlands. *Geologie & Mijnbouw*, 63(4), pp. 351 – 354.
- BERENDSEN, H.J.A. (1984)(c) The evolution of the fluvial area in the western part of the Netherlands from 1000-1300 AD. *Geologie & Mijnbouw*, 63(3), pp. 231 – 240.

- BERENDSEN, H.J.A. (2007) History of geological mapping of the Holocene Rhine-Meuse delta, the Netherlands., pp. 165 – 177.
- BERENDSEN, H.J.A. & W.H. ZAGWIJN (1984) Some conclusions reached at the symposium on geological changes in the western Netherlands during the period 1000-1300 AD. *Geologie & Mijnbouw*, 63, pp. 225 – 229.
- BERENDSEN, H.J.A. & E. STOUTHAMER (2000) Late Weichselian and Holocene palaeogeography of the Rhine-Meuse delta, The Netherlands. *Palaeogeography, Palaeoclimatology, Palaeoecology*, 161(3 – 4), pp. 311 – 335.
- BERENDSEN, H.J.A. & E. STOUTHAMER (2001) *Palaeogeographic development of the Rhine-Meuse delta, The Netherlands*, Assen: Koninklijke Van Gorcum.
- BERENDSEN, H.J.A. & K.P. VOLLEBERG (2007) New prospects in geomorphological and geological mapping of the Rhine-Meuse delta – Application of detailed digital elevation maps based on laser altimetry. *Netherlands Journal of Geosciences – Geologie & Mijnbouw*, 86(1), pp. 15 – 22.
- BERENDSEN, H.J.A., T.E. TÖRNQVIST & H.J.T. WEERTS (1986) De geologisch-geomorfologische kaart van de Bommelerwaard. In *Het landschap van de Bommelerwaard*. pp. 15 – 20.
- BERENDSEN, H.J.A., W.Z. HOEK & E. SCHORN (1995) Late Weichselian and Holocene river channel changes of the rivers Rhine and Meuse in the Netherlands (Land van Maas en Waal). *Paläoklimaforschung/Palaeoclimate Research*, 14, pp. 151 – 171.
- BERENDSEN, H.J.A., K.M. COHEN & E. STOUTHAMER (2001) The geological-geomorphological map and palaeogeographic maps of the Rhine-Meuse delta. In H.J.A. Berendsen & E. Stouthamer, eds. *Palaeogeographic development of the Rhine-Meuse delta, The Netherlands*. Assen: Koninklijke Van Gorcum, pp. 49 – 50.
- BERENDSEN, H.J.A., K.M. COHEN & E. STOUTHAMER (2007) The use of GIS in reconstructing the Holocene palaeogeography of the Rhine-Meuse delta, The Netherlands. *International Journal of Geographical Information Science*, 21(5), pp. 589 – 602.
- BERTRAND, S. & C. BAETEMAN (2005) Sequence mapping of Holocene coastal lowlands: the application of the Streif classification system in the Belgian coastal plain. *Quaternary International*, 133 – 134, pp. 151 – 158.
- BIANCHI, T.S. (2016) *Deltas and humans: A long relationship how threatened by global change*, Oxford University Press.
- BICKET, A. & L. TIZZARD (2015) A review of the submerged prehistory and palaeolandscapes of the British Isles. *Proceedings of the Geologists' Association*, 126, pp. 643 – 663.
- BIELEMANS J. (1987) Boeren op het Drentse zand 1600-1910. Een nieuwe visie op de “oude” landbouw. *AAG Bijdragen*, 29.
- BISSCHOPS, J.H., J.P. BROERTJES & W. DOBMA (1985) *Toelichtingen bij de geologische kaart van Nederland 1: 50.000. Blad Eindhoven West (51W)*, Haarlem: Rijks Geologische Dienst.
- BOHNCKE, S.J.P. (1991) *Palaeohydrological changes in the Netherlands during the last 13.000 years*.
- BORGER, G. (1992) Draining-digging-dredging; the creation of a new landscape in the peat areas of the low countries. In J. Verhoeven, ed. *Fens and bogs in the Netherlands: vegetation, history, nutrient dynamics and conservation*. Dordrecht/London/Boston: Kluwer Academic Publishers, pp. 131 – 172.
- BOS, I.J. & E. STOUTHAMER (2011) Spatial and temporal distribution of sand-containing basin fills in the Holocene Rhine-Meuse delta, the Netherlands. *The Journal of Geology*, 119(6), pp. 641 – 660.
- BOS, I.J., H. FEIKEN, F. BUNNIK & J. SCHOKKER (2009) Influence of organics and clastic lake fills on distributary channel processes in the distal Rhine-Meuse delta (The Netherlands). *Palaeogeography, Palaeoclimatology, Palaeoecology*, 284(3 – 4), pp. 355 – 374.
- BOS, I.J., F.S. BUSSCHERS & W.Z. HOEK (2012) Organic-facies determination: a key for understanding facies distribution in the basal peat layer of the Holocene Rhine-Meuse delta, The Netherlands. *Sedimentology*, 59(2), pp. 676 – 703.
- BOSCH J.H.A (1990) *Toelichtingen bij de Geologische kaart van Nederland 1:50.000. Blad Assen West (12W) en Blad Assen Oost (12O)*, Haarlem.

- BOUMAN, M.T.I.J., L.P. VERNIERS & K. VAN KAPPEL (2012) Location, the construction and preservation of Roman burial mounds in the Dutch river delta. In W. Bebermeier, R. Hebenstreit, E. Kaiser, & J. Krause, eds. *Landscape Archaeology. Proceedings of the International Conference Held in Berlin, 6th – 8th June 2012, eTopoi Special Volume 3*, pp. 155 – 159.
- BREIER, M. (2013) Getting around in the past: historical road modelling. In K. Kriz, W. Cartwright, & M. Kinberger, eds. *Understanding different geographies, lecture notes in geoinformation and cartography*. Berlin, Heidelberg: Springer, pp. 215 – 226.
- BREW, D.S., T. HOLT, K. PYE & R. NEWSHAM (2000) Holocene sedimentary evolution and palaeocoastlines of the Fenland embayment, eastern England. *Geological Society, London, Special Publications*, 166(1), pp. 253 – 273.
- BRIERLEY, G.J., R.J. FERGUSON & K.J. WOOLFE (1997) What is a fluvial levee? *Sedimentary Geology*, 114(1 – 4), pp. 1 – 9.
- BRINKKEMPER, O. (2013) Pollenonderzoek waterputten W3 en W4. In E. Mittendorf, B. Vermeulen, & M. van der Wal, eds. *Op Kloostergronden. Archeologisch, (bouw)historisch en landschappelijk onderzoek naar het erf De Olthof en de naastgelegen watermolen in Epse-Noord, Rapportage Archeologie Deventer 38*. pp. 92 – 98.
- BRONK RAMSEY, C. & S. LEE (2013) Recent and planned developments of the program OxCal. *Radiocarbon*, 55(2 – 3), pp. 720 – 730.
- BROSTRÖM, A., M.-J. GAILLARD, M. IHSE & B.V. ODGAARD (1998) Pollen-landscape relationships in modern analogues of ancient cultural landscapes in southern Sweden – a first step towards quantification of vegetation openness in the past. *Vegetation History and Archaeobotany*, 7(4), pp. 189 – 201.
- BROUWER BURG, M. (2013) Reconstructing “total” paleo-landscapes for archaeological investigation: An example from the central Netherlands. *Journal of Archaeological Science*, 40(5), pp. 2308 – 2320.
- BROUWERS, W., E. JANSMA & M. MANDERS (2013) Romeinse scheepsresten in Nederland. *Archeobrief*, 17(4), pp. 13 – 27.
- BROUWERS, W., E. JANSMA & M. MANDERS (2015) Middeleeuwse scheepsresten in Nederland: de Vroege Middeleeuwen (500-1050). *Archeobrief*, 19(3), pp. 6 – 24.
- BROWN, A.G. (1997) *Alluvial geoarchaeology: floodplain archaeology and environmental change*, Cambridge University Press.
- BROWN, A.G. (2008) Geoarchaeology, the four dimensional (4D) fluvial matrix and climatic causality. *Geomorphology*, 101(1 – 2), pp. 278 – 297.
- BRUINS, H.J. (1981) Vechten tegen het zand: stuifzandbestrijding in de marken langs de Overijsselse Vecht. *Bijdragen uit het land van IJssel en Vecht*, pp. 7 – 21.
- BRYANT, M., P. FALK & C. PAOLA (1995) Experimental study of avulsion frequency and rate of deposition. *Geology*, 23(4), pp. 365 – 368.
- BUISMAN, J. & A. VAN ENGELEN (1996) *Duizend jaar weer, wind en water in de Lage Landen: Dl. 2: 1300-1450*, Franeker: Van Wijnen.
- BUISMAN, J. & A. VAN ENGELEN (1998) *Duizend jaar weer, wind en water in de Lage Landen: Dl. 3: 1450-1575*, Franeker: Van Wijnen.
- BUISMAN, J. & A. VAN ENGELEN (2000) *Duizend jaar weer, wind en water in de Lage Landen: Dl. 4: 1575-1675*, Franeker: Van Wijnen.
- BUNGENSTOCK, F. & H.J.T. WEERTS (2010) The high-resolution Holocene sea-level curve for Northwest Germany: global signals, local effects or data-artefacts? *International Journal of Earth Sciences*, 99(8), pp. 1687 – 1706.
- BÜNTGEN, U., W. TEGEL, K. NICOLUSSI, M. MCCORMICK, D. FRANK, V. TROUET, J.O. KAPLAN, F. HERZIG, K.-U. HEUSSNER, H. WANNER, J. LUTERBACHER & J. ESPER (2011) 2500 years of European climate variability and human susceptibility. *Science*, 331(6017), pp. 578 – 582.
- BÜNTGEN, U., V.S. MYGLAN, F.C. LJUNGQVIST, M. MCCORMICK, N. DI COSMO, M. SIGL, J. JUNGCLAUS, S. WAGNER, P.J. KRUSIC, J. ESPER, J.O. KAPLAN, M.A.C. DE VAAN, J. LUTERBACHER, L. WACKER, W.

- TEGEL & A.V. KIRDYANOV (2016) Cooling and societal change during the Late Antique Little Ice Age from 536 to around 660 AD. *Nature Geoscience*, pp. 1 – 6.
- BURROUGH, P.A. (1986) Principles of geographical information systems for land resources assessment. *Geocarto International*, 1(3), p.54.
- BUSSCHERS, F.S., R.T. VAN BALEN, K.M. COHEN, C. KASSE, H.J.T. WEERTS, J. WALLINGA & F.P.M. BUNNIK (2008) Response of the Rhine-Meuse fluvial system to Saalian ice-sheet dynamics. *Boreas*, 37(3), pp. 377 – 398.
- BUTZER, K.W. (1982) *Archaeology as human ecology: method and theory for a contextual approach*, Cambridge University Press.
- BUTZER, K.W. (2008) Challenges for a cross-disciplinary geoarchaeology: The intersection between environmental history and geomorphology. *Geomorphology*, 101(1 – 2), pp. 402 – 411.
- CARMIGGELT, A. & A.J. GUIRAN (1997) Prestedelijke bewoningssporen en vondsten uit het trace van de Willemsspoortunnel te Rotterdam: prehistorie, Romeinse tijd en Middeleeuwen (vóór circa 1150). In A. Carmiggelt, A. Guiran, & M. Van Trierum, eds. *BOORbalans 3 Archeologisch onderzoek in het trace van de Willemsspoortunnel te Rotterdam*. pp. 73 – 112.
- CASPARIE, W.A. & W. GROENMAN-VAN WAATERINGE (1980) Palynological analysis of Dutch barrows. *Palaeohistoria*, 22, p.7 – 66.
- CASPARIE, W.A. & J.G. STREEFKERK (1992) Climatological, stratigraphic and palaeo-ecological aspects of mire development. In *Fens and bogs in the Netherlands: vegetation, history, nutrient dynamics and conservation*. Springer, pp. 81 – 129.
- CASTEL, I.I.Y. (1991) *Late Holocene eolian drift sands in Drenthe (the Netherlands)*. Utrecht University.
- CASTEL, I.I.Y., E.A. KOSTER & R.T. SLOTBOOM (1989) Morphogenetic aspects and age of Late Holocene eolian drift sands in Northwest Europe. *Zeitschrift für Geomorphologie*, 33, pp. 1 – 26.
- CAZANACLI, D. & N.D. SMITH (1998) A study of morphology and texture of natural levees-Cumberland Marshes, Saskatchewan, Canada. *Geomorphology*, 25(1 – 2), pp. 43 – 55.
- CHARMAN, D.J. (2010) Centennial climate variability in the British Isles during the mid-late Holocene. *Quaternary Science Reviews*, 29(13 – 14), pp. 1539 – 1554.
- CHEYETTE, F.L. (2008) The disappearance of the ancient landscape and the climatic anomaly of the early Middle Ages: a question to be pursued. *Early Medieval Europe*, 16(2), pp. 127 – 165.
- CITTER, C. (2012) Modelli predittivi e archeologia postclassica: vecchi strumenti e nuove prospettive. In F. Redi & A. Forgone, eds. *Atti del VI convegno nazionale della SAMI, L' Aquila*,. Firenze, pp. 3 – 6.
- CLARKE, M.L. & H.M. RENDELL (2009) The impact of North Atlantic storminess on western European coasts: a review. *Quaternary International*, 195(1), pp. 31 – 41.
- CLARKE, M.L. & H.M. RENDELL (2011) Atlantic storminess and historical sand drift in Western Europe: Implications for future management of coastal dunes. *Journal of Coastal Conservation*, 15(1), pp. 227 – 236.
- CLARKE, M., H.M. RENDELL, J.-P. TASTET, B. CLAVÉ & L. MASSÉ (2002) Late-Holocene sand invasion and North Atlantic storminess along the Aquitaine Coast, southwest France. *The Holocene*, 12, pp. 231 – 238.
- CLARKE, M.L., H.M. RENDELL & M.L. CLARKEL (2006) North Atlantic Oscillation on sand invasion. *The Holocene*, 3(2006), pp. 341 – 355.
- CLAVÉ, B., L. MASSÉ, P. CARBONEL & J.P. TASTET (2001) Holocene coastal changes and infilling of the La Perroche marsh (French Atlantic coast). *Oceanologica Acta*, 24(4), pp. 377 – 389.
- CLEMMENSEN, L.B., K. PYE, A. MURRAY & J. HEINEMEIER (2001) Sedimentology, stratigraphy and landscape evolution of a Holocene coastal dune system, Lodbjerg, NW Jutland, Denmark. *Sedimentology*, 48(1), pp. 3 – 27.
- CLEMMENSEN, L.B., M. BJØRNSSEN, A. MURRAY & K. PEDERSEN (2007) Formation of aeolian dunes on Anholt, Denmark since AD 1560: A record of deforestation and increased storminess. *Sedimentary Geology*, 199(3 – 4), pp. 171 – 187.

- CLEMMENSEN, L.B., A. MURRAY, J. HEINEMEIER & R. DE JONG (2009) The evolution of Holocene coastal dunefields, Jutland, Denmark: A record of climate change over the past 5000 years. *Geomorphology*, 105(3 – 4), pp. 303 – 313.
- CLEVERINGA, J. (2000) *Reconstruction and modelling of Holocene coastal evolution of the western Netherlands*. Universiteit Utrecht.
- CNOSSEN, J. (1958) Enige opmerkingen omtrent het ontstaan van het beneden-Boornegebied. *Boor & Spade*, pp. 24 – 38.
- COHEN, K.M. (2003) *Differential subsidence within a coastal prism – Late-Glacial-Holocene tectonics in the Rhine-Meuse delta, the Netherlands*, Utrecht.
- COHEN, K.M. (2005) 3D geostatistical interpolation and geological interpretation of paleo-groundwater rise in the Holocene coastal prism in the Netherlands. In *River deltas – Concepts, Models and Examples*. SEMP, pp. 341 – 364.
- COHEN, K.M., M.J.P. GOUW & J.P. HOLTEN (2005) Fluvio-deltaic floodbasin deposits recording differential subsidence within a coastal prism (central Rhine–Meuse delta, The Netherlands). *Special Publications IAS*, 35, pp. 295 – 320.
- COHEN, K.M., E. STOUTHAMER, W.Z. HOEK, H.J.A. BERENDSEN & H.F.J. KEMPEN (2009) *Zand in banen – zanddiepte kaarten van het Rivierengebied en het IJsseldal in de provincies Gelderland en Overijssel*.
- COHEN, K.M., E. STOUTHAMER, H.J. PIERIK & A.H. GEURTS (2012) Digitaal Basisbestand Paleogeografie van de Rijn-Maas Delta/Rhine-Meuse Delta Studies' Digital Basemap for Delta Evolution and Palaeogeography.
- COHEN, K.M., P.L. GIBBARD & H.J.T. WEERTS (2014)(a) North Sea palaeogeographical reconstructions for the last 1 Ma. *Netherlands Journal of Geosciences – Geologie & Mijnbouw*, 93(1 – 2), pp. 7 – 29.
- COHEN, K.M., S. ARNOLDUSSEN, G. ERKENS, Y.T. POPTA & L.J. TAAL (2014)(b) *Archeologische verwachtingskaart uiterwaarden rivierengebied*, Deltares rapport 1207078, Utrecht.
- COHEN, K.M., W.H.J. TOONEN & H.J.T. WEERTS (2016) *Overstromingen van de Rijn gedurende het Holoceen: relevantie van de grootste overstromingen voor archeologie van het Nederlandse rivierengebied*, Deltares report 1209091, Utrecht.
- COHEN, K.M., R. DE BRUIJN, V. MARGES, S. DE VRIES, H.J. PIERIK, P.C. VOS, G. ERKENS & M.P. HIJMA (2017)(a) *Production of buried-landscape maps for Holocene-covered Netherlands, Map layer T0123 for the RCE Kenniskaart portal*, Deltares rapport 1210450-000-BGS-0013. Utrecht, 105 pp.
- COHEN, K.M., R. DAMBRINK, R. DE BRUIJN, V.C. MARGES, G. ERKENS, H.J. PIERIK, K. KOSTER, J. STAFLEU, J. SCHOKKER & M.P. HIJMA (2017)(b) Mapping buried Holocene landscapes: past lowland environments, palaeoDEMs and preservation in GIS. *Nederlandse Archeologische Rapportage* 55, pp. 73-95
- CORENBLIT, D., E. TABACCHI, J. STEIGER & A.M. GURNELL (2007) Reciprocal interactions and adjustments between fluvial landforms and vegetation dynamics in river corridors: A review of complementary approaches. *Earth-Science Reviews*, 84(1 – 2), pp. 56 – 86.
- COSTAS, S., S. JEREZ, R.M. TRIGO, R. GOBLE & L. REBÊLO (2012) Sand invasion along the Portuguese coast forced by westerly shifts during cold climate events. *Quaternary Science Reviews*, 42, pp. 15 – 28.
- CUNLIFFE, B. (2004) *Facing the Ocean. The Atlantic and its Peoples*, Oxford.
- CUNNINGHAM, A.C., M.A.J. BAKKER, S. VAN HETEREN, B. VAN DER VALK, A.J.F. VAN DER SPEK, D.R. SCHAART & J. WALLINGA (2011) Extracting storm-surge data from coastal dunes for improved assessment of flood risk. *Geology*, 39(11), pp. 1063 – 1066.
- DAVID, B. & J. THOMAS (2016) *Handbook of landscape archaeology*, Routledge.
- DAVIS, J.R. & M. MCCORMICK (2008) *The Long Morning of Medieval Europe. New Directions in Early Medieval Studies*, Hampshire: Ashgate.
- DAVIS, R.A. & M.O. HAYES (1984) What is a wave-dominated coast? *Marine Geology*, 60(1 – 4), pp. 313 – 329.
- DE BAKKER, H. (1970) Purposes of soil classification. *Geoderma*, 4, pp. 195 – 208.
- DE BAKKER, H. & J. SCHELLING (1966) Systeem van bodemclassificatie voor Nederland: de hogere niveaus.

- DE BAKKER, H. & J. SCHELLING (1989) *Systeem van bodemclassificatie voor Nederland. De hogere niveaus, 2e gewijzigde druk*, Wageningen: PUDOC.
- DE BOER, A.G., W.N.H. LAAN, W. WALDUS & W.K. VAN ZIJVERDEN (2008) LIDARbased surface height measurements: applications in archaeology. In B. Fischer & A. Dakouri, eds. *Beyond Illustration: 2d and 3d Digital Technologies as Tools for Discovery in Archaeology. British Arch. Rep. Int. Series 1805*. pp. 69 – 77.
- DE BOER, T.A. & L.J. PONS (1960) *Bodem en grasland in de Vijfheerenlanden*, Bennekom.
- DE BONT, C. (2008) *Vergeten land: ontginning, bewoning en waterbeheer in de westnederlandse veengebieden (800-1350)*, Wageningen.
- DE GANS, W. & K. VAN GIJSEL (1996) The Late-Weichselian morphology of The Netherlands and its influence on the Holocene coastal development D.J. Beets, M.M. Fischer, & W. De Gans, eds. *Mededelingen Rijks Geologische Dienst*, 57, pp. 11 – 25.
- DE GROOT, T.A.M., H.A. VAN ADRICHEM BOOGAERT, M.M. FISCHER, B. KLIJNSTRA, H.M. VAN MONTFRANS, H. UIL, M.W. TER WEE, M.J. VAN WEEPEREN & J.G. ZANDSTRA (1987) *Toelichtingen bij de Geologische Kaart van Nederland 1:50.000, Blad Heerenveen West (11W) en Oost (11O)*, Haarlem.
- DE JONG, J. (1982) Chronostratigraphic subdivision of the Holocene in the Netherlands. In J. Mangerud, H. Birks, & Jäger, K-D, eds. *Uppsala*. pp. 71 – 74.
- DE JONG, J.D., B.P. HAGEMAN & F.F.E. VAN RUMMELEN (1960) De Holocene afzettingen in het deltagebied. *Geologie & Mijnbouw*, 39, pp. 654 – 660.
- DE KEYZER, M. (2016) All we are is dust in the wind: The social causes of a “subculture of coping” in the late medieval coversand belt. *Journal for the History of Environment and Society* 1, 1(1), pp. 1 – 35.
- DE KEYZER, M. & M.D. BATEMAN (in review) Reconstructing the causes of historical sand drifts in Breckland (East Anglia, England). *The Holocene*.
- DE LANGEN, G., H.A. GROENENDIJK & W. SCHWARZ (2013) Tussen klei en zand: leven en werken in de veengebieden/Zwischen Marsch und Geest: Leben und Arbeiten in den Moorgebieten. In *De archeologie van het Friese kustgebied/Die Archäologie des friesischen Küstenraums*. pp. 173 – 187.
- DE MULDER, E.F.J. & J.H.A. BOSCH (1982) Holocene stratigraphy, radiocarbon datings and paleogeography of central and northern north-holland (the Netherlands). *Mededelingen Rijks Geologische Dienst*, 36(3), pp. 111 – 160.
- DE ROO, H. (1953) De bodemgesteldheid van Noord-Kennemerland. *Verslagen van landbouwkundige onderzoeken*, 59(3), p.202.
- DE SMET, L.A.H. (1962) *Het Dollardgebied, bodemkundige en landbouwkundige onderzoeken in het kader van de bodemkartering. De Bodemkartering van Nederland, Verslagen Landbouwkundig Onderzoek*. Den Haag.
- DE VRIES, F., W.J.M. DE GROOT, T. HOOGERLAND & J. DENNEBOOM (2003) *De bodemkaart van Nederland digitaal; Toelichting bij inhoud, actualiteit en methodiek en korte beschrijving van additionele informatie*, Wageningen.
- DEEBEN, J., B. GROENEWOUDT, D. HALLEWAS, C. VAN ROOIJEN & P. ZOETBROOD (2005) Op zoek naar de archeologische voorraad. In M.H. Van den Driesch & W.J.H. Willems, eds. *Innovatie in de Nederlandse archeologie. Liber amicorum voor Roel W. Brandt*. Gouda, p. 37 – 54.
- DEGEAI, J.P., B. DEVILLERS, L. DEZILEAU, H. OUESLATI & G. BONY (2015) Major storm periods and climate forcing in the Western Mediterranean during the Late Holocene. *Quaternary Science Reviews*, 129, pp. 37 – 56.
- DEKKER, C. (1983) Het Kromme Rijngebied in de middeleeuwen. *Stichtse Historische Reeks*, 9.
- DEN HELD, A.J., M. SCHMITZ & G. VAN WIRDUM (1992) Types of terrestrializing fen vegetation in the Netherlands. In J. Verhoeven, ed. *Fens and Bogs in the Netherlands*. Kluwer, pp. 237 – 321.
- DEN OUDEN, J., U.G.W. SASS-KLAASSEN & P. COPINI (2007) Dendrogeomorphology – a new tool to study drift-sand dynamics. *Netherlands Journal of Geosciences*, 86(4), pp. 355 – 363.

- DENYS, S. (2007) *De contrasterende Holocene sediment successie langsheen het westelijk en oostelijk deel van de Belgische kust: oorzaak en gevolgen*. Brussel.
- DERESE, C., D. VANDENBERGHE, N. EGGERMONT, J. BASTIAENS, R. ANNAERT & P. VAN DEN HAUTE (2010) A medieval settlement caught in the sand: Optical dating of sand-drifting at Pulle (N Belgium). *Quaternary Geochronology*, 5(2 – 3), pp. 336 – 341.
- DERMODY, B.J., H.J. DE BOER, M.F.P. BIERKENS, S.L. WEBER, M.J. WASSEN & S.C. DEKKER (2011) Revisiting the humid Roman hypothesis: novel analyses depict oscillating patterns. *Climate of the Past Discussions*, 7(4), pp. 2355 – 2389.
- DIJKMANS, J.W.A. & A.G. WINTLE (1991) Methodological Problems in Thermoluminescence Dating of Weichselian Coversand and Late Holocene Drift Sand from the Lutterzand Area, the Netherlands. *Geologie & Mijnbouw/Netherlands Journal of Geosciences*, 70(1), pp. 21 – 33.
- DIJKMANS, J.W.A., A.G. WINTLE & V. MEJDAHL (1988) Some thermoluminescence properties and dating of eolian sands from the Netherlands. *Quaternary Science Reviews*, 7(3 – 4), pp. 349 – 355.
- DIJKMANS, J.W.A., J.M. VAN MOURIK & A.G. WINTLE (1992) Thermoluminescence dating of aeolian sands from polycyclic soil profiles in the southern Netherlands. *Quaternary Science Reviews*, 11(1 – 2), pp. 85 – 92.
- DIJKSTRA, M. (2011) *Rondom de mondingen van Rijn & Maas. Landschap en bewoning tussen de 3e en 9e eeuw in Zuid-Holland, in het bijzonder de Oude Rijnstreek*, Sidestone Press.
- DONDERS, T.H., F.P.M. BUNNIK & M.T.I.J. BOUMAN (2010) *De Nederlandse biostratigrafie database, v1.0: pollen biozones*, Utrecht.
- DOORENBOSCH, M. (2013) *Ancestral heaths: reconstructing the barrow landscape in the Central and Southern Netherlands*, Sidestone Press.
- DOORENBOSCH, M. & J.M. VAN MOURIK (2016) The impact of ancestral heath management on soils and landscapes: a reconstruction based on paleoecological analyses of soil records in the middle and southeast Netherlands. *Soil*, 2, pp. 311 – 324.
- DUBOIS, G. (1924) *Recherches sur les terrains quaternaires du Nord de la France*. Lille.
- EBBING, J. & C. LABAN (1996) Geological history of the offshore part of the Western Scheldt area, since Eemian times. In D.J. Beets, M.M. Fischer, & W. De Gans, eds. *Coastal studies on the Holocene of the Netherlands*. Haarlem: Rijks Geologische Dienst, pp. 251 – 267.
- EBBING, J.H.J., H.J.T. WEERTS & W.E. WESTERHOFF (2003) Towards an integrated land – sea stratigraphy of the Netherlands. *Quaternary Science Reviews*, 22(15 – 17), pp. 1579 – 1587.
- EDELMAN, C.H., L. ERINGA, K.J. HOEKSEMA, J.J. JANTZEN & P.J.R. MODDERMAN (1950) *Een bodemkartering van de Bommelerwaard boven den Meidijk*, STIBOKA.
- EGBERTS, H. (1950) *De bodemgesteldheid van de Betuwe*, Wageningen.
- EIMERMANN, E., L. VERNIERS & K. VAN CAMPENHOUT (2009) *Archeologisch onderzoek aan de Tiendweg – Volkstuinencomplex Groenakker, gemeente Gouda Een Inventariserend Veldonderzoek in de vorm van proefsleuven*, EISMA, D. & W. DE WOLFF (1980) The development of the westernmost part of the Wadden Sea in historical time. In *Geomorphology of the Wadden Sea area*. Rotterdam: Balkema, pp. 95 – 103.
- ENGELS, S., M. BAKKER, S. BOHNCKE, C. CERLI, W. HOEK, B. JANSSEN, T. PETERS, H. RENSSEN, D. SACHSE, J. VAN AKEN, V. VAN DEN BOS, B. VAN GEEL, R. VAN OOSTROM, T. WINKELS & M. WOLMA (2016) Centennial-scale lake-level lowstand at Lake Uddelermeer (The Netherlands) indicates changes in moisture source region prior to the 2.8-kyr event. *The Holocene*, 26(7), pp. 1 – 17.
- ENTE, P.J., J. KONING & R. KOOPSTRA (1986) *Flevobericht 258: De bodem van Oostelijk Flevoland*, Lelystad.
- ERKENS, G. & K.M. COHEN (2009) Quantification of intra-Holocene sedimentation in the Rhine-Meuse delta: a record of variable sediment delivery. In G. Erkens, ed. *Sediment dynamics in the Rhine catchment*. Utrecht, pp. 117 – 172.

- ERKENS, G., T. HOFFMANN, R. GERLACH & J. KLOSTERMANN (2011) Complex fluvial response to Lateglacial and Holocene allogenic forcing in the Lower Rhine Valley (Germany). *Quaternary Science Reviews*, 30(5 – 6), pp. 611 – 627.
- ERKENS, G., W.H.J. TOONEN, K.M. COHEN & M.A. PRINS (2013) Unravelling mixed sediment signals in the floodplains of the Rhine catchment using end member modelling of grain size distributions. In *ICFS proceedings 2010*.
- ERKENS, G., M.J. VAN DER MEULEN & H. MIDDELKOOP (2016) Double trouble: subsidence and CO₂ respiration due to 1,000 years of Dutch coastal peatlands cultivation. *Hydrogeology Journal*, 24(3), pp. 551 – 568.
- ERVYNCK, A., C. BAETEMAN, H. DEMIDDELE, Y. HOLLEVOET, M. PIETERS, J. SCHELVIS, D. TYS, V. STRYDONCK & F. VERHAEGHE (1999) Human occupation because of a regression, or the cause of a transgression: A critical review of the interaction between geological events and human occupation in the Belgian coastal plain during the first millennium AD. *Probleme der Küstenforschung im südlichen Nordseegebiet*, 26, pp. 97 – 121.
- EVANS, G. (1965) Intertidal flat sediments and their environments of deposition in the Wash. *Quarterly Journal of the Geological Society*, 121(1 – 4), pp. 209 – 240.
- FABER J.A. (1965) Population changes and economic development in the northern Netherlands: a historical survey. *A.A.G. Bijdragen*, 12, pp. 47 – 110.
- FAN, D. (2012) Open-Coast Tidal Flats. In R.A. Davis & R.W. Dalrymple, eds. *Principles of Tidal Sedimentology*. Dordrecht Heidelberg London New York: Springer Science, pp. 187 – 230.
- FARRELL, K.M. (2001) Geomorphology, facies architecture, and high-resolution, non-marine sequence stratigraphy in avulsion deposits, Cumberland Marshes, Saskatchewan. *Sedimentary Geology*, 139(2), pp. 93 – 150.
- FILGUEIRA-RIVERA, M., N.D. SMITH & R.L. SLINGERLAND (2007) Controls on natural levee development in the Columbia River, British Columbia, Canada. *Sedimentology*, 54(4), pp. 905 – 919.
- FISK, H.N. (1947) *Fine-grained alluvial deposits and their effects on Mississippi River activity*, Vicksburg, MS.
- FITCH, S., K. THOMSON & V. GAFFNEY (2005) Late Pleistocene and Holocene depositional systems and the palaeogeography of the Dogger Bank, North Sea. *Quaternary Research*, 64(2), pp. 185 – 196.
- FLEMMING, B.W. (2012) Siliciclastic Back-Barrier Tidal Flats. In R.A. Davis & R.W. Dalrymple, eds. *Principles of Tidal Sedimentology*. Dordrecht Heidelberg London New York: Springer Science, pp. 231 – 268.
- FOVET, É. & K. ZAKŠEK (2014) Path Network Modelling and network of agglomerated settlements: a case study in Languedoc (South eastern France). In S. Polla & P. Verhagen, eds. *Computational approaches to the study of movement in archaeology. Theory, practice and interpretation of factors and effects of long term landscape formation and transformation*. Berlin: de Gruyter, pp. 43 – 72.
- FRENZEL, B. (1994) Evaluation of land surfaces cleared from forests in the Roman Iron Age and the time of migrating Germanic tribes based on regional pollen diagrams. *Gustav Fischer Verlag*.
- FRENZEL, B., L. REISCH & B. GLÄSE (1992) Evaluation of land surfaces cleared from forests by prehistoric man in Early Neolithic times and the time of migrating Germanic tribes. *Gustav Fischer Verlag*.
- FREY, R.W. & P.B. BASAN (1985) Coastal Salt Marshes. In R.A. Davis, ed. *Coastal Sedimentary Environments*. New York, Berlin, Heidelberg, Tokyo: Springer-Verlag, pp. 225 – 301.
- FUNABIKI, A., Y. SAITO, V.V. PHAI, H. NGUYEN & S. HARUYAMA (2012) Natural levees and human settlement in the Song Hong (Red River) delta, northern Vietnam. *The Holocene*, 22(6), pp. 637 – 648.
- GAO, S. & M.B. COLLINS (2014) Holocene sedimentary systems on continental shelves. *Marine Geology*.
- GEHRELS, W.R. (2010) Sea-level changes since the Last Glacial Maximum: an appraisal of the IPCC Fourth Assessment Report. *Journal of Quaternary Science*, 25(1), pp. 26 – 38.
- GEITL, R., M. DONEUS & M. FERA (2008) Cost Distance Analysis in an Alpine Environment: Comparison of Different Cost Surface Modules. In A. Poluschny, K. Lambers, & I. Herzog, eds. *Layers of Perception. Proceedings*

- of the 35th International Conference on Computer Applications and Quantitative Methods in Archaeology (CAA). Berlin, pp. 342 – 350.
- GERRETS, D.A. (2010) *Op de grens van land en water: dynamiek van landschap en samenleving in Frisia gedurende de Romeinse tijd en de Volksverhuizingstijd*, Barkhuis.
- GILBERTSON, D.D. (1999) Atlantic Coastline: 14,000 Years of Diverse Geomorphological, Climatic and Human Impacts. *Journal of Archaeological Science*, pp. 439 – 469.
- GIOSAN, L., J.P. DONNELLY, S. CONSTANTINESCU, F. FILIP, I. OVEJANU, A. VESPREMEANU-STROE, E. VESPREMEANU & G.A.T. DULLER (2006) Young Danube delta documents stable Black Sea level since the middle Holocene: Morphodynamic, paleogeographic, and archaeological implications. *Geology*, 34(9), p.757.
- GIOSAN, L., P.D. CLIFT, M.G. MACKLIN, D.Q. FULLER, S. CONSTANTINESCU, J.A. DURCAN, T. STEVENS, G. A.T. DULLER, A.R. TABREZ, K. GANGAL, R. ADHIKARI, A. ALIZAI, F. FILIP, S. VANLANINGHAM & J.P.M. SYVITSKI (2012) Fluvial landscapes of the Harappan civilization. *Proceedings of the National Academy of Sciences*, 109(26), pp.E1688 – E1694.
- GOLDBERG, P. & R.I. MACPHAIL. (2008) *Practical and theoretical geoarchaeology*, Blackwell Science.
- GOODBRED, S.L. & S.A. KUEHL (1999) Holocene and modern sediment budgets for the Ganges-Brahmaputra river system: Evidence for highstand dispersal to flood-plain, shelf, and deep-sea depocenters.
- GOTTSCHALK, M.K.E. (1975) *Storm Surges and River Floods in The Netherlands I (the period 1400–1600)*, Assen: van Gorcum.
- GOUDIE, A. (2006) *The human impact on the natural environment* sixth edit, Blackwell Science.
- GOUW, M.J.P. (2007) Alluvial architecture of fluvio-deltaic successions: a review with special reference to Holocene settings. *Netherlands Journal of Geosciences – Geologie & Mijnbouw*, 86(3), pp. 211 – 227.
- GOUW, M.J.P. (2008) Alluvial architecture of the Holocene Rhine-Meuse delta (the Netherlands). *Sedimentology*, 55(5), pp. 1487 – 1516.
- GOUW, M.J.P. & G. ERKENS (2007) Architecture of the Holocene Rhine-Meuse delta (the Netherlands) – A result of changing external controls. *Netherlands Journal of Geosciences – Geologie & Mijnbouw*, 86(1), pp. 23 – 54.
- GRIEDE, J.W. (1978) *Het ontstaan van Frieslands Noordhoek: een fysisch-geografisch onderzoek naar de Holocene ontwikkeling van een zoekleigebied*. Vrije Universiteit Amsterdam.
- GROENWOUDT, B.J. (1989) Prehistorische woonplaatsen in een landschap. *Tijdschrift voor landschapsecologie en milieukunde*, 6, pp. 301 – 316.
- GROENWOUDT, B.J. (1994) *Prospectie, waardering en selectie van archeologische vindplaatsen: een beleidsgerichte verkenning van middelen en mogelijkheden*. Amsterdam: Amsterdam University.
- GROENWOUDT, B.J., H. VAN HAASTER, R. VAN BEEK & O. BRINKKEMPER (2007) Towards a reverse image. Botanical research into the landscape history of the eastern Netherlands (1100 B.C. – A.D. 1500). *Landscape History*, 29(1), pp. 17 – 33.
- GROENHUIJZEN, M.R., J.W.H.P. VERHAGEN (2015) Exploring the dynamics of transport in the Dutch Limes. *eTopoi Journal for Ancient Studies*, 1, pp. 15 – 47.
- GROENHUIJZEN, M.R., J.W.H.P. VERHAGEN (2016) Testing the robustness of local network metrics in research on archeological local transport networks. *Frontiers in Digital Humanities*, 3(6).
- GROENMAN-VAN WAATERINGE, W. (1986) Grazing possibilities in the Neolithic of the Netherlands based on palynological data.
- GROENMAN-VAN WAATERINGE, W. (1992) Palynology and archaeology: the history of a plaggen soil from the Veluwe, The Netherlands. *Review of Palaeobotany and Palynology*, 73(1 – 4), pp. 87 – 98.
- GROOTHEDDE, M. (2013) *Een vorstelijke palts te Zutphen?: macht en prestige op en rond het plein's-Gravenhof van de Karolingische tijd tot aan de stadsrechtverlening*, Leiden: Medieval Archaeology, Faculty of Archaeology, Leiden University.

- GUCCIONE, M.J. (2008) Impact of the alluvial style on the geoarcheology of stream valleys. *Geomorphology*, 101(1 – 2), pp. 378 – 401.
- GUIRAN, A. (1996) Rotterdam: gasfabriek Kralingen. *Archeologische kroniek van Holland over 1995*, Holland 28, pp. 343 – 344.
- GUIRAN, A. (1997) Geologische waarnemingen in het tracé van de Willemsspoortunnel en de bewoningsgeschiedenis van Rotterdam. In A. Carmiggelt, A. Guiran, & M. Van Trierum, eds. *BOORbalans 3 Archeologisch onderzoek in het trace van de Willemsspoortunnel te Rotterdam*. Rotterdam, pp. 25 – 43.
- GUNNINK, J.L., D. MALJERS, S.F.V. GESSEL, A. MENKOVIC & H.J. HUMMELMAN (2013) Digital Geological Model (DGM): a 3D raster model of the subsurface of the Netherlands. *Netherlands Journal of Geosciences*, 92(1), pp. 33 – 46.
- HACK-TEN BROEKE, M.J.D., C.V. BEEK, T. HOOGLAND, M. KNOTTERS, J.P. MOL-DIJKSTRA, R.L.M. SCHILS, A. SMIT & F. DE VRIES (2009) *Kaderrichtlijn bodem: basismateriaal voor eventuele prioritaire gebieden*, Wageningen.
- HAGEMAN, B.P. (1963) De profieltype-legenda van de nieuwe geologische kaart voor het zeelei- en rivierkleigebied. *Tijdschrift voor het Koninklijk Nederlands Aardrijkskundig Genootschap, Tweede Reeks*, 80, pp. 217 – 229.
- HAGEMAN, B.P. (1964) *Toelichtingen bij de Geologische kaart van Nederland 1:50.000. Blad Goeree en Overflakkee*, Haarlem.
- HAGEMAN, B.P. (1969) Development of the western part of the Netherlands during the Holocene. *Geologie & Mijnbouw*, 48, pp. 373 – 388.
- HAJEK, E.A. & M.A. WOLINSKY (2012) Simplified process modeling of river avulsion and alluvial architecture: Connecting models and field data. *Sedimentary Geology*, 257, pp. 1 – 30.
- HALLEWAS, D. (1986) Zuid-Holland. *Regionaal Historisch tijdschrift Holland*, 18(6).
- HALSALL, G. (2007) *Barbarian migrations and the Roman West*, 376 – 568, Cambridge University Press.
- HAMEROW, H.F. (2002) *Early Medieval Settlements. The archaeology of Rural Communities in Northwest Europe 400-900*, Oxford.
- HANEBUTH, T.J.J., U. PROSKE, Y. SAITO, V.L. NGUYEN & T.K.O. TA (2012) Early growth stage of a large delta – Transformation from estuarine-platform to deltaic-progradational conditions (the northeastern Mekong River Delta, Vietnam). *Sedimentary Geology*, 261 – 262, pp. 108 – 119.
- HAVINGA, A.J. (1969) A physiographic analysis of a part of the Betuwe, a Dutch river clay area. *Mededelingen Landbouwhogeschool Wageningen*, 69(3), p.47.
- HAVINGA, A.J. & A. OP 'T HOF (1983) *Physiography and formation of the Holocene floodplain along the lower course of the Rhine in the Netherlands*, Landbouwhogeschool Wageningen.
- HEEREN, S. (2009) *Romanisering van rurale gemeenschappen in de civitas Batavorum: de casus Tiel-Passewaaij*. Amersfoort: Vrije Universiteit, Amsterdam.
- HEEREN, S. (2015) The depopulation of the Lower Rhine region in the 3rd century: An archaeological perspective. In N. Roymans, T. Derks, & H. Hiddink, eds. *The Roman villa of hoogeloon and the archaeology of the periphery*, Amsterdam Archaeological Studies 22. Amsterdam, pp. 269 – 292.
- HEIDINGA, H.A. (1984)(a) Indications of severe drought during the 10th-century AD from an inland dune area in the central Netherlands. *Geologie & Mijnbouw*, 63(3), pp. 241 – 248.
- HEIDINGA, H.A. (1984)(b) *De Veluwe in de vroege middeleeuwen: aspecten van de nederzittingsarcheologie van Kootwijk en zijn buien*.
- HEIDINGA, H.A. (1987) *Medieval settlement and economy north of the Lower Rhine: archeology and history of Kootwijk and the Veluwe (the Netherlands)*, Van Gorcum Ltd.
- HEIRI, O., A. LOTTER & G. LEMKE (2001) Loss on ignition as a method for estimating organic and carbonate content in sediments: reproducibility and comparability of results. *Journal of paleolimnology*, 25, pp. 101 – 110.

- HEITMULLER, F.T., P.F. HUDSON & R.H. KESEL (2017) Overbank sedimentation from the historic A.D. 2011 flood along the Lower Mississippi River, USA. *Geology*, 45(2), pp. 107 – 110.
- HELLER, P.L. & C. PAOLA (1996) Downstream changes in alluvial architecture: an exploration of controls on channel-stacking patterns. *Journal of Sedimentary Research*, 66(2).
- HENDRIKS, J., H. VAN ENCKEVORT & M.J. NICASIE (2017) De overgang van de laat-Romeinse tijd naar de vroege middeleeuwen in Zuid-Nederland. *Nederlandse Archeologische Rapporten (NAR)*.
- HENDRIKX, P. (1983) *Rijn en Maas: landschap en bewoning van de Romeinse tijd tot ca. 1000*. University of Amsterdam.
- HERZOG, I. (2013)(a) Theory and Practice of Cost Functions. In F. Contreras, M. Farjas, & F.J. Melero, eds. *Fusion of Cultures. Proceedings of the 38th Annual Conference on Computer Applications and Quantitative Methods in Archaeology, Granada, Spain, April 2010. BAR International Series 2494*. Granada, pp. 375 – 282.
- HERZOG, I. (2013)(b) Least-cost networks. In G. Earl, T. Sly, A. Chrysanthi, P. Murrieta-Flores, C. Papadopoulos, I. Romanowska, & D. Wheatley, eds. *Archaeology in the Digital Era. CAA 2012, Proceedings of the 40th Annual Conference of Computer Applications and Quantitative Methods in Archaeology (CAA)*. Southampton, pp. 240 – 51.
- HERZOG, I. (2013)(c) Calculating Accessibility. In G. Earl, T. Sly, A. Chrysanthi, P. Murrieta-Flores, C. Papadopoulos, I. Romanowska, & D. Wheatley, eds. *Archaeology in the Digital Era. Volume II, e-Papers from the 40th Conference on Computer Applications and Quantitative Methods in Archaeology*. Southampton, pp. 720 – 734.
- HERZOG, I. (2014) Least-cost Paths – Some Methodological Issues. *Internet Archaeology*, 36.
- HERZOG, I. & A. POSLUSCHNY (2011) Tilt-slope-dependent Least Cost Path Calculations Revisited. In E. Jerem, F. Redő, & V. Szeverényi, eds. *On the Road to Reconstructing the Past. Proceedings of the 36th CAA conference 2008 in Budapest*. Budapest, pp. 212 – 218.
- HESEL, R., J. STOLTE & M.J. RIKSEN (2011) *Huidige maatregelen tegen water -en winderosie in Nederland*, Wageningen.
- HESELINK, A.W., H.J.T. WEERTS & H.J.A. BERENDSEN (2003) Alluvial architecture of the human-influenced river Rhine, The Netherlands. *Sedimentary Geology*, 161(3 – 4), pp. 229 – 248.
- HEYVAERT, V.M.A. & C. BAETEMAN (2007) Holocene sedimentary evolution and palaeocoastlines of the Lower Khuzestan plain (southwest Iran). *Marine Geology*, 242(1 – 3), pp. 83 – 108.
- HEYVAERT, V.M.A. & J. WALSTRA (2016) The role of long-term human impact on avulsion and fan development. *Earth Surface Processes and Landforms*, 41(15), pp. 2137 – 2152.
- HIDDINK, H.A. (2003) Het grafritueel in de Late IJzertijd en Romeinse tijd in het Maas-Demer-Scheldegebied, in het bijzonder van twee grafvelden bij Weert. *Zuidnederlandse Archeologische Rapporten (ZAR)*, 11.
- HIJMA, M.P. & K.M. COHEN (2011) Holocene transgression of the Rhine river mouth area, The Netherlands/Southern North Sea: palaeogeography and sequence stratigraphy. *Sedimentology*, 58(6), pp. 1453 – 1485.
- HIJMA, M.P., K.M. COHEN, G. HOFFMANN, A.J.F.V. DER SPEK & E. STOUTHAMER (2009) From river valley to estuary: the evolution of the Rhine mouth in the early to middle Holocene (western Netherlands, Rhine-Meuse delta). *Netherlands Journal of Geosciences*, 88(1), pp. 13 – 53.
- HIJMA, M.P., A.J.F. VAN DER SPEK & S. VAN HETEREN (2010) Development of a mid-Holocene estuarine basin, Rhine-Meuse mouth area, offshore The Netherlands. *Marine Geology*, 271(3 – 4), pp. 198 – 211.
- HILGERS, A. (2007) *The chronology of Late Glacial and Holocene dune development in the northern Central European lowland reconstructed by optically stimulated luminescence (OSL) dating*.
- HILL, C.L. (2014) Rivers: Environmental Archaeology. In *Encyclopedia of Global Archaeology*. New York: Springer, pp. 6343 – 6351.
- HOBO, N. (2015) *The sedimentary dynamics in natural and human-influenced delta channel belts*. Utrecht: Utrecht University.
- HOEK, W.Z. (1997) Late-glacial and early Holocene climatic events and chronology of vegetation development in the Netherlands. *Vegetation History and Archaeobotany*, 6(4), pp. 197 – 213.

- HOFFMANN, T., G. ERKENS, K.M. COHEN, P. HOUBEN, J. SEIDEL & R. DIKAU (2007) Holocene floodplain sediment storage and hillslope erosion within the Rhine catchment. *The Holocene*, 17(1), pp. 105 – 118.
- HOMEIER, H. (1977) Einbruch und weitere Entwicklung des Dollart bis um 1600. *Jahresbericht 1976 der Forschungsstelle für Insel- und Küstenschutz der Niedersächsischen Wasserwirtschaftsverwaltung, Nordeney*, pp. 39 – 81.
- HORSTEN, F.H. (2005) *Doorgaande wegen in Nederland, 16e tot 19e eeuw. Een historische wegenatlas*.
- HOWARD, A.J., S.J. KLUIVING, M. ENGEL & V.M. HEYVAERT (2015) Geoarchaeological records in temperate European river valleys: Quantifying the resource, assessing its potential and managing its future. *Quaternary International*, 367, pp. 42 – 50.
- HUDSON, P.F. (2004) Geomorphic context of the prehistoric Huastec floodplain environments: Lower Punuco basin, Mexico. *Journal of Archaeological Science*, 31(8), pp. 653 – 668.
- HUDSON, P.F. & F.T. HEITMULLER (2003) Local- and watershed-scale controls on the spatial variability of natural levee deposits in a large fine-grained floodplain: Lower Punuco Basin, Mexico. *Geomorphology*, 56(3 – 4), pp. 255 – 269.
- HUDSON, P.F., H. MIDDELKOOP & E. STOUTHAMER (2008) Flood management along the Lower Mississippi and Rhine Rivers (The Netherlands) and the continuum of geomorphic adjustment. *Geomorphology*, 101(1 – 2), pp. 209 – 236.
- JACOBS, E., A. PAVLOVIC, O. BRINKKEMPER & P. VAN RIJN (2001) *Een archeologisch onderzoek van een dam met duikers uit de Romeinse Tijd*.
- JAMES, E. (1988) The Northern World in the Dark Ages. In G. Holmes, ed. *The Oxford illustrated history of Medieval Europe*. Oxford: Oxford University Press.
- JANSMA, E. (2013) Towards sustainability in dendroarchaeology: the preservation, linkage and reuse of tree-ring data from the cultural and natural heritage in Europe. In N. Bleicher, J. Koninger, H. Schlichtherle, & M. Woltersdorf, eds. *DENDRO -Chronologie, -Typologie, -Ökologie*. pp. 169 – 176.
- JANSMA, E., R.J. VAN LANEN, P. BREWER & R. KRAMER (2012) The DCCD: a digital data infrastructure for tree-ring research. *Dendrochronologia*, 30(4), p.249 – 251.
- JANSMA, E., M.T.I.J. GOUW-BOUMAN, R.J. VAN LANEN, H.J. PIERIK, K.M. COHEN, B.J. GROENEWOUDT, W.Z. HOEK, E. STOUTHAMER & H. MIDDELKOOP (2014) The Dark Age of the Lowlands in an interdisciplinary light: people, landscape and climate in The Netherlands between AD 300 and 1000. *European Journal of Post – Classical Archaeologies*, 4, pp. 473 – 478.
- JANSSEN, C.R. (1972) The palaeoecology of plant communities in the Dommel valley, North Brabant, Netherlands. *The Journal of Ecology*, 60(2), pp. 411 – 437.
- JARRETT, J.T. (1976) *Tidal prism – inlet area relationships*, General Investigation of Tidal Inlets, Coastal Engineering Research Center, US Army Corps of Engineers, Report no. 3, pp. 32.
- JELGERSMA, S. (1961) Holocene sea level changes in the Netherlands. *Mededelingen Rijks Geologische Stichting*, 6(7), p.100.
- JELGERSMA, S. (1979) Sea-level changes in the North Sea basin. In E. Oele, R.T.E. Schüttenhelm, & A. Wiggers, eds. *The Quaternary History of the North Sea*. Upsala: Acta Univ. Upsala Symp. Annum Quingentesimum Celebrantis, pp. 233 – 248.
- JELGERSMA, S. (1983) The Bergen inlet, transgressive and regressive holocene shoreline deposits in the northwestern Netherlands. *Geologie & Mijnbouw*, 62(3), pp. 471 – 486.
- JELGERSMA, S. & P.J. ENTE (1977) Genese van het Holocene. In C.J. van Staaldin, ed. *Geologisch onderzoek van het Nederlandse Waddengebied*. Haarlem: Rijks Geologische Dienst, pp. 23 – 36.
- JELGERSMA, S., J. DE JONG, W.H. ZAGWIJN & J.F. VAN REGTEREN ALTENA (1970) The coastal dunes of western Netherlands; geology, vegetational history and archaeology. *Mededelingen Rijks Geologische Dienst*, pp. 93 – 167.

- JELGERSMA, S., M.J.F. STIVE & L. VAN DER VALK (1995) Holocene storm surge signatures in the coastal dunes of the western Netherlands. *Marine Geology*, 125, pp. 95 – 110.
- JONES, L.S. & S.A. SCHUMM (1999) Causes of avulsion: an overview. In N.D. Smith & J. Rogers, eds. *Fluvial Sedimentology VI*. International Association of Sedimentologists, p. 171 – 178.
- JONGEPIER, I., T. SOENS, E. THOEN, V. VAN EETVELDE, P. CROMBÉ & M. BATS (2011) The brown gold: A reappraisal of medieval peat marshes in Northern Flanders (Belgium). *Water History*, 3(2), pp. 73 – 93.
- JUNGERIUS, P.D. & M.J.P.M. RIKSEN (2010) Contribution of laser altimetry images to the geomorphology of the Late Holocene inland drift sands of the European Sand Belt. *Baltica*, 23(1), pp. 59 – 70.
- KALIS, A., S. KARG, J. MEURERS-BALKE & H. TEUNISSEN-VAN OORSCHOT (2008) Mensch und Vegetation am Unteren Niederrhein während der Eisen- und Römerzeit. In M. Müller, H.-J. Schalles, & N. Zieling, eds. *Colonia Ulpia Traiana, Xanten und sein Umland in römischer zeit*. pp. 31 – 48.
- KAPLAN, J.O., K.M. KRUMHARDT & N. ZIMMERMANN (2009) The prehistoric and preindustrial deforestation of Europe. *Quaternary Science Reviews*, 28(27 – 28), pp. 3016 – 3034.
- KARSSENBERG, D. & J.S. BRIDGE (2008) A three-dimensional numerical model of sediment transport, erosion and deposition within a network of channel belts, floodplain and hill slope: extrinsic and intrinsic controls on floodplain dynamics and alluvial architecture. *Sedimentology*, 55(6), pp. 1717 – 1745.
- KASSE, C. (1995) Younger Dryas cooling and fluvial response (Maas River, the Netherlands). *Geologie & Mijnbouw*, 74, pp. 251 – 256.
- KASSE, C. (2002) Sandy aeolian deposits and environments and their relation to climate during the Last Glacial Maximum and Lateglacial in northwest and central Europe. *Progress in Physical Geography*, 26(4), pp. 507 – 532.
- KEUNEN, L. (2011) Middeleeuwse dorpsvorming in Oost-Nederland. Een verkenning van de historische relatie tussen hoven, kerken en dorpen. *Historisch-Geografisch Tijdschrift*, 29(2), pp. 60 – 72.
- KIDEN, P., L. DENYS & P. JOHNSTON (2002) Late Quaternary sea-level change and isostatic and tectonic land movements along the Belgian-Dutch North Sea coast: geological data and model results. *Journal of Quaternary Science*, 17(5 – 6), pp. 535 – 546.
- KISS, T., V.G. OROSZI, G. SIPOS, K. FIALA & B. BENYHE (2011) Accelerated overbank accumulation after nineteenth century river regulation works: A case study on the Maros River, Hungary. *Geomorphology*, 135(1 – 2), pp. 191 – 202.
- KLASZ, G., W. RECKENDORFER, H. GABRIEL, C. BAUMGARTNER, R. SCHMALFUSS, & D. GUTKNECHT (2014) Natural levee formation along a large and regulated river: The Danube in the National Park Donau-Auen, Austria. *Geomorphology*, 215, pp. 20 – 33.
- KLEINHANS, M.G., H.J.T. WEERTS & K.M. COHEN (2010) Avulsion in action: Reconstruction and modelling sedimentation pace and upstream flood water levels following a Medieval tidal-river diversion catastrophe (Biesbosch, The Netherlands, 1421 – 1750 AD). *Geomorphology*, 118(1 – 2), pp. 65 – 79.
- KLEINHANS, M.G., R.I. FERGUSON, S.N. LANE & R.J. HARDY (2013) Splitting rivers at their seams: Bifurcations and avulsion. *Earth Surface Processes and Landforms*, 38(1), pp. 47 – 61.
- KLUIVING, S.J. & E. GUTTMANN-BOND (2012) *Landscape archaeology between art and science: From a multi- to an interdisciplinary approach*, Amsterdam.
- KLUIVING, S.J., F. LEHMKUHL & B. SCHÜTT (2012) Landscape archaeology at the LAC 2010 conference. *Quaternary International*, 251, pp. 1 – 6.
- KLUIVING, S.J., M.E. BEKKEMA & N.G.A.M. ROYMANS (2015) Mass migration through soil exhaustion: Transformation of habitation patterns in the southern Netherlands (1000 BC-500 AD). *Catena*, 132, pp. 139 – 150.
- KNOL, E. (1993) *De Noordnederlandse kustlanden in de vroege middeleeuwen*. Groningen: Vrije Universiteit Amsterdam.

- KOBASHI, T., K. KAWAMURA, J.P. SEVERINGHAUS, J.M. BARNOLA, T. NAKAEGAWA, B.M. VINTHER, S.J. JOHNSEN & J.E. BOX (2011) High variability of Greenland surface temperature over the past 4000 years estimated from trapped air in an ice core. *Geophysical Research Letters*, 38(21).
- KOLB, C.R. (1963) Sediments forming the bed and banks of the Lower Mississippi River and their effects on river migration. *Sedimentology*, 2, p.227 – 234.
- KOLSTRUP, E. (1997) Wind blown sand and palynological records in past environments. *Aarhus Geoscience*, 7, pp. 91 – 100.
- KOOISTRA, L.I., M.V. DINTER, M.K. DÜTTING & P.V. RIJN (2013) Could the local population of the Lower Rhine delta supply the Roman army? Part 1: The archaeological and historical framework. *JALC*, 4(2), pp. 5 – 23.
- KOOMEN, A.J.M. & G.J. MAAS (2004) *Geomorfologische Kaart Nederland (GKN); Achtergrond document bij het landsdekkende digitale bestand*, Wageningen.
- KOPP, R.E., C.C. HAY, C.M. LITTLE & J.X. MITROVICA (2015) Geographic variability of sea-level change. *Current Climate Change Reports*, 1(3), pp. 192 – 204.
- KOSIAN, M.C., R.J. VAN LANEN & H.J.T. WEERTS (2016) Dorestads' rise and fall: how the local landscape influenced the growth, prosperity and disappearance of an early-medieval emporium. In H. Willemsen, A. Kik, ed. *Golden Middle Ages in Europe. New Research into Early-Medieval Communities and Identities*. Brepols Publishers.
- KOSSMANN, E.H. (1986) *De Lage Landen 1780-1890*, Amsterdam.
- KOSTER, E.A. (1978) *De stuifzanden van de Veluwe: een fysisch-geografische studie (The aeolian drift sands of the Veluwe, Central Netherlands); a physical geographical study*. Universiteit van Amsterdam.
- KOSTER, E.A. (1982) Terminology and lithostratigraphic division of (surficial) sandy eolian deposits in the Netherlands - an evaluation. *Geologie & Mijnbouw*, 61(2), pp. 121 – 129.
- KOSTER, E.A. (2005) Recent advances in luminescence dating of Late Pleistocene (Cold-Climates) aeolian sand and loess deposits in western Europe. *Permafrost and Periglacial Processes*, 16(1), pp. 131 – 143.
- KOSTER, E.A. (2009) The "European Aeolian Sand Belt": Geoconservation of Drift Sand Landscapes. *Geoheritage*, 1(2 – 4), pp. 93 – 110.
- KOSTER, E.A., I.I.Y. CASTEL & R.L. NAP (1993) Genesis and sedimentary structures of late Holocene aeolian drift sands in northwest Europe. *Geological Society Special Publication*, 72, pp. 247 – 267.
- KOSTER, K., J. STAFLEU & K.M. COHEN (2016)(a) Generic 3D interpolation of Holocene base-level rise and provision of accommodation space, developed for the Netherlands coastal plain and infilled palaeovalleys. *Basin Research*, pp. 1 – 23.
- KOSTER, K., G. ERKENS & C. ZWANENBURG (2016)(b) A new soil mechanics approach to quantify and predict land subsidence by peat compression. *Geophysical Research Letters*, 43(20), pp. 10792 – 10799.
- KOSTER, K., G. DE LANGE, R. HARTING, E. DE HEER, & H. MIDDELKOOP (2017) Characterizing the void ratio and compressibility of Holocene peat with CPT for assessing coastal-deltaic subsidence, in: Koster (Ed.), 3D characterization of Holocene peat in the Netherlands: Implications for coastal-deltaic subsidence.
- KOZARSKI, S. & B. NOWACZYK (1991) Lithofacies variation and chronostratigraphy of Late Vistulian and Holocene aeolian phenomena in northwestern Poland. *Zeitschrift für Geomorphologie*, 90, pp. 107 – 122.
- KRUIVER, P., E. VAN DEDEM, R. ROMIJN, G. DE LANGE, M. KORFF, J. STAFLEU, J.L. GUNNINK, J.J. RODRIGUEZ-MAREK, A., BOMMER, J. VAN ELK & D. DOORNHOF (2017) An integrated shear-wave velocity model for the Groningen gas field. *The Netherlands, Bulletin of Earthquake Engineering*, 15(9), pp.3355 – 3580.
- KUIJT, I. & N. GORING-MORRIS (2002) Foraging, farming, and social complexity in the Pre-Pottery Neolithic of the southern Levant: a review and synthesis. *Journal of World Prehistory*, 16(4), pp. 361 – 440.
- KVAMME, K.L. (1988) Development and testing of quantitative models. In W.J. Judge & L. Sebastian, eds. *Quantifying the present and predicting the past: theory, method, and application of archaeological predictive modelling*. Denver, pp. 324 – 428.

- LAMB, H. (1972) The cold Little Ice Age climate of about 1550 to 1800. In *Climate: present, past and future*. London: Methuen & Co., p. 107.
- LAMBECK, K., H. ROUBY, A. PURCELL, Y. SUN & M. SAMBRIDGE (2014) Sea level and global ice volumes from the Last Glacial Maximum to the Holocene. *Proceedings of the National Academy of Sciences of the United States of America*, 111(43), pp. 15296 – 15303.
- LARSEN, A. (2016) The mouldboard plough in the Danish area 200 – 1500 AD. In J. Klapste, ed. *Agrarian technology in the medieval landscape (Proceedings Ruralia X, 9 – 15 September 2013, Slovakia)*. pp. 225 – 236.
- LASCARIS, M.A. (1999) Zandverstuivingen op de noordwestelijke Veluwe. *Historisch geografisch tijdschrift*, pp. 54 – 63.
- LASCARIS, M.A. & A.M.J. DE KRAKER (2013) Dikes and other hydraulic engineering works from the Late Iron Age and Roman period on the coastal area between Dunkirk and the Danish Bight. In E. Thoen, G. Borger, A. M. J. de Kraker, T. Soens, D. Tys, L. Ervoet, & H. J. Weerts, eds. *Landscapes or seascapes? The history of the coastal environment in the North Sea area reconsidered*. CORN Publication Series 13, pp. 177 – 198.
- LECCE, S.A. (1997) Spatial patterns of historical overbank sedimentation and floodplain evolution, Blue River, Wisconsin. *Geomorphology*, 18, pp. 265 – 277.
- LEENDERS, K.A.H.W. (2016) Datering zandverstuiving in Zuid-Brabant.
- LENSELINK, G. & R. KOOPSTRA (1994) Ontwikkelingen in het Zuiderzeegebied; van Meer Flevo, via de Almere-lagune, tot Zuiderzee. In M. Rappol & C.M. Soonius, eds. *In de Bodem van Noord- Holland*. Amsterdam: Lingua Terra, pp. 129 – 138.
- LEOPOLD, L.B. & M.G. WOLMAN (1960) River meanders. *Geological Society of America Bulletin*, 71(6), pp. 769 – 793.
- LESOURD, S., P. LESUEUR, J.C. BRUN-COTTAN, J.P. AUFFRET, N. POUPINET & B. LAIGNEL (2001) Morphosedimentary evolution of the macrotidal Seine estuary subjected to human impact. *Estuaries and Coasts*, 24(6), pp. 940 – 949.
- LEWIN, J. & P.J. ASHWORTH (2014) The negative relief of large river floodplains. *Earth-Science Reviews*, 129, pp. 1 – 23.
- LIVINGSTONE, I. & A. WARREN (1996) *Aeolian geomorphology: an introduction*, Longman.
- LJUNGQVIST, F.C. (2010) A new Reconstruction of Temperature Variability in the Extra-Tropical Northern Hemisphere During the Last Two Millennia. *Geografiska Annaler: Series A, Physical Geography*, 92(3), pp. 339 – 351.
- LLOBERA, M. (2000) Understanding movement: a pilot model towards the sociology of movement. In G. R. Lock, ed. *Beyond the map: archaeology and spatial technologies*. Amsterdam: IOS Press, pp. 65 – 84.
- LONG, A.J., J.B. INNES, J.M. LLOYD, M.M. RUTHERFORD, I. SHENNAN, J.R. KIRBY & M.J. TOOLEY (1998) Holocene sea-level change and coastal evolution in the Humber estuary, eastern England: an assessment of rapid coastal change. *The Holocene*, 8(2), pp. 229 – 247.
- LONG, A.J., M.P.P. WALLER & P. STUPPLES (2006) Driving mechanisms of coastal change: Peat compaction and the destruction of late Holocene coastal wetlands. *Marine Geology*, 225(1 – 4), pp. 63 – 84.
- LOUWE KOOIJMANS, L.P. (1974) *The Rhine/Meuse delta: four studies on its prehistoric occupation and Holocene geology*. Leiden: Leiden University.
- LOUWE KOOIJMANS, L.P. (1995) Prehistory or paradise? Prehistory as a reference for modern nature development, the Dutch case. *Mededelingen Rijks Geologische Dienst*, 52, pp. 415 – 424.
- LOUWE KOOIJMANS, L.P., P.W. VAN DEN BROEKE, H. FOKKENS & A. VAN GIJN (2011) *Nederland in de prehistorie*. Amsterdam.
- MACKLIN, M.G. (1999) Holocene river environments in prehistoric Britain: human interaction and impact. *Journal of Quaternary Science*, 14(6), pp. 521 – 530.

- MACKLIN, M.G., W.H.J. TOONEN, J.C. WOODWARD, M.A.J. WILLIAMS, C. FLAUX, N. MARRINER, K. NICOLL, G. VERSTRAETEN, N. SPENCER & D. WELSBY (2015) A new model of river dynamics, hydroclimatic change and human settlement in the Nile Valley derived from meta-analysis of the Holocene fluvial archive. *Quaternary Science Reviews*, 130(December), pp. 109 – 123.
- MAGILLIGAN, F.J. (1985) Historical Floodplain Sedimentation in the Galena River Basin, Wisconsin and Illinois. *Annals of the Association of American Geographers*, 75(4), pp. 583 – 594.
- MAKASKE, B., H.J.A. BERENDSEN & M.H.M. VAN REE (2007) Middle Holocene Avulsion-Belt Deposits in the Central Rhine-Meuse Delta, The Netherlands. *Journal of Sedimentary Research*, 77, pp. 110 – 123.
- MAKASKE, B., D.G. SMITH & H.J.A. BERENDSEN (2002) Avulsions, channel evolution and floodplain sedimentation rates of the anastomosing upper Columbia River, British Columbia, Canada. *Sedimentology*, 49(5), pp. 1049 – 1071.
- MAKASKE, B., G.J. MAAS & D.G.V. SMEERDIJK (2008) The age and origin of the Gelderse IJssel. *Netherlands Journal of Geosciences – Geologie & Mijnbouw*, 87(4), pp. 323 – 337.
- MAKASKE, B., B.H.P. MAATHUIS, C.R. PADOVANI, C. STOLKER, E. MOSSELMAN & R.H.G. JONGMAN (2012) Upstream and downstream controls of recent avulsions on the Taquari megafan, Pantanal, south-western Brazil. *Earth Surface Processes and Landforms*, 37(12), pp. 1313 – 1326.
- MANN, M. (2003) Little Ice Age. In M.C. MacCracken & J.S. Perry, eds. *Encyclopedia of Global Environmental Change, Volume 1, The Earth System: Physical and Chemical Dimensions of Global Environmental Change*. John Wiley & Sons.
- MARKUS, W.C. (1984) Bodemkaart van Nederland 1: 50.000: *Toelichtingen bij kaartblad 38 West Gorinchem*, Wageningen.
- MARRINER, N., C. MORHANGE & J.P. GOIRAN (2010) Coastal and ancient harbour geoarchaeology. *Geology Today*, 26(1), pp. 21 – 27.
- MARRINER, N., C. FLAUX, C. MORHANGE & J.D. STANLEY (2013) Tracking Nile Delta Vulnerability to Holocene Change. *PLoS ONE*, 8(7), pp. 1 – 9.
- MARTINIUS, A.W. & J.H. VAN DEN BERG (2011) *Atlas of sedimentary structures in estuarine and tidally-influenced river deposits of the Rhine-Meuse-Scheldt system: Their application to the interpretation of analogous outcrop and subsurface depositional systems*, Houten: EAGE Publications.
- MARZOLF, J.E. (1988) Controls on late Paleozoic and early Mesozoic eolian deposition of the western United States. *Sedimentary Geology*, 56(1), pp. 167 – 191.
- MASELLI, V. & F. TRINCARDI (2013) Man made deltas. *Scientific reports*, 3 (1926).
- MATHYS, M. (2009) *The Quaternary geological evolution of the Belgian Continental Shelf, southern North Sea*. UGent.
- MAUZ, B. & F. BUNGENSTOCK (2007) How to reconstruct trends of late Holocene relative sea level: A new approach using tidal flat clastic sediments and optical dating. *Marine Geology*, 237(3 – 4), pp. 225 – 237.
- MCCORMICK, M. (2007) *Origins of the European Economy. Communications and Commerce AD 300-900*, New York.
- MCCORMICK, M. (2008) Discovering the Early Medieval Economy. In J.R. Davis & M. McCormick, eds. *The Long Morning of Medieval Europe. New Directions in Early Medieval Studies*. Ashgate, Hampshire, pp. 13 – 18.
- MCCORMICK, M., U. BÜNTGEN, M.A. CANE, E.R. COOK, K. HARPER, P. HUYBERS, T. LITT, S.W. MANNING, P.A. MAYEWSKI, A.F.M. MORE, K. NICOLUSSI & W. TEGEL (2012) Climate change during and after the Roman Empire: reconstructing the past from scientific and historical evidence. *Journal of Interdisciplinary History*, 43(2), pp. 169 – 220.
- MCEVEDY, C. & R. JONES (1978) *Atlas of World Population History, Facts on File*, Harmondsworth: Penguin Books Ltd.
- MENKE, U., E. VAN DE LAAR & G. LENSELINK (1998) *Flevobericht 415 – De geologie en bodem van zuidelijk Flevoland*.

- METCALFE, S.E., S. ELLIS, B.P. HORTON, J.B. INNES, J. MCARTHUR, A. MITLEHNER, A. PARKES, J.S. PETHICK, J. REES, J. RIDGWAY, M.M. RUTHERFORD, I. SHENNAN & M.J. TOOLEY (2000) The Holocene evolution of the Humber Estuary: reconstructing change in a dynamic environment. *Geological Society, London, Special Publications*, 166(1), pp. 97 – 118.
- MIALL, A.D. (1985) Architectural-element analysis: A new method of facies analysis applied to fluvial deposits. *Earth-Science Reviews*, 22(4), pp. 261 – 308.
- MIEDEMA, M. (1983) *Vijffentwintig eeuwen bewoning in het terpengebied ten noordoosten van Groningen*. Amsterdam: Free University Amsterdam.
- MIKKELSEN, J.H., R. LANGOHR & R.I. MACPHAIL (2007) Soilscape and land-use evolution related to drift sand movements since the Bronze Age in Eastern Jutland, Denmark. *Geoarchaeology*, 22(2), pp. 157 – 181.
- MINDERHOUD, P.S.J., K.M. COHEN, W.H.J. TOONEN, G. ERKENS & W.Z. HOEK (2016) Improving age-depth models of fluvio-lacustrine deposits using sedimentary proxies for accumulation rates. *Quaternary Geochronology*, 33, pp. 35 – 45.
- MISSIAEN, T., I. JONGEPIER, K. HEIRMAN, T. SOENS, V. GELORINI, J. VERNIERS, J. VERHEGGE & P. CROMBÉ (2016) Holocene landscape evolution of an estuarine wetland in relation to its human occupation and exploitation: Waasland Scheldt polders, northern Belgium. *Netherlands Journal of Geosciences*, 96(1), pp. 35 – 62.
- MODDERMAN, P.J.R. (1948) Oudheidkundige aspecten van de Bodemkartering. *Boor & Spade*, pp. 209 – 212.
- MOHRIG, D., P.L. HELLER, C. PAOLA & W.J. LYONS (2000) Interpreting avulsion process from ancient alluvial sequences: Guadalupe-Matarranya system (northern Spain) and Wasatch Formation (western Colorado). *Geological Society of America Bulletin*, 112(12), pp. 1787 – 1803.
- MOREE, J. & M. VAN TRIERUM (1992) Rotterdam-Terbregge. In P. Woltering & W. Hessing, eds. *Archeologische kroniek van Holland over 1991*. pp. 361 – 362.
- MOREE, J., A. CARMIGGELT, T. GOOSSENS, A. GUIRAN, F. PETERS & M. VAN TRIERUM (2002) Archeologisch onderzoek in het Maasmondegebied: archeologische kroniek 1991-2000. In A. Carmiggelt, A. Guiran, & M. Van Trierum, eds. *BOORbalans 5 Bijdragen aan de bewoningsgeschiedenis van het Maasmondegebied*. Rotterdam, pp. 87 – 213.
- MOREE, J., A. SCHOONHOVEN & M. VAN TRIERUM (2010) Archeologisch onderzoek van het BOOR in het Maasmondegebied: archeologische kroniek 2001-2006. In A. Carmiggelt, M. Van Trierum, & D. Wesselingh, eds. *BOORbalans 6 Bijdragen aan de bewoningsgeschiedenis van het Maasmondegebied*. pp. 77 – 240.
- MURRAY, A.S. & A.G. WINTLE (2003) The single aliquot regenerative dose protocol: potential for improvements in reliability. *Radiation measurements*, 37(4), pp. 377 – 381.
- MURRIETTA-FLORES, P. (2012) Understanding human movement through spatial technologies. The role of natural areas of transit in the Late Prehistory of South-western Iberia. *Trabajos de Prehistoria*, 69(1), pp. 103 – 122.
- NEEFJES, J., R. VAN BEEK & R. ELFRING (2011) *Cultuurhistorische atlas van de Vecht: biografie van Nederlands grootste kleine rivier*.
- NICHOLAS, A.P., D.E. WALLING, R.J. SWEET & X. FANG (2006) New strategies for upscaling high-resolution flow and overbank sedimentation models to quantify floodplain sediment storage at the catchment scale. *Journal of Hydrology*, 329(3 – 4), pp. 577 – 594.
- NIEUWHOF, A. & M. SCHEPERS (2016) Living on the Edge: Synanthropic Salt Marshes in the Coastal Area of the Northern Netherlands from around 600 BC. *Archaeological Review from Cambridge*, 32(2).
- NIU, M., T. HEATON, P.G. BLACKWELL & C.E. BUCK (2013) The Bayesian approach to radiocarbon calibration curve estimation: the IntCal13, Marine13, and SHCal13 methodologies. *Radiocarbon*, 55(4), pp. 1905 – 1922.
- NOOREN, K., W.Z. HOEK, H. VAN DER PLICHT, M. SIGL, M.J. VAN BERGEN, D. GALOP, N. TORRESCANO-VALLE, G. ISLEBE, A. HUIZINGA, T. WINKELS & H. MIDDELKOOP (2016) Explosive eruption of El Chichón volcano (Mexico) disrupted 6th century Maya civilization and contributed to global cooling. *Geology*, 44(2), pp. 175 – 178.

- NUMAN, A.M. (2005) *Noord-Hollandse kerken en kapellen in de Middeleeuwen, ca. 720 – 1200. Een archeologische, bouwhistorische en historische inventarisatie*, Zutphen.
- O'BRIEN, M.P. (1931) Estuary tidal prisms related to entrance areas. *Civil Eng.*, 1, pp. 738 – 739.
- O'BRIEN, M.P. (1969) Equilibrium flow areas of inlets on sandy coasts. *Journal of the Waterways and Harbors Division, Proceedings of the American Society of Civil Engineers*, 95(ww1), p.43 – 53.
- OELE, E., W. APON, R. FISCHER, M.M., HOOGENDOORN, C.S. MESDAG, E.F.J. DE MULDER, B. OVERZEE, A. SESÖREN & W.E. WESTERHOFF (1983) Surveying the Netherlands, Sampling Techniques, Maps and their application. *Geologie & Mijnbouw*, 62, pp. 355 – 372.
- OOST, A.P. (1995) *Dynamics and sedimentary development of the Dutch Wadden Sea with emphasis on the Frisian inlet*. Utrecht.
- ORFORD, J.D., P. WILSON, A.G. WINTLE, J. KNIGHT & S. BRALEY (2000) Holocene coastal dune initiation in Northumberland and Norfolk, eastern UK: climate and sea-level changes as possible forcing agents for dune initiation. *Geological Society London Special Publications*, 166, pp. 197 – 217.
- OSTERKAMP, W.R., C.R. HUPP & M. STOFFEL (2012) The interactions between vegetation and erosion: new directions for research at the interface of ecology and geomorphology. *Earth Surface Processes and Landforms*, 37(1), pp. 23 – 36.
- OTVOS, E.G. (2000) Beach ridges – definitions and significance. *Geomorphology*, 32, pp. 83 – 108.
- OTVOS, E.G. (2012) Coastal barriers – nomenclature, processes, and classification issues. *Geomorphology*, 139 – 140, pp. 39 – 52.
- OUDEHOEF, J.W.M., A.A.A. VERHOEVEN & I. SCHUURING (2013) *Tiel rond 1000: Analyse van vier opgravingen in de Tielse binnenstad*, Amsterdam.
- OUT, W.A. (2009) *Sowing the seed?: human impact and plant subsistence in Dutch wetlands during the Late Mesolithic and Early and Middle Neolithic (5500-3400 cal BC)*, Leiden: Leiden University Press.
- PAPING, R. (2009) Urbanisatie en de-urbanisatie in Nederland 1400-1850. *Paper presented at 'Dag van de Historische Demografie'*, Tilburg, 4 december 2009.
- PEETERS, J.H.M. (2007) *Hoge Vaart A 27 in context: towards a model of Mesolithic – Neolithic land use dynamics as a framework for archaeological heritage management*. University of Amsterdam.
- PENNINGTON, B.T., J. BUNBURY & N. HOVIUS (2016) Emergence of Civilization, Changes in Fluvio-Deltaic Style, and Nutrient Redistribution Forced by Holocene Sea-Level Rise. *Geoarchaeology*, 31(3), pp. 194 – 210.
- PHILLIPS, J.D. (2003) Sources of nonlinearity and complexity in geomorphic systems. *Progress in Physical Geography*, 27(1), pp. 1 – 23.
- PIERIK, H.J. & R.J. VAN LANEN (2017) Roman and early-medieval habitation patterns in a delta landscape: the link between settlement elevation and landscape dynamics. *Quaternary International* (in press).
- PIERIK, H.J., K.M. COHEN & E. STOUTHAMER (2016) A new GIS approach for reconstructing and mapping dynamic Late Holocene coastal plain palaeogeography. *Geomorphology*, 270, pp. 55 – 70.
- PIERIK, H.J., K.M. COHEN, P.C. VOS, A.J.F. VAN DER SPEK & E. STOUTHAMER (2017)(a) Late Holocene coastal-plain evolution of the Netherlands: the role of natural preconditions in human-induced sea ingresses. *Proceedings of the Geologists' Association*, 128(2), pp. 180 – 197.
- PIERIK, H.J., E. STOUTHAMER & K.M. COHEN (2017)(b) Natural levee evolution in the Rhine-Meuse delta, the Netherlands, during the first millennium CE. *Geomorphology*, 295, pp. 215 – 234.
- PIJLS, F.W.G. (1948) *Een gedetailleerde bodemkartering van de gemeente Didam*. Wageningen: Landbouwhogeschool Wageningen.
- PONS, L.J. (1953) Oevergronden als Middeleeuwse afzettingen en overslag gronden als dijk doorbraakafzettingen in het rivierkleigebied. *Boor en Spade*, 7, pp.97 – 111.
- PONS, L.J. (1957) *De geologie, de bodenvorming en de waterstaatkundige ontwikkeling van het Land van Maas en Waal en een gedeelte van het Rijk van Nijmegen*. Wageningen.

- PONS, L.J. (1965) De Zeekleigronden. In *De bodem van Nederland: toelichting bij de bodemkaart van Nederland schaal 1:200.000*. Wageningen: STIBOKA, pp. 23 – 59.
- PONS, L.J. (1966) *De bodemkartering van het Land van Maas en Waal en een gedeelte van het Rijk van Nijmegen*, Wageningen.
- PONS, L.J. (1992) Holocene peat formation in the lower parts of the Netherlands. In J.T.A. Verhoeven, ed. *Fens and bogs in the Netherlands: vegetation, history, nutrient dynamics and conservation*. Kluwer, pp. 7 – 79.
- PONS, L.J. & A.J. WIGGERS (1959/1960) *De Holocene wordingsgeschiedenis van Noordholland en het Zuiderzee gebied*.
- PONS, L.J. & I.S. ZONNEVELD (1965) *Soil ripening and soil classification: initial soil formation of alluvial deposits with a classification of the resulting soils*, Wageningen: Veenman.
- PONS, L.J. & M.F. VAN OOSTEN (1974) *De Bodem van Noordholland. Toelichting bij blad 5 van de Bodemkaart van Nederland, schaal 1: 200.000*, STIBOKA.
- PONS, L.J., S. JELGERSMA, A.J. WIGGERS & J. DE JONG (1963) Evolution of the Netherlands coastal area during the Holocene. In J. de Jong, ed. *Verhandelingen van het KNGMG Transactions of the jubilee convention – part two*. 's Gravenhage: Koninklijk Nederlands Geologisch Mijnbouwkundig Genootschap, pp. 197 – 207.
- PRUISSERS, A.P. & W. DE GANS (1985) *De bodem van Leidschendam*, Haarlem.
- PYE, K. & A. NEAL (1993) Late Holocene dune formation on the Sefton coast, northwest England. *The Dynamics and Environmental Context of Aeolian Sedimentary Systems*, 72, pp. 201 – 217.
- PYE, K. & H. TSOAR (2008) *Aeolian sand and sand dunes*, Springer Science & Business Media.
- RAEMAEEKERS, D.C. (2005) Het Vroeg -en Midden-Neolithicum in Noord-, Midden -en West-Nederland. In J. Deebe, E. Drenth, M. van Oursouw, & L. Verhart, eds. *De Steentijd van Nederland*. pp. 261 – 282.
- RAMSEY, C.B. (2009) Bayesian analysis of radiocarbon dates. *Radiocarbon*, 51(1), pp. 337 – 360.
- RAPP, G.R. & C.L. HILL (2006) *Geoarchaeology: the earth-science approach to archaeological interpretation*, Yale University Press.
- RAPPOL, M. (1987) Saalian till in The Netherlands: A review. In J.J.M. van der Meer, ed. *Tills and Glaciotectonics*. Rotterdam: Balkema, pp. 3 – 21.
- RAVI, S., D.D. BRESHEARS, T.E. HUXMAN & P. D'ODORICO (2010) Land degradation in drylands: Interactions among hydrologic-aeolian erosion and vegetation dynamics. *Geomorphology*, 116(3 – 4), pp. 236 – 245.
- REGNAULD, H., S. JENNINGS, C. DELANEY & L. LEMASSON (1996) Holocene sea-level variations and geomorphological response: An example from northern Brittany (France). *Quaternary Science Reviews*, 15(8 – 9), pp. 781 – 787.
- REIMER, P.J., E. BARD, A. BAYLISS, J.W. BECK, P.G. BLACKWELL, C. BRONK RAMSEY, C.E. BUCK, H. CHENG, R.L. EDWARDS, M. FRIEDRICH & P.M. GROOTES (2013) IntCal13 and Marine13 radiocarbon age calibration curves 0-50,000 years cal BP. *Radiocarbon*, 55(4), pp. 1869 – 1887.
- REINECK, H.-E. & I.B. SINGH (1980) *Depositional Sedimentary Environments: With Reference to Terrigenous Clastics* second, Berlin: Springer-Verlag.
- RENSINK, E., J.-W. DE KORT, J. VAN DOESBURG, L. THEUNISSEN & J. BOUWMEESTER (2016) *Digitaal informatiesysteem Prospectie op Maat: Werkwijze en verantwoording*, Amersfoort.
- RIEU, R., S. VAN HETEREN, A.J.F. VAN DER SPEK & P.L. DE BOER (2005) Development and preservation of a Mid-Holocene tidal-channel network offshore the Western Netherlands. *Journal of Sedimentary Research*, 75(3), pp. 409 – 419.
- RIKSEN, M., R. KETNER-OOSTRA, C. VAN TURNHOUT, M. NIJSSEN, D. GOOSSENS, P.D. JUNGERIUS & W. SPAAN (2006) Will we lose the last active inland drift sands of Western Europe? The origin and development of the inland drift-sand ecotype in the Netherlands. *Landscape Ecology*, 21(3 SPEC. ISS.), pp. 431 – 447.
- ROELEVELD, W. (1974) The Holocene Evolution of the Groningen Marine-Clay District. *Berichten van de Rijksdienst voor het Oudheidkundig Bodemonderzoek*, 24, pp. 1 – 133.

- ROEP, T.B. (1984) Progradation, erosion and changing coastal gradient in the coastal barrier deposits of the western Netherlands. *Geologie & Mijnbouw*, 63(3), pp. 249 – 258.
- ROEP, T.B. & D.J. BEETS (1988) Sea level rise and paleotidal levels from sedimentary structures in the coastal barriers in the western Netherlands since 5600 BP. *Geologie & Mijnbouw*, 67(1988), pp. 53 – 60.
- ROORDA, I.M. & R. WIEMER (1992) The ARCHIS project: Towards a new national archaeological record in the Netherlands. In C. Larsen, ed. *Sites and monuments: National Archaeological Records*. Copenhagen, pp. 117 – 122.
- ROSSI, V., A. AMOROSI, G. SARTI & M. POTENZA (2011) Influence of inherited topography on the Holocene sedimentary evolution of coastal systems: An example from Arno coastal plain (Tuscany, Italy). *Geomorphology*, 135(1 – 2), pp. 117 – 128.
- ROYMANS, N. & F. GERRITSEN (2002) Landscape, ecology and mentalitas: a long-term perspective on developments in the Meuse-Demer-Scheldt region. *Proceedings of the prehistorical society*, 68, pp. 257 – 287.
- RUTTE, R. & M. IJSSELSTIJN (2014) 1000 – 1500 – Stadswording aan waterwegen: de grote stedenboom. In R. Rutte & J. E. Abrahamse, eds. *Atlas van de verstedelijking van Nederland. 1000 jaar ruimtelijke ontwikkeling*. Thoth Publishers. Bussum, pp. 170 – 185.
- RUTTE, R. & J.E. ABRAHAMSE (2015) *Atlas of the Dutch urban landscape. A millennium of spatial development*, Thoth Publishers.
- SALVADOR, A. (1994) *International Stratigraphic Guide. A Guide to stratigraphic classification, terminology, and procedure*. Second ed., Trondheim/Boulder.
- SCHELLING, J. (1955) *Stuifzandgronden: Inland-dune sand soils*, Wageningen.
- SCHELLING, J. (1970) Soil genesis, soil classification and soil survey. 4(4).
- SCHIFFER, M.B. (1976) *Behavioral archaeology*, New York: Academic Press.
- SCHIFFER, M.B. (1987) *Formation processes of the archaeological record*, Salt Lake City: University of Utah Press.
- SCHLANGER, S.H. (1992) Recognizing persistent places in Anasazi settlement systems. In J. Rossignol & L. Wandsnider, eds. *Space, time, and archaeological landscapes*. New York: Plenum Press, pp. 91 – 112.
- SCHNEEWEISS, J. & T. SCHATZ (2014) The impact of landscape change on the significance of political centres along the lower Elbe River in the 10th century A.D. *Quaternary International*, 324, pp. 20 – 33.
- SCHOKKER, J., H.J.T. WEERTS, W.E. WESTERHOFF, H.J.A. BERENDSEN & C. DEN OTTER (2007) Introduction of the Boxtel formation and implications for the Quaternary lithostratigraphy of the Netherlands. *Geologie & Mijnbouw/Netherlands Journal of Geosciences*, 86(3), pp. 197 – 210.
- SCHOORL, H. (1999) *De convexe kustboog: Texel, Vlieland, Terschelling: bijdragen tot de kennis van het westelijk Waddengebied en de eilanden Texel, Vlieland en Terschelling*.
- SCHOTHORST, C. (1977) Subsidence of low moor peat soils in the western Netherlands. *Geoderma*, 17, pp. 265 – 291.
- SCHUBERT, S.D., M.J. SUAREZ, P.J. PEGION, R.D. KOSTER & J.T. BACMEISTER (2004) On the cause of the 1930s Dust Bowl. *Science*, 303(5665), pp. 1855 – 1859.
- SEVINK, J., E.A. KOSTER, B. VAN GEEL & J. WALLINGA (2013) Drift sands, lakes, and soils: The multiphase Holocene history of the Laarder Wasmeren area near Hilversum, the Netherlands. *Geologie & Mijnbouw/Netherlands Journal of Geosciences*, 92(4), pp. 243 – 266.
- SHEN, Z., T.E. TÖRNQVIST, B. MAUZ, E.L. CHAMBERLAIN, A.G. NIJHUIS & L. SANDOVAL (2015) Episodic overbank deposition as a dominant mechanism of floodplain and delta-plain aggradation. *Geology*, 43(10), pp. 875 – 878.
- SHEPARD, F. (1932) Sediments on continental shelves. *Geol. Soc. America Bulletin*, 4(43), p.1017 – 1040.
- SIMM, D.J. & D.E. WALLING (1998) Lateral variability of overbank sedimentation on a Devon flood plain. *Hydrological Sciences Journal*, 43(5), pp. 715 – 732.
- SLICKER VAN BATH, B.H. (1957) *Een samenleving onder spanning, geschiedenis van het platteland in Overijssel*, Assen.

- SLINGERLAND, R. & N.D. SMITH (1998) Necessary conditions for a meandering-river avulsion. *Geology*, 26(5), pp. 435 – 438.
- SMITH, D.E., S. HARRISON, C.R. FIRTH & J.T. JORDAN (2011) The early Holocene sea level rise. *Quaternary Science Reviews*, 30(15 – 16), pp. 1846 – 1860.
- SMITH, N.D. & M. PEREZ-ARLUCEA (2008) Natural levee deposition during the 2005 flood of the Saskatchewan River. *Geomorphology*, 101(4), pp. 583 – 594.
- SMITH, N.D., T.A. CROSS, J.P. DUFFICY & S.R. CLOUGH (1989) Anatomy of avulsion. *Sedimentology*, 36, pp. 1 – 23.
- SMITH, N.D., M. PÉREZ-ARLUCEA, D.A. EDMONDS & R.L. SLINGERLAND (2009) Elevation adjustments of paired natural levees during flooding of the Saskatchewan River. *Earth Surf. Process. Landf.*, 34(8), pp. 1060 – 1068.
- SORREL, P., M. DEBRET, I. BILLEAUD, S.L. JACCARD, J.F. MCMANUS & B. TESSIER (2012) Persistent non-solar forcing of Holocene storm dynamics in coastal sedimentary archives. *Nature Geoscience*, 5(12), pp. 892 – 896.
- SPEK, T. (1996) Die bodenkundliche und landschaftliche Lage von Siedlungen, Äckern und Gräberfeldern in Drenthe (nördliche Niederlande). Eine Studie zur Standortwahl in vorgeschichtlicher, frühgeschichtlicher und mittelalterlicher Zeit (3400 v. Chr. – 1500 n. Chr.). *Siedlungsforschung; Archeologie, Geschichte, Geographie*, (14), pp. 95 – 193.
- SPEK, T. (2004) *The open field village landscape in Drenthe: a historical-geographical study*, Stichting Matrijs.
- SPEK, T., W. GROENMAN-VAN WAATERINGE, M. KOOISTRA & L. BAKKER (2003) Formation and land-use history of celtic fields in north-west Europe: An interdisciplinary case study at Zeijen, The Netherlands. *European Journal of Archaeology*, 6(2), pp. 141 – 173.
- STAFLEU, J., D. MALJERS, F.S. BUSSCHERS, J.L. GUNNINK, J. SCHOKKER, R.M. DAMBRINK, H.J. HUMMELMAN & M.L. SCHIJF (2013) *GeoTop modelling*, Utrecht.
- STAFLEU, J., D. MALJERS, J.L. GUNNINK, A. MENKOVIC & F.S. BUSSCHERS (2011) 3D modelling of the shallow subsurface of Zeeland, the Netherlands. *Netherlands Journal of Geosciences*, 90(4), pp. 293 – 310.
- STANLEY, D.J. & A.G. WARNE (1993) Nile Delta: Geological Recent and Impact Evolution. *Science*, 260(5108), pp. 628 – 634.
- STANLEY, D.J. & A.G. WARNE (1994) Worldwide initiation of holocene marine deltas by deceleration of sea-level rise. *Science (New York, N.Y.)*, 265(5169), pp. 228 – 231.
- STARING, W.C.H. (1858-1867) Geologische kaart van Nederland 1:200.000 in 19 bladen, uitgevoerd door het Topographisch Bureau van Oorlog, uitgegeven op last van Z.M. den Koning. A.C. Kruseman, Haarlem.
- STECKHAN, H. (1950) Bodenabtragung durch Wind in Niedersachsen – eine Gefahr für die Landeskultur. *Neues Archiv für Niedersachsen*, 17, pp. 320 – 335.
- STEENBEEK, R. (1990) *On the balance between wet and dry: vegetation horizon development and prehistoric occupation: a palaeoecological-micromorpho – logical study in the Dutch river area*. Amsterdam: Vrije Universiteit Amsterdam.
- STEFANI, M. & S. VINCENZI (2005) The interplay of eustasy, climate and human activity in the late Quaternary depositional evolution and sedimentary architecture of the Po Delta system. *Marine Geology*, 222 – 223, pp. 19 – 48.
- STOOTHAMER, E. (2001) Sedimentary products of avulsions in the Holocene Rhine–Meuse Delta, The Netherlands. *Sedimentary Geology*, 145(1 – 2), pp. 73 – 92.
- STOOTHAMER, E. & H.J.A. BERENDSEN (2001) Avulsion Frequency, Avulsion Duration, and Interavulsion Period of Holocene Channel Belts in the Rhine-Meuse Delta, The Netherlands. *Journal of Sedimentary Research*, 71(4), pp. 589 – 598.
- STOOTHAMER, E. & H.J.A. BERENDSEN (2007) Avulsion: The relative roles of autogenic and allogenic processes. *Sedimentary Geology*, 198(3 – 4), pp. 309 – 325.

- STOUTHAMER, E., K.M. COHEN & M.J.P. GOUW (2011) Avulsion and its implications for fluvial-deltaic architecture: Insights from the Holocene Rhine-Meuse Delta. In S.K. Davidson, S. Leleu, & C.P. North, eds. *From River to Rock Record: The preservation of fluvial sediments and their subsequent interpretation*. Society for Sedimentary Geology, Special Publication 97, pp. 215 – 231.
- STREIF, H. (1972) The results of stratigraphical and facial investigations in the coastal Holocene of Woltzetzen/Ostfriesland, Germany. *Geologiska Föreningen i Stockholm Förhandlinga*, 94(2), pp. 281 – 299.
- STREIF, H. (1978) A new method for the representation of sedimentary sequences in coastal regions. *Coastal Engineering Proceedings*, 1(16), pp. 1245 – 1256.
- SUGITA, S., M.J. GAILLARD & A. BROSTRÖM (1999) Landscape openness and pollen records: a simulation approach. *The Holocene*, 9(4), pp. 409 – 421.
- SUGITA, S., T. PARSHALL, R. CALCOTE & K. WALKER (2010) Testing the Landscape Reconstruction Algorithm for spatially explicit reconstruction of vegetation in northern Michigan and Wisconsin. *Quaternary Research*, 74(5), pp. 289 – 300.
- SYVITSKI, J.P.M. & Y. SAITO (2007) Morphodynamics of deltas under the influence of humans. *Global and Planetary Change*, 57(3 – 4), pp. 261 – 282.
- SYVITSKI, J.P., C.J. VÖRÖSMARTY, A.J. KETTNER & P. GREEN (2005) Impact of humans on the flux of terrestrial sediment to the global coastal ocean. *Science*, 308(5720), pp. 376 – 380.
- SYVITSKI, J.P.M., A.J. KETTNER, I. OVEREEM, E.W.H. HUTTON, M.T. HANNON, G.R. BRAKENRIDGE, J. DAY, C. VÖRÖSMARTY, Y. SAITO, L. GIOSAN & R.J. NICHOLLS (2009) Sinking deltas due to human activities. *Nature Geoscience*, 2(10), pp. 681 – 686.
- TAMURA, T. (2012) Beach ridges and prograded beach deposits as palaeoenvironment records. *Earth-Science Reviews*, 114(3 – 4), pp. 279 – 297.
- TAMURA, T., Y. SAITO, V. LAP NGUYEN, T.K. OANH TA, M.D. BATEMAN, D. MATSUMOTO & S. YAMASHITA (2012) Origin and evolution of interdistributary delta plains; insights from Mekong River Delta. *Geology*, 40(4), pp. 303 – 306.
- TANABE, S., Y. SAITO, Q. LAN VU, T.J.J. HANEBUTH, Q. LAN NGO & A. KITAMURA (2006) Holocene evolution of the Song Hong (Red River) delta system, northern Vietnam. *Sedimentary Geology*, 187(1 – 2), pp. 29 – 61.
- TANABE, S., T. NAKANISHI, Y. ISHIHARA & R. NAKASHIMA (2015) Millennial-scale stratigraphy of a tide-dominated incised valley during the last 14 kyr: Spatial and quantitative reconstruction in the Tokyo Lowland, central Japan. *Sedimentology*, 62(7), pp. 1837–1872.
- TAVERNIER, R. (1946) L' évolution du Bas Escaut au Pléistocène supérieur. *Géologie: Bulletin de la Société Belge de Géologie*.
- TAVERNIER, R. (1948) Les formations quaternaires de la Belgique en rapport avec l' évolution morphologique du pays. *Bulletin de la Société belge de Géologie*, 62, pp. 609 – 641.
- TEN ANSCHER, T.J. (2012) *Leven met de Vecht: Schokland-P14 en de Noordoostpolder in het Neolithicum en de Bronstijd*. Amsterdam: Universiteit van Amsterdam.
- TEN CATE, J.A.M. & G.C. MAARLEVELD (1977) *Geomorfologische kaart van Nederland – schaal 1:50.000. Toelichting op de legenda*, Wageningen/Haarlem.
- TER BRUGGE, J.P. (2002) Duikers gemaakt van uitgeholde boomstammen in het Maasmondgebied in de Romeinse tijd. In A. Carmiggelt, J. Guiran, & M. Van Trierum, eds. *BOORbalans 5 Bijdragen aan de bewoningsgeschiedenis van het Maasmondgebied*. pp. 63 – 86.
- TER WEE, M.W. (1976) *Toelichtingen bij de Geologische kaart van Nederland 1:50.000. Blad Sneek (10W, 10O)*, Haarlem.
- TESCH, P. (1930) *Eenige toelichting bij de Geologische kaart van Nederland 1: 50.000.*,

- TESCH, P. (1942) Toelichtingen bij de Geologische Kaart van Nederland. Mededeeling nr. 1: De geologische kaart van Nederland en hare beteekenis voor verschillende doeleinden. *Mededelingen van de Geologische Stichting*, serie D(1), p.38.
- TEUNISSEN, D. (1988) De bewoningsgeschiedenis van Nijmegen en omgeving, haar relatie tot de landschapsbouw en haar weerspiegeling in palynologische gegevens. *Mededelingen van de afdeling Biogeologie van de Discipline Biologie van de Katholieke Universiteit van Nijmegen*, 15, p.108.
- TEUNISSEN, D. (1990) Palynologisch onderzoek in het oostelijk rivierengebied – een overzicht. *Mededelingen van de afdeling Biogeologie van de Discipline Biologie van de Katholieke Universiteit van Nijmegen*, 16, p.163.
- THEUWS, F. (1989) Middeleeuwse parochiecentra in de Kempen 1000-1350. In A.A.A.Verhoeven & F. Theuws, eds. *Het Kempenproject 3. De Middeleeuwen centraal*. Waalre, pp. 97 – 216.
- THONON, I., H. MIDDELKOOP & M. VAN DER PERK (2007) The influence of floodplain morphology and river works on spatial patterns of overbank deposition. *Netherlands Journal of Geosciences*, 86(1), pp. 63 – 75.
- TOLKSDORF, J.F. & K. KAISER (2012) Holocene aeolian dynamics in the European sand-belt as indicated by geochronological data. *Boreas*, 41(3), pp. 408 – 421.
- TOONEN, W.H.J. (2013) *A Holocene flood record of the Lower Rhine*. Utrecht University.
- TOONEN, W.H.J., M.G. KLEINHANS & K.M. COHEN (2012) Sedimentary architecture of abandoned channel fills. *Earth Surface Processes and Landforms*, 37(4), pp. 459 – 472.
- TOONEN, W.H.J., T.H. DONDEERS, B. VAN DER MEULEN, K.M. COHEN & M.A. PRINS (2013) A composite Holocene palaeoflood chronology of the Lower Rhine. In *A Holocene flood record of the Lower Rhine*. Utrecht, pp. 137 – 150.
- TOONEN, W.H.J., T.G. WINKELS, K.M. COHEN, M.A. PRINS & H. MIDDELKOOP (2015) Lower Rhine historical flood magnitudes of the last 450 years reproduced from grain-size measurements of flood deposits using End Member Modelling. *Catena*, 130, pp. 69-81.
- TOONEN, W.H.J., S. VAN ASSELEN, E. STOUTHAMER & N.D. SMITH (2016) Depositional development of the Muskeg Lake crevasse splay in the Cumberland Marshes (Canada). *Earth Surface Processes and Landforms*, 41(1), pp. 117 – 129.
- TOONEN, W.H.J., S.A. FOULDS, M.G. MACKLIN & J. LEWIN (2017) Events, episodes, and phases: Signal from noise in flood-sediment. *Geology*, 45(4), pp. 331 – 334.
- TÖRNQVIST, T.E. (1990) Fluvial activity, human activity and vegetation (2300-600 yr BP) near a residual channel in the Tielerwaard (central Netherlands). *Berichten van de Rijksdienst voor het Oudheidkundig Bodemonderzoek*, 40, pp. 223 – 241.
- TÖRNQVIST, T.E. (1993) *Fluvial sedimentary geology and chronology of the Holocene Rhine-Meuse delta, the Netherlands*. Utrecht University.
- TÖRNQVIST, T.E. & G.J. VAN DIJK (1993) Optimizing sampling strategy for radiocarbon dating of Holocene fluvial systems in a vertically aggrading setting. *Boreas*, 22(2), pp. 129 – 145.
- TÖRNQVIST, T.E. & J.S. BRIDGE (2002) Spatial variation of overbank aggradation rate and its influence on avulsion frequency. *Sedimentology*, 49(5), pp. 891 – 905.
- TÖRNQVIST, T.E., D.J. WALLACE, J.E.A. STORMS, J. WALLINGA, R.L. VAN DAM, M. BLAAUW, M.S. DERKSEN, C.J.W. KLERKS, C. MEIJNEKEN & E.M.A. SNIJDERS (2008) Mississippi Delta subsidence primarily caused by compaction of Holocene strata. *Nature Geoscience*, 1(3), pp. 173 – 176.
- VAKARELOV, B.K. & R. BRUCE AINSWORTH (2013) A hierarchical approach to architectural classification in marginal-marine systems: Bridging the gap between sedimentology and sequence stratigraphy. *AAPG Bulletin*, 97(7), pp. 1121 – 1161.
- VAN ASSELEN, S. (2011) The contribution of peat compaction to total basin subsidence: implications for the provision of accommodation space in organic-rich deltas. *Basin Research*, 23(2), pp. 239 – 255.

- VAN ASSELEN, S., D. KARSSSENBERG & E. STOUTHAMER (2011) Contribution of peat compaction to relative sea-level rise within Holocene deltas. *Geophysical Research Letters*, 38(24).
- VAN ASSELEN, S., K.M. COHEN & E. STOUTHAMER (2017) The impact of avulsion on groundwater level and peat formation in delta floodbasins during the middle-Holocene transgression in the Rhine-Meuse delta, The Netherlands. *The Holocene*, (in press).
- VAN BAVEL, B.J.P. (1999) Transitie en continuïteit. De bezitsverhoudingen en de plattelandseconomie in het westelijke gedeelte van het Gelderse riviereengebied ca. 1300 – ca. 1570. *Werken Gelre*, 52.
- VAN BAVEL, B.J.P. (2010) *Manors and Markets, Economy and Society in the Low Countries 500-1600*, Oxford University Press.
- VAN BEEK, R. (2009) *Reliëf in tijd en ruimte. Interdisciplinair onderzoek naar bewoning en landschap van Oost-Nederland tussen vroege prehistorie en middeleeuwen*. Wageningen University.
- VAN BEEK, R. & B.J. GROENEWOUDT (2011) An Odyssey along the River Vecht in the Dutch-German border area. A Regional Analysis of Roman-period Sites in Germania Magna. *Germania*, 89(1 – 2), pp. 157 – 190.
- VAN BEEK, R., M.T.I.J. GOUW-BOUMAN & J.A.A. BOS (2015)(a) Mapping regional vegetation developments in Twente (the Netherlands) since the Late Glacial and evaluating contemporary settlement patterns. *Netherlands Journal of Geosciences*, 94(3), pp. 1 – 27.
- VAN BEEK, R., G.J. MAAS & E. VAN DEN BERG (2015)(b) Home Turf: an interdisciplinary exploration of the long-term development, use and reclamation of raised bogs in the Netherlands. *Landscape History*, 36(2), pp. 5 – 34.
- VAN DASSELAAR, M. (2006) *Archeologisch onderzoek bij de aanleg van riolering aan de Gouderaksedijk te Gouda*, Rapport AO4-348-R, ArcheoMedia bv, Capelle aan de IJssel.
- VAN DE PLASSCHE, O. (1982) Sea-level change and water-level movements in the Netherlands during the Holocene. *Mededelingen Rijks Geologische Dienst*, 36(1), pp. 1 – 93.
- VAN DE PLASSCHE, O. (1985) Time-Limit Assessment of some Holocene Transgressive and Regressive Periods in the Northern Netherlands. *Eiszeitalter und Gegenwart*, 35, pp. 43 – 48.
- VAN DE PLASSCHE, O., B. MAKASKE, W.Z. HOEK, M. KONERT & J. VAN DER PLICHT (2010) Mid-Holocene water-level changes in the lower Rhine-Meuse delta (western Netherlands): Implications for the reconstruction of relative mean sea-level rise, palaeoriver-gradients and coastal evolution. *Geologie & Mijnbouw/Netherlands Journal of Geosciences*, 89(1), pp. 3 – 20.
- VAN DEN BERG, J.H., C.J.L. JEUKEN & A.J.F. VAN DER SPEK (1996) Hydraulic processes affecting the morphology and evolution of the Westerschelde estuary. In K. F. Nordstrom & C. T. Roman, eds. *Estuarine Shores: Evolution. Environments and Human Alterations*. John, Wiley and Sons, pp. 157 – 184.
- VAN DEN BERG, M.W. & C. DEN OTTER. (1993) *Toelichtingen bij de geologische kaart van Nederland 1: 50.000, blad Almelo Oost/Denekamp (28O/29)*, Haarlem.
- VAN DEN BIGGELAAR, D.F.A.M. (2017) *New land, old history: past landscapes and hominin activity covering the last 220,000 years in Flevoland, The Netherlands*. Vrije Universiteit Amsterdam.
- VAN DEN BIGGELAAR, D.F.A.M., S.J. KLUIVING, R.T. VAN BALEN, C. KASSE, S.R. TROELSTRA & M.A. PRINS (2014) Storms in a lagoon: Flooding history during the last 1200 years derived from geological and historical archives of Schokland (Noordoostpolder, the Netherlands). *Netherlands Journal of Geosciences*, 93(4), pp. 175-196.
- VAN DER HAMMEN, T., MAARLEVELD, G.C., J.C. VOGEL & W.H. ZAGWIJN (1967) Stratigraphy, climatic succession and radiocarbon dating of the last glacial in the Netherlands. *Geologie & Mijnbouw*, 46(3), pp. 79 – 95.
- VAN DER HEIJDEN, P. (2016) *Romeinse wegen in Nederland*, Utrecht: Matrijs.
- VAN DER MEIJ, M. (2014) *De geomorfologie van het Gelderse riviereengebied – actualisering van de geomorfologische kaart*, Wageningen.
- VAN DER MEULEN, M.J., J.C. DOORNENBAL, J.L. GUNNINK, J. STAFLEU & J. SCHOKKER (2013) 3D geology in a 2D country: perspectives for geological surveying in the Netherlands. *Netherlands Journal of Geosciences*, 92(4), pp. 217 – 241.

- VAN DER MOLEN, J. & H.E. DE SWART (2001)(a) Holocene wave conditions and wave-induced sand transport in the southern North Sea. *Continental Shelf Research*, 21(16 – 17), pp. 1723 – 1749.
- VAN DER MOLEN, J. & H.E. DE SWART (2001)(b) Holocene tidal conditions and tide-induced sand transport in the southern North Sea. *Journal of Geophysical Research*, 106(5), pp. 9339 – 9362.
- VAN DER MOLEN, J. & B. VAN DIJCK (2000) The evolution of the Dutch and Belgian coasts and the role of sand supply from the North Sea. *Global and Planetary Change*, 27(1 – 4), pp. 223 – 244.
- VAN DER MOLEN, P. & S. HOEKSTRA (1988) A palaeoecological study of a hummock-hollow complex from Engbertsdijkveen, in the Netherlands. *Review of Palaeobotany and Palynology*, 56(3 – 4), p.213 – 274.
- VAN DER SPEK, A.J.F. (1995) Reconstruction of tidal inlet and channel dimensions in the Frisian Middelzee, a former tidal basin in the Dutch Wadden Sea. *Tidal Signatures in Modern and Ancient Sediments: International Association of Sedimentologists, Special Publication*, (24), p.239 – 258.
- VAN DER SPEK, A.J.F. (1996) Holocene depositional sequences in the Dutch Wadden Sea south of the island of Ameland. *Mededelingen Rijks Geologische Dienst*, 57, pp. 41 – 78.
- VAN DER SPEK, A.J.F. (1997) Tidal asymmetry and long-term evolution of Holocene tidal basins in The Netherlands: simulation of palaeo-tides in the Schelde estuary. *Marine Geology*, 141(1 – 4), pp. 71 – 90.
- VAN DER SPEK, A.J.F. & D.J. BEETS (1992) Mid-Holocene evolution of a tidal basin in the western Netherlands: a model for future changes in the northern Netherlands under conditions of accelerated sea-level rise? *Sedimentary Geology*, 80, pp. 185 – 197.
- VAN DER SPEK, A.J.F., J. CLEVERINGA & S. VAN HETEREN (2007) From transgression to regression; coastal evolution near The Hague, the Netherlands, around 5000 BP. *Coastal Sediments '07*, pp. 1 – 13.
- VAN DER VALK, L. (1992) *Mid-and Late-Holocene coastal evolution in the beach-barrier area of the Western Netherlands*. Amsterdam: Vrije Universiteit Amsterdam.
- VAN DER VALK, L. (1996)(a) Geology and sedimentology of Late Atlantic sandy, wave-dominated deposits near The Hague (South-Holland, the Netherlands): a reconstruction of an early prograding coastal sequence. *Mededelingen Rijks Geologische Dienst*, 57, pp. 201 – 227.
- VAN DER VALK, L. (1996)(b) Coastal barrier deposits in the central Dutch coastal plain. *Mededelingen Rijks Geologische Dienst*, 57, pp. 133 – 199.
- VAN DER VELDE, H.M. (2004) Landschapsordening in de Vroege Middeleeuwen. Het ontstaan van het middeleeuwse cultuurlandschap in Oost-Nederland. In R.M. Van Heeringen, E.H.P. Cordfunke, M. Ilsink, & H. Sarfatij, eds. *Geordend landschap. 3000 jaar ruimtelijke ordening in Nederland*. Hilversum, pp. 43 – 59.
- VAN DIJK, G.J., H.J.A. BERENDSEN & W. ROELEVELD (1991) Holocene water level development in The Netherlands' river area; implications for sea-level reconstruction. *Geologie & Mijnbouw*, 70, pp. 311 – 326.
- VAN DINTER, M. (2013) The Roman Limes in the Netherlands: How a delta landscape determined the location of the military structures. *Geologie & Mijnbouw/Netherlands Journal of Geosciences*, 92(1), pp. 11 – 32.
- VAN DINTER, M. & W.K. VAN ZIJVERDEN (2010) Settlement and land use on crevasse splay deposits; geoarchaeological research in the Rhine-Meuse Delta, the Netherlands. *Geologie & Mijnbouw/Netherlands Journal of Geosciences*, 89(1), pp. 21 – 34.
- VAN DINTER, M., L.I. KOOISTRA, M.K. DÜTTING, P.V. RIJN & C. CAVALLO (2014) Could the local population of the Lower Rhine delta supply the Roman army? Part 2: Modelling the carrying capacity using archaeological, palaeo-ecological and geomorphological data. *JALC*, pp. 5 – 50.
- VAN DINTER, M., K.M. COHEN, W.Z. HOEK, E. STOUTHAMER, E. JANSMA & H. MIDDELKOOP (2017) Late Holocene lowland fluvial archives and geoarchaeology: Utrecht's case study of Rhine river abandonment under Roman and Medieval settlement. *Quaternary Science Reviews*, 166, pp. 227-265.
- VAN ES, W.A. (1981) *De Romeinen in Nederland*, Bussum.
- VAN ES, W.A. & W.J.H. VERWERS (2010) Early Medieval settlements along the Rhine: precursors and contemporaries of Dorestad. *Journal of Archaeology in the Low Countries*, 2(1), pp. 5 – 39.

- VAN GEEL, B., O. BRINKKEMPER, E.J. WEEDA & J. SEVINK (2017) Formation, vegetation succession and acidification of a Mid-Holocene moorland pool in the western Netherlands. *Netherlands Journal of Geosciences*, 96(1), pp. 17 – 27.
- VAN GEEL, B., J. BUURMAN & H.T. WATERBOLK (1996) Archaeological and palaeoecological indications of an abrupt climate change in The Netherlands, and evidence for climatological teleconnections around 2650 BP. *Journal of Quaternary Science*, 11(6), pp. 451 – 460.
- VAN GIFFEN, A.E. (1940) Die Wurtenforschung in Holland. Probleme der Küstenforschung im südlichen Nordseegebiet. 1, pp. 70 – 86.
- VAN GIJN, A.L. & H.T. WATERBOLK (1984) The colonization of the salt marshes of Friesland and Groningen: the possibility of a transhumant prelude. *Palaeohistoria*, 26, p.22.
- VAN HELVOORT, P.J. (2003) Complex confining layers: A physical and geochemical characterization of heterogeneous unconsolidated fluvial deposits using a facies-based approach. *Netherlands, Geographical Studies*, 321, p.147.
- VAN HETEREN, S., D.J. HUNTLEY, O. VAN DE PLASSCHE & R.K. LUBBERTS (2000) Optical dating of dune sand for the study of sea-level change. *Geology*, 28(5), p.411.
- VAN HETEREN, S., A.J.F. VAN DER SPEK & B. VAN DER VALK (2011) Evidence and Implications of Middle- To Late- Holocene Shoreface Steepening Offshore the Western Netherlands. *Coastal Sediments '11*, pp. 188 – 201.
- VAN LANEN, R.J. (2016) Historische routes in Nederland. Een multidisciplinaire zoektocht naar verdwenen en langdurig gebruikte routetrajecten. *Tijdschrift voor Historische Geografie (THG)*, 1(1), pp. 12 – 29.
- VAN LANEN, R.J. (2017) *Changing ways: Patterns of habitation, connectivity, and persistence in the northwestern European Lowlands during the first millennium AD*. Utrecht University.
- VAN LANEN, R.J. & H.J. PIERIK (2017) Calculating connectivity patterns in delta landscapes: modelling Roman and early-medieval route networks and their stability in dynamic lowlands. *Quaternary International*.
- VAN LANEN, R.J., M.C. KOSIAN, B.J. GROENEWOUDT & E. JANSMA (2015)(a) Finding a way: Modeling landscape prerequisites for Roman and early-medieval routes in the Netherlands. *Geoarchaeology*, 30(3), pp. 200 – 222.
- VAN LANEN, R.J., M.C. KOSIAN, B.J. GROENEWOUDT, T. SPEK & E. JANSMA (2015)(b) Best travel options: Modelling Roman and early-medieval routes in the Netherlands using a multi-proxy approach. *Journal of Archaeological Science: Reports*, 3, pp. 144 – 159.
- VAN LANEN, R.J., E. JANSMA, J. VAN DOESBURG & B.J. GROENEWOUDT (2016)(a) Roman and early-medieval long-distance transport routes in north-western Europe: Modelling frequent-travel zones using a dendroarchaeological approach. *Journal of Archaeological Science*, 73, pp. 120 – 137.
- VAN LANEN, R.J., GROENEWOUDT, B.J., T. SPEK & E. JANSMA (2016)(b) Route persistence. Modelling and quantifying historical route-network stability from the Roman period to early-modern times (AD 100 – 1600): a case study from the Netherlands. *Archaeological and Anthropological Sciences*, pp. 1 – 16.
- VAN LIERE, W.J. (1948) *De bodemgesteldheid van het Westland*. Wageningen University.
- VAN LIERE, W.J. (1950) Upper Holocene transgressions in the neighbourhood of the mouth of the Meuse. *Boor & Spade*.
- VAN LONDEN, H. (2006) *Midden-Delfland: the roman native landscape past and present*. Amsterdam University.
- VAN LOON, A.J. & A.J. WIGGERS (1975) Holocene lagoonal silts (formerly called “sloef”) from the Zuiderzee. *Sedimentary Geology*, 13, pp. 47 – 55.
- VAN MOURIK, J.M. (1988) Landschap in beweging: Ontwikkeling en bewoning van een stuifzandlandschap in de Kempen. *Netherlands Geographical Studies*, 74, p.191.
- VAN MOURIK, J.M., K.G.J. NIEROP & D.A.G. VANDENBERGHE (2010) Radiocarbon and optically stimulated luminescence dating based chronology of a polycyclic driftsand sequence at Weerterbergen (SE Netherlands). *Catena*, 80(3), pp. 170 – 181.

- VAN MOURIK, J.M., R.T. SLOTBOOM & J. WALLINGA (2011) Chronology of plagic deposits; palynology, radiocarbon and optically stimulated luminescence dating of the Posteles (NE-Netherlands). *Catena*, 84(1 – 2), pp. 54 – 60.
- VAN MUNSTER, B. (2012) *Landscape changes in the Netherlands during the Late Roman period and the Early Middle Ages (A.D. 270-525), a multi disciplinary approach combining changes in demography, physical landscape and climate*, Amersfoort.
- VAN OORSCHOT, M., M.G. KLEINHANS, G. GEERLING & H. MIDDELKOOP (2015) Distinct patterns of interaction between vegetation and morphodynamics. *Earth Surface Processes and Landforms*, 41(6), pp. 791 – 808.
- VAN RUMMELEN, F.F.F.E. (1965) *Toelichtingen bij de Geologische kaart van Nederland 1:50.000. Bladen Zeeuwsch-Vlaanderen West en Oost*, Haarlem.
- VAN RUMMELEN, F.F.F.E. (1970) *Toelichtingen bij de Geologische kaart van Nederland 1:50.000. Blad Schouwen-Duiveland*, Haarlem.
- VAN RUMMELEN, F.F.F.E. (1972) *Toelichtingen bij de Geologische kaart van Nederland 1:50.000. Blad Walcheren*, Haarlem.
- VAN RUMMELEN, F.F.F.E. (1978) *Toelichtingen bij de Geologische kaart van Nederland 1:50.000. Blad Beveland*, Haarlem.
- VAN STAALDUINEN, C.J. (1979) *Toelichtingen bij de geologische kaart van Nederland 1:50.000. Blad Rotterdam West (37W)*, Haarlem.
- VAN STRAATEN, L.M.J.U. (1965) Coastal barrier deposits in South-and North-Holland in particular in the areas around Scheveningen and IJmuiden. *Mededelingen Rijks Geologische Dienst – Nieuwe Serie*, 17, pp. 41 – 75.
- VAN STRAATEN, L.M.J.U. & P.H. KUENEN (1957) Accumulation of fine grained sediments in the dutch wadden sea. *Geologie & Mijnbouw*, 19, pp. 329 – 354.
- VAN STRAATEN, L.M.J.U. & P.H. KUENEN (1958) Tidal action as a cause of clay accumulation. *Journal of Sedimentary Petrology*, 28(4), pp. 406 – 413.
- VAN TRIERUM, M. (1986) *Landschap en bewoning rond de Bernisse in de IJzertijd en de Romeinse Tijd*, Rotterdam.
- VAN VLIET-LANOË, B., J. GOSLIN, A. HÉNAFF, B. HALLÉGOUËT, C. DELACOURT, E. LE CORNEC & M. MEURISSE-FORT (2015) Holocene formation and evolution of coastal dunes ridges, Brittany (France). *Comptes Rendus – Geoscience*.
- VAN WALLENBURG, C. (1966) *De bodem van Zuid-Holland, toelichting bij blad 6 van de bodemkaart van Nederland schaal 1: 200.000*, Wageningen.
- VAN ZIJVERDEN, W.K. (2013) The palaeoenvironment of eastern West-Frisia: a critical review. *Studien zur nordeuropäischen Bronzezeit*, 1, pp. 161 – 169.
- VAN ZIJVERDEN, W.K. (2017) *After the deluge, a palaeogeographical reconstruction of bronze age West-Frisia (2000-800 BC)*. Leiden University.
- VANDENBERGHE, D.A.G., C. DERESE, C. KASSE & P. VAN DEN HAUTE (2013) Late Weichselian (fluvio-)aeolian sediments and Holocene drift-sands of the classic type locality in Twente (E Netherlands): A high-resolution dating study using optically stimulated luminescence. *Quaternary Science Reviews*, 68, pp. 96 – 113.
- VANGHELUWE, D. & T. SPEK (2008) De laatmiddeleeuwse transitie van landbouw en landschap in de Noord-Brabantse Kempen. *Historisch-Geografisch Tijdschrift*, 26(1), pp. 1 – 23.
- VEENENBOS, J.S. (1949) De bodemkartering van de Friese knipkleigronden. *Boor & Spade*, pp. 76 – 86.
- VEENENBOS, J.S. & J. SCHUYLENBORGH (1951) Het knip- of knikverschijnsel van kleigronden. *Boor & Spade*, pp. 24 – 39.
- VERA, H. (2011) *Dat men het goed van den ongeboornen niet mag verkoopen, Gemene gronden in de Meierij van Den Bosch tussen hertog en hertgang 1000 – 2000*, Oisterwijk: Uitgeverij BOXpress.

- VERBRAECK, A. (1970) *Toelichtingen bij de Geologische kaart van Nederland 1:50.000. Blad Gorinchem Oost (380)*, Haarlem.
- VERBRAECK, A. (1984) *Toelichtingen bij de Geologische kaart van Nederland 1:50.000. Blad Tiel (39W/O)*, Haarlem.
- VERBRAECK, A. & J.H. BISSCHOPS (1971) *Toelichtingen bij de geologische kaart van Nederland 1:50.000. Blad Willemstad Oost (43O)*, Haarlem.
- VERHAGEN, J.W.H.P. (2007) *Case studies in archaeological predictive modelling*, Leiden: Leiden University Press.
- VERHAGEN, J.W.H.P. (2013) On the Road to Nowhere? Least Cost Paths, Accessibility and the Predictive Modelling Perspective. In F. Contreras, M. Farjas, & J. F. Melero, eds. *Proceedings of the 38th Annual Conference on Computer Applications and Quantitative Methods in Archaeology*. Granada/Oxford: Archaeopress, pp. 383 – 390.
- VERHAGEN, J.W.H.P. & A. BORSBOOM (2009) The design of effective and efficient trial trenching strategies for discovering archaeological sites. *Journal of Archaeological Science*, 36(8), p.1807 – 1815.
- VERHAGEN, J.W.H.P. & T.G. WHITLEY (2011) Integrating Archaeological Theory and Predictive Modeling: a Live Report from the Scene. *Journal of Archaeological Method and Theory*, 19, pp. 49 – 100.
- VERHAGEN, J.W.H.P. & C.F. JENESON (2012) A Roman Puzzle. Trying to Find the Via Belgica with GIS. Thinking beyond the Tool: Archaeological Computing & the Interpretive Process. *BAR International Series*, 2344, pp. 123 – 130.
- VERHAGEN, J.W.H.P., I. VOSSEN, M.R. GROENHUIJZEN & J. JOYCE (2016) Now you see them, now you don't: Defining and using a flexible chronology of sites for spatial analysis of Roman settlement in the Dutch river area. *Journal of Archaeological Science: Reports*, 10, pp. 309 – 321.
- VERLINDE, A.D. (1987) *Die Gräber und Grabfunde der späten Bronzezeit und frühen Eisenzeit in Overijssel*. Leiden University.
- VERLINDE, A.D. (2004) De Germaanse nederzetting te Denekamp binnen een regionaal archeologisch kader van de Romeinse tijd. *OHB*, 119, p.57 – 92.
- VERSTRAETEN, G., N. BROOTHAERTS, M. VAN LOO, B. NOTEBAERT, K. D'HAEN, B. DUSAR & H. DE BRUE (2017) Variability in fluvial geomorphic response to anthropogenic disturbance. *Geomorphology*, 294, pp. 20-39.
- VERWERS, W.J.H. (1998) *North Brabant in Roman and Early Medieval Times: Habitation History*. VU University Amsterdam.
- VINK, A., H. STEFFEN, L. REINHARDT & G. KAUFMANN (2007) Holocene relative sea-level change, isostatic subsidence and the radial viscosity structure of the mantle of northwest Europe (Belgium, the Netherlands, Germany, southern North Sea). *Quaternary Science Reviews*, 26(25 – 28), pp. 3249 – 3275.
- VINK, T. (1926) *De Lekstreek – Een aardrijkskundige verkenning van een bewoond deltagebied*, Amsterdam: Paris.
- VIS, G.G., K.M. COHEN, W.E. WESTERHOFF, J.H. VEEN, M.P. HIJMA, A.J.F. VAN DER SPEK & P.C. VOS (2015) Paleogeography. In I. Shennan, A. J. Long, & B. Horton, eds. *Handbook of Sea-Level Research*. Wiley-Blackwell, pp. 514 – 534.
- VLAM, A.W. (1942) *Historisch-morfologisch onderzoek van eenige Zeeuwsche eilanden*. Leiden University.
- VLETTER, W.F. (2013) Predictive modelling of unknown road and path networks. In W. Neubauer, I. Trinks, R. Salisbury, & C. Einwögerer, eds. *Archaeological Prospection. Proceedings of the 10th International Conference – Vienna*. pp. 321 – 323.
- VLETTER, W.F. (2014) (Semi) automatic extraction from airborne laser scan data of roads and paths in forested areas, *Proc. SPIE*.
- VLETTER, W.F. & R.J. VAN LANEN (in review) Finding “Hidden” Routes. Applying a Multi-Modelling Approach on Lost Route and Path Networks: an Example from the Veluwe Region in the Netherlands, Rural Landscapes.
- VON NAGY, C. (1997) The geoarchaeology of settlement in the Grijalva delta, Olmec to Aztec: settlement patterns in the ancient Gulf lowlands, pp. 253 – 277.
- VOS, P.C. (2006) Toelichting bij de nieuwe paleogeografische kaarten van Nederland. *Nationale Onderzoeksagenda Archeologie*, pp. 1 – 15.

- VOS, P.C. (2008) The geological development of the Oer-IJ area. In M.S.M. Kok, ed. *The homecoming of religious practice: an analysis of offering sites in the wet low-lying parts of the landscape in the Oer-IJ area (2500 BC-AD 450)*. pp. 81 – 95.
- VOS, W.K. (2009) *Bataafs platteland; het Romeinse nederzettingslandschap in het Nederlandse Kromme-Rijng gebied*. Vrije Universiteit Amsterdam.
- VOS, P.C. (2015)(a) *Origin of the Dutch coastal landscape – Long-term landscape evolution of the Netherlands during the Holocene described and visualized in national, regional and local palaeogeographical map series*, Groningen: Barkhuis.
- VOS, P.C. (2015)(b) Flooding history of the Southwestern Netherlands. In P. C. Vos, ed. *Origin of the Dutch coastal landscape – Long-term landscape evolution of the Netherlands during the Holocene described and visualized in national, regional and local palaeogeographical map series*. Groningen: Barkhuis, pp. 82 – 97.
- VOS, P.C. & R.M. VAN HEERINGEN (1997) Holocene geology and occupation history of the Province of Zeeland. *Mededelingen Nederlands Instituut voor Toegepaste Geowetenschappen TNO*, 59, pp. 5 – 109.
- VOS, P.C. & B.A.M. BAARDMAN (1999) The Subatlantic evolution of the coastal area around the Wijnaldum-Tjitsma terp. In *The excavations at Wijnaldum. Reports on Frisia in Roman and Medieval times*. Rotterdam: Balkema, pp. 33 – 72.
- VOS, P.C. & W.P. VAN KESTEREN (2000) The long-term evolution of intertidal mud flats in the northern Netherlands during the Holocene; natural and anthropogenic processes. *Continental Shelf Research*, 20, pp. 31 – 38.
- VOS, P.C. & D.A. GERRETS (2005) Archaeology: a major tool in the reconstruction of the coastal evolution of Westergo (northern Netherlands). *Quaternary International*, 133 – 134, pp. 61 – 75.
- VOS, P.C. & F.D. ZEILER (2008) Overstromingsgeschiedenis van zuidwest-Nederland, interactie tussen natuurlijke en antropogene processen. *Grondboor & Hamer*, 62(3/4), pp. 86 – 95.
- VOS, P.C. & Y. EIJSKOOT (2011) Geologie. In Eijsskoot, Brinkkemper, & De Ridder, eds. *RAM-rapport 200 Vlaardingen – De Vergulde Hand West Onderzoek van archeologische resten van de middenbronstijd tot en met de late middeleeuwen*. Amersfoort: Rijksdienst voor het Cultureel Erfgoed, pp. 69 – 146.
- VOS, P.C. & S. DE VRIES (2013) 2e generatie palaeogeografische kaarten van Nederland (versie 2.0). Deltares, Utrecht.
- VOS, P.C. & E. KNOL (2015) Holocene landscape reconstruction of the Wadden Sea area between Marsdiep and Weser. *Netherlands Journal of Geosciences*, 94(2), pp. 157 – 183.
- VOS, P.C. & Y. EIJSKOOT (2015) Palaeo-environmental investigations at the archaeological site Vergulde Hand West in Vlaardingen (Port of Rotterdam). In P.C. Vos, ed. *Origin of the Dutch coastal landscape – Long-term landscape evolution of the Netherlands during the Holocene described and visualized in national, regional and local palaeogeographical map series*. Groningen: Barkhuis, pp. 264 – 293.
- VOS, P.C., E.C. RIEFFE & E.E.B. BULTEN (2007) *Nieuwe geologische kaart van Den Haag en Rijswijk*, Den Haag, Rijswijk.
- VOS, P.C., J. DE KONING & R. VAN EERDEN (2015)(a) Landscape history of the Oer-IJ tidal system, Noord-Holland (The Netherlands). *Netherlands Journal of Geosciences*, 94(4), pp. 295 – 332.
- VOS, P.C., F.P.M. BUNNIK, K.M. COHEN & H. CREMER (2015)(b) A staged geogenetic approach to underwater archaeological prospection in the Port of Rotterdam (Yangtzehaven, Maasvlakte, The Netherlands): A geological and palaeoenvironmental case study for local mapping of Mesolithic lowland landscapes. *Quaternary International*, 367, pp. 4 – 31.
- VOS, P.C., M. VAN DER HEIJDE & E. STURMAN (2015)(c) Landscape reconstruction of the Bronze Age site De Druppels found on a salt-marsh ridge of the Westfriese-inlet system; a case study north of Alkmaar (Noord-Holland). In P. C. Vos, ed. *Origin of the Dutch coastal landscape – Long-term landscape evolution of the Netherlands during the Holocene described and visualized in national, regional and local palaeogeographical map series*. Groningen: Barkhuis, pp. 294 – 319.

- WALLINGA, J., F. DAVIDS & J.W.A. DIJKMANS (2007) Luminescence dating of Netherlands sediments. *Geologie & Mijnbouw/Netherlands Journal of Geosciences*, 86(3), pp. 179 – 196.
- WALLINGA, J., J.M. VAN MOURIK & M.L.M. SCHILDER (2013) Identifying and dating buried micropodzols in Subatlantic polycyclic drift sands. *Quaternary International*, 306, pp. 60 – 70.
- WARTENBERG, W., A. VÖTT, H. FREUND, H. HADLER, M. FRECHEN, T. WILLERSHÄUSER, S. SCHNAIDT, P. FISCHER & L. OBROCKI (2013) Evidence of isochronic transgressive surfaces within the Jade Bay tidal flat area, southern German North Sea coast – Holocene event horizons of regional interest. *Zeitschrift für Geomorphologie – Supplementary Issues*, 57, pp. 229 – 256.
- WATERBOLK, H.T. (1964) Podsolierungserscheinungen bei Grabhügeln. *Palaeohistoria*, 10, p.87 – 102.
- WATERBOLK, H.T. (1980) Hoe oud zijn de Drentse dorpen? Problemen van nederzettingscontinuïteit in Drenthe van de bronstijd tot in de middeleeuwen. *Westerheem*, 29, pp. 190 – 212.
- WATERS, M.R. (2008) Alluvial chronologies and archaeology of the Gila River drainage basin, Arizona. *Geomorphology*, 101(1), pp. 332 – 341.
- WEERTS, H.J.T. (1996) Fluvial, aeolian and organic facies units in the Rhine-Meuse delta. In H.J.T. Weerts, ed. *Complex confining layers – Architecture and hydraulic properties of Holocene and Late-Weichselian deposits in the fluvial Rhine-Meuse delta, the Netherlands*. Utrecht, pp. 15 – 56.
- WEERTS, H.J.T. & H.J.A. BERENDSEN (1995) Late Weichselian and Holocene fluvial palaeogeography of the southern Rhine-Meuse delta (the Netherlands). *Geologie & Mijnbouw*, 74(3), pp. 199 – 212.
- WEERTS, H.J.T., P. CLEVERINGA, F.D.D. LANG & W.E. WESTERHOFF (2000) *De lithostratigrafische indeling van Nederland – Formaties uit het Tertiair en Kwartair Versie 2000*, Utrecht.
- WEERTS, H.J.T., W.E. WESTERHOFF, P. CLEVERINGA, M.F.P. BIERKENS, J.G. VELDKAMP & K.F. RIJSDIJK (2005) Quaternary geological mapping of the lowlands of The Netherlands, a 21st century perspective. *Quaternary International*, 133 – 134, pp. 159 – 178.
- WESTERHOFF, W.E., E.F.J. MULDER & W. DE GANS (1987) *Toelichtingen bij de Geologische kaart van Nederland 1:50.000 – Alkmaar West/Oost (190/W)*, Haarlem.
- WESTERHOFF, W.E., T.E. WONG & M.C. GELUK (2003) De opbouw van de ondergrond. In E.F.J. De Mulder, M.C. Geluk, I. Ritsema, W.E. Westerhoff, & T.E. Wong, eds. *De ondergrond van Nederland*. Utrecht: De ondergrond van Nederland, vol. 7. Nederlands Instituut voor Toegepaste Geowetenschappen TNO, p. 247 – 352.
- WHITE, D.A. & S.B. BARBER (2012) Geospatial modeling of pedestrian transportation networks: a case study from precolumbian Oaxaca, Mexico. *Journal of Archaeological Science*, 39, pp. 2684 – 2696.
- WICKHAM, C. (2009) *The Inheritance of Rome: A History of Europe from 400 to 1000*, Allen Lane.
- WIEMER, R. (2002) Standardisation: the key to archaeological data quality. In L. García Sanjuan & D.W. Wheatley, eds. *Mapping the Future of the Past, Managing the Spatial Dimension of the European Archaeological resource*. Sevilla, pp. 103 – 108.
- WIGGERS, A.J. (1955) *De wording van het Noordoostpoldergebied – Een onderzoek naar de fysisch-geografische ontwikkeling van een sedimentair gebied*. Zwolle.
- WILKINSON, T. (2000) Settlement and land use in the zone of uncertainty in upper Mesopotamia, pp. 3 – 35.
- WILLEMS, W.J.H. (1986) *Romans and Batavians. A Regional Study in the Dutch Eastern River Area*. University of Amsterdam.
- WILLEMSE, N.W. & B.J. GROENEWOUDT (2012) Resilience of Meta-Stable Landscapes? The Non-Linear Response of Late Glacial Aeolian Landforms to Prehistoric Reclamation along Dutch River Valleys. *Landscape Archaeology. Proceedings of the International Conference Held in Berlin, 6th – 8th June 2012*, 3, pp. 245 – 255.
- WILSON, P., J. MCGOURTY & M.D. BATEMAN (2004) Mid- to late-Holocene coastal dune event stratigraphy for the north coast of Northern Ireland. *The Holocene*, 14(2004), pp. 406 – 416.
- WINTLE, A.G. (2008) Luminescence dating: Where it has been and where it is going. *Boreas*, 37(4), pp. 471 – 482.

- WOLTHUIS, T.I. & S. ARNOLDUSSEN (2015) IJzertijdbewoning: een toetsing van de bewoningsmodellen voor locatiekeuze en demografie. *Bijdragen in de studie van de metaaltijden*, 2, pp. 171 – 185.
- WORSTER, D. (1979) *Dust bowl: the southern plains in the 1930s*, Oxford University Press.
- WU, L., C. ZHU, C. ZHENG, F. LI, X. WANG, L. LI & W. SUN (2014) Holocene environmental change and its impacts on human settlement in the shanghai area, East China. *Catena*, 114, pp. 78 – 89.
- ZAGWIJN, W.H. (1984) The formation of the Younger Dunes on the west coast of The Netherlands (AD 1000-1600). *Geologie & Mijnbouw*, 63, pp. 259 – 269.
- ZAGWIJN, W.H. (1986) *Nederland in het Holoceen*, Den Haag: Sdu.
- ZAGWIJN, W.H. & C.J. VAN STAALDUINEN (1975) *Toelichting bij geologische overzichtskaarten van Nederland*, Rijks Geologische Dienst.
- ZAKŠEK, K., E. FOVET, L. NUNNIGER & T. PODOBNIKAR (2008) Path Modelling and Settlement Pattern. In A. Poluschny, K. Lambers, & I. Herzog, eds. *Layers of perception. Proceedings of the 35th International Conference on Computer Applications and Quantitative Methods in Archaeology (CAA)*. Bonn, pp. 309 – 315.
- ZECCHIN, M., G. BRANCOLINI, L. TOSI, F. RIZZETTO, M. CAFFAU & L. BARADELLO (2009) Anatomy of the Holocene succession of the southern Venice lagoon revealed by very high-resolution seismic data. *Continental Shelf Research*, 29(10), pp. 1343 – 1359.
- ZHANG, Q., C. ZHU, C.L. LIU & T. JIANG (2005) Environmental change and its impacts on human settlement in the Yangtze Delta, PR China. *Catena*, 60(3), pp. 267 – 277.
- ZOETBROOD, P., C. VAN ROOIJEN, R. LAUWERIER, G. VAN HAAFF & A. VAN AS (2006) *Uit balans: Wordingsgeschiedenis en analyse van het bestand van wettelijk beschermde archeologische vindplaatsen*, Amersfoort.
- ZONNEVELD, I.S. (1960) *De Brabantse Biesbosch*. Wageningen University.

About the author

Harm Jan Pierik was born in Zwolle (the Netherlands) on 24 July 1986. In 2004 he came to Utrecht to study Earth Sciences, and obtained his Bachelor's degree in 2007 and his Master's degree Physical Geography in 2010 (both cum laude). After his graduation he worked as a junior researcher to upgrade the Rhine-Meuse delta channel belt map and on a project on dike safety and bank stability of the river Lek. He also worked on several mapping projects for the Geological Survey of the Netherlands. In 2012 he started at the archaeological company Vestigia as a physical geographer, studying landscape history around the entire Netherlands. In 2013 he came back to Utrecht University to do this PhD on the natural landscape evolution of the Netherlands during the first millennium AD. He currently works as a postdoc on the historical evolution of the Ems-Dollard estuary at Utrecht University.

Peer reviewed publications

Journal articles as first author

- PIERIK, H.J., R.J. VAN LANEN, M.T.I.J. GOUW-BOUMAN, B.J. GROENEWOUDT, J. WALLINGA & W.Z. HOEK (in review) Controls on late Holocene drift-sand dynamics: the dominant role of human pressure in the Netherlands. *The Holocene*.
- PIERIK, H.J. & R.J. VAN LANEN (2017) Roman and early-medieval habitation patterns in a delta landscape: the link between settlement elevation and landscape dynamics. *Quaternary International* (in press).
- PIERIK, H.J., K.M. COHEN, P.C. VOS, A.J.F. VAN DER SPEK & E. STOUTHAMER (2017) Late Holocene coastal-plain evolution of the Netherlands: the role of natural preconditions in human-induced sea ingressions. *Proceedings of the Geologists' Association*, 128(2), pp. 180–197.
- PIERIK, H.J., E. STOUTHAMER & K.M. COHEN (2017) Natural levee evolution in the Rhine-Meuse delta, the Netherlands, during the first millennium CE. *Geomorphology*, 295, pp. 215–234.
- PIERIK, H.J., K.M. COHEN & E. STOUTHAMER (2016) A new GIS approach for reconstructing and mapping dynamic Late Holocene coastal plain palaeogeography. *Geomorphology*, 270, pp. 55–70.

Journal articles as co-author

- DE HAAS, T., H.J. PIERIK, A.J.F. VAN DER SPEK, K.M. COHEN, B. VAN MAANEN & M.G. KLEINHANS (in review) Holocene evolution of tidal systems in the Netherlands: effects of rivers, coastal boundary conditions, eco-engineering species, inherited relief and human interference. *Earth Science Reviews*.
- JANSMA, E., R.J. VAN LANEN & H.J. PIERIK (2017) Travelling through a river delta: a landscape-archaeological reconstruction of river development and long-distance connections in the Netherlands during the first millennium AD. *Medieval Settlement Research*, 32 (in press).
- JANSMA, E., M.T.I.J. GOUW-BOUMAN, R.J. VAN LANEN, H.J. PIERIK, K.M. COHEN, B.J. GROENEWOUDT, W.Z. HOEK, E. STOUTHAMER & H. MIDDELKOOP (2014) The Dark Age of the Lowlands in an interdisciplinary light: people, landscape and climate in The Netherlands between AD 300 and 1000. *European Journal of Post - Classical Archaeologies*, 4, pp. 473–478.
- VAN LANEN, R.J. & H.J. PIERIK (2017) Calculating connectivity patterns in delta landscapes: modelling Roman and early-medieval route networks and their stability in dynamic lowlands. *Quaternary International* (in press).